

# Contrast-Enhanced Digital Mammography (CEDM)

Jacopo Nori  
Maninderpal Kaur  
*Editors*

---

# Contrast-Enhanced Digital Mammography (CEDM)

---

Jacopo Nori · Maninderpal Kaur  
Editors

# Contrast-Enhanced Digital Mammography (CEDM)

 Springer

*Editors*

Jacopo Nori  
Diagnostic Senology Unit,  
Department of Radiology  
Azienda Ospedaliero Universitaria  
Careggi  
Florence  
Italy

Maninderpal Kaur  
Department of Radiology  
Kuala Lumpur Hospital  
Kuala Lumpur  
Malaysia

ISBN 978-3-319-94552-1      ISBN 978-3-319-94553-8 (eBook)  
<https://doi.org/10.1007/978-3-319-94553-8>

Library of Congress Control Number: 2018949153

© Springer International Publishing AG, part of Springer Nature 2018

This work is subject to copyright. All rights are reserved by the Publisher, whether the whole or part of the material is concerned, specifically the rights of translation, reprinting, reuse of illustrations, recitation, broadcasting, reproduction on microfilms or in any other physical way, and transmission or information storage and retrieval, electronic adaptation, computer software, or by similar or dissimilar methodology now known or hereafter developed.

The use of general descriptive names, registered names, trademarks, service marks, etc. in this publication does not imply, even in the absence of a specific statement, that such names are exempt from the relevant protective laws and regulations and therefore free for general use.

The publisher, the authors, and the editors are safe to assume that the advice and information in this book are believed to be true and accurate at the date of publication. Neither the publisher nor the authors or the editors give a warranty, express or implied, with respect to the material contained herein or for any errors or omissions that may have been made. The publisher remains neutral with regard to jurisdictional claims in published maps and institutional affiliations.

This Springer imprint is published by the registered company Springer Nature Switzerland AG  
The registered company address is: Gewerbestrasse 11, 6330 Cham, Switzerland



*I dedicate this to my wife, Rossella, and my daughter, Viola, who tirelessly fostered my growth and blessed me with constant love, support and encouragement.*

*Si volo possum!*

*Jacopo Nori*

*To my parents, Ranbir and Harjit, who love and support me endlessly,*

*To my brother, Surinder, who inspires me,*

*To my daughter, Suneha, who makes it all worthwhile, I love you.*

*Maninderpal Kaur*

---

## Preface

As in all disciplines, learning in radiology is a lifelong process. The continuous development and application of new and improved technologies and imaging modalities is part of the allure of the speciality, but it can also be one of its greatest challenges. For breast radiologists, these new “cutting-edge” technologies have the potential to impact profoundly the ease and confidence of breast imaging interpretation and offer a more efficient diagnostic workup of patients suffering from breast disease.

Contrast-enhanced digital mammography (CEDM) is a breast imaging technique based on dual energy acquisition, combining mammography with iodine-based contrast agents to display contrast uptake in breast lesions. It improves the sensitivity and specificity of breast cancer detection by providing higher foci to breast-gland contrast and better lesion delineation than digital mammography. Preliminary results suggest that CEDM is comparable to breast magnetic resonance imaging (MRI) for evaluating the extent and size of lesions and detecting multicentric and multifocal lesions. It thus has the potential to become a readily available, fast and cost-effective examination.

The purpose of this book is to serve as a basic introduction to breast CEDM and to add depth to the growing knowledge of this relatively new technology. Thus, the text walks the reader through the basics of CEDM, making it accessible also to beginners. We have included chapters on how to set up a breast CEDM unit and the physics behind this technology. We have tried to be comprehensive in coverage of all aspects of CEDM from the review of literature, to the interpretation tips and its limitations. Our book also discusses the comparison of both functional breast imaging modalities, which are MRI and CEDM, as well as the role of CEDM in the diagnosis and staging of breast cancer. From a detailed outline of equipment prerequisites for obtaining high-quality CEDM images to instructions on how to optimize image quality in the artefacts section, the book covers the topics that are most relevant to performing this examination. The second part of this book is an atlas where we have thoroughly described imaging features of benign, premalignant and malignant breast diseases.

This book would not have come to life without the help of many people. Firstly, we would like to thank Vittorio Miele, MD, chief of the imaging section at Careggi University Hospital in Florence, Italy, for supporting our vision and getting us on track with the team at Springer, particularly Antonella Cerri, Corinna Parravicini, Manasseh Johnson, Prakash Marudhu and Vishal Anand who guided us through this process.

We are grateful to all the individuals who had the incredible vision and drive to develop this amazing technique. In particular, we would like to thank Bob Martins, who helped us to put together an exceptional team of contributing authors from Europe, Asia and the USA, who were equally passionate about this modality as we were. Thank you to all our co-authors for combining to make this outstanding work.

We would also like to acknowledge the gracious help of the Fiorenzo Fratini Onlus Association for providing us with the funding of the initial CEDM unit in Careggi. Our individual practices were the initial sites to have this modality tested in our respective countries. We felt that our collective experiences with this new technology and the knowledge we gained as a result could prove quite valuable to other breast imaging specialists.

We are extremely grateful to our colleagues and residents who have shared our vision of the value of CEDM. Our clinical work could not have been achieved without our dedicated and highly skilled staff and breast imaging technologists at Careggi University Hospital and Kuala Lumpur Hospital. We would also like to thank our colleagues in the departments of Surgery, Oncology and Pathology, whom we work closely with everyday. Most importantly, we are highly indebted to our patients, from whom we learn, and are an invaluable source of information that we can now share with all our readers.

We sincerely hope that this book is well received and provides meaningful information to our readers. Please provide us with any suggestions, constructive criticism, comments or corrections for a future edition. We look forward to your thoughts (be nice, we are quite sensitive).

Finally, this book would not have been possible without the support and encouragement of our families, who recognized our love for teaching and spared us the time away from family to pursue our passion. We hope that our children will see this book and understand that from effort and dedication come knowledge and satisfaction.

Kuala Lumpur, Malaysia  
Florence, Italy

Maninderpal Kaur  
Jacopo Nori

---

# Contents

## Part I Principles and Clinical Aspects of CEDM

<b>1 Introduction</b> . . . . .	3
Maninderpal Kaur and Jacopo Nori	
<b>2 Mammographic Breast Density and Its Effects on Imaging</b> . . . . .	9
Vincenzo Lattanzio and Angela Maria Guerrieri	
<b>3 Physics and Practical Considerations of CEDM</b> . . . . .	17
Andrew P. Smith	
<b>4 Contrast Media in CEDM</b> . . . . .	25
Felix Diekmann and Rüdiger Lawaczeck	
<b>5 An Overview of the Literature on CEDM</b> . . . . .	35
Diego De Benedetto and Chiara Bellini	
<b>6 Comparison Between Breast MRI and Contrast-Enhanced Digital Mammography</b> . . . . .	47
Marc B. I. Lobbes	
<b>7 Implementation of Contrast-Enhanced Mammography in Clinical Practice</b> . . . . .	57
Maninderpal Kaur, Claudia Lucia Piccolo, and Shantini Arasaratnam	
<b>8 Artefacts in CEDM</b> . . . . .	75
Maninderpal Kaur, Claudia Lucia Piccolo, and Victor Chong Xing Dao	
<b>9 CEDM Lexicon and Imaging Interpretation Tips</b> . . . . .	93
Giulia Bicchierai, Federica Di Naro, and Francesco Amato	
<b>10 Pitfalls and Limitations</b> . . . . .	119
Cecilia Boeri, Valeria Selvi, and Carlotta Checcucci	

## Part II CEDM in Clinical Practice

<b>11 Benign Lesions</b> . . . . .	139
Ermanno Vanzi, Federica Di Naro, and Chiara Bellini	

---

<b>12 High-Risk (B3) Lesions</b> .....	169
Giulia Bicchierai, Jacopo Nori, and Francesco Amato	
<b>13 Malignant Lesions</b> .....	185
Jacopo Nori, Chiara Bellini, and Claudia Piccolo	
<b>14 Clinical Cases</b> .....	215
Jacopo Nori, Maninderpal Kaur, Marc B. I. Lobbes, Felix Diekmann, Giulia Bicchierai, and Diego de Benedetto	
<b>Index</b> .....	255

---

## Abbreviations

ABUS	Automated breast ultrasound
ACR	American College of Radiology
AD	Architectural distortions
ADC	Apparent diffusion coefficient
ADH	Atypical ductal hyperplasia
AEC	Automatic exposure control
AGD	Average glandular dose
AI	Aromatase inhibitors
ALH	Atypical lobular hyperplasia
BC	Breast cancer
BCT	Breast conservative therapy
BI-RADS	Breast Imaging Reporting and Data System
BPE	Background parenchymal enhancement
CC	Cranio-caudal
CE2D	Contrast-enhanced 2D mammography
CE3D	Contrast-enhanced 3D mammography
CEDM	Contrast-enhanced digital mammography
CEM	Contrast-enhanced mammography
CESM	Contrast-enhanced spectral mammography
CI	Confidence interval
CIN	Contrast-induced nephrotoxicity
CNB	Core needle biopsy
CSL	Complex sclerosing lesions
CT	Computed tomography
Cu	Copper
DBT	Digital breast tomosynthesis
DCE	Dynamic contrast enhanced
DCE-MRI	Dynamic contrast-enhanced MRI
DCIS	Ductal carcinoma in situ
DWI	Diffusion-weighted imaging
eGFR	Glomerular filtration rate
EUREF	European Reference Organisation for Quality Assured Breast Screening and Diagnostic Services
ESUR	European Society of Uroradiology
FA	Fibroadenoma
FC	Fibrocystic change
FDA	Food and Drug Administration

---

FEA	Flat epithelial atypia
FFDM	Full-field digital mammography
FFMG	Full-field mammography
GE	General electric
HE	High-energy
HHUS	Hand-held ultrasound
IDC	Infiltrative/invasive ductal cancer
IDC-NOS	Invasive ductal carcinoma, not otherwise specified
ILC	Invasive lobular carcinoma
IV	Intravenous
KeV	kilo-electron volts
MBD	Mammographic breast density
MBI	Molecular breast imaging
MD	Mammographic density
MIBB	Swiss Minimally Invasive Biopsy Group
MIP	Maximum intensity projection
MLO	Medio-lateral oblique
MMG	Mammography
Mo	Molybdenum
MRI	Magnetic resonance imaging
MQSA	Mammography Quality Standards Act
NAC	Neoadjuvant chemotherapy
NME	Non-mass Enhancement
NOS	Not otherwise specified
NPV	Negative predictive value
PACS	Picture Archiving and Communication System
PCC	Pearson's correlation coefficient
pCR	Pathologic complete response
PET	Positron-emission mammography
PL	Papillary lesion
PPV	Positive predictive value
PT	Phyllodes tumour
QC	Quality control
Rh	Rhodium
RS	Radial scar
SCC	Six class categories
SI	Subtraction images
TAM	Tamoxifen
TCEM	Temporal contrast-enhanced mammography
TDLU	Terminal ductal-lobular unit
US	Ultrasound
U.S.	United States
VABB	Vacuum-assisted breast biopsy
WHO	World Health Organization

---

**Part I**

**Principles and Clinical Aspects of CEDM**





# Introduction

1

Maninderpal Kaur and Jacopo Nori

Contrast-enhanced digital mammography (CEDM) is a revolutionary technique in breast imaging that uses contrast-enhanced recombined images for the assessment of tumour angiogenesis, in a similar manner as magnetic resonance imaging (MRI) (Fig. 1.1). CEDM is the only imaging modality that provides contrast-enhanced images, which are similar to MRI and complement it with the morphological information obtained from the high-resolution, low-energy image that is comparable to full-field digital mammography (FFDM).

Our departments at Careggi University Hospital, Florence, Italy, and Kuala Lumpur Hospital (KLH), Malaysia, pioneered the first CEDM units in our countries in September 2016 and September 2017, respectively. Based on our initial clinical experience, we observed that CEDM allows highly sensitive functional assessment and localization of lesions with lower imaging costs and shorter imaging acquisition and interpretation times compared to MRI.

The primary objective of any diagnostic breast-imaging modality is to accurately define

the presence, type, and extent of the disease to optimize patient management decisions. The choice between mastectomy and breast-conserving surgery depends on numerous factors, including the location, size, and grade of the tumour, multifocality or multicentricity, and the ratio of the tumour size to the breast volume.

Currently, mammography remains the gold standard for screening of breast cancer; however, mammography brings its share of limitations, particularly in denser breasts, where its sensitivity in cancer detection is reduced. The continued development of digital X-ray systems has enabled additional techniques such as breast tomosynthesis to overcome this limitation, resulting in improved cancer detection and reduction of false-positive findings. Breast tomosynthesis combined with other breast-imaging modalities such as ultrasound has further improved the diagnostic accuracy.

MRI, which entails the use of a contrast medium to highlight the neovascularity of breast cancer induced by angiogenesis, is currently considered the most sensitive breast cancer detection modality. However, the widespread use of MRI is limited by its high cost, variable accessibility, and patient contraindications. In addition, the side effects and unknown long-term toxicity related to gadolinium are areas of concern, resulting in the need for alternative imaging modalities for functional imaging of the breast with different contrast media.

---

Maninderpal Kaur (✉)  
Department of Radiology, Kuala Lumpur Hospital,  
Kuala Lumpur, Malaysia

J. Nori  
Diagnostic Senology Unit, Department of Radiology,  
Azienda Ospedaliero Universitaria Careggi,  
Florence, Italy  
e-mail: [jakopo@tin.it](mailto:jakopo@tin.it)

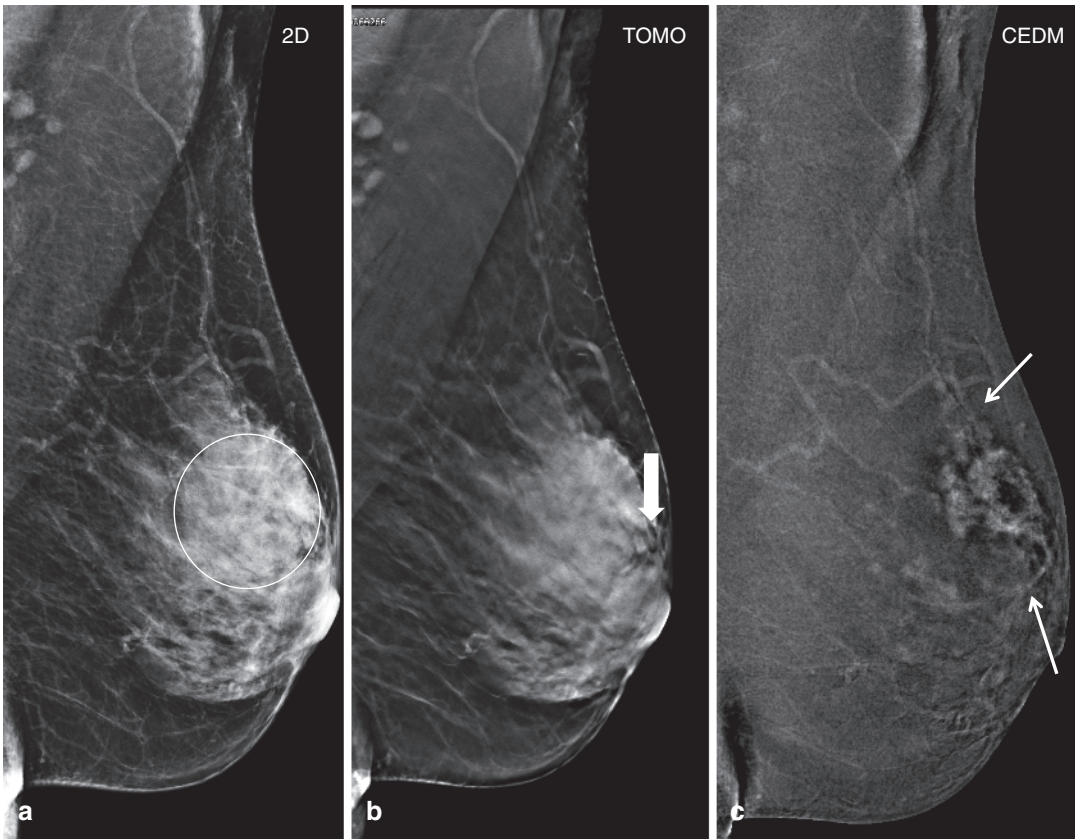


**Fig. 1.1** A 54-year-old woman with personal history of biopsy-proven invasive ductal carcinoma presented for preoperative staging. (a) 2D low-energy MLO view with dense breast parenchymal pattern showing an asymmetrical area of increased density (with respect to the other side, not shown) particularly in the left upper quadrant

(circle). (b) Tomosynthesis MLO view reveals a subtle architectural distortion in the upper quadrant (*block arrow*). (c) CEDM recombined image demonstrates an enhancing mass with central necrosis and surrounding neoangiogenesis (*arrows*). CEDM contrast-enhanced digital mammography, MLO mediolateral oblique

CEDM is a favourable alternative to MRI in terms of cost-effectiveness and space allocation, as CEDM can be performed in the existing mammography suite. The adoption of CEDM into imaging practices requires only minor modifications of the existing equipment to obtain full CEDM capability. In breast-imaging practices that own mammography systems with CEDM capability, CEDM implementation requires only the purchase of a software upgrade from the vendor and the insertion of a copper filter into the existing mammography unit. A standard contrast power injector is also required. Widespread adoption of this technique is potentially rapid given that most of the current generation mammography units incorporate CEDM capability.

CEDM uses a dual energy technique to generate a high-resolution, low-energy digital mammography image and a high-energy contrast-enhanced image that provides information on lesion vascularity. Subsequently, these two images are recombined into one image, resulting in a digital subtracted image of the relative distribution of iodine in the breast (Fig. 1.2).

Because CEDM allows both the characterization and localization of lesions, many of the additional conventional diagnostic imaging views become unnecessary, thereby improving workflow and reducing patient anxiety. In our clinical practice, we have observed that the improved lesion characterization leads to more precise

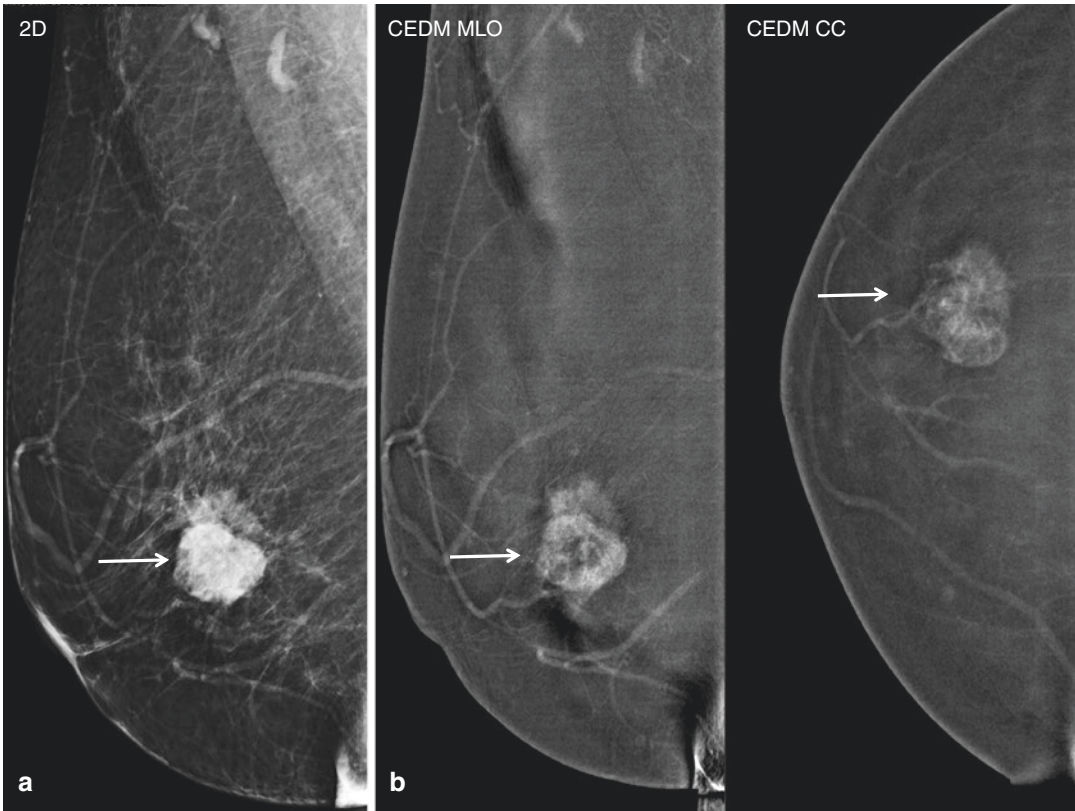


**Fig. 1.2** A 46-year-old woman with a biopsy-proven invasive carcinoma. **(a)** 2D low-energy right MLO view shows a lobulated mass with indistinct margins (*arrow*). **(b)** CEDM recombined images in MLO and CC view

demonstrates heterogeneous enhancement of the lobulated mass in the right upper outer quadrant. *CEDM* contrast-enhanced digital mammography, *CC* craniocaudal, *MLO* mediolateral oblique

biopsy planning with an increased positive predictive value for biopsy.

CEDM is a relatively new technique; therefore, there is a lack of familiarity with this technology and uncertainty regarding how to incorporate this modality into existing breast-imaging practices. Individuals who perform or refer patients for breast-imaging studies must understand the physics of CEDM, the indications for CEDM, how to obtain and interpret the images, and the outcomes of CEDM in specific scenarios. This book was created to satisfy that need.

Because CEDM is an emerging technology, with the United States (US) Food and Drug Administration's (FDA's) approval of the first commercial system as recent as 2011, the scientific literature related to CEDM is relatively limited. We are therefore fortunate to feature

esteemed breast-imaging colleagues who have published valuable research on CEDM as contributing authors to this book. CEDM is rapidly evolving, and our goal is to provide readers with a clinical understanding of the essentials of this modality.

This book is organized into two parts. The first part covers the theoretical aspects of CEDM, while the second part comprises of a clinical imaging atlas, in which we discuss the commonly seen benign, premalignant (B3), and malignant lesions in our clinical practice and their appearance on CEDM in our clinical experience.

In Chapter 2, we discuss the basics of breast imaging, which constitute mammography. In this chapter, Vincenzo Lattanzio, who has vast experience in 2D mammography and breast tomosynthesis (3D mammography), provides readers

with a valuable insight on mammographic breast density and its effect on imaging and breast cancer risk.

Obtaining ideal CEDM images is a collaborative effort between a radiologist and technologist. Chapter 3, which is contributed by Andrew Smith of Hologic, Bedford, USA, who has expertise in medical physics, provides readers an overview of the physics of CEDM, including the process of obtaining a CEDM image. Understanding the physics behind this novel technique will help our readers be better prepared to address the inevitable equipment variations that may develop over time.

We are fortunate to have Felix Diekmann of St. Joseph-Stift Bremen, Germany, who has been very active in clinical research regarding CEDM, share his experience regarding contrast media in CEDM in Chapter 4.

Chapter 5 provides readers with an overview of the available literature on CEDM. In this chapter, Diego De Benedetto analyses the available literature and divides it into subsections to compare different modalities as well as breast density and clinical indications, allowing readers to easily review the literature.

MRI, the most accurate breast-imaging modality to date, is compared with the exciting new CEDM technique in Chapter 6. Marc Lobbes of Maastricht University Medical Centre, the Netherlands, who has conducted exhaustive work and clinical research on both imaging modalities, provides his valuable perspective on these two imaging modalities, which have comparable sensitivity rates. The clinical indications of breast CEDM are also presented in this chapter, including high-risk screening, breast cancer staging, assessment of residual disease, CEDM after breast cancer treatment, and other clinical scenarios.

Implementing CEDM into the reader's clinical practice requires appropriate planning and staff training. Based on our clinical experience of configuring a CEDM unit at Careggi University Hospital and KLH, we systematically describe how to configure a breast CEDM programme in Chapter 7. We also review the basic steps of performing a contrasted mammography procedure.

Marc Lobbes was kind enough to share his experience of configuring a CEDM unit at his centre. This chapter therefore provides readers with a detailed account of the issues that must be considered at the initial stages of configuring a CEDM unit from the combined experiences of three large breast-imaging units and how to address them.

The artefacts observed in CEDM that we have personally encountered in our practice are addressed in Chapter 8. We provide images of the artefact types that we have encountered at our centres. With input from a medical physicist, Andrew Smith, we identify the reasons these artefacts occurred, and we describe the possible ways to eliminate them.

CEDM does not yet have a dedicated BI-RADS lexicon and classification system; therefore, we employ the morphological descriptors from the MRI BI-RADS lexicon reporting system for our CEDM cases, with some exceptions, of course. In Chapter 9, we provide a step-by-step guide to CEDM image interpretation.

The final chapter in Part I discusses the pitfalls and limitations of CEDM, which supplements but does not replace mammography. A negative CEDM does not spare the need for biopsy of a lesion that is suspicious based on mammography, ultrasound, or physical examination. The drawbacks of CEDM include patient exposure to iodinated contrast materials and the risks from radiation exposure. CEDM also features no commercially available system to biopsy regions of suspicious enhancement under CEDM guidance. These limitations are discussed at length in this chapter.

Part II provides a clinical imaging atlas of breast CEDM in which features of benign lesions, high-risk (B3) lesions, and invasive breast cancers are discussed in detail. We have strived to obtain optimal images, maintaining the highest resolution possible to demonstrate the various cases presented.

We end this book with case examples illustrating a wide variety of cases from three large centres actively performing CEDM in Europe and one centre in Asia, thus providing readers with a wide variety of cases. As a breast radiologist from

Malaysia who has worked extensively with CEDM cases in Italy and now on cases here in Malaysia, I found it interesting to survey the vast difference in the clinical presentation of cases between the two regions. Due to a lack of awareness (particularly in rural areas) and cultural issues, breast cancer cases present at much later stages in Malaysia; thus, we see cases with much larger lesions and more extensive disease processes than the cases in Europe. Therefore, we aim to provide a variety of high-quality images of a wide variety of lesions, representing a spectrum of benign, premalignant, and malignant findings in this final section.

Both at Careggi University Hospital and Kuala Lumpur Hospital, we have successfully implemented CEDM into our daily practice as a diagnostic, staging, and treatment response tool. Our systems come with a combination of 2D FFDM, 3D tomosynthesis and contrast-enhanced 2D imaging, which provide us improved localization and morphologic evaluation of enhancing lesions. This capability is valuable in surgical planning and has reduced the number of unnecessary breast biopsies at our centres.

We observed strong patient acceptance with CEDM relative to MRI due to their familiarity with the mammography procedure and the fact that CEDM is more accessible and affordable.

For radiologists embarking on a breast CEDM programme, it may be helpful to start with women who have proven breast cancer, to look for additional ipsilateral and contralateral disease. An essential component of any breast CEDM programme is the ability to perform localization and a biopsy of the lesions identified only by CEDM. Unfortunately, there is still no technology available to perform CEDM-guided biopsy; however, considering how rapidly this technology is evolving, we anticipate this capability soon becoming available.

The use of CEDM alone in symptomatic patients could decrease the radiation dose, and we expect that with future technological advancements, improvements in contrast visualization will be available at lower radiation doses. We are certain that CEDM will ultimately reduce medical costs by decreasing unnecessary costly follow-up tests and interventions.

Based on our clinical experience, CEDM is a suitable alternative to MRI for the diagnosis of symptomatic patients and the improvement of the preoperative assessment of breast cancer. CEDM is an exceptional advancement in breast cancer imaging and is expected to play an integral role in the diagnostic armamentarium of any breast cancer centre.





# Mammographic Breast Density and Its Effects on Imaging

# 2

Vincenzo Lattanzio and Angela Maria Guerrieri

## 2.1 Introduction

Mammographic breast density (MBD) is a term used to define the proportion of radiologically dense tissue in the breast, such as glandular tissue and stromal tissue, and the variable amount of water contained within the breast. This proportional representation varies greatly from one person to another due to natural structural characteristics and other factors such as age, sex hormones, menopause and specific therapies such as hormonal replacement therapy and genetic predisposition. MBD is a “dynamic” representation of radiopaque glandular and fibrous tissue unlike fat tissue, which is radiolucent.

Interest on this topic has grown since then and has recently become controversial; therefore, a decision was made to divide breast density values into categories to provide homogenous guidelines for interpretation in clinical practice.

As mammographic images are 2D representations (*area-based*) of a 3D entity (*volume-based*), new methods to measure MBD have been developed in recent years [2, 3].

These methods can be classified based on (a) the evaluation process (visual, semi-automated, fully-automated), (b) measurement of specific parameters that are area-based or volume-based and (c) qualitative or quantitative analysis (Table 2.2).

## 2.2 MBD Assessment Methods

Breast cancer derives from glandular tissue; thus, the probability of breast cancer is higher when there is a larger glandular component than fat tissue. Since the mid-1970s, this knowledge has encouraged many scientists to study different methods to measure breast composition and to study its correlation with breast cancer [1].

### 2.2.1 Visual Methods

In 1976, John Wolfe, a pioneer of MBD studies, published the first two works based on a qualitative and descriptive evaluation of breast density (*pattern-based*). He proposed a four-category classification for the different parenchymal patterns (N1, P1, P2, DY). In the N1 pattern, the breast consists almost entirely of fat, the P1 and P2 patterns represent increasing ductal prominence, and in the DY pattern, the breast parenchyma consists of diffuse or extensive nodular densities. There was a lower risk of cancer in less-dense breasts (N1, P1), and a higher risk of cancer in denser breasts (P2, DY). It was observed

V. Lattanzio (✉) · A. M. Guerrieri  
Breast Imaging Center, “Senologia e Salute Srl-  
Centro di Diagnosi e Prevenzione”, Bari, Italy

that the risk of cancer was 37-fold higher in women with a density of DY than in those women with fatty breasts (N1 group) [4, 5].

Later, in 1977, Laszlo Tabar developed an alternative system of qualitative measurement, defining five categories (Patterns I, II, III, IV, V) with different associated cancer risks [6]. Patterns IV and V, which are denser, were those associated with higher risk of developing breast cancer.

Wolfe’s qualitative method was not reproducible [7, 8], so Boyd et al. proposed a quantitative method based on the percentage of mammographic density (*area-based*). It is based on a radiologist’s assessment of the proportion of dense breast tissue relative to the breast areas. The classification is known as six class categories (SCC) where the density proportions are Class 1,

0%; Class 2, 0–10%; Class 3, 10–25%; Class 4, 25–50%; Class 5, 50–75%; and Class 6, 75–100% [9]. The visual estimate of mammographic density (MD) permitted the identification of cases at higher risk based on a higher percentage value.

The American College of Radiology (ACR), with its Breast Imaging Reporting and Data System (BI-RADS), developed a new visual method that divided breasts into four categories to standardize the evaluation and interpretation of MD by the radiologist. The ACR classification criteria have changed in different editions [10–12]. In edition IV, percentage values were added to the descriptive categories and edition V, released by BIRADS in 2013, defined four new categories, a, b, c and d (Fig. 2.1), and the quantitative evaluation (% gland) was replaced by an

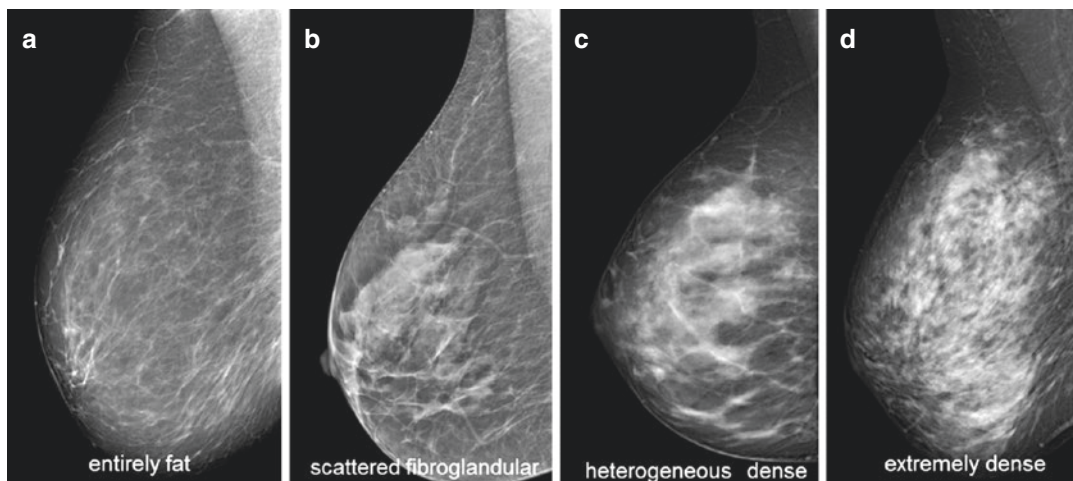


**Fig. 2.1** Breast composition according to BI-RADS 5th edition. (a) Almost entirely fatty. (b) Scattered areas of fibroglandular density. (c) Heterogeneously dense. (d) Extremely dense

**Table 2.1** BI-RADS categories for mammographic breast density

Classification of breast composition BI-RADS® (ACR)		
BI-RADS® 3rd edition	BI-RADS® 4th edition	BI-RADS® 5th edition
(1) Almost entirely fatty	(1) Almost entirely fatty (MBD < 25%)	(a) Breasts are almost entirely fatty
(2) Scattered fibroglandular	(2) Scattered fibroglandular (MBD 25–50%)	(b) There are scattered areas of fibroglandular density
(3) Heterogeneously dense	(3) Heterogeneously dense (MBD 51–75%)	(c) The breasts are heterogeneously dense, which may obscure small masses
(4) Extremely dense	(4) Extremely dense (MBD > 75%)	(d) The breasts are extremely dense, which lowers the sensitivity of mammography

evaluation of “masking risk”; masking risk refers to the probability that breast density may result in the misdetection of an underlying carcinoma (Table 2.1).

### 2.2.2 Computer-Assisted Methods

The problem with this subjective classification is the significant variability (intra- and interobserver), regardless of the system used. As a result of these limitations, new software have been developed for the semi-automated or fully-automated evaluation of breast density [13] to obtain objective measures that are easily used in clinical practice (Table 2.2).

Among these, CUMULUS is a computerized model developed by Yaffe and other researchers [14] that allows the radiologist to estimate the density area on a full-field digital mammography (FFDM), analysing every single pixel.

Such methods, developed in the last 20 years, have been regarded as the gold standard for the quantitative measurement of breast density. Many studies have demonstrated the high repeatability

of CUMULUS [15, 16], and based on the results obtained, the probability of developing cancer is four- to sixfold higher in women with dense breasts than in women with fatty breasts. In the most important study to date [17], three quantitative methods (BI-RADS, CUMULUS and IMAGEJ) and three fully automated volumetric measurement methods (VOLPARA, QUANTRA and SXA) have been investigated. It was concluded that the latter methods represent a valuable alternative to quantify density and obtain a more precise assessment of the risk of developing cancer.

One of the fundamental criticisms of these methods, which is also applied to objective measurement methods, is that they evaluate 3D characteristics using 2D images [18]; evaluation parameters are influenced by breast positioning (CC, MLO), depth and the superimposition of dense tissue as well as the level of compression.

Growing interest from both industry and researchers highlights the necessity of defining a standardized evaluation method to measure breast density and, hence, the risk of breast cancer, although this goal appears difficult and demanding.

**Table 2.2** Mammographic breast density measurement systems

MBD assessment			Method
Visual	Area	Parenchymal patterns	WOLFE TABAR
		Qualitative	BI-RADS
		Semi-quantitative	BOYD Visual analogue scale
Semi-automated	Area	Quantitative	CUMULUS MADENA
Fully-automated	Area	Quantitative	AutoDensity DenSeeMammo Densitas IMAGEJ iReveal STRATUS Libra MedDensity
			Volumetric



## 2.3 Breast Density: Clinical Relevance

In clinical practice, the relevance of this topic is related to:

1. The complexity of mammography interpretation for the radiologist when the breast is dense, which causes a reduction in the sensitivity of the test due to the masking effect, especially for lesions that are not visible or palpable, often leading to a delay in diagnosis.
2. The fact that breast density is an important and independent risk factor for breast cancer (BC).

Therefore, we affirm that a high percentage of glandular tissue reduces the diagnostic accuracy of mammography and increases the risk of developing BC.

### 2.3.1 Masking Effect

Breast cancer demonstrates the same radiologic attenuation as fibroglandular tissue. The detection of small lesions can be difficult in breasts with high density; therefore, under such conditions, the sensitivity of mammography is reduced. Recent studies have shown that sensitivity values differ between analogic systems (film-screen) and digital systems (FFDM) [19, 20].

Moreover, we note that there are clinical outcomes (tumour size and disease interval) that confirm the effect of breast density on the diagnosis of BC [21].

The number of BCs screen-detected at >15 mm grows with increasing breast density [22]. It seems clear that there is an association between elevated breast density and decreased sensitivity and specificity of 2D FFDM (masking effect), which is related to diagnostic delay and the detection of tumours at advanced stages, as well as biological predisposition to BC in breasts with a high percentage of glandular tissue.

The masking effect of MBD determines growth in a certain percentage of interval cancers

(cancers discovered in the period between regular mammographic controls) in women with dense breasts, who may benefit from a more personalized screening programme [23]. Interval carcinomas can even be caused by different factors that are not related to MBD, such as innate biological characteristics, anatomical location or misinterpretation of the radiologist [42–44].

In 2006, McCormack's meta-analysis [24] confirmed the importance of the masking effect due to MBD and reaffirmed that the risk of malignancy is four- to sixfold higher in women with denser breasts (>75%) than in women with less glandular components (<5%).

### 2.3.2 Independent Risk Factors

Many studies have already established that MBD constitutes an independent risk factor for BC, persisting for 8–10 years after the first evaluation [17, 25, 26]. Breast density is associated with an increased risk of local and loco-regional relapse of BC, but it was not shown to have any influence on metastasis or survival [27, 28]; the results from larger studies confirmed that higher density is not related to increased mortality for BC [29, 30].

Although breast density is considered an independent risk factor for BC, risk can be determined by different factors; the foremost factor seems to be genetic predisposition (65%) [1], and some genetic polymorphisms contribute to the multifactorial genesis of many types of BC [31–33]. Other factors include age, lifestyle (age/number of pregnancies, nutrition), hormonal layout and replacement hormonal therapy [34].

MBD is also a potential marker for the treatment responses of drugs used to cure and prevent BC, such as tamoxifen (TAM) and aromatase inhibitors (AI), as these therapies result in a reduction in breast density. Recently, to analyse the role of these drugs, a new study was conducted to automatically measure MBD. In this study, a group of women with BC treated with TAM and AI was compared with a control group of healthy women who did not receive any

treatment [35] and volume-based measurement was shown to elucidate changes in MBD during therapy; therefore, MBD can be used as a prognostic marker [36]. Further studies are being performed to evaluate if changes in density are a biomarker of BC risk [37].

## 2.4 Diagnostic Tools

MBD assessment has clinical utility for identifying women at increased risk of developing breast cancer and/or having reduced mammographic sensitivity. Certain difficulties associated with the limitations of conventional mammography

(film-screen and FFDM) may arise in the diagnosis of BC in dense breasts. Thus, more research involved in investigating standardized criteria to identify women at risk who may benefit from supplemental screening, prevention or genetic analysis is necessary. To date, there is still a lack of sufficient *evidence-based* proof regarding the correct interpretation of dense breast, how MBD should be measured and the best imaging modality for individual women.

There has been a notable effort within the scientific community to optimize breast screening according to individual risk, using the most advanced technologies available (Figs. 2.2 and 2.3). Interest in this topic has increased after

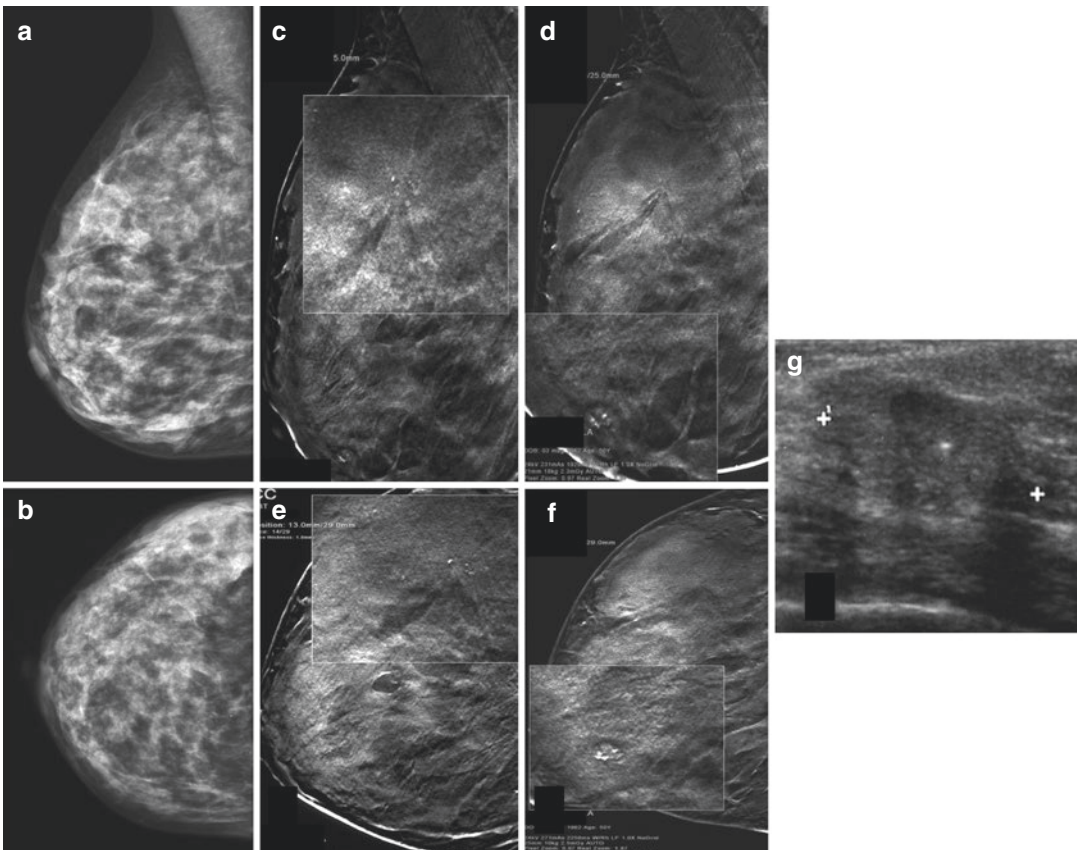


**Fig. 2.2** DBT study in a 51-year-old asymptomatic woman. (a, b) FFDM: MLO and CC views demonstrating extremely dense breast parenchyma with no radiologic abnormality. (c–f) DBT, MLO and CC views show two different lesions: a stellate architectural distortion in upper outer aspect (invasive ductal carcinoma, G1 with

tubular and in situ aspects) and a circumscribed lesion with intralésional calcifications in the lower inner aspect (intraductal papilloma with calcinosis). (g) Ultrasound shows a hypoechoic ill-defined 0.8 cm lesion in upper outer quadrant

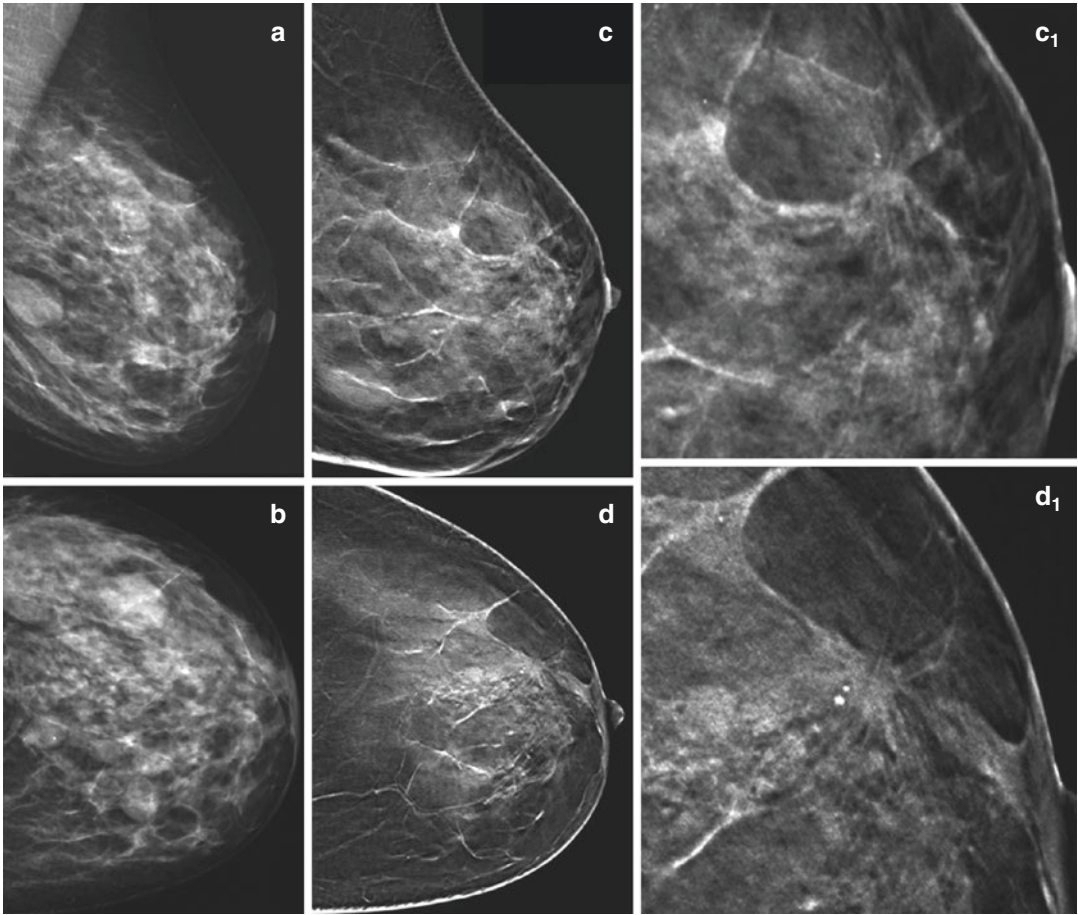


**Fig. 2.3** DBT screening study in a 47-year-old asymptomatic woman. (a, b) FFDM: MLO and CC views of an extremely dense breast parenchyma demonstrating well-circumscribed opacities in the left breast. DBT

MLO (c, c<sub>1</sub>) and CC (d, d<sub>1</sub>) views show a stellate lesion in the upper outer quadrant, behind the nipple. The pathology of this lesion was an invasive tubular carcinoma, G2

the launch of the campaign called “Are you dense?” [38], promoted in the United States to spread information about the risk associated with high MBD and the utility of supplemental screening. As of 2017, 31 U.S. states have adopted legislations requiring radiologists to specify breast density in the medical report.

To overcome the limitations of MBD, new imaging modalities in addition to screening mammography have been studied, such as handheld ultrasound (HHUS). Automated breast ultrasound system (ABUS) and digital breast tomosynthesis (DBT), which are based on morphological criteria, and magnetic resonance

imaging (MRI) and molecular imaging (MBI) which are based on functional criteria. In a study published in 2016, Melnikow et al. [39] analysed the results of 18 studies that reported rates of additional cancers detected in association with supplemental screening and concluded that supplemental tests added to screening mammography in women with dense breasts, identified additional BC but also increased the number of false-positives. DBT, which is a relatively novel technique, may reduce recall rates (range, 0.8–3.6/100 screens) and has the potential to increase BC detection (range, 0.5–2.7/1000 screens) [40, 41].

## Conclusion

At this moment, we can state that MBD is a hot topic of medical research that remains controversial. It is therefore necessary to define standardized methods of measurement to guarantee the objective evaluation of BC risk and to identify diagnostic strategies and therapies personalized for individual women.

## References

- Boyd NF, Martin LJ, Rommens JM, et al. Mammographic density: a heritable risk factor for breast cancer. *Methods Mol Biol.* 2009;472:343–60.
- Ng K-H, Lau S. Vision 20/20: mammographic breast density and its clinical applications. *Med Phys.* 2015;42:7059–77.
- Ekpo EU, Hogg P, Highnam R, McEntee MF. Breast composition: measurement and clinical use. *Radiography.* 2015;21:324–33.
- Wolfe JN. Risk for breast cancer development determined by mammographic parenchymal pattern. *Cancer.* 1976;37:2486–92.
- Wolfe JN. Breast patterns as an index of risk for developing breast cancer. *Am J Roentgenol.* 1976;126:1130–7.
- Gram IT, Funkhouser E, Tabar L. The Tabar classification of mammographic parenchymal patterns. *Eur J Radiol.* 1997;24:131–6.
- Egan RL, Mosteller RC. Breast cancer mammography patterns. *Cancer.* 1977;40:2087–90.
- Whitehead J, Carlile T, Kopecky KJ, Thompson DJ, Gilbert FI, Present AJ, Threatt BA, Krook P, Hadaway E. The relationship between Wolfe's classification of mammograms, accepted breast cancer risk factors, and the incidence of breast cancer. *Am J Epidemiol.* 1985;122:994–1006.
- Boyd NF, Jensen HM, Cooke G, Han HL. Relationship between mammographic and histological risk factors for breast cancer. *J Natl Cancer Inst.* 1992;84:1170–9.
- ACR. Breast imaging reporting and data system® (BI-RADS®). 3rd ed. Reston: American College of Radiology; 1998.
- ACR. Breast imaging reporting and data system® (BI-RADS®). 4th ed. Reston: American College of Radiology; 2003.
- ACR. Breast imaging reporting and data system® (BI-RADS®) Atlas. 5th ed. Reston: American College of Radiology; 2014.
- Tagliafico G, Tosto S, Chiesa F, Martinoli C, Derchi LE, Calabrese M. Mammographic density estimation: comparison among BI-RADS categories, a semi-automated software and a fully automated one. *Breast.* 2009;18(1):35–40.
- Byng JF, Boyd NF, Fischell E, Iong RA, Yaffe MJ. The quantitative analysis of mammographic densities. *Phys Med Biol.* 1994;39:1629–38.
- Harvey JA, Bovbjerg VE. Quantitative assessment of mammographic breast density: relationship with breast cancer risk. *Radiology.* 2004;230:29–41.
- Boyd NF, Lockwood GA, Byng JW, Tritchler DL, Yaffe MJ. Mammographic densities and breast cancer risk. *Cancer Epidemiol Biomark Prev.* 1998;7:1133–44.
- Eng A, Gallant Z, Shepherd J, McCormack V, Li J, Dowsett M, Vinnicombe S, Steve A, dos-Santos-Silva I. Digital mammographic density and breast cancer risk: a case-control study of six alternative density assessment methods. *Breast Cancer Res.* 2014;16:439.
- Kopans DB. Basic physics and doubts about relationship between mammographically determined tissue density and breast cancer risk. *Radiology.* 2008;246(2):348–53.
- Pisano ED, Hendrick RE, Yaffe MJ, Baum JK, Acharyya S, Cormack JB, Hanna LA, Conant EF, Fajardo LL, Bassett LW, et al. Diagnostic accuracy of digital versus film mammography: exploratory analysis of selected population subgroups in DMIST. *Radiology.* 2008;246:376–83.
- Prummel MV, Muradali D, Shumak R, Majpruz V, Brown P, Jiang H, Done SJ, Yaffe MJ, Chiarelli AM. Digital compared with screen-film mammography: measures of diagnostic accuracy among women screened in the Ontario breast screening program. *Radiology.* 2016;278:356–73.
- Arora N, King T, Jacks L, et al. Impact of breast density on the presenting features of malignancy. *Ann Surg Oncol.* 2010;17:211–8.
- Nickson C, Kavanagh AM. Tumor size at detection according to different measures of mammographic breast density. *J Med Screen.* 2009;16:140–6.
- Bae MS, Moon WK, Chang JM, et al. Breast cancer detected with screening US: reasons for nondetection at mammography. *Radiology.* 2014;270(2):369–77.
- McCormack VA, dos Santos Silva I. Breast density and parenchymal patterns as markers of breast cancer risk: a meta-analysis. *Cancer Epidemiol Biomark Prev.* 2006;15:1159–69.
- Boyd NF, Guo H, Martin LJ, Sun L, Stone J, Fishell E, Jong RA, Hislop G, Chiarelli A, Minkin S, et al. Mammographic density and the risk and detection of breast cancer. *N Engl J Med.* 2007;356:227–36.
- Bertrand KA, Tamimi RM, Scott CG, Jensen MR, Pankratz VS, Visscher D, Norman A, Couch F, Shepherd J, Fan B, et al. Mammographic density and risk of breast cancer by age and tumor characteristics. *Breast Cancer Res.* 2013;15:R104.
- Park CC, Remberg J, Chew K, Moore D, Kerliwadowske K. High mammographic breast density is independent predictor of local but not distant recurrence after lumpectomy and radiotherapy for invasive breast cancer. *Int J Radiat Oncol Biol Phys.* 2009;73:75–9.



28. Eriksson L, Czene K, Rosenberg L, Humphreys K, Hall P. Possible influence of mammographic density on local and locoregional recurrence of breast cancer. *Breast Cancer Res.* 2013;15(4):R56.
29. Gierach GL, Ichikawa L, Kerlikowske K, Brinton LA, Farhat GN, Vacek PM, Weaver DL, Schairer C, Taplin SH, Sherman ME. Relationship between mammographic density and breast cancer death in the breast cancer surveillance consortium. *J Natl Cancer Inst.* 2012;104:1218–27.
30. Zhang S, Ivy JS, Diehl KM, Yankaskas BC. The association of breast density with breast cancer mortality in African American and white women screened in community practice. *Breast Cancer Res Treat.* 2013;13781:273–83.
31. Dumas I, Diorio C. Polymorphism in genes involved in the estrogen pathway and mammographic density. *BMC Cancer.* 2010;10:636.
32. Peng S, Lü B, Ruan W, Zhu Y, Sheng H, Lai M. Genetic polymorphism and breast cancer risk: evidence from meta-analyses, pooled analyses, and genome-wide association studies. *Breast Cancer Res Treat.* 2011;127(2):309–24.
33. Lindström S, Vachon CM, Li J, et al. Common variants in ZNF365 are associated with both mammographic density and breast cancer risk. *Nat Genet.* 2011;43(3):185–7. Pearce MS, Tennant PW, Mann KD, et al. Lifecourse predictors of mammographic density: the Newcastle Thousand Families Cohort Study. *Breast Cancer Res Treat* 2012;131(1):187–95.
34. Parce MS, Tennant PW, Mann KD, Pollard TM, McLean L, Kaye B, Parker L. Lifecourse predictors of mammographic density: the Newcastle thousand families cohort study. *Breast Cancer Res Treat.* 2012;131(1):187–95.
35. Engmann NJ, Scott C, Jensen MR, Ma L, Brandt KR, Mahmoudzadeh A, Maikov S, Whaley DH, Hruska C, Wu FF, et al. Longitudinal changes in volumetric breast density with tamoxifen and aromatase inhibitors. *Cancer Epidemiol Biomark Prev.* 2017;26(6):930–7.
36. Li J, Humphreys K, Eriksson L, Edgren G, Czene K, Hall P. Mammographic density reduction is a prognostic marker of response to adjuvant tamoxifen therapy in postmenopausal patients with breast cancer. *J Clin Oncol.* 2013;31:2249–56.
37. Shawky MS, Martin H, Hugo HJ, Lloyd T, Britt KL, Redfern A, Thompson EW. Mammographic density: a potential monitoring biomarker for adjuvant and preventative breast cancer endocrine therapies. *Oncotarget.* 2017;8:5578–91.
38. Are You Dense Inc. Are you dense? Exposing the best-kept secret. <https://www.areyoudense.org>. Accessed 28 Mar 2017.
39. Melnikow J, et al. Supplemental screening for breast cancer in women with dense breasts: a systematic review for the US preventive services task force. *Ann Intern Med.* 2016;164:268–78.
40. Tagliafico AS, Calabrese M, Mariscotti G, Durando M, Tosto S, Monetti F, Airaldi S, Bignotti B, Nori J, Bagni A, Signori A, Sormani MP, Houssami N. Adjunct screening with Tomosynthesis or Ultrasound in women with mammography—negative dense breast: interim report of a prospective comparative Trial. *J Clin Oncol.* 2016;34(16):1882–8.
41. Bernardi D, Belli P, Benelli E, Brancato B, Bucchi L, Calabrese M, Carbonaro LA, Caumo F, Cavallo-Marincola B, Clauser P, Fedato C, Frigerio A, Galli V, Giordano L, Giorgi Rossi P, Golinelli P, Morrone D, Mariscotti G, Martincich L, Montemezzi S, Naldoni C, Paduos A, Panizza P, Pediconi F, Querci F, Rizzo A, Saguatti G, Tagliafico A, Trimboli RM, Zappa M, Zuiani C, Sardanelli F. Digital breast tomosynthesis (DBT): recommendations from the Italian College of Breast Radiologists (ICBR) by the Italian Society of Medical Radiology (SIRM) and the Italian Group for Mammography Screening (GISMa). *Radiol Med.* 2017;122(10):723–30. <https://doi.org/10.1007/s11547-017-0769-z>.
42. Aiello EJ, Buist DSM, White E, et al. Association between mammographic breast density and breast cancer tumor characteristics. *Cancer Epidemiol Biomark Prev.* 2005;14:662–8.
43. Gail MH, Brinton LA, Byar DP, Corle DK, Green SB, Schairer C, Mulvihill JJ. Projecting individualized probabilities of developing breast cancer for white females who are being examined annually. *J Natl Cancer Inst.* 1989;81(24):1879–86.
44. Gail MH. Twenty-five years of breast cancer risk models and their applications. *J Natl Cancer Inst.* 2015;107(5):d42.



# Physics and Practical Considerations of CEDM

# 3

Andrew P. Smith

## 3.1 Introduction

Contrast mammography comprises a clinical and acquisition protocol that images the distribution of iodine in the breast following the injection of an iodinated contrast agent. The imaging can be done either in 2D or tomosynthesis modes. Confusingly, there are many commonly used acronyms for this method. Contrast-enhanced spectral mammography (CESM), contrast-enhanced digital mammography (CEDM), contrast-enhanced mammography (CEM), and contrast-enhanced 2D mammography (CE2D) all mean essentially the same thing. These all refer to a 2D iodine imaging procedure. If the imaging is done in 3D, such as tomosynthesis, the procedure is known as contrast-enhanced 3D mammography (CE3D). In this book, we shall refer to the procedure as CEDM.

## 3.2 Physics Theory

Iodine in the breast is usually administered in the form of an iodinated contrast agent. Iodine is a metal that has high X-ray absorption due to its heavy atomic weight; however, the actual physical amount of iodine that is present in breast

tissue, in grams, is small, relative to the mass of other absorbing materials in the breast such as fibrous and glandular tissue, so special methods of imaging are needed to be able to visualize the iodine.

Historically, one of the earlier proposals for imaging iodine in the breast used a method known as background subtraction [1]. In this method, a first image of the breast (background image) was acquired, prior to the administration of iodine and therefore without any iodine present in the breast, using standard mammography equipment and techniques. Then the iodine was injected, and a second image was acquired. The subtraction of the two images subtracts out all the adipose and fibroglandular tissues, which are unchanged in the two acquisitions, leaving an image that consists solely of the changes between the two exposures, which is the iodine uptake. This method suffers from a practical issue that requires that the breast positioning remain completely unchanged between the two images which typically occur minutes apart. Even the smallest motion will cause the subtraction to create large artifacts. Due to this problem, the method of background subtraction is not used in any commercially available mammography systems.

A second method overcomes this limitation and is known as dual-energy subtraction [2]. With this method, two images are taken in rapid succession (seconds apart), at different X-ray energies, and the subtraction yields an image of

---

A. P. Smith  
Image Research, Breast and Skeletal Health,  
Hologic, Inc., Marlborough, MA, USA  
e-mail: [Andrew.Smith@hologic.com](mailto:Andrew.Smith@hologic.com)

the iodine. Due to the short time interval between the two exposures, patient motion artifacts are minimized. This imaging method is available on several commercial mammography systems and can be performed in either 2D or 3D imaging modes.

The physics behind the dual-energy subtraction method is based on what is known as k-edge imaging. All materials have X-ray absorption properties that vary based on X-ray energy; however these absorptions change slowly for adipose and fibroglandular tissues in the mammographic energy range, whereas the absorption changes very rapidly for iodine for X-rays having energies near 33 kilo-electron volts (keV), which is in the range of typical mammography exposures. The k-edge of iodine is approximately 33 keV. An X-ray having an energy just above the k-edge is easily absorbed by one of the iodine atom's electrons, and an X-ray having an energy below the k-edge is less easily absorbed.

The behavior is illustrated schematically in the following figure (Fig. 3.1) [3].

Two images are acquired, ideally one with X-ray energies just above the k-edge at 33 keV and the other just below 33 keV. When one of these images are subtracted from the other, the visibility of the tissue and fat disappears, because the absorption of these two components and hence their visual appearance are almost identical in the two acquisitions. However, the amount of iodine seen in the two images varies considerably, due to the large difference in

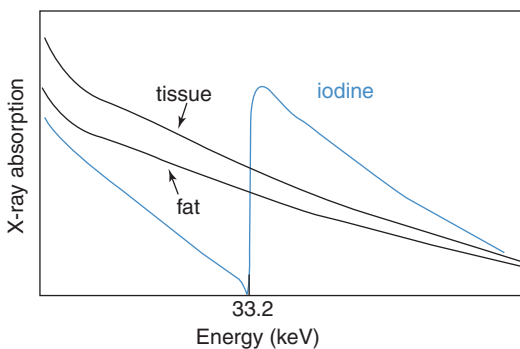


**Fig. 3.1** Absorption of adipose and fibroglandular tissue, and iodine (I), as a function of X-ray energy

absorption, and results in an image of the breast's iodine distribution following the subtraction. If the technique is working well, the subtracted image will have no tissue or fat visible, and the sole component in the image represents the iodine.

This theory is a little more complicated in practice, because X-ray tubes and X-ray filters do not produce X-rays of a single energy. Rather, they generate X-rays with a range of energies, and the resultant subtracted image does not completely subtract out the fibroglandular tissue. By careful selection of the X-ray filters and of the X-ray tubes operating voltage kVp, however, one can produce X-rays that are reasonably monoenergetic, enough so for the procedure to work.

Figure 3.2 illustrates the low- and high-energy X-ray spectra from a commercial CEDM system. The blue curve in the graph shows the distribution of X-rays that are produced in a standard mammography exposure using 28 kVp on a tungsten anode X-ray tube, and a rhodium (Rh) X-ray filter, and one can see that X-rays are generated having energies from about 10 to 25 keV, with most of them in the range of 20 keV. An image taken using this X-ray energy spectrum is known as the low-energy exposure. The red curve shows the X-ray spectrum that comes from a tungsten anode X-ray tube at 45 kVp using a copper (Cu) X-ray filter, and it has X-rays that range from 25 to 45 keV. This is known as the high-energy exposure. The high-energy spectrum has X-rays that are mostly above the iodine k-edge of 33 keV, and the low-energy X-rays are mostly below the 33 keV energy. Therefore, a subtraction of the two images can take advantage of iodine's rapidly changing absorption near its k-edge (Fig. 3.2).

In a practical commercial system, these two exposures happen automatically in rapid sequence during a dual-energy exposure, with the first exposure being a more-or-less typical mammogram using standard X-ray filters, and following that exposure a different filter, commonly copper, is introduced into the system, the

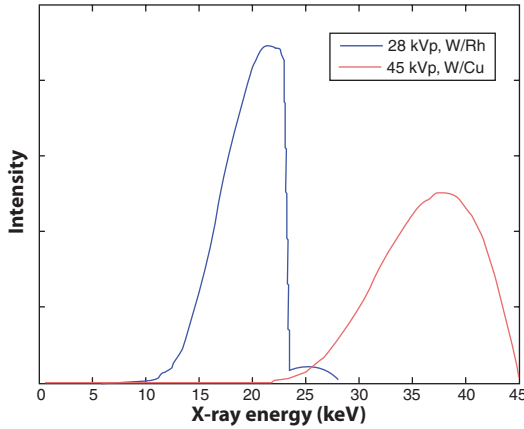


**Fig. 3.2** X-ray spectra for the low- and high-energy beams used in dual-energy imaging

kilovoltage is raised to 45–49 kVp, and the second, high-energy exposure occurs. The short time between the low- and high-energy exposure minimizes the likelihood of patient motion, and hence subtraction artifacts, between the two images.

### 3.3 Generating the Iodine Image

The dual-energy acquisition results in two raw images—the low- and high-energy mammograms. There is iodine present in both images; however it is hard to visually discern this due to the overwhelming structure noise caused by normal fibroglandular tissues. The low-energy image is typically taken using the same X-ray filters, kVp ranges, and dose levels, as normal mammograms, and can be substituted for a normal 2D mammogram during the diagnostic process [4].

The iodine image is created as a subtraction of one image from the other. Normally, the difference is made from the logarithm of the two images, as the logarithm image is proportional to the X-ray absorption in the breast, as seen in the following equation:

$$\text{Iodine Image} = \log(\text{High Energy Image}) * k - \log(\text{Low Energy Image})$$

The constant “ $k$ ” is determined by the equipment manufacturer so that the adipose and fibroglandular tissues subtract out as fully as possible in the resultant iodine image.

The following figure shows an example of the low- and high-energy images, and of the final subtracted iodine image. The low-energy image appears similar to a normal mammogram. The high-energy image is relatively low contrast due to the high kV used for the exposure, and one can faintly see the regions where there is uptake of the iodine. In the subtracted image, one mainly only sees the iodine in the lesion, and in this example also some blood vessels that had iodine remaining in them. The images in this example were acquired at about 2 minutes postinjection, early in the imaging procedure, which could explain the presence of iodine in the vessels.

Typically, only the low-energy and the subtracted images are viewed and saved by the system (Fig. 3.3).

### 3.4 Exposure Techniques and Radiation Dose

Exposures are commonly made using automatic exposure control. The kVp range for the low-energy mammogram is the typical one used in mammography—25–35 kVp—whereas the high-energy image uses a much higher tube voltage, typically 45–49 kVp. The X-ray filters for the low-energy image are the common ones used in mammography, and the X-ray filter for the high-energy exposure is most commonly copper.

The dose for the low kV image is within the range used in a normal mammogram, and the dose for the high-energy exposure is commonly around 25–50% of the dose for the low-energy exposure. Thus, the patient radiation exposure for one iodine image is under about 1.5 times that for a normal screening exposure. Because this type of imaging is most commonly performed on symptomatic patients, the small additional radiation may not be of great concern.



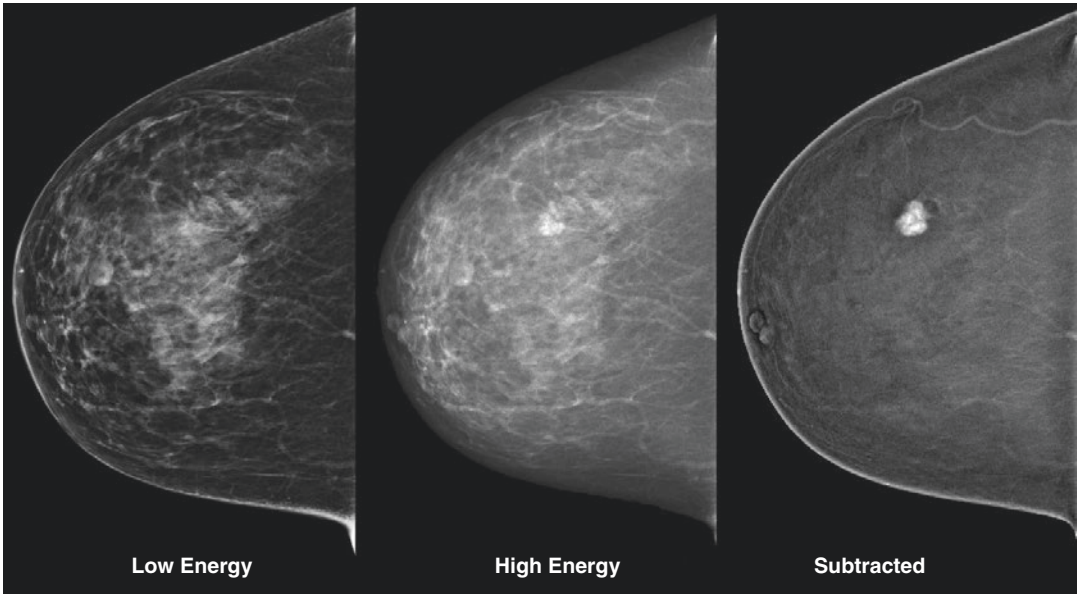


**Fig. 3.3** Low-energy (left), high-energy (middle), and subtracted (right) images from the CEDM acquisition



**Fig. 3.4** Example of iodine lesion visibility in a very dense breast

### 3.5 Dense Breast Imaging

One of the advantages of contrast-enhanced mammography is that it is primarily insensitive to breast density. The fibroglandular tissues subtract out during the image processing, leaving

visibility of the iodine lesions unaffected, even in dense breasts.

Figure 3.4 shows an example of this. The 2D LCC and LMLO images reveal areas of dense tissue, but the CEDM images easily show the lesion located in these areas.

### 3.6 Imaging Procedure Workflow

The basic procedure of a contrast examination is:

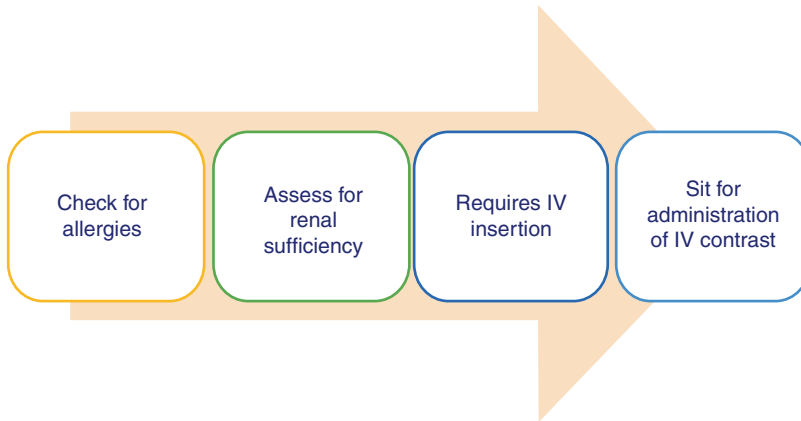
- Evaluate the patient for renal sufficiency and allergies to iodine.
- Perform the injection of the iodine.
- Wait approximately 2 minutes for the iodine to distribute throughout the breast.
- Perform the contrast imaging, in a 6-minutes imaging window.

Figure 3.5 shows the steps commonly performed during the contrast agent administration.

In terms of evaluation of the suitability of the patient for the procedure, refer to contrast media guidelines where appropriate [5, 6]. The injection is commonly performed using a power injector, to facilitate delivery of a bolus of the iodine.

Refer to the datasheets for the pharmaceutical, for dosage information and any warnings. The literature reports that typical doses of iodine are 1.5 cc/kg of body weight, and the injection can be done at 3 cc/s [7]. One typically waits approximately 2 minutes postinjection before beginning the imaging sequence [8]. The patient's breast is not compressed during the injection or during the 2-minutes wait, to allow the iodine to flow into the breast, and the patient can be seated to help minimize vasovagal reactions. The iodine imaging is commonly performed within a 6-minutes imaging window, before significant redistribution of the iodine and its background occurs.

During the imaging window, multiple images can be acquired, depending upon the clinical protocol. One must separately perform imaging on both the left and right breast if both breasts are needed for evaluation, unlike MRI where both breasts are imaged during the one scan. Figure 3.6



**Fig. 3.5** Example of workflow for iodine contrast administration

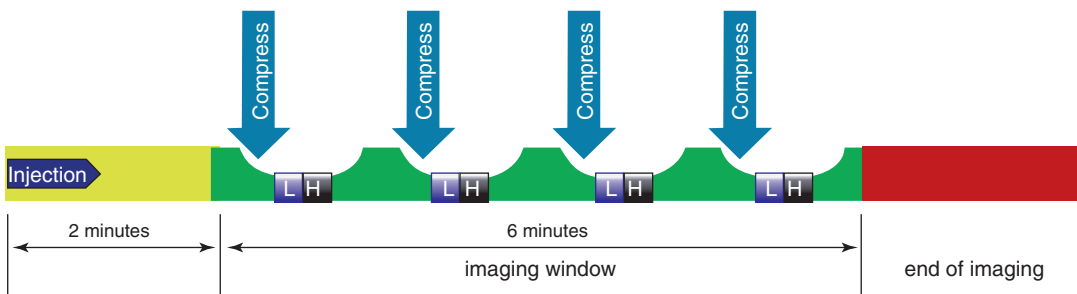


**Fig. 3.6** Time sequence of the contrast procedure

illustrates an example of the time sequence of the procedure, showing four projections taken. These can be, for example, CC and MLO of both breasts.

### 3.7 2D and 3D Iodine Imaging

In addition to 2D iodine imaging, it is possible to perform the procedure as part of a tomosynthesis examination.

There are two methods that have been proposed to accomplish this. One is performing the 2D iodine as part of a 2D/3D combo examination. In this method, there are three exposures taken in rapid sequence: the tomosynthesis scan followed by the low and high 2D exposures. The result of this is a 2D regular mammogram and a 2D iodine image, as described previously, and additionally a tomosynthesis volume. The acquisition sequence is illustrated in Fig. 3.7.

The iodine contrast agent is present in the tomosynthesis image, but cannot be easily detected, just as was seen with the 2D regular mammogram, because the tomosynthesis image is not a subtraction image. Because the 2D and the tomosynthesis images are taken in the same compression, they are co-registered, and if the lesion with iodine uptake is correlated to a tomosynthesis-detected lesion, the iodine lesion can be localized in three dimensions using the tomosynthesis images. This combo iodine imaging procedure has higher radiation than either a normal combo examination or a normal 2D contrast examination because it involves three exposures: the low- and high-energy 2D images and the

tomosynthesis scan. If the tomosynthesis image uses about the same dose as the low-energy mammogram, then the radiation of this combo procedure is about 25 % =  $(1 + 1 + 0.5)/(1 + 1)$  times higher than a normal combo exam, which has a dose of two times relative to a 2D mammogram.

Another method of acquiring 3D contrast information is to acquire a 3D dual-energy image directly. This can be done by acquiring, for each of the tomosynthesis projection angles, two exposures, one being the low energy and the other the high energy. The final 3D contrast image can be calculated either by directly reconstructing separately the low- and high-energy 3D exams and subtracting the two volume reconstructions or by an angle-by-angle subtraction of the low- and high-energy projections and then reconstructing the subtracted projections. This method results in two image sets: the standard low-energy 3D image and the subtracted contrast 3D image. This allows localization of any 3D-visible contrast lesion, and it accomplishes this at lower radiation exposure than the combo iodine imaging, as it requires only two raw images: the low- and high-energy 3D images.

The clinical performance of contrast-enhanced tomosynthesis has not been shown to be significantly different from contrast-enhanced mammography [8]. This is perhaps not surprising. The advantage of normal tomosynthesis compared to digital mammography is due to the reduction in overlapping structures. With contrast mammography, there are essentially no overlapping structures, which would represent overlapping contrast-enhancing lesions. The lesions can be seen directly in either 2D or 3D contrast images.

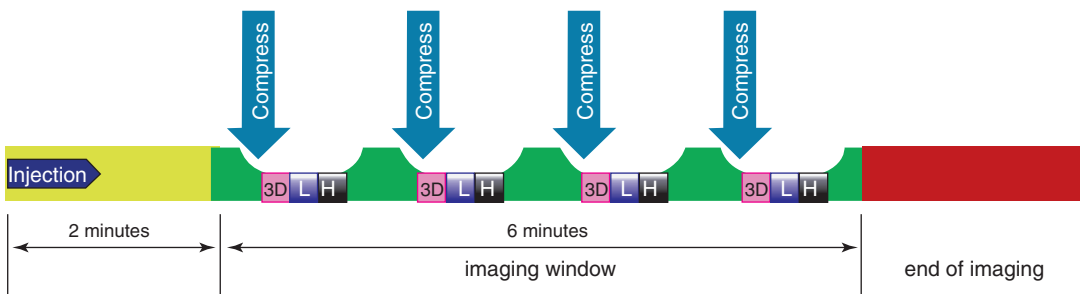


**Fig. 3.7** Time sequence of a combo contrast procedure

However, there still potentially are advantages to contrast-enhanced tomosynthesis and a contrast combo study, compared to contrast-enhanced mammography, and these relate to the ability to localize and potentially biopsy a lesion detected on the contrast image.

### 3.8 Technical Comparison to Gadolinium MRI Breast Imaging

Initial comparisons of the clinical efficacy of CEDM to gadolinium-contrast breast MRI indicate similar sensitivity and specificity in the detection of breast cancer, although there are uncertainties in these comparisons due to relatively small numbers of cases [9].

The technical differences are more easily enumerated. Some advantages of CEDM over MRI are that the procedure can sometimes be performed in women contraindicated for MRI due to claustrophobia, women unable to lie prone, and women who have metallic implants that preclude MRI. The CEDM procedure is also faster, and less costly. In preference comparisons, women preferred CEDM compared to MRI [10]. It can also be an advantage that the CEDM procedure can be performed on the same X-ray machine that is used for the evaluation of symptomatic patients and for upright tomosynthesis-guided biopsy. Advantages of MRI compared to CEDM are the ability to image both breasts at one time, ease of acquiring dynamic wash-in/wash-out information, and no X-ray radiation exposure. Gadolinium also has, compared to iodine, a lower incidence of allergic reactions to the contrast agent, although the observed accumulation of gadolinium in brain tissue is of pos-

sible concern due to its unknown long-term health consequence [11].

## References

1. Jong RA, Yaffe MJ, Skarpathiotakis M, et al. Contrast-enhanced digital mammography: initial clinical experience. *Radiology*. 2003;228(3):842–50.
2. Lewin JM, Isaacs PK, Vance V, et al. Dual-energy contrast-enhanced digital subtraction mammography: feasibility. *Radiology*. 2003;229(1):261–8.
3. Figure courtesy of John M Lewin, MD. The Women's Imaging Center, 3773 Cherry Ck N Dr, Suite 101, Denver CO 80209, john.lewin@thewomensimaging-center.net.
4. Francescone MA, Jochelson MS, Dershaw DD, et al. Low energy mammogram obtained in contrast-enhanced digital mammography (CEDM) is comparable to routine full-field digital mammography (FFDM). *Eur J Radiol*. 2014;83(8):1350–5.
5. See, for example. <https://www.acr.org/Clinical-Resources/Contrast-Manual>.
6. Stacul F, van der Molen AJ, Reimer P, et al. Contrast induced nephropathy: updated ESUR contrast media safety committee guidelines. Contrast media safety committee of European Society of Urogenital Radiology (ESUR). *Eur Radiol*. 2011;21(12):2527–41.
7. Lewis TC, Pizzitola VJ, Giurescu ME, et al. Contrast-enhanced digital mammography: a single-institution experience of the first 208 cases. *Breast J*. 2017;23(1):67–76.
8. Chou CP, Lewin JM, Chiang CL, et al. Clinical evaluation of contrast-enhanced digital mammography and contrast enhanced tomosynthesis—comparison to contrast-enhanced breast MRI. *Eur J Radiol*. 2015;84(12):2501–8.
9. Patel BK, Lobbes MBI, Lewin J. Contrast enhanced spectral mammography: a review. *Semin Ultrasound CT MR*. 2018;39(1):70–9.
10. Phillips J, Miller MM, Mehta TS, et al. Contrast-enhanced spectral mammography (CESM) versus MRI in the high-risk screening setting: patient preferences and attitudes. *Clin Imaging*. 2017;42:193–7.
11. McDonald RJ, McDonald JS, Kallmes DF, et al. Intracranial gadolinium deposition after contrast-enhanced MR imaging. *Radiology*. 2015;275(3):772–82.



## 4.1 Basic Considerations

The basic concept that creates contrast in X-ray images is the different absorption of X-rays by different tissues. For example, dense breast glandular tissue does absorb far more X-rays in comparison to fatty tissue. In many experimental designs, the X-ray absorption of dense breast glandular tissue is similar to that of water. Unfortunately the difference in the X-ray absorption between tissues is very little and hence the similarity between the image contrast of tumorous tissue in comparison to glandular tissue in dense breasts.

As described in the chapter on physics by Andrew Smith, the underlying idea for the use of contrast media is to increase the absorption of X-rays in certain tissues, which accumulate large amounts of contrast media. This effect may be achieved by direct application or injection of contrast media into the specific structures (e.g. in the case of galactography, when contrast media is injected into dilated milk ducts) [1] or by indirect application into supplying vessels (intraarterial or intravenous injection).

The improved visualization of breast cancer and certain benign changes of the breast tissue with the use of contrast media (e.g. within CT scans of the thorax) have been well established before contrast media was introduced specifically for the assessment of breast structures. A study by Teifke et al. in 1994 [2] demonstrated how different tissues within the breast differ in their response to contrast media after application of an iodine-containing contrast agent in computer tomography examinations (CT). Based on these observations, it is possible to calculate the concentration of iodine that is required to be visualized in a mammography procedure. To detect a so-called enhancement or, in other words, an accumulation of iodine-containing contrast agent within a certain structure, it is necessary to visualize a minimum of approximately 2–3 mg/dL (milligrams per decilitre) of iodine. This concentration of iodine can be visualized by various methods. In Chapter 3, Andrew Smith has already mentioned the “temporal subtraction”, which is used in MRI, and “energy subtraction”. Since temporal subtraction nicely demonstrates some differences and principles of contrast-enhanced digital mammography (CEDM), we will describe it again in our chapter with some examples.

---

F. Diekmann (✉)  
Department of Radiology, St. Joseph-Stift Bremen,  
Bremen, Germany  
e-mail: [FDiekmann@sjs-bremen.de](mailto:FDiekmann@sjs-bremen.de)

R. Lawaczek  
Bayer AG, Berlin, Germany

### 4.1.1 Temporal Subtraction

Initial studies to assess the visualization of contrast media in digital mammography were performed using the “temporal subtraction” [3–5] technique. Using the analogy of techniques that have been established from MRI, in temporal contrast mammography, an initial plain image followed by an image after intravenous administration of contrast media is obtained, maintaining identical positioning of the breast. Subsequently, the plain image is subtracted logarithmically from the post-contrast image. The aim of the resulting image is to solely visualize the contrast enhancement as shown in Fig. 4.1. The tumour in this case is only visible within the subtracted image, while plain mammography failed to delineate the tumour. This is the difference in comparison to MRI, where the tumour is usually visualized even in non-subtracted images. Moreover one should always have a look at the tumour in the non-subtracted images in MRI as this makes it easier to differentiate between artefacts and real tumours. In CEDM, differences in the grey values are often far below 100. Taking into account that the dynamic range of a normal digital mammography is about more than 65 thousand grey levels, it is obvious that we need a very constant detector for this procedure; however, the small differences in the greyscale are not perceivable with the human eye without post-processing algorithms. As mentioned above, on MR images, enhancing tumours are usually also visible on the non-subtracted images; with respect to this limitation, one can expect that the assessment of contrast-enhancing breast tumours in the presence of motion artefacts or other artefacts is more difficult in digital mammography in comparison to MRI.

Figure 4.1 demonstrates contrast enhancement within a tumour in the recombined image, which is not visualized on plain mammography. This image also illustrates another drawback of CEDM, where the complex positioning of the breast in mammography is a disadvantage in comparison to the prone position in MRI. While in MRI, the chest wall is well visualized; in mammography, tumours near the chest wall like in this

example are only visualized when the breast is optimally positioned.

The limitations of positioning in mammography are particularly apparent in a case of “temporal subtraction” as shown in Fig. 4.1, while the problem of motion artefacts in temporal subtraction is better demonstrated in Fig. 4.2. The tumour in this case is only visualized, because it is located in an area that is not affected by the motion artefacts. To get information about the dynamics of the contrast enhancement, several images taken 60, 120 and 180 seconds after intravenous administration of contrast agent have been obtained. Motion artefacts in this case are seen to increase over time. A maximum compression of the breast for 3 minutes would reduce the motion artefacts, but would at the same time have an impact on the contrast enhancement, and would not be tolerable for the patient. Motion artefacts are identified by very bright and very dark areas close to each other as seen in Fig. 4.2, with the temporal subtraction exaggeration. As a result of the above-mentioned limitations of using temporal subtraction, at present the dual-energy contrast-enhanced digital mammography (CEDM) or contrast-enhanced spectral mammography (CESM), which shows far less motion artefacts, is the preferred procedure.

### 4.1.2 Contrast-Enhanced Digital Mammography (CEDM)

As described by Andrew Smith in Chapter 3, a second possibility to visualize contrast media in digital mammography is by the dual-energy mammography technique. Whereby, initial intravenous administration of contrast media is followed by the sequential generation of low- and high-energy images. To avoid motion artefacts, both exposures can be generated by a single action without the need for further interventions by the user. The contrast agent in use currently is iodine, with a K-edge at 33.13 keV. This characteristic of iodine can be utilized to create a high-energy and a low-energy image using different filters for the X-rays. Using copper filters, the high-energy image can be obtained, while the



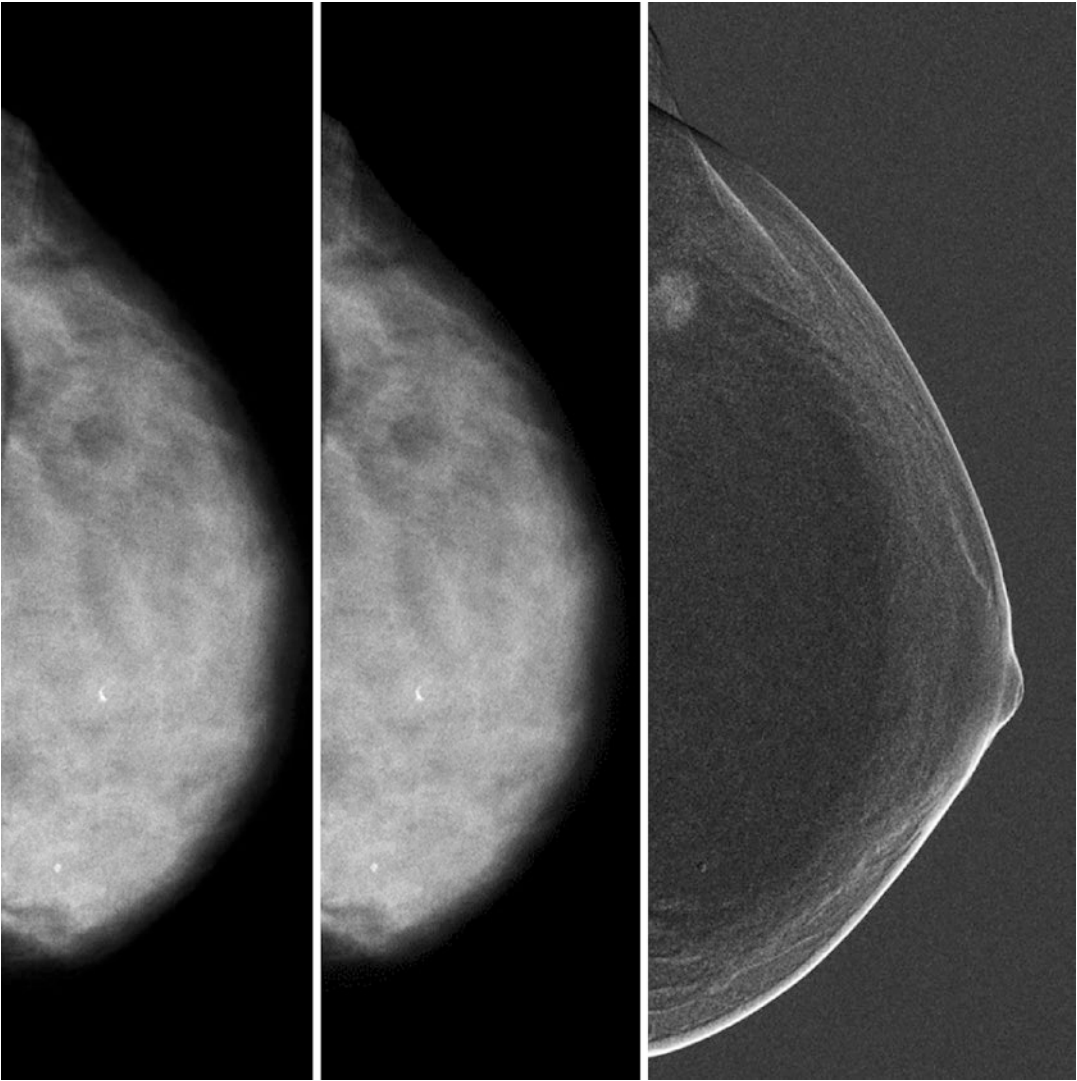


**Fig. 4.1** Digital mammography obtained using 49 kV before and after intravenous administration of contrast media and visualization of the tumour within the recombined image

conventional molybdenum or tungsten anodes with molybdenum or rhodium filters can be used to obtain a low-energy image. A wheel carrying different filters is placed in the gantry of a CEDM unit, which rotates during the exposures to allow for switching between both energy levels (Fig. 4.3).

Thus the resultant high- and low-energy images may be ideally recombined in a way that only the contrast enhancement is visible in the final image.

### 4.1.3 Timing of the Image Acquisition After Contrast Media Application

It has been demonstrated by the example of temporal subtraction in Fig. 4.2 that there are different approaches for the timing of the image acquisition in CEDM. In Fig. 4.2, images have been obtained with a delay of 60, 120 and 180 seconds after contrast administration [6]. The aim of this approach was; firstly, to detect

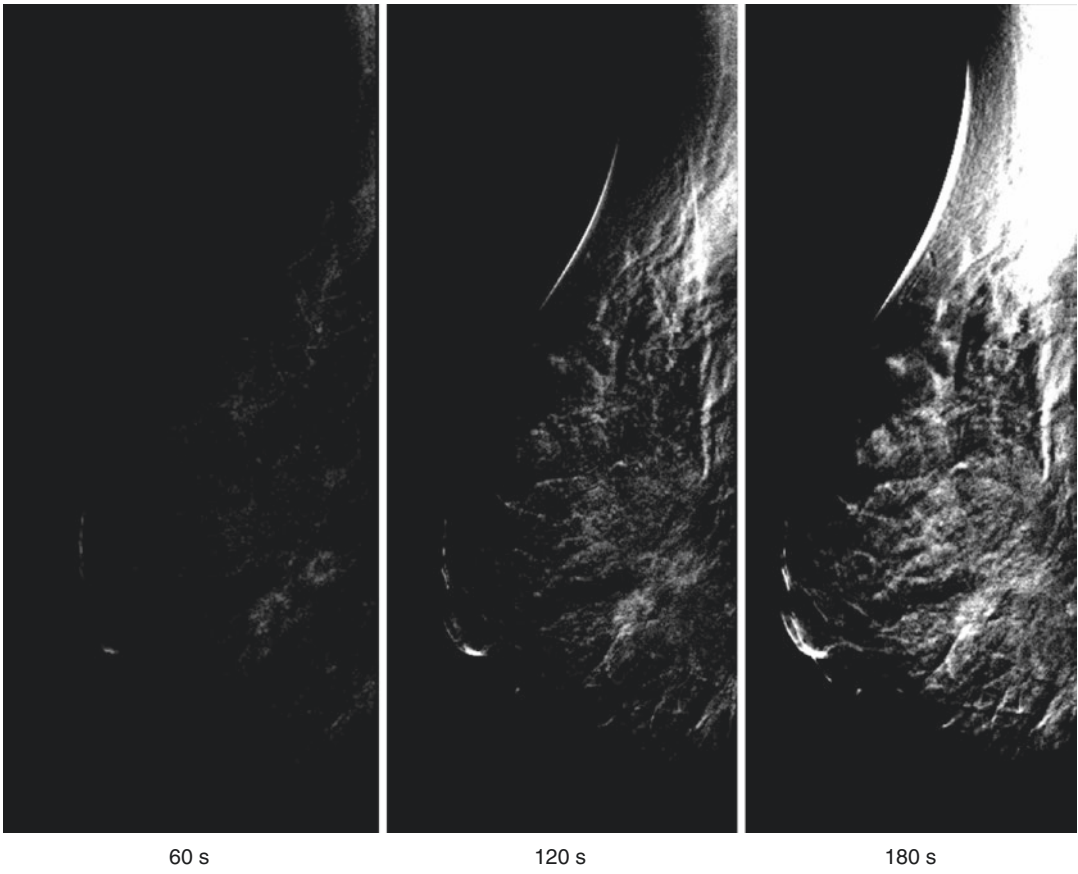


**Fig. 4.2** Temporal subtraction 60, 120 and 180 seconds after contrast administration



**Fig. 4.3** Installation of an additional copper filter for CEDM into the gantry enabling the mammography device to create high-energy images



the optimal timing for the visualization of contrast media and secondly, to assess the diagnostic value of dynamic contrast enhancement in contrasted mammography as has been proven in MRI. Even the very first studies of CEDM (initially using temporal subtraction) have shown that contrast enhancement of iodine-containing contrast agents can be visualized over a long period of time [4]. This was followed by studies using various different protocols of contrast media application and delays, most of which have been published with very limited sample

size. At present, the protocol that has gained acceptance is the one in which the images in craniocaudal (CC) view are obtained approximately 2 minutes and images in mediolateral oblique (MLO) view are obtained approximately 4 minutes after contrast administration. This also complies with theoretical simulations of contrast enhancement in tumours. Figure 4.4a shows the schematic diagram of the pharmacokinetic simulation, which simulates contrast enhancement. Figure 4.4b depicts the resulting graph for the currently used protocol of 1.5 mL

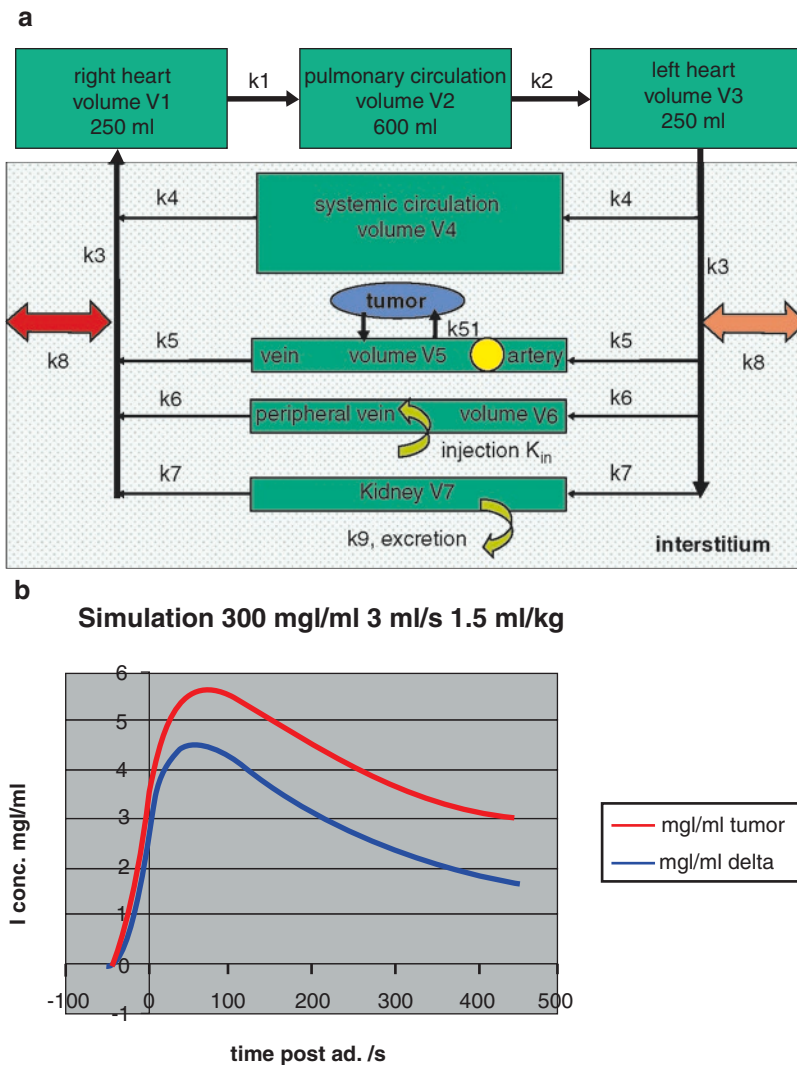


**Fig. 4.4** (a) Schematic diagram of the pharmacokinetic simulation of the contrast medium concentration in a number of organs and in the tumor.  $k_1$ – $k_7$  are constants for the in- and outflow of blood of organs and tumor ( $k_{51}$ ),  $k_8$  describes the exchange with the interstitium. (b) Example

of a resulting graph using the pharmacokinetic simulation. Approx. 100–200 seconds after contrast administration, the enhancement reaches a maximum. Upper curve represents concentration in the tumor; lower curve represents difference to the interstitium of the surrounding tissue

of contrast media per kilogram body weight at a flow rate of 3 mL/s via intravenous injection.

These theoretical considerations have coincided with our experience from the use of CEDM in our daily clinical practice. Contrast enhancement depends on various factors such as tissue-specific constants ( $k_1$ – $k_8$  in Fig. 4.4a) as well as individual cardiac function (such as ejection fraction of the heart, etc.). In our opinion, a good approach is to analyse the images during acquisition on the screen and to add delayed images if necessary. Case 1 of the case files in Chapter 14 shows an example, in which the tumour is hardly visible on the initial craniocaudal image while multiple arteries are filled with contrast. These findings suggest that the initial image acquisition has been performed too early; hence the tumour is better visualized on the additional delayed image.

#### **4.1.4 Interventions: Contrast Enhancement During the Use of a Compression Paddle with Opening for Wire Localization**

As we have discussed in Section 4.1.3, the contrast enhancement within tumours of the breast is often visible for a substantial period of time. This is an important factor to perform mammography-guided interventions of the breast. While MRI-guided interventions are often time-consuming and expensive due to the use of special non-magnetic tools, mammography-guided interventions of the breast are more feasible with respect to economic and medical considerations. Apart from that, mammography is the standard method for the detection of breast cancer. Therefore, the correlation of contrast enhancement with mammographically visible structures is an advantage, particularly for follow-up assessments. A comparison of MRI findings with mammography findings is often difficult, and matches may deviate in the range of more than 1 cm. In our opinion, among the most important advantage of

CEDM in comparison with MRI is the strong correlation between the mammographic images with the area of enhancement seen in CEDM. Case 3 of the case files in Chapter 14 is an example for this correlation between the native mammography finding and the enhancing lesion in CEDM.

A major drawback of interventions in CEDM is the dependence of contrast enhancement on object thickness. For mammographically guided interventions, normally a special compression paddle with an opening is used. The interventional device (basically a needle) can be placed through this opening in the paddle. Due to the soft composition of breast tissue, it tends to protrude through the opening while compression is performed. This “protrusion” of the breast tissue causes severe artefacts in the recombined image and hence significantly hampers the performance of an intervention. An example for an interventional wire localization procedure, in which a tumour and a satellite lesion have been localized using CEDM, is shown in Fig. 4.5. In this case, the focally increased object thickness has not been adjusted manually, and thus artefacts have compromised the recombined image. The artefact may be reduced significantly by lowering the protrusion of breast tissue through the opening of the compression paddle. This can be achieved by wrapping the compression paddle with a sterile bandage to cover the hole. Case 4 of the case files in Chapter 14 shows an example for an intervention procedure with the compression paddle prepared in such a way. Using this technique, CEDM-guided interventions may be performed in a simple and cost-effective way. However, there are still no standard CEDM-guided procedures available from the vendors in the market. This is especially important, when the alternative use of MRI is limited due to limited timing schedules or even restricted due to individual contraindications like pacemakers, claustrophobia, etc.

For all the described examples, iodine was used as a contrast agent. Unfortunately iodine has some disadvantages compared to the gadolinium used in MRI, which we have to consider.

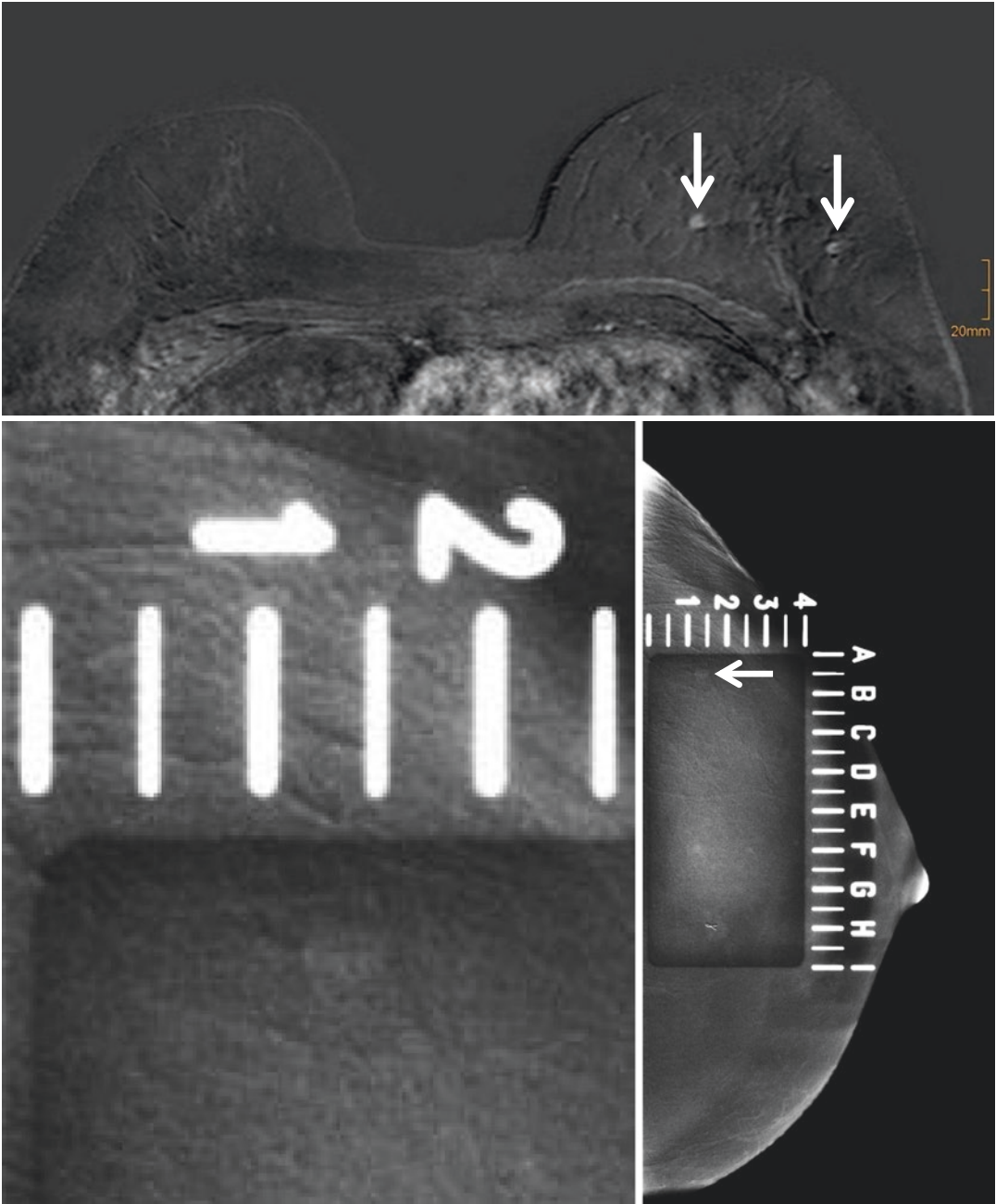


**Fig. 4.5** Example of MRI with two lesions (*arrows*); lesions are hard to visualize in the background of the white artefact due to difference in the thickness of the breast at the opening of the mammography paddle in the CEDM technique below

#### 4.1.5 Medical Considerations to Iodine-Containing Contrast Agents in Comparison to Gadolinium-Based Contrast Media

Different recommendations exist for the use of iodine-containing contrast agents. One of the most used and best known guidelines for contrast administration in Europe is the guideline of the European Society of Uroradiology (ESUR). The requirements for the use of iodine-containing contrast agents have been defined exhaustively in these guidelines. Before administration of contrast agents, a risk assessment regarding allergies, thyroid gland dysfunction and kidney function is recommended. With respect to the workflow of contrast-enhanced examinations, it is important to evaluate which patients need blood testing prior to contrast administration. In most hospitals this means that the examination cannot be performed during the first visit (“one-stop shop”), but a separate appointment to perform the CEDM has to be made, or at least some delay in the workflow is necessary. Additionally for every contrast administration, emergency drugs need to be made available. After contrast administration, patients need to be monitored for at least 30 minutes to assess for acute as well as for delayed adverse events. Non-ionic contrast media should be used. Most users prefer contrast agents with a concentration of around 300 mg/mL, because higher osmolarities seem to increase the risk of adverse events. The contrast agent should be administered at body temperature because this is more comfortable for the patients and also seems to lower the risk of adverse events. According to the actual guidelines in the ESUR, the following risk constellations are relative contraindications to perform CEDM:

- Known eGFR <60 mL/min/1.73 m<sup>2</sup>.
- Age >70 years.
- Any of the following patient history:
  - Kidney surgery.
  - Proteinuria.
  - Diabetes mellitus.

- Hypertension.
- Gout.
- Recent use of nephrotoxic agents.

Additionally, it is important to consider the individual risk of allergic reactions and thyroid gland dysfunction. With respect to allergic reactions, it is especially important to identify if any previous moderate or severe adverse effects have been observed after contrast administration or if the patient suffers from asthma or other treated allergies. As for thyroid gland dysfunction, a blood test should be performed especially in patients with untreated Morbus Basedow (Graves’ disease), multinodular goitre or thyroid autonomy, with a special focus on elderly patients who live in iodine-deficient areas. In our hospital, we avoid performing CEDM in all these cases.

---

## 4.2 Future Developments of Contrast Media in CEDM

### 4.2.1 Dynamics of Contrast Media

Assessment of contrast media dynamics is widely performed in MRI [7]. Investigations show that a prolonged contrast enhancement is more likely consistent with benign lesions, while a so-called wash out (fast enhancement within the first minute followed by a decrease of enhancement) is a sign of malignancy [8]. Initial studies of contrast dynamics in contrast-enhanced mammography resulted in limited success [6]. A possible explanation for it is that the visualization of contrast enhancement is dependent of object thickness. In the commonly used method of CEDM, contrast enhancement is measured within the full thickness of a given lesion. This would be comparable to a measurement of MRI contrast enhancement in “maximum intensity projection”. In MRI, the established method to assess contrast enhancement is imaging within selected slices. Froeling et al. [9] were the first to attempt the assessment of contrast enhancement within a limited number of overlapping slices in “contrast-enhanced tomosynthesis” which showed promising results for the evaluation of contrast dynamics in mam-

mography. They used a photon-counting detector that allowed the simultaneous generation of contrast-enhanced images and tomosynthesis. Because each tomosynthesis exposure with this technique may be performed within seconds, any movement artefacts, timing artefacts (alteration of contrast enhancement during the scan) and overlapping artefacts were minimized. According to the results of this study, the overall dynamics of the contrast enhancement seems to be similar to that observed in MRI but slightly less pronounced [9].

### 4.2.2 Other Contrast Media

As described in Figs. 4.1 and 4.2, artefacts may hamper the performance of CEDM. While contrast enhancement in MRI can usually be differentiated from artefacts by comparison with the unenhanced image, this is not possible in most cases of CEDM. As shown in Fig. 4.1, there is very limited visualization of contrast enhancement in the non-subtracted images. This is due to the limited contrast between iodine in comparison to breast tissue in the low-energy image that is used in mammography. Within the recombined or subtracted image, the contrast enhancement is visualized. As mentioned in the chapter on the basic physics of CEDM by Andrew Smith, while the X-ray absorption of iodine is on one hand ideal for the use in mammography due to its K-edge, however, on the other hand, the X-ray absorption of iodine is quite low at the energy levels typically used in mammography. Initial examinations of using contrast media in mammography focused on the identification of specific elements other than iodine to be used in contrast-enhanced mammography [10]. It has been shown that bismuth and zirconium are possibly more suitable than iodine for the use in mammography. To date, no approved intravenous contrast agents containing these elements exist,

and the development of a new contrast media is very expensive. Hence, it can be estimated that such developments will follow the distribution of CEDM and the resulting growing market of a specific contrast media.

## References

1. Diekmann F. Spectral tomosynthesis—galactography with photon counting detector. *Rofo*. 2013;185(9):880–1.
2. Teifke A, Schweden F, Cagil H, Kauczor HU, Mohr W, Thelen M. Spiral computerized tomography of the breast. *Rofo*. 1994;161(6):495–500.
3. Diekmann F, Diekmann S, Taupitz M, Bick U, Winzer KJ, Hüttner C, Muller S, Jeunehomme F, Hamm B. Use of iodine-based contrast media in digital full-field mammography—initial experience. *Rofo*. 2003;175(3):342–5.
4. Jong RA, Yaffe MJ, Skarpathiotakis M, Shumak RS, Danjoux NM, Gunesevara A, Plewes DB. Contrast-enhanced digital mammography: initial clinical experience. *Radiology*. 2003;228(3):842–50.
5. Diekmann F, Freyer M, Diekmann S, Fallenberg EM, Fischer T, Bick U, Pöllinger A. Evaluation of contrast-enhanced digital mammography. *Eur J Radiol*. 2011;78(1):112–21. <https://doi.org/10.1016/j.ejrad.2009.10.002>. Epub 2009 Nov 19.
6. Diekmann F, Diekmann S, Jeunehomme F, Muller S, Hamm B, Bick U. Digital mammography using iodine-based contrast media: initial clinical experience with dynamic contrast medium enhancement. *Investig Radiol*. 2005;40(7):397–404.
7. Kuhl CK, Mielcareck P, Klaschik S, Leutner C, Wardelmann E, Gieseke J, Schild HH. Dynamic breast MR imaging: are signal intensity time course data useful for differential diagnosis of enhancing lesions? *Radiology*. 1999;211(1):101–10.
8. Bick U. Typical and unusual findings in MR mammography. *Rofo*. 2000;172(5):415–28.
9. Froeling V, Diekmann F, Renz DM, Fallenberg EM, Steffen IG, Diekmann S, Lawaczeck R, Schmitzberger FF. Correlation of contrast agent kinetics between iodinated contrast-enhanced spectral tomosynthesis and gadolinium-enhanced MRI of breast lesions. *Eur Radiol*. 2013;23(6):1528–36.
10. Diekmann F, Sommer A, Lawaczeck R, Diekmann S, Pietsch H, Speck U, Hamm B, Bick U. Contrast-to-noise ratios of different elements in digital mammography: evaluation of their potential as new contrast agents. *Investig Radiol*. 2007;42(5):319–25.





# An Overview of the Literature on CEDM

# 5

Diego De Benedetto and Chiara Bellini

## 5.1 Introduction

The first bibliographical approach to contrast-enhanced mammography may be complicated by the variety of abbreviations and acronyms referring to this procedure, such as CESM (contrast-enhanced spectral mammography), CEDM (contrast-enhanced digital mammography), dual-energy mammography, TCEM (temporal contrast-enhanced mammography) and CEM (contrast-enhanced mammography).

To date, there are fewer than 100 CEDM studies published in medical journals in the most important international biomedical databases. These studies are very heterogeneous in terms of their different methodologies, few being prospective studies, while the majority were retrospective and were performed on small population samples.

The sampling design in CEDM leads to an increased risk of bias, because it is a diagnostic examination given to an ultra-selected population with a high prevalence of disease, thus misrepresenting the pretest probability of suffering from breast cancer.

From the beginning, two procedures have been described: one approach involving temporal

subtraction known as temporal contrast-enhanced mammography (TCEM) and a new approach, which has replaced the first, based on dual-energy subtraction known as contrast-enhanced digital mammography (CEDM).

In TCEM, the temporal subtraction technique consists of the acquisition of high-energy single images in a single projection before and after contrast medium injection, at an interval of 1 minutes. The pre-contrast image is then subtracted from the post-contrast image, offering the possibility of kinetic analysis of the enhancement pattern of breast lesions, similar to breast MRI. Unfortunately, many studies demonstrated that this first technical approach had a variety of issues, one of the most important being the long duration of breast compression, which led to patient discomfort and to altered perfusion of the contrast medium for vascular stasis, which did not permit the enhancement of some hyper-vascularized lesions. Another disadvantage was the ability to study only one breast at a time in a unilateral manner with each single projection.

Currently, TCEM has been replaced by CEDM. The dual-energy technique consists of the acquisition of a pair of low-energy images (25–33 peak kilovoltage; kVp) with silver (Ag) or rhodium (Rh) filters and high-energy images (45–49 kVp) with copper filters (Cu) only after contrast medium injection. The recombined image, which contains information on the iodine distribution, is produced from the spectral sub-

---

D. De Benedetto (✉) · C. Bellini  
Diagnostic Senology Unit, Department of Radiology,  
Azienda Ospedaliero Universitaria Careggi,  
Florence, Italy  
e-mail: chiara.bellini3@stud.unifi.it

traction of these images. The acquisition of CEDM images starts 2 minutes after the intravenous administration of iodinated contrast medium and is completed within 8 minutes. During these 6 minutes, the high-energy (HE) and low-energy (LE) coupled images are obtained with craniocaudal (CC) and mediolateral oblique (MLO) projections of each breast. The main advantage of the dual-energy technique is the ability to study bilateral breasts in all the four mammographic projections; this also allows better visualization of contrast enhancement because breast compression occurs just 2 minutes after injection of the iodinated agent, thus reducing patient discomfort.

## 5.2 Literature Review of the Diagnostic Accuracy of CEDM

From a “historical” point of view, although it may appear to be a relatively new technique in breast imaging, CEDM was first studied and performed more than 10 years ago. Lewin et al. published the first introductory study of the feasibility in 2003; the authors performed CEDM on 26 patients with suspected breast lesions detected by full-field digital mammography (FFDM), acquiring images from just a single MLO projection. They identified 13 invasive carcinomas, 11 of which demonstrated intense contrast enhancement. After this study, CEDM was defined as a promising and research-worthy new tool for breast imaging [1].

It has been 15 years since the introduction of this technique, and many more studies investigating CEDM have been published since then, evaluating both the sensitivity and specificity. According to an accurate literature analysis, the sensitivity of CEDM varies from 86 to 100%, which are very high values with elevated agreement and homogeneity between studies (Table 5.1, Fig. 5.1).

The results concerning the specificity of CEDM are discordant, with variable values. This may be attributed to the intrinsic features of different studies, which are very heterogeneous with

**Table 5.1** Comparison of sensitivity and specificity (%) results in clinical studies from 2003 to 2017

Author	Year	Sensitivity	Specificity
Lewin	2003	92	83
Dromain	2011	92	56
Jochelson	2013	96	
Helal	2013	94	67
Fallenberg	2014	95	
Cheung	2014	93	68
Luczynska	2014	100	41
Badr	2014	95	85
Mokhtar	2014	97	50
Luczynska	2015	100	
Kamal	2015		83
Lobbes	2015	100	88
Fallenberg	2016		94
Lalji	2016		70
Li	2016	100	
Luczynska	2016	100	
Lobbes	2016	96	
Mori	2016	86	
Cheung	2016		97
Wang	2016	95	65
Tardivel	2016		74
Tsigginou	2016	92	
Tennant	2016		81
Fallenberg	2017	94	
Patel	2017	97	58

small population samples and insufficient initial familiarity of radiologists with this new technique (Table 5.1, Fig. 5.2).

## 5.3 CEDM in Comparison with FFDM Alone and FFDM + US

Lobbes et al. [2] demonstrated that CEDM is an excellent tool for problem-solving. In this study, two radiologists examined 113 patients referred for CEDM from screening, due to suspicious lesions identified by FFDM. They observed that the diagnostic performance was higher with CEDM than with FFDM. When CEDM was compared with FFDM, CEDM was found to have 100% (+3%) sensitivity, 88% (+46%) specificity, 76% (+37%) positive predictive value (PPV) and 100% (+3%) negative predictive value (NPV). In particular, CEDM was demonstrated to be very

**Fig. 5.1** Comparison of sensitivity (%) results in clinical studies from 2003 to 2017

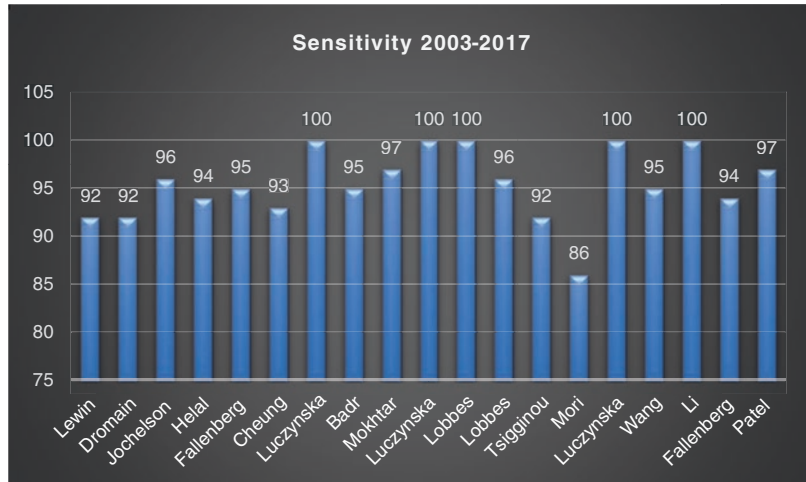
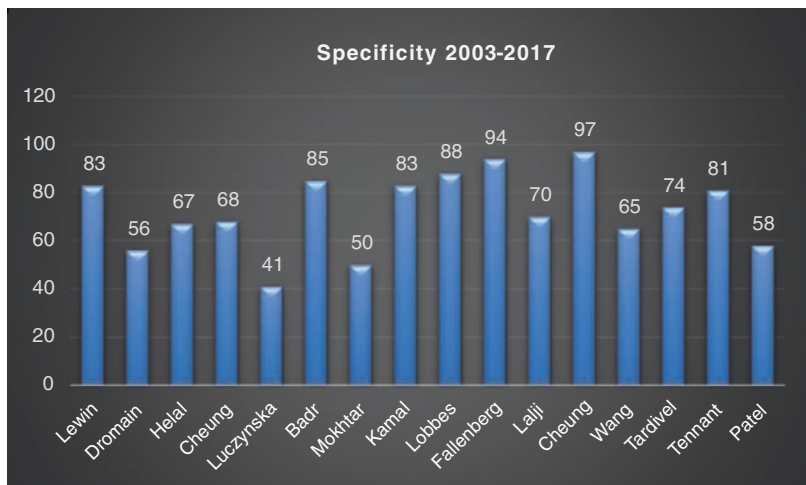


**Fig. 5.2** Comparison of specificity (%) results in clinical studies from 2003 to 2017



useful for improving specificity, thus reducing the number of false-positive cases.

Another very interesting result was the high NPV, suggesting that the absence of contrast enhancement excluded breast malignancies.

In a follow-up study, Lalji et al. [3] obtained similar results where 10 radiologists with different levels of experience in CEDM retrospectively examined 199 patients referred from screening. CEDM presented, in comparison to FFDM, a sensitivity of 97% (+4%) and a specificity of 70% (+34%). These data confirmed Lobbes’ first observations, and they also demonstrated that CEDM has hardly any learning curve, making its implementation into daily clinical practice safe and feasible.

In a meta-analysis, Tagliafico et al. [4] reviewed all studies on CEDM sensitivity and specificity using the PRISMA (Preferred Reporting Items for Systematic Reviews and Meta-Analyses) system [5], which consists of a checklist of 27 items that act as eligibility criteria.

Out of 643 studies inspected, only eight studies met the 27 criteria and were included in the review. Of these eight studies, four were prospective and four were retrospective studies.

The authors obtained values of 98% for sensitivity and approximately 58% for specificity, including three studies with values below 40%, which is not acceptable in clinical practice.



The limitations and pitfalls of this review were the heterogeneity (prospective and retrospective) of the eight studies, which included the fact that three of the studies were from the same working group (Luczynska) and that specificity was evaluated in only six of the studies, while sensitivity was evaluated in all eight studies.

Another limitation was the risk of bias in the population sampling, as stated above. However, the study by Lobbes et al. [2] was considered to have a reasonably low risk of bias because it was a prospective study, which included patients from screening programmes.

Since low-energy CEDM images present the same physical characteristics (same KVP) as FFDM, some studies [6–8] have focused on comparing the CEDM low energy and FFDM images to demonstrate their equivalence in terms of diagnostic accuracy.

These studies agreed that there are no statistically significant differences between low-energy images and FFDM.

In particular, the aim of the study by Lalji et al. [6] was to evaluate the quality of low-energy (LE) CEDM images and compare them with FFDM, following the 20 EUREF criteria.

Two independent expert radiologists observed 147 cases of FFDM and LE CEDM images. No statistically significant differences were observed in the quality scores of the two images for 17 out of 20 criteria, thus indicating that the LE CEDM images were just as accurate as FFDM images.

In a study by Fallenberg et al. [7], CEDM alone had the same sensitivity as CEDM + FFDM with just a 6.2% increase in average glandular dose (AGD). The author suggests that when CEDM is available, FFDM can be avoided, resulting in 61% reduction of the radiation dose, particularly in women with dense breasts.

Based on these results, Tennant et al. [9], proposed have proposed to use LE CEDM images as the first line of examination in patients with palpable masses to reduce radiation exposure.

Five radiologists retrospectively evaluated 100 CEDM exams, initially analysing just the LE images and then the recombined images 3 weeks after the full exam.

ROC analysis showed an improved overall performance of CEDM over LE CEDM alone, with an area under the curve of 0.93 versus 0.83. CEDM showed increased sensitivity (95% versus 84%) and specificity (81% versus 63) compared to LE CEDM alone, with all five readers showing improved accuracy.

Tumour size estimation with CEDM was significantly more accurate than with LE CEDM alone, the latter tending to undersize lesions. In 75% of cases, CEDM was regarded as a useful or significant aid in diagnosis.

Although this study was run as a double-blinded experiment, all five readers knew that patients were symptomatic and that lesions were large in size, thus leading to a minimum risk of bias.

Regarding the indications for CEDM, EUSOBI [10] (European Society of Breast Imaging) states that “On the basis of still preliminary results, CEDM can be considered as an alternative to contrast-enhanced MRI in the case of contraindications to MRI (including the presence of MRI-unsafe devices in the patient’s body, claustrophobia and obesity preventing the patient from entering the magnet) or to gadolinium-based contrast injection as well as local conditions of difficult MRI availability due to interesting results obtained by comparing CESM and MRI in the same patients”. Therefore, CEDM shares the same potential clinical indications as MRI.

In a study by Cheung et al. [11], they inferred that CEDM might be used as a valid device for the evaluation of calcifications. In this study, 59 women with suspicious microcalcifications (BI-RADS 4) without an associated mass, referred from screening, were analysed to verify the potential correlation between the type of suspicious microcalcification and contrast enhancement.

In total, 37 microcalcifications (amorphous microcalcifications) were classified as low concern and 22 as intermediate (20 pleomorphic microcalcifications) or high concern (two linear microcalcifications).

Of the 59 microcalcifications, 22 were diagnosed as cancers, 19 were atypical lesions, and 18 were benign lesions (Table 5.2).

When microcalcifications were classified as high concern, they were more likely to demonstrate enhancement in CEDM. However, the presence of enhancement was not inevitably suggestive of malignancy, because benign microcalcifications may also show contrast enhancement.

Ten of the 37 amorphous microcalcifications had associated enhancement; five were diagnosed as cancerous and five as non-cancerous. Of the 22 intermediate- and high-risk microcalcifications,

16 (15 cancerous, 1 non-cancerous lesion) showed enhancement (Fig. 5.3).

The true positive rate of intermediate- and high-concern microcalcifications was significantly higher than that of low-concern lesions (93.75% vs. 50%). Overall, the diagnostic sensitivity of enhancement was 90.9%, with 83.78% specificity, 76.92% positive predictive value, 93.94% negative predictive value and 86.4% accuracy.

The potential bias of this study is based on the small number of cases and patient sample size. Subsequently, Cheung and colleagues [12] conducted a study with a larger cohort, enrolling 94 patients, thus confirming their previous results.

CEDM can also be used as an efficient diagnostic tool for the evaluation of architectural distortions detected by FFDM or tomosynthesis. Suspicious mammographic distortions with contrast enhancement in CEDM are worthy of further histological characterization, whereas the absence of enhancement may prevent unnecessary biopsies.

The retrospective study done by Bhavika Patel et al. on 45 women with 49 distortions [13] was among the most significant study to date for this

**Table 5.2** Histological diagnosis of 59 microcalcifications detected by FFDM, grouped by the presence or absence of enhancement

Histological diagnosis	Presence of enhancement	Absence of enhancement
IDC (7)	7 (100%)	0
DCIS (15)	13 (87%)	2 (13%)
ADH (6)	3 (50%)	3 (50%)
FEA (13)	0	13 (100%)
Benign (18)	3 (17%)	15 (83%)

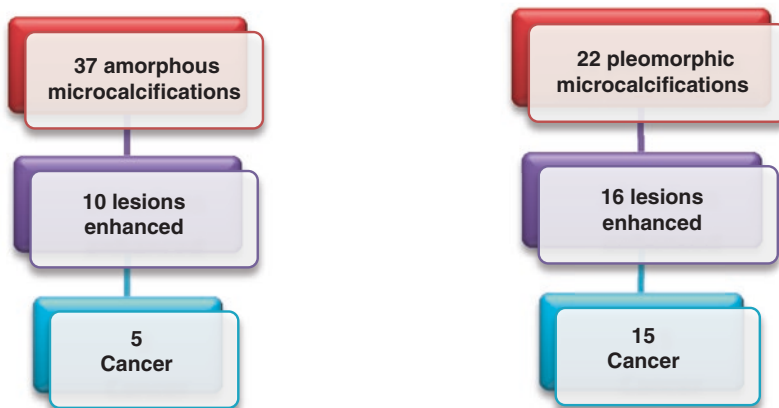


**Fig. 5.3** Of the 22 pleomorphic microcalcifications, 16 showed brilliant enhancement in CEDM, out of which 15 were histologically proven to be malignant lesions. Of the 37 amorphous microcalcifications, only 10 showed enhancement, out of which 5 were histologically proven

to be malignant lesions. This result shows a strong correlation between pleomorphic calcifications and malignancy, especially if the lesions present as enhancement on CEDM

indication, despite its limitation of a small sample population size.

The authors observed that architectural distortions (AD) detected by tomosynthesis and showed contrast enhancement on CEDM were more often associated with the presence of malignant lesions; thus, contrast media allows us to better characterize suspicious findings, increasing the sensitivity and specificity.

Thirty-seven (75.5%) ADs exhibited associated enhancement, with a resulting PPV of 78.4% (29/37), sensitivity of 96.7% (29/30), specificity of 57.9% (11/19) and NPV of 91.7% (11/12). The false-positive rate was 21.6% (8/37), and the false-negative rate was 8.3% (1/12). The accuracy was 81.6% (40/49) (Fig. 5.4).

The high sensitivity and NPV of CEDM in patients with AD are very promising for the diagnosis of malignancy and thereby avoiding unnecessary biopsies, respectively.

### 5.4 CEDM in Dense Breasts

As already discussed in chapter 2 by Vincenzo Lattanzio, it is a well-known fact that increased breast parenchymal density is the main limitation of FFDM as a diagnostic test. To solve this problem, we compared FFDM findings with other imaging modalities such as ultrasonography, tomosynthesis and MRI. CEDM is a promising additional tool for radiologists to overcome the difficulties associated with interpretation of very dense breasts.

Fallenberg et al., conducted a study on this topic [7], in which they compared the sensitivity of FFDM, CEDM and the combination of FFDM + CEDM.

The final outcome showed a better sensitivity for CEDM than FFDM in dense breasts (93% vs. 72%), and similar values were obtained for CEDM in the comparison with the combined

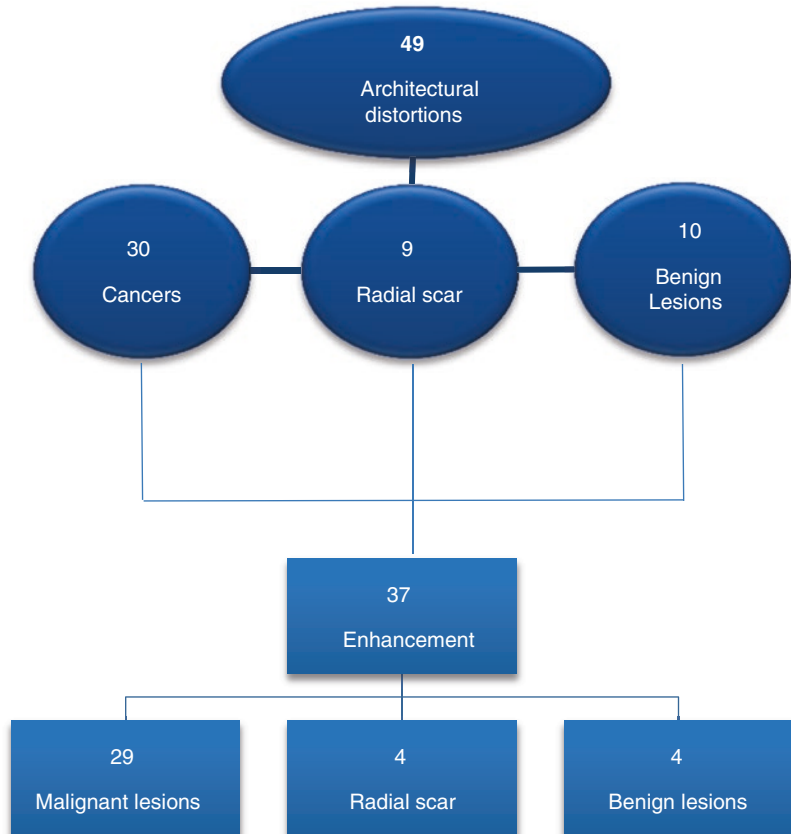


**Fig. 5.4** Correlation between architectural distortions (AD) enhancing in CEDM and malignancy: AD with strong contrast enhancement are more likely associated with malignant lesions than the ones without enhancement, with a positive predictive value of 78.4%

examination of FFDM + CEDM (94%). CEDM was proposed as an alternative, first-line examination to study dense breasts (Table 5.3).

Since then, there are other studies that have verified Fallenberg's results. In a study by Mori et al. [14], the authors suggested that CEDM offers better clinical performance than FFDM. The use of CEDM may decrease false-negative cases, especially for women with dense breasts. A total of 143 breasts on 72 women who underwent CEDM and FFDM were analysed, and 58 (40.6%) of 143 breasts were diagnosed with breast cancer based on histopathology.

CEDM revealed eight false-negative cases among 58 breast cancer cases (sensitivity of 86%) and five false-positive cases (specificity of 94%). The accuracy of CEDM was 91%.

FFDM was found to detect 31 true-positives among 58 breast cancer cases (sensitivity of 53%) and false-positives in 12 cases (specificity of 86%). FFDM missed malignancies in 27 breasts. Of these 27 cases missed on FFDM, 25 of them were dense breasts, in which 20 (80.0%) were found to be positive on CEDM (Table 5.4).

Cheung et al. [15] analysed 100 lesions (72 breast malignancies and 28 benign lesions) in 89 females. The use of CEDM in their study improved cancer diagnosis compared to FFDM in terms of sensitivity (71.5–92.7%) and specificity (51.8–67.9%) (Table 5.4).

**Table 5.3** CEDM alone improved cancer diagnosis compared to FFDM and FFDM + CEDM: a comparison of the sensitivities of the three techniques

Density	FFDM (%)	CEDM alone (%)	FFDM + CEDM (%)
Dense breast	72	93	94
Non-dense breast	86	97	97

CEDM is also a valuable tool for problem-solving in cases of inconclusive findings on conventional imaging. Tardivel et al. [16] retrospectively subjected 195 patients with inconclusive lesions detected by conventional imaging to undergo a CEDM examination. Contrast agent allowed the authors to identify and characterize new lesions. Out of the 195 cases, 41 patients (21%) modified their therapeutic plan with more extensive surgery ( $n = 21$ ) or neoadjuvant chemotherapy ( $n = 1$ ), while unnecessary biopsy was avoided in the 20 patients with negative CEDM findings. The use of CEDM improved cancer diagnosis compared with conventional imaging based on the higher sensitivity (94%) and specificity (74%), with the PPV and NPV being at 91% and 81%, respectively. CEDM can easily be performed as a clinical assessment after positive breast cancer screening and may significantly change the diagnostic and treatment strategy through breast cancer staging.

Another important factor evaluated in the literature is the average glandular dose (AGD) absorbed in CEDM. Fallenberg et al. [7] obtained rather interesting results, where they observed that in very dense breasts (ACR4), the AGD of CEDM was significantly lower than that of FFDM (Table 5.5).

Fallenberg's explanation of this result was "At equal thickness under compression, a dense breast will absorb more in the upper parts (closer to the tube) and 'shields' the lower parts in a way. To still have a reasonable number of photons at the detector level, one way is to compensate by increasing kVp, which lowers the absorbed dose. AGD for a 100% glandular breast is estimated to be 20% lower than for a 50/50 glandular breast; the latter absorbs 20% less than a 0% glandular breast".

Conversely, James et al. [17] demonstrated how AGD increases with very dense breasts in

**Table 5.4** In dense breasts, CEDM offers superior clinical performance compared to FFDM: comparison of sensitivity and specificity values

Study	Patients	Sensitivity CEDM (%)	Specificity CEDM (%)	Sensitivity FFDM (%)	Specificity FFDM (%)
Cheung 2014	89	93	68	71	52
Mori 2017	72	86	94	53	86

**Table 5.5** In very dense breasts (ACR 4), average glandular dose (AGD) in CEDM was significantly lower than in FFDM

Dense breast	FFDM mGy	CEDM mGy
ACR 1	1.16	2.40
ACR 2	1.68	2.06
ACR 3	1.75	1.87
ACR 4	2.21	1.37

**Table 5.6** Average glandular dose in CEDM increases with breast density, to a greater extent compared with FFDM

Density	FFDM mGy	CEDM mGy
Non-dense breast phantoms	1.00	1.6
Dense breast phantoms	1.3	2.1

phantoms and patients with varying breast thickness and density. Non-dense phantoms had a mean AGD of 1.0 mGy with 2D FFDM and 1.6 mGy with CEDM, while dense breast phantoms had a mean AGD of 1.3 mGy with 2D FFDM and 2.1 mGy with CEDM. At a compressed thickness of 4.5 cm, radiation exposure from CEDM was approximately 25% higher in dense breast phantoms than in non-dense breast phantoms.

The dose in dense phantoms at a compressed thickness of 6 cm was approximately 42% higher than the dose in non-dense phantoms at a compressed thickness of 4.5 cm (Table 5.6). Therefore, these findings were in contrast with the study done by Fallenberg and colleagues.

Many studies have evaluated AGD, with variable and noncomparable results. Some studies have been performed with a CEDM prototype unit in which exposure settings were manually set, while others were performed with automatic control of exposition, and additional studies were dependent on breast thickness and glandularity.

Despite this high variability between the studies, all the results obtained were under the radiation dose limits set by the Mammography Quality Standards Act (MSQA).

## 5.5 CEDM in Comparison with MRI

CEDM has proven to be an effective alternative to MRI for functional imaging of the breast, to assess hyper-vascularized tissues that may be related to tumour angiogenesis. Many experts have focused on comparing these two examinations.

The sensitivity is the same for both CEDM and MRI, but there is still limited available data on the specificity. Fallenberg's study was the only one, which compared the specificity between these two modalities, and they observed a specificity of 94% in CEDM in comparison to 88% in MRI [18] (Table 5.7).

The first study to compare CEDM and MRI was performed by Jochelson et al. [19]. Each technique identified 50 out of 52 lesions with the same sensitivity (96%), but CEDM had a lower sensitivity for detecting ipsilateral additional lesions than MRI; specifically, CEDM identified 14 lesions out of 25 (56%), and MRI identified 22 (88%).

CEDM showed a higher PPV (97% vs. 85%), thus increasing the specificity: there were just two false-positives with CEDM and 13 false-positives with MRI. These results may be explained by the differential timing of acquisition between the two techniques and the differing molecular composition of the contrast media (iodinate in CEDM and paramagnetic in MRI). Iodinated contrast in CEDM persists for more than 10-minutes in breast glandularity, allowing better visualization of lesions with slow enhancement.

Subsequently, Luczynska et al. [20] enrolled 102 patients (identified by conventional mammography) into a CEDM/MRI study, and 118 lesions were identified by the combination of CEDM and breast MRI. The sensitivity was 100% with CEDM and 93% with breast MRI. The accuracy was 79% with CEDM and 73% with breast MRI. ROC curve areas based on BI-RADS were 0.83 for CEDM and 0.84 for breast MRI. These results showed that CEDM has a high NPV and false-positive rate similar to that of breast MRI.

**Table 5.7** Comparison between CEDM and MRI in terms of sensitivity and specificity: the sensitivity is similar and very high for both MRI and CEDM, whereas the specificity is significantly higher for CEDM, although only one study has compared the two techniques. The positive predictive value (PPV) is also higher for CEDM than for MRI, reducing the number of false-positive (FP) cases.

Investigator	Patients	Age (mean)	No. of cancers	Sensitivity		Specificity		PPV	
				MRI (%)	CEDM (%)	MRI	CEDM	MRI	CEDM
Jochelson 2012	72	49.6	52	96	96	–	–	85%	97%
Fallenberg 2014	80	–	80	97	100	–	–	–	–
Luczynska 2015	102	–	81	93	100	–	–	74%	77%
Fallenberg 2016	155	53	273	95	94	88%	94%	–	–
Li 2017	48	56	62	100	100	–	–	94%	97%

Li et al. [21] retrospectively compared the diagnostic performance of CEDM and MRI for breast cancer detection. This study enrolled 48 women who underwent both CEDM and MRI exams, performed within 30 days. The parameters of the study were to determine the sensitivity, PPV, lesion size, morphology (using the breast MRI BI-RADS lexicon), index lesion and background enhancement (from 0, no enhancement, to 3, marked/moderate enhancement, according to the guidelines from ACR BI-RADS 5th edition).

In this study, CEDM identified 64 lesions, all visible by MRI as well, of which 62 were malignant findings and two were benign lesions. MRI identified 66 lesions, two more than CEDM, which were found to be benign lesions upon pathology. The sensitivity was 100% for both techniques, but CEDM had a better PPV (97% vs. 94%) and a lower false-positive rate (2/64 vs. 4/66). The morphology of the malignant findings was 100% consistent between CEDM and MRI. The authors concluded that CEDM had a higher PPV and a lower BPE than MRI and potentially represents a new innovative alternative to MRI.

Another important two-centre study performed by Fallenberg et al. [18] aimed to demonstrate that CEDM alone is not inferior to MRI and is superior to FFDM for breast cancer detection. Six independent breast radiologists examined the FFDM, CEDM and MRI images of 187 patients.

Twenty-three of 187 were ineligible, and the remaining 155 were included. The authors found

**Table 5.8** Assessment of lesion size measurements by comparing the three different modalities, FFDM, MRI and CEDM, with postoperative histological results as the gold standard

Technique	Lesions	Average (mm)	SD
FFDM	59	27.31	22.18
CEDM	59	31.62	24.41
MRI	59	27.72	21.51
Size pathology	59	32.51	29.02

that the sensitivity of FFDM alone (0.81) was significantly lower than that of CEDM (0.94) and MRI (0.95), and the MRI sensitivity was higher than that of CEDM alone and CEDM + FFDM; the MRI specificity (0.88) was lower than that of other modalities (CEDM, 0.94, and FFDM 0.95). The benefits of CEDM alone and MRI alone were particularly evident in dense breast. CEDM alone and with MRI showed no significant differences in ROC curves, demonstrating that it is an accurate alternative to MRI.

In another study by Fallenberg [22], the measurements of the size of the index cancer were compared between FFDM, CEDM, MRI and postoperative histology in 59 cases for which the index cancer was depicted with all three imaging techniques and final histology findings were available.

There was a slight underestimation of the tumour size using FFDM and MRI compared to CEDM and pathology (Table 5.8).

These results confirmed that CEDM has a good correlation with postoperative histology for size assessment.



Lobbes et al. also concluded that CEDM is not inferior to MRI for tumour size assessment. Using the surgical specimen as a gold standard, the authors evaluated 57 CEDM examinations and compared them with MRI exams. They found that Pearson's correlation coefficient was  $>0.9$  for CEDM vs. histopathology with  $p < 0.0001$ , which was the same value calculated for MRI, with a mean difference of 0.03 mm (vs. 2.12 mm for MRI), and there was no additional benefit to performing MRI after CEDM in any case [23].

## 5.6 Review of the Literature on New Potential Clinical Indications

Based on the available literature, the efficiency and accuracy of CEDM, which are comparable to those of MRI, have already been proven; therefore researchers are now focussing on expanding its clinical indications. Currently, EUSOBI guidelines have concluded that CEDM should be performed when there are contraindications to MRI [10].

Beyond the diagnostic efficiency of CEDM, Patel et al. defined new potential clinical indications [24]. The authors focused on two potential indications, which are monitoring the response of neoadjuvant chemotherapy (NAC) and "personalized" screening. The authors demonstrate not only the efficiency of CEDM in comparison to MRI for evaluating the perioperative chemotherapy (ChT) but also the usefulness of CEDM as an alternative tool in patients with pacemakers, severe claustrophobia and other MRI contraindications.

We also analysed the study by El Said et al., which included 21 patients undergoing NAC [25]; this study reported six false-negative cases, but the authors suggested that this was due to residual small tumour foci receiving nutrients by diffusion instead of new angiogenic vessels and not due to a lack of CEDM sensitivity.

Other studies have been performed to evaluate CEDM efficacy in evaluating residual tumour post-NAC. One important retrospective study by Barra FR et al. [26] involved the analysis of eight

lesions in eight patients who received NAC as part of their treatment before undergoing surgery. Three radiologists assessed the size of the residual tumour by CEDM and FFDM separately and then correlated the residual tumour size with the pathological response in surgical specimens.

The authors used low-energy CEDM images (for FFDM) and recombined images to measure suspicious findings. The results indicated a higher sensitivity (83.3% vs. 50%), specificity (100% vs. 50%), PPV (100% vs. 50%) and NPP (66% vs. 25%) for CEDM.

The correlation between CEDM and surgical specimens was statistically significant and differed from FFDM, with an underestimation of lesion size in 37.5% vs. 50% of cases, an overestimation by both techniques in 37.5% of cases and correct assessment in 25% vs. 12.5% of cases. Additionally, the interobserver agreement was slightly better for CEDM, increasing the diagnostic performance of all readers.

A second, larger study sought to compare CEDM and MRI for the evaluation of tumour response to NAC. This prospective study enlisted 54 women with breast cancer who were indicated for NAC. CEDM and MRI were performed three times: before NAC, after 3 months and after 6 months, just before surgery. To evaluate tumour response, seven independent radiologists measured the size of the residual lesion by both CEDM and MRI and compared it to the surgical specimen (gold standard). Response to therapy was assessed according to the parameters set in the RECIST criteria: complete response (CR, no residual lesion), partial response (PR, reduction  $\geq 30\%$  of largest dimension), stable disease (SD,  $<30\%$  reduction,  $<20\%$  increase) and progressive disease (PD  $\geq 20\%$  increase). Forty-six patients of 54 completed the study. CEDM better predicted pCR than MRI (Lin's coefficient of 0.81 vs. 0.59). Both methods underestimated the residual size (4.1 mm in CEDM vs. 7.5 mm in MRI). For the evaluation of CR, CEDM sensitivity and sensibility were 100% and 84% vs. 87% and 60% for MRI, respectively.

This study confirms that CEDM is as reliable as MRI for monitoring the response to NAC [27].



The second diagnostic potential indication was to use CEDM to perform a personalized individual screening programme for each woman [23]. Since dense breast has a higher risk of developing cancer than fatty breast parenchyma, and CEDM alone or CEDM + FFDM has better diagnostic accuracy than FFDM alone, many women with dense breast parenchyma may benefit from this additional screening [7, 14].

Additionally, in a recent study by Convington et al., the authors discussed the possibility of personalizing screening procedures for each patient depending on breast density and the potential lifetime risk of developing cancer [28]. MRI is the standard screening modality in high-risk women, such as BRCA1 and BRCA2 mutation carriers [29]. However, supplemental screening with MRI is only cost-effective if the risk is more than 20%. Since CEDM is approximately 25% cheaper than the cost of an MRI, it may be an important tool in those women with intermediate lifetime risk, such as women with dense breasts [30].

There is still no commercially available system to obtain biopsies under CEDM guidance at present. However, to our knowledge it should be available in due time. For now, researchers have tried placing a clip at the site of a suspicious enhancement with CEDM guidance and then performed a stereotactic core needle biopsy targeting the clip [28].

Potentially greater cost savings than MRI also supports the implementation of CEDM. A study by Bhavika Patel and colleagues in Mayo Clinic, Arizona, stated that the total cost of MRI screening was \$954, encompassing contrast administration, contrast medium costs and computer-assisted detection with prior FFDM, whereas the cost for a CEDM examination was \$196 because it was not necessary to conduct a separate FFDM study given the equivalency of the low-energy CEDM image. Therefore, with CEDM implementation, the savings amount would be \$750 per examination and \$1.1 billion annually, a cost that is 80% cheaper than MRI with comparable performance [30]. In our experience, at our centre at AOU Careggi, a breast MRI costs approximately €245, whereas CEDM

costs only €95 and thus a CEDM examination is approximately 60% cheaper.

In conclusion, based on the review of the available literature, results have shown that CEDM is more sensitive and specific than conventional mammography for the detection of breast cancer. Additionally, it has a sensitivity that is comparable to MRI for the detection of primary breast cancers. Given its low cost, potential broad availability and ability to be used in women who cannot undergo MRI, CEDM has proven to be a promising addition to current breast imaging techniques.

---

## References

1. Lewin JM, Isaacs PK, Vance V, Larke FJ. Dual-energy contrast-enhanced digital subtraction mammography: feasibility. *Radiology*. 2003;229(1):261–8.
2. Lobbes MB, Lalji U, Houwers J, Nijssen EC, Nelemans PJ, van Roozendaal L, Smidt ML, Heuts E, Wildberger JE. Contrast-enhanced spectral mammography in patients referred from the breast cancer screening programme. *Eur Radiol*. 2014;24(7):1668–76.
3. Lalji UC, Houben IP, Prevos R, Gommers S, van Goethem M, Vanwetswinkel S, Pijnappel R, Steeman R, Frotscher C, Mok W, Nelemans P, Smidt ML, Beets-Tan RG, Wildberger JE, Lobbes MB. Contrast-enhanced spectral mammography in recalls from the Dutch breast cancer screening program: validation of results in a large multireader, multicase study. *Eur Radiol*. 2016;26(12):4371–9.
4. Tagliafico AS, Bignotti B, Rossi F, Signori A, Sormani MP, Valdora F, Calabrese M, Houssami N. Diagnostic performance of contrast-enhanced spectral mammography: systematic review and meta-analysis. *Breast*. 2016;28:13–9. <https://doi.org/10.1016/j.breast.2016.04.008>. Epub 2016 May 7.
5. Libera A, Altman DG, Tetzla J, Mulrow C, Gøtzsche PC, Ioannidis JPA, Clarke M, Devereaux PJ, Kleijnen J, Moher D. PRISMA Statement per il reporting di revisioni sistematiche e meta-analisi degli studi che valutano gli interventi sanitari: spiegazione ed elaborazione. *Evidence*. 2015;7(6):e1000115.
6. Lalji UC, Jeukens CR, Houben I, Nelemans PJ, van Engen RE, van Wylick E, Beets-Tan RG, Wildberger JE, Paulis LE, Lobbes MB. Evaluation of low-energy contrast-enhanced spectral mammography images by comparing them to full-field digital mammography using EUREF image quality criteria. *Eur Radiol*. 2015;25(10):2813–20.
7. Fallenberg EM, Dromain C, Diekmann F, Renz DM, Amer H, Ingold-Heppner B, Neumann AU, Winzer KJ, Bick U, Hamm B, Engelken F. Contrast-enhanced

- spectral mammography: does mammography provide additional clinical benefits or can some radiation exposure be avoided? *Breast Cancer Res Treat.* 2014;146(2):371–81.
8. Francescone MA, Jochelson MS, Dershaw DD, Sung JS, Hughes MC, Zheng J, Moskowitz C, Morris EA. Low energy mammogram obtained in contrast-enhanced digital mammography (CEDM) is comparable to routine full-field digital mammography (FFDM). *Eur J Radiol.* 2014;83(8):1350–5.
  9. Tennant SL, James JJ, Cornford EJ, Chen Y, Burrell HC, Hamilton LJ, Girio-Fragkoulakis C. Contrast-enhanced spectral mammography improves diagnostic accuracy in the symptomatic setting. *Clin Radiol.* 2016;71(11):1148–55.
  10. Sardanelli F, Fallenberg EM, Clauser P, Trimboli RM, Camps-Herrero J, Helbich TH, Forrai G, European Society of Breast Imaging (EUSOBI), with language review by Europa Donna—The European Breast Cancer Coalition. Mammography: an update of the EUSOBI recommendations on information for women. *Insights Imaging.* 2017;8(1):11–8.
  11. Cheung YC, Tsai HP, Lo YF, Ueng SH, Huang PC, Chen SC. Clinical utility of dual-energy contrast-enhanced spectral mammography for breast microcalcifications without associated mass: a preliminary analysis. *Eur Radiol.* 2016;26(4):1082–9.
  12. Cheung YC, Juan YH, Lin YC, Lo YF, Tsai HP, Ueng SH, Chen SC. Dual-energy contrast-enhanced spectral mammography: enhancement analysis on BI-RADS 4 non-mass microcalcifications in screened women. *PLoS One.* 2016;11(9):e0162740.
  13. Patel BK, Naylor ME, Kosiorek HE, Lopez-Alvarez YM, Miller AM, Pizzitola VJ, Pockaj BA. Clinical utility of contrast-enhanced spectral mammography as an adjunct for tomosynthesis-detected architectural distortion. *Clin Imaging.* 2017;46:44–52.
  14. Mori M, Akashi-Tanaka S, Suzuki S, Daniels MI, Watanabe C, Hirose M, Nakamura S. Diagnostic accuracy of contrast-enhanced spectral mammography in comparison to conventional full-field digital mammography in a population of women with dense breasts. *Breast Cancer.* 2017;24(1):104–10.
  15. Cheung YC, Lin YC, Wan YL, Yeow KM, Huang PC, Lo YF, Tsai HP, Ueng SH, Chang CJ. Diagnostic performance of dual-energy contrast-enhanced subtracted mammography in dense breasts compared to mammography alone: interobserver blind-reading analysis. *Eur Radiol.* 2014;24(10):2394–403.
  16. Tardivel AM, Balleyguier C, Dunant A, Delaloue S, Mazouni C, Mathieu MC, Dromain C. Added value of contrast-enhanced spectral mammography in Postscreening assessment. *Breast J.* 2016;22(5):520–8.
  17. James JR, Pavlicek W, Hanson JA, Boltz TF, Patel BK. Breast radiation dose with CESM compared with 2D FFDM and 3D Tomosynthesis mammography. *AJR Am J Roentgenol.* 2017;208(2):362–72.
  18. Fallenberg EM, et al. Contrast-enhanced spectral mammography vs. mammography and MRI—clinical performance in a multi-reader evaluation. *Eur Radiol.* 2017;27(7):2752–64.
  19. Jochelson MS, Dershaw DD, Sung JS, Heerd AS, Thornton C, Moskowitz CS, Ferrara J, Morris EA. Bilateral contrast-enhanced dual-energy digital mammography: feasibility and comparison with conventional digital mammography and MR imaging in women with known breast carcinoma. *Radiology.* 2013;266(3):743–51.
  20. Łuczyszka E, Heinze-Paluchowska S, Hendrick E, Dyczek S, Ryś J, Herman K, Blecharz P, Jakubowi J. Comparison between breast MRI and contrast-enhanced spectral mammography. *Med Sci Monit.* 2015;21:1358–67.
  21. Li L, et al. Contrast-enhanced spectral mammography (CESM) versus breast magnetic resonance imaging (MRI): a retrospective comparison in 66 breast lesions. *Diagn Interv Imaging.* 2017;98(2):113–23.
  22. Fallenberg EM, Dromain C, Diekmann F, Engelken F, Krohn M, Singh JM, Ingold-Heppner B, Winzer KJ, Bick U, Renz DM. Contrast-enhanced spectral mammography versus MRI: initial results in the detection of breast cancer and assessment of tumour size. *Eur Radiol.* 2014;24(1):256–64.
  23. Lobbes MBI, et al. The quality of tumor size assessment by contrast-enhanced spectral mammography and the benefit of additional breast MRI. *J Cancer.* 2015;6(2):144–50.
  24. Patel BK, Lobbes MB, Lewin J. Contrast enhanced spectral mammography: a review. *Semin Ultrasound CT MRI.* 2018;39:70–9.
  25. ElSaid NAE, Mahmoud HGM, Salama A, et al. Role of contrast enhanced spectral mammography in predicting pathological response of locally advanced breast cancer post neo-adjuvant chemotherapy. *Egypt J Radiol Nucl Med.* 2017;48(2):519–27.
  26. Barra FR, et al. Accuracy of contrast-enhanced spectral mammography for estimating residual tumor size after neoadjuvant chemotherapy in patients with breast cancer: a feasibility study. *Radiol Bras.* 2017;50(4):224–30.
  27. Iotti V, et al. Contrast-enhanced spectral mammography in neoadjuvant chemotherapy monitoring: a comparison with breast magnetic resonance imaging. *Breast Cancer Res.* 2017;19:106.
  28. Covington MF, et al. The future of contrast-enhanced mammography. *AJR.* 2018;210:292–300.
  29. Pataky R, et al. Cost-effectiveness of MRI of breast cancer screening in BRCA1/2 mutation carriers. *BMC Cancer.* 2013;13:339.
  30. Patel BK, et al. Potential cost savings of contrast-enhanced digital mammography. *AJR.* 2017;208:W231–7.



# Comparison Between Breast MRI and Contrast-Enhanced Digital Mammography

6

Marc B. I. Lobbes

Nowadays, breast magnetic resonance imaging (MRI) is regarded to be the most sensitive breast imaging modality, both in terms of breast cancer detection and the assessment of disease extent preoperatively. Dedicated breast MRI was first introduced in the late 1980s. In the first attempts, distinction between benign and malignant breast lesions was made based on differences in T1 and T2 relaxation times [1]. However, initial studies showed that there was an important overlap in these parameters between benign and malignant breast lesions. Soon after, the requirement for using contrast agents was demonstrated by Heywang et al., who showed that malignant lesions showed a significant enhancement within 5 minutes after contrast administration [2]. The importance of contrast administration was further emphasized by Kuhl et al., who showed that differentiation between benign and malignant lesions could be further optimized by studying the signal intensity time curves during dynamic, contrast-enhanced breast MRI [3]. Technical developments in the last decade, such as improved coil designs, increased magnetic field strengths and optimization of sequence protocols, have further improved the diagnostic performance of breast MRI.

When tumours are still in their earliest stages and are still small, they depend on simple diffusion to acquire the necessary nutrients. When they continue to grow, this process is becoming insufficient, causing hypoxic changes. This results in the excretion of angiogenic factors, triggering adjacent blood vessels to sprout new capillaries towards the tumour. These can supply tumours with their own blood supply, restoring their nutritional needs for further growth. However, these newly formed vessels are often disorganized and rapidly formed, causing them to be ‘leaky’ to contrast agent. Consequently, contrast agents can extravasate into the tumour interstitium, causing them to enhance when dedicated imaging is being applied. This is not only the principle behind breast MRI but also contrast-enhanced dual-energy mammography or CEDM [4].

According to international guidelines [5–7], the indications for performing dynamic, contrast-enhanced breast MRI are the following: (1) inconclusive findings during conventional imaging (such as full-field digital mammography and ultrasound), (2) preoperative staging, (3) evaluation of patients with unknown primary cancer, (4) response monitoring of breast cancer patients treated with neoadjuvant systemic therapy (NST), (5) imaging after breast-conservative therapy, (6) screening of high-risk patients, (7) evaluation of breast implants and (8) imaging-guided breast biopsies. As discussed before, the principles of

---

M. B. I. Lobbes  
Department of Radiology and Nuclear Medicine,  
Maastricht University Medical Center,  
Maastricht, The Netherlands  
e-mail: [marc.lobbes@mumc.nl](mailto:marc.lobbes@mumc.nl)

breast MRI and CEDM are comparable, and there is an increasing amount of scientific evidence that indications for CEDM are also comparable. In terms of patient's tolerance, CEDM was even preferred by patients over breast MRI [8]. However, it should be emphasized that CEDM is still a rather novel imaging technique, and consequently, scientific support for these indications is often based on retrospective studies or studies with relatively small sample sizes.

---

## 6.1 Inconclusive Findings During Conventional Breast Imaging

Although chance findings can occur in every imaging exam, the most common population to have inconclusive findings on conventional breast imaging are women that participated in breast cancer screening programs. In most programs, standard mammographic views are acquired and studied by radiologists, who can recall patients for additional exams when a suspect breast lesion is detected.

Lobbes et al. studied the performance of CEDM in women recalled from the national breast cancer screening [9]. In this study, they showed that using CEDM for this purpose in a clinical setting is feasible: of the 116 women eligible to undergo CEDM, 113 indeed underwent this exam. They found that CEDM was significantly better than full-field digital mammography, with the following diagnostic performance parameters (and their comparison to conventional mammography in brackets): sensitivity, 100% (+3%); specificity, 88% (+46%); positive predictive value (PPV), 76% (+37%); and negative predictive value (NPV), 100% (+3%). However, two radiologists experienced in evaluating CEDM exams read all the CEDM exams in this study.

In a subsequent study, Lalji et al. used 199 novel consecutive cases and had them reviewed by a panel of ten radiologists: four had extensive CEDM experience, three were experienced breast radiologists without any experience in reading CEDM exams, and the remaining three readers were residents [10]. Again, CEDM increased the diagnostic accuracy in all readers, with sensitiv-

ity and specificity for all readers of 97% (+4%) and 70% (+34%), respectively. The area under the ROC curve for CEDM was 0.833 (+0.188 as compared to full-field digital mammography). Hence, they concluded that the initial results were confirmed even when using radiologists with less experience in reading CEDM exams.

To be used as a problem-solving tool in case of inconclusive findings during conventional breast imaging, the modality of choice needs to have a high sensitivity (preferably with a high specificity as well). When directly compared to breast MRI, CEDM has a comparable sensitivity. Jochelson et al. studied 52 women that underwent both CEDM and breast MRI and found that sensitivity was equal: 96% [11]. However, CEDM suffered from less false-positive findings when compared to breast MRI. In a multi-reader study using three different readers, Fallenberg et al. studied a total of 604 breast lesions (273 malignancies) and concluded that the area under the ROC curve for CEDM was significantly higher than for full-field digital mammography (0.84 versus 0.79) and comparable to breast MRI (0.85) [12]. A study performed by Li et al. included 48 women and showed that both CEDM and breast MRI had a sensitivity of 100% for detecting breast cancers [13].

In conclusion, these results show that CEDM is an excellent problem-solving tool (Fig. 6.1), with a sensitivity to detect breast cancer that is equal to breast MRI. In addition, some studies suggest that even its specificity is higher, resulting in less false-positive findings when used for this indication.

---

## 6.2 Preoperative Staging of Breast Cancer Patients

For preoperative staging purposes, it is important that the image modality of choice can delineate the tumour extent as accurate as possible. Currently, breast MRI is regarded to be the most accurate modality for this indication, it being superior to other conventional imaging methods such as full-field digital mammography or ultrasound [14].



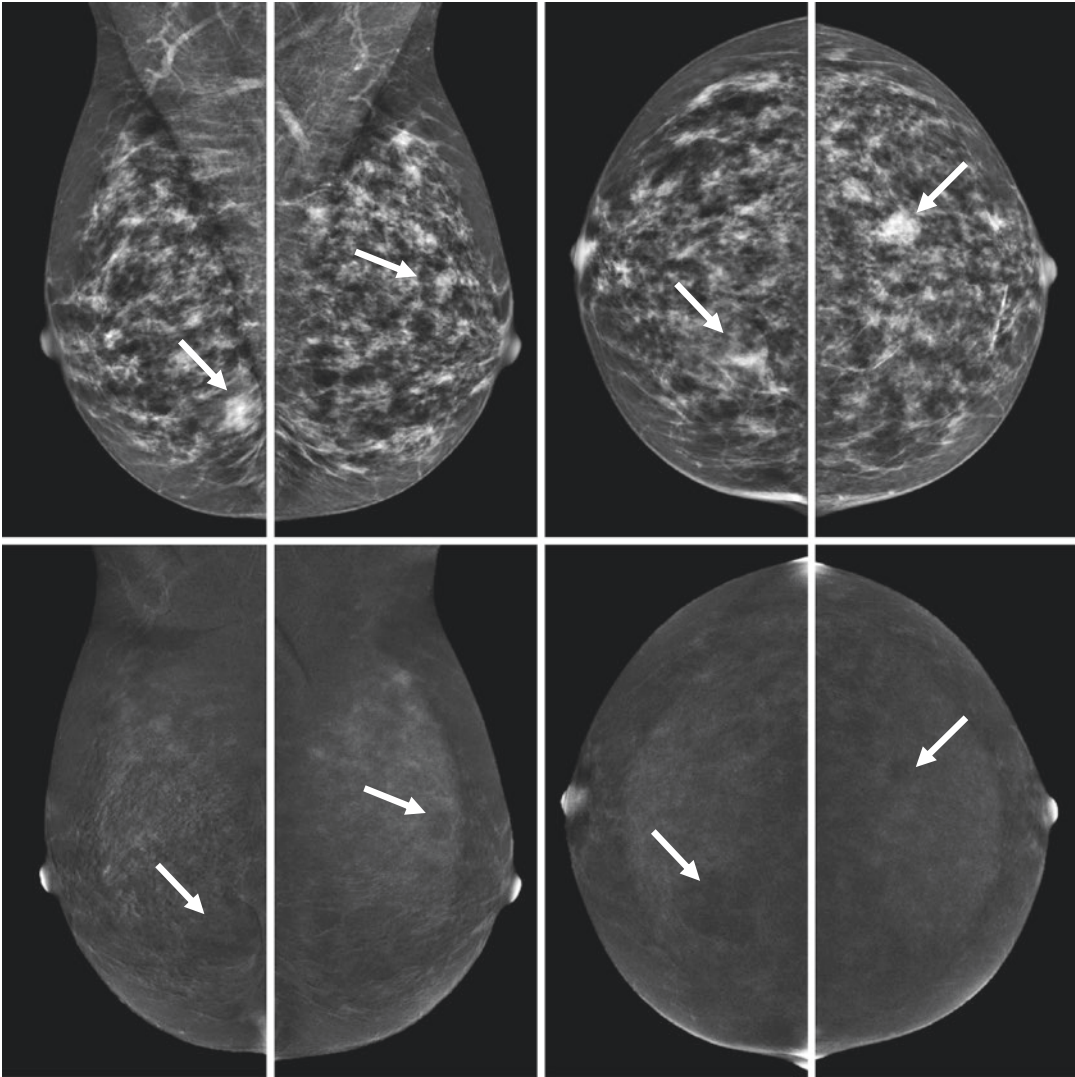


**Fig. 6.1** A 50-year-old female with ill-defined, partly obscured masses in both breasts (*arrows*). On the recombined images (*bottom row*), no enhancement is observed. More specifically, negative enhancement (more pro-

nounced blackening when compared to the adjacent fibroglandular tissue) was described, which is sometimes defined as an ‘eclipse sign’. This is the typical image of cysts, and no further imaging is needed for this diagnosis

Fallenberg et al. were the first to study the correlation between tumour size measurement performed with CEDM and breast MRI [15]. In this study of 80 patients, histopathological results served as the gold standard. The correlation was expressed as the Pearson’s correlation coefficient (PCC), it being 0.603 for full-field digital mammography. The numbers were superior for breast MRI with a PCC of 0.654. CEDM seemed to perform best in their study with a PCC of 0.733.

However, correlation does not automatically imply good agreement, which is equally important in these kinds of analyses. Although the PCC can be high, agreement can still be limited due to a structural over- or underestimation of the technique of choice.

In a subsequent study by Lobbes et al., tumour size measurements performed with CEDM were compared to histopathological results for 87 patients [16]. In 57 patients, an additional breast

MRI was available. In their study, both imaging modalities showed an excellent agreement with tumour size measurements performed on surgical specimens. For breast MRI, the PCC was slightly higher: 0.915 (for CEDM the PCC was 0.905). However, using Bland-Altman plots, they showed that breast MRI suffered from a slight systematic overestimation of tumour size measurements (mean difference with histopathological measurements of 2.12 mm), whereas CEDM did not (mean difference 0.03 mm). Presumably, this small difference does not have any impact on surgical outcomes, which was also studied. Using a  $2 \times 2$  contingency table to assess the frequency distribution of a relevant size discrepancy of  $>1$  cm between breast MRI or CEDM and histopathological results, they did not observe any advantage of performing an additional breast MRI exam after CEDM in any of the 57 cases.

However, the assessment of invasive lobular cancers is always a challenge, and previous studies have shown that especially in these cancer types, the ability of breast MRI to delineate tumour extent is optimal and might even lead to fewer mastectomies (when compared to patients with invasive lobular carcinoma that did not undergo breast MRI) [17]. Van Nijnatten et al. showed that for the assessment of invasive lobular cancer extent, both breast MRI and CEDM showed comparable results. The mean difference in tumour diameter measurement as compared to histopathological results was 5.5 mm (PCC 0.816) for breast MRI and 5.0 mm (PCC 0.853) for CEDM (Van Nijnatten: <http://dx.doi.org/10.1594/ecr2018/C-1490>). In this study, breast MRI detected seven more lesions than CEDM, of which five were false-positive findings and two were considered malignant (one 12 mm grade I ductal carcinoma in situ (at only 9 mm distance towards to primary index tumour) and one 8 mm invasive breast cancer of no special type). In summary, breast MRI should still be recommended for the evaluation of disease extent in invasive lobular cancers as there is more scientific evidence for its efficiency. However, CEDM might be an interesting alternative if breast MRI is not

feasible for whatever reason, albeit at the expense of less sensitivity but higher specificity (Fig. 6.2).

Another important issue in preoperative evaluation of breast cancer is the assessment of multifocal or contralateral disease. However, there are no studies published that studied the accuracy of both breast MRI and CEDM in their ability to detect multifocal or contralateral breast cancer. From experience, similar findings can be observed in both breast MRI and CEDM regarding multifocal disease, but this still must be objectively studied. Although no direct comparative study between CEDM and breast MRI exists for the evaluation of contralateral disease, Houben et al. studied the impact of finding additional breast lesions only observed by using CEDM ('CEDM-only' lesions) in women recalled from screening [18]. In this study, 70 CEDM-only lesions were detected (the majority being mammographically occult or presenting as a minimal sign on mammography) in 839 patients. Of these 70 lesions, 54.3% proved to be additional foci of breast cancer, suggesting that when CEDM would be used as a primary preoperative staging method, contralateral breast cancer can be detected reliably, even when this is mammographically occult or difficult to detect.

---

### 6.3 Evaluation of Patients with Unknown Primary Cancer

This indication refers to a group of patients diagnosed with metastases (in the axillae or elsewhere in the body), in whom a primary tumour cannot be identified. As CEDM is a novel technique and no studies have been published yet regarding this topic, it seems logical that similar findings might be observed as in breast MRI. Schorn et al. demonstrated that breast MRI was of added value in these patients even when a first evaluation using full-field digital mammography and ultrasound was negative. In this study, breast MRI detected breast cancer in almost 50% of the cases [19]. When metastases are found in the axillae in

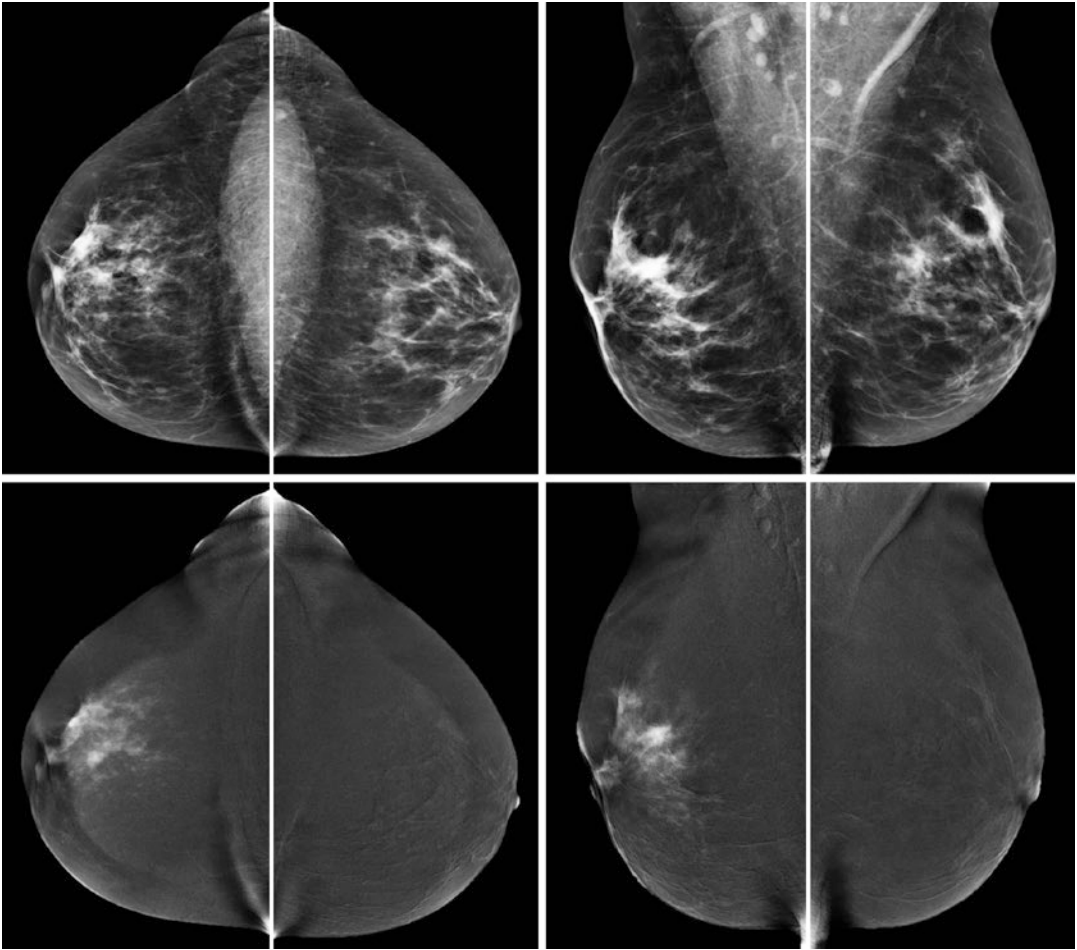


**Fig. 6.2** A 72-year-old female with a suspicious nipple retraction of the right nipple. On CEDM, an asymmetry or architectural distortion is observed next to the nipple retraction, which is difficult to delineate on the low-energy images (*top row*). However, on the recombined

images (*bottom row*), the true disease extent can be appreciated much easier by the larger area of non-mass enhancement behind the right nipple. Final histopathological results showed invasive lobular carcinoma

patients without an unknown primary tumour, breast MRI detects cancer in even 86% of the cases [20]. However, the sample sizes of these studies were small, but they emphasized the benefit of performing an additional breast MRI even when full-field digital mammography and/or ultrasound is negative. As discussed before, the sensitivity for detecting breast cancer is comparable to breast MRI. In our institute, we therefore perform ('one-stop-shop') CEDM in all patients with an unknown primary tumour as part of their work-up protocol.

#### 6.4 Response Monitoring of Breast Cancer Patients Treated with Neoadjuvant Chemotherapy

Neoadjuvant chemotherapy is the administration of systemic chemotherapy prior to surgery, as opposed to adjuvant chemotherapy, where the treatment is given after breast cancer surgery. Neoadjuvant chemotherapy has been predominantly used to reduce tumour burden to enable breast conservative surgery where otherwise a



mastectomy would have been performed. However, neoadjuvant chemotherapy also enabled us to study the response to therapy *in vivo* using different imaging modalities. It also holds important prognostic information, as the absence of residual disease correlates with good prognosis. Finally, it can create time to perform genetic testing with the option of bilateral mastectomy if proven positive.

Previous studies have shown that breast MRI is the most suitable imaging modality to study response to neoadjuvant chemotherapy [21]. Two recent studies have published initial results on the diagnostic performance of CEDM for response monitoring of breast cancer patients treated with neoadjuvant chemotherapy.

ElSaid et al. were the first to report on the ability of CEDM to predict pathological response in patients treated with neoadjuvant chemotherapy [22]. In 21 women diagnosed with stage II and III breast cancer, CEDM was performed after completion of therapy (no CEDM at baseline or halfway through the courses was performed). Pathological complete response (pCR) was achieved in 28.5% of these women. The sensitivity of detecting pCR with CEDM was 100% according to their calculations, with a specificity of 83%. Although the sample size of this population was small, it showed the potential of CEDM as response monitoring tool for patients treated with neoadjuvant chemotherapy.

Iotti et al. performed a more detailed prospective study on this topic and studied 46 cases of women treated with neoadjuvant chemotherapy [23]. These women underwent both CEDM and breast MRI as part of their response evaluation. They concluded that CEDM predicted pCR better than MRI (Lin's coefficients of 0.81 and 0.59, respectively), with both modalities tending to underestimate the extent of residual disease. Breast MRI tended to have a larger underestimation than CEDM (4.5 mm for CEDM, 7.5 mm for breast MRI). For assessing complete response, sensitivity and specificity of CEDM were 100 and 84%, whereas for breast

MRI, sensitivity and specificity were 87% and 60%, respectively.

Although these initial results are promising, there is still insufficient evidence to completely replace breast MRI by CEDM as response monitoring tool. Studies using breast MRI for this indication have shown that breast cancer phenotype and the treatment regimen used can be of influence of the accuracy of breast MRI to monitor response to therapy [24]. It is to be expected that similar limitations will occur using CEDM. However, current available studies suffer from too small sample sizes to draw any final conclusions on this topic. Larger studies are needed to study the performance of CEDM in response monitoring of women treated with neoadjuvant chemotherapy. Nevertheless, these initial results show that response monitoring using CEDM should be considered when there are contraindications for performing a breast MRI exam (Fig. 6.3).

---

## 6.5 Imaging After Breast Conservative Therapy

During the past decades, breast conservative therapy (BCT) has been increasingly used, especially with the introduction of neoadjuvant chemotherapy treatment. However, postoperative scarring and the effects of radiotherapy can cause coarse architectural distortions and asymmetries that can be difficult to evaluate on follow-up mammographic exams. Although no studies have been published using CEDM for this indication, similar advantages and limitations might be expected as we know from breast MRI. In a previous section, it was already discussed that the sensitivity for detecting breast cancer using CEDM is equal to breast MRI. Hence, CEDM might be used as well when a local recurrence is suspected and should present itself with increased enhancement on the recombined images in the surgical area. Scarring and fibrous tissue does not show any enhancement on breast MRI and is not expected to show enhancement on CEDM images as well.

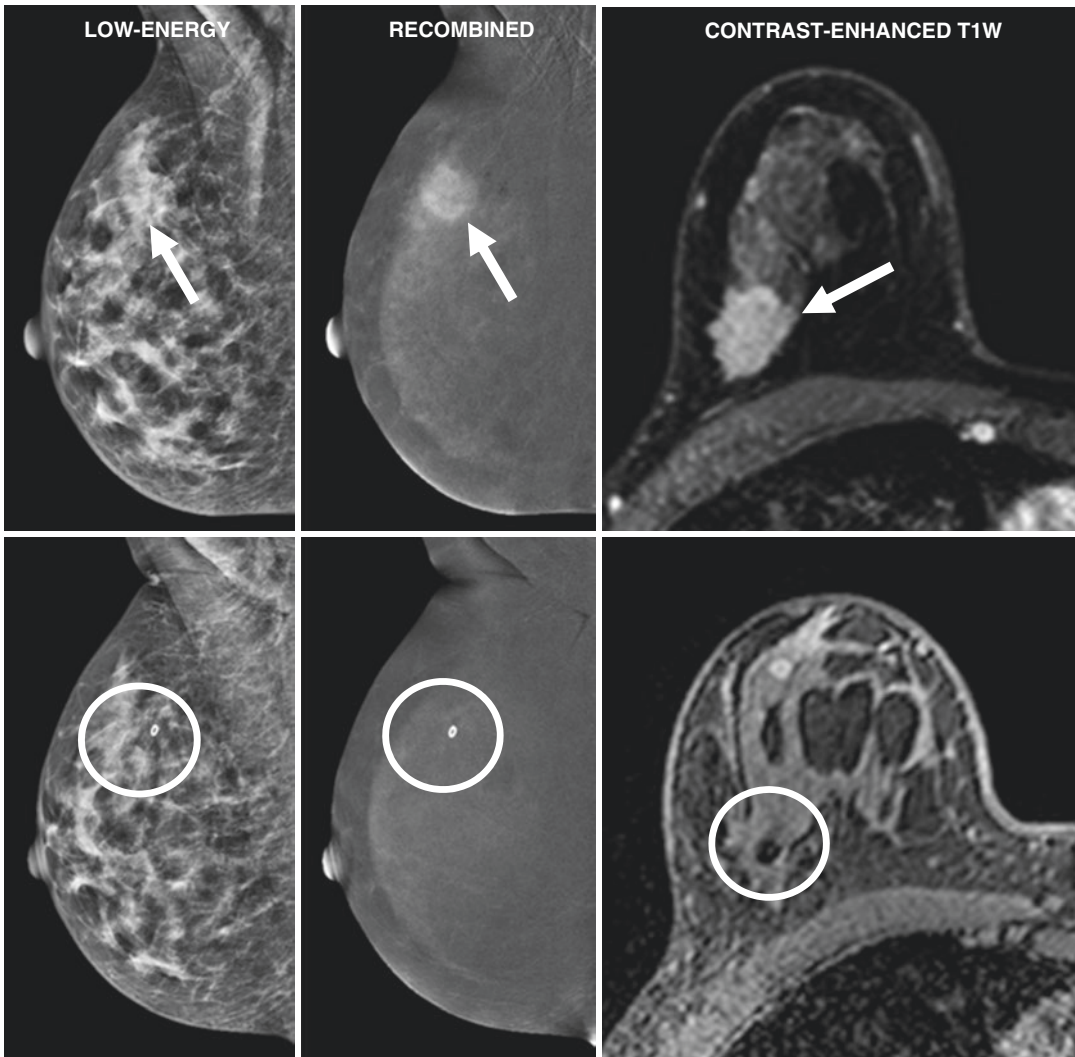


**Fig. 6.3** A 54-year-old female diagnosed with an invasive breast cancer of no special type (NST) in the right breast, visible as an ill-defined irregular and enhancing mass (arrows). The cancer is visible on both CEDM and breast MRI exams (top row). After being treated with neoadjuvant chemotherapy, CEDM and breast MRI were per-

formed just prior to surgery (bottom row). The former tumour location is represented by the clip placement (circle). At this site, no masses or enhancement is detected anymore. Final histopathological results showed complete response (pCR)

However, if CEDM is performed to soon after surgery (e.g. for positive surgical resection margins), one can expect diffuse non-specific enhancement caused by healing processes (similar to breast MRI). Future studies should provide us with more insights on the ability of CEDM to study the postoperative breast.

## 6.6 Screening of High-Risk Patients

Breast MRI plays an important role in periodical screening of women at high or intermediate risk for breast cancer. Specific screening programs using breast MRI are recommended for these

women by both American and European guidelines [5, 25, 26]. These programs were based on the results of several studies that showed that breast MRI detected additional cancers in these women: up to 15 cancers per 1000 women at intermediate or high risk for developing breast cancer [27]. Of all breast cancer detected in these women, approximately 45% were detected by breast MRI [28, 29].

However, breast MRI is an expensive imaging modality, and current protocols are time-consuming in the screening setting. Also, breast MRI slots may not be widely available, and women with contraindications for performing breast MRI, such as claustrophobia or metal implants, cannot be imaged. In addition, studies have shown that small traces of gadolinium can be detected in the brain and bone of patients that underwent MRI exams [30]. Although no relevant side effects of this accumulation have thus far been described, the use of gadolinium-based contrast agents, especially in a screening setting, is a topic of debate.

Due to the similarity of the underlying principle, CEDM might also be considered as imaging tool to screen women at intermediate or high risk for developing breast cancer. Jochelson et al. performed a pilot study on this topic, studying 307 women undergoing both CEDM and breast MRI [31]. In the first screening round, three cancers were detected, which were all visible on breast MRI. Only two of these were detected on CEDM, but none of them were visible on the low-energy images (suggesting that they were mammographically occult). After 2 years of imaging follow-up, another five cancers (non-palpable) were detected. The positive predictive value for both imaging techniques was comparable: 15% for CEDM (95% confidence interval (CI) 2–45%) versus 14% for breast MRI (95% CI 3–36%). Specificities of CEDM and breast MRI were 94.7 and 94.1%. Consequently, the authors concluded that CEDM could be considered as an alternative imaging tool when breast MRI for these women is not available. However, the results were based on a single-centre study so validation in larger and preferably multicentre trials is needed.

## 6.7 Evaluation of Breast Implants

Breast implant might cause intracapsular or extracapsular ruptures, requiring them to be explanted and perhaps replaced. The clinical evaluation of breast implant integrity is difficult, and numerous imaging modalities have been evaluated for detection of implant ruptures. Breast MRI, using dedicated implant sequence protocols which differ from ‘oncologic’ sequence protocols, is the most accurate technique for the evaluation of implant integrity, with a sensitivity for detecting ruptures of 80–90% (specificity, 90–97%; [32]). It is important to realize that the sequences for assessing implant integrity are based on non-contrast-enhanced protocols, and performing a CEDM without contrast would be like performing a ‘plain’ mammography exam. CEDM would only be useful in the oncological setting with patients having breast implants. However, performing CEDM in women with breast implants gives large artefacts, mainly in the (post-processing of the) recombined images, refraining us from studying any areas of enhancement in these areas. In women with breast implants, breast MRI will continue to be the preferred imaging modality.

## 6.8 Imaging-Guided Breast Biopsy Procedures

When suspicious breast lesions are only detected on breast MRI, MR-guided vacuum-assisted core biopsy can be considered for final diagnosis [33]. Although rare, CEDM can show enhancing lesions on the recombined images only, without any substrate on the low-energy images or during targeted ultrasound. In these cases, CEDM-guided breast biopsy is recommended, but although under development, this is currently not (yet) feasible. A technical challenge that needs to be tackled is, for example, the time required for targeting a lesion in a small field of view. If this procedure takes too long (e.g. small lesions in large breasts), the enhancement of the lesion

might have diminished to a level where it becomes difficult to visualize. From clinical experience, enhancing lesions on CEDM are often visible on breast MRI as well, making them suitable for MR-guided biopsy. If they have no correlate on the low-energy CEDM images and a subsequently breast MRI (usually performed some days later) does not show any suspicious findings, the observed abnormality is most likely to be benign, and short-term imaging follow-up is recommended to exclude breast cancer. However, this strategy requires easy access to the MRI facilities and the ability to perform MRI-guided biopsies.

## References

1. Raush DR, et al. How to optimize clinical breast MR imaging practices and techniques on your 1.5T-system. *Radiographics*. 2006;26(5):1469–84.
2. Heywang SH, et al. MR imaging of the breast with Gd-DTPA: use and limitations. *Radiology*. 1989;171(1):95–103.
3. Kuhl CK, et al. Dynamical breast MR imaging: are signal intensity time course data useful for differential diagnosis of enhancing lesions. *Radiology*. 1999;211(1):101–10.
4. Lobbes MBI, et al. Contrast-enhanced mammography: techniques, current results, and potential indications. *Clin Radiol*. 2013;68(9):935–44.
5. Mann RM, et al. Breast MRI: guidelines from the European Society of Breast Imaging. *Eur Radiol*. 2008;18(7):1307–18.
6. Sardanelli F, et al. Magnetic resonance imaging of the breast: recommendations from the EUSOMA working group. *Eur J Canc*. 2010;46(8):1296–316.
7. Yeh ED, et al. Breast magnetic resonance imaging: current clinical indications. *Magn Reson Imaging Clin N Am*. 2010;18(2):155–69.
8. Hobbs MM, et al. Contrast-enhanced spectral mammography (CESM) and contrast enhanced MRI (CEMRI): patient preferences and tolerance. *J Med Imaging Radiat Oncol*. 2015;59(3):300–5.
9. Lobbes MBI, et al. Contrast-enhanced spectral mammography in patients referred from the breast cancer screening programme. *Eur Radiol*. 2014;24(7):1668–76.
10. Lalji UC, et al. Contrast-enhanced spectral mammography in recalls from the Dutch breast cancer screening program: validation of results in a large multireader, multicase study. *Eur Radiol*. 2016;26(12):4371–9.
11. Jochelson MS, et al. Bilateral contrast-enhanced dual-energy digital mammography: feasibility and comparison with conventional digital mammography and MR imaging in women with known breast carcinoma. *Radiology*. 2013;266(3):743–51.
12. Fallenberg EM, et al. Contrast-enhanced spectral mammography vs. mammography and MRI—clinical performance in a multi-reader evaluation. *Eur Radiol*. 2017;27(7):2752–64.
13. Li L, et al. Contrast-enhanced spectral mammography (CESM) versus breast magnetic resonance imaging (MRI): a retrospective comparison in 66 breast lesions. *Diagn Interv Imaging*. 2017;98(2):113–23.
14. Gruber IV, et al. Measurement of tumour size with mammography, sonography and magnetic resonance imaging as compared to histological tumour size in primary breast cancer. *BMC Cancer*. 2013;13:328.
15. Fallenberg EM, et al. Contrast-enhanced spectral mammography versus MRI: initial results in the detection of breast cancer and assessment of tumour size. *Eur Radiol*. 2014;24(1):256–64.
16. Lobbes MBI, et al. The quality of tumour size assessment by contrast-enhanced spectral mammography and the benefit of additional breast MRI. *J Cancer*. 2015;6(2):144–50.
17. Lobbes MBI, et al. Breast MRI increases the number of mastectomies for ductal cancers, but decreases them for lobular cancers. *Breast Cancer Res Treat*. 2017;162(2):353–64.
18. Houben IPL, et al. Contrast-enhanced spectral mammography as work-up tool in patients recalled from breast cancer screening has low risks and might hold clinical benefits. *Eur J Radiol*. 2017;94:31–7.
19. Schorn C, et al. MRI of the breast in patients with metastatic disease of unknown primary. *Eur Radiol*. 1999;9(3):470–3.
20. Orel SG, et al. Breast MR imaging in patients with axillary node metastases and unknown primary malignancy. *Radiology*. 1999;212(2):543–9.
21. Marinovich ML, et al. Agreement between MRI and pathologic breast tumor size after neoadjuvant chemotherapy, and comparison with alternative tests: individual patient data meta-analysis. *BMC Cancer*. 2015;15:662.
22. ElSaid NAES, et al. Role of contrast enhanced spectral mammography in predicting pathological response of locally advanced breast cancer post neoadjuvant chemotherapy. *Egypt J Radiol Nucl Med*. 2017;48(2):519–27.
23. Iotti V, et al. Contrast-enhanced spectral mammography in neoadjuvant chemotherapy monitoring: a comparison with breast magnetic resonance imaging. *Breast Cancer Res*. 2017;19(1):106.
24. Lobbes M, Prevos R, Smidt M. Response monitoring of breast cancer patients receiving neoadjuvant chemotherapy using breast MRI—a review of current knowledge. *J Cancer Ther Res*. 2012. <https://doi.org/10.7243/2049-7962-1-34>.
25. Mann RM, et al. Breast MRI: EUSOBI recommendations for women’s information. *Eur Radiol*. 2015;25(12):3669–78.

26. Saslow D, et al. American Cancer Society guidelines for breast cancer screening with MRI as an adjunct to mammography. *CA Cancer J Clin.* 2007;57(2):75–89.
27. Kuhl C, et al. Prospective multicenter cohort study to refine management recommendations for women at elevated familial risk of breast cancer: the EVA trial. *J Clin Oncol.* 2010;28(9):1450–7.
28. Obdeijn IM, et al. Should we screen BRCA1 mutation carriers only with MRI? A multicenter study. *Breast Cancer Res Treat.* 2014;144(3):577–82.
29. Riedl CC, et al. Triple-modality screening trial for familial breast cancer underlines the importance of magnetic resonance imaging and questions the role of mammography and ultrasound regardless of patient mutation status, age, and breast density. *J Clin Oncol.* 2015;33(10):1128–35.
30. Murata N, et al. Gadolinium tissue deposition in brain and bone. *Magn Reson Imaging.* 2016;34(10):1359–65.
31. Jochelson MS, et al. Comparison of screening CEDM and MRI for women at increased risk for breast cancer: a pilot study. *Eur J Radiol.* 2017;97:37–43.
32. Juanpere S, et al. Imaging of breast implants—a pictorial review. *Insights Imaging.* 2011;2(6):653–70.
33. Heywang-Köbrunner SH, et al. Interdisciplinary consensus on the uses and technique of MR-guided vacuum-assisted breast biopsy (VAB): results of a European consensus meeting. *Eur J Radiol.* 2009;72:289–94.





# Implementation of Contrast-Enhanced Mammography in Clinical Practice

# 7

Maninderpal Kaur, Claudia Lucia Piccolo,  
and Shantini Arasaratnam

Contrast-enhanced digital mammography (CEDM) was first introduced to clinical use by Lewin et al. in 2003 [1]; since then, the use of CEDM in clinical practice has evolved with increasing equipment installation, clinical experience and clinical application.

The principle behind CEDM is similar to that of breast magnetic resonance imaging [2] as they both assess tumour neoangiogenesis; therefore, with some exceptions, most of the indications for breast MRI apply to CEDM.

CEDM is increasingly being adopted in breast-imaging centres, largely due to early clinical studies demonstrating this technology's ability to provide both anatomic and functional information of breast parenchyma similar to MRI but at a lower cost and shorter duration of examination. Because such capability can be an added feature to the newer generation mammogram machines, we expect that the use of CEDM will increase. However, there is limited guidance regarding how to best implement this technology, and there are no standard guidelines for the clinical use of CEDM. In this chapter, we discuss the implementation of CEDM into the clinical practice setting, with a review of the available

literature and perspectives from our large tertiary academic hospital.

Since the implementation of CEDM in 2016, Careggi University Hospital in Florence, Italy, has performed approximately 800 examinations. CEDM is now being conducted almost daily as an essential part of the diagnostic workup, in which a majority (75%) of our cases have a breast cancer diagnosis, and imaging is performed to evaluate the extent of disease. Twenty-five percent of CEDM cases are performed for additional diagnostic evaluation of inconclusive imaging findings on mammography. The remainder of our indications includes an assessment of the response to neoadjuvant chemotherapy (NAC), patients with a history of breast cancer and screening of high-risk patients for whom MRI is contraindicated.

## 7.1 Configuring a Contrast-Enhanced Digital Mammography (CEDM) Unit

The U.S. Food and Drug Administration (FDA) approved contrast-enhanced mammography systems in 2011, with the first system to be approved being the GE Essential SenoBright system (GE Healthcare), known as contrast-enhanced spectral mammography (CESM). Subsequently, in 2013, the Hologic Dimensions I-View (Hologic) system was approved, which is known as

---

Maninderpal Kaur (✉) · S. Arasaratnam  
Department of Radiology, Kuala Lumpur Hospital,  
Kuala Lumpur, Malaysia

C. L. Piccolo  
Department of Medicine and Health Science,  
University of Molise, Campobasso, Italy



contrast-enhanced digital mammography (CEDM). Other vendors are currently working on prototypes. Most current-generation mammography systems are frequently delivered with CEDM capability, reflecting the feasibility of implementing CEDM into breast-imaging practice in terms of equipment costs and space allocation.

CEDM can be performed in the existing mammography suite for practices that own a CEDM-capable mammography system. Implementation requires only the acquisition of a standard contrast power injector, purchase of a software upgrade from the vendor and insertion of a copper filter into the existing mammography unit [3, 4]. Hence, this is the beauty of incorporating CEDM, as it is just a technology application that is uploaded into an existing mammogram unit, precluding the need for additional space, and it fits nicely without disruption into the workflow.

For practices that do not own a CEDM-capable mammography system, the acquisition costs are higher. However, implementing a CEDM-capable mammography unit would definitely be beneficial for any breast-imaging centre because the system can provide the unit with standard 2D and 3D mammography as well as a CEDM upgrade capability and can also perform stereotactic-guided procedures.

### 7.1.1 Patient Issues

Breast CEDM patients comprise a subset of patients who have issues, typically because they have a known cancer, have a relatively high risk for cancer or have an issue on their mammogram that requires further testing. As a result, these patients are generally anxious. Performing an MRI examination for these patients can exacerbate this anxiety, as they would have to wait for an opening in the MRI examination schedule; in contrast, CEDM can be performed on the same day in the existing mammography suite. The presence of a CEDM unit at our centres has allowed us to image patients quickly because we can perform CEDM on the same day that a patient is referred to us for a suspicious breast mass; therefore, we

avoid any delay involved with the patient receiving an MRI examination.

CEDM examinations can be added to a full breast-imaging schedule at our breast units in Careggi University Hospital and Kuala Lumpur Hospital (KLH) with little disruption to our schedule, similar to the case of a breast ultrasound (US). At our centres, we observed that the total “room time” to perform a CEDM is approximately 20 minutes.

Hobbs et al. [5] studied the differences in patient preference and tolerance between CEDM and MRI. Although patients graded breast compression or positioning and contrast administration less favourably for CEDM, in general, they still expressed a preference for CEDM over breast MRI. Based on the experience at our centres, we observed a greater ease of scheduling, faster imaging and interpretation times, and improved patient compliance and tolerance when we performed CEDM compared with those of MRI.

CEDM is particularly useful for patients with claustrophobia, leading to higher satisfaction among patients and referring clinicians than that seen in MRI. CEDM may also be beneficial for patients with other contraindications to MRI such as body habitus, table weight limits and the presence of pacemakers.

Patient anxiety can be reduced by providing information about the CEDM procedure during the consultation along with a patient fact card explaining what to expect (Fig. 7.1). The radiologist or referring physician should inform and counsel patients to ensure that there are no absolute contraindications for CEDM contrast agents. It is also helpful to explain in advance the necessity of injecting contrast; as such a discussion would exclude any prior history of reaction to contrast. Proper patient screening, adequate prophylactic measures and training of staff to cope with hypersensitivity reactions can prevent certain adverse reactions or their complications. Radiologists should be familiar with all potential adverse renal events, including contrast-induced nephropathy, and should plan strategies with the referring physicians to lower their incidences [6].



**DEPARTMENT OF RADIOLOGY**

**KUALA LUMPUR HOSPITAL**

**JALAN PAHANG**

**50586 KUALA LUMPUR**

**TEL : 03-26155930**

**FAX : 03-26984035**

**WEBSITE: [xray@hkl.gov.my](mailto:xray@hkl.gov.my)**

## **Contrast Enhanced Digital Mammography (CEDM)**

### **Patient Information Sheet**

This leaflet aims to answer some frequently asked questions about CEDM in Kuala Lumpur Hospital. If you have any further questions, please feel free to speak to a member of the breast imaging team caring for you.

#### **What is CEDM?**

CEDM uses an iodinated contrast dye, in combination with mammography, to make cancers that are not visible on standard mammograms to show up as enhancing areas. The contrast is injected into an arm vein.

#### **Why might I need a CEDM and what are the benefits?**

Your doctor may recommend that you have a CEDM for:

- Evaluating any breast lump that was found during a physical examination or previous imaging.
- Breast cancer screening for women who are at increased risk for developing breast cancer and for women who have dense breasts.

In multiple studies, CEDM equaled MRI in its ability to detect breast cancer and is superior to both standard mammography and breast ultrasound, especially in women with dense breasts.

#### **What are the risks of a CEDM?**

People who get CEDMs are exposed to slightly more radiation than people who get regular mammograms, however, the extra dose is still within the dose recommendations for diagnostic purposes.

Some people can have an allergic reaction to IV contrast. Most reactions are mild, such as hives, however, some people can have more serious reactions, such as shortness of breath or facial swelling.

**Fig. 7.1** Patient fact card

**Who shouldn't get a CEDM?**

CEDMs aren't safe for everyone. Do inform us promptly:

- If you are pregnant/breastfeeding
- If you are allergic to iodine/seafood
- If you have renal (kidney) failure or asthma

**Before your CEDM**

If you are older than 70 years, or have any underlying kidney disease or diabetes, you will need to have a blood test called serum creatinine. You will be exempted from this test if you have had a serum creatinine done within 3 months before your CEDM.

**On the day of your CEDM**

We recommend you to be fasted for at least 4 hours prior to your scheduled appointment as the contrast may cause some mild nausea.

Do not put on any deodorant, powder, lotion, perfume or cream before your CEDM.

After a brief interview, you will be required to sign an informed consent giving us permission to administer the contrast media. An intravenous (IV) line will then be inserted into a vein in your arm by the doctor or nurse, through which the IV contrast will be given.

It is normal to have a warm sensation and a metallic taste in your throat as you are getting the IV contrast. At this point, do let the nurse or technologist know if you feel any pain at your IV site or have any other unusual symptoms.

Two minutes after injection of the IV contrast, the mammograms will be performed.

The entire procedure will not normally last more than 20 minutes.

**After your CEDM**

Once the CEDM examination is completed, you will be asked to sit in the waiting room. Your radiologist will inform you if you need any additional imaging such as an ultrasound or biopsy.

Once all the additional imaging is completed and if you have no reaction to the contrast media, a nurse will remove your IV line and place a bandage (Band-Aid®) over the area.

It is advisable to drink at least 6 to 8 glasses of water after the examination, as it would help to remove the contrast from your kidneys.

Most people will be informed of the results of the CEDM on the same day and a report of your examination will be sent to your doctor within a few days after your test.

**Fig. 7.1** (continued)

Before a patient undergoes a CEDM examination, the patient and referring physician should possess a clear understanding of the potential outcomes. The patient must be aware that CEDM is a complementary test that may generate additional workup with a complementary ultrasonography, with the possibility of a core needle biopsy due to findings on the CEDM.

As CEDM is an adjunctive test that is used only in specific clinical situations in view of the added radiation doses received, patient self-referral for breast CEDM should be discouraged. The physicians should also be made aware that there will be an added radiation dose to the breast during the procedure [7]. Therefore, it may be helpful initially to designate a single radiologist to screen and protocol all referred breast CEDM cases to ensure that the appropriate patients are being scanned. This approach would include requests from clinicians who may not initially understand the importance of careful patient selection. We found it helpful to provide referring physicians with a presentation on this new technique available at our centre in addition to providing them with a memo on the appropriate indications for CEDM referrals.

### 7.1.2 Radiologist and Technologist Considerations

As with any new imaging modality, training is an important factor in the implementation process. CEDM was implemented at our centres in Careggi University Hospital and KLH by our existing mammography technologists who were trained to perform CEDM, and there was no need to hire additional technologists. The radiologists, technologists and physicists are required to undergo training in CEDM, which is typically offered through application training provided by the vendors.

Initially, it may be useful to scan patients with known cancers to develop a sense of confidence and build a knowledge base. Additionally, these patients are likely going to the operating room, regardless, and any additional information that the CEDM examination provides will likely only help them.

Nursing support may be beneficial for placement of the intravenous (IV) line and assistance with management of contrast reactions; thus, a dedicated nurse is always present during CEDM procedures at our centres. A radiologist or other licensed physician must always be present in the mammography suite during CEDM imaging to evaluate and treat any contrast-associated reaction.

Another important consideration for technologists is that the timeline of 6 minutes to complete all imaging is sufficient to acquire all four standard mammographic views. Emphasizing this point to technologists is important, because patients may experience increased anxiety when they feel rushed through the imaging process, frequently resulting in motion artefacts on the recombined images. Apprehension among the technologists at our centres was particularly apparent when we began implementing the CEDM unit; however, this apprehension lessened with increasing experience.

Contrast splatter mimicking calcifications is another artefact that we occasionally observe. At Careggi University Hospital and KLH, we ensure that a nurse or medical officer inserts the intravenous line and performs contrast administration away from the mammogram machine, after which patient positioning is performed by the technician. Marc Lobbes of the Maastricht University Medical Centre reported that his centre expressly ensures that the technologist handling contrast administration does not perform patient positioning; additionally, the technologist uses gloves that are discarded prior to image acquisition.

### 7.1.3 Radiation Dose Considerations

Among the limitations of CEDM is the added radiation dose involved in the examination. Dromain et al. [8] were the first to report on the CEDM radiation dose, for which they observed an increase of a 20% higher radiation dose in CEDM relative to full-field digital mammography (FFDM).

Subsequently, Jeukens et al. [7] demonstrated that the average glandular dose for CEDM was 2.80 mGy relative to 1.55 mGy for routine FFDM.

More recently, James et al. [9] performed phantom studies to observe the radiation exposure in both dense and non-dense breast tissue. In their study, CEDM was found to increase the average glandular dose at a mean breast thickness of 63 mm by approximately 0.9 mGy and 0.5 mGy relative to 2D FFDM and 3D tomosynthesis, respectively; however, the additional radiation exposure was still below the dose limit of 3 mGy set by the US Mammography Quality Standards Act (MQSA) guidelines. James et al. concluded that the benefits obtained by the additional contrast images offset the additional radiation.

Yakoumakis et al. [10] reported that the low-energy mammography is the main contributor to the total glandular breast dose in CEDM. At our centre in KLH, when patients older than 40 years of age are referred for a suspicious breast mass, we immediately perform CEDM because the low-energy image obtained in the CEDM examination is equivalent to that of a standard mammogram. Therefore, the only added radiation dose received would be the high-energy exposure, which is minimal. However, the additional dose should always be kept in mind when deciding to use this examination.

### **7.1.4 Examination Interpretation and Results Communication**

For radiologists, in addition to training on the technical aspects, a learning curve is also required for image interpretation. Lalji et al. [11] demonstrated that CEDM requires a minimal learning curve to effectively interpret studies in their study, which included ten readers; among which were radiologists who were experienced in reading CEDM exams, experienced breast radiologists without any prior experience in CEDM and radiology residents. Even in our setting, we have observed CEDM to be relatively straightforward to interpret compared

with the interpretation of FFDM alone and MRI. Radiologists will generally observe a decrease in recall rates and also fewer short-term follow-up cases. To breast radiologists, CEDM images look familiar and may be faster to interpret than MRI images, with a mean total image interpretation time of 1–2 minutes [3, 4]. As with mammographic interpretation, communication with the referring physician about the final recommendation is necessary in CEDM studies. Considering the ease of interpretation of CEDM examinations, the radiologist can inform patients of the results of the CEDM procedure on the same day. At our centre, we have a consultation room adjacent to the CEDM examination room where we interpret the images immediately after the procedure and provide patients with their reports before they leave. If a new lesion is found on CEDM, we can immediately perform a complementary US, and an US-guided core biopsy procedure can be performed during the same sitting. This capability markedly reduces patient anxiety and waiting time.

---

## **7.2 Performing Contrast-Enhanced Imaging of the Breast**

### **7.2.1 Patient Handling**

Prior to performing a CEDM examination, patients should be provided with thorough instructions regarding the procedure and informed of potential adverse reactions to iodinated contrast media. An informed consent should be obtained from patients before the administration of contrast media. After a careful assessment of the patient's medical history, including known allergies, particularly to iodinated contrast media, and a laboratory evaluation of renal function, peripheral intravenous (IV) access is obtained in the antecubital fossa, preferably with a 22-gauge needle. A dose of 1.5 mL/kg of iodinated contrast material (300–370 mg iodine/mL) is administered by a power injector at a rate of 2–3 mL/s. A 20-mL saline bolus is administered following contrast injection to achieve a significant bolus

administration and optimal delivery of contrast to tissues, thus improving image quality.

After contrast injection is completed, the connecting tubing is detached from the patient, while the catheter remains in place until the end of the examination. The acquisition of the images begins 2 minutes after contrast injection, and care must be taken to complete the examination within 8 minutes following contrast media injection. During this time, the patient is monitored for any adverse reaction to the iodinated contrast material. A 2 minute delay after injection is essential, as applying compression too early may result in retained contrast media within vessels outside the breast, preventing the contrast from flowing in sufficiently and producing a bolus in major vessels that is visible in early images.

At our centres, the entire CEDM procedure takes approximately 20 minutes, after which the patient changes her clothes and waits for us to review the images before she is called to the consultation room, where the results are explained to her. If any areas of abnormal enhancement are detected based on the CEDM, the patient is immediately subjected to a second-look US to locate the lesion, and US-guided core biopsy is performed.

This process takes approximately 30 minutes post-procedure, which is sufficient time for us to observe any contrast reaction that may occur, and the IV line is kept in place in case any severe contrast reactions are observed.

### 7.2.2 Contrast Reactions

Although the use of contrast media is generally considered safe and beneficial in medical imaging, such use occasionally results in adverse events in patients. A 0.6% reaction rate to IV injections of non-ionic contrast media has been reported [12].

All life-threatening contrast reactions typically occur immediately or within 20 minutes after contrast administration; therefore, it is necessary to observe the patient post-contrast administration. General precautions should be taken to ensure that the likelihood of severe adverse reac-

tions is minimal, such as ensuring that patients are adequately hydrated and that emergency equipment is available in the CEDM suite [6].

All staff involved with the CEDM unit should have up-to-date anaphylaxis training and the contact information for the institution's emergency response team. They should know the location of emergency monitoring equipment and medications. The American College of Radiology recently designed a contrast reaction card that summarizes the important steps for managing an acute reaction to contrast agents, which is available on their website. Each card is the size of a driver's licence, which has been distributed to all our staff associated with the CEDM unit of our centre in KLH. According to Marc Lobbes, the Maastricht University Medical Centre performs annual training to cope with these reactions, which has worked well for their centre.

### 7.2.3 Image Acquisition

Image acquisition includes full-field exposures obtained at high and low energies using standard craniocaudal (CC) and mediolateral oblique (MLO) projections of each breast. The imaging protocol is typically configured in the system, and the order of image acquisition has not been shown to be relevant. Each facility must determine their own CEDM protocol to stimulate a consistent protocol. At KLH, we perform the CC projection on the suspected side first, in an attempt to capture early arterial enhancement and minimize false-negative results from early wash-out; subsequently, the contralateral breast is imaged in CC view and then followed by the MLO projections of both breasts. If enhancement is seen on the suspected side, we obtain an image after 8 minutes in the delayed phase to assess the enhancement kinetics that may provide additional information regarding the likelihood of malignancy. Although there is still no evidence that the kinetics in CEDM is similar to that of breast MRI, based on our experience at Careggi University Hospital and KLH, the incorporation of a delayed acquisition provides a relatively accurate guide to the lesion morphology.



The low-energy mammograms are performed at the same peak kilovoltage (kVp) as full-field digital mammography (FFDM) at 25–33 kVp and with the same filtration of either rhodium or silver. The high-energy acquisition is performed at a higher value of 45–49 kVp, optimized to the *k*-edge of iodine and using a copper filter. In 2002, Skarpathiotakis et al. [13] compared aluminium, molybdenum and copper filters for CEDM and concluded that copper is a suitable choice because it is relatively transparent to X-rays at energies where iodine attenuates them most heavily, thereby providing high contrast. They also inferred that due to a *k*-edge of copper at 9 keV, high attenuation occurs at low energies, thereby reducing the dose to the breast from relatively low-energy X-rays.

Recombined images are produced by the cancellation of background breast tissue and sent to the picture archiving and communication system (PACS) together with the low-energy images.

### 7.3 Clinical Applications

A detailed description and background of the clinical indications of CEDM are comprehensively discussed in Chapter 6. We provide here a brief summary of the clinical indications with a note on our clinical experience for each indication.

#### 7.3.1 Inconclusive Findings in Conventional Imaging

Occasionally, a mammographic finding may be inconclusive even when additional problem-solving views and sonograms have been obtained. This situation arises because the diagnostic accuracy of FFDM is highly dependent on the fibroglandular density of breast parenchyma [14]. Additional imaging is typically required in response to difficult-to-interpret mammograms, such as in cases of a focal asymmetry, evaluation of architectural distortion and differentiation between a scar and a recurrent cancer.

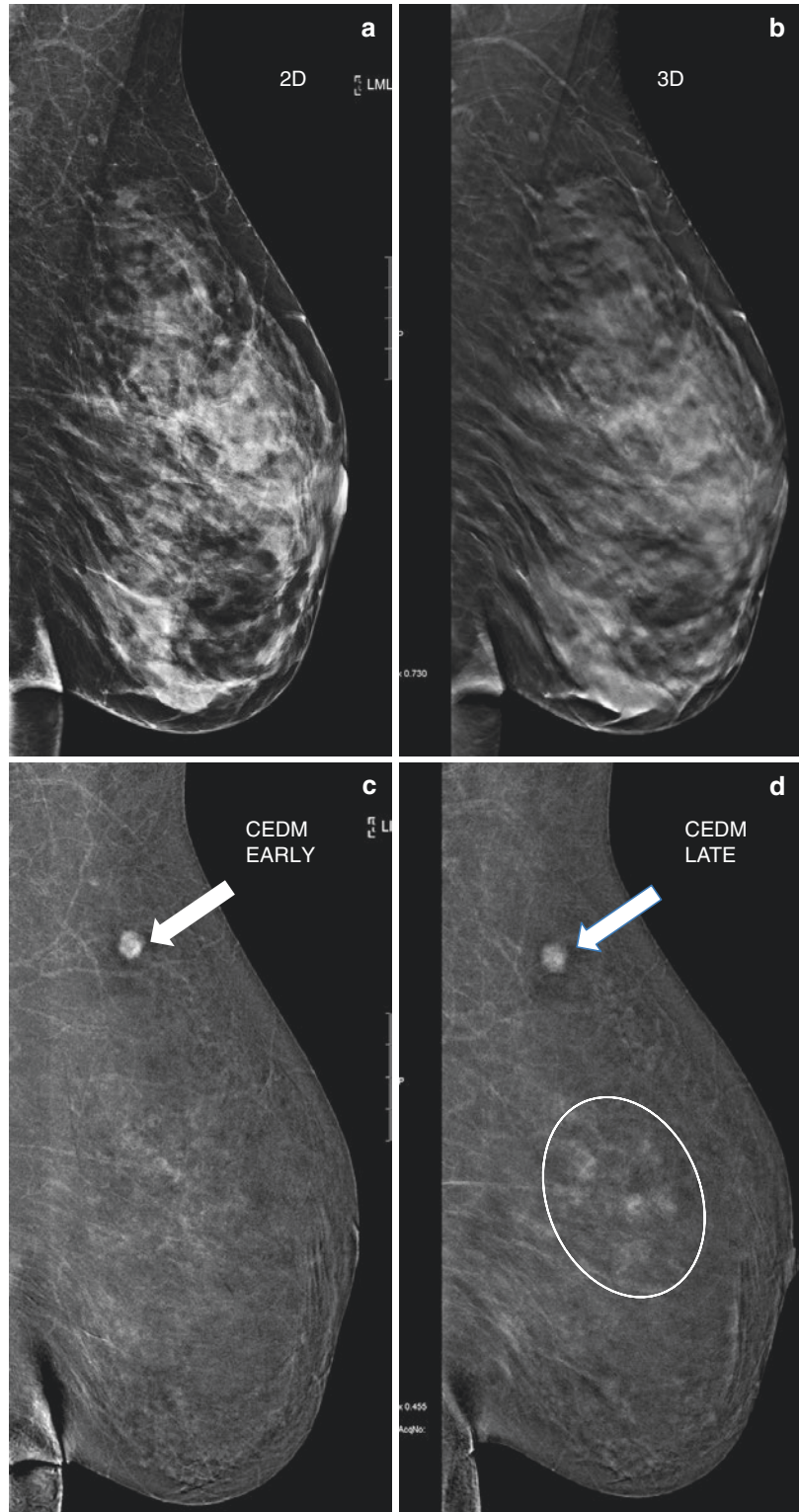
Several studies have been conducted to compare the feasibility of CEDM with that of

conventional breast imaging in breast cancer detection; these studies showed that CEDM detects more malignant tumours than does mammograms [2, 8, 11, 15–17].

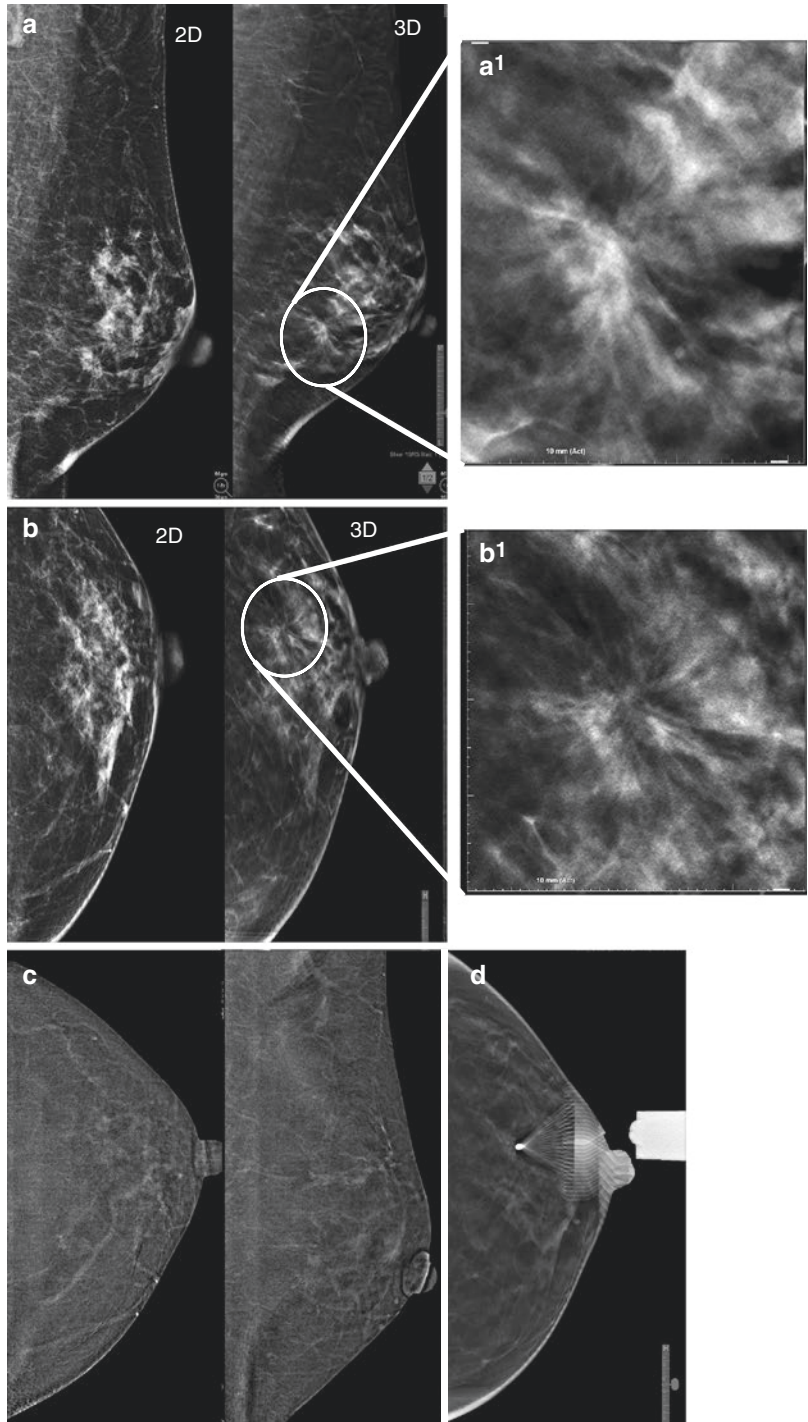
Also notable is the comparison of CEDM to MRI in the diagnosis of cancer, regarding which very limited literature is available. A cornerstone in this context was laid by Fallenberg et al. [18], who demonstrated that bilateral dual-energy CEDM and MRI are superior to mammogram in breast tumour detection, with CEDM performing slightly better than MRI, exhibiting an increase in lesion detection by 17.5% relative to FFDM and 2.6% relative to MRI. In this report, the authors also demonstrated that CEDM has an excellent correlation with respect to the evaluation of the extent of the disease. They also observed that CEDM recognized two cancers undetected by MRI, an invasive lobular carcinoma (ILC) and an invasive ductal carcinoma (IDC), plus ductal carcinoma in situ (DCIS). They inferred that in the absence of neoangiogenesis, contrast media moved into the ducts by diffusion as the possible explanation for the enhancement of DCIS in CEDM. That study suggested that longer time delays between contrast injection and CEDM exposure can result in stronger enhancement and better visibility of DCIS in CEDM compared to MRI because the amount of contrast reaching the tissue by diffusion is time-dependent. The authors concluded that the significant role of delayed acquisition of contrast-enhanced images in CEDM allowed better visibility of certain cancers relative to MRI, particularly when neovascularization is absent and only mild or low enhancement is present due to diffusion of the contrast media into the ducts. At Careggi University Hospital, we have also observed that some lower grade tumours are enhanced more vividly in the second mammographic view than in the first view (Fig. 7.2).

However, note that a negative CEDM does not preclude the need to biopsy indeterminate or suspicious calcifications identified on mammography. Whether calcifications are indeterminate or suspicious (thus requiring biopsy) should be determined solely on the mammographic features of the calcifications (Figs. 7.3 and 7.4).

**Fig. 7.2** Delayed enhancement. A 59-year-old female, in whom CEDM was done as preoperative staging for a biopsy proven, left infiltrating tubular carcinoma. **(a, b)** No demonstrable lesion seen on 2D and 3D mediolateral oblique views. **(c, d)** CEDM recombined image in mediolateral oblique view in early and delayed phase. The examination demonstrates a faint area of non-mass enhancement (NME) in the mid to upper quadrant that is more prominent in the delayed acquisition (*circle*) corresponding to the region that was previously biopsied. There is another intensely enhancing nodule seen at the axillary tail (*arrow*), which shows wash-out in the delayed acquisition. A second-look ultrasound was performed where the axillary tail lesion was identified and biopsied. *Diagnosis: The pathology of the axillary tail lesion (arrow) was also an Infiltrating Tubular Carcinoma.*



**Fig. 7.3** Problem-solving. A 46-year-old woman was recalled from screening for an architectural distortion in the left lower outer quadrant. (a) 2D and 3D mediolateral oblique views. (b) 2D and 3D craniocaudal views. It is observed that the architectural distortions are more clearly seen on the 3D tomosynthesis images (*circles*) (a<sup>1</sup>, b<sup>1</sup>) and 3D magnified views of the distortions. (c) CEDM recombined images show no enhancement. (d) Tomosynthesis guided biopsy of the distortion was still performed. *Diagnosis: The pathology of the architectural distortion was fibrocystic change*





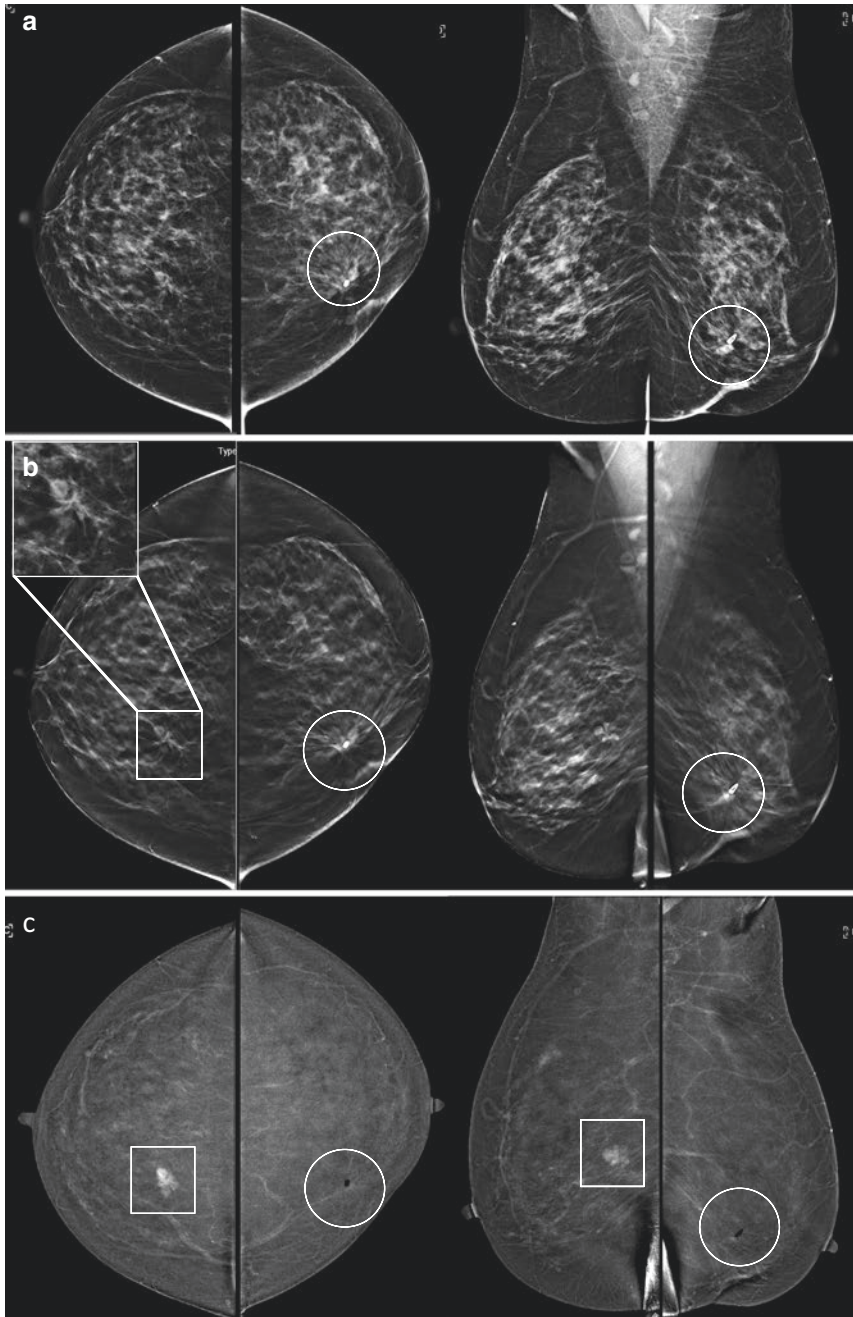


**Fig. 7.4** Problem-solving. A 60-year-old female, on follow-up since 12 years post-surgery for left ductal carcinoma in situ (DCIS). (a) 2D craniocaudal and mediolateral oblique views show a focal distortion (*circle*) seen at the left surgical scar site. (b) 3D craniocaudal and mediolateral oblique views demonstrate a more prominent area of distortion (*circle*) at the surgical scar. (c) CEDM recombined images show an intensely enhancing lesion in the right breast (*box*); however, no enhancement is seen at the region of surgical scar (*circle*) in the left

breast. The examination demonstrated an enhancing lesion in the right upper inner quadrant with no enhancement seen at the apparent suspicious lesion of the left breast. Retrospective assessment of the 3D images revealed a subtle architectural distortion in the right breast (*magnified view*). A second-look ultrasound was performed where this lesion was identified and biopsied.

*Diagnosis: The pathology of the right breast lesion was an invasive ductal carcinoma*

### 7.3.2 Preoperative Staging

Breast conservative surgery is the current trend for treatment of small tumours with a favourable lesion-to-breast volume ratio. Therefore, it is essential to provide accurate preoperative radiological quantification of the tumour to prevent early recurrences and to avoid re-excision for positive excision margins on histology. For women in whom the mammogram, ultrasound and physical examination indicate that the tumour is sufficiently small to allow lumpectomy and conservation surgery, further evaluation with additional imaging may demonstrate more extensive tumours than previously suspected. This information can be helpful for the surgeons to accurately plan the amount of tissue to be included in the lumpectomy or in suggesting the need for mastectomy.

At Careggi University Hospital and KLH, the majority of our CEDM examinations are done for preoperative staging. A significant number of cases have undergone a change of management post-CEDM based on the localization of additional lesions. In KLH, all patients undergoing breast conservation surgery are subjected to a CEDM prior to operation, and patients who are referred to us for highly suspicious masses are subjected to a CEDM immediately. The low-energy image is considered the patient's mammogram. We found that this approach enabled improved biopsy accuracy, particularly in the presence of multifocal lesions (Fig. 7.5).

Tennant et al. [19] concluded that CEDM provided immediately available, clinically useful information in patients with suspicious lesions. There was a higher sensitivity, specificity and size accuracy for breast cancer detection and staging demonstrated using CEDM as a primary mammographic investigation in clinically suspicious lesions.

Fallenberg et al. [18] suggested that initially using CEDM alone in symptomatic patients could decrease the radiation dose.

### 7.3.3 Assessment of Response to Neoadjuvant Chemotherapy

In women with large primary breast carcinomas, preoperative neoadjuvant chemotherapy (NAC) is increasingly being used to shrink tumour size to facilitate mastectomy or breast conservation. The determination of tumour size after treatment is important to the surgeon to enable complete removal of the tumour without residual cancer in the breast at the time of lumpectomy. MRI [2] is currently the modality of choice for monitoring tumour response and for assessing residual disease after NAC, being more accurate than mammography, ultrasound and clinical examination [20].

A recent study by Iotti et al. [21] compared the diagnostic performance of CEDM with respect to MRI; the authors concluded that CEDM was as reliable as MRI in assessing the response to NAC and can be considered an alternative when MRI is contraindicated or unavailable. In another study, Barra et al. [22] compared CEDM with FFDM in the evaluation of response to NAC and ultimately concluded that a positive CEDM indicates the presence of residual tumour after NAC.

In our clinical experience at Careggi University Hospital, we observed that CEDM could serve as an alternative to breast MRI to monitor the responsiveness to NAC, as depicted in Fig. 7.6.

### 7.3.4 Screening of High-Risk Patients

When addressing genetic risk, to date, MRI remains the most sensitive examination for the detection of breast cancer in both women at average and increased risk, yielding 15 cancers for every 1000 women at intermediate (15–20%) or high (>20%) risk. Several studies have demonstrated that in approximately 45% of women with

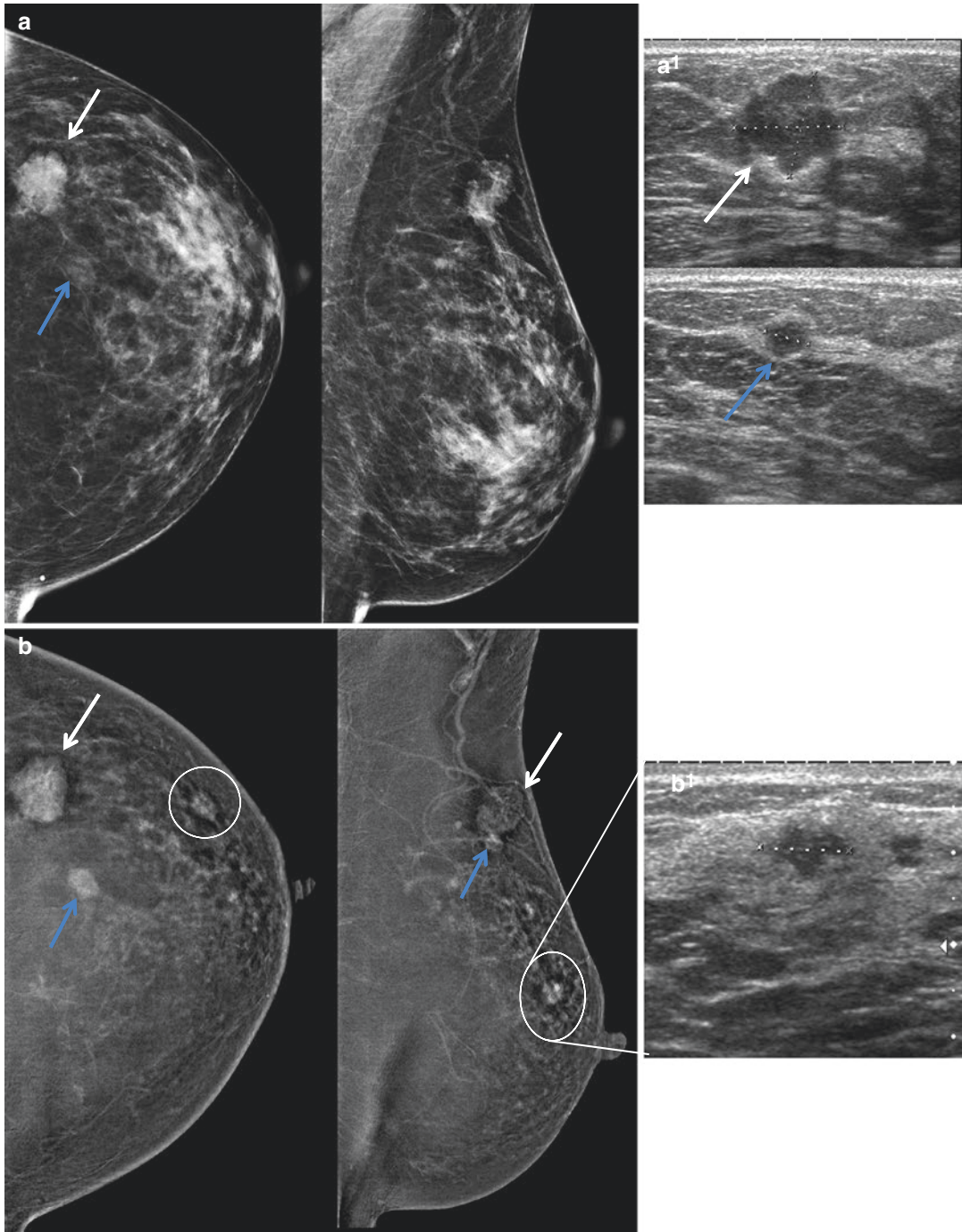


**Fig. 7.5** Preoperative staging. A 45-year-old woman with a biopsy confirmed invasive ductal carcinoma in the left breast. **(a, a<sup>1</sup>)** 2D craniocaudal and mediolateral oblique views with corresponding ultrasound images, demonstrating a dominant mass in the left upper outer quadrant (*white arrow*) with a small satellite nodule (*blue arrow*) less than 2 cm away from the index lesion. The patient was scheduled for a breast conservation surgery, and CEDM was

performed for preoperative assessment. **(b)** CEDM-recombined images in craniocaudal and mediolateral oblique views demonstrated a small enhancing nodule (*circle*) approximately 5 cm from the index lesion. **(b<sup>1</sup>)** A second-look ultrasound was performed, and a subtle suspicious hypoechoic lesion was identified and biopsied. *Diagnosis: the pathology was an invasive ductal carcinoma, not otherwise specified*



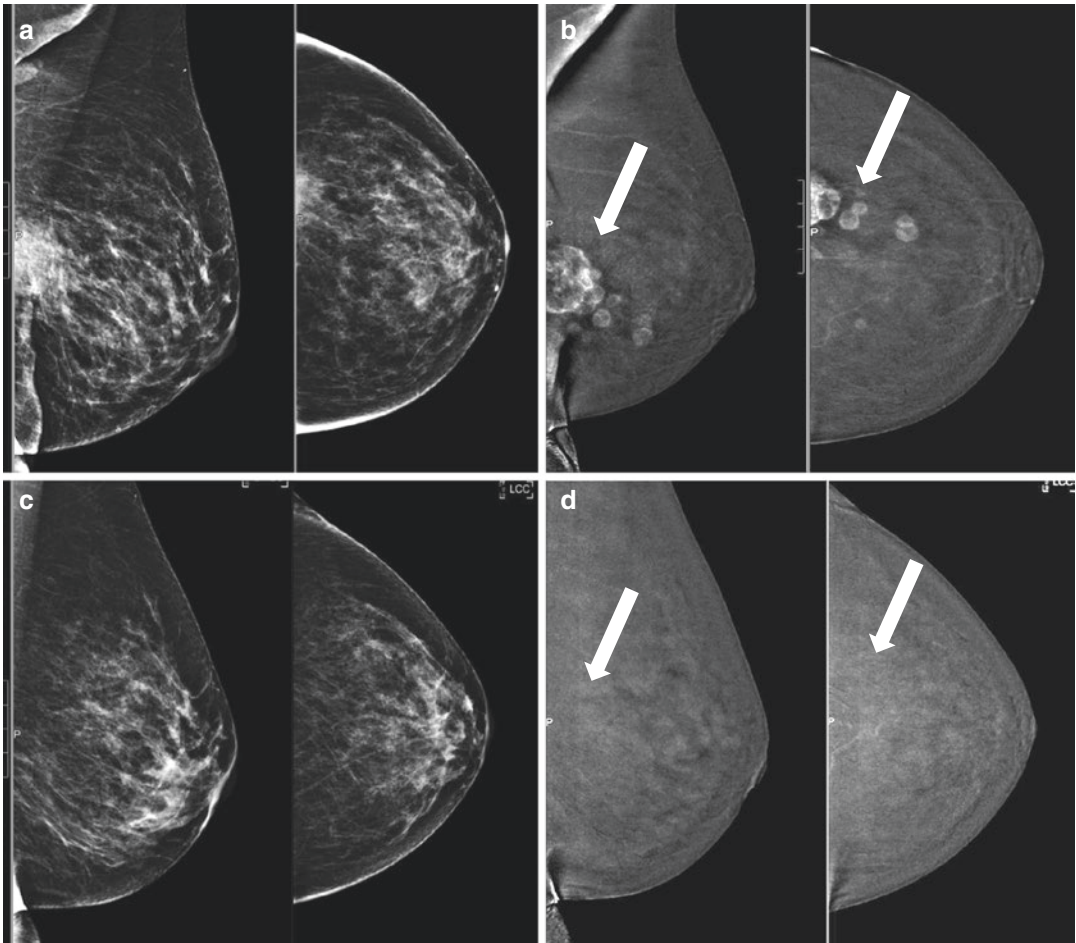


**Fig. 7.6** Response to chemotherapy. A 62-year-old woman with a palpable mass underwent core biopsy yielding invasive ductal carcinoma. CEDM examinations were performed during the patient's course of preoperative neoadjuvant chemotherapy. (a) Mediolateral oblique and craniocaudal low-energy and (b) recombined images of CEDM done pre-neoadjuvant chemotherapy assess-

ment revealed an irregular heterogeneously enhancing mass (*arrow*) with associated satellite nodules in the lower outer quadrant. (c) After six cycles of chemotherapy, mediolateral oblique and craniocaudal low-energy and (d) recombined images of a repeat CEDM demonstrated no enhancing areas with complete response of the tumour to chemotherapy

intermediate or high genetic risk, breast cancers were detected only by MRI [7, 23, 24]. These results led to specific screening programmes for high-risk women, including annual mammography and MRI, developed and recommended by the American Cancer Society and the European Society of Breast Imaging [25]. However, MRI may not be an option in this group of patients due to its high cost and low availability. Previous studies have suggested CEDM application in the

screening of these patients, with the first pilot study performed by Jochelson and colleagues [25], who concluded that this technique could be valuable as a supplemental imaging modality for women at increased risk for breast cancer who do not meet the criteria for MRI or in whom access to MRI is limited.

However, few studies have been published about this topic until now, and the main concern regarding performing CEDM in patients at high

risk of developing breast cancer is the radiation exposure involved. There has been no conclusive study for performing CEDM in high-risk patients, and this indication remains to be studied in a larger population.

At our centres, we tend to avoid performing CEDM on patients who are highly sensitive to the effects of radiation. So far, we have performed CEDM on only several patients with the BRCA 1 mutation; such patients had dense breasts and were contraindicated for breast MRI (Fig. 7.7).

### 7.3.5 Unknown Primary Cancer

Occult primary breast cancer presenting as isolated ipsilateral axillary metastases without evidence of tumour in the breast on physical examination or mammography accounts for approximately 0.3–0.8% of breast cancers [26].

MRI has been the only imaging modality that can reliably identify breast cancers that have evaded detection by mammography and physical examination [27, 28]. To date, there is no literature available for CEDM in identifying unknown primary cancer; however, we assume that the accuracy of breast cancer detection in this group of patients would be similar to MRI. We have performed CEDM in several cases of occult primary malignancy at Careggi and KLH, and we observed satisfactory results.

---

## 7.4 Future of Contrast-Enhanced Mammography

There is a growing body of evidence supporting CEDM use for various clinical indications, with levels of sensitivity and specificity on par with those of breast MRI. CEDM should therefore be considered for expanded clinical use at other breast-imaging centres in the near future. Future research with larger sample populations for CEDM as an adjunct or alternative to mammography, US, MRI or a combination of these

modalities will affect the expanded use of CEDM.

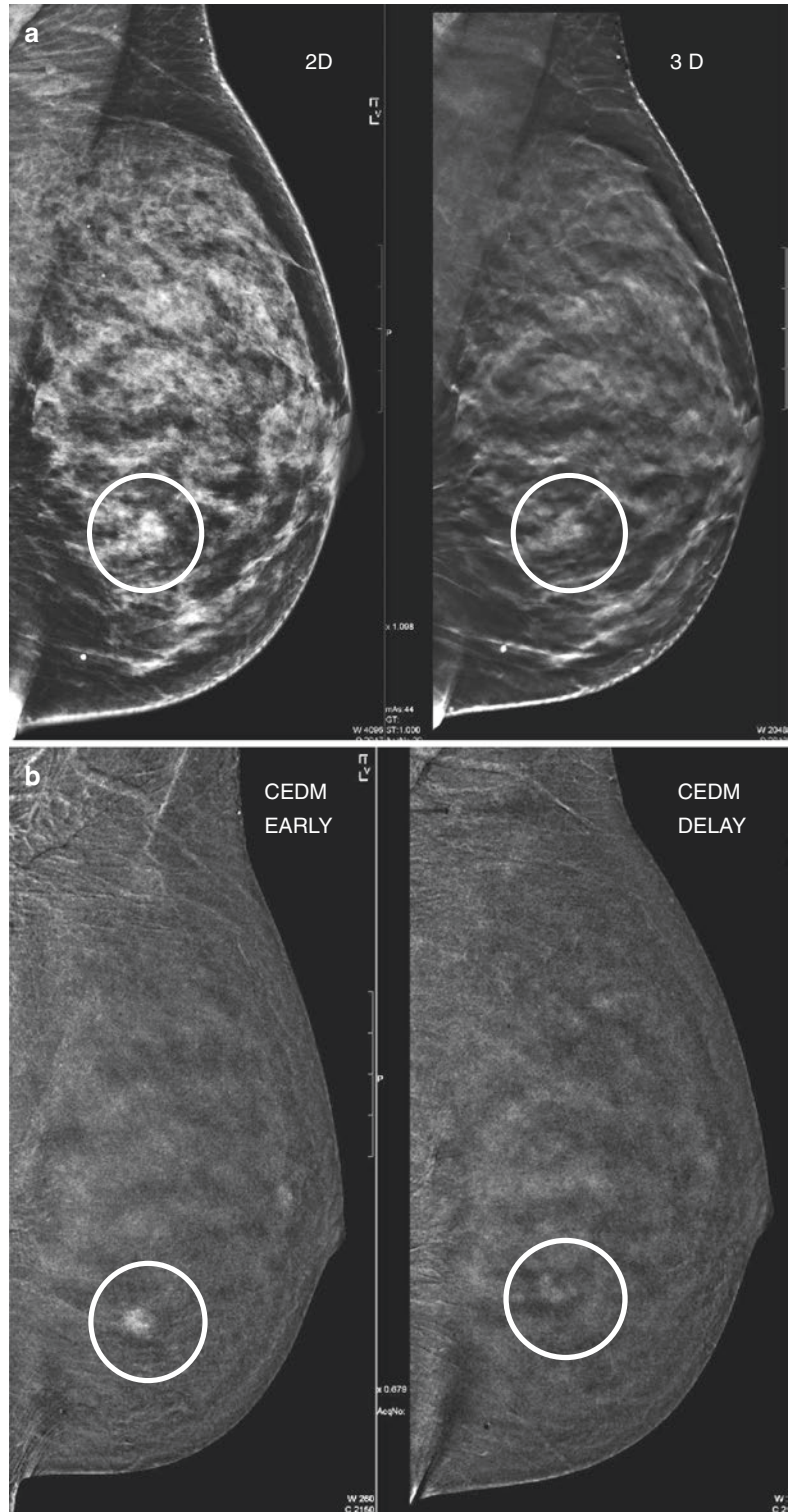
The time required to perform a CEDM examination is shorter than that required for MRI, as is the time required for lesion interpretation with CEDM. These are among the main reasons CEDM is being used more frequently in breast cancer diagnosis. Although CEDM is currently available at a minority of breast-imaging practices, widespread adoption could be rapid, given that many current-generation mammography systems are delivered with CEDM capability.

CEDM provides functional information similar to MRI at a lower cost and greater ease of implementation. Bhavika Patel et al. [4], using data obtained from the Mayo Clinic in Arizona, suggested that CEDM is faster to perform and interpret and has lower equipment acquisition and maintenance costs than does MRI. They also observed that if CEDM was deemed a viable substitute for breast MRI, such capability could lower the overall imaging costs of the healthcare system by more than one billion US dollars annually. Even at our centre in Careggi University Hospital, we observed a 60% reduction in the cost of a CEDM examination compared with that of an MRI.

CEDM is likely to be among the modalities offering the best value compared with other costlier emerging imaging technologies, such as automated whole-breast ultrasound, contrast-enhanced breast ultrasound, abbreviated breast MRI, molecular breast imaging, positron emission mammography (PET) and breast computed tomography (CT).

The limitations of CEDM are discussed comprehensively in Chapter 10. The technique's disadvantages include patient exposure to iodinated contrast material, as well as the potential low-risk associated with contrast-induced reactions and radiation exposure. Unlike MRI, there is no commercially available system to biopsy regions of suspicious enhancement under CEDM guidance [29]. To our knowledge, however, there is evidence that a commercial CEDM-guided biopsy system will become available in due time.

**Fig. 7.7** High-risk screening. A 40-year-old woman with a strong family history of breast cancer and personal history of BRCA2 gene mutation. She has severe claustrophobia and refused to undergo a breast MRI examination. (a) 2D low-energy and 3D tomosynthesis in MLO projections show relatively dense breast parenchymal pattern with a subtle area of increased density (*circle*) in the lower quadrant of the left breast. (b) CEDM-recombined image in the early and late phase in MLO projection. The examination shows an irregular enhancing mass demonstrating a rapid wash-out. The lesion was identified on a second look ultrasound and an US-guided biopsy was performed. *Diagnosis: the pathology was an infiltrating lobular carcinoma*



## References

- Lewin JM, Isaacs PK, Vance V, Larke FJ. Dual-energy contrast-enhanced digital subtraction mammography: feasibility. *Radiology*. 2003;229(1):261–8.
- Klionsky DJ, Abdelmohsen K, Abe A, Abedin MJ, Abeliovich H, Acevedo Arozena A, et al. Guidelines for the use and interpretation of assays for monitoring autophagy (3rd edition). *Autophagy*. 2016;12(1):1–222.
- Covington MF, Pizzitola VJ, Lorans R, Pockaj BA, Northfelt DW, Appleton CM, et al. The future of contrast-enhanced mammography. *AJR Am J Roentgenol*. 2018;210(2):292–300.
- Patel BK, Gray RJ, Pockaj BA. Potential cost savings of contrast-enhanced digital mammography. *AJR Am J Roentgenol*. 2017;208(6):W231–W7.
- Hobbs MM, Taylor DB, Buzynski S, Peake RE. Contrast-enhanced spectral mammography (CESM) and contrast enhanced MRI (CEMRI): patient preferences and tolerance. *J Med Imaging Radiat Oncol*. 2015;59(3):300–5.
- Katrina R, Beckett AKM, Langer JM. Safe use of contrast media: what the radiologist needs to know. *Radiographics*. 2015;35(6):1738–50.
- Jeukens CR, Lalji UC, Meijer E, Bakija B, Theunissen R, Wildberger JE, et al. Radiation exposure of contrast-enhanced spectral mammography compared with full-field digital mammography. *Investig Radiol*. 2014;49(10):659–65.
- Dromain C, Thibault F, Muller S, Rimareix F, Delalogue S, Tardivon A, et al. Dual-energy contrast-enhanced digital mammography: initial clinical results. *Eur Radiol*. 2011;21(3):565–74.
- James JR, Pavlicek W, Hanson JA, Boltz TF, Patel BK. Breast radiation dose with CESM compared with 2D FFDM and 3D Tomosynthesis mammography. *AJR Am J Roentgenol*. 2017;208(2):362–72.
- Yakoumakis E, Tzamicha E, Dimitriadis A, Georgiou E, Tsapaki V, Chalazonitis A. Dual-energy contrast-enhanced digital mammography: patient radiation dose estimation using a Monte Carlo code. *Radiat Prot Dosim*. 2015;165(1–4):369–72.
- Lalji UC, Houben IP, Prevos R, Gommers S, van Goethem M, Vanwetswinkel S, et al. Contrast-enhanced spectral mammography in recalls from the Dutch breast cancer screening program: validation of results in a large multireader, multicase study. *Eur Radiol*. 2016;26(12):4371–9.
- Wang CL, Cohan RH, Ellis JH, Caoili EM, Wang G, Francis IR. Frequency, outcome, and appropriateness of treatment of nonionic iodinated contrast media reactions. *AJR Am J Roentgenol*. 2008;191(2):409–15.
- Skarpathiotakis M, Yaffe MJ, Bloomquist AK, Rico D, Muller S, Rick A, et al. Development of contrast digital mammography. *Med Phys*. 2002;29(10):2419–26.
- Carney PA, Miglioretti DL, Yankaskas BC, Kerlikowske K, Rosenberg R, Rutter CM, et al. Individual and combined effects of age, breast density, and hormone replacement therapy use on the accuracy of screening mammography. *Ann Intern Med*. 2003;138(3):168–75.
- Lobbes MB, Smidt ML, Houwers J, Tjan-Heijnen VC, Wildberger JE. Contrast enhanced mammography: techniques, current results, and potential indications. *Clin Radiol*. 2013;68(9):935–44.
- Mori M, Akashi-Tanaka S, Suzuki S, Daniels MI, Watanabe C, Hirose M, et al. Diagnostic accuracy of contrast-enhanced spectral mammography in comparison to conventional full-field digital mammography in a population of women with dense breasts. *Breast Cancer*. 2017;24(1):104–10.
- Cheung YC, Lin YC, Wan YL, Yeow KM, Huang PC, Lo YF, et al. Diagnostic performance of dual-energy contrast-enhanced subtracted mammography in dense breasts compared to mammography alone: interobserver blind-reading analysis. *Eur Radiol*. 2014;24(10):2394–403.
- Fallenberg EM, Dromain C, Diekmann F, Engelken F, Krohn M, Singh JM, et al. Contrast-enhanced spectral mammography versus MRI: initial results in the detection of breast cancer and assessment of tumour size. *Eur Radiol*. 2014;24(1):256–64.
- Tennant SL, James JJ, Cornford EJ, Chen Y, Burrell HC, Hamilton LJ, et al. Contrast-enhanced spectral mammography improves diagnostic accuracy in the symptomatic setting. *Clin Radiol*. 2016;71(11):1148–55.
- Rosen EL, Blackwell KL, Baker JA, Soo MS, Bentley RC, Yu D, et al. Accuracy of MRI in the detection of residual breast cancer after neoadjuvant chemotherapy. *AJR Am J Roentgenol*. 2003;181(5):1275–82.
- Iotti V, Ravaioli S, Vacondio R, Coriani C, Caffarri S, Sghedoni R, et al. Contrast-enhanced spectral mammography in neoadjuvant chemotherapy monitoring: a comparison with breast magnetic resonance imaging. *Breast Cancer Res*. 2017;19(1):106.
- Barra FR, de Souza FF, Camelo R, Ribeiro ACO, Farage L. Accuracy of contrast-enhanced spectral mammography for estimating residual tumor size after neoadjuvant chemotherapy in patients with breast cancer: a feasibility study. *Radiol Bras*. 2017;50(4):224–30.
- Francescone MA, Jochelson MS, Dershaw DD, Sung JS, Hughes MC, Zheng J, et al. Low energy mammogram obtained in contrast-enhanced digital mammography (CEDM) is comparable to routine full-field digital mammography (FFDM). *Eur J Radiol*. 2014;83(8):1350–5.
- Fallenberg EM, Dromain C, Diekmann F, Renz DM, Amer H, Ingold-Heppner B, et al. Contrast-enhanced spectral mammography: does mammography provide additional clinical benefits or can some radiation exposure be avoided? *Breast Cancer Res Treat*. 2014;146(2):371–81.
- Jochelson MS, Pinker K, Dershaw DD, Hughes M, Gibbons GF, Rahbar K, et al. Comparison of screening CEDM and MRI for women at increased



- risk for breast cancer: a pilot study. *Eur J Radiol.* 2017;97:37–43.
26. Morris EA, Schwartz LH, Dershaw DD, van Zee KJ, Abramson AF, Liberman L. MR imaging of the breast in patients with occult primary breast carcinoma. *Radiology.* 1997;205(2):437–40.
  27. Olson JA Jr, Morris EA, Van Zee KJ, Linehan DC, Borgen PI. Magnetic resonance imaging facilitates breast conservation for occult breast cancer. *Ann Surg Oncol.* 2000;7(6):411–5.
  28. Lieberman S, Sella T, Maly B, Sosna J, Uziely B, Sklair-Levy M. Breast magnetic resonance imaging characteristics in women with occult primary breast carcinoma. *Isr Med Assoc J.* 2008;10(6):448–52.
  29. Ali-Mucheru M, Pockaj B, Patel B, Pizzitola V, Wasif N, Stucky CC, et al. Contrast-enhanced digital mammography in the surgical management of breast cancer. *Ann Surg Oncol.* 2016;23(Suppl 5):649–55.



Maninderpal Kaur, Claudia Lucia Piccolo,  
and Victor Chong Xing Dao

An artefact is typically defined as any feature in an image or sequence that misrepresents the object in the field of view. Artefact manifestations include an additional unexpected signal on the image or sequence, a lack of signal or image distortion.

As with any imaging modality, artefacts in contrast-enhanced digital mammography (CEDM) can interfere with image quality, and their effects can vary from negligible to severe, possibly leading to unnecessary procedures or hiding underlying abnormalities. Although some of these artefacts are similar to those observed with full-field digital mammography (FFDM), many are unique to CEDM.

It is critical for radiologists and technologists to be familiar with the various CEDM artefacts and to understand their causes to minimize or eliminate potential negative effects on image interpretation. This strategy not only improves image quality but also reduces imaging time, which can improve both the workflow and patient experience.

To date, there is limited published literature available reviewing the artefacts related to CEDM [1, 2]. We have categorized the artefacts observed in

CEDM into four categories, namely, FFDM-related factors, contrast-related factors, CEDM-related factors, and quality-control (QC)-related artefacts.

In this chapter, we survey examples of artefacts and other factors that interfere with image acquisition observed with CEDM in our clinical practices at Careggi University Hospital and Kuala Lumpur Hospital (KLH), and we highlight the necessary steps to reduce and eliminate these artefacts.

## 8.1 FFDM-Related Factors

The low-energy (LE) image obtained in CEDM resembles a full-field digital mammogram (FFDM) even though iodinated contrast media is already present within the breast [3]. Therefore, it is necessary to address some of the artefacts that have been described for FFDM that are commonly observed in our CEDM experience. Ayyala et al. [4] exhaustively illustrated many of the artefacts related to FFDM and divided them into three different categories:

- Patient-related factors (motion artefacts, hair artefacts, antiperspirant artefacts, and air artefacts).
- Hardware-related factors (field inhomogeneity, detector-associated artefacts, collimator misalignment, grid lines, grid misplacements, underexposure, and vibration artefacts).

---

Maninderpal Kaur (✉) · V. C. X. Dao  
Department of Radiology, Kuala Lumpur Hospital,  
Kuala Lumpur, Malaysia

C. L. Piccolo  
Department of Medicine and Health Science,  
University of Molise, Campobasso, Italy



- Software processing artefacts (“breast-within-a-breast” artefacts, vertical processing bars, loss of edge, and high-density artefacts).

We highlight the artefacts that are common to CEDM.

### 8.1.1 Motion

As with any imaging modality, patient motion can affect image quality [4–9]. The risk of motion artefacts is greater in CEDM than that in other techniques because CEDM involves sequential acquisition of low-energy (LE) and high-energy (HE) images, thereby increasing the time of exposure and resulting in an increased likelihood of patient motion [2].

Patient motion degrades image quality, resulting in blurring of radiopaque structures present in the breast as well as lesion margins. Patient motion between the LE and HE images adversely affects the subtraction process, which relies on

accurate registration between the two images, and results in imperfect parenchymal suppression with greater anatomical noise.

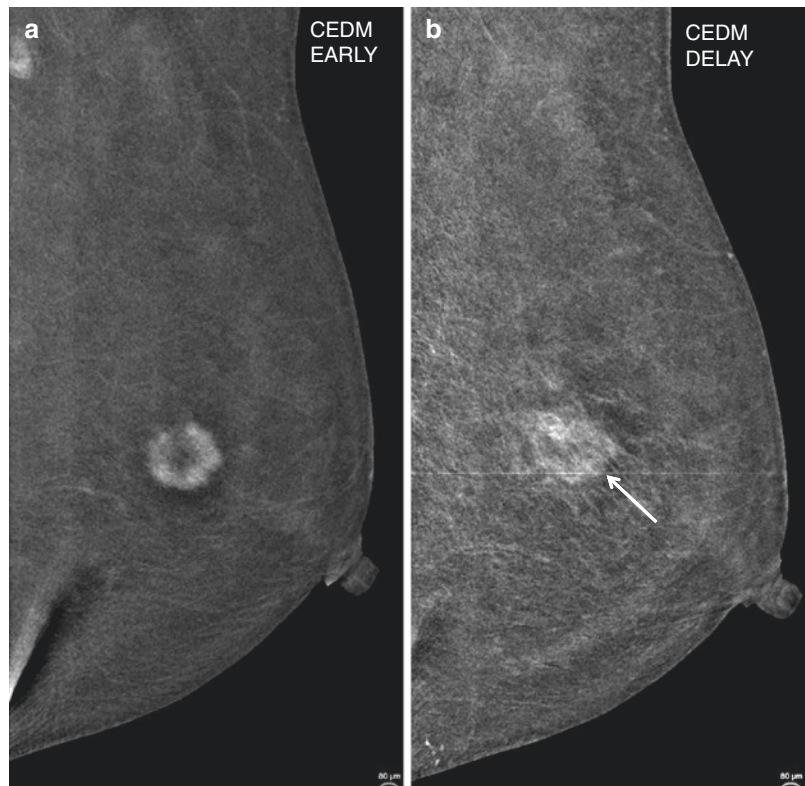
These artefacts are commonly observed in clinical practice. To minimize the patient motion, which is the most common cause of blurring (Fig. 8.1), the technologist should apply adequate compression during the examination and remind patients to remain still during image acquisition.

Adequate compression is essential for mammography and has many benefits, including decreasing motion artefacts, reducing scatter, improving X-ray penetration, and reducing dose [10].

### 8.1.2 Hair Artefacts

Similar to the case of analogue studies, patients can create image artefacts related to their clothing, hairstyle, or jewellery. To avoid unnecessary added image acquisitions and radiation exposure, it is important to ensure that the patient’s

**Fig. 8.1 Motion artefact:** A 49-year-old woman with biopsy-proven invasive ductal carcinoma in the left breast underwent CEDM as part of a staging workup. **(a)** CEDM-recombined image in MLO view demonstrates an intensely enhancing well-demarcated round mass in the upper quadrant of the left breast. **(b)** CEDM delay was performed to assess the enhancement kinetics, but due to motion artefacts, the margins of the mass are blurred. *CEDM* contrast-enhanced digital mammography, *MLO* mediolateral oblique



hair is pulled back, as hair overlying the breast is represented in the image and may potentially obscure important abnormalities (Fig. 8.2). Other subject-related factors to note and remove prior to image acquisition are pieces of clothing, glasses, and any accessories that the patient is wearing that can project on the image. It is important to position the patient suitably to ensure that her chin or shoulders are out of the imaging field of view [9].

### 8.1.3 Antiperspirant Artefacts

Antiperspirant artefacts are important to recognize since their appearance can be mistaken for

unusual lesions or calcifications in the axillary region of the breast, possibly leading to unnecessary testing and procedures (Fig. 8.3). It is important for technologists to recognize this artefact and to ask the patient to clean the axilla or skinfolds before the subsequent image acquisition is performed [4, 11].

Reminding patients to clean their breast and axilla before imaging is crucial to minimize these common artefacts. A patient fact card that can be given to the patient upon scheduling the CEDM appointment, informing them of all the necessary precautions to be taken prior to the examination day, is helpful to avoid such artefacts from occurring. An example of such a patient fact card is shown in Fig. 7.1 of Chapter 7.

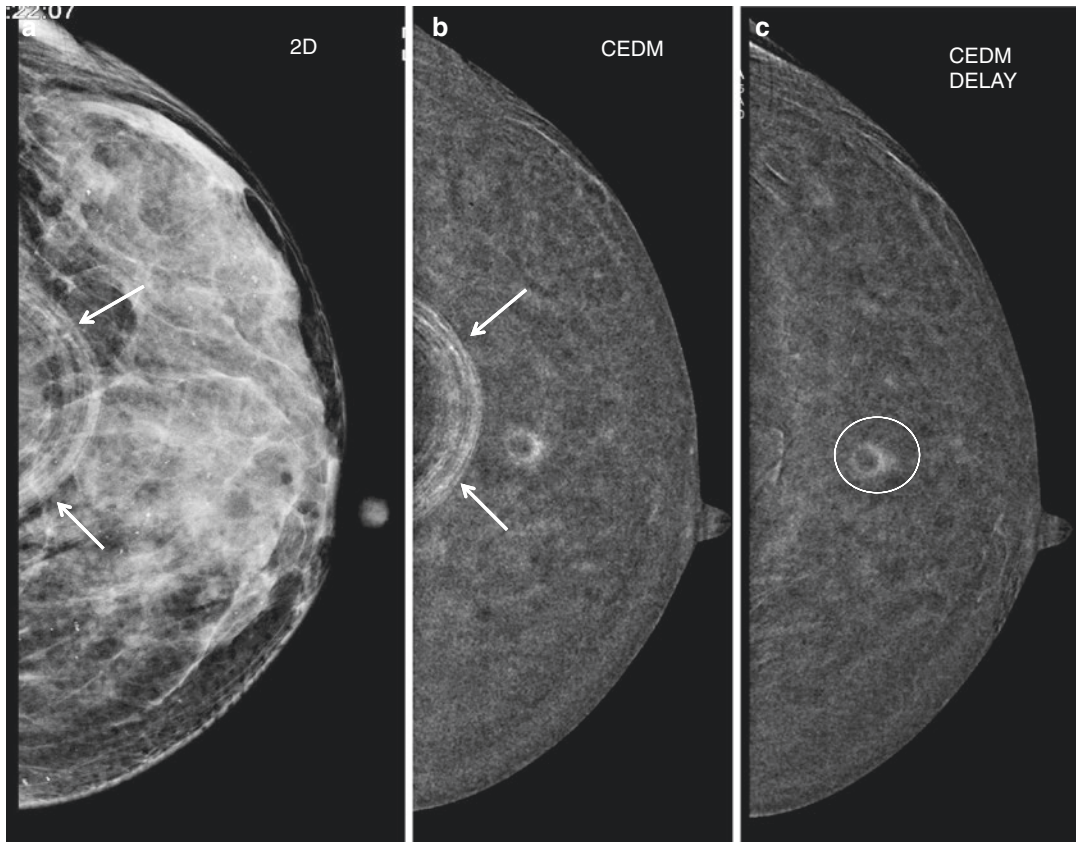


**Fig. 8.2 Hair artefact:** CC views of a 46-year-old woman with biopsy-proven invasive ductal carcinoma in the left breast underwent CEDM as part of a staging workup. (a) LE image shows a well-defined opacity (*arrows*) in the left posterior central quadrant. (b) The opacity which was related to the patient's hair is seen to appear more pro-

nounced in the early recombined CEDM images. (c) We subsequently instructed the patient to tie her hair back before proceeding with a delay CEDM acquisition, thus eliminating the opacity. A post-biopsy rim artefact (*circle*) is also present in these images. *CEDM* contrast-enhanced digital mammography, *LE* low energy, *CC* craniocaudal

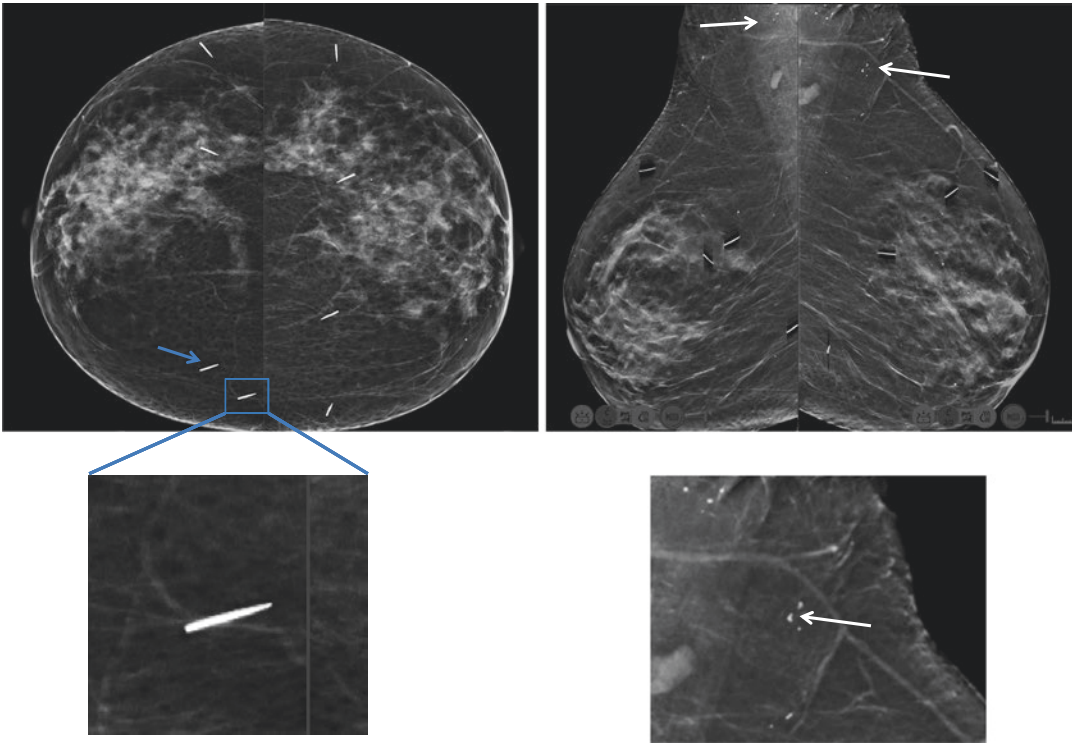


**Fig. 8.3 Antiperspirant artefact:** Bilateral mammograms in CC and MLO views show small, faint radiopaque densities in the axilla region on the MLO view caused by antiperspirant (*white arrows*). The artefact was eliminated through removal of the antiperspirant. Also observed in this mammogram are multiple linear metallic densities (*blue arrow and blue box*) projected over both breasts, measuring approximately 5 mm, in keeping with charm needles. These charm needles can be identified by their fine needle shape with a broader base and a pointed tapering tip (*magnified view*). Charm needles or “susuk” are needles made of gold or other precious metals that are inserted subcutaneously in various parts of the body to act as talismans. The practice of inserting susuk is an indis-

putably cultural and superstitious traditional belief common in the Southeast Asian region, particularly in Malay culture, and is typically observed in the people of Malaysia, Thailand, Singapore, Indonesia, and Brunei. Their insertion is presumed to bring beauty, and for this reason, they are most commonly identified in the craniofacial regions and breasts of women. Most susuk wearers are secretive about their hidden talismans, but these gold or silver needles are being discovered with increasing frequency now that radiographs are used more widely. An understanding of this practice and an awareness of its existence are important to avoid misdiagnosis and mismanagement of these patients. *MLO* mediolateral oblique, *CC* craniocaudal

#### 8.1.4 Air Gap and Other High-Attenuation Artefacts

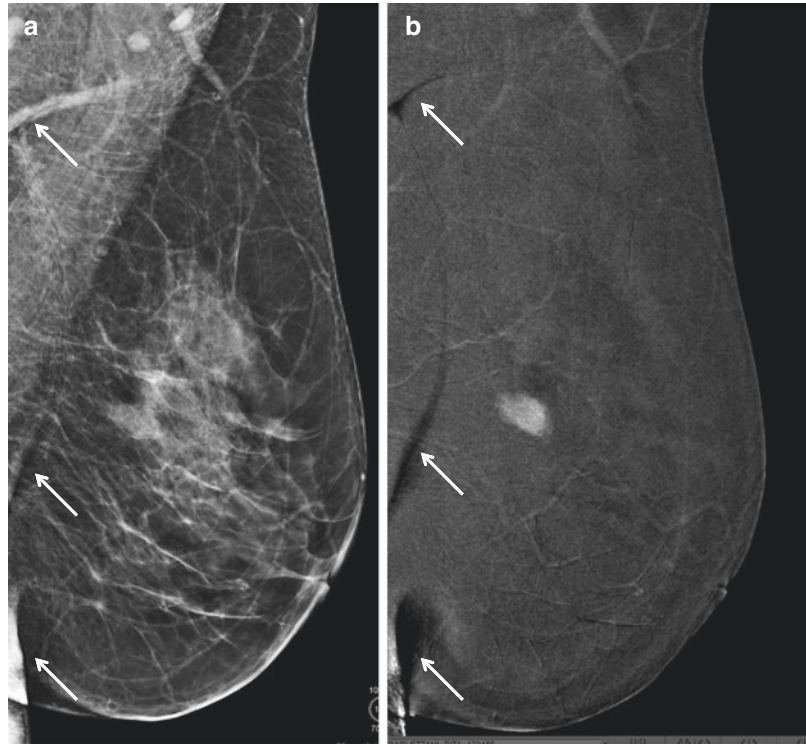
In our experience with CEDM, the air gap is the most common artefact. This artefact is caused by partial contact between the skin and the detector or compression paddle, which creates a dark artefact in the configuration of the area of incomplete contact, possibly hiding underlying abnormalities [12]. Imperfect contact may also be the result from improper compression or skinfolds and is

commonly observed at the skinfolds of the axilla (Fig. 8.4).

Placing markers after breast biopsy is common. These highly attenuating objects can show a variable appearance depending on a demetal function, which has been turned off by default in the current systems [12]. We have noticed a dark halo appearance around high-attenuation items, such as post-biopsy markers, mole markers, scar markers, pacemakers, and chest ports, which is caused by image processing filters. The manufac-



**Fig. 8.4 Air artefact:** A 51-year-old woman with biopsy-proven invasive ductal carcinoma in the left breast underwent CEDM as part of a staging workup. **(a)** LE image in MLO projection. **(b)** CEDM-recombined image in MLO projection. The vertically oriented black lines (*white arrows*) in the superior and inferior aspect of the left breast posteriorly arise from air trapped in the axillary and inframammary folds. *CEDM* contrast-enhanced digital mammography, *MLO* mediolateral oblique, *LE* low energy



turer's latest software release has a demetal algorithm to remove these dense markers and prevent this artefact.

In our clinical setting, we place bowtie titanium markers during vacuum-assisted biopsy procedures and barbell non-metallic markers during US-guided procedures. The barbell marker, despite being non-metallic, is still sufficiently dense to create an artefact (Fig. 8.5).

## 8.2 Contrast-Related Factors

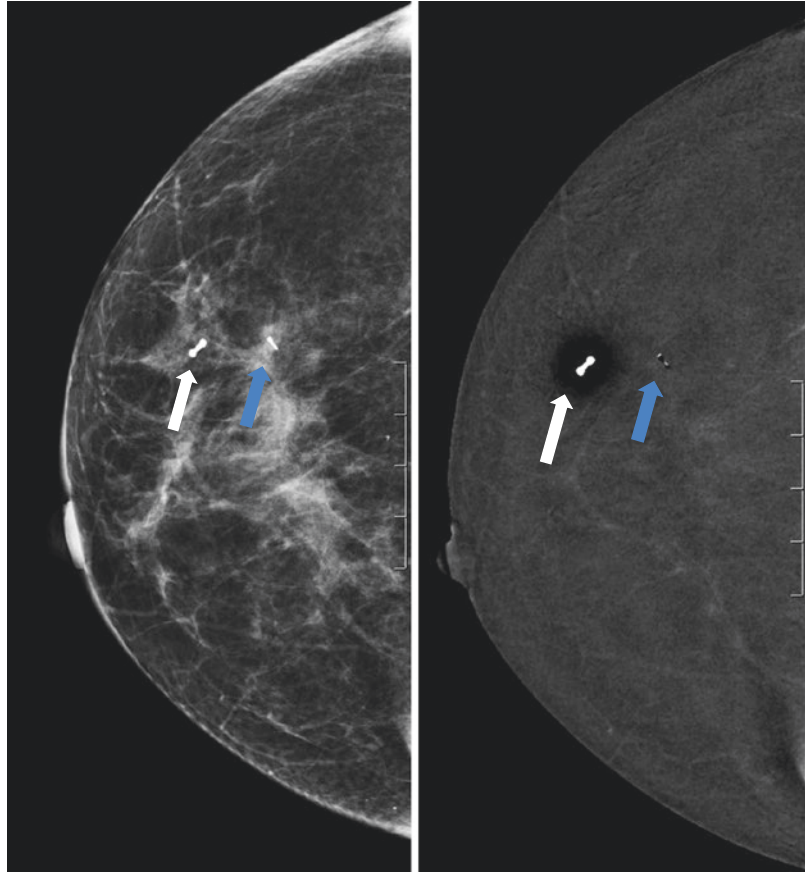
Several contrast-related factors can affect the image quality in CEDM, such as the delivery rate of the contrast agent, the correct timing of the administration relative to breast compression, and the image acquisition. Similar to the case of MRI, physiological processes, such as the menstrual cycle phase, may also contribute to the degree of background parenchymal enhancement in CEDM [13].

### 8.2.1 Contrast Splatter

In a CEDM examination, it is critical to pay close attention to the technique during contrast administration to prevent contrast contamination. The contrast is administered via a power injector to the venous access in the patient's arm through a connecting tube. While disconnecting the tubing, small droplets of contrast may splatter onto the adjacent equipment and give the appearance of small white dots, specifically on the recombined images, sometimes simulating the appearance of calcifications (Fig. 8.6), which may lead to unnecessary procedures. Therefore, it is important to carefully analyse the rest of the images to avoid mistakenly classifying splatter artefacts as true calcifications. Taking precautions, such as disconnecting the injector at an appropriate distance from the mammography unit and wiping the imaging surfaces of the unit between patients, reduces the possibility of such artefacts from occurring.

**Fig. 8.5 High-attenuation artefact:**

An example of two markers with differences in artefact appearance. The posteriorly located marker (*blue arrow*) is a bowtie marker that we use for vacuum-assisted breast biopsy (VABB) procedures consisting of a titanium marker, while the anteriorly located (*white arrow*) marker is a non-metallic barbell marker consisting of natural minerals and carbon-coated zirconium oxide. The anteriorly located marker closer to the skin demonstrates a surrounding dark halo that is not observed with the titanium marker. This is caused by image processing filters, which cause the marker to have a prominent dark halo surrounding it



A study by Gluskin et al. [14] suggested that if this finding is encountered in clinical practice, several circumstances may suggest that this finding is only an artefact:

- If a non-mass enhancement is observed on only one view and does not persist on additional or repeat imaging after cleaning the breast.
- If the suspicious calcifications do not persist on magnification views.
- If the suspicious non-mass enhancement does not persist on repeated contrast-enhanced studies, such as CEDM or MRI [2, 14].

We also observed that when the intravenous (IV) line is still in place at the patient's antecubital fossa and the patient is positioned with her arm resting on the side of the detector for the mediolateral oblique (MLO) projection, contrast contamination commonly occurs due to the close

proximity of the patient's arm to the detector. This contamination is typically resolved by cleaning the patient's breast and the detector prior to subsequent imaging.

An important point to note is that while calcifications are white on FFDM and LE CEDM, they appear black on CEDM-recombined images. Therefore, anything that resembles calcifications on recombined images should raise the suspicion of an artefact and the patient's breast and detector should be cleaned prior to further imaging.

### 8.2.2 Abnormal Timing of the Contrast Bolus

In CEDM, image acquisition starts 2 minutes after the beginning of the contrast administration, and all the images are acquired within 8–10 minutes from the time of injection [15].

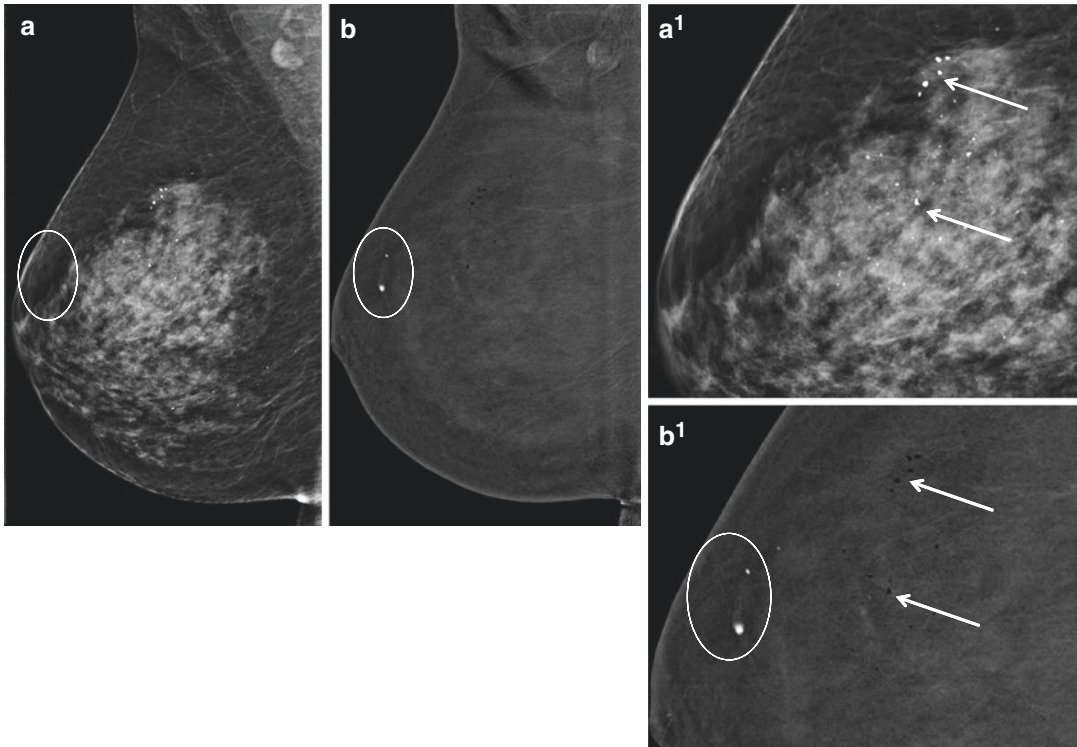


**Fig. 8.6 Contrast splatter:** A 55-year-old woman underwent a CEDM examination for inconclusive findings on mammogram. (**a**, **a<sup>1</sup>**) LE and (**b**, **b<sup>1</sup>**) recombined CEDM images of the right breast in the MLO projection, showing small droplets of contrast splattered on the detector plate before starting the CEDM examination. Splattered droplets of contrast are detected on the recombined images as small white dots, simulating the appear-

ance of calcifications (*circle*); no correlating abnormality is detected at the same level on the LE image (*circle*). Note that although calcifications appear white on FFDM and LE CEDM (*arrows*), they appear black on CEDM-recombined images (*arrows*). *CC* craniocaudal, *CEDM* contrast-enhanced digital mammography, *FFDM* full-field digital mammography, *LE* low energy

Therefore, an incorrect timing of contrast bolus or image acquisition can result in suboptimal image quality and false-negative examination [2]. Any image obtained prior to 2 minutes post-contrast administration results in retained contrast outside the breast, as the contrast media cannot reach the breast due to premature compression. Images taken after the 8-minute timeline result in a false-negative result as the contrast has dispersed from the breast by that point.

### 8.2.3 Transient Retention of Contrast in the Vein

A mild retention of contrast in the veins is common in clinical practice but is frequently transient

and unilateral (Fig. 8.7). This artefact is probably related to breast compression but offers no limitation to image interpretation. This phenomenon typically disappears by the time the ipsilateral MLO projection is obtained. However, if it is related to central venous occlusion, the retention of contrast in the veins is prolonged and observed bilaterally [2].

## 8.3 CEDM-Related Factors

CEDM-related factors include the following: negative contrast enhancement, halo artefact, ripple artefacts, misregistration artefact, skin-line enhancement, and enhancing skin lesion artefacts [1, 2]. Here, we discuss the various



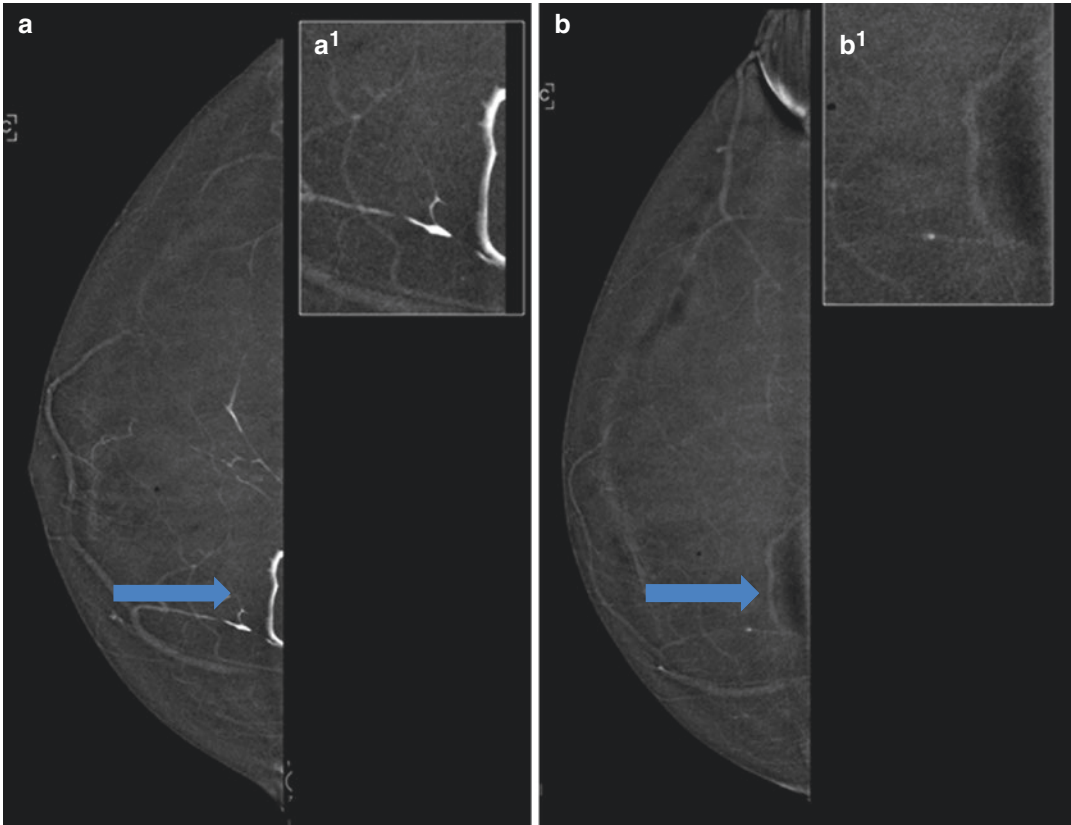


**Fig. 8.7 Transient retention of contrast in the vein:** A 63-year-old woman undergoing CEDM for the evaluation of an enhancing mass in the upper-central quadrant of the left breast (*not shown*). CEDM-recombined images of the right breast in CC projection. (**a, a<sup>1</sup>**) Early phase of CEDM showing linear branching hyperdensities in the inner

quadrants of the right breast (*blue arrows*), representing mild transient retention of intravenous contrast in the veins. (**b, b<sup>1</sup>**) Shows that this phenomenon typically disappears by the time the same projection is acquired in the late phase. *CEDM* contrast-enhanced digital mammography, *CC* craniocaudal

CEDM-related artefacts that we have encountered in our clinical experience.

### 8.3.1 Negative Contrast Enhancement

Negative contrast enhancement cannot be considered a true artefact, as it is actually a natural consequence of the acquisition technique. When a cyst (Figs. 8.8 and 8.9) or a macrocalcification (Fig. 8.9) is not enhanced in the recombined image, a rim-enhancing hypodensity arises with respect to the background: a “negative contrast enhancement”, also referred to as an “eclipse sign” as it resembles a full solar eclipse on the

recombined images. Generally, this condition does not compromise image interpretation [2]. Based on our experience at Careggi University Hospital, in addition to cysts and calcifications, this type of artefact is also encountered in cases of post-biopsy haematoma (Fig. 8.10), characterized by a peripheral enhancement of the granulation tissue surrounding the non-enhancing haematinic collection.

### 8.3.2 Halo Artefact

This artefact, also known as the “breast-within-a-breast” artefact, tends to occur in women with thick breasts. The artefact occurs due to

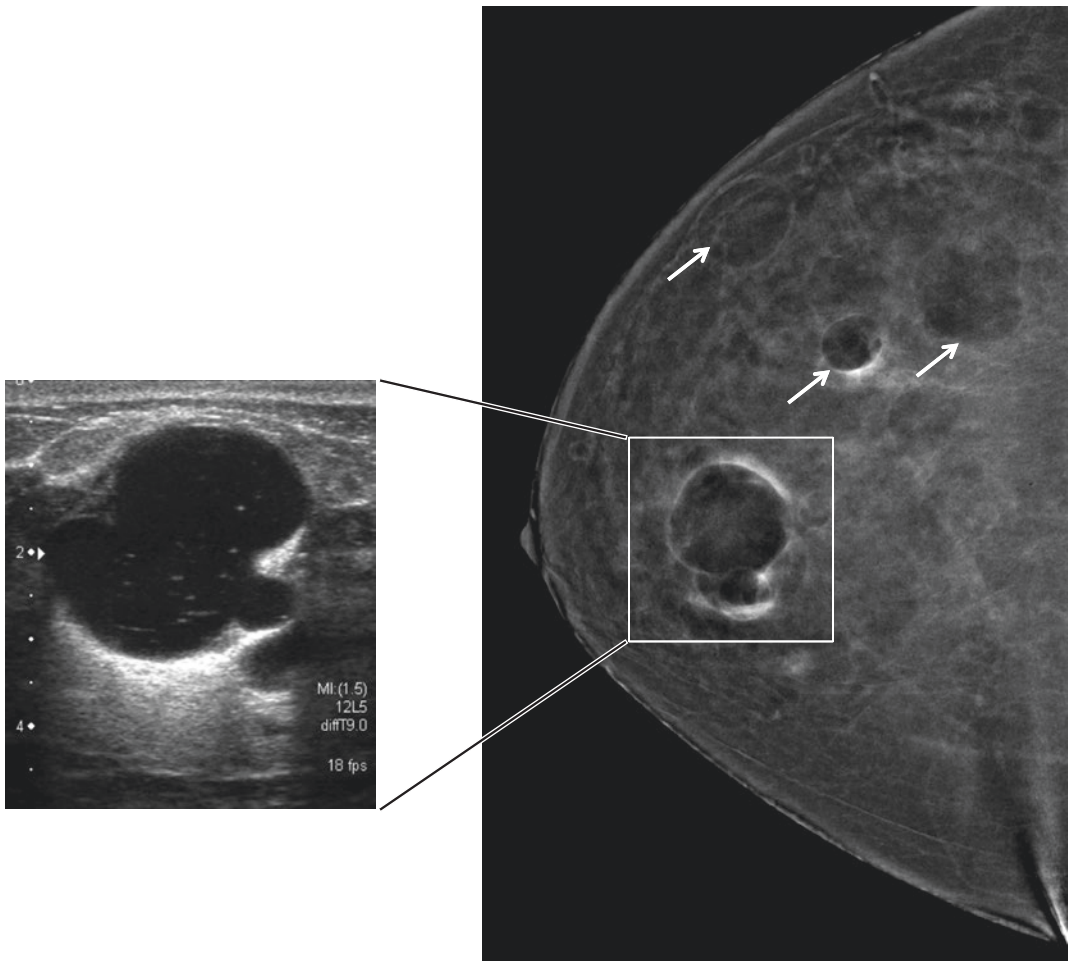


**Fig. 8.8 Negative contrast enhancement:** A 51-year-old female presented with a palpable right breast lump. CEDM of the right breast in CC projection displays several lesions (*arrows*) with a rim enhancement pattern and central non-enhancement on the recombined image; these lesions appear darker with respect to the background, a phenomenon often referred to as “negative contrast

enhancement” or an “eclipse sign”. One of these features (*box*) is characterized by a strong peripheral enhancement. An ultrasound confirmed the findings of a cyst with internal debris, suggestive of an infected benign cyst. *CEDM* contrast-enhanced digital mammography, *CC* craniocaudal

the rapid change in breast tissue thickness from the chest wall to the edge of the breast, causing the software processing algorithm to create a false exaggerated boundary. Technical factors caused by the presence of scatter radiation, which is non-uniform throughout the breast and has different characteristics between the LE and HE acquisitions, also play a role in this artefact, which is typically observed on the

recombined images and appears as a thin curvilinear area of increased density paralleling the edge of the breast [2, 4, 16, 17]. However, this artefact does not interfere with diagnostic interpretation of the images. These software processing artefacts are vendor specific, and we have not encountered this artefact in our cases performed at Careggi University Hospital and KLH.

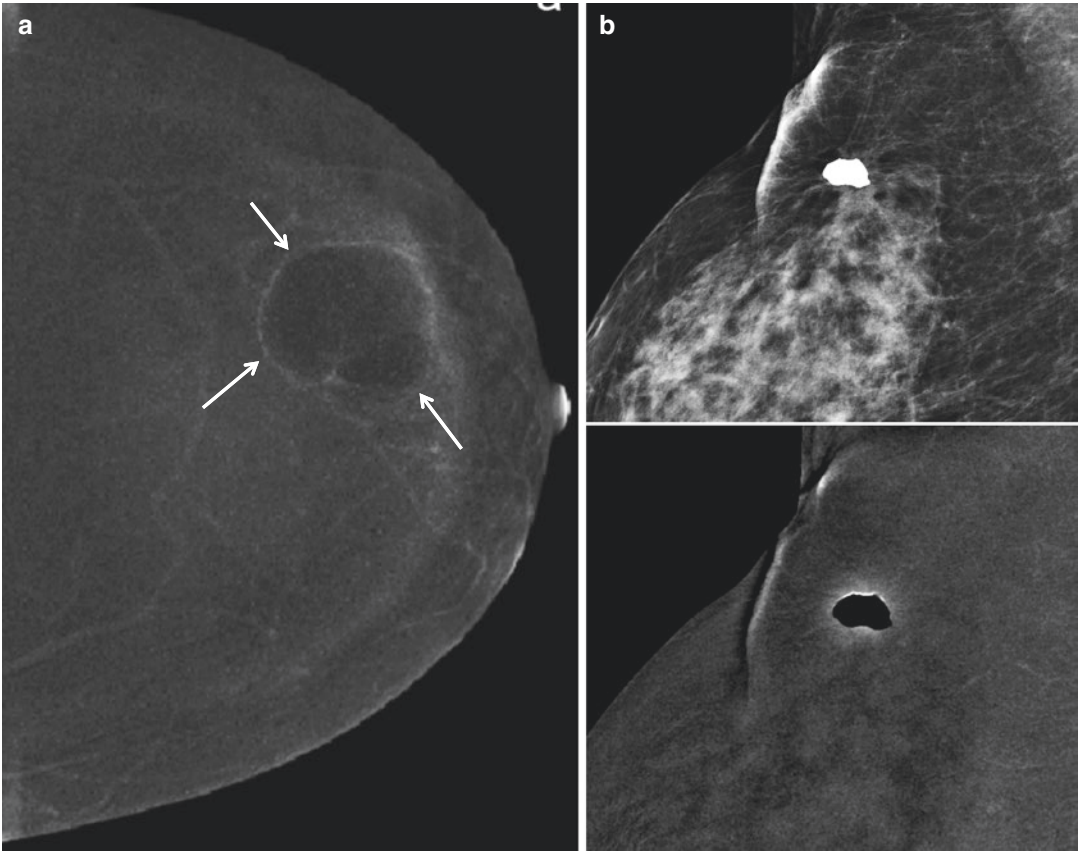


**Fig. 8.9 Negative contrast enhancement:** When a (a) cyst or (b) coarse calcification is imaged, it appears darker with respect to the background and is often referred to as

“negative contrast enhancement” or the “eclipse sign” because it resembles a full solar eclipse on the recombined CEDM image

### 8.3.3 Ripple Artefact

The ripple artefact, which is commonly observed on the recombined images, consists of faint alternating black and white lines appearing on the mediolateral oblique (MLO) projections of both breasts in the recombined images (Fig. 8.11). Dromain et al. [17] attributed this artefact to patient motion, most likely caused by the short interval between the LE and HE exposures. The artefact is commonly observed on the inferior portion of the MLO view because the inferior parts of the breasts are typically less well compressed, as suggested by Hill et al. [18], resulting in a mismatch of the exposures and an incom-

plete suppression of anatomical noise on the recombined images.

As this artefact is most frequently observed in the inferior quadrant of the left MLO projection, Bhimani et al. [2] suggested that it arises from cardiac pulsations transmitted through the chest wall. The ripple artefact does not compromise the quality of the image, but it is possible to decrease its effect by reducing patient anxiety during the procedure.

Providing patients with information about the procedure is a suitable first step towards reducing their fears. Talking the patient through their experience also helps greatly. Six minutes is adequate time for the technologist to obtain the four

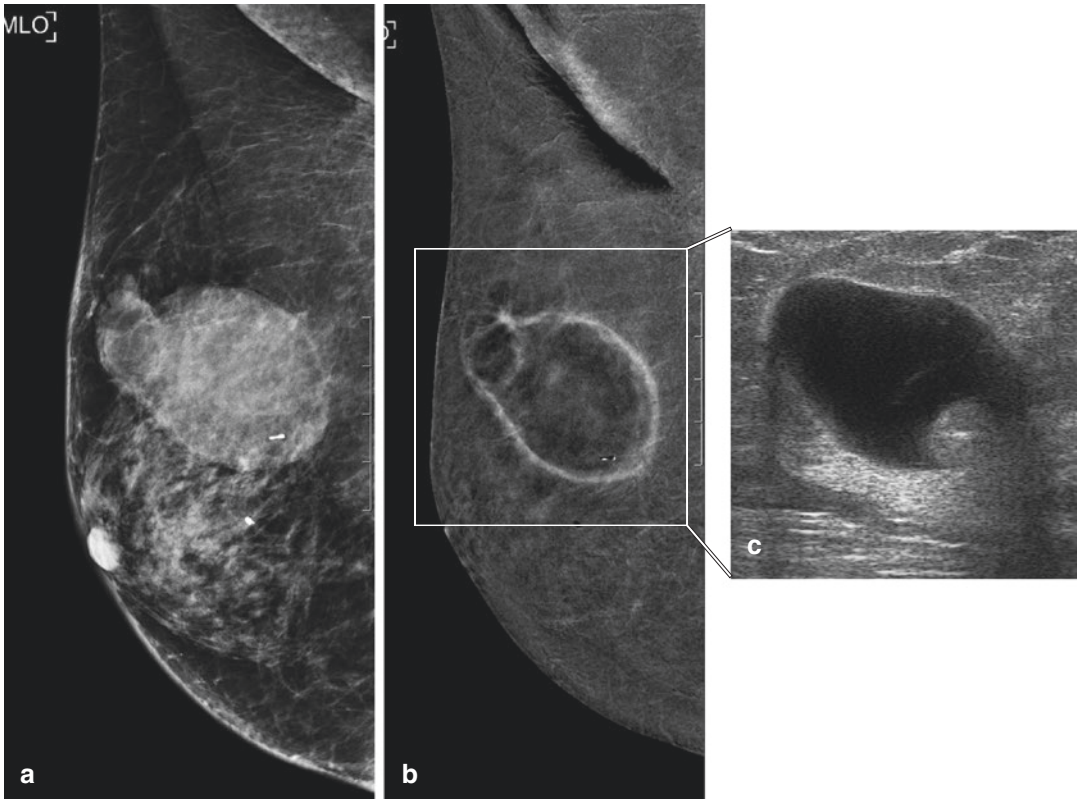


**Fig. 8.10 Negative contrast enhancement:** A 51-year-old patient, treated with a left breast carcinoma, presented with a new suspicious cluster of calcifications in the upper outer quadrant of the right breast. She was subjected to a vacuum-assisted breast biopsy (VABB). (a) LE in MLO projection shows a large lobulated area of increased density at the site of the VABB with a radiopaque marker

within. (b) CEDM-recombined image in MLO projection shows a lobulated area of ring enhancement corresponding to the post-biopsy granulation tissue with central “negative contrast enhancement”. (c) Ultrasound confirming the post-biopsy haematoma with a marker in situ. *CEDM* contrast-enhanced digital mammography, *LE* low energy, *MLO* mediolateral oblique

standard mammographic views; thus, to avoid increasing the patient’s anxiety, operators need not rush through the procedure.

### 8.3.4 Skin-Line Enhancement Artefact and Enhancing Skin Lesions

The skin is predominately non-enhancing on CEDM but may show a thin line of enhancement known as the “skin-line enhancement artefact” or “skyline artefact”. These features are

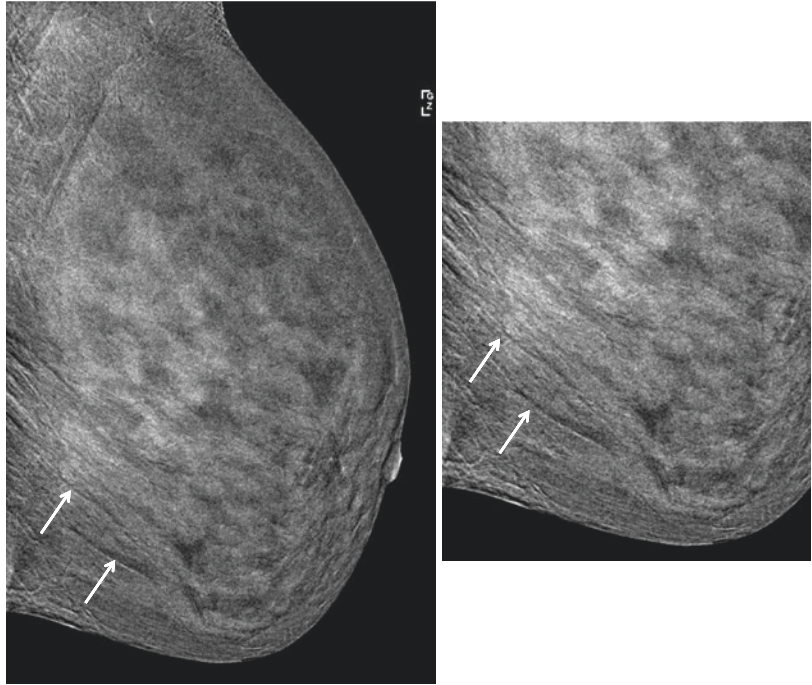
commonly observed in the CC images relative to the MLO projection and are reported to be associated with the difference in skin thickness and scatter radiation, which is non-uniform throughout the breast (Fig. 8.12). Given the variable appearance of the skin on the recombined images, any findings of skin enhancement and thickening observed on the recombined images should be correlated with the low-energy image [1].

Vascular skin lesions such as cherry angiomas can appear as an enhancing intraparenchymal breast lesion on CEDM, mimicking a

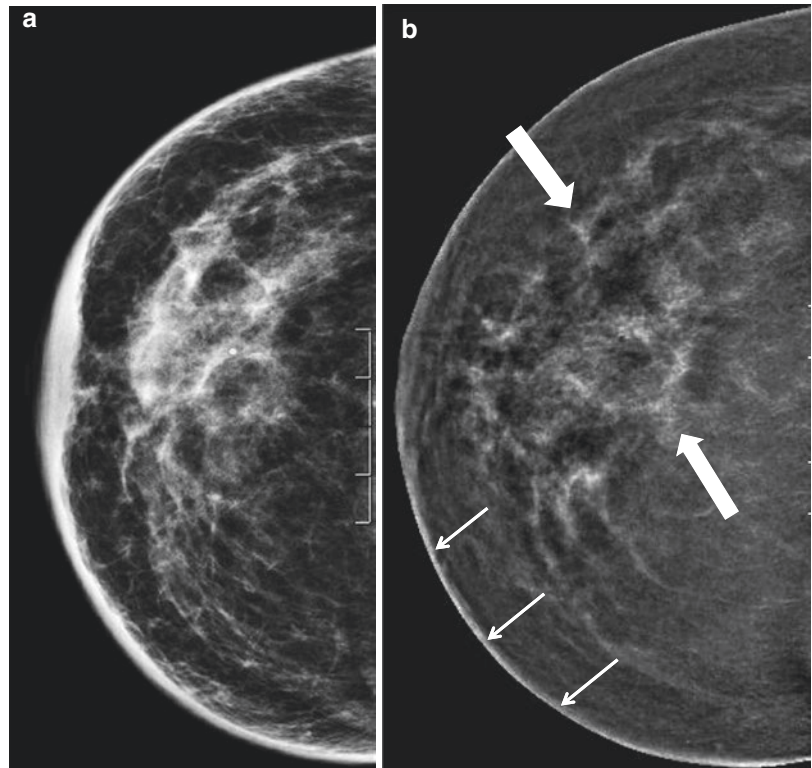


**Fig. 8.11 Ripple**

**artefact:** A 65-year-old woman received CEDM due to abnormal findings in the right breast on screening mammography (*not shown*). The white arrows point to faint alternating fine black and white ripple-like lines layered upon the breast parenchyma on the “left” MLO-recombined image (better observed on the magnification view), which are possibly related to cardiac pulsations. *CEDM* contrast-enhanced digital mammography, *MLO* mediolateral oblique

**Fig. 8.12 Skyline**

**artefact:** A 53-year-old woman with biopsy-proven invasive carcinoma in the right breast underwent CEDM as part of a staging workup. (a) The LE image shows pathologic skin thickening, and (b) the recombined CC view shows areas of non-mass enhancement of a biopsy-proven breast carcinoma (*block arrows*); the recombined image is also seen to illustrate a thin line of skin enhancement (*arrows*) that illustrates a “skyline appearance”. *LE* low energy, *CC* craniocaudal



suspicious lesion. We have encountered such enhancing lesions in our clinical practice with cherry angiomas and skin tags (Fig. 8.13). Therefore, the technologist must identify such lesions and place markers on any potentially enhancing skin lesion.

### 8.3.5 Misregistration Artefacts

A specific type of motion artefact observed exclusively on the recombined images is the

misregistration artefact, which is the result of motion between the LE and HE images; even minimal motion causes misalignment of the images, resulting in imprecise subtraction. These signals are alternately additive and cancel each other out, resulting in an alternating bright and dark appearance, illustrating a “zebra artefact”, which is secondary to motion-causing misregistration.

Misregistration is commonly observed in relation to surgical clips, vessels, and calcifications (Fig. 8.14).

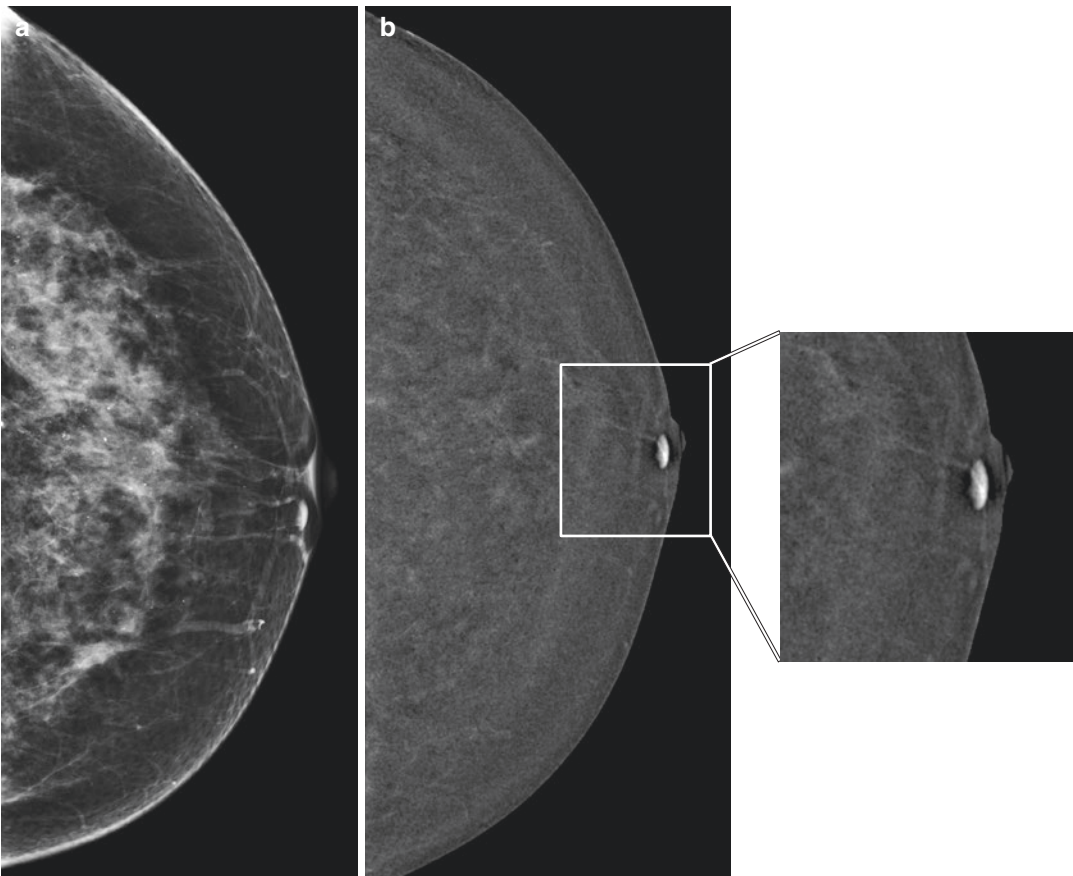


**Fig. 8.13 Cherry angioma:** A 45-year-old woman had a CEDM due to abnormal findings in the right breast (*not shown*) on screening mammography. (a) The left CC LE image shows an oval density in the subcutaneous tissue in the periareolar region suggestive of a skin lesion, and (b)

the recombined image shows a small oval area of intense enhancement (*box*) in the periareolar region, mimicking an enhancing mass. On further clinical examination of the breast, the oval enhancing lesion was confirmed to be a cherry angioma. *LE* low energy, *CC* craniocaudal



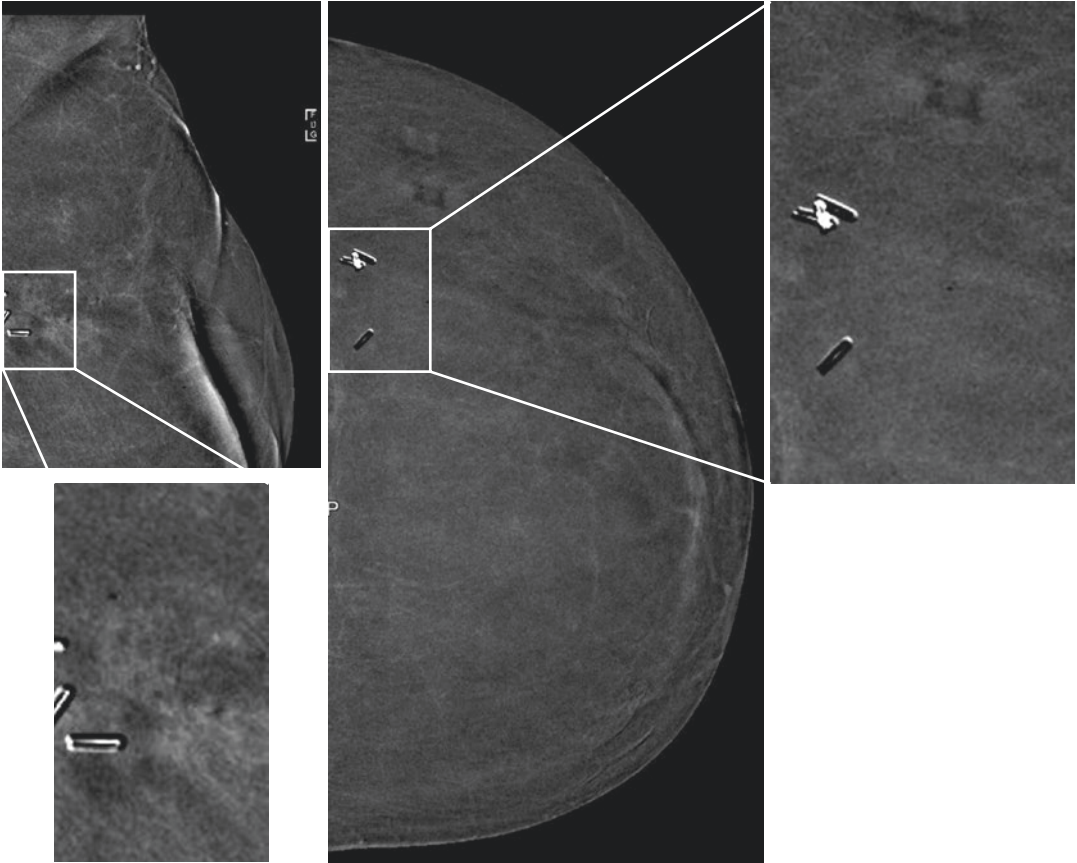


**Fig. 8.14 Misregistration artefact:** Recombined images from two patients, who had previous surgeries for breast cancer, show misregistration artefacts. Surgical

clips observed on the magnified recombined images show side-by-side bright and dark lines, often described as “zebra artefacts” from the misregistration

#### 8.4 Artefacts Related to the Quality-Control (QC) Process

According to the U.S. Mammography Quality Standards Act (MQSA), every U.S. facility must adhere to the recommended protocols for QC of mammographic equipment to ensure optimal image quality. While not a requirement outside the USA, understanding and following the vendor-dependent QC processes, recognizing artefacts that can occur during various steps, and having fundamental knowledge to correct these artefacts that may result in a suboptimal image are critical to ensure optimal image quality.

Working together, a qualified physicist, technologist, and radiologist are all responsible for meeting the MQSA requirements, ensuring that the images produced by the equipment meet regulatory standards, thereby ensuring optimal images for interpretation and maximizing the detection of early malignancies.

It is important to train all technologists and arrange specific times for the daily QC processes and specific days for the weekly QC processes. The weekly QC step should be performed at the end of the week after the last scheduled patient listed for that week or early at the beginning of the week before the scheduled patients are seen. Figure 8.15 shows an artefact encountered when a gain calibration QC, which did not complete

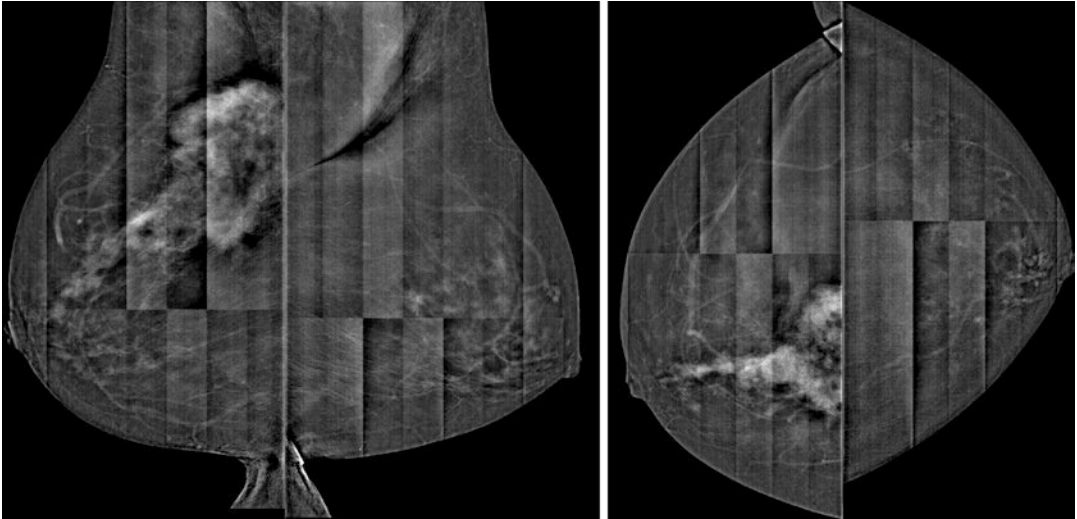


**Fig. 8.15 Gain calibration artefact:** A 51-year-old woman presented with a palpable abnormality in her right breast. The CEDM examination revealed these grossly pixelated artefacts only on the recombined images of all four mammographic views. We then determined that the gain calibration QC step was performed just prior to our CEDM schedule. Therefore, this artefact is the result of an

incomplete gain calibration QC step superimposed in this CEDM examination. Thus, it is important not to perform the QC step before a CEDM schedule, and if this step has been done, to ensure that the system is tested on a phantom prior to scanning a patient, as such artefacts severely degrade the images. *CEDM* contrast-enhanced digital mammography, *QC* quality control

properly, was performed prior to a CEDM procedure. The artefact has severely degraded the image quality, compromising the image interpretation.

Therefore, to avoid such situations from occurring, if a QC step has been performed prior to a scheduled list of patients, it is important to test the system on a phantom prior to performing a CEDM procedure, as once the contrast has been injected, obtaining optimal images within the CEDM time limit is crucial. In fact, it is a good practice to always follow a QC calibration with a phantom image prior to any patient imaging, not just CEDM imaging, to ensure that the calibration was executed properly.

#### 8.4.1 Ghosting Artefact

A ghosting artefact results when a latent image from a prior exposure is superimposed on a newly acquired image. The rapid acquisition of images

in CEDM can cause the lingering latent signal from one exposure to project on the subsequent exposures, resulting in an apparent incomplete erasure of the previous image, which is known as the image lag (Fig. 8.16).

Recalibrating the machine to remove the memory of the previous image and acquiring a test image to ensure that the artefact is no longer present can rectify this complication. However, this is not possible due to the limited timeline for imaging in CEDM; therefore, this effect can be reduced by a longer delay between the four image acquisitions. This artefact is not usually seen under normal conditions.

Detector saturation in the skin region due to a high detector signal causes the skin artefact observed in the diseased right breast in Fig. 8.16. This artefact is predominantly observed in the right breast, as this was the larger breast with the underlying pathology which could not be optimally compressed.

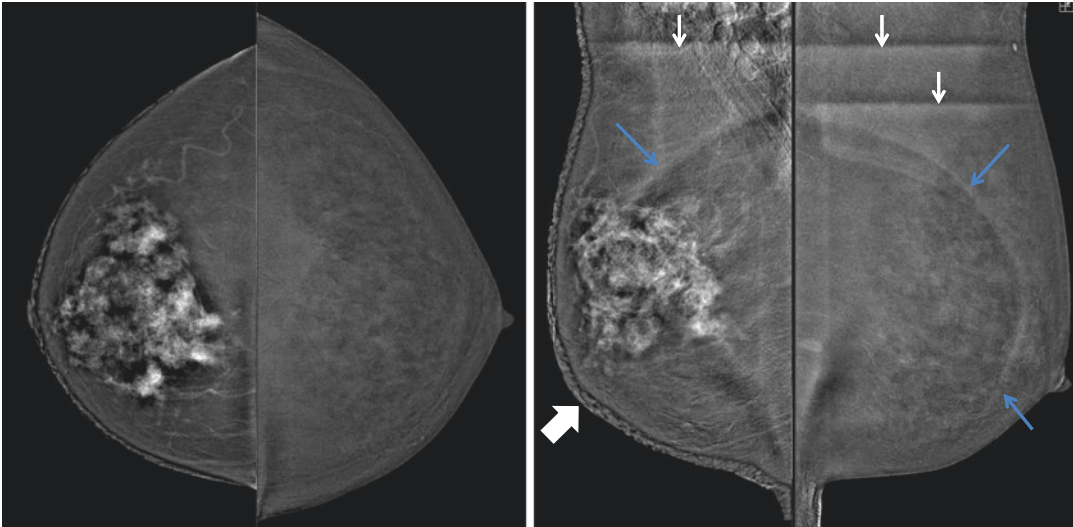


**Fig. 8.16 Ghosting artefact:** A 62-year-old woman presented with a right breast lump. The CEDM recombined images in this examination were acquired in the following sequence: right CC, left CC, right MLO, and left MLO. A single right axillary line (*white arrows*) was observed in the right MLO, and a double left axillary line (*white arrows*) was observed in the left MLO. These lines repre-

sent ghosting from shifting of the paddle in the three positions, i.e., CC, right MLO, and left MLO. Ghosting of the CC view (*blue arrows*) of the previously imaged breast projected within the MLO images is also evident. The skin artefact observed in the diseased right breast (*black arrow*) is caused by detector saturation in the skin region due to a high detector signal

### Conclusion

Both patient and technical factors may lead to unwanted artefacts at CEDM, and as the use of CEDM in clinical practice is rapidly gaining popularity, there is a greater need for radiologists and technologists to be aware of the artefacts associated with this relatively new technology.

Although some of these artefacts are similar to those observed in mammography, many artefacts are unique to CEDM, specifically artefacts due to software processing errors or contrast administration issues. In addition, CEDM also depends on combining images acquired with various X-ray energy spectra resulting in CEDM-specific artefacts.

It is important that the technologist, radiologist, and physicist become familiar with the spectrum of CEDM artefacts and pay careful attention to QC procedures to ensure optimal image quality. Recognizing and understanding the cause of patient-related and technical artefacts allow the CEDM imaging

technologist and radiologist to work together to optimize the image quality and avoid interpretive pitfalls.

This chapter presents the commonly encountered patient-related and technical artefacts that may result in reduced image quality and ways to recognize and reduce them. We have also included a detailed pictorial of some of the common artefacts that we have encountered in our clinical practice in Careggi University Hospital, Italy, and Kuala Lumpur Hospital, Malaysia.

### References

1. Yagil Y, Shalmon A, Rundstein A, Servadio Y, Halshok O, Gotlieb M, et al. Challenges in contrast-enhanced spectral mammography interpretation: artefacts lexicon. *Clin Radiol.* 2016;71(5):450–7.
2. Bhimani C, Li L, Liao L, Roth RG, Tinney E, Germaine P. Contrast-enhanced spectral mammography: modality-specific artifacts and other factors which may interfere with image quality. *Acad Radiol.* 2017;24(1):89–94.

3. Lalji UC, Jeukens CR, Houben I, Nelemans PJ, van Engen RE, van Wylick E, et al. Evaluation of low-energy contrast-enhanced spectral mammography images by comparing them to full-field digital mammography using EUREF image quality criteria. *Eur Radiol.* 2015;25(10):2813–20.
4. Ayyala RS, Chorlton M, Behrman RH, Kornguth PJ, Slanetz PJ. Digital mammographic artifacts on full-field systems: what are they and how do I fix them? *Radiographics.* 2008;28(7):1999–2008.
5. Daniaux M, De Zordo T, Santner W, Amort B, Koppelstatter F, Jaschke W, et al. Dual-energy contrast-enhanced spectral mammography (CESM). *Arch Gynecol Obstet.* 2015;292(4):739–47.
6. Dromain C, Balleyguier C, Adler G, Garbay JR, Delaloge S. Contrast-enhanced digital mammography. *Eur J Radiol.* 2009;69(1):34–42.
7. Jochelson MS, Dershaw DD, Sung JS, Heerd AS, Thornton C, Moskowitz CS, et al. Bilateral contrast-enhanced dual-energy digital mammography: feasibility and comparison with conventional digital mammography and MR imaging in women with known breast carcinoma. *Radiology.* 2013;266(3):743–51.
8. Lobbes MB, Smidt ML, Houwers J, Tjan-Heijnen VC, Wildberger JE. Contrast enhanced mammography: techniques, current results, and potential indications. *Clin Radiol.* 2013;68(9):935–44.
9. Geiser WR, Haygood TM, Santiago L, Stephens T, Thames D, Whitman GJ. Challenges in mammography: part 1, artifacts in digital mammography. *AJR Am J Roentgenol.* 2011;197(6):W1023–30.
10. Jayadevan R, Armada MJ, Shaheen R, Mulcahy C, Slanetz PJ. Optimizing digital mammographic image quality for full-field digital detectors: artifacts encountered during the QC process. *Radiographics.* 2015;35(7):2080–9.
11. Chaloeykitti L, Muttarak M, Ng KH. Artifacts in mammography: ways to identify and overcome them. *Singap Med J.* 2006;47(7):634–40; quiz 41.
12. Lewis TC, Patel BK, Pizzitola VJ. Navigating contrast-enhanced digital mammography. *Appl Radiol.* 2017;46(3):21–8.
13. Sogani J, Morris EA, Kaplan JB, D'Alessio D, Goldman D, Moskowitz CS, et al. Comparison of background parenchymal enhancement at contrast-enhanced spectral mammography and breast MR imaging. *Radiology.* 2017;282(1):63–73.
14. Gluskin J, Click M, Fleischman R, Dromain C, Morris EA, Jochelson MS. Contamination artifact that mimics in-situ carcinoma on contrast-enhanced digital mammography. *Eur J Radiol.* 2017;95:147–54.
15. Bhimani C, Matta D, Roth RG, Liao L, Tinney E, Brill K, et al. Contrast-enhanced spectral mammography: technique, indications, and clinical applications. *Acad Radiol.* 2017;24(1):84–8.
16. Choi JJ, Kim SH, Kang BJ, Choi BG, Song B, Jung H. Mammographic artifacts on full-field digital mammography. *J Digit Imaging.* 2014;27(2):231–6.
17. Dromain C, Thibault F, Muller S, Rimareix F, Delaloge S, Tardivon A, et al. Dual-energy contrast-enhanced digital mammography: initial clinical results. *Eur Radiol.* 2011;21(3):565–74.
18. Hill ML, Mainprize JG, Carton AK, Saab-Puong S, Iordache R, Muller S, et al. Anatomical noise in contrast-enhanced digital mammography. Part II. Dual-energy imaging. *Med Phys.* 2013;40(8):081907.



# CEDM Lexicon and Imaging Interpretation Tips

# 9

Giulia Bicchierai, Federica Di Naro,  
and Francesco Amato

## 9.1 Introduction

At present, there are still no standardized interpretation criteria for the evaluation of breast lesions by CEDM. Different patterns of contrast uptake and the morphology descriptors of enhancing lesions, which allow the characterization of benign and malignant breast lesions with CEDM, are still undergoing research. Given the analogy between dynamic contrast-enhanced MRI (DCE-MRI) and CEDM, some studies published in the literature have tried to assess whether it is possible to apply the MRI BI-RADS lexicon morphology descriptors instituted by the American College of Radiology (ACR) to address a lack of standardization and uniformity in mammography practice reporting by CEDM. Previous authors have concluded that it is possible to apply MRI morphology descriptors to characterize lesions observed by CEDM with only a few exceptions, which we will analyse in this chapter. Therefore, based on our experience with CEDM and the data published in the international literature, it is recommended to use a well-defined and standardized lexicon of morphology descriptors,

similar to the MRI BI-RADS lexicon, to characterize breast lesions by CEDM.

Indeed, the use of a standardized lexicon for this new diagnostic technique provides accurate lesion description and characterization. It also provides a standard terminology to facilitate communication between radiologists and clinicians, resulting in a positive impact on management decision-making and outcome assessment.

In this chapter, we will describe how we apply the MRI BI-RADS lexicon to CEDM and discuss the differences that must be addressed.

In a CEDM study, we not only must analyse recombined images but also low-energy (LE) images, which are analogous to conventional digital mammography; therefore, we use the standard lexicon of mammography to describe a lesion seen in LE images and the MRI BI-RADS lexicon to describe a lesion seen in recombined images. We usually begin our report by describing the breast density, i.e. almost entirely fat, scattered areas of fibroglandular densities, heterogeneously dense or extremely dense, in addition to pertinent imaging findings seen in LE images (Fig. 9.1).

The next section of our CEDM reporting template describes the findings from the recombined image, in which the background parenchymal enhancement (BPE) is described in four categories, similar to MRI BPE: minimal (<25% enhancement), mild (25–50% enhancement),

---

G. Bicchierai (✉) · F. Di Naro · F. Amato  
Diagnostic Senology Unit, Department of Radiology,  
Azienda Ospedaliero Universitaria Careggi,  
Florence, Italy



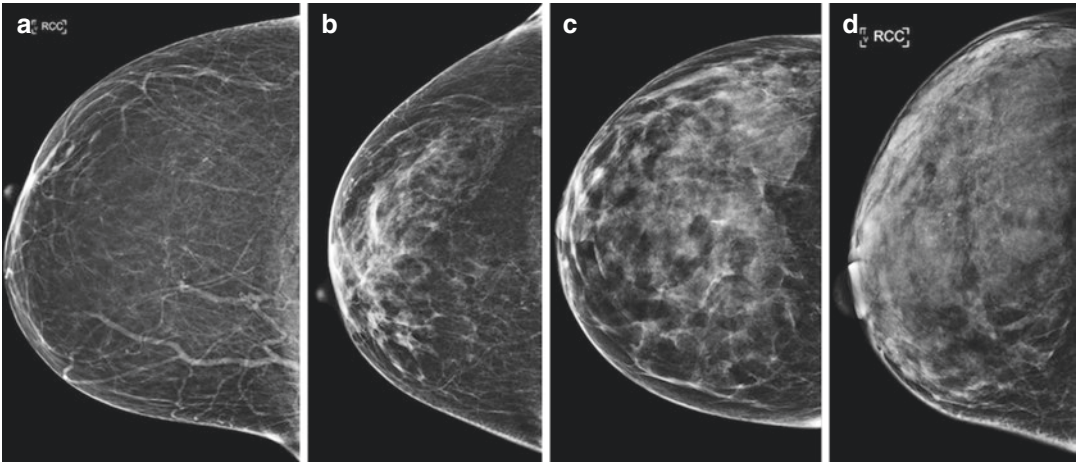


**Fig. 9.1** Breast density. (a) Cranio-caudal low-energy view of an almost entirely fat breast; (b) cranio-caudal low-energy view of a breast with scattered areas of fibro-

glandular densities; (c) cranio-caudal low-energy view of a heterogeneously dense breast; and (d) cranio-caudal low-energy view of an extremely dense breast

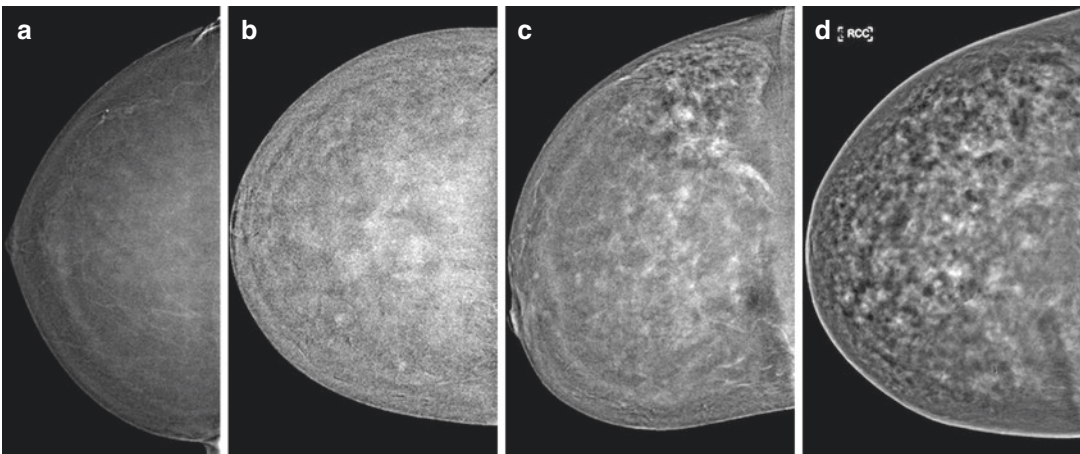


**Fig. 9.2** Breast background parenchymal enhancement (BPE). (a) Cranio-caudal recombined image of minimal BPE, <25% enhancement; (b) cranio-caudal recombined image of a mild BPE, 25–50% enhancement; (c) cranio-

caudal recombined image of moderate BPE, 50–75% enhancement; and (d) cranio-caudal recombined image of marked BPE, >75% enhancement

moderate (50–75% enhancement) or marked (>75% enhancement) (Fig. 9.2).

At our centre, we also make it a point to analyse the kinetic enhancement pattern for each lesion with delayed acquisition. The delayed acquisition is obtained more than 8 minutes from the beginning of the administration of the contrast medium, falling in the phase of the study in which the contrast is dispersing from the breast. Delayed

acquisition allows us to evaluate the subjective kinetics of lesion enhancement in addition to the morphological analysis data, which may help to characterize the lesions [1–4] (Fig. 9.3).

Regarding patterns of enhancement seen by CEDM, we classify the lesions seen in subtracted images into three main groups (similar to MRI): focus, mass and non-mass enhancement [1–4].

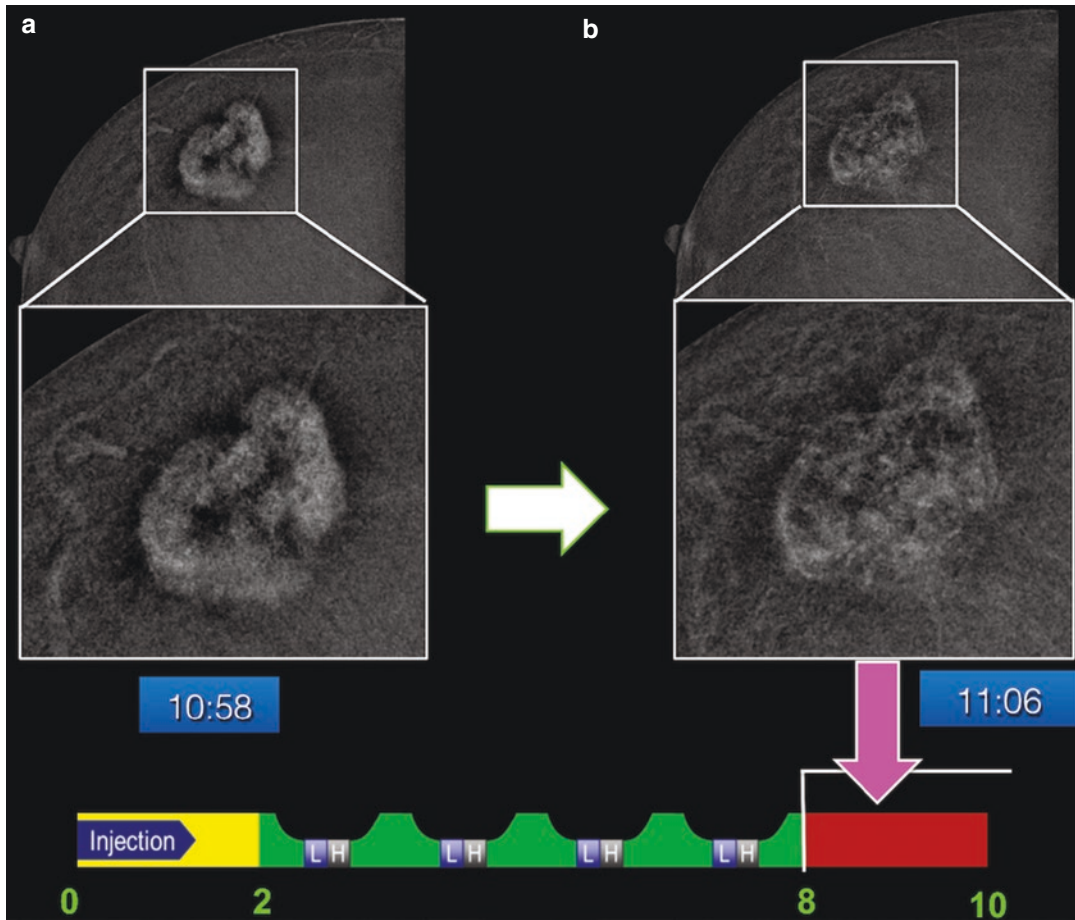


**Fig. 9.3** CEDM examination of pathology-proven ductal invasive carcinoma of the right breast. Note the strong washout of contrast agent in the cancer, leading to decreased enhancement intensity in the late-phase image,

acquired 8 minutes after the injection of contrast medium. (b) Compared with the first acquisition, acquired 2 minutes after the injection (a)

## 9.2 Focus

A focus is a single tiny punctate enhancement that is non-specific and too small to be characterized. A focus is smaller than 5 mm and is clearly not a space-occupying lesion or a mass. The morphologic descriptors of an enhancing focus include:

- Single or multiple
- Unilateral or bilateral
- Faint or intense enhancement

Morphological descriptors that suggest a greater positive predictive value for malignancy are the presence of a single, unilateral focus with

**Table 9.1** Focus morphology descriptors

Number	Spatial Distribution	Intensity of Enhancement
Single	Unilateral	Faint
Multiple	Bilateral	Intense

an intense enhancement, which we observe in the first imaging acquisitions 2 minutes after the contrast medium is administered (Table 9.1, Fig. 9.4).

When we see a focus of enhancement, we should immediately review the LE images to search for a correlation with mammography findings: for example, a subtle cluster of microcalcifications or an architectural distortion that may have been missed,

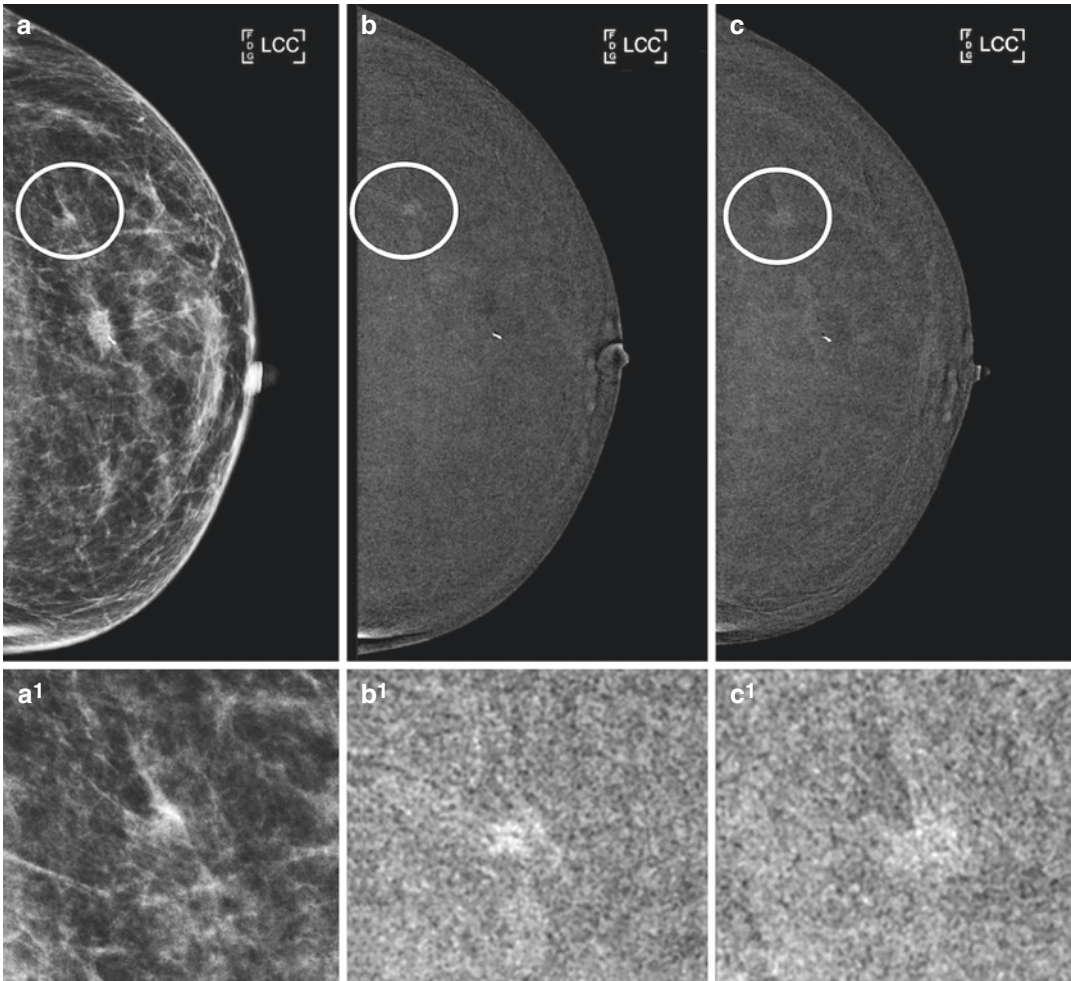


**Fig. 9.4** A single intensely enhancing focus in the upper outer quadrant of the left breast in a 73-year-old woman with previous homolateral breast biopsy with benign outcome. **(a)** Cranio-caudal low-energy view with magnification **(a<sup>1</sup>)** shows an irregular opacity at the focal

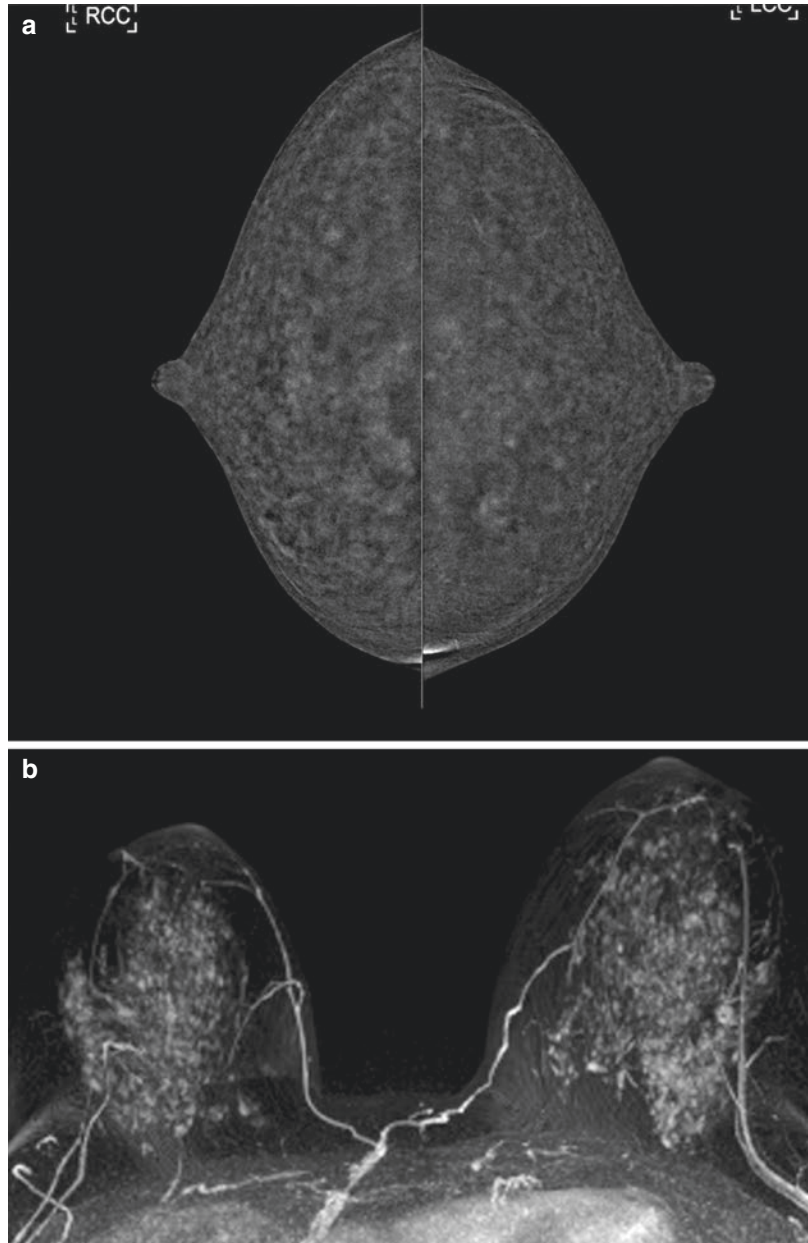
enhancement zone; **(b)** recombined CEDM view with magnification **(b<sup>1</sup>)**; and **(c)** late recombined CEDM view with magnification **(c<sup>1</sup>)**. The opacity was then subjected to stereotactic VABB and found to be a microinvasive, not otherwise specified carcinoma and in situ carcinoma

corresponding to the area of enhancement. We should also perform a second-look ultrasound to search for a possible lesion to biopsy, and further management of the foci depends on the risk status of the patient, ranging from follow-up to further diagnostic tests. An appreciable focus, which is only seen in delayed images and not during the early phase, with progressive enhancement kinetics is more closely related to benignity. The presence of multiple, bilateral and faint foci is also usually related to benignity. Based on the available literature, the presence of multiple and bilateral foci by

MRI is considered to be associated with background parenchymal enhancement (BPE); however, with CEDM, the discriminating element is the intensity of the focal enhancement. In CEDM, multiple bilateral intensely enhancing foci may be related to malignancy (i.e. multicentric invasive ducts or invasive lobular carcinomas), particularly if they exhibit different sizes and distributions in both breasts. In these cases, it is therefore recommended to add further diagnostic or interventional techniques to characterize the foci before considering them to be associated with BPE [2–13] (Fig. 9.5).



**Fig. 9.5** Many bilateral faint enhancing foci related to BPE in a 45-year-old woman with familiarity for breast cancer. **(a)** CEDM cranio-caudal view recombined images and **(b)** MRI maximum intensity projection reconstruction (MIP) images. The images are perfectly superimposable across the two techniques



### 9.3 Mass

A mass is a three-dimensional space-occupying lesion that displaces tissue.

Morphology descriptors of enhancing mass lesions include:

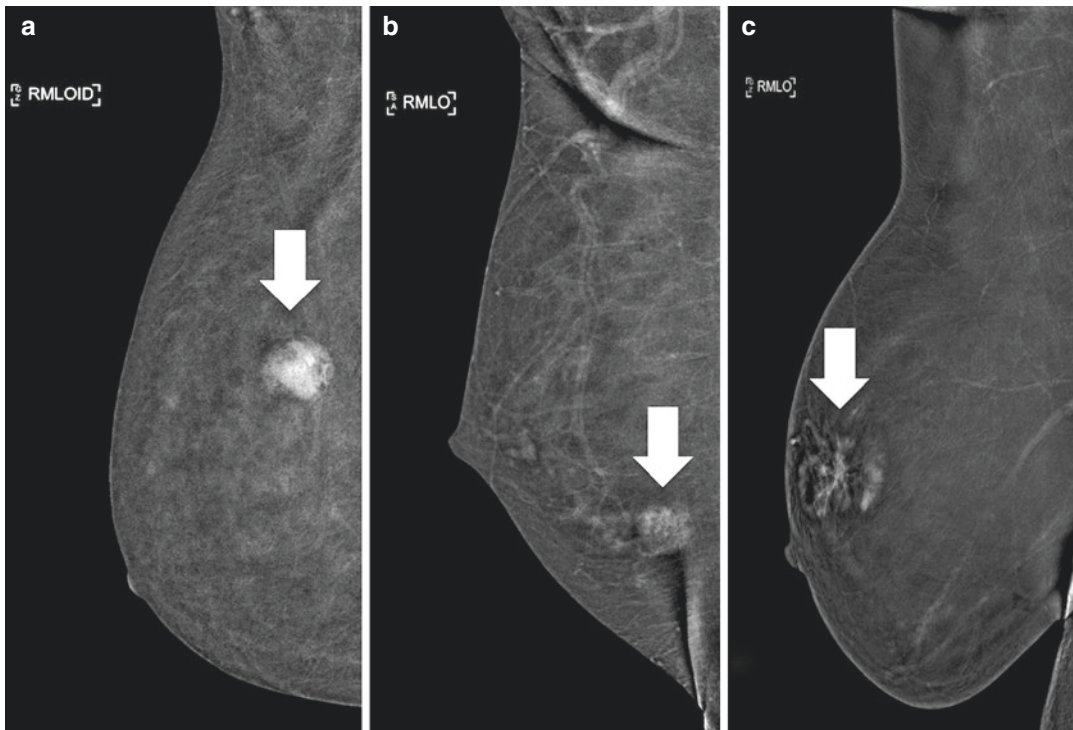
- Mass shape: round, oval and irregular
- Mass margin: circumscribed and non-circumscribed (irregular or spiculated)

- Internal enhancement characteristics: homogeneous, heterogeneous, rim enhancement and dark internal septations
- Degree of enhancement: faint, moderate and intense

It is important to note that the margin analysis of a mass is dependent on spatial resolution and the spatial resolution of CEDM (similar to mammography) is higher than MRI. In general, margin

**Table 9.2** Mass morphology descriptors

Shape	Margin	Internal Enhancement	Intensity of Enhancement
Round	Circumscribed	Homogeneous	Faint
Oval	Non-circumscribed	Heterogeneous	Moderate
Irregular		Rim enhancement	Intense
		Dark internal septations	

**Fig. 9.6** Medio-lateral oblique CEDM recombined views in (a) a lesion with regular margins, (b) a lesion with irregular margins, and (c) a lesion with spiculated margins

and shape analysis of a mass should be performed with the first post-contrast image to avoid the subsequent effects of washout or progressive enhancement of the surrounding normal breast tissue, which can obscure lesion analysis. Morphological descriptors that have a greater positive predictive value for a malignant mass in CEDM are irregular shape, non-circumscribed margins and heterogeneous internal enhancement (Table 9.2, Figs. 9.6 and 9.7).

Homogeneous enhancement is confluent and uniform; heterogeneous enhancement is non-uniform with areas of variable signal intensity.

In contrast to the MRI BI-RADS lexicon, the internal enhancement pattern of mass lesions in CEDM has a lower specificity and a high number of false-positive and false-negative cases, particularly related to rim enhancement.

In breast MRI, we have the advantage of referring back to non-contrast T<sub>1</sub>- and T<sub>2</sub>-weighted



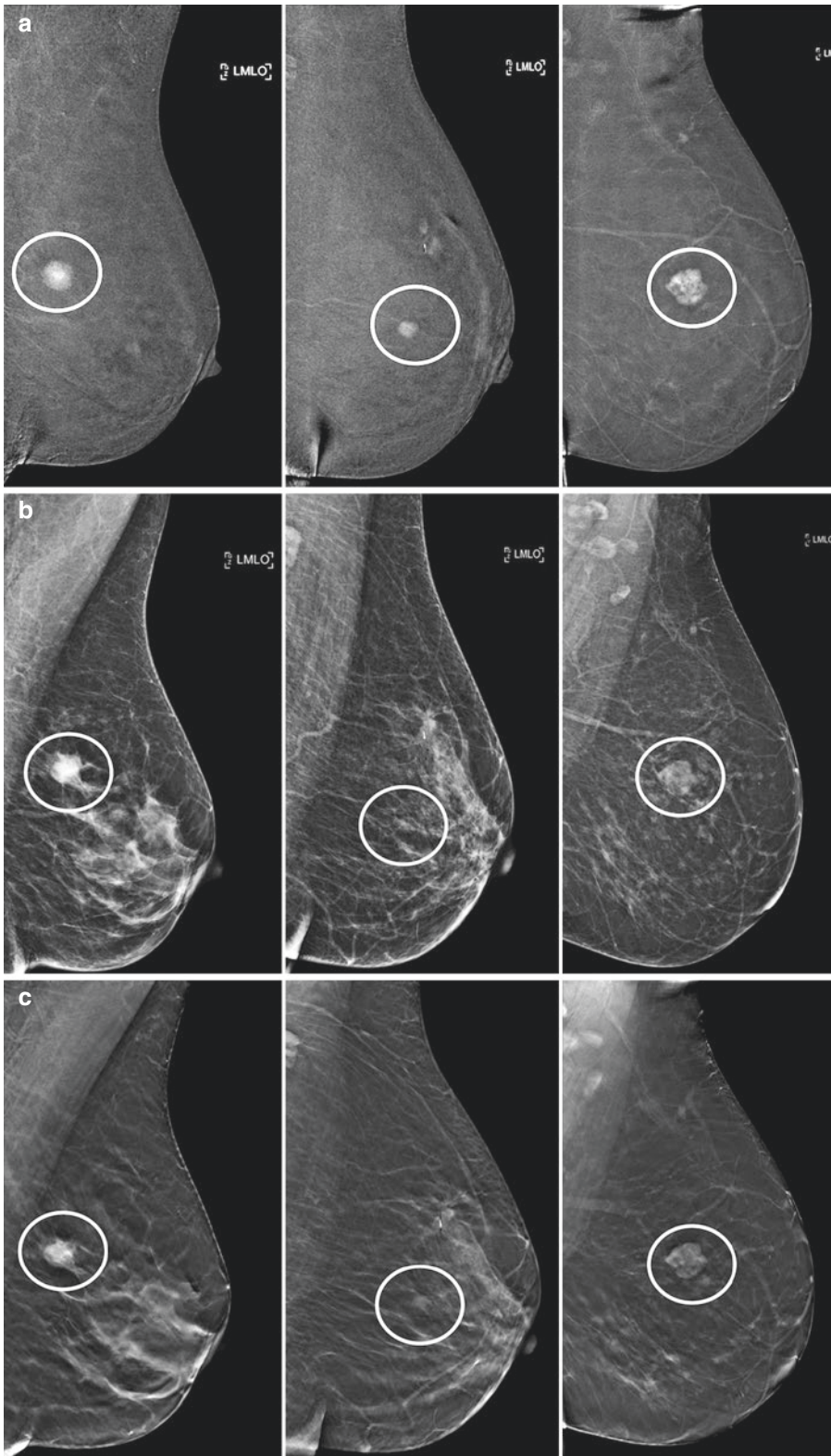


**Fig. 9.7** (a) CEMM study in lesions with round, oval or irregular shape; (b) low-energy lesions with round, oval or irregular shape; and (c) tomosynthesis slices in lesions with round, oval or irregular shape

images in lesions that show rim enhancement, where we can easily recognize benign lesions such as inflammatory cysts or post-biopsy haematoma that cause false-positive results. However, this is not feasible with CEDM, although it is sufficient to add an ultrasound

examination of these lesions to recognize false-positive lesions and increase the specificity of this descriptor (Figs. 9.8 and 9.9).

The descriptors of a mass that have a higher correlation with benignity are round or of oval shape, well-circumscribed margins with dark

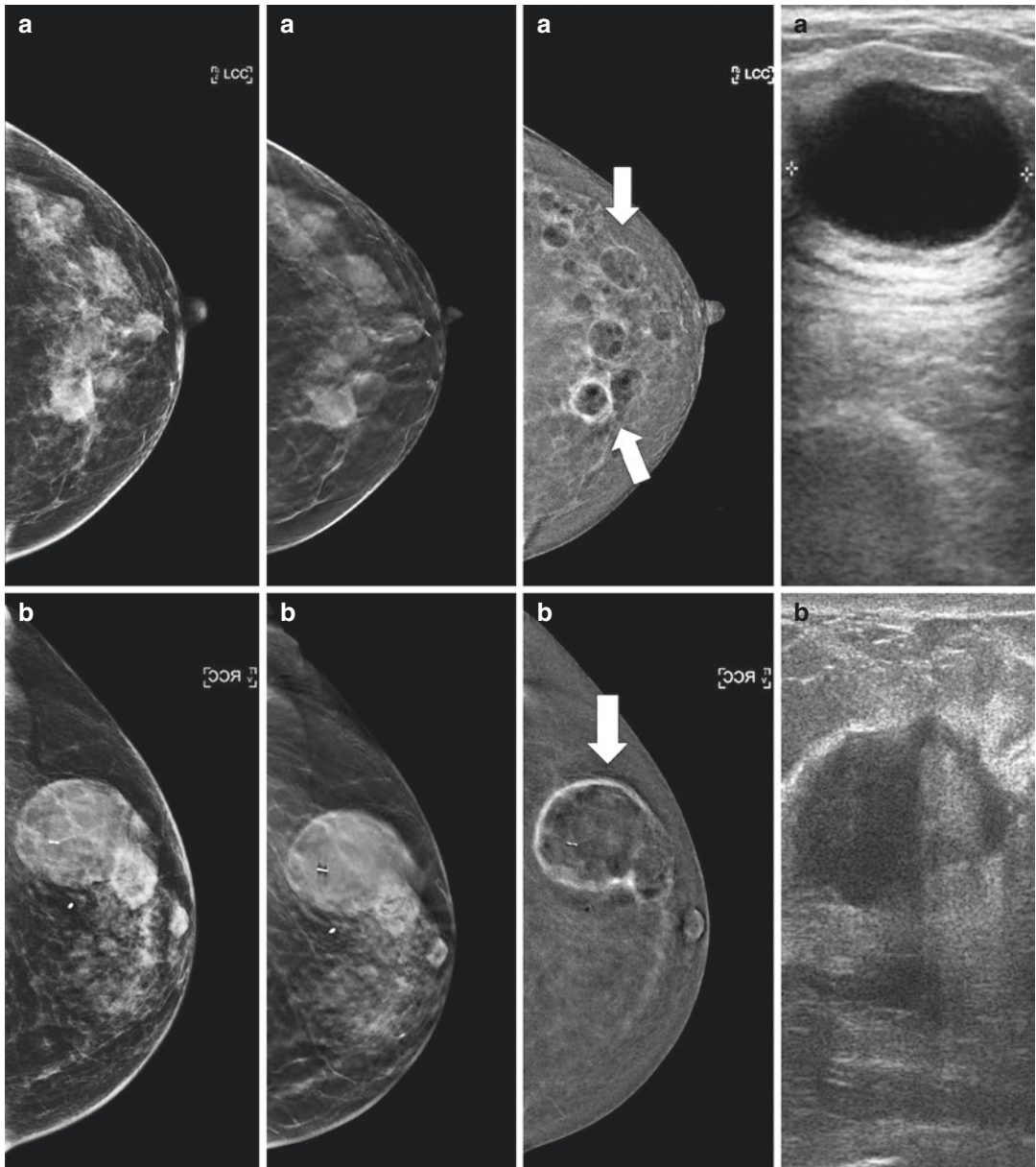


**Fig. 9.8** Two cases of false-positive rim enhancement due to benign lesions. (a) Simple cyst lesions in low-energy CEDM views, tomosynthesis slice, CEDM recombined image and corresponding ultrasound image; (b) a post-

biopsy haematoma with contextual clip in low-energy CEDM views, tomosynthesis slice, CEDM recombined image and corresponding ultrasound image

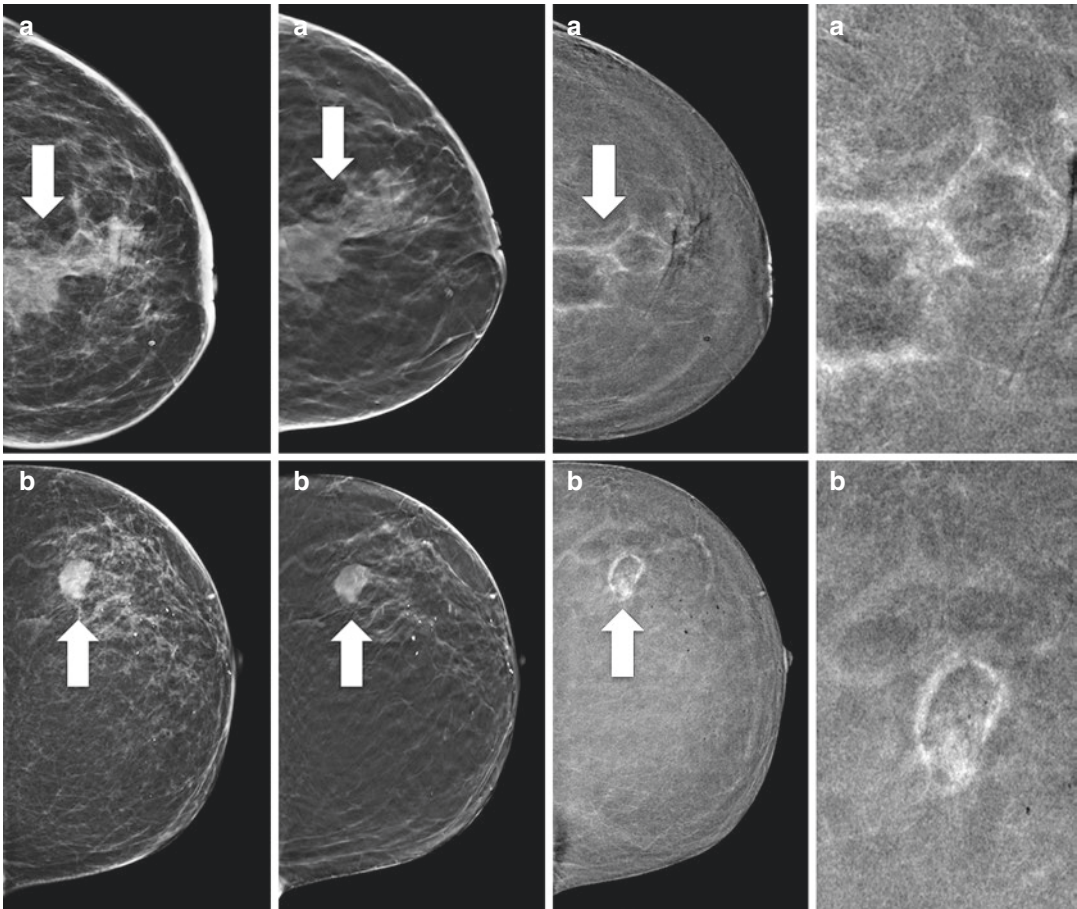


**Fig. 9.9** Two cases of true-positive rim enhancement due to malignant lesions. (a) Breast angiosarcoma in low-energy CEDM views, tomosynthesis slice, CEDM recom-

bined image with magnification; (b) invasive carcinoma in low-energy CEDM views, tomosynthesis slice, CEDM recombinant image with magnification

internal septations, which are characteristic of fibroadenomas.

Homogeneous enhancement is suggestive of a benign process; however, particularly in small lesions, this pattern can also be a presentation of invasive cancer as reported in some studies published in the literature [8, 9, 11–13]. After evaluating all morphology descriptors of enhancing mass lesions, we concluded that irregular shape, non-circumscribed margins (irregular and spiculated) and “heterogeneous” internal enhancement were the highest predictors of malignancy, although at the same time, we were unable to exclude malignancy based on either a rounded or oval shape or a homogeneous pattern of enhancement (Figs. 9.10, 9.11 and 9.12).

In CEDM, another important descriptor of mass lesions is the intensity of enhancement. Despite being a subjective parameter, all previous literature evaluating the intensity of enhancement demonstrated a high inter-reader reproducibility and a statistically significant association with malignancy. Therefore, a mass with moderate or intense enhancement is suspicious of malignant transformation, which is observed most frequently in invasive carcinomas. However, a mass with faint or no enhancement is most frequently observed in benign lesions (Fig. 9.13).

In our clinical practice in Careggi, Italy, we have observed another descriptor that can help us to characterize a mass: the evaluation of enhancement



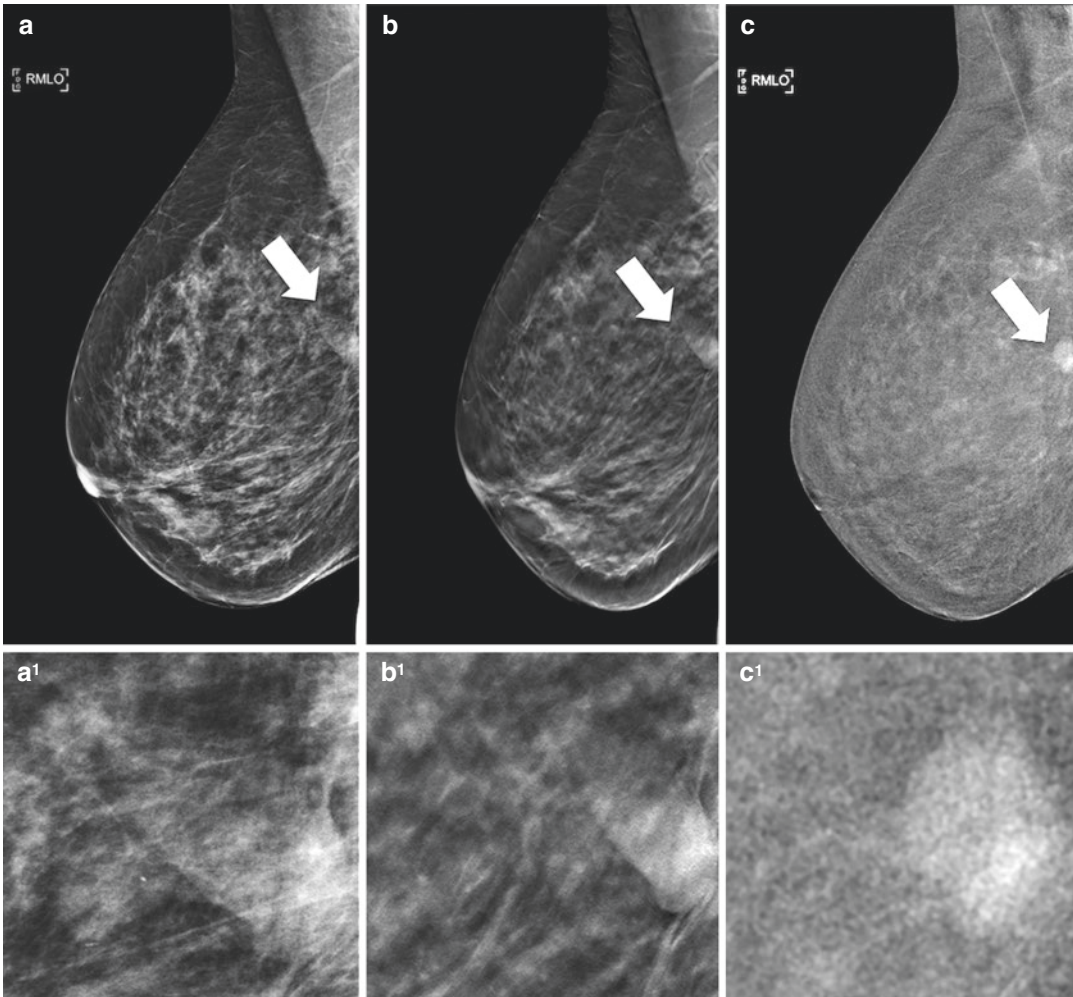


**Fig. 9.10** Homogeneous enhancement in a benign lesion (fibroadenoma); (a) medio-lateral oblique low-energy view with magnification (a<sup>1</sup>); (b) tomosynthesis slice with magnification (b<sup>1</sup>); (c) medio-lateral oblique recombined CEDM view with magnification (c<sup>1</sup>)

kinetics. In the case of a well-defined mass that may quite possibly be benign, the enhancement kinetics pattern may help one decide if a biopsy is required or if it is safe to recommend a follow-up of the lesion. Unlike MRI, we can only make a subjective non-quantitative evaluation of the kinetics with CEDM.

To perform kinetic analysis, we compare the early image (within the first 8 minutes of maximal contrast enhancement) with the delayed image acquired after the eighth minute starting from the administration of contrast medium. We have observed that malignant lesions demonstrate a greater intensity of enhancement in early

images with washout seen in the delayed acquisition images. Conversely, if a lesion demonstrates a progressive enhancement pattern, this suggests benignity. Similar to MRI, there are some exceptions to this rule, such as in papillary lesions, which are highly vascularized benign lesions that may demonstrate a rapid washout of contrast agent, while some malignant lesions, such as lobular carcinoma, may have delayed progressive enhancement. Our evaluation must therefore take into consideration a combination of all morphological data and those data derived from kinetics [2–13] (Figs. 9.14, 9.15, 9.16 and 9.17).

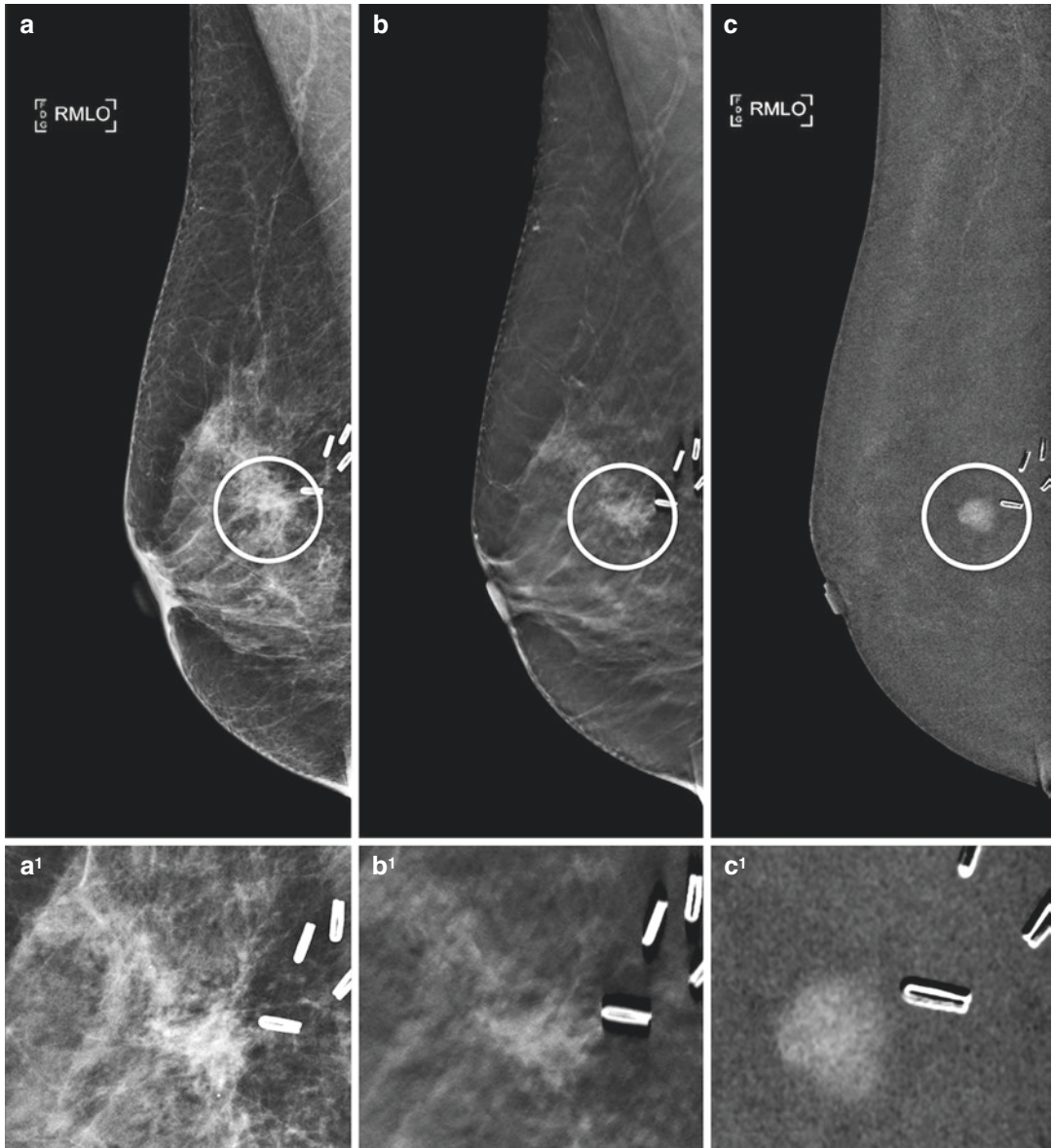


**Fig. 9.11** Homogeneous enhancement in a malignant lesion (CDI); (a) medio-lateral oblique low-energy view with magnification (a<sup>1</sup>); (b) tomosynthesis slice with magnification (b<sup>1</sup>); (c) medio-lateral oblique recombined CEDM view with magnification (c<sup>1</sup>)



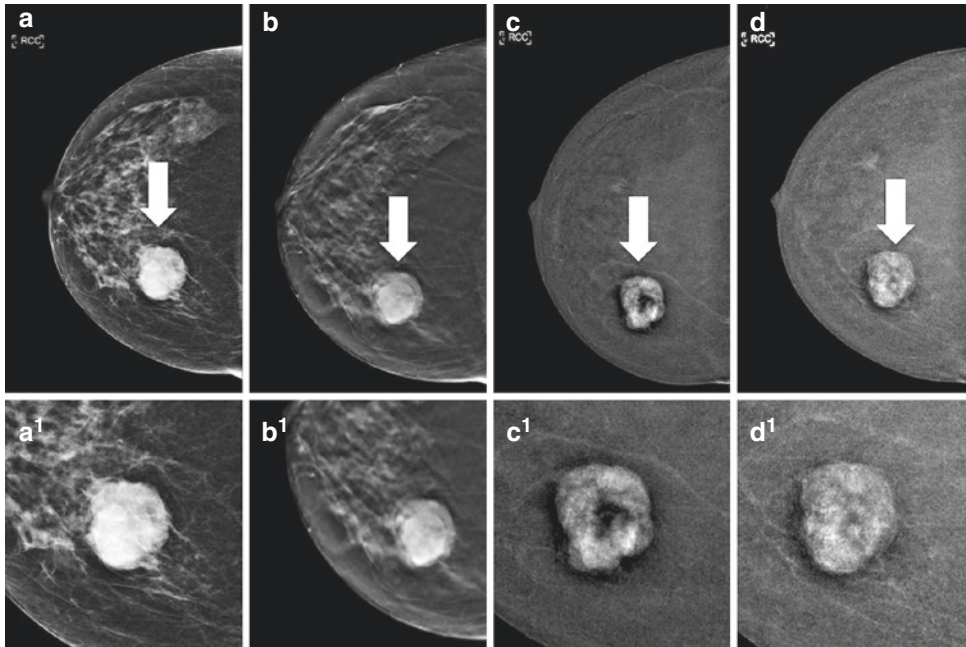


**Fig. 9.12** Heterogeneous enhancement in a malignant lesion (CDI); (a) cranio-caudal low-energy view with magnification (a<sup>1</sup>); (b) tomosynthesis slice with magnifi-

cation (b<sup>1</sup>); (c) cranio-caudal recombined early CEDM view with magnification (c<sup>1</sup>); (d) cranio-caudal recombined late CEDM view with magnification (d<sup>1</sup>)

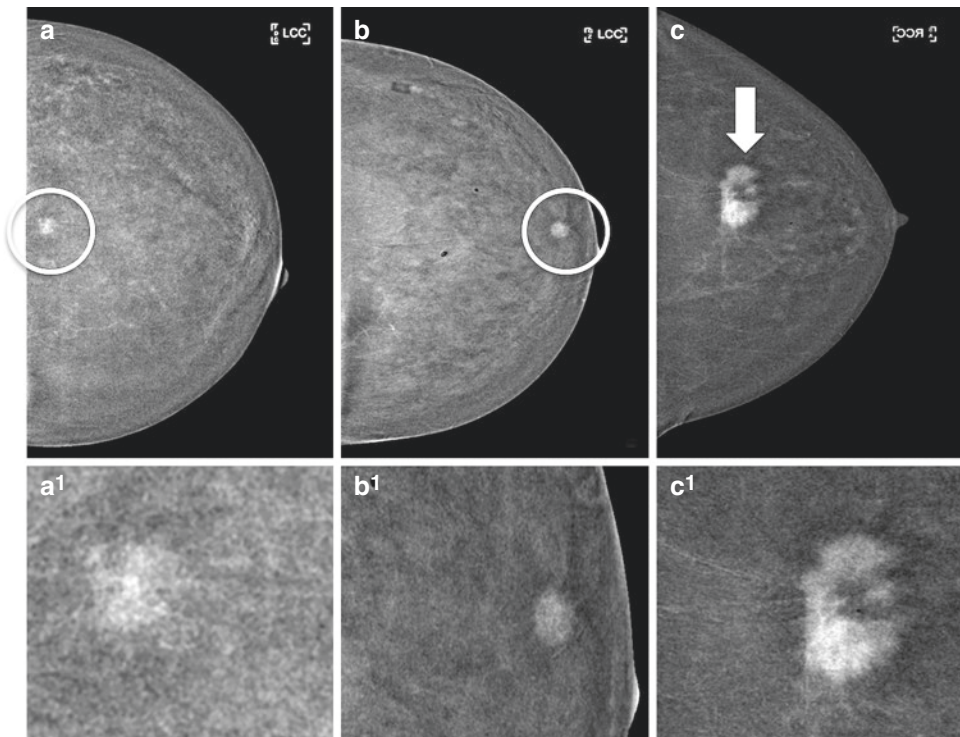


**Fig. 9.13** Three mass lesions with different degrees of intensity of enhancement; (a) cranio-caudal recombined CEDM view with magnification (a<sup>1</sup>) shows a mass with faint enhancement; (b) cranio-caudal recombined CEDM

view with magnification (b<sup>1</sup>) shows a mass with moderate enhancement; and (c) cranio-caudal recombined CEDM view with magnification (c<sup>1</sup>) shows a mass with intense enhancement

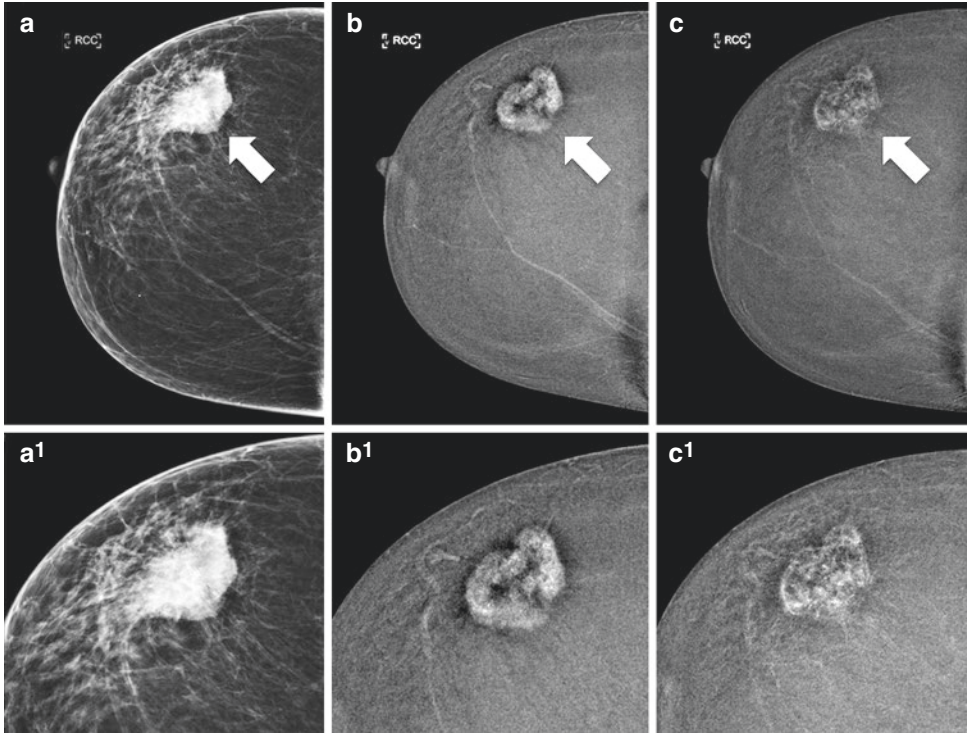


**Fig. 9.14** CEDM study in a 62-year-old woman with an invasive ductal carcinoma of the right breast. (a) Cranio-caudal low-energy view with magnification (a<sup>1</sup>); (b) cranio-caudal early recombined image with magnification (b<sup>1</sup>) shows a mass

with heterogeneous enhancement in the right upper outer breast. (c) Cranio-caudal late recombined view with magnification (c<sup>1</sup>) shows a rapid washout of the mass with less intensity of enhancement in this late view than in the early view

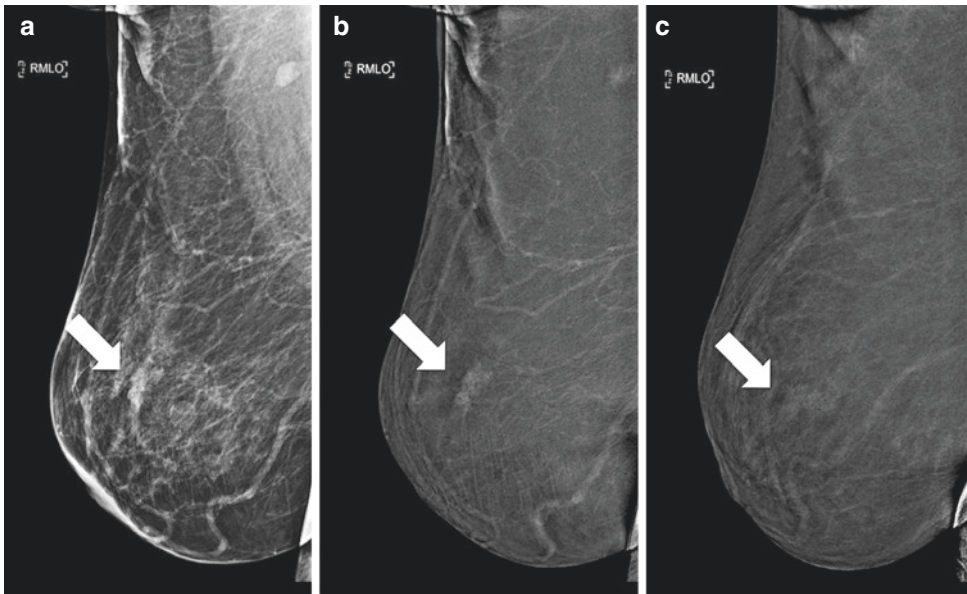


**Fig. 9.15** CEDM study in a 51-year-old woman with a papillary lesion in the right breast. (a, d) Medio-lateral oblique and cranio-caudal low-energy views; (b, e) medio-lateral oblique and cranio-caudal early recombined

images show a 2.0 cm oval mass with intense enhancement in the right central outer breast; (c, f) medio-lateral oblique and cranio-caudal late views shows less intensity of enhancement of the lesion during washout



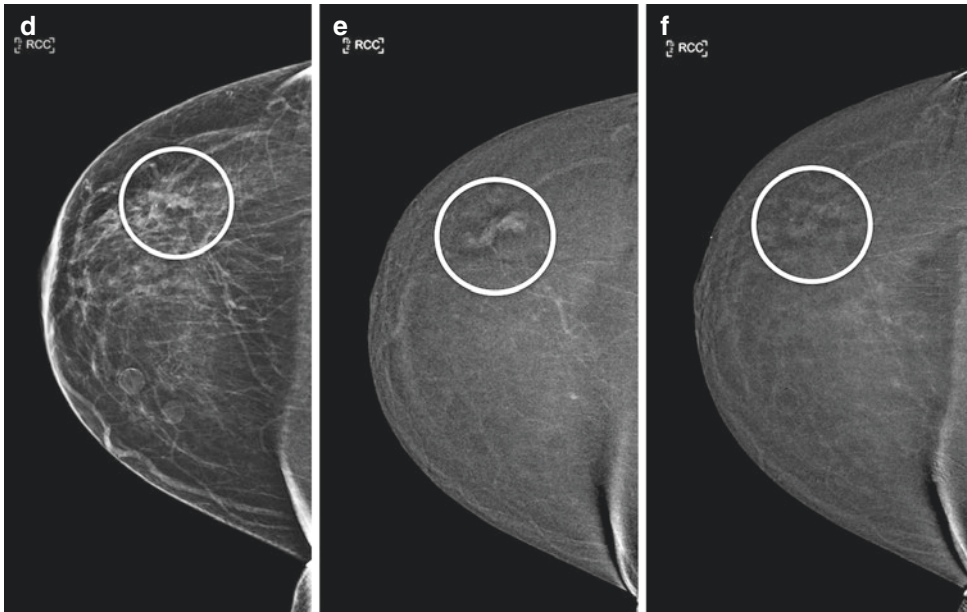


**Fig. 9.15** (continued)

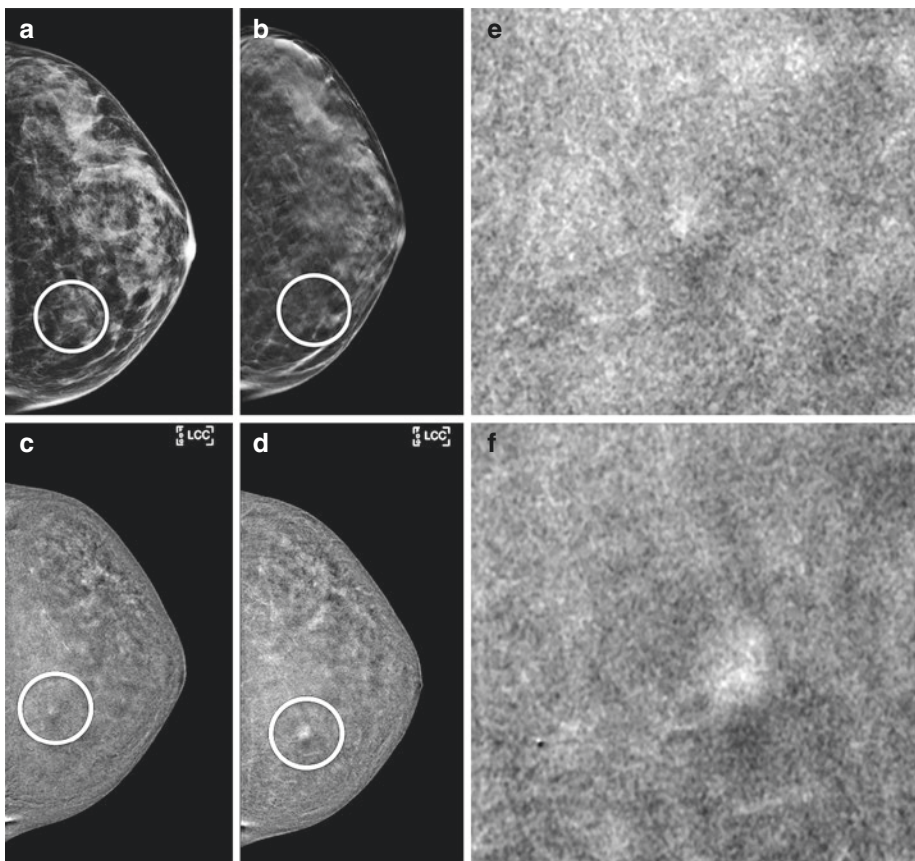


**Fig. 9.16** CEDM study in a 48-year-old woman with a fibroadenoma in the left lower inner breast. **(a)** Cranio-caudal low-energy view; **(b)** cranio-caudal tomosynthesis slice; **(c)** cranio-caudal early recombined image with

magnification **(e)**; **(d)** cranio-caudal late recombined image with magnification **(f)** showing progressive enhancement of the lesion increasing over time

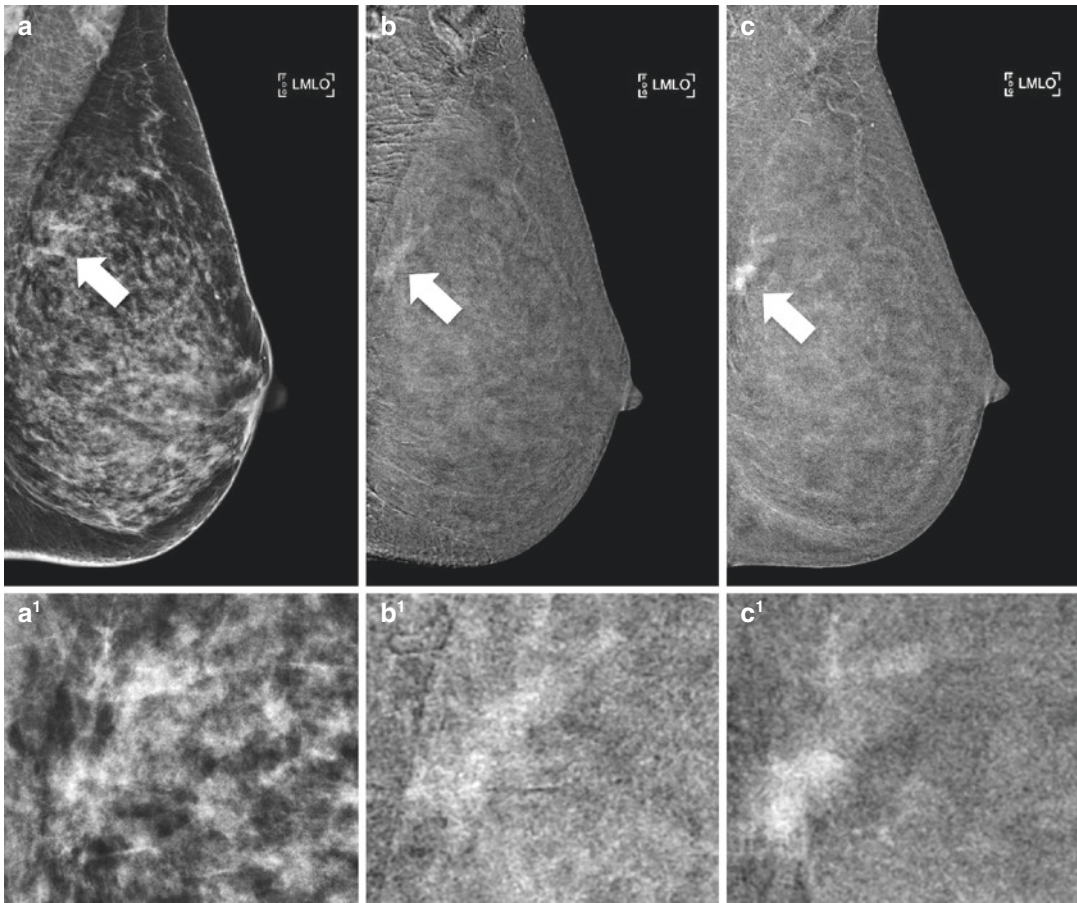


**Fig. 9.17** CEDM study in a 50-year-old woman with a lobular carcinoma in the left upper outer breast. (a) Medio-lateral oblique low-energy view, with magnification (a<sup>1</sup>); (b) medio-lateral oblique early recombined image showing a mass with heterogeneous enhance-

ment, ill-defined margins and moderate enhancement in the left upper outer breast, with magnification (b<sup>1</sup>); (c) medio-lateral oblique late recombined images showing progressive enhancement of the malignant mass

## 9.4 Non-mass Enhancement

According to the fifth edition of the *ACR BI-RADS Atlas*, non-mass enhancement (NME) is defined as an area of enhancement that is distinct from the surrounding parenchyma, larger than a focus but without space-occupying effect features. NME shows stippled or patchy normal gland tissue or fat inside. It is neither a 3D mass nor does it have distinct features of a mass, and it is typically interspersed with non-enhancing fatty or glandular tissue. NME is usually not detected in pre-contrast images, even when correlated with post-contrast images, and it follows the

distribution of glandular tissue. This imaging entity is unique to MRI and CEDM and is not usually detected by mammography and US. NME refers to an enhancing abnormality that is separate from background parenchymal enhancement (BPE), which is a hormonal mediated enhancement of healthy breast tissue. The most common causes of NME are fibrocystic changes, focal adenosis, inflammatory changes, hormonal stimulation and intraductal or diffuse cancer, particularly invasive lobular carcinoma.

Non-mass enhancement is characterized by its distribution within the breast as well as its internal enhancement patterns.

Distribution descriptors for NME in CEDM are similar to the distribution descriptors in MRI and are characterized as:

- Focal area
- Linear
- Segmental
- Regional
- Multiregional
- Diffuse

In the revised new lexicon [1], the terms “linear” and “linear branching” replace “ductal” as descriptors to describe enhancement in a line, with or without branching (Fig. 9.18). The remaining descriptors are unchanged in the lexicon (Table 9.3).

Focal NME is defined as a single small, confined abnormal enhancing area occupying less than 25% of a given breast quadrant. In focal NME, fat or normal glandular tissue is generally interspersed between the abnormally enhancing components; this presentation differs from that of a focus (Fig. 9.19).

Linear NME is described as an enhancement along a line that does not conform to a ductal pattern, and it can be seen as a sheet rather than a line or may extend across the breast. This pattern of NME is considered suspicious for cancer and is usually suggestive of ductal carcinoma in situ (DCIS); however, it is also seen in atypical ductal hyperplasia, lobular carcinoma in situ and other benign findings (Fig. 9.20).

Segmental NME is a triangular or wedge-shaped area of enhancement with its apex directed towards the nipple, and it usually represents the substantial involvement of a single branching duct system (Fig. 9.21).

Regional NME is defined as the involvement of more than 25% of a quadrant of the breast, not conforming to a ductal distribution, being patchy or geographic in appearance and lacking convex borders.

It is more likely to be associated with benign lesions such as fibrocystic changes.

Multiregional NME is an enhancement that involves large tissue volumes and is separated by either normal breast tissues or fat. Multiregional NME may represent benign changes and is most

often attributable to background enhancement. However, when multiple regional distribution of enhancement is seen unilaterally, it is a feature of a multicentric breast carcinoma, such as invasive ductal carcinoma (IDC) or invasive lobular carcinoma (ILC) (Fig. 9.22).

Diffuse NME is defined as widely scattered yet more or less evenly distributed enhancements appearing through the breast fibroglandular tissue.

Internal enhancement patterns of NME in CEDM are similar to those patterns used in MRI and are characterized as (Fig. 9.23):

- Homogeneous
- Heterogeneous
- Clumped
- Clustered ring

The terms “homogeneous” and “heterogeneous” have similar definitions for both masses and NME. In particular, homogeneous enhancement is a uniform enhancement pattern that tends to be confluent and separated by areas of normal breast parenchyma or fat. It is rarely observed by CEDM. Heterogeneous enhancement is a more commonly observed pattern seen in CEDM; it is defined as a non-uniform enhancement in a random pattern and is considered suspicious of malignancy.

Clumped enhancement patterns appear as an aggregate of enhanced masses or foci that may appear confluent, without a shape or margin to be defined as a mass (Fig. 9.24).

Clumped enhancement is defined as a cobblestone pattern of enhancement or beaded enhancement and appears as grape-like clusters that are well-differentiated from BPE and multiple masses, in which the masses are not spatially continuous or independent.

In CEDM, like in MRI, this pattern is suspicious for cancer, which is typically DCIS because it appears as irregularly heaped-up tumour cells expanding a duct. Indeed a segmental distribution is more suggestive of malignancy [14].

The clustered ring enhancement pattern is a predominantly peripheral enhancement and is similar to rim enhancement for masses. This pattern shows less specificity by CEDM than by



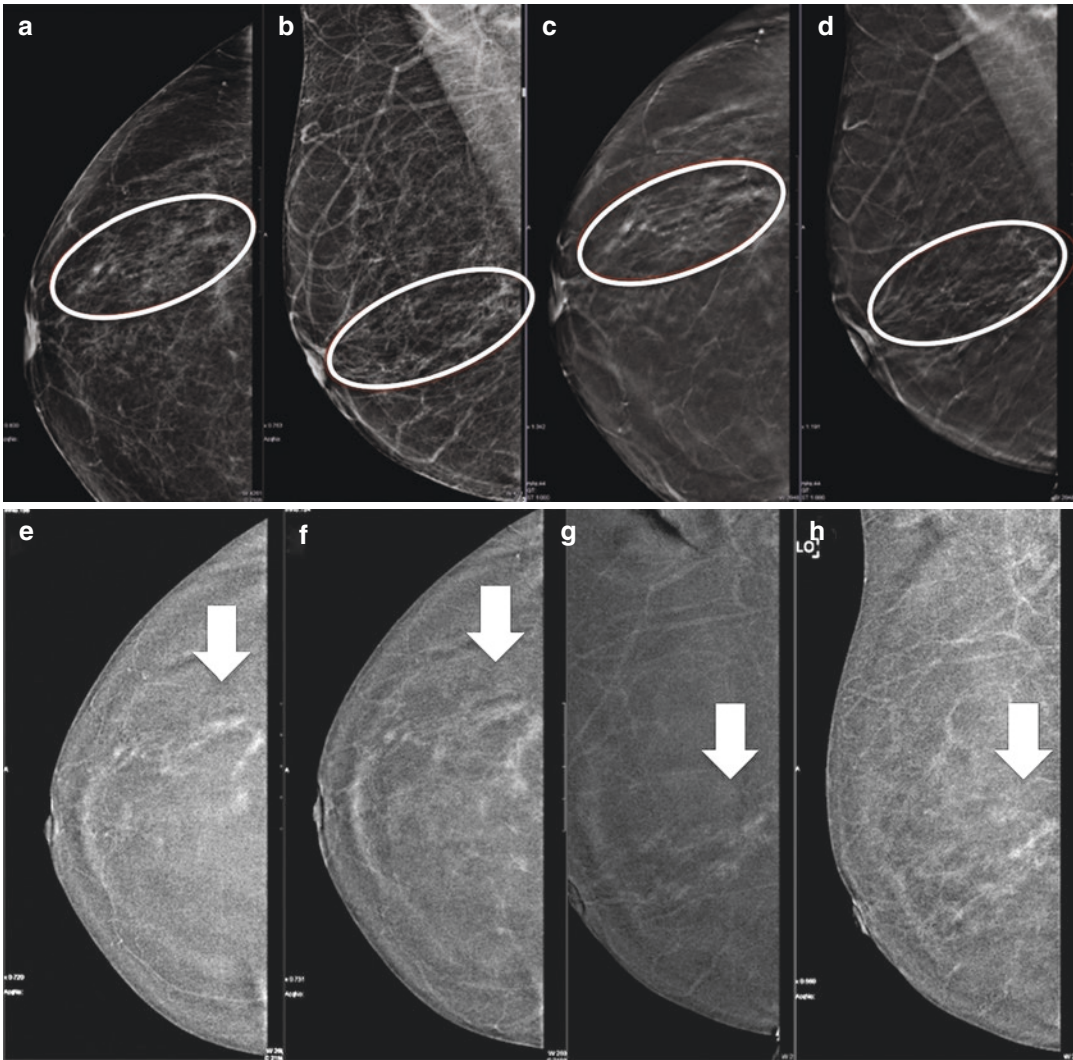


**Fig. 9.18** Pre-surgical staging in a patient with a BI-RADS 5 lesion in the lower outer quadrant of the right breast, already biopsied. (a–b) Mammograms in CC and MLO projections show a cluster of fine pleomorphic microcalcifications with a linear distribution (white circle). (c–d) DBT in the CC and MLO projection better enhances the microcalcifications distribution and pattern (white circle). (e–f) CEDM in the early

phase and late phase in the CC projection. (g–h) CEDM in the early and late phase in the MLO projection. The examination clearly depicts a mild and diffuse enhancement in the lower outer quadrant of the right breast, tracing the location of the microcalcifications: the enhancement kinetics is progressive, as demonstrated by the comparison between the two phases. The histological results showed a CDIS

**Table 9.3** Non-mass enhancement morphology descriptors

Spatial Distribution	Internal Enhancement	Symmetry
Focal	Homogeneous	Symmetric
Linear	Heterogeneous	Asymmetric
Segmental	Clumped	
Regional	Clustered ring	
Multiregional		
Diffuse		

MRI, with many false-positive results related to inflammatory alterations of the breast.

Clustered ring enhancement pattern describes “minute ring enhancements” seen on high spatial resolution sequences within an area of heterogeneous NME. The pathologic processes most frequently associated with this enhancement pattern are ductal carcinoma in situ and invasive cancers associated with ductal carcinoma in situ. One possible pathophysiologic explanation for this

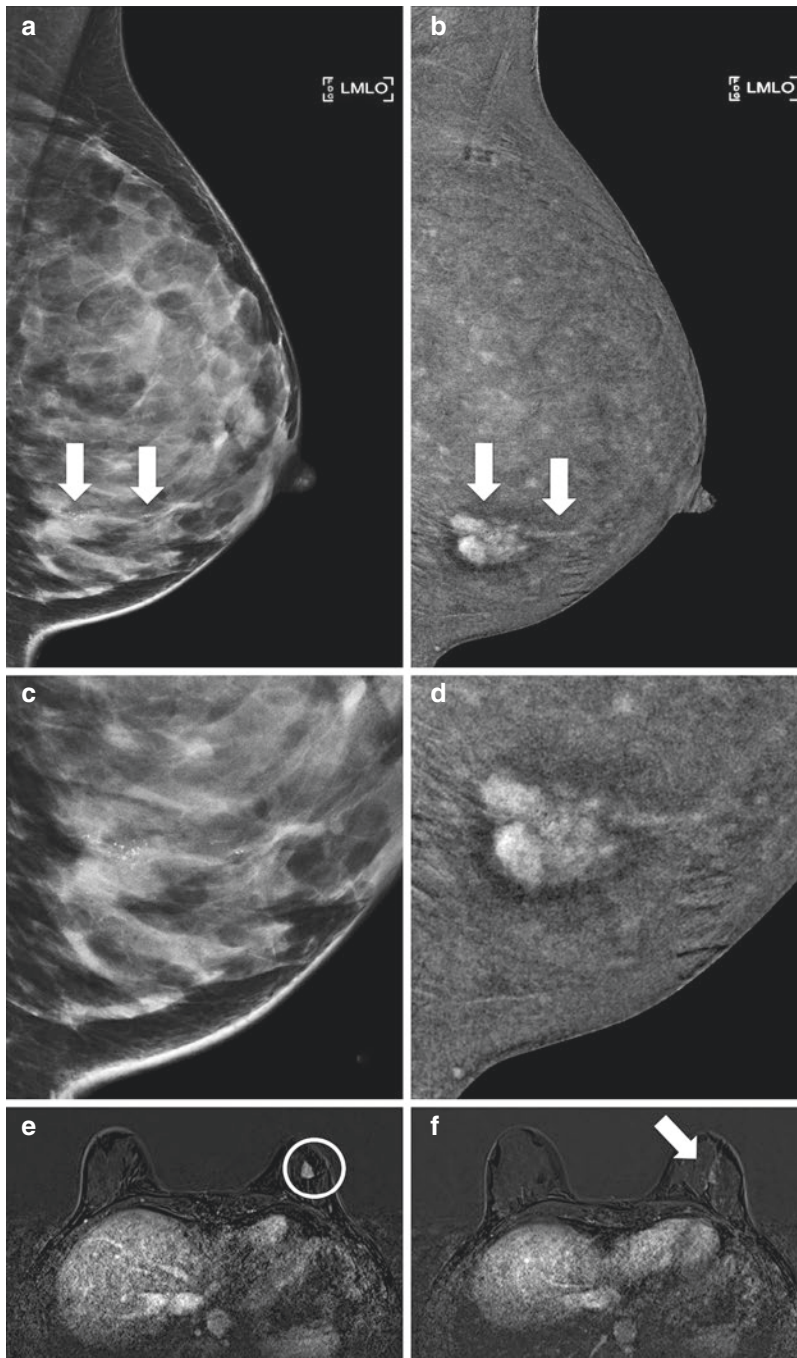


**Fig. 9.19** CEDM and MRI studies in a 58-year-old woman with an invasive (IDC) and in situ (DCIS) ductal carcinoma of the left breast. (a) Mediolateral oblique low-energy view, with magnification (c); (b) mediolateral oblique early recombined image with magnification (d) showing a mass with heterogeneous enhancement in the left lower outer breast associated superior and at the

front of location with a linear non-mass enhancement. (e) Post-contrast axial T1 MRI slice showing the mass enhancement; (f) post-contrast axial T1 MRI slice showing the linear non-mass enhancement cranially with respect to the mass, perfectly superimposable with CEDM images. The mass depicts the IDC component, and the linear NME depicts the associated DCIS

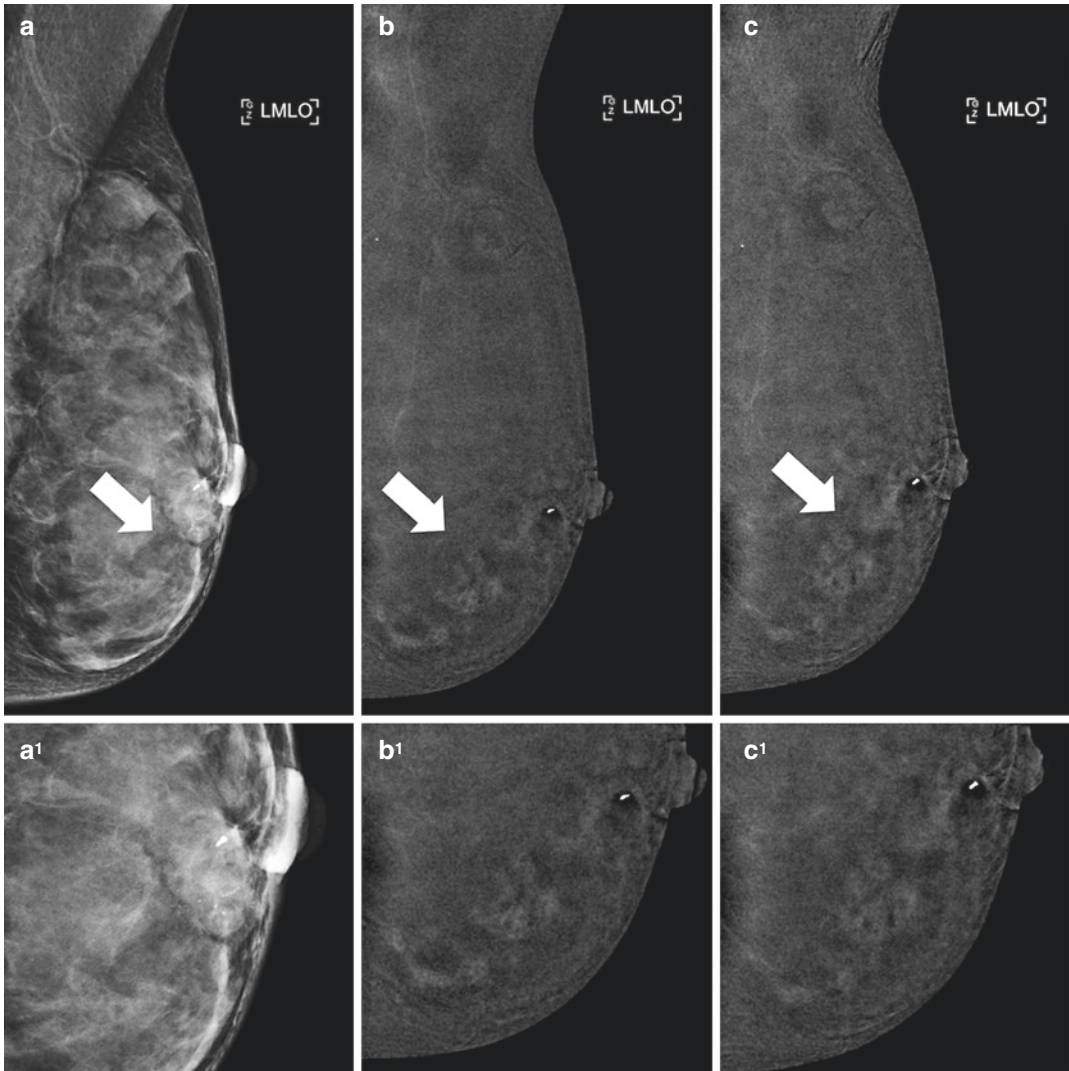


**Fig. 9.20** Regional non-mass enhancement in the left lower outer breast. (a) Medio-lateral oblique low-energy view, with magnification (a<sup>1</sup>) showing fine linear microcalcifications and a post-biopsy marker; (b) medio-lateral oblique early recombined image with magnification (b<sup>1</sup>); (c) medio-lateral oblique late recombined image with magnification (c<sup>1</sup>). This regional NME underlies a multi-focal CDIS



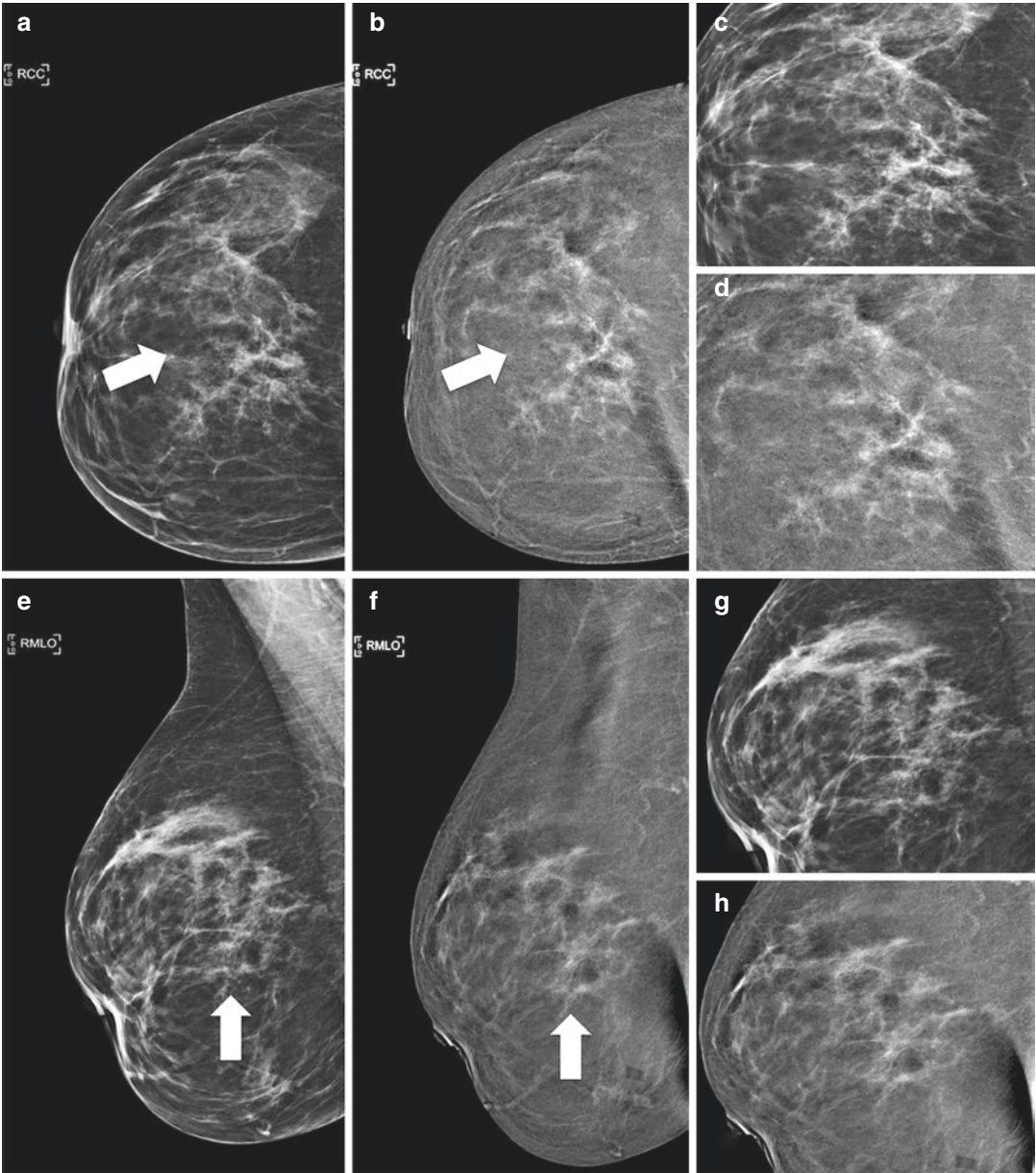


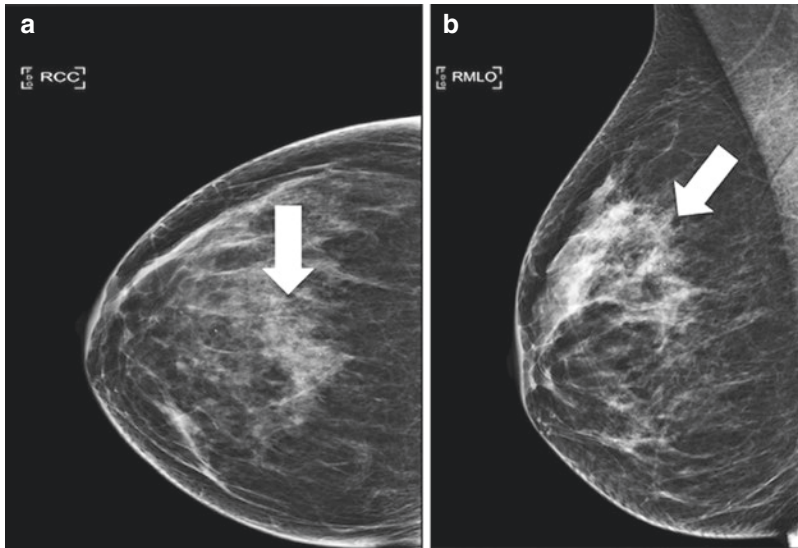
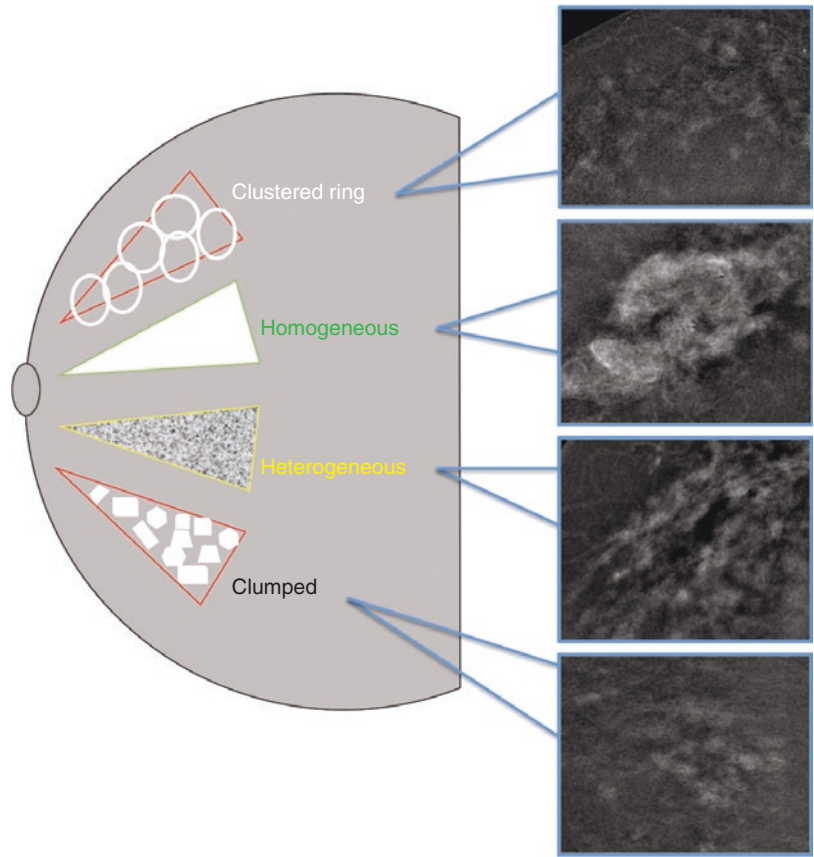
**Fig. 9.21** One example of multiregional non-mass enhancement in the right upper outer and central breast; (a, e, c, g) cranio-caudal and medio-lateral oblique low-energy views with magnification (b, f, d, h) cranio-caudal

and medio-lateral oblique late recombined images with magnification showing a multiregional NME that represents a multicentric CDI

finding is that an intraductal carcinoma with an abundant blood supply exhibits a washout kinetic pattern, whereas contrast media that have accumulated in the periductal stroma demonstrate a more persistent kinetic pattern. Tozaki and colleagues [15] described this pattern in 63% of

malignant lesions, compared with only 4% of benign lesions. The specificity of this pattern for malignancy was found to be 63%, and a washout kinetics pattern was seen in 55% of malignant lesions with clustered ring enhancement. The authors also showed that the combination of

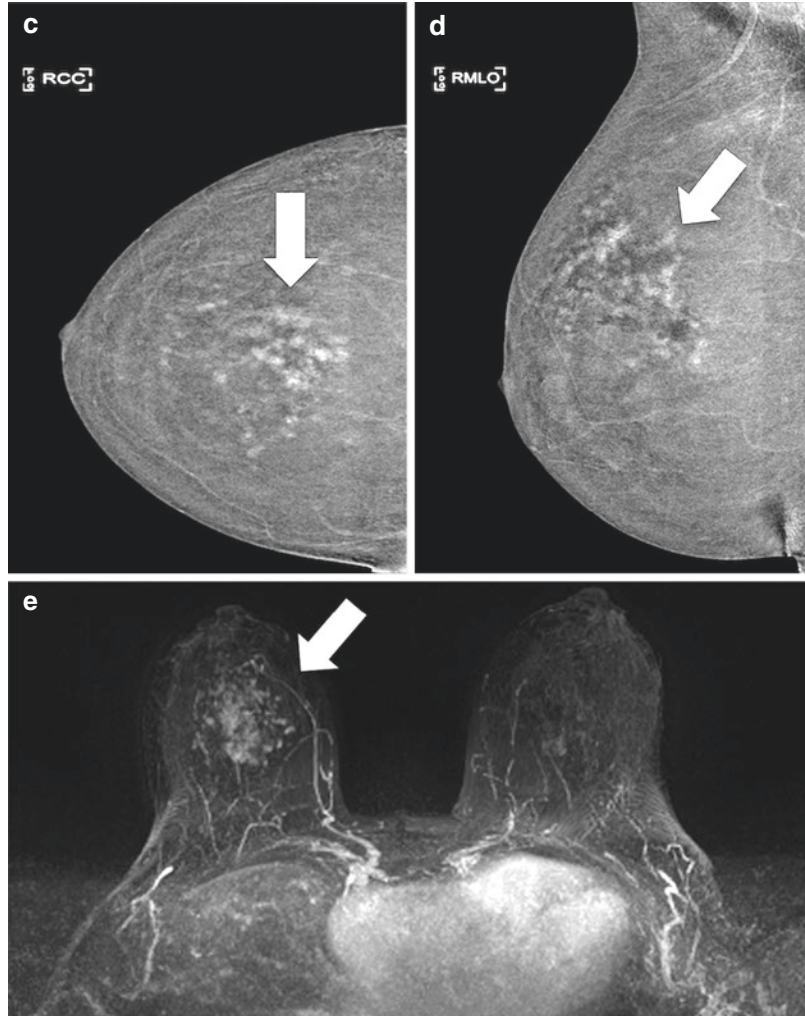
**Fig. 9.22** Distribution descriptors for NME in CEDM



**Fig. 9.23** One example of clumped non-mass enhancement in the right upper and central breast; (a, b) cranio-caudal and medio-lateral oblique low-energy views; (c, d) cranio-caudal and medio-lateral oblique recombined

images showing a clumped NME that represents a multicentric CDI and CDIS; (e) MRI maximum intensity projection (MIP) reconstruction shows a clumped NME exactly overlapping CEDM images



**Fig. 9.23** (continued)

clustered ring enhancement and a clumped internal architecture had a statistically significant association with malignancy.

Another important element helpful for further characterization of NME in CEDM is the symmetry of the enhancement areas between both breasts.

Symmetric enhancement is described as similar, mirror distribution enhancement in both breasts, while more pronounced enhancement in one breast compared to the other is seen in asymmetric NME enhancement.

Bilateral symmetric NME in any distribution is highly suggestive of benign changes or part of the background parenchymal enhancement, while markedly asymmetric enhancement is con-

sidered suspicious of malignancy [2–4, 16–25] (Fig. 9.25).

In summary, morphology descriptors of NME, which are more suggestive of benign lesions in CEDM, are a symmetric distribution, multiple regions or diffuse distribution and homogeneous internal enhancement. However, the descriptors that are related to malignancy are an asymmetric NME in a focal, linear, segmental or regional distribution with heterogeneous or clumped internal enhancement.

NMEs are characterized by their distribution within the breast as well as their internal enhancement patterns, which, when combined, may contribute to improved diagnosis. However, similar to

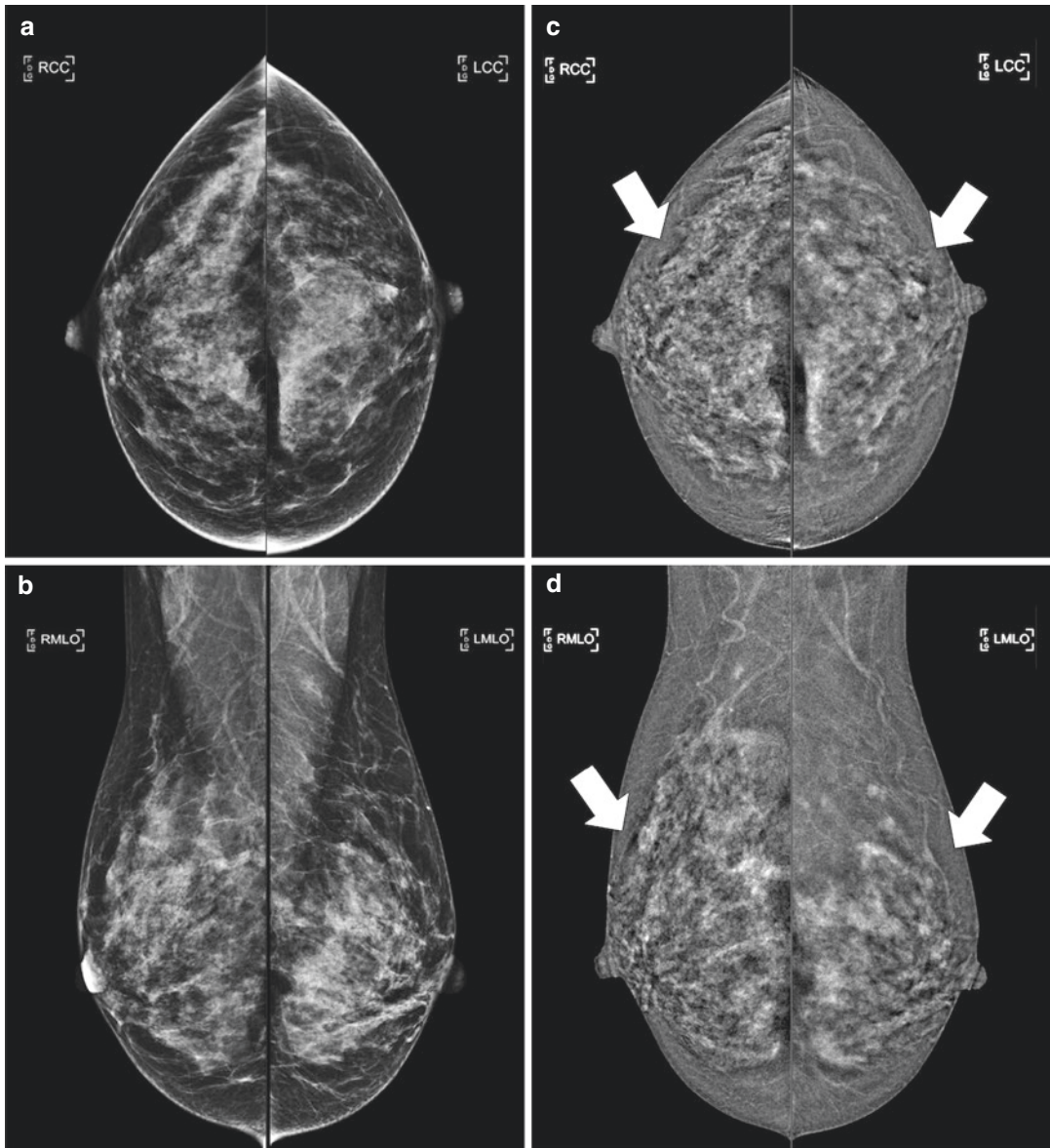


**Fig. 9.24** An example of bilateral symmetric non-mass enhancement in a patient with a heterogeneous dense breast; (a, b) cranio-caudal and medio-lateral oblique

low-energy views; (c, d) cranio-caudal and medio-lateral oblique recombined images showing a symmetric NME due to background parenchymal enhancement

MRI, it is more difficult to characterize a NME by CEDM with respect to a mass because the evaluation of enhancement is more subjective and the morphology descriptors give more false-positive results; therefore, we recommend adding another diagnostic tool for the characterization of NME.

When we see an area of NME by CEDM, it is very important to analyse the low-energy

images to search for abnormalities such as microcalcifications, which may be associated with the area corresponding to the NME in the SI. An important advantage of CEDM over MRI is the potential to identify intraparenchymal microcalcifications in the LE and to evaluate their morphology and distribution and eventual enhancement patterns in the SI. This

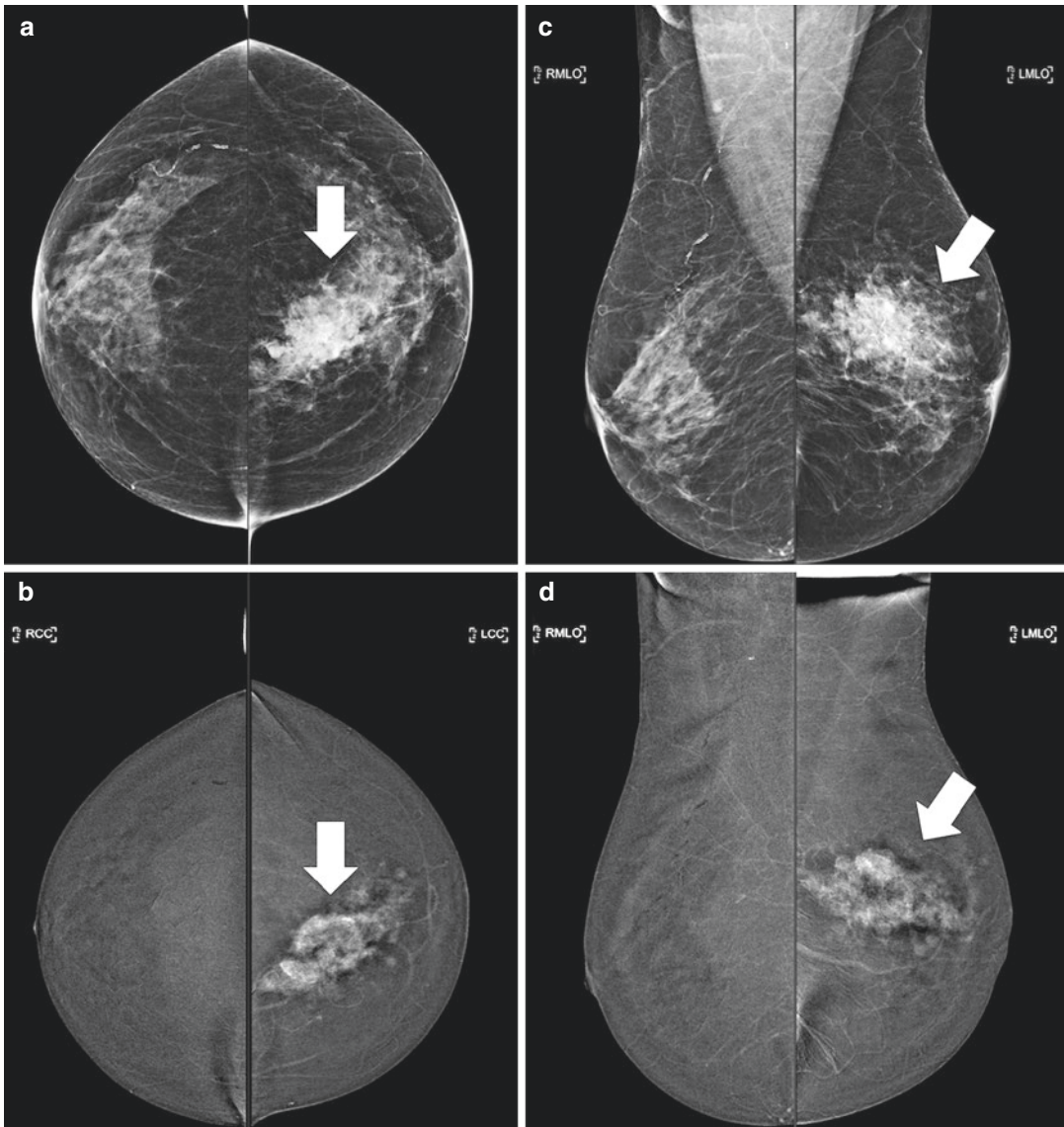


**Fig. 9.25** An example of marked asymmetric non-mass enhancement; (**a, c**) cranio-caudal and medio-lateral oblique low-energy views; (**b, d**) cranio-caudal and

medio-lateral oblique recombined images showing an asymmetric heterogeneous regional NME due to an invasive carcinoma

also facilitates any subsequent biopsy procedures (Table 9.4).

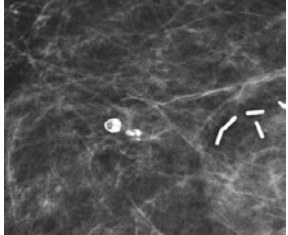
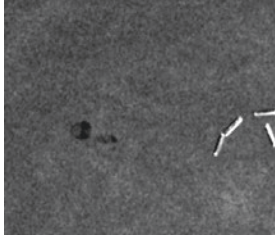
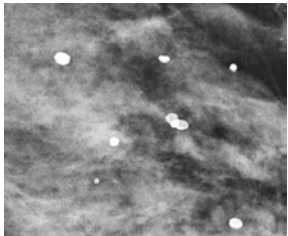
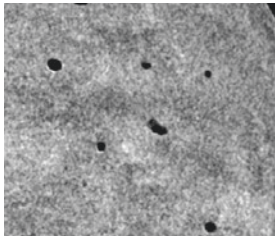
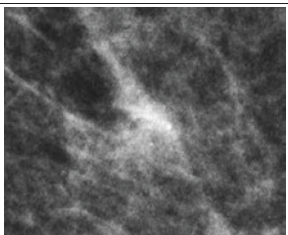
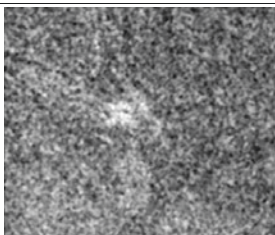
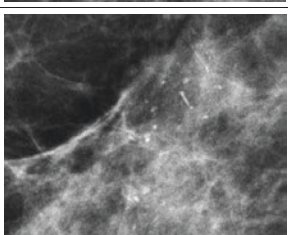
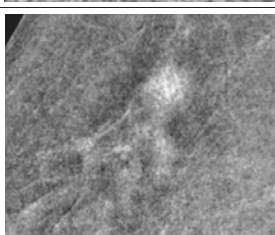
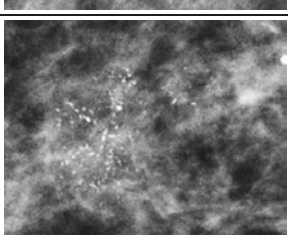
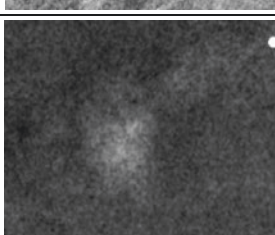
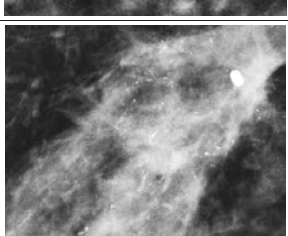
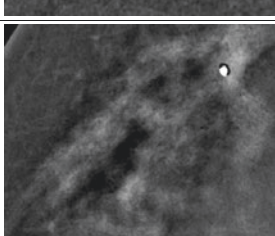
In conclusion, the preliminary results from the sparse literature available on CEDM, encompassing studies by Kamal et al. and Knogler et al. [2–4], have concluded that the MRI BI-RADS descriptors of contrast-enhancing lesions can be applied for the morphologic analysis of enhancing lesions observed by CEDM.

Good differentiation between benign and malignant lesions is possible with the application of the MRI BI-RADS descriptors to CEDM. Partial discrepancies in interpretation do not influence the final BI-RADS score.

However, studies with large patient numbers investigating contrast kinetics by CEDM are necessary.



**Table 9.4** Correlation between microcalcification morphology in the LE and eventual enhancement pattern in the SI

Low-Energy Images	Recombined Images	Description
		<p>Benign calcifications: dystrophic calcifications, coarse irregular 'lava-shaped'. They are seen in the irradiated breast and show no enhancement in the recombined images.</p>
		<p>Benign calcifications: lucent centered round or oval calcifications that range from under 1 mm to over a centimetre. They are the result of fat necrosis or calcified debris in ducts and show no enhancement in the recombined images.</p>
		<p>Suspicious calcifications: amorphous or indistinct calcifications 'without a clearly defined shape or form', showing faint enhancement in recombined images. Biopsy reveals a DCIS.</p>
		<p>Suspicious calcifications: coarse heterogeneous, formerly called coarse granular; irregular and conspicuous calcifications showing moderate enhancement in the recombined images. Biopsy reveals a B3 lesion (ADH).</p>
		<p>High probability of malignancy: fine pleomorphic calcifications that vary in size and shape and are usually more conspicuous than amorphous calcifications, showing moderate enhancement in the recombined images. Biopsy reveals an invasive carcinoma.</p>
		<p>High probability of malignancy: fine linear branching Thin, linear or curvilinear irregular calcifications. Their appearance suggests filling of the lumen of a duct, i.e., 'casting' calcifications, showing intense enhancement in the recombined images. Biopsy reveals an IDC.</p>

## References

- Morris EA, Comstock CE, Lee CH, et al. ACR BI-RADS<sup>®</sup> magnetic resonance imaging. In: D'Orsi CJ, editor. ACR BI-RADS<sup>®</sup> atlas, breast imaging reporting and data system. Reston, VA: American College of Radiology; 2013.
- Mohamed Kamal R, Hussien Helal M, Wessam R, Mahmoud Mansour S, Godda I, Alieldin N. Contrast-enhanced spectral mammography: impact of the qualitative morphology descriptors on the diagnosis of breast lesions. *Eur J Radiol.* 2015;84(6):1049–55.
- Kamal RM, Helal MH, Mansour SM, et al. Can we apply the MRI BI-RADS lexicon morphology descriptors on contrast-enhanced spectral mammography? *Br J Radiol.* 2016;12:20160157.
- Knogler T, et al. Application of BI-RADS descriptors in contrast-enhanced dual-energy mammography: comparison with MRI. *Breast Care (Basel).* 2017;12(4):212–6. <https://doi.org/10.1159/000478899>.
- Berg WA, Campassi C, Langenberg P, Sexton MJ. Breast imaging reporting and data system inter- and intraobserver variability in feature analysis and final assessment. *AJR Am J Roentgenol.* 2000;174:1769–77.
- Timmers JMH, van Doorne-Nagtegaal HJ, Zonderland HM, van Tinteren H, Visser O, Verbeek ALM, et al. The breast imaging reporting and data system (BI-RADS) in the Dutch breast cancer screening programme: its role as an assessment and stratification tool. *Eur Radiol.* 2012;22:1717–23.
- Kuczyrska E, Heinze-Paluchowska S, Hendrick E, Dyczek S, Herman K, Blecharz P, et al. Comparison between breast MRI and contrast enhanced spectral mammography. *Med Sci Monit.* 2015;21:1358–67.
- Kuhl C. Concepts for differential diagnosis in breast MR imaging. *Magn Reson Imaging Clin N Am.* 2006;14:305–28.
- Millet I, Pages E, Hoa D, Merigeaud S, Doyon FC, Prat X, et al. Pearls and pitfalls in breast MRI. *Br J Radiol.* 2012;85:197–207.
- Liberman L, Mason G, Morris EA, Dershaw DD. Does size matter? Positive predictive value of MRI-detected breast lesions as a function of lesion size. *AJR Am J Roentgenol.* 2006;186:426–30.
- Schnall MD, Blume J, Bluemke DA, De Angelis GA, De Bruhl N, Harms S, et al. Diagnostic architectural and dynamic features at breast mr imaging: multicenter study. *Radiology.* 2006;238:42–53.
- Tozaki M, Igarashi T, Fukuda K. Positive and negative predictive values of BI-RADS-MRI descriptors for focal breast masses. *Magn Reson Med Sci.* 2006;5:7–15.
- Nunes LW, Schnall MD, Siegelman ES, Langlotz CP, Orel SG, Sullivan D, et al. Diagnostic performance characteristics of architectural features revealed by high spatial-resolution MR Imaging of the breast. *AJR Am J Roentgenol.* 1997;169:409–15.
- Agrawal G, et al. Significance of breast lesion descriptors in the ACR BI-RADS MRI lexicon. *Cancer.* 2009;115(7):1363–80.
- Tozaki M, Igarashi T, Fukuda K. Breast MRI using the VIBE sequence: clustered ring enhancement in the differential diagnosis of lesions showing non-masslike enhancement. *AJR Am J Roentgenol.* 2006;187(2):313–21.
- Yabuuchi H, Matsuo Y, Kamitani T, Setoguchi T, Okafuji T, Soeda H, et al. Non-mass-like enhancement on contrast-enhanced breast MR imaging: lesion characterization using combination of dynamic contrast-enhanced and diffusion-weighted MR images. *Eur J Radiol.* 2010;75:e126–32.
- El Khoury M, Lalonde L, David J, Labelle M, Mesurolle B, Trop I. Breast imaging reporting and data system (BI-RADS) lexicon for breast MRI: interobserver variability in the description and assignment of BI-RADS category. *Eur J Radiol.* 2015;84:71–6.
- Gity M, Moghadam KG, Halali AH, Shakiba M. Association of different MRI BI-RADS descriptors with malignancy in non mass-like breast lesions. *Iran Red Crescent Med J.* 2014;16:e26040.
- Kuhl C. The current status of breast MR imaging. Part I. Choice of technique, image interpretation, diagnostic accuracy, and transfer to clinical practice. *Radiology.* 2007;244:356–78.
- Mahoney MC, Gatsonis C, Hanna L, DeMartini WB, Lehman C. Positive predictive values of BI-RADS MR imaging. *Radiology.* 2012;264:51–8.
- Lewin J, Larke F, Hendrick RE. Dual-energy contrast-enhanced digital subtraction mammography: development and clinical results of a new technique for breast cancer detection. *Radiology.* 2001;221:339.
- Dromain C, Balleyguier C. Contrast-enhanced digital mammography. In: Bick U, Diekmann F, editors. *Digital mammography.* Berlin: Springer; 2010. p. 187–98.
- Fallenberg EM, Dromain C, Diekmann F, Engelken F, Krohn M, Singh JM, et al. Contrast-enhanced spectral mammography versus MRI: initial results in the detection of breast cancer and assessment of tumor size. *Eur Radiol.* 2014;24(1):256–64.
- Morris EA. Illustrated breast MR lexicon. *Semin Roentgenol.* 2001;36:238–49.
- Łuczyska E, Niemiec J, Hendrick E, et al. Degree of enhancement on contrast enhanced spectral mammography (CESM) and lesion type on mammography (MG): comparison based on histological results. *Med Sci Monit.* 2016;22:3886–93.





In this chapter, we will focus on the pitfalls and limitations of contrast-enhanced digital mammography (CEDM) based on our clinical experience and the current literature.

A brief summary of the main points to be analysed in this chapter has been outlined in Table 10.1.

**Table 10.1** Summary of the main points analysed in the chapter

	Pitfalls and limitations of CEDM
1	Radiation exposure
2	Contrast-related factors
	<i>Possibility of allergic reactions</i>
	<i>Absolute or relative contraindications in the case of underlying medical illness</i>
	<i>Fasting required</i>
3	Lack of technology to biopsy the abnormal areas of enhancement
4	False negatives
	<i>Limited assessment of posterior extent of masses</i>
	<i>Poorly vascularized tumours</i>
	<i>Malignant microcalcifications with no underlying mass</i>
5	False positives
6	Background parenchymal enhancement
7	Lesser degree of diagnostic performance in breast prosthesis

C. Boeri (✉) · V. Selvi · C. Checcucci  
Diagnostic Senology Unit, Department of Radiology,  
Azienda Ospedaliero Universitaria Careggi,  
Florence, Italy  
e-mail: [boeric@aou-careggi.toscana.it](mailto:boeric@aou-careggi.toscana.it)

## 10.1 Radiation Exposure

Dual-energy contrast-enhanced digital mammography acquisitions are based on the *k*-edge of iodine, which is at approximately 33 kilo-electron volts (keV). For each mammographic view, a low-energy exposure (25–33 keV) and a high-energy exposure (45–49 keV) are sequentially obtained [1]. Subsequently, a recombination algorithm is used to generate a subtracted image that gives an image of the relative distribution of iodine in the breast while fully subtracting the adipose and fibroglandular tissues [1, 2]. In the recombined image, mainly the iodine in the lesions with neoangiogenesis is visualized [3].

For low-energy exposure, Silver (Ag) or rhodium (Rh) filters should be used; for high-energy exposure, it is preferable to shift to copper (Cu) filters, which allow the absorption of soft unnecessary radiation and preserve the photons around the iodine absorption energy [2].

As expected, CEDM would involve a higher radiation dose than conventional mammography; this increase has been documented between 20 and 80% greater than that of conventional mammography (Table 10.2). The dose is frequently calculated as AGD, which is the acronym for Average Glandular Dose (unit of measure: milligray: mGy). Despite the increase, the additional radiation exposure was still below the dose limit of 3 mGy set by the Mammography Quality Standards Act (MSQA) guidelines [4–6].

**Table 10.2** CEDM radiation dose literature review: CEDM radiation dose has been documented to be between 20 and 80% higher than that of conventional mammography (AGD, average glandular dose; CBT compressed breast thickness; FFDM full field digital mammography)

Author	Lewin J. M. et al. [23]	Dromain C. et al. [22]	Badr S. et al. [3]	Houben et al. [7]
<b>Title</b>	Dual-energy contrast-enhanced digital subtraction mammography: feasibility	Dual-energy contrast-enhanced digital mammography: initial clinical results of a multireader, multicase study	Dual-energy contrast-enhanced digital mammography in routine clinical practice in 2013	Contrast-enhanced spectral mammography as a workup tool in patients recalled from breast cancer screening has low risks and might hold clinical benefits
<b>Year</b>	2003	2012	2014	2017
<b>Aim of the study</b>	Application of CEDM in patients with mammographic or clinical findings that warranted biopsy	Comparison of the diagnostic accuracy of CEDM as an adjunct to mammography (FFDM) $\pm$ ultrasonography (US) with the diagnostic accuracy of FFDM $\pm$ US alone	Description of CEDM techniques with advantages and disadvantages, review of the literature, personal clinical experience	Evaluation of additional findings by CEDM alone; considerations on advantages/disadvantages of this technique
<b>No of patients</b>	26	110	104	839
<b>CEDM AGD</b>	Not reported	Mean dose per image 0.7–3.6 mGy	Mean dose per image 2.65 mGy (1.07–4.76 mGy, SD 0.78 mGy)	Median radiation dose per complete exam 6.0 mGy (0.9–23.4 mGy)
<b>FFDM AGD</b>	Not reported	Calculated values in good agreement with published data from Wu et al. [24] (mean difference of 3%)	1.72 mGy per image ([0.74–7.82], SD 0.96 mGy)	Not calculated
<b>CBT(mm)</b>	Not reported	Not reported	Mean CBT = 56 mm	Median CBT 58.8 (range, 11–220 mm; SD, 21 mm)
<b>CEDM dose versus FFDM</b>	Increase (CEDM dose 0.7 mGy above that needed for FFDM for a 50% glandular–50% fat breast with compressed thickness of 4.5 cm)	Increase (CEDM dose 1.2 times higher than FFDM dose)	Increase (CEDM dose 1.54 times higher than FFDM dose)	Increase (CEDM dose versus FFDM dose-FFDM dose extrapolated from literature datas)

Author	Fallenberg E.M. et al. [25]	Jeukens S. et al. [8]	James J. et al. [11]	Jochelson M. et al. [10]
<b>Title</b>	Contrast-enhanced spectral mammography: does mammography provide additional clinical benefits or can some radiation exposure be avoided?	Radiation exposure of contrast-enhanced spectral mammography compared with full-field digital mammography	Breast radiation dose with CEDM compared with 2D FFDM and 3D tomosynthesis mammography	Bilateral contrast-enhanced dual-energy digital mammography: feasibility and comparison with conventional digital mammography and MR imaging in women with known breast carcinoma
<b>Year</b>	2014	2014	2017	2013
<b>Aim of the study</b>	Comparison CEDM with FFDM and combined CEDM + FFDM in terms of detection and size estimation of histologically proven breast cancers, to assess the potential to reduce radiation exposure	Measurement of the dose increase of CEDM with respect to FFDM	Comparison of radiation dose of CEDM versus FFDM and tomosynthesis (evaluation on patient-single left craniocaudal projection and using phantom)	Evaluation of the feasibility of performing CEDM and evaluation of its performance with respect to FFDM and MRI in women with known breast cancer
<b>No of patients</b>	118	47 patients underwent CEDM, 715 FFDM	173 patients underwent CEDM, 6214 FFDM	52
<b>CEDM AGD</b>	Mean dose per image 1.89 mGy Mean dose 2.80 mGy for a single CEDM exposure	Patients: mean dose $3.0 \pm 1.1$ mGy per image Phantom: mean AGD 1.6 mGy per image	Not reported	
<b>FFDM AGD</b>	Mean dose per image 1.78 mGy	Mean dose 1.55 mGy for an FFDM exposure	Patients: mean dose $1.8 \pm 0.9$ mGy per image Phantom: mean AGD 1.0 mGy per image	Not reported
<b>CBT(mm)</b>	Mean CEDM CBT = 55.4 mm (SD 12.9) (mean FFDM CBT = 53.6, SD 13.6 mm)	Mean CEDM CBT = 58.4 mm (mean FFDM CBT, 56.1 mm)	Mean CEDM CBT = 63 mm (mean FFDM CBT, 47 mm)	Not reported
<b>CEDM dose versus FFDM</b>	Not unequivocal results (CEDM dose 6.2% higher than FFDM, but in very dense breasts, AGD of CEDM was significantly lower than FFDM)	Increase (CEDM dose 81% higher than that for FFDM)	Increase (patients: CEDM dose 70% higher than that for FFDM; Non-dense phantom, compressed thickness of 4, 5 and 6 cm: CEDM Dose 37.5% and 36.2%, respectively, higher than FFDM; dense phantom, compressed thickness of 4.5 and 6 cm: CEDM doses 33.3% and 35.4% higher than FFDM, respectively)	Increase (CEDM dose 20% higher than that for routine FFDM or the equivalent of one additional view)

The benefits obtained by the additional contrast images offset the additional radiation. If we assess the lifetime attributable risk (LAR) of cancer after a single exposure from CEDM, the risk of inducing tumour development due to this increased dose is negligible. Houben et al. [7] calculated the LAR per 100,000 persons to be 0.002–0.0003% for breast cancer incidence and 0.02–0.001% for breast cancer mortality; additionally, Jeukens et al. [8] have also reported results that are consistent with these percentages.

The dose increase is primarily due to the need for dual acquisition of low- and high-energy, per CEDM image.

Notably, an increase in the thickness of the breast, which is a function of the size of the breast and the compression of the machine, leads to an increase in the dose received by the patient [8–10]. James et al. [11] reported statistical evaluations indicating that breast thickness is a major factor in the received dose. The dose given also depends on the composition of the gland (% fat, % gland) [9, 10]. In particular, James et al. [11] measured the radiation dose in both dense and non-dense phantoms at different thicknesses. Higher doses were observed in dense phantoms than in non-dense phantoms at the same compression thicknesses; the overall CEDM radiation dose (mGy) was measured as 12.5% and 35% higher in the dense phantom than in the non-dense phantom at 4.5 and 6 cm, respectively.

Fallenberg et al. [12] drew different conclusions from their study; firstly, they found that the average dose increase for a CEDM examination compared to mammography was only 6.2%. Secondly, they found that at an equal breast thickness, the AGD of CEDM decreased with increasing breast density, while the AGD of mammography increased. This trend led to the finding that the AGD of CEDM was lower than that of 2D full-field digital mammography (FFDM) in very dense breasts (BIRADS 4). The main reasons for this discrepancy may be differential exposure control leading to different exposure settings. For example, Dromain et al. and Fallenberg et al. used a prototype

CEDM unit in which exposure settings were manually set depending on breast thickness and glandularity following a table of predefined exposure values [11, 13]. However, the equipment used in more recent studies consists of commercially available imaging devices in which breast thickness is a factor for automatic exposure settings [8, 11]. Moreover, different vendors now apply different dose calculation algorithms to calculate the AGD; therefore, this would explain the discrepancies observed between the changes found in dose across thickness or modalities. A breast density of 50:50 (fat/parenchyma) is applied as a default in the Hologic system, while General Electric (GE) Healthcare systems use density, as detected by the automatic exposure control (AEC), for the exposure technique setting [11]. Additionally, the Hologic Selenia Dimensions system has the option to acquire CEDM images in the combo mode, which includes 2D (a low-energy image which is basically a mammogram), 3D (tomosynthesis) and CEDM.

Studies have been aimed to lower the radiation dose administered in CEDM. Dose optimization can be achieved by studying multiple variables (contrast agent and target/filter material used, kilovolt and milliampere-second) [8].

One potential strategy is to modify the settings for low-energy images because it has been reported that the low-energy images are the main contributors to the total glandular breast dose [13, 14], while the high-energy acquisition accounts only for 25% of the total dose [3]. James et al. [11] showed that low-energy CEDM had an AGD that was slightly higher than FFDM in both dense and in non-dense phantoms, even if similar exposure techniques were used; the authors found a statistically significant difference between compression thicknesses of 60 and 80 mm. Jeukens et al. [8] obtained similar results by observing higher CEDM exposure for compressed breast thicknesses of 30–75 mm.

Dose reduction can be achieved by optimizing low-contrast scans by varying CEDM exposure settings via manual programming, bearing in mind that, depending on the clinical indication, a

lower-quality image may have to be acceptable [8, 15].

Francescone et al. [1] compared findings (e.g. masses, calcifications) obtained by CEDM and FFDM and demonstrated that low-energy CEDM images are equivalent to standard FFDM despite the presence of intravenous iodinated contrast and consequently proposed the idea that FFDM can be replaced by CEDM given the reduction in the overall dose to the patient. Lalji et al. [16] have also described the equivalence between low-energy CEDM images and conventional mammography images. The authors scored CEDM and FFDM images using European Reference Organisation for Quality Assured Breast Screening and Diagnostic Services (EUREF) criteria and did not find any difference for 17 of 20 EUREF criteria (CEDM scored worse only for the criterion regarding the sharpness of the pectoral muscle) [5].

---

## 10.2 Contrast-Related Factors

### 10.2.1 Possibility of Allergic Reaction

As was extensively detailed in the preceding segment, the working principles of CEDM and its exciting results are based on the administration of iodinated contrast media. This exposes patients to potential risks and adverse effects of administering the contrast medium itself [7, 13, 17, 18].

Before a patient undergoes a CEDM examination, the referring physician and radiologist must balance the likelihood of an adverse event with the benefits of the examination.

Allergic reactions to iodinated contrast media have decreased significantly since the adoption of non-ionic contrast media, with an estimated incidence of 0.6% for overall allergic adverse reactions and 0.04% for severe reactions [7, 19].

Houben et al. [7] in a study of 839 women, who underwent CEDM after a screening recall, reported a 0.6% incidence of adverse allergic reaction (four cases of mild reactions presenting

urticaria and one moderate reaction presenting urticaria and complaining of shortness of breath, treated with an immediate administration of intravenous corticosteroids).

Patients who have had a prior allergic-like reaction to contrast media have an approximately five-fold increased risk of developing an allergic-like reaction if exposed to the same class of contrast media again; this is considered the greatest risk factor for predicting future adverse events. There is no evidence of cross-reactivity between different classes of contrast media. Instead, patients with unrelated allergies are at a two- to threefold increased risk of an allergic-like contrast reaction. It has been documented that patients with shellfish or povidone-iodine (e.g. Betadine) allergies do not present greater risk from iodinated contrast media than patients with other allergies. A history of asthma or atopic diathesis increases the likelihood of an allergic-like contrast reaction. There is also some evidence that contrast reactions are more common in anxious patients and that reassuring an anxious patient before contrast media injection may mitigate the likelihood of a mild contrast reaction [19, 20].

It is therefore important to carefully evaluate the patient's allergy history when booking the CEDM exam and to prescribe a corticosteroid prophylaxis preparation if the patient has history of allergies, although there are actually no sufficiently strong studies to evaluate the efficacy of premedication for the prevention of moderate or severe reactions [17, 19].

Our institutional guidelines suggest that the patient assumes:

- *On the day before the examination, a tablet of methylprednisolone (16 mg) in the morning after breakfast and a tablet of cetirizine hydrochloride 10 mg or levocetirizine 5 mg in the evening*
- *On the day of the examination, a tablet of methylprednisolone (16 mg) in the morning after breakfast and a tablet of cetirizine hydrochloride 10 mg or levocetirizine 5 mg 1 hour before the exam*



### 10.2.2 Absolute or Relative Contraindications in the Case of Some Medical Illnesses

Accurate screening and selection strategies are the first line of prevention against the risks of both allergic and non-allergic adverse events. Prior to booking the examination, other factors, including the presence of renal failure, previous renal transplantation, diabetes and hyperthyroidism, must be considered.

To avoid acute and post-contrast acute kidney injury and contrast-induced nephrotoxicity (CIN), serum creatinine concentration measurement is the most common method to obtain information about renal function, even if normal serum creatinine levels are maintained until the glomerular filtration rate (eGFR) is reduced by nearly 50%.

For these reasons, calculation of the eGFR or creatinine clearance is a more accurate measurement. The American College of Radiology (ACR) guidelines recommend evaluating renal function only if:

- *Patient age is >60.*
- *There is a history of renal disease, including dialysis, kidney transplant, single kidney, renal cancer or renal surgery.*
- *There is a history of hypertension requiring medical therapy.*
- *There is a history of diabetes mellitus.*

Many institutions require the evaluation of serum creatinine in all patients who undergo CEDM examinations.

Furthermore, there is no agreement regarding the acceptable maximum interval between baseline renal function assessment and contrast medium injection in patients at high risk of CIN. It may be appropriate to consider a 30-day interval in outpatients and a shorter interval for inpatients, for those patients with a new risk factor and for those patients with a heightened risk of renal dysfunction.

In the case of a post-contrast acute kidney injury, the common criteria for diagnosis are a

$\geq 0.3$  mg/dL ( $>26.4$   $\mu\text{mol/L}$ ) increase in serum creatinine within 48 hours or a  $\geq 50\%$  ( $\geq 1.5$ -fold) above baseline within 7 days. Serum creatinine usually begins to rise within 24 hours after the intravascular administration of iodinated contrast medium and peaks within 4 days. It is unusual for patients to develop permanent renal dysfunction, and often serum creatinine returns to baseline within 7–10 days. Several studies have shown that patients with post-contrast acute kidney injury, including those with only transient injury, tend to have longer hospital stays, higher mortality and higher incidences of cardiac and neurologic events than other patients.

Thus, according to ACR guidelines, even if there is no absolute contraindication for the administration of intravascular iodinated contrast medium in at-risk patients, patients with acute kidney insufficiency or severe chronic kidney disease are considered at risk for contrast-induced nephropathy, and alternative imaging strategies are suggested.

For diabetic patients, it is important to consider that even if eventual metformin assumption does not confer an increased risk of contrast-induced nephrotoxicity, there is the possibility of developing lactic acidosis in patients who develop acute kidney insufficiency after contrast injection while taking metformin.

Among patients with altered thyroid function, the development of thyrotoxicosis in patients with a history of hyperthyroidism after exposure to iodinated contrast medium is a rare complication. In such cases, restricting the use of contrast medium or premedicating is not recommended. Special care must be taken with patients with acute thyroid storm and considering radioactive iodine therapy or in patients undergoing radioactive iodine imaging of the thyroid gland. In the first group of patients, iodinated contrast medium should be avoided; corticosteroid premedication is not suggested. In the second group of patients, the administration of iodinated contrast medium can interfere with uptake of the treatment and diagnostic dose. If iodinated contrast

medium was administered, the ideal suggested washout period is 3–4 weeks for patients with hyperthyroidism and 6 weeks for patients with hypothyroidism.

Patients with severe cardiac disease (angina, congestive heart failure symptoms with minimal exertion, severe aortic stenosis, cardiac arrhythmias, primary pulmonary hypertension, severe cardiomyopathy even if compensated) may be at increased risk for a non-allergic cardiac event if an allergic-like or non-allergic contrast reaction occurs. These events occur very rarely, and ACR guidelines do not suggest any premedication in this group of patients [19, 20].

### 10.2.3 Fasting Required

As a general precaution, patients are told not to eat or drink 6 hours prior to the examination. We have observed many patients complain of nausea immediately after intravenous infusion of contrast media due to a metallic taste that they experience during the procedure. However, we have not had any patients vomit during the procedure.

## 10.3 Lack of Technology to Biopsy Abnormal Areas of Enhancement

Unlike MRI, there is no commercially available system to biopsy regions of suspicious enhancement under CEDM guidance. This is one of the main limitations of CEDM because the radiologist is not able to directly carry out biopsies on the suspected breast pathologic areas highlighted by contrast enhancement during a CEDM exam. Thus, when a suspected area of enhancement seen on CEDM is not found in the mammogram or on second-look ultrasound scan, the only possibility is to carry out a breast MRI and then perform a biopsy under MRI guidance. This results in delays in the diagnostic procedure and additional patient anxiety [3, 18].

Badr et al. [3] reported the case of one patient who, for this reason, after undergoing CEDM

examination, was subjected to MRI biopsy on a suspected pathologic area of enhancement. The biopsy examination failed due to incomplete coincidence between the enhancement area by CEDM and MRI.

Based on our experience of CEDM in Careggi Hospital (Florence), we have always managed to find the abnormal areas of enhancement seen on CEDM during a second-look at the tomosynthesis images.

## 10.4 False-Negative Lesions

### 10.4.1 Limited Assessment of the Posterior Extent of Masses

Due to the limited field of view of CEDM, there is no possibility of accurately studying masses that have a predominant posterior extension [2, 3, 18]; in particular, chest wall invasion, internal mammary adenopathy [18] and deep or axillary tumours [2] are better seen on MRI.

According to Lalji et al. [16], who compared CEDM (in particular the low energy contrast-enhanced spectral mammography images) and FFDM according to EUREF criteria, sharp visualization of the pectoral muscle is not good for either CEDM or FFDM, although results are worse with CEDM than with FFDM. Instead for the visualization of Cooper's ligaments and vascular structures in the subcutaneous and prepectoral areas, the results were favourable with no statistically significant difference between CEDM (low energy contrast-enhanced spectral mammography images) and FFDM. However, the initial clinical experience of other authors has led to the observation that CEDM is better than conventional mammography for the study of posterior masses [21].

Based on our clinical experience, we have observed some difficulty in studying posteriorly extended masses with CEDM; in such cases, the diagnostic methods of choice are ultrasound and/or magnetic resonance imaging (Figs. 10.1, 10.2, and 10.3).

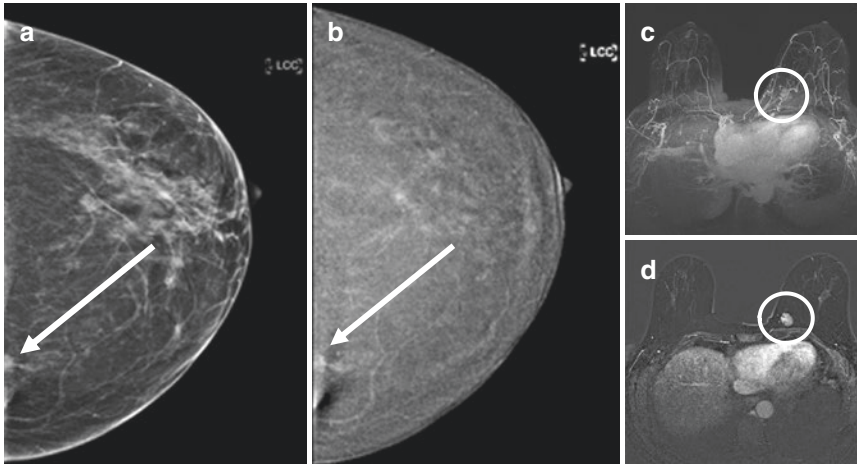


**Fig. 10.1** Pre-surgical evaluation in a 54-year-old patient with a biopsy-proven left breast cancer. (a) Left low-energy images in CC view show an ill-defined deep-seated opacity at the left lower inner quadrant (LIQ). The entire extent of the lesion is not visualized, as the posterior portion is not included in the field of view (*arrow*). (b) CEDM recombined image (CC view) shows a faintly enhancing

irregular mass at the left LIQ (*arrow*), unable to assess the posterior extent of the lesion. Also note the presence of the axillary line artefact further obscuring the lesion. (c, d) Patient underwent an MRI for a complete pre-surgical staging. MRI clearly shows an irregular mass with inhomogeneous enhancement at the left LIQ (*circle*). MRI was able to exclude chest wall infiltration

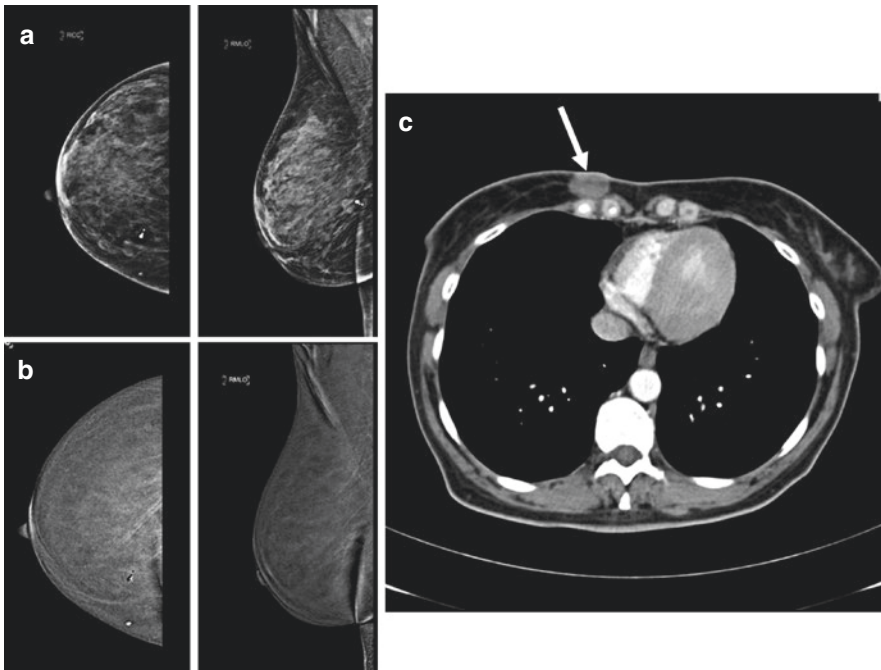
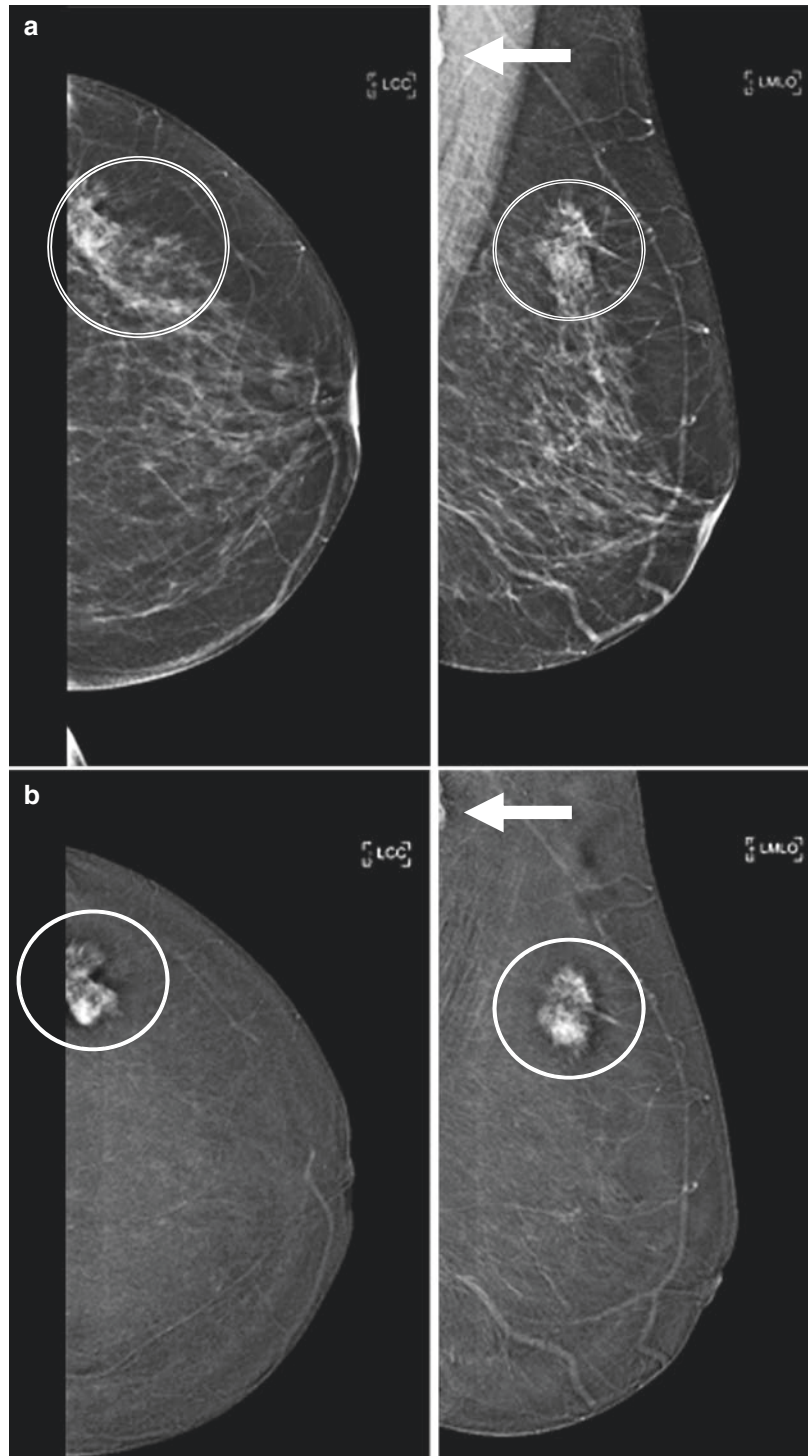


**Fig. 10.2** Pre-surgical staging in a 55-year-old patient, with a palpable right breast lesion. Patient underwent conventional mammography and ultrasound examinations; the ultrasound examination identified the lesion, and an ultrasound biopsy revealed an invasive carcinoma. (a) The low-energy images (CC and MLO view) show a normal breast, with no demonstrable mass. The

lesion is deep-seated and is not included in mammographic field of view. (b) In the CEDM examination (CC and MLO view), there are no enhancing masses. CEDM shows a negative contrast enhancement artefact in the right breast due to a coarse calcification. (c) Patient underwent CT for staging, which shows the deep-seated mass (*arrow*)

**Fig. 10.3** Pre-surgical staging in a 60-year-old patient with a palpable lesion at the left upper outer quadrant (UOQ) and a metastatic axillary lymph node; an ultrasound guided biopsy confirmed it is an invasive carcinoma. (a) Low-energy image (CC and MLO view) shows an irregularly shaped opacity with spiculated margins at the left UOQ (*circle*). (b) CEDM (CC and MLO view) shows an inhomogeneous mass enhancement with irregular shape (*circle*). There appears to be an enhancing lymph node in the axilla, the full extent of which is not visualized in this study (*arrow*). Unlike MRI, CEDM does not allow assessment of axillary lymph nodes, due to the limitations of the mammographic field of view. Thus, a second-look ultrasound examination is always advisable to assess lymph node involvement



### 10.4.2 Poorly Vascularized Tumours

Enhancement detected by CEDM corresponds to the hypervascularization of lesions. In the case of poorly vascular masses, CEDM misses the anatomic substrate interacting with the contrast medium [2, 3].

Badr et al. [3] reported their clinical experience with a false-negative case for a lymphangitic carcinomatosis. The patient, a 55-year-old woman with previous total left mastectomy for ductal carcinoma and surgically treated recurrence on the scar tissue, presented a right axillary adenopathy in a follow-up PET-CT. The mammograms and ultrasound scan were normal; furthermore, the CEDM examination was negative due to the poor vascularization of the lesion. Instead, breast MRI detected a non-mass retroareolar enhancement, and the diagnosis of lymphangitis carcinomatosis was made through MRI biopsy (Fig. 10.4).

### 10.4.3 Malignant Microcalcifications with No Underlying Mass

Low-energy CEDM images give us information about microcalcifications; however microcalcifications are seen as dark foci in the recombined images [2]. (they do not take up contrast, and therefore they are subtracted in the recombined images). Enhancement occurs only in the presence of an underlying vascularized area and are seen as areas of non-mass enhancement. For this reason, some authors have suggested that CEDM should not be used to study calcifications [9, 22]. However, based on our experience at Careggi Hospital (Florence), we have observed favourable results with suspicious calcifications on CEDM.

---

## 10.5 False Positives

### 10.5.1 Benign Lesion Enhancement

This topic has already been described in the chapter of benign lesions in Chapter 11 of the book (Part II). Even benign lesions could exhibit enhancement after the administration of contrast medium in CEDM due to hypervas-

cularization [2, 3, 7, 18]. Benign lesions usually exhibit typical features such as well-demarcated lesion margins and shape that suggest benignity, but in some cases such patterns may be missing. In such situations, it is necessary to perform a complementary ultrasound scan, to obtain a correct diagnosis. However, in cases of doubt, an ultrasound-guided biopsy should be performed for a definitive diagnosis (Figs. 10.5 and 10.6).

---

## 10.6 Background Parenchymal Enhancement

Background parenchymal enhancement (BPE) is seen as several diffuse, non-specific enhancing areas. These areas are usually multiple and bilateral. There is likely a correlation between breast pattern and the hormonal cycle of the patient [2].

Our clinical experience confirms this finding and we have personally observed that BPE is more pronounced in the premenopausal group of women, while postmenopausal women have lower BPE levels. In most instances, it is simple to recognize BPE because of its distribution (multiple, bilateral, symmetric areas of enhancement). Rarely, BPE may be a misleading element when interpreting CEDM images because it may hide an enhancing area suggestive of malignancy or, conversely, it may appear as an area of enhancement, which is demonstrated to be false by pathology. Based on our practice, these limitations are improved with increased experience of the radiologist with CEDM (Figs. 10.7 and 10.8)

---

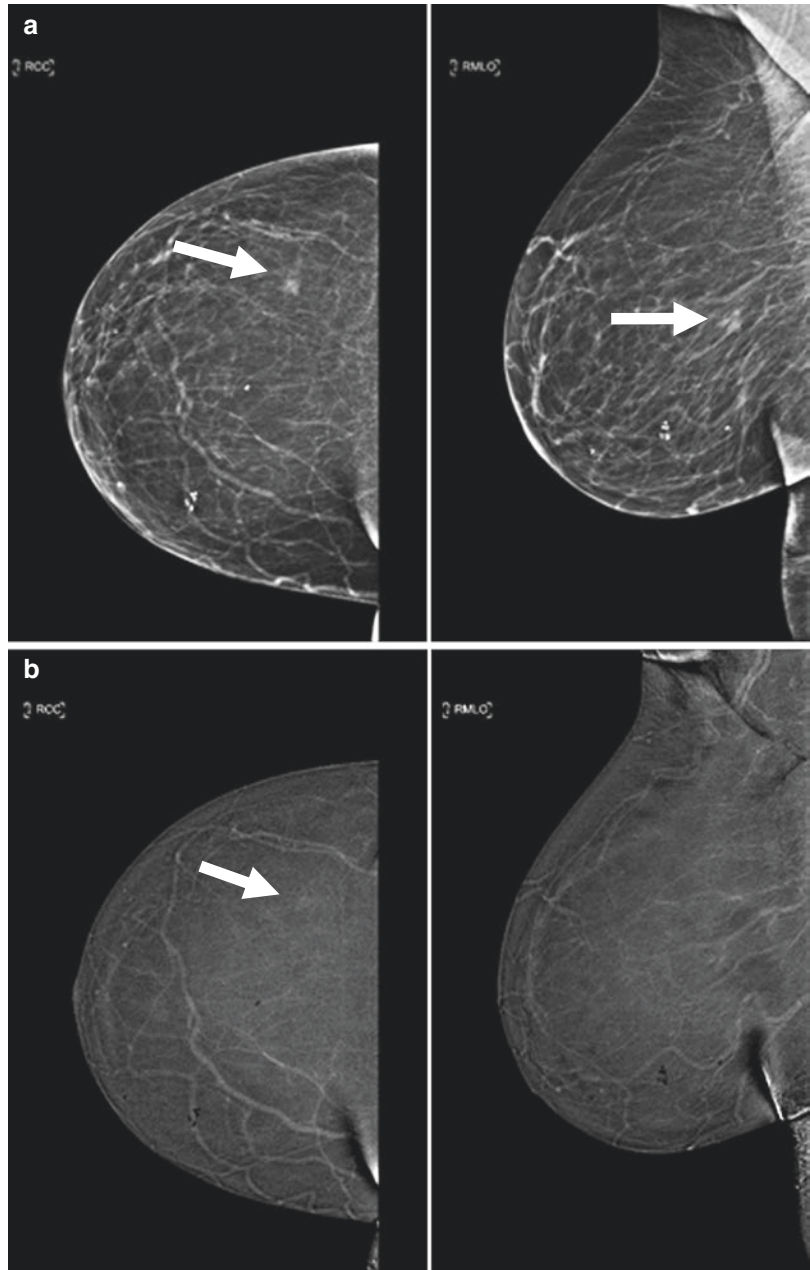
## 10.7 Lesser Degree of Diagnostic Performance in Breast Prosthesis and Siliconomas

As breast prosthesis produces severe artefacts on CEDM recombined images, patients with breast prosthesis and surgical implants are considered a contraindication for CEDM. This was confirmed in our clinical experience with breast implants producing severe artefacts in the recombined images.



**Fig. 10.4** Pre-surgical staging of a 72-year-old patient with a lesion seen in the right breast as seen on screening mammography.

(a) Low-energy image (CC and MLO view) shows a small opacity with irregular shape and margins, at the right outer central quadrant CQ (*arrow*). (b) CEDM (CC and MLO view) recombined image shows a faint enhancement (*arrow*), detectable only in CC projection. By the time the MLO projection was performed, the contrast in the lesion had already washed out. The CEDM finding in this case was not clear and not sufficient to characterize the lesion. An ultrasound-guided biopsy confirmed that the mammographic opacity was an intraductal carcinoma



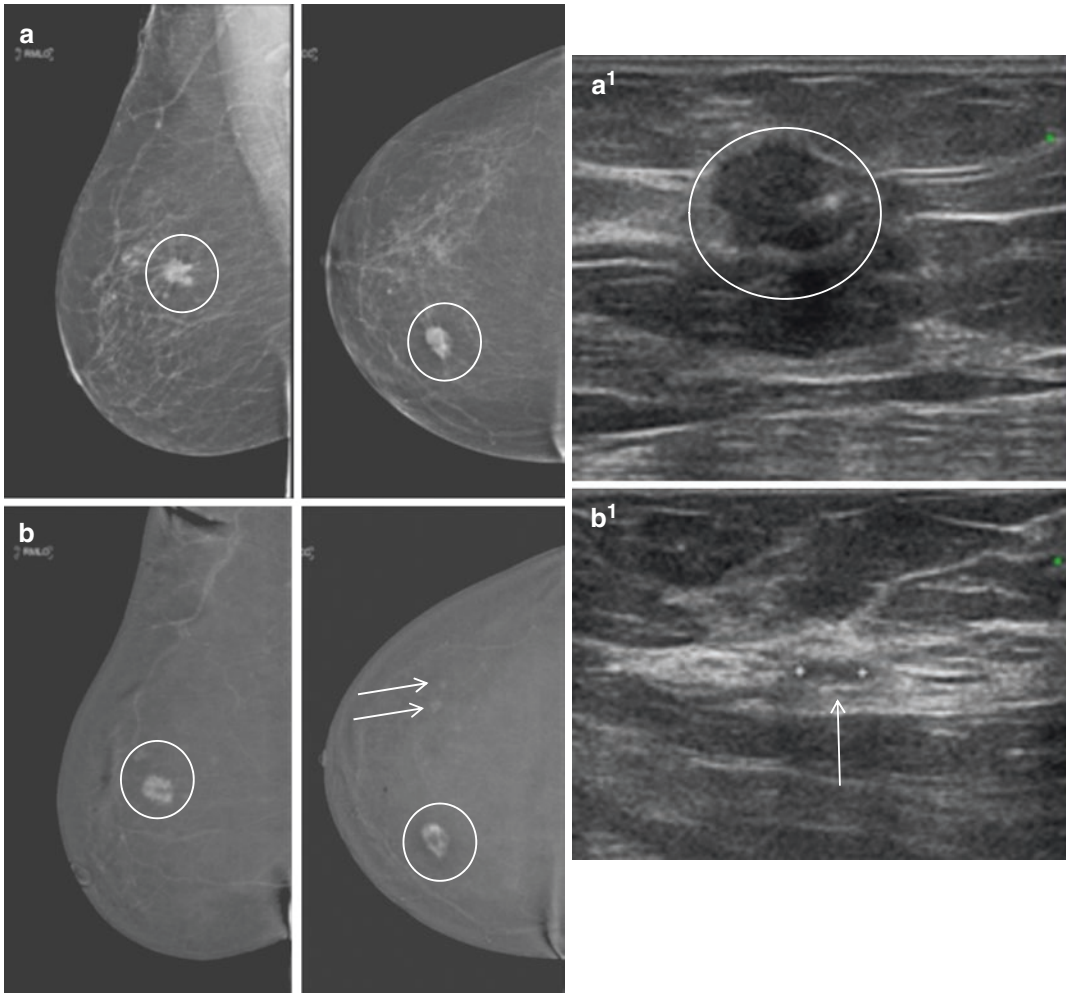


**Fig. 10.5** Pre-surgical staging in a 73-year-old patient with a palpable right breast mass. **(a–a<sup>1</sup>)** Low-energy (CC and MLO view) and ultrasound images show an ill-defined opacity (*circle*) at the right upper inner quadrant. **(b)** CEDM recombined image (CC and MLO view)

demonstrates intense mass enhancement of the lesion (*circle*). In the outer quadrant, there are two other small well-defined faintly enhancing lesions (*arrow*). **(b<sup>1</sup>)** A second-look ultrasound was performed; these lesions were seen as small benign appearing lymph nodes

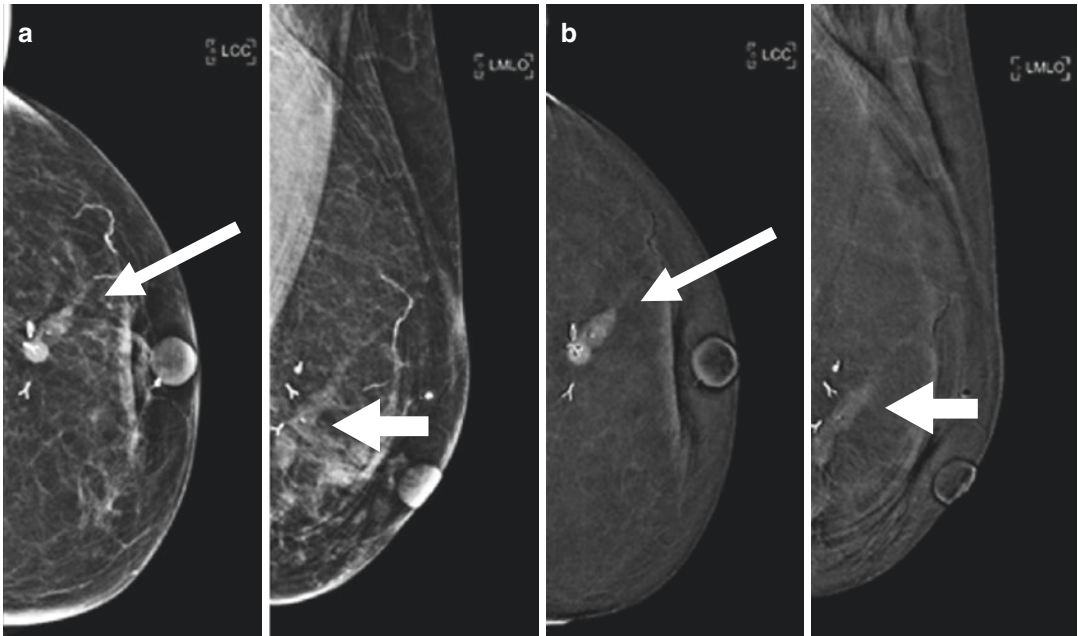


**Fig. 10.6** A 78-year-old patient, with previous left quadrantectomy for breast cancer, on routine yearly follow-up. **(a)** The low-energy image (CC and MLO view) shows lobular opacity with surgical clips in situ, at the left central quadrant, at the same location of the previous

quadrantectomy (*arrow*). **(b)** CEDM recombinant image (CC and MLO view) reveals an intensely enhancing mass that corresponds to the opacity (*arrow*). A biopsy examination under ultrasound guidance was performed, and the result of which was an extensive area of inflammation

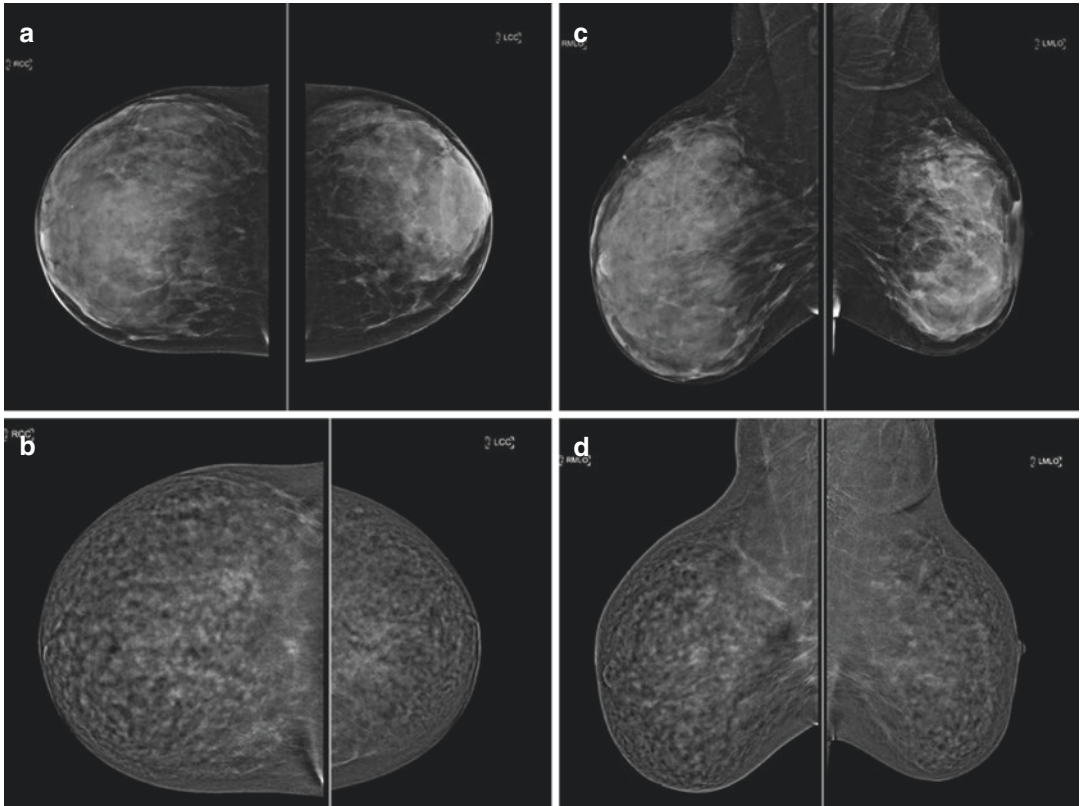


**Fig. 10.7** A 36-year-old patient with a strong family history of breast cancer had a CEDM for screening, as she was claustrophobic and unable to undergo an MRI. (a, c) Low-energy images of the breast (CC and MLO view) appear dense and present isolated calcifi-

cations of benign appearance. (b, d) CEDM recombinated image (CC and MLO view) shows severe background parenchymal enhancement, which is of a stippled type, symmetric and bilateral. No obvious enhancing mass seen

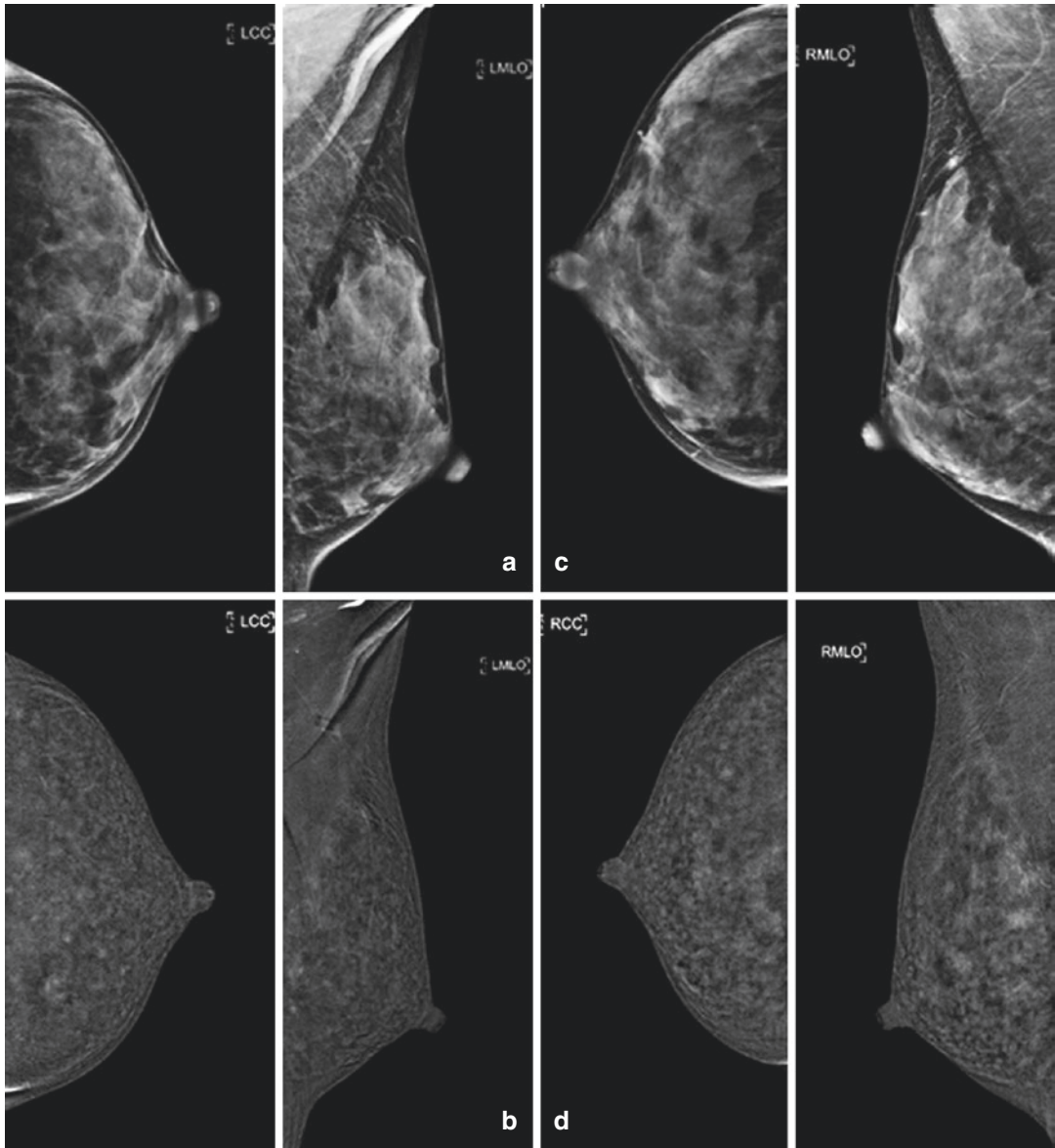


**Fig. 10.8** A 46-year-old woman had an ultrasound investigation done at a private centre, which showed a suspicious hypoechoic nodularity in the left upper outer quadrant. CEDM was performed as a precautionary diagnostic investigation. A later biopsy conducted under ultrasound guidance had outcome B2 (fibrocystic mastopathy).

(a, c) Low-energy images (CC and MLO view) shows dense breast parenchyma; it does not show suspicious masses nor suspicious calcifications. (b, d) CEDM (CC and MLO view) shows an intense bilateral background enhancement, which is symmetrical, but no suspicious enhancing lesions



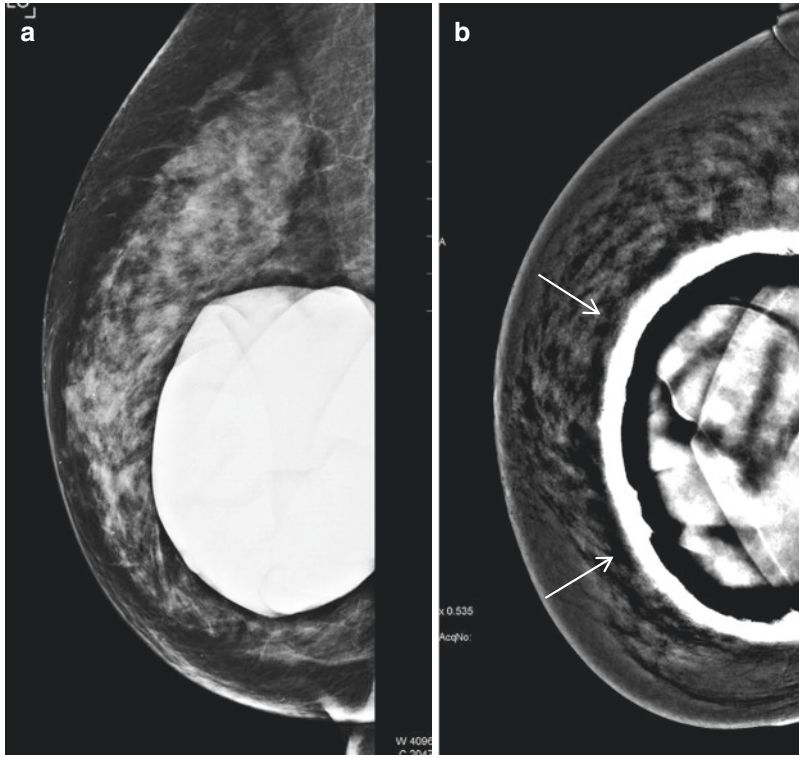


**Fig. 10.9** A 43-year-old with previous history of left breast cancer and left mastectomy, on routine follow-up. Patient is severely claustrophobic and was unable to undergo MRI. (a) Low-energy image demonstrating right breast prosthesis in situ with relatively dense breast parenchyma. (b) CEDM recombined image showing severe artefacts from the prosthesis in the right breast and reduced ability to identify any obvious pathology

Travesio et al. [2] reported the diagnosis of breast carcinoma with CEDM in only 50% of studied patients with prosthesis.

The presence of siliconomas is another important limitation. Due to the features of this material, the CEDM recombined images are completely rendered of non-diagnostic quality [2]. Based on our experience, breast MRI is still the best modality to study siliconomas or breast implants (Fig. 10.9).

## References

1. Francescone MA, Jochelson MS, Dershaw DD, Sung JS, Hughes MC, Zheng J, Moskowitz C, Morris EA. Low energy mammogram obtained in contrast-enhanced digital mammography (CEDM) is comparable to routine full-field digital mammography (FFDM). *Eur J Radiol.* 2014;83(8):1350–5.
2. Travesio Aja MM, Rodríguez Rodríguez M, Alayón Hernández S, Vega Benítez V, Luzardo OP. Dual-energy contrast-enhanced mammography. *Radiologia.* 2014;56(5):390–9.
3. Badr S, Laurent N, Régis C, Boulanger L, Lemaille S, Poncelet E. Dual-energy contrast-enhanced digital mammography in routine clinical practice in 2013. *Diagn Interv Imaging.* 2014;95(3):245–58.
4. Mammography Quality Standards Act, Quality standards. 21 CFR §900.12(e)(5)(vi).
5. EUREF European Guidelines –EUREF. European Reference Organisation for quality assured Breast Screening and Diagnostic Services, European Guidelines for Quality Assurance in Breast Cancer Screening and Diagnosis, fourth edition supplement. 2013.
6. American Association of Physicists in Medicine, AAPM position statement on radiation risks from medical imaging procedures. Policy Number PP25-A; 2011.

7. Houben IPL, Van de Voorde P, Jeukens CRLPN, Wildberger JE, Kooreman LF, Smidt ML, Lobbes MBI. Contrast-enhanced spectral mammography as work-up tool in patients recalled from breast cancer screening has low risks and might hold clinical benefits. *Eur J Radiol*. 2017;94:31–7.
8. Jeukens CR, Lalji UC, Meijer E, Bakija B, Theunissen R, Wildberger JE, Lobbes MB. Radiation exposure of contrast-enhanced spectral mammography compared with full-field digital mammography. *Invest Radiol*. 2014;49(10):659–65.
9. Dromain C, Thibault F, Muller S, Rimareix F, Delalogue S, Tardivon A, Balleyguier C. Dual-energy contrast-enhanced digital mammography: initial clinical results. *Eur Radiol*. 2011;21(3):565–74.
10. Jochelson MS, Dershaw DD, Sung JS, Heerdt AS, Thornton C, Moskowitz CS, Ferrara J, Morris EA. Bilateral contrast-enhanced dual-energy digital mammography: feasibility and comparison with conventional digital mammography and MR imaging in women with known breast carcinoma. *Radiology*. 2013;266(3):743–51.
11. James JR, Pavlicek W, Hanson JA, Boltz TF, Patel BK. Breast radiation dose with CESM compared with 2D FFDM and 3D Tomosynthesis mammography. *AJR Am J Roentgenol*. 2017;208(2):362–72.
12. Fallenberg EM, Dromain C, Diekmann F, Renz DM, Amer H, Ingold-Heppner B, Neumann AU, Winzer KJ, Bick U, Hamm B, Engelken F. Contrast-enhanced spectral mammography as work-up tool in patients recalled from breast cancer screening has low risks and might hold clinical benefits. *Breast Cancer Res Treat*. 2014;146(2):371–81.
13. Patel BK, Gray RJ, Pockaj BA. Potential cost savings of contrast-enhanced digital mammography. *AJR Am J Roentgenol*. 2017;208(6):W231–7.
14. Tzamicha E, Yakoumakis E, Tsalafoutas IA, Dimitriadis A, Georgiou E, Tsapaki V, Chalazonitis A. Dual-energy contrast-enhanced digital mammography: glandular dose estimation using a Monte Carlo code and voxel phantom. *Phys Med*. 2015;31(7):785–91.
15. Dromain C, Canale S, Saab-Puong S, Carton AK, Muller S, Fallenberg EM. Optimization of contrast-enhanced spectral mammography depending on clinical indication. *J Med Imaging (Bellingham)*. 2014;1(3):033506.
16. Lalji UC, Jeukens CR, Houben I, Nelemans PJ, van Engen RE, van Wylick E, Beets-Tan RG, Wildberger JE, Paulis LE, Lobbes MB. Evaluation of low-energy contrast-enhanced spectral mammography images by comparing them to full-field digital mammography using EUREF image quality criteria. *Eur Radiol*. 2015;25(10):2813–20.
17. Daniaux M, De Zordo T, Santner W, Amort B, Koppelstätter F, Jaschke W, Dromain C, Oberaigner W, Hubalek M, Marth C. Dual-energy contrast-enhanced spectral mammography (CESM). *Arch Gynecol Obstet*. 2015;292(4):739–47.
18. Bhimani C, Matta D, Roth RG, Liao L, Tinney E, Brill K, Germaine P. Contrast-enhanced spectral mammography: technique, indications, and clinical applications. *Acad Radiol*. 2017;24(1):84–8.
19. American College of Radiology Committee on drugs and contrast media. *ACR Manual on contrast media, Version 10.3*. 2017.
20. ESUR guidelines. <http://www.esur.org/esur-guidelines/>.
21. Thibault F, Balleyguier C, Tardivon A, Dromain C. Contrast enhanced spectral mammography: better than MRI? *Eur J Radiol*. 2012;81(Suppl 1):S162–4.
22. Dromain C, Thibault F, Diekmann F, Fallenberg EM, Jong RA, Koomen M, Hendrick RE, Tardivon A, Toledano A. Dual-energy contrast-enhanced digital mammography: initial clinical results of a multireader, multicase study. *Breast Cancer Res*. 2012;14(3):R94.
23. Lewin JM, Isaacs PK, Vance V, Larke FJ. Dual-energy contrast-enhanced digital subtraction mammography: feasibility. *Radiology*. 2003;229(1):261–8.
24. Wu X, Barnes GT, Tucker DM. Spectral dependence of glandular tissue dose in screen-film mammography. *Radiology*. 1991;179(1):143–8.
25. Fallenberg EM, Dromain C, Diekmann F, Renz DM, Amer H, Ingold-Heppner B, Neumann AU, Winzer KJ, Bick U, Hamm B, Engelken F. Contrast-enhanced spectral mammography: does mammography provide additional clinical benefits or can some radiation exposure be avoided? *Breast Cancer Res Treat*. 2014;146(2):371–81.

---

## Part II

# CEDM in Clinical Practice



# Benign Lesions

# 11

Ermanno Vanzi, Federica Di Naro,  
and Chiara Bellini

## 11.1 Introduction

Benign breast lesions deserve attention because of their high prevalence. Breast cancer is the most common malignancy in women in developed countries; however, the vast majority of lesions that occur in the breasts are benign. Most of the patients who present with a clinical breast problem, usually have a benign lesion. Diagnosis of a benign disease of the breast is usually accomplished with mammography, ultrasound (US), magnetic resonance imaging (MRI) or needle biopsies, thereby eliminating the need for surgery [1–3].

Benign breast lesions have been comprehensively studied, and most of these lesions are not associated with an increased risk of breast cancer; therefore, unnecessary surgical procedures should be avoided [3–7]. It is very important for radiologists to recognize benign breast lesions and to distinguish them from both in situ and invasive cancer and, in certain cases, to assess a patient's risk of developing breast cancer so that the most appropriate treatment modality is established in every case [8–10].

Contrast-enhanced digital mammography (CEDM), which uses an iodinated contrast agent that has preferential uptake in regions of increased vascularity, provides physiological information that complements the morphological information obtained through conventional mammography [11, 12].

Invasive carcinomas usually present as enhancing lesions on CEDM; however, this presentation is not specific, and there is a significant percentage of benign lesions that produces similar false-positive results on CEDM [12, 13]. Benign lesions usually present as a weak or medium enhancement, rather than the strong enhancement pattern that is a typical indicator of malignant transformation [14]. However, there is no reliable CEDM enhancement pattern that is helpful in defining false-positive lesions.

## 11.2 CEDM Benign Findings

Similarities between benign and malignant lesion characteristics on mammography and ultrasound are well known. Breast MRI has not managed to resolve the issues of lesion specificity; and even if the typical appearance of benign breast conditions is well established, there are cases where it is still extremely difficult to differentiate benign lesions from malignant tumours; CEDM is no exception to this rule. Ultrasound examination

E. Vanzi (✉) · F. Di Naro · C. Bellini  
Diagnostic Senology Unit, Department of Radiology,  
Azienda Ospedaliero Universitaria Careggi,  
Florence, Italy

(US) is the usual supplemental imaging technique to evaluate enhancing breast lesions on CEDM. It is usually followed by an ultrasound-guided core biopsy whenever there is a suspicion of malignancy.

Accumulating evidence has shown that CEDM is emerging as a new technique for the early diagnosis of breast cancer with a diagnostic accuracy comparable to that of breast MRI [15].

CEDM has recently been introduced as an adjunct and a potential alternative to MRI with some advantages, such as lower costs, shorter acquisition times, easier availability and the absence of typical MRI contraindications such as claustrophobia or the presence of metallic implants and cardiac pacemakers [12, 15].

However, as with MRI, CEDM is associated with many false-positive findings, which are benign breast-enhancing lesions that, not only extend the length of the workup, but can also lead to additional imaging studies and increased patient anxiety. Additionally, these false-positive findings may lead to unnecessary biopsies and interventions [13, 14].

Attempts have been made to identify features of benign and malignant lesions by CEDM to reduce false-positive findings and thus improve specificity. Although there is still no evidence that the kinetics in CEDM is similar to that of breast MRI, based on our experience, the morphologic features and enhancement kinetics of breast lesions may be used as descriptive methods for reducing false-positive findings [11–13].

## 11.3 Benign Breast Lesions

### 11.3.1 Fibroadenoma

Fibroadenoma is the most common benign tumour of the breast and occurs in up to 25% of asymptomatic women [1]. It is usually a disease of the early reproductive life; the peak incidence is between the ages of 15 and 35 years. The lesion is a hormone-dependent neoplasm that persists during reproductive years, increases with pregnancy or with oestrogen therapy and decreases after menopause [8].

Although most frequently unilateral, multiple fibroadenomas occur bilaterally in 20% of cases [5].

Macroscopically, the lesion is a well-circumscribed firm mass usually <3 cm in diameter. If the tumour assumes massive proportions (>10 cm), more commonly observed in female adolescents, it is called “giant fibroadenoma” [5].

Microscopically, fibroadenomas consist of a proliferation of epithelial and mesenchymal elements.

Approximately 50% of fibroadenomas contain other proliferative changes of the breast, such as sclerosing adenosis, adenosis and duct epithelial hyperplasia. Fibroadenomas that contain these elements are called “complex fibroadenomas”. Simple fibroadenomas are not associated with any increased risk of breast cancer. However, women with complex fibroadenoma may have a slightly higher risk for subsequent cancer [16].

When a suspicious fibroadenoma is identified upon examination or imaging, it is recommended to have a percutaneous core biopsy for histologic confirmation, as ultrasound alone cannot differentiate between fibroadenoma and a phyllodes tumour [16].

If a biopsy-proven fibroadenoma is stable and asymptomatic, it can be observed with routine examination. If the fibroadenoma increases in size, surgical excision is recommended to rule out a malignant change or a phyllodes tumour [17].

#### 11.3.1.1 Fibroadenoma Findings

Fibroadenoma is the most common sharply marginated breast mass among women in their teens, twenties and early thirties.

- *On mammography*, fibroadenomas appear as well-defined round, oval or lobulated masses, with the most common pattern of calcification devolving into coarser popcorn-shaped features. Calcifications may also present as crushed stone-like calcifications, which make differentiation from malignancy more difficult.



US is usually the next step towards characterization of the lesion.

- *On US*, a fibroadenoma appears as a well-circumscribed elliptic mass that is either hypoechoic or isoechoic and has uniform echogenicity.

The lesion is typically larger in the transverse than in the anteroposterior direction and has very well-demarcated margins. A fibroadenoma may have no effect on ultrasound transmission, or acoustic enhancement or shadowing may be observed in US images [18, 19].

- *On MRI*, fibroadenomas are hypointense or isointense lesions on T1-weighted images, and they are hypointense or hyperintense on T2-weighted images. Septations occur in approximately half of fibroadenomas and have been reported to be a strong indicator of this diagnosis. With gadolinium, the majority of fibroadenomas are hyperintense, with slow initial contrast enhancement followed by a persistent delayed phase, but some have rapid enhancement and either a plateau or a washout phase [5, 18, 19].
- *In our experience with CEDM*, fibroadenomas show a faint, homogeneous enhancement with well-defined margins, and a persistent enhancement is seen in the delayed phase. Non-enhancing internal septations, similar to those seen on MRI, may be observed (Figs. 11.1, 11.2, 11.3, 11.4, and 11.5).

### 11.3.2 Breast Cysts

Breast cysts are the most common non-proliferative breast disease and are seen in over one-third of women aged 35–50 years, with 20–25% having a palpable mass [5, 6].

Simple cysts are derived from the terminal duct lobular unit and are fluid-filled round or ovoid masses.

Ultrasonography is the preferred imaging modality for breast cysts, providing an accurate evaluation of cyst content and complexity.

Ultrasonography allows for characterization into simple, complicated and complex cysts. Features that increase the likelihood of malignancy include a thickened cyst wall, thick septations, solid internal components and hyperechogenicity of the internal fluid.

Complex cysts are defined by ultrasound criteria as masses with the presence of intracystic solid components and thick walls or septa. Complex cysts have a relatively higher risk of malignancy ranging from 5 to 23% and should therefore be evaluated with a tissue biopsy [20].

#### 11.3.2.1 Simple Cyst Findings

Simple cysts are the most common masses seen in the breast in young woman and result from dilatation and effacement of the terminal duct lobular unit.

They are benign and have no risk of malignancy. No intervention is necessary for simple cysts.

However, if they are large and cause pain, aspiration may be necessary for pain relief. If the fluid is clear, no investigation is needed; however, if the fluid is haemorrhagic, it should be sent for cytologic analysis [20].

- *On mammography*, they typically show a circumscribed round, oval or lobulated mass with well-defined margins.
- *On US*, ultrasonography is the preferred imaging modality for breast cysts, providing an accurate evaluation of cyst content and complexity. Ultrasonography allows for characterization as simple, complicated and complex cysts.

Simple cysts are well-circumscribed, anechoic, have a thin echogenic capsule, increased through transmission, have thin edge shadows and lack internal solid components.

- *On MRI*, these cysts follow fluid signals in all sequences, are iso- or hypointense to the breast parenchyma on T1-weighted images and are very hyperintense on T2-weighted images and do not enhance after gadolinium;

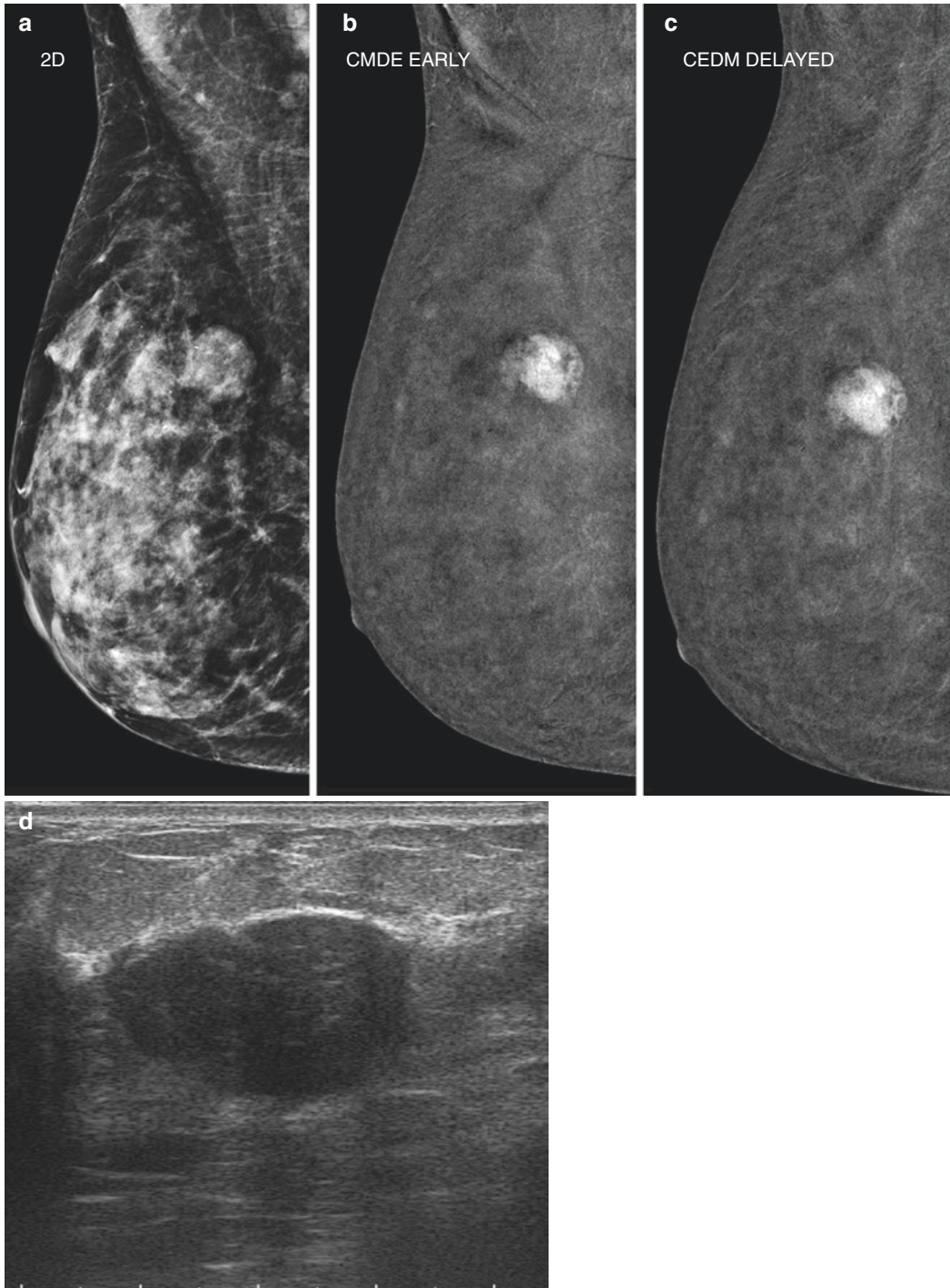


**Fig. 11.1** An enhancing fibroadenoma. **(a)** Low Energy CEDM image (LE CEDM) in MLO view showing a well-defined round opacity in the upper quadrant of the right breast. **(b–c)** CEDM recombined images showing a solitary well-defined mass enhancement in the early phase, and it demonstrates a progressive and persistent enhance-

ment in the delayed phase. **(d)** Ultrasound (US) shows a well-defined, oval, homogeneously hypoechoic mass suggestive of a benign mass. *CEDM* contrast-enhanced digital mammography, *LE* low energy, *MLO* mediolateral oblique, *US* ultrasound

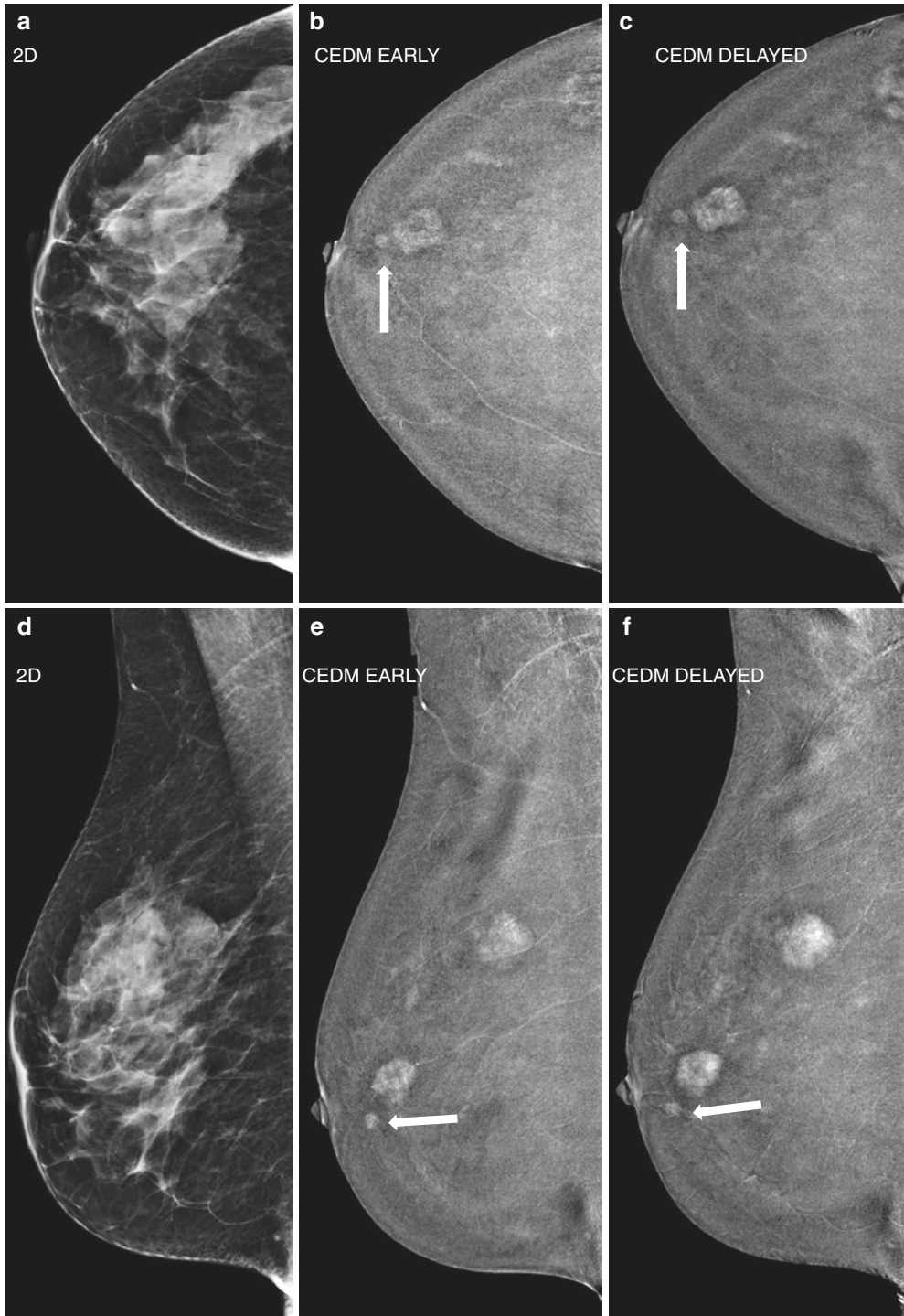


**Fig. 11.2** Enhancing fibroadenomas and papilloma. (a and d) LE CEDM images in CC and MLO views show a round opacity in the upper outer quadrant of the right breast. (b and e) CEDM recombined images in early phase show three masses with well-defined margins, demonstrating a faint, early homogeneous enhancement, the two larger with internal septations are typical fibroadeno-

mas, the smaller mass in the retroareolar zone is a papilloma (white arrow). (c and f) CEDM recombined images in delayed phase, in CC and MLO views, show the classic progressive and persistent enhancement of benign lesions. CEDM contrast-enhanced digital mammography, LE low energy, CC craniocaudal, MLO mediolateral oblique



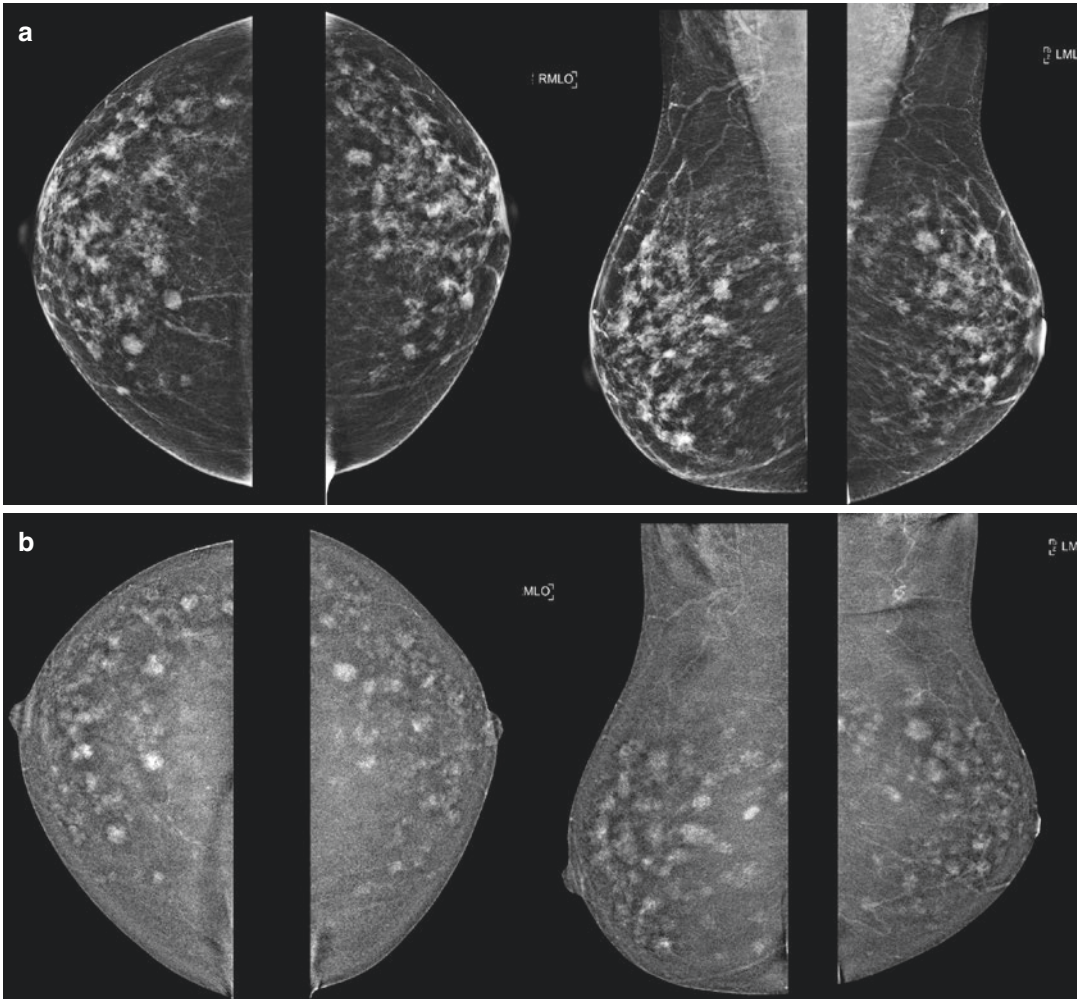


**Fig. 11.3** Multiple fibroadenomas. (a) LE CEDM images in CC and MLO views show multiple bilateral opacities with well-defined margins. (b) CEDM recombined images demonstrate multiple well defined bilateral homogeneously enhancing masses. (c) Second-look US showed

many hypoechoic nodules with benign features. An ultrasound-guided core biopsy revealed multiple fibroadenomas. *CEDM* contrast-enhanced digital mammography, *LE* low energy, *CC* craniocaudal, *MLO* mediolateral oblique, *US* ultrasound

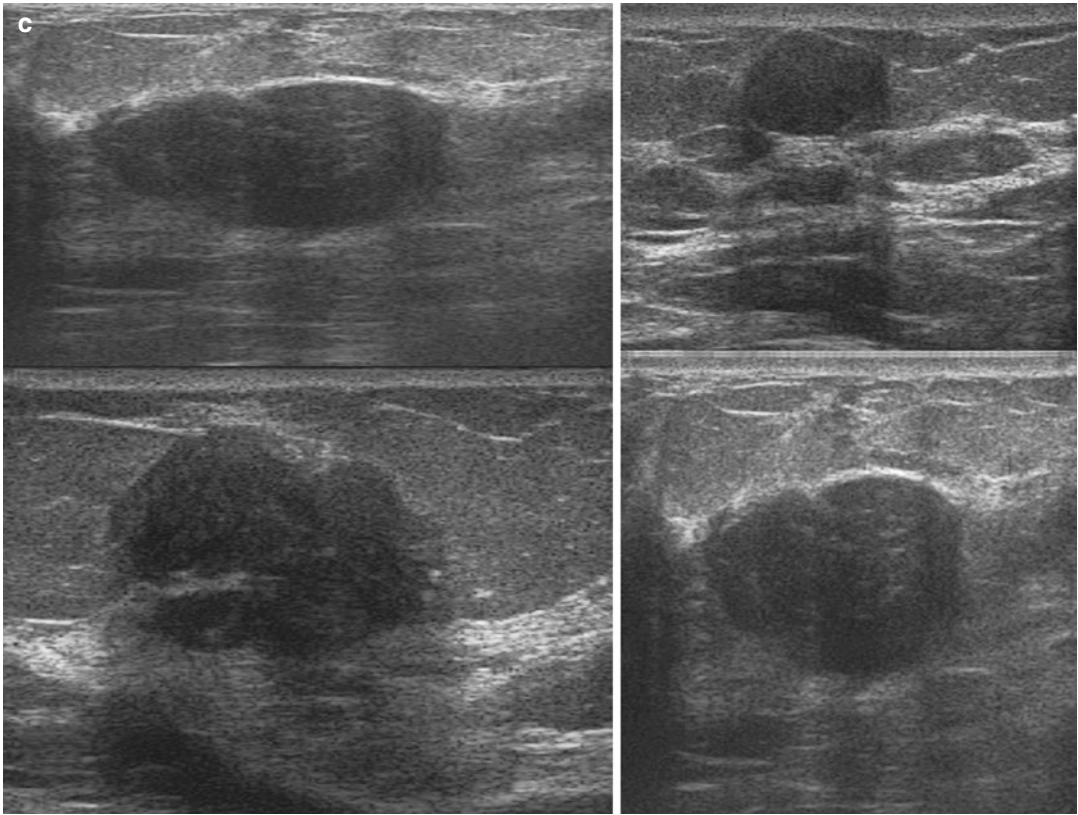


**Fig. 11.3** (continued)

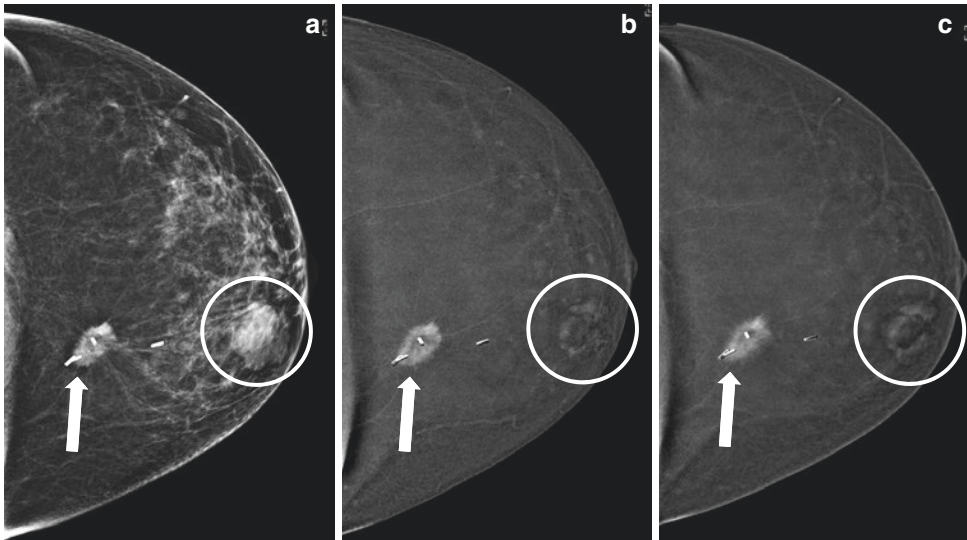


**Fig. 11.4** Different enhancing patterns of benign and malignant lesions on CEDM in the same breast. **(a)** LE CEDM image in CC view of the left breast shows a deep opacity with ill-defined margins and another well-circumscribed opacity in the retroareolar region. **(b, c)** CEDM recombined images in early and delayed phases show an intense heterogeneous

enhancement of the posteriorly located mass with spiculated and ill-defined margins (*white arrow*), whose pathology was invasive ductal carcinoma. The retroareolar oval mass with internal dark non-enhancing septations was consistent with a fibroadenoma (*white circle*). CEDM contrast-enhanced digital mammography, CC craniocaudal



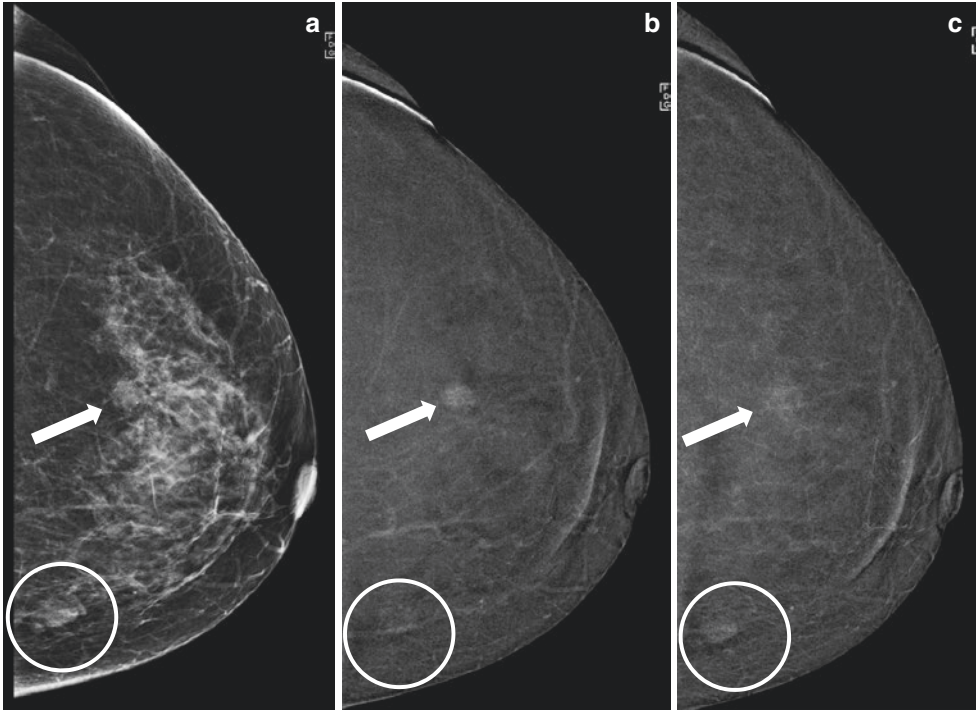


**Fig. 11.5** Different enhancing patterns of benign and malignant lesions in the same breast on CEDM images. (a) LE CEDM image of the left breast in CC view demonstrates a well-circumscribed opacity in the inner quadrant posteriorly (*white circle*) and another opacity with ill-defined margins located more anteriorly and more centrally (*white arrow*). (b, c) CEDM recombined images in

early and delayed phases show early enhancement and wash-out of the mass centrally located (*white arrow*) and a progressive delayed enhancement of the mass in the inner quadrant (*white circle*) which are typical enhancement features of invasive carcinoma (*white arrow*) and fibroadenoma (*white circle*), respectively. CEDM contrast-enhanced digital mammography, CC craniocaudal

however, the periphery of the cyst may enhance if there is surrounding pericystic inflammation [6, 8].

- *In our experience with CEDM*, the findings consist of round areas of radiolucency with regular margins in keeping with the absence of enhancement, with possible peripheral enhancement in recombined images, which is also called “rim enhancement”. The enhancement could also be described as “eclipse sign”, because it resembles a full solar eclipse (Figs. 11.6 and 11.7).

### 11.3.2.2 Complicated Cyst Findings

A complicated cyst is a cyst that contains low-level internal echoes or fluid-fluid or fluid-debris

levels that include cell debris, proteins, cholesterol, blood and epithelial cells.

The risk of malignancy with complicated cysts is 0.2%, but they should be aspirated to confirm diagnosis after imaging [7, 8].

- *On mammography*, these complicated cysts show the same characteristic findings of simple cysts.
- *On US*, complicated cysts have most, but not all, of the ultrasonographic criteria of a simple cyst: they may have homogeneous internal echoes but lack solid components, thick walls or septa and do not demonstrate increased vascularity.
- *On MRI*, a complicated cyst may have intermediate or high signals on T1-weighted

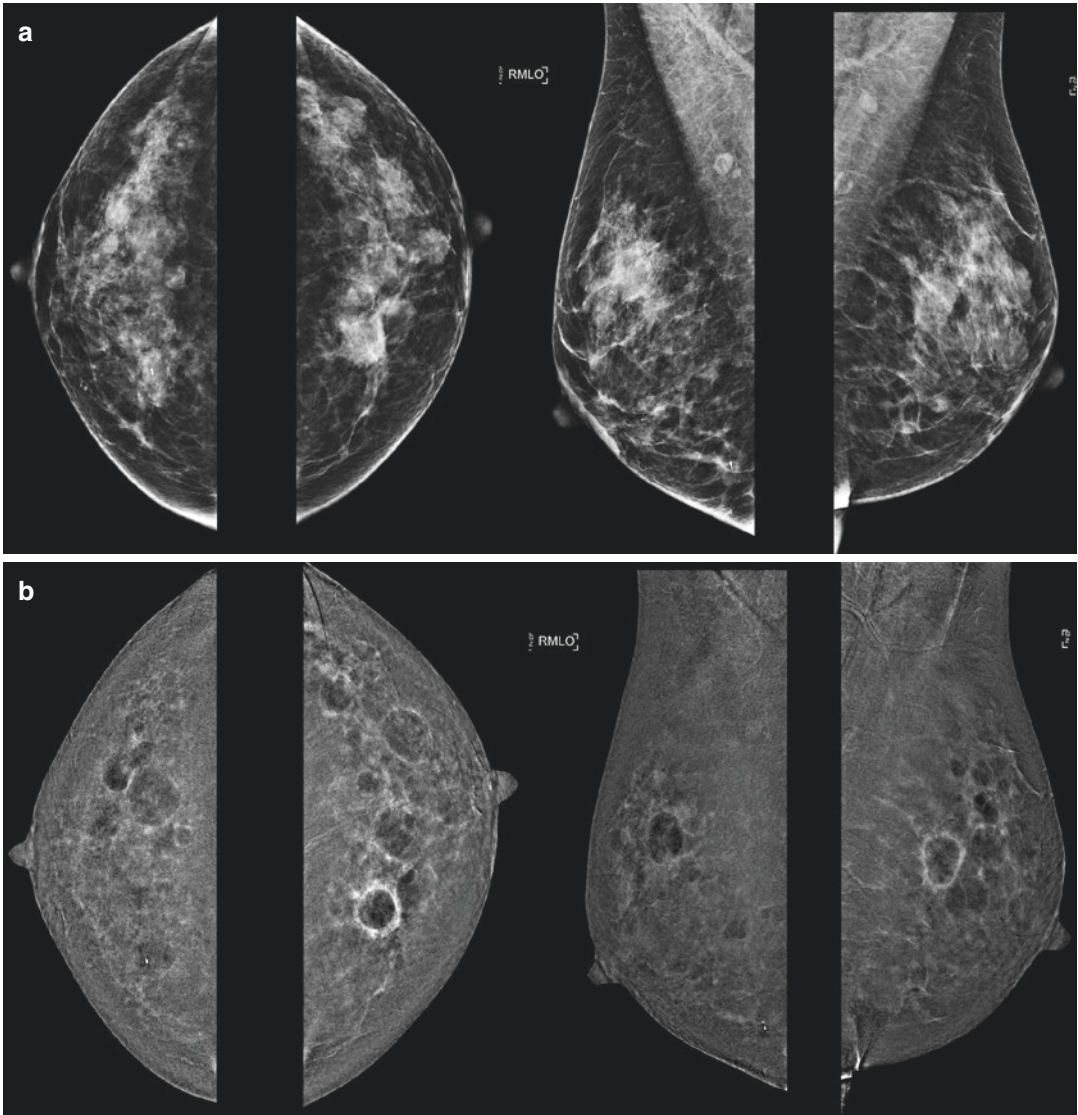


**Fig. 11.6** Rim enhancement pattern of cysts. (a) LE CEDM images in CC and MLO views of both breasts show multiple scattered round opacities, with circumscribed margins. (b) CEDM recombined images show multiple bilateral radiolucent areas, surrounded by thin

uniform wall enhancement in keeping with simple cysts. There are some, which have thick rim enhancement suggestive of cysts with peripheral inflammation. *CEDM* contrast-enhanced digital mammography, *LE* low energy, *CC* craniocaudal, *MLO* mediolateral oblique

images due to proteinaceous contents or blood products. Their appearance on T2-weighted images is variable depending on the cyst contents [17, 20, 21].

- *In our experience with CEDM*, the findings are similar to those observed for simple cysts; complex cysts appear as focal areas of radiolucency

with thick irregular peripheral enhancement also called “rim enhancement” (Fig. 11.8).

### 11.3.2.3 Complex Cyst Findings

To avoid confusion with a complicated cyst, the current preferred term for complex breast cysts is a combination of solid and cystic mass. Complex

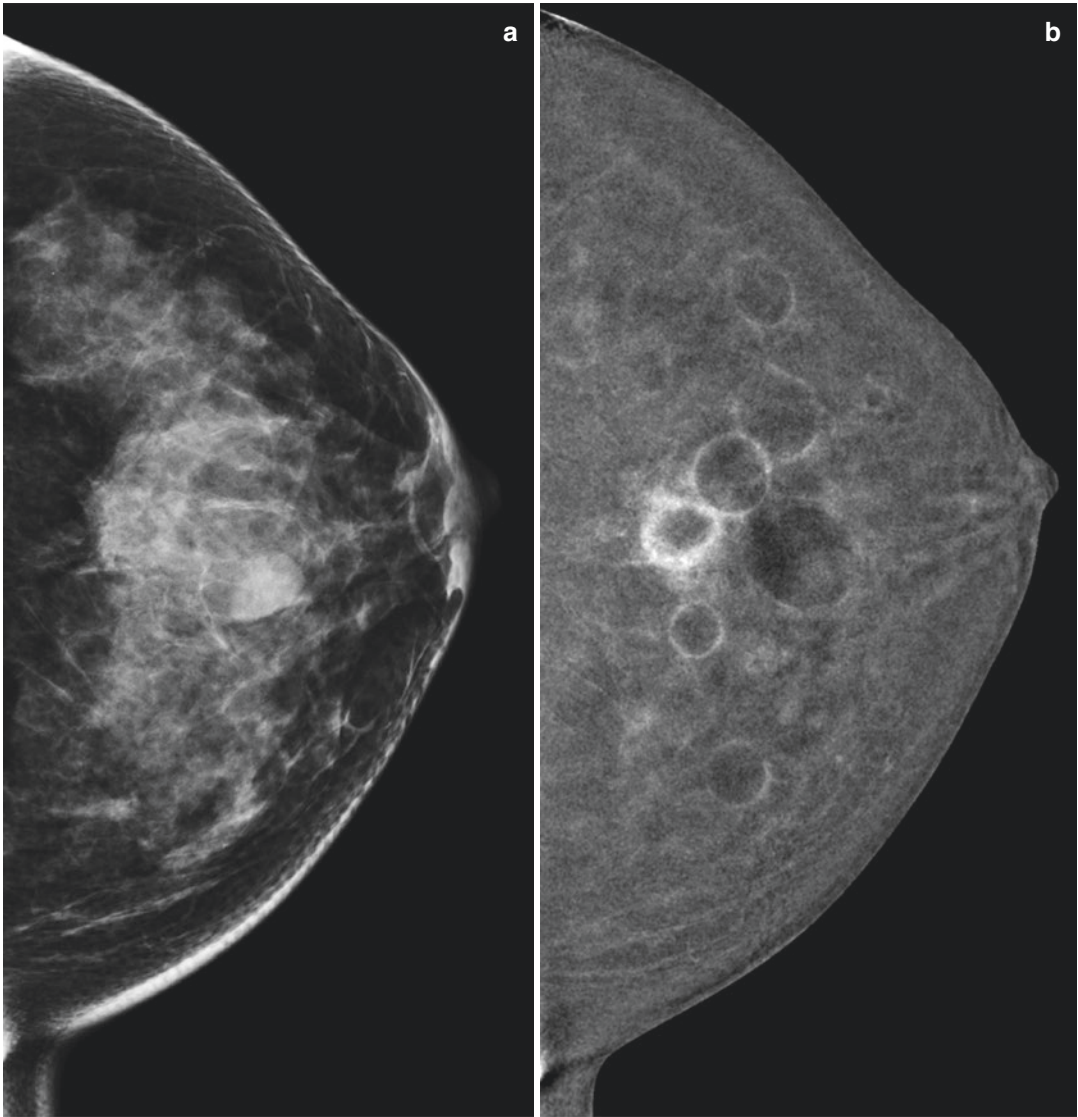


**Fig. 11.7** Rim enhancement pattern of cysts. (a) LE CEDM image of the left breast in CC view shows multiple scattered round opacities, with circumscribed margins. (b) CEDM recombined image shows multiple radiolucent round areas in the left breast, surrounded by

thin uniform rim enhancement in simple cysts, while sometimes a thick rim enhancement can be seen in case of cysts with peripheral inflammation. *CEDM* contrast-enhanced digital mammography, CC craniocaudal

cysts have a relatively higher risk of malignancy, ranging from 5 to 23%, and therefore should be evaluated with tissue biopsy [20].

The cysts that fall in these categories are galactoceles, haematomas, fat necrosis, abscesses, necrotic tumours, papillary tumours, atypical ductal hyperplasia and ductal carcinoma in situ (DCIS).

- *On mammography*, these cysts show the same characteristic findings as simple cysts.
- *On US*, these cysts contain thick wall, thick septae or intracystic masses that are characteristic of complex breast cysts [20].
- *In our experience with CEDM*, the findings are similar to those observed for simple cysts; complex cysts appear as focal areas of radiolucency



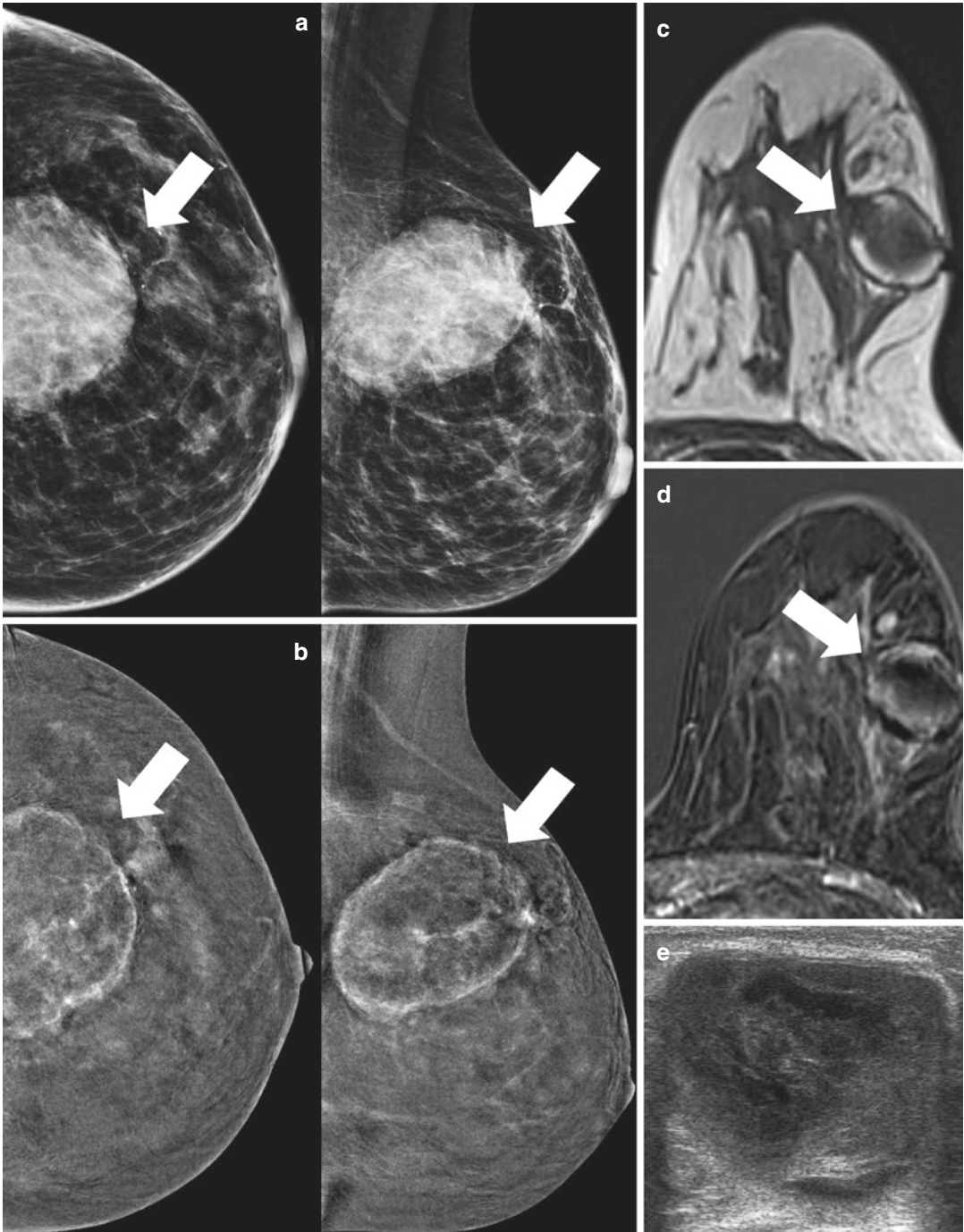


**Fig. 11.8** Post-biopsy haematoma. (a) LE CEDM images, in CC and MLO views, of the left breast show a large, oval, post biopsy opacity suggestive of a breast haematoma. (b) CEDM recombined CC and MLO images demonstrate a large oval rim-enhancing lesion with slight central enhancement in keeping with complex cystic features. (c) MRI T1-weighted pre-contrast image shows a mass with in-

homogeneous hyperintensity. (d) MRI FAT SAT T1-weighted post-contrast image shows rim enhancement. (e) US images show a well circumscribed elliptic mass with inhomogeneous echogenicity, compatible with a post biopsy haematoma. *LE CEDM* low energy contrast-enhanced digital mammography, *MRI* magnetic resonance imaging, *CC* craniocaudal, *MLO* mediolateral oblique, *US* ultrasound

with thick irregular peripheral enhancement also called “rim enhancement” (Fig. 11.9). Occasionally, we may also observe intracystic enhancement due to the associated solid components.

### 11.3.3 Fibrocystic Changes

Fibrocystic changes are the most frequently encountered benign breast findings and occur most often in women of reproductive age between 20 and 50 years. Patients often present with a his-

tory of bilateral, menstrual-related, tender and nodular breasts, most often localized to the upper outer quadrants [5–7, 10].

Exact pathogenesis is unclear but hormonal imbalance with oestrogen predominance seems to be a relevant factor in their development [7].

Fibrocystic changes have no single histopathologic definition. It includes several histopathologic categories such as microcystic and macrocystic formations, hyperplasia of the ductal epithelium, apocrine metaplasia, papillomatosis, ductal ectasia, sclerosing adenosis and stromal fibrosis.

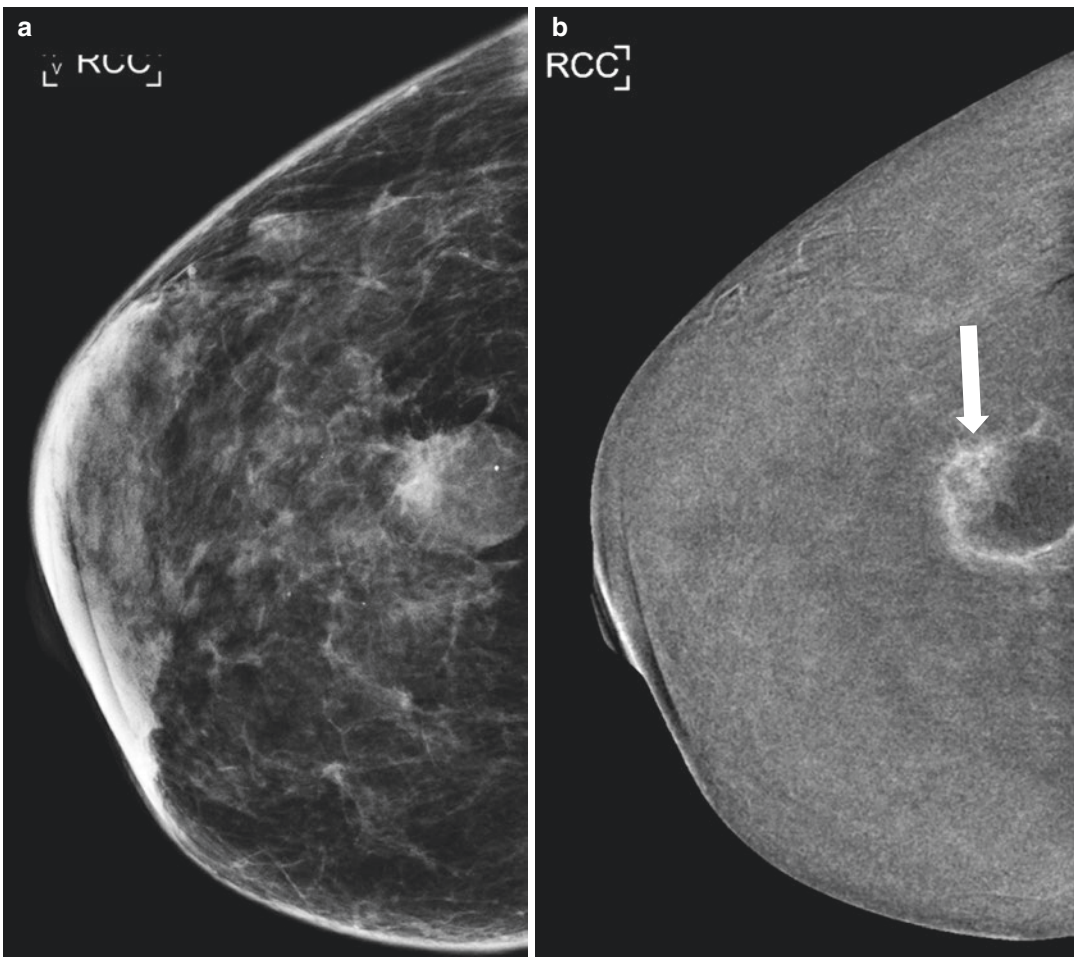


**Fig. 11.9** Complex cysts. (a) LE CEDM image in CC view of the right breast shows a solitary, oval, central opacity with well-defined margins. (b) CEDM recombined image in CC view shows peripheral thin rim enhancement

with an internal enhancing nodule. Pathology: Complex cyst containing a B3 solid mass, lobular intraepithelial neoplasia (LIN). CEDM contrast-enhanced digital mammography, CC craniocaudal, MLO mediolateral oblique



As a result of these indistinct clinical and pathological findings, some authors have even questioned the validity of referring to fibrocystic change as a disease or even the use of the term [7].

Given the importance of determining if a clinical “fibrocystic lesion” is a risk factor for the subsequent development of breast cancer, lesions are further characterized under the histologic classification system proposed by DuPont and Page as non-proliferative lesions, proliferative lesions without atypia and proliferative lesions with atypia [16, 22, 23].

Breast cancer risk for these benign lesions is then classified according to histology. There is no elevated risk in women with biopsy-proven non-proliferative lesions. Proliferative disease without atypia and with atypical ductal/lobular hyperplasia is associated with a small increased breast cancer risk ranging from 1.2 to 2.0% and 3.7 to 5.3%, respectively [19, 22, 23].

### 11.3.3.1 Fibrocystic Changes Findings

Fibrocystic changes are usually defined as cystic degeneration of the breast parenchyma associated or not associated with fibrosis, adenosis and ductal or lobular hyperplasia [20].

Generally, fibrocystic changes consist of palpable lumps in the breast, associated with breast pain or tenderness, that fluctuate with the menstrual cycle.

- *On mammography*, findings associated with fibrocystic disease are asymmetrical densities, architectural distortions (sclerosing adenosis) and microcalcifications (adenosis, apocrine metaplasia, ductal hyperplasia) with opacities corresponding to cysts, focal fibrosis or nodular adenosis [18, 24, 25].
- *On ultrasound*, fibrocystic change consists of cysts (anechogenic for simple cyst, or echogenic for complicated or complex cysts, or often clustered microcysts), scattered echogenic foci due to microcalcifications (associated or not associated with cysts), solid masses and discrete masses due to fibrosis (homo-

neous/inhomogeneous ovoid mass or irregular mass with shadowing) [24, 25].

- *On MRI*, fibrocystic disease demonstrates a wide spectrum of morphologic and kinetic features. Fibrocystic disease commonly occurs as a diffuse type of non-mass-like regional enhancing lesion, with a benign enhancement pattern. They may also present as a focal mass-type lesion with enhancement kinetics usually showing rapid up-slope mimicking a breast cancer [26].
- *In our experience with CEDM*, findings of fibrocystic change are seen as areas of non-mass-like parenchymal enhancement, usually of regional distribution, without specific characteristics, similar to their appearance on MRI that requires a second-look ultrasound to discriminate between benign or suspicious lesions (Figs. 11.10, 11.11, 11.12, and 11.13).

### 11.3.4 Hamartoma

Breast hamartomas are benign lesions also known as fibroadenolipoma or adenolipoma. They are uncommon tumour-like masses that have varying amounts of glandular, adipose and fibrous tissue. They present as encapsulated painless masses found upon screening mammography. The classic mammographic finding is a circumscribed area consisting of a mixture of both glandular tissue and lipomatous elements surrounded by a thin translucent zone [3, 27].

Hamartomas do not have specific diagnostic features upon histology with the exception of a nodular distribution of fat tissue within a fibrotic stroma that extends between individual lobules [3, 27].

#### 11.3.4.1 Hamartoma Findings

- *On mammography*, hamartomas are typically seen as oval or round masses, inhomogeneous with radio-opaque and radiotransparent areas reflecting the presence of tissues that differ in density, well-defined by a thin radio-opaque pseudocapsule and surrounded by breast parenchyma displaced by the mass [27].

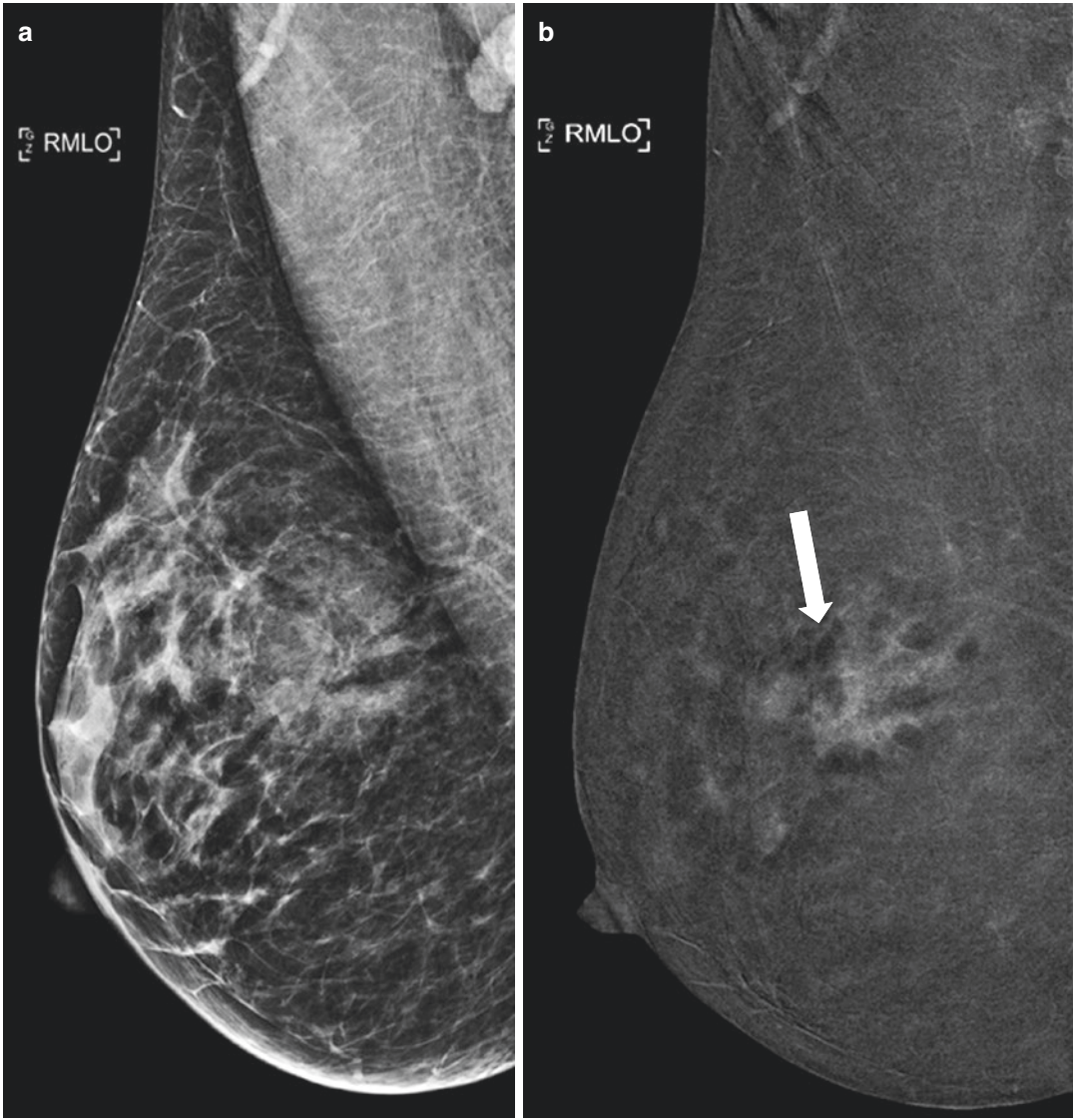


**Fig. 11.10** CEDM images of different enhancement patterns of fibrocystic changes. (a) LE CEDM image in MLO view of the right breast shows a large opacity with ill-defined margins in the upper quadrant. (b) CEDM recombined

image shows an intense heterogeneous area of non-mass enhancement that was biopsied with the histologic result of fibrocystic changes. CEDM contrast-enhanced digital mammography, MLO mediolateral oblique

The mass typically resembles a “slice of salami” with a “breast within a breast” appearance.

- *On US*, hamartomas appear as solid, well-defined, oval formations lying parallel to the skin plane. They are inhomogeneous with hypoechoic areas intermixed with hyperechoic

band-like or nodular areas, reflecting the presence of adipose, epithelial and fibrous connective tissues. Because hamartomas resemble the normal breast tissue, it is sometimes difficult to delineate their margins [28–31].

- *On MRI*, hamartomas may present heterogeneous signal intensity on T1- and T2-weighted

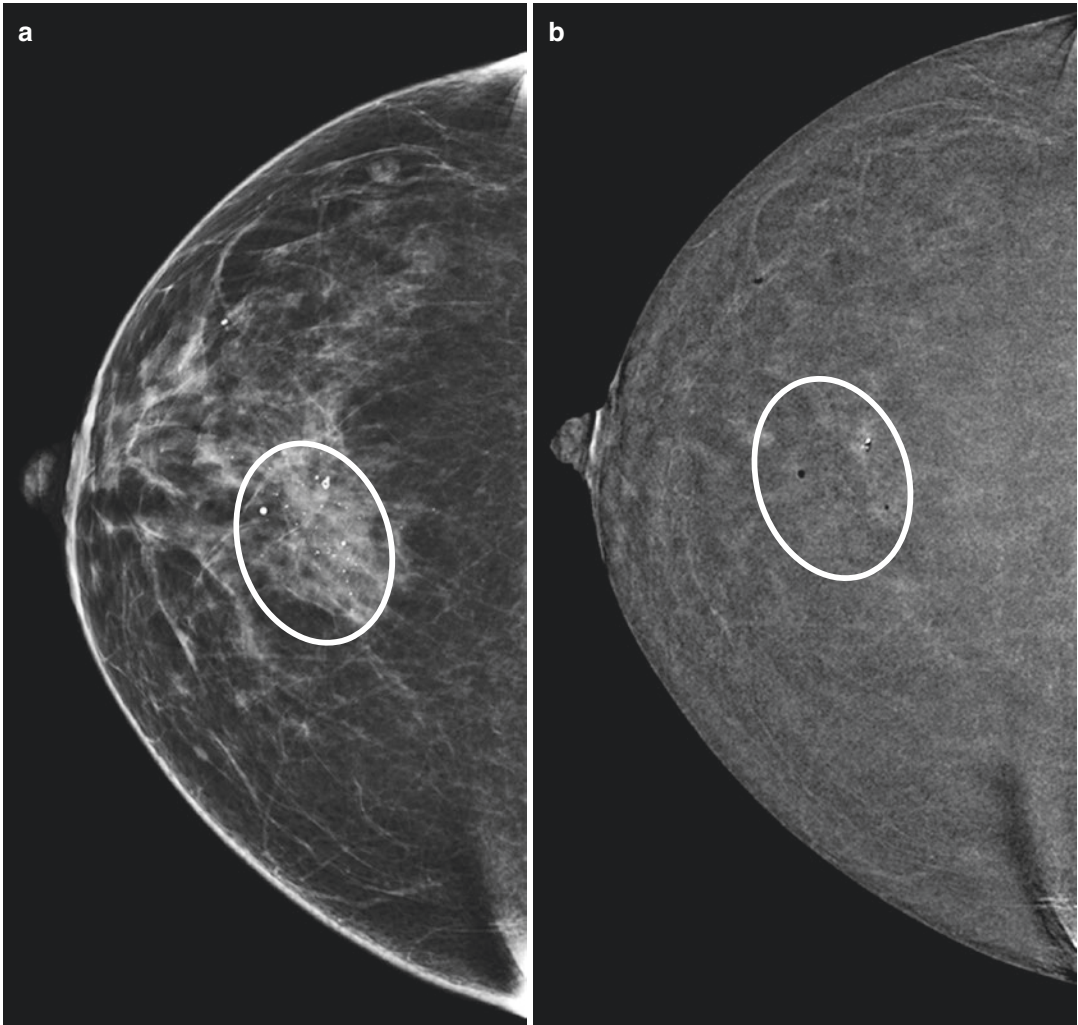


**Fig. 11.11** CEDM images of different enhancement patterns of fibrocystic changes. (a) LE CEDM image in CC view of the right breast shows an opacity with ill-defined margins and calcifications. (b) CEDM recombined image

shows no enhancement in the same area in keeping with non-enhancing fibrocystic change. *CEDM* contrast-enhanced digital mammography, *CC* craniocaudal, *MLO* mediolateral oblique

sequences, reflecting the presence of glandular and adipose tissue components and a thin capsule. After the administration of contrast medium, hamartomas show a gradual, progressive enhancement with a type I kinetic curve [32].

- *In our experience with CEDM*, similar to MRI, hamartomas demonstrate slow heterogeneous initial enhancement pattern with a persistent delayed phase on the recombined CEDM images (Fig. 11.14).

### 11.3.5 Intraductal Papilloma (Without Atypia)

Papillomas are hyperplastic epithelial lesions composed of a central fibrovascular core covered by epithelium. Papillomas may be central, involving larger subareolar ducts, and are usually solitary or peripheral papillomas that involve terminal duct lobular units and are usually multiple. The epithelial component of papillomas can harbour a spectrum of morphologic changes ranging



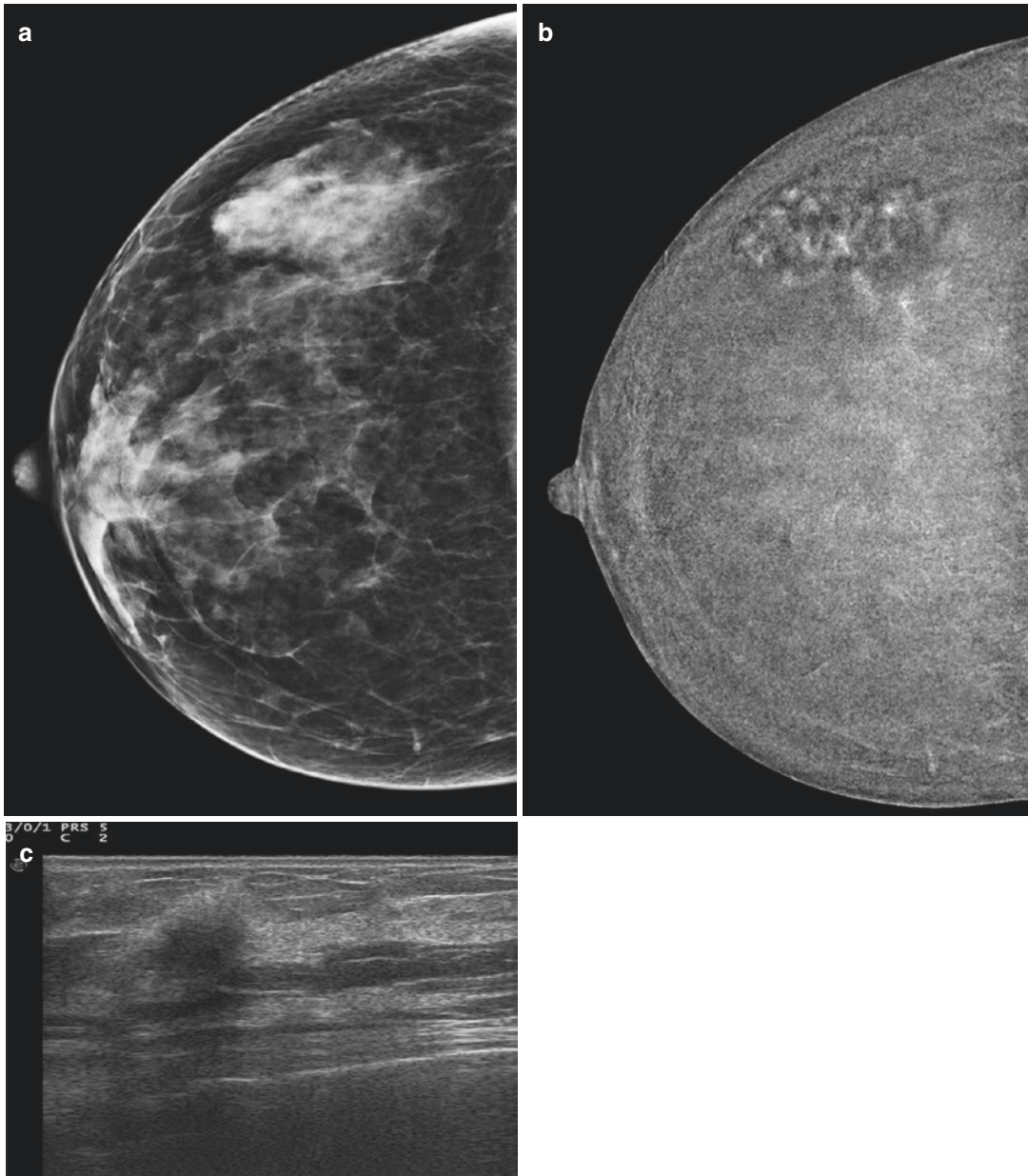


**Fig. 11.12** CEDM images of different enhancement patterns of fibrocystic changes. (a) LE CEDM image in CC view of the right breast shows an asymmetric oval opacity at the upper outer quadrant. (b) CEDM recombined image shows a faint heterogeneous area of non-mass enhance-

ment in the same quadrant. (c) US shows a pseudonodular area, which was subsequently biopsied with the histologic result of fibrocystic changes. *CEDM* contrast-enhanced digital mammography, *CC* craniocaudal, *MLO* mediolateral oblique, *US* ultrasound



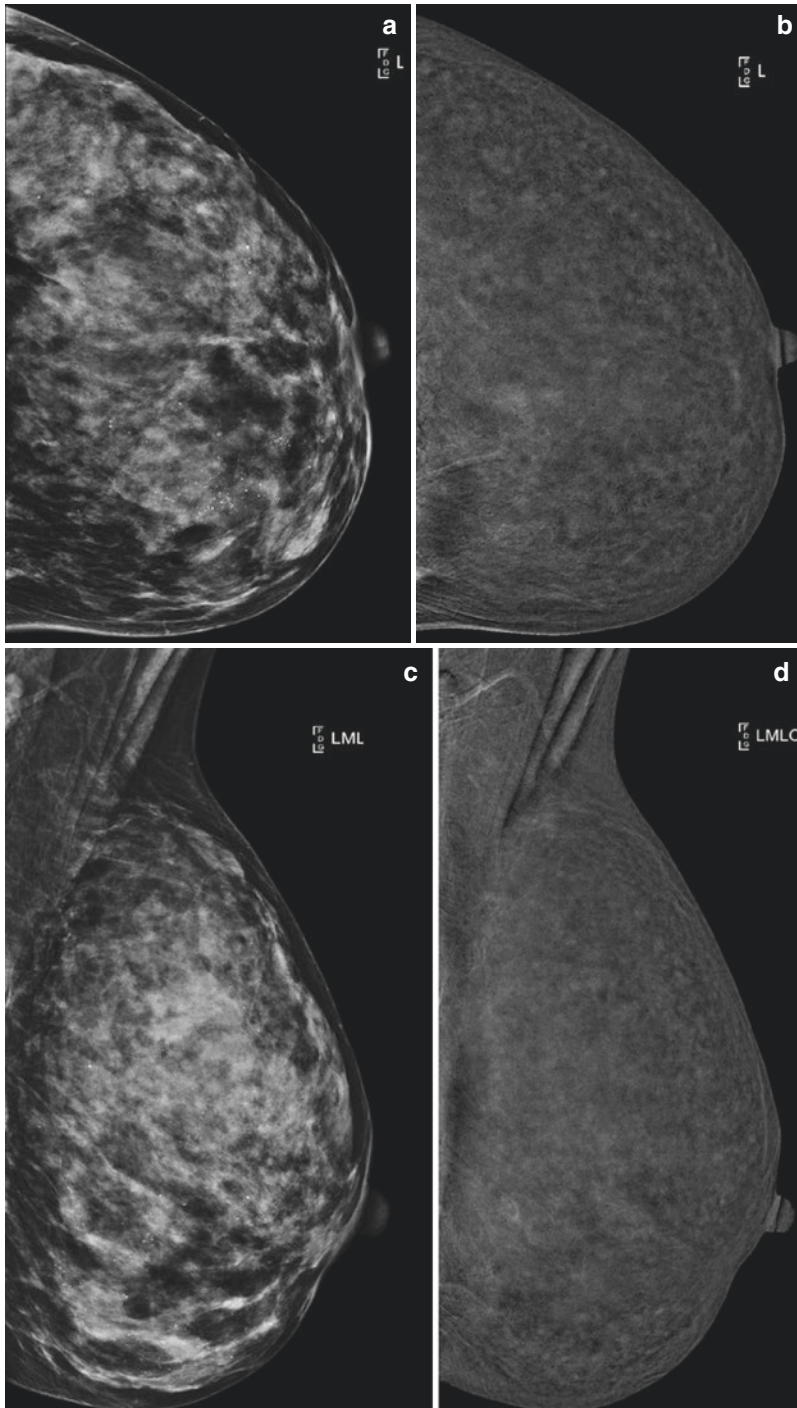


**Fig. 11.13** CEDM images of calcifications with segmental distribution on fibrocystic changes. (a and c) LE CEDM images in CC and MLO views of the left breast show pleomorphic calcifications with segmental distribution, in the lower inner quadrant (a<sup>1</sup>). (b and d) CEDM

recombined images in CC and MLO views show no enhancement in the same area (b<sup>1</sup>). Vacuum-assisted biopsy was performed and the pathology result was fibrocystic change. CEDM contrast-enhanced digital mammography, CC craniocaudal, MLO mediolateral oblique

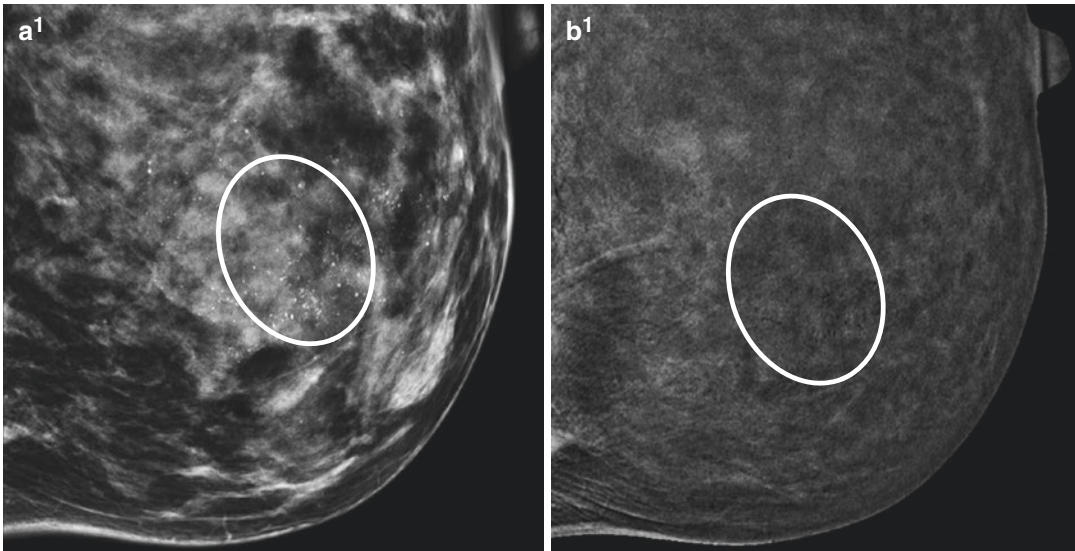


**Fig. 11.13** (continued)

from metaplasia to hyperplasia, atypical hyperplasia and in situ or invasive carcinoma. Given this risk of atypia and malignancy, the traditional recommendation after core needle biopsy of papilloma is surgical excision. However, there are recent reports concerning the potential safety of observation in patients diagnosed with solitary papilloma without atypia upon biopsy [33–35].

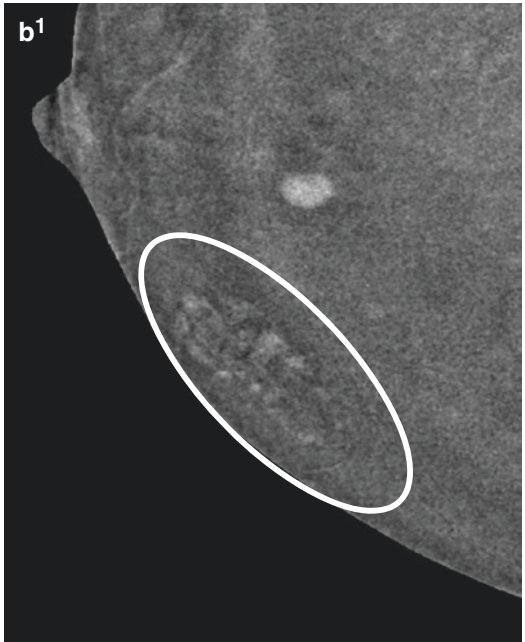
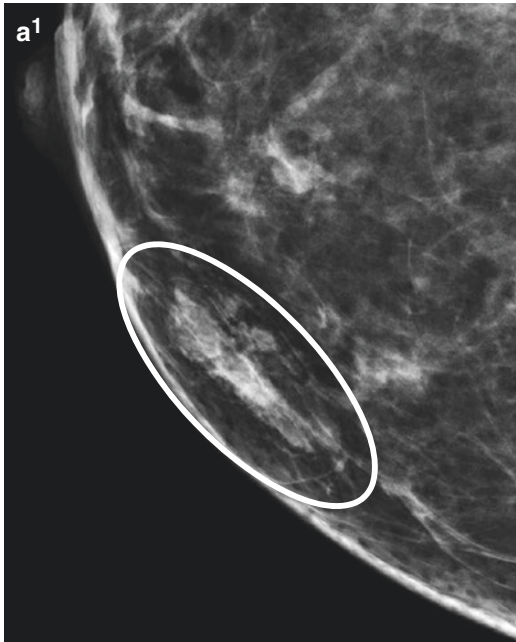
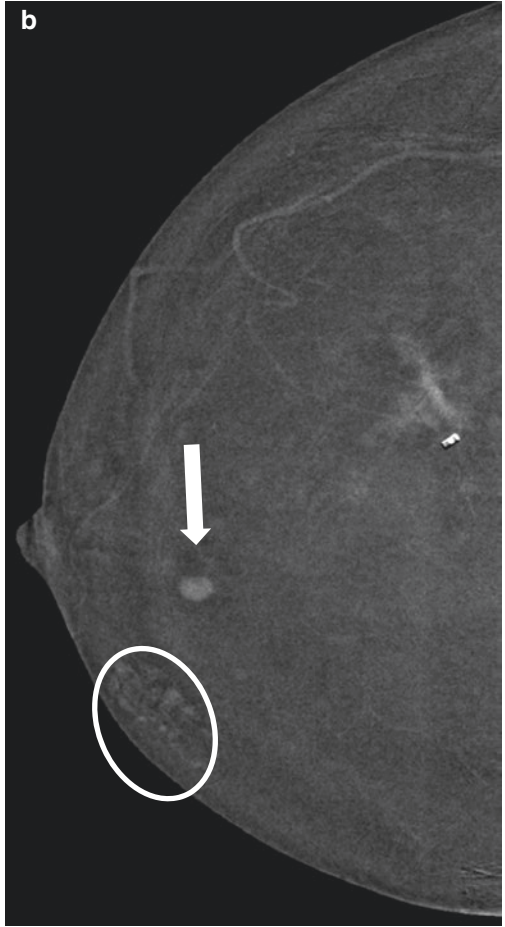
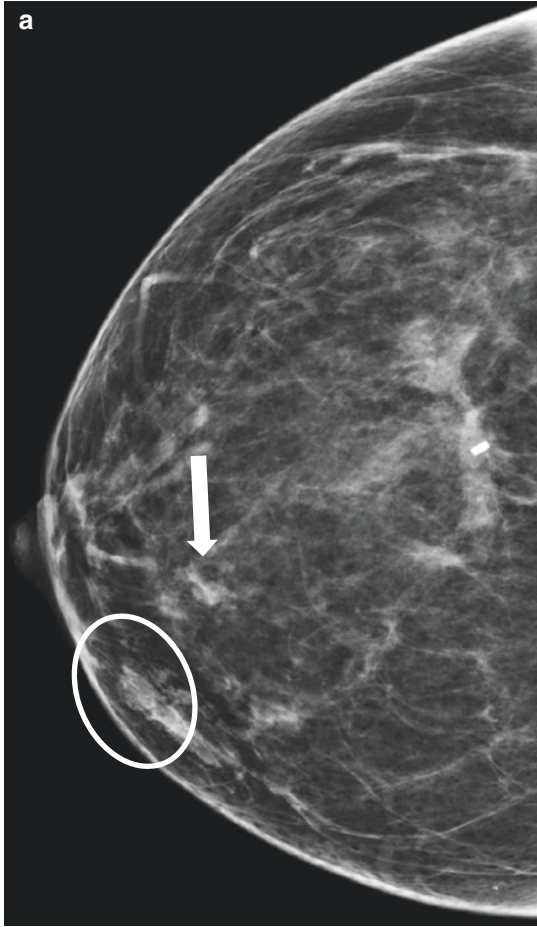
### 11.3.5.1 Intraductal Papilloma Findings

Intraductal papilloma is usually a retroareolar or central benign lesion, often associated with bloody or clear nipple discharge [23].

- *On mammography*, when small and located in the retroareolar regions, intraductal papillomas can be occult due to the breast density. Larger lesions may appear as a round- or oval-shaped masses with well-circumscribed margins, associated with benign calcifications [36].
- *On galactography*, intraductal papillomas appear as well-defined mural-based filling defects with smooth or lobulated contours [36].
- *On US*, intraductal papillomas are seen as well-defined solid nodules or mural-based nodules within a dilated duct [36].
- *On MRI*, intraductal papillomas are shown as enhancing nodules with or without intraductal

---

**Fig. 11.14** CEDM images of a hamartoma and other findings of benign and high risk B3 lesions in the same breast. (a) LE CEDM image in CC view of the right breast shows three findings: (1) (a<sup>1</sup>) an oval opacity (white circle) corresponding to a hamartoma in the inner quadrant. (2) a second lesion is a well-defined round mass (white arrow) corresponding to a fibroadenoma in the retro-areolar region. (3) thirdly, an area of distortion deeply in the central quadrant (b) CEDM recombined image show three different enhancing patterns from the inner quadrant to the outer quadrant: (1) (b<sup>1</sup>) A faintly enhancing oval mass with regular margins (white circle) corresponding to a hamartoma, (2) A round well-defined enhancing mass (white arrow) in keeping with a fibroadenoma (B2 lesion), (3) An area of non-mass enhancement corresponding to a radial scar (B3 lesion). *CEDM* contrast-enhanced digital mammography, *CC* craniocaudal



components that may have high signal on T1-weighted images if the duct contains proteinaceous debris or haemorrhage. A round filling defect may be seen within the duct. Papillomas enhance avidly with gadolinium. The enhancement of these nodules may be uniform or irregular with either washout or plateau kinetics, making differentiation from invasive malignancies potentially difficult [36].

- *In our experience with CEDM*, intraductal papillomas demonstrate peri- or retroareolar, ductal and homogeneous enhancement in the recombined images (Figs. 11.15 and 11.16).

### 11.3.6 Fat Necrosis

Fat necrosis is a benign non-suppurative inflammatory process of the adipose tissue. It is important to diagnose because it can often mimic breast carcinoma. Fat necrosis is most commonly the result of trauma or surgery to the breast [3].

Examination and imaging of fat necrosis may be concerning for malignancy due to dense palpable masses, erythema, skin retraction and skin thickening.

It is sometimes necessary to biopsy the lesion to confirm diagnosis, although with experience it is possible to delineate this diagnosis particularly when oil cysts are present.

Conservative management is recommended unless there is a serious cosmetic distortion of the breast, in which case surgery can be considered [37].

#### 11.3.6.1 Fat Necrosis Findings

- *On mammography*, fat necrosis can present as oil cysts x-ray transparency, coarse calcifications, focal asymmetries, microcalcifications or spiculated masses. The mass usually appears as a radiolucent mass with linear and curvilinear calcifications. Sometimes, the cal-

cifications are of concern due to their shape and distribution: branching, rod-like, angular or pleomorphic-clustered calcifications are sometimes indistinguishable from those of malignancy.

Occasionally, the reparative fibrotic reactions may replace all of the radiolucent necrotic fat, resulting in the appearance of a focal asymmetric density, a focal dense mass or an irregular spiculated mass upon mammography [38].

- *On US*, fat necrosis may present as a solid mass or a complex mass with echogenic nodules, a complex mass with echogenic bands, an anechoic mass with posterior acoustic enhancement, an anechoic mass with shadowing or an isoechoic mass. The margins range from well-circumscribed to indistinct or spiculated.

- *On MRI*, fat necrosis usually shows signal of heterogeneous intensity on T1weighted sequences, which may be due to its haemorrhagic and inflammatory content. Calcifications are sometimes seen on MRI as areas of absence of signal. Fibrosis may appear as high, intermediate or low signal on T1weighted images. Post-gadolinium, fat necrosis can enhance and be focal or diffuse and homogeneous or heterogeneous. Enhancement depends on the intensity of the inflammatory process. The fat suppression sequence is important for identifying enhancing breast cancers or enhancing regions of fat necrosis because the high signal of fat interferes with the detection of enhancing lesions. Enhancement patterns may vary from slow, gradual enhancement to rapid enhancement [38].

- *In our experience with CEDM*, similar to MRI, fat necrosis appears as focal or diffuse areas of enhancement, with either a homogeneous or heterogeneous pattern of enhancement on CEDM recombined images (Figs. 11.17, 11.18 and 11.19).



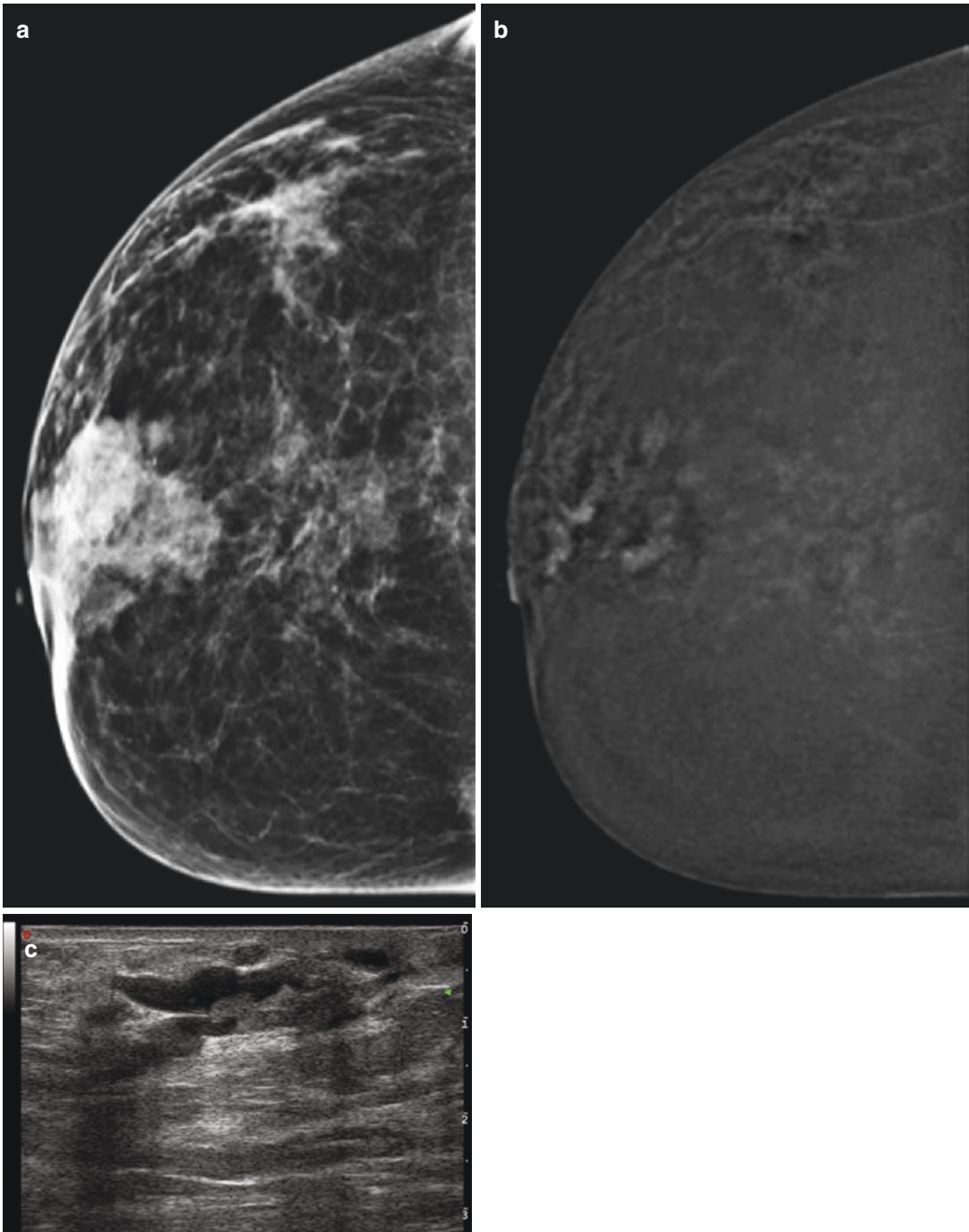


**Fig. 11.15** CEDM images of intraductal papillomas. (a) LE CEDM image in CC view of the right breast shows a retroareolar irregular opacity. (b) CEDM recombined image in CC view shows a segmental area of non-mass enhancement in the periareolar region. (c) US demon-

strates an anechoic dilated duct with an intraductal hyperechoic mass. US-guided biopsy was performed, and the pathology result was intraductal papilloma. *CEDM* contrast-enhanced digital mammography, *CC* craniocaudal, *MLO* mediolateral oblique, *US* ultrasound

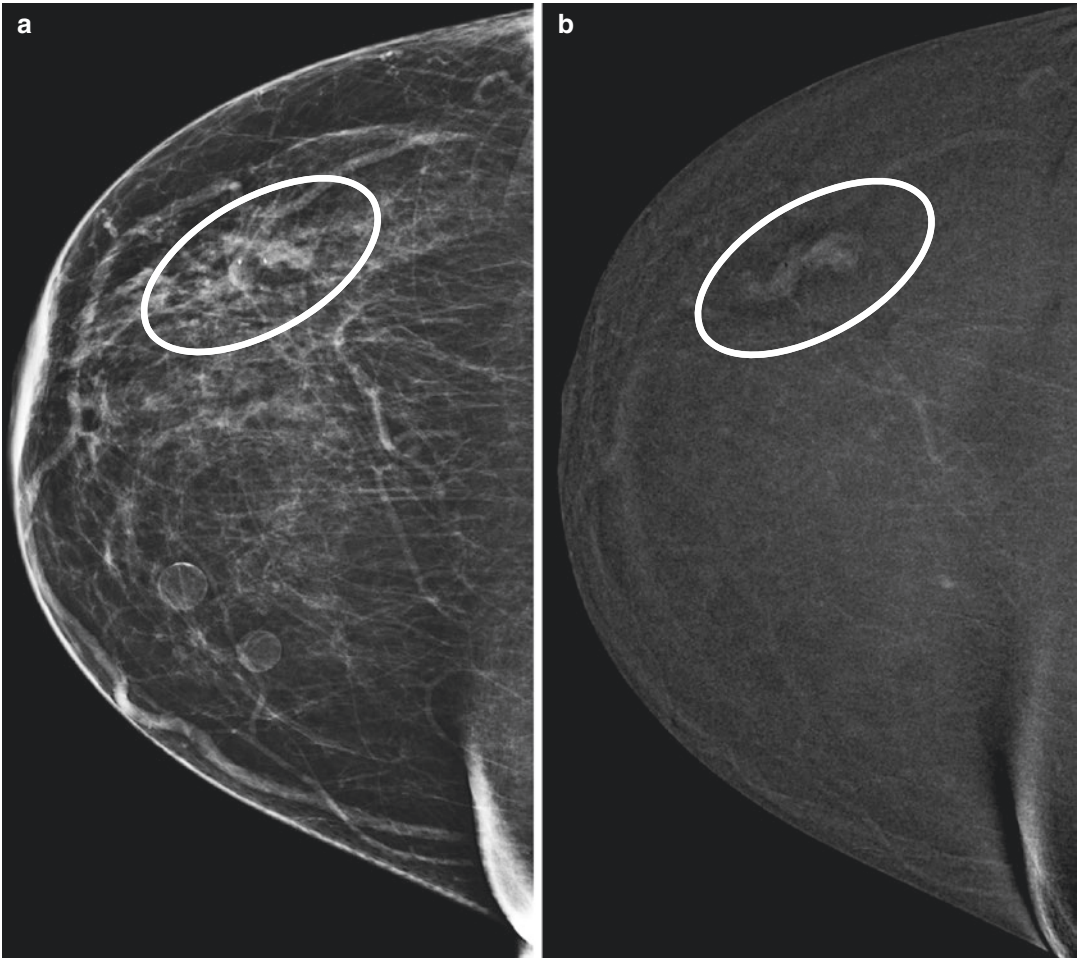


**Fig. 11.16** CEDM images of intraductal papillomas. (a and c) LE CEDM images in CC and MLO views show an oval opacity in the upper outer quadrant of the right breast. (b and d) CEDM recombined images demonstrate a faint, ill-defined, elongated enhancing mass that was biopsied

under sonographic guidance. The pathology was an intraductal papilloma. *CEDM* contrast-enhanced digital mammography, *CC* craniocaudal, *MLO* mediolateral oblique, *US* ultrasound



Fig. 11.16 (continued)

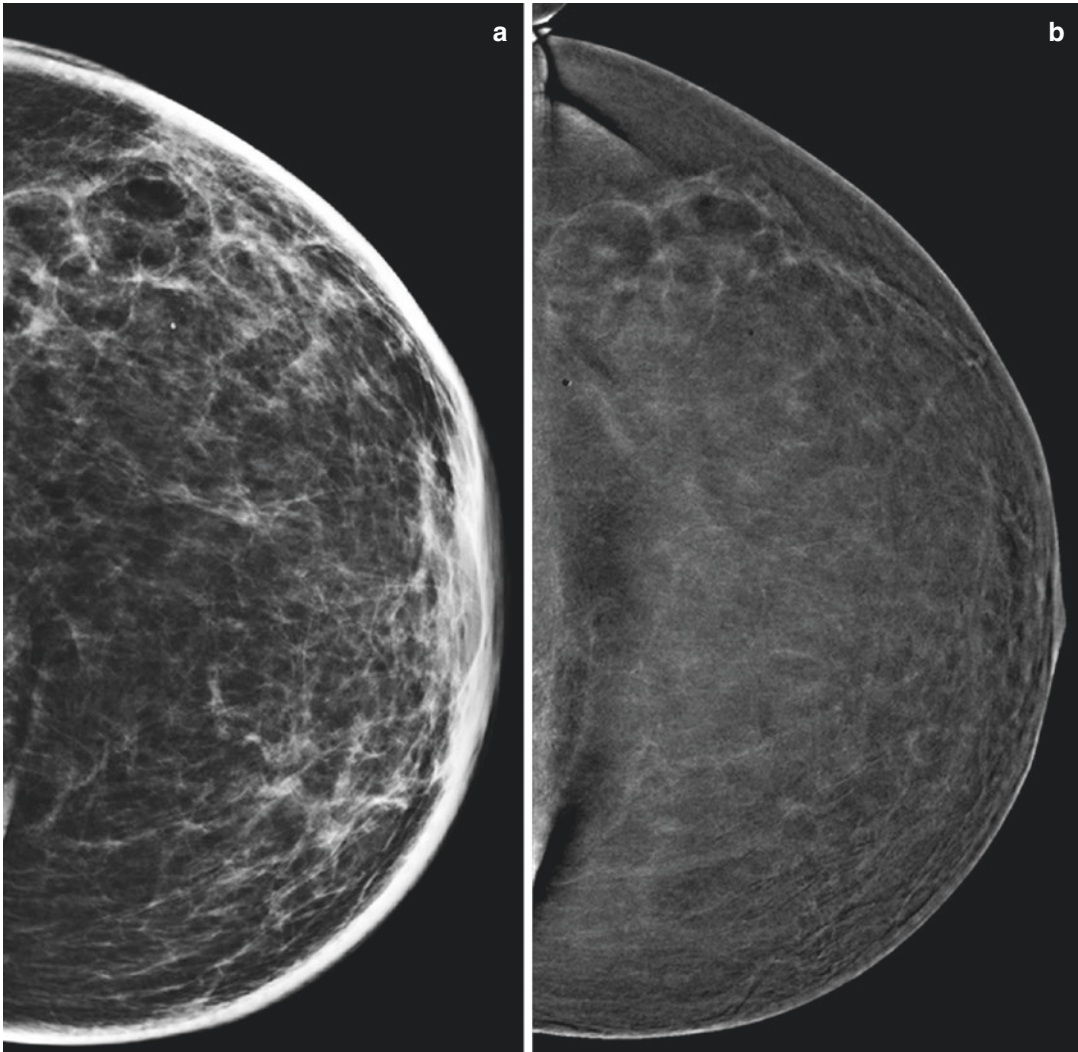


**Fig. 11.17** CEDM images of different patterns of fat necrosis. (a and c) LE CEDM images of the left breast in CC and MLO views show a surgical scar of a previous quadrantectomy with a round area of radiolucency on the upper outer quadrant, better seen on the magnification view (a<sup>1</sup>). (b and d) CEDM recombined images demon-

strate an area of radiotransparency surrounded by low-intensity peripheral enhancement in keeping with an oil cyst, better seen on the magnification view (b<sup>1</sup>). *CEDM* contrast-enhanced digital mammography, *CC* craniocaudal, *MLO* mediolateral oblique



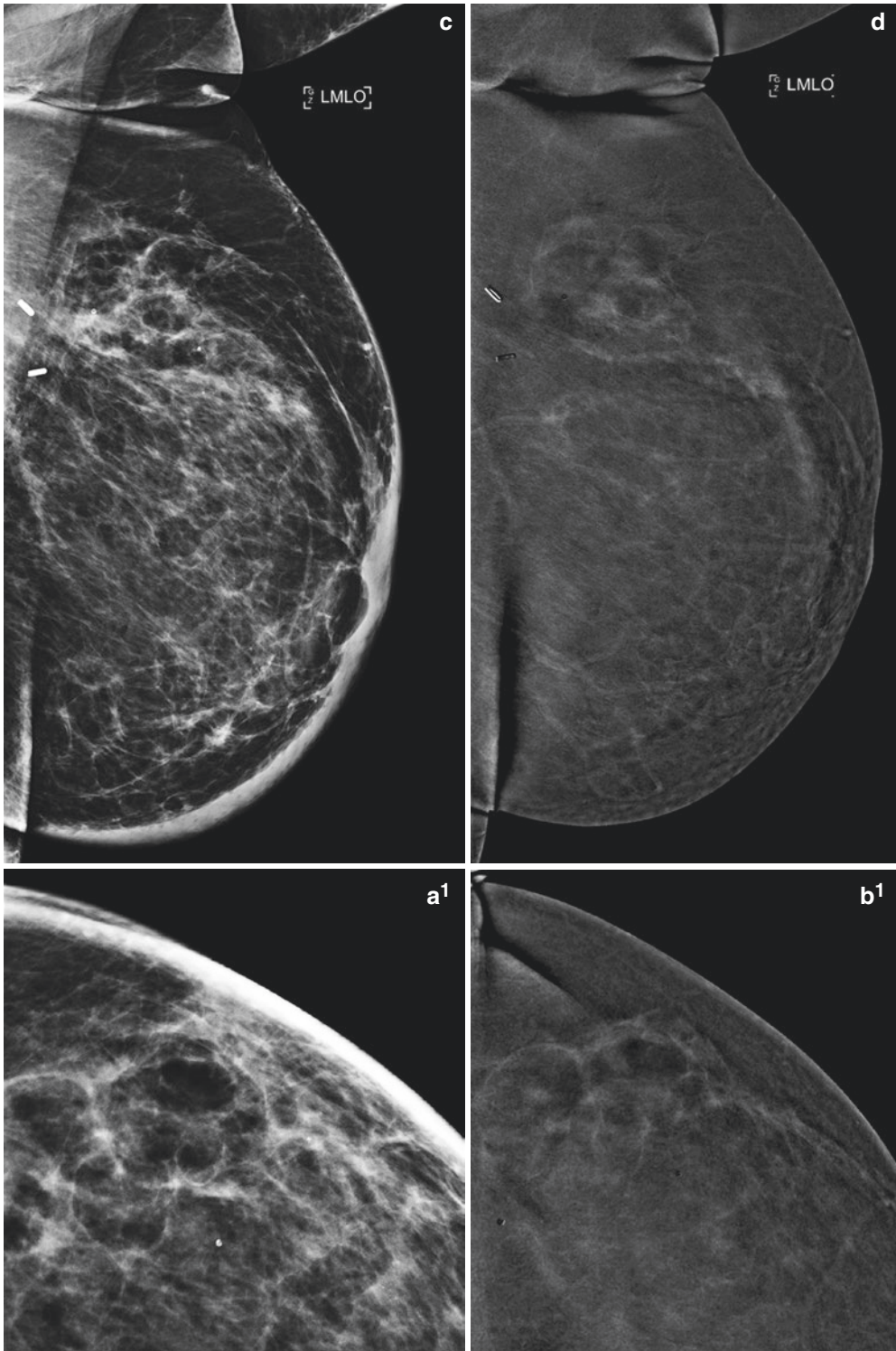
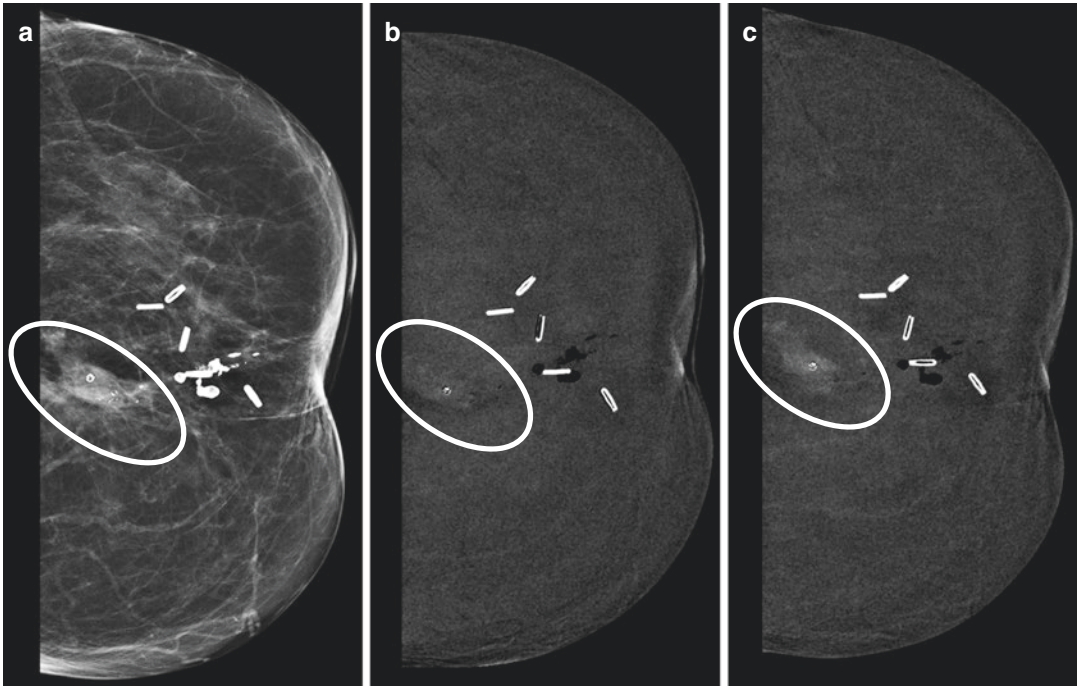
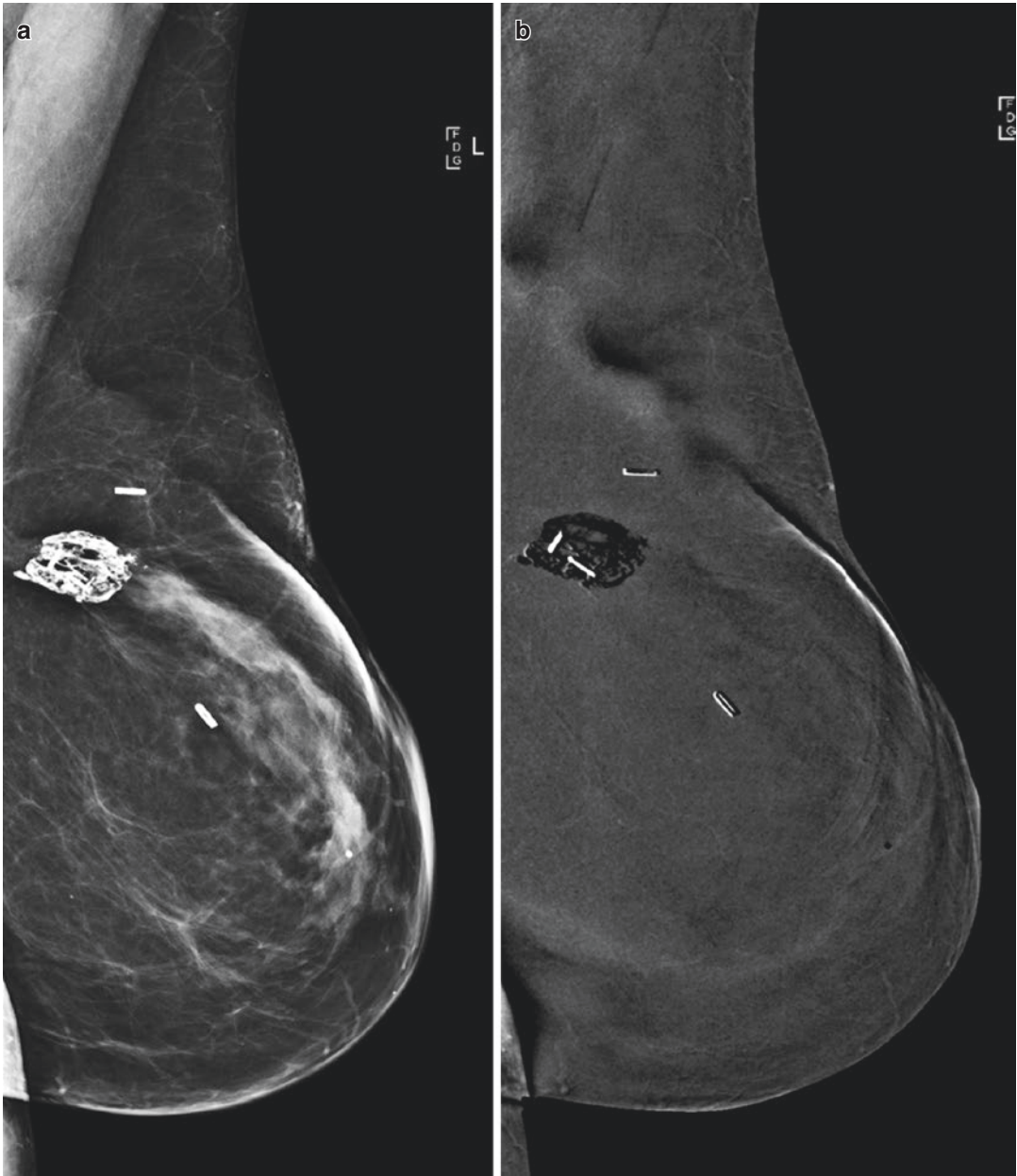


Fig. 11.17 (continued)



**Fig. 11.18** CEDM images of different patterns of fat necrosis. **(a)** LE CEDM image in CC view of the left breast shows a surgical scar of a previous quadrantectomy with a posteriorly located opacity located in the central quadrant behind the surgical clips. **(b–c)** CEDM recom-

bined images in early and delayed phases demonstrate a slow progressive enhancement corresponding to inflammation and fat necrosis. *CEDM* contrast-enhanced digital mammography, *CC* craniocaudal



**Fig. 11.19** CEDM images of different patterns of fat necrosis. (a) LE CEDM image in MLO view of the left breast shows a post quadrantectomy surgical scar with liponecrotic macrocalcifications in the upper outer quadrant near to the axilla. (b) CEDM recombined image in

MLO view shows no enhancement of the area, with an artefact typically seen with coarse calcifications known as “negative contrast enhancement”. CEDM contrast-enhanced digital mammography, MLO mediolateral oblique

## Conclusion

Although the introduction of CEDM has increased both the sensitivity and specificity of the detection of breast cancer over digital mammography and ultrasonography, the specificity of CEDM, similar to breast MRI, is still limited because some benign lesions have features that are indistinguishable from cancers [39–41].

The specificity of CEDM can be improved by combining morphological and dynamic characteristics and correlating CEDM presentation with clinical, mammographic and ultrasonographic features, although in our experience biopsy is usually necessary for further differentiation in many of these benign enhancing findings [42].

## References

- Guray M, Sahin A. Benign breast diseases: classification, diagnosis, and management. *Oncologist*. 2006;11(5):435–49.
- Putti TC, Pinder SE, et al. Breast pathology practice: most common problems in a consultation service. *Histopathology*. 2005;47:445–57.
- Miltenburg DM, Speights VO Jr. Benign breast disease. *Obstet Gynecol Clin North Am*. 2008;35:285–300.
- Neal L, Tortorelli CL, et al. Clinician's guide to imaging and pathologic findings in benign breast disease. *Mayo Clin Proc*. 2010;85:274–9.
- Pearlman MD, Griffin JL. Benign breast disease. *Obstet Gynecol*. 2010;116:747–58.
- Santen RJ, Mansel R. Benign breast disorders. *N Engl J Med*. 2005;353:275–85.
- Goehring C, Morabia A. *Epidemiol Rev*. 1997;19:310–27.
- Runruang B, Kelley J. Benign breast diseases: epidemiology, evaluation and management. *Clin Obstet Gynecol*. 2011;54:110–24.
- Hartmann LC, Sellers TA, et al. Benign breast disease and the risk of breast cancer. *N Engl J Med*. 2005;353:229–37.
- Bartow SA, Pathak DR, Black WC, et al. Prevalence of benign, atypical and malignant breast lesions in populations at different risk for breast cancer. A forensic autopsy study. *Cancer*. 1987;60:2751–60.
- Smith A. The principles of contrast mammography. [Info@hologic.com](mailto:Info@hologic.com).
- Lobbes MB, Smidt ML, et al. Contrast enhanced mammography: techniques, current results, and potential indications. *Clin Radiol*. 2013;68:935–44.
- Diekmann F, Freyer M, et al. Evaluation of contrast enhanced digital mammography. *Eur J Radiol*. 2011;78:112–21.
- Kamal R, Helal M, et al. Can we apply the MRI BI-RADS lexicon morphology descriptors on contrast-enhanced spectral mammography? *Br J Radiol*. 2016;89(1064):20160157.
- Jochelson MS, Dershaw DD, Sung JS, et al. Bilateral contrast enhanced dual-energy digital mammography: feasibility and comparison with conventional digital mammography and MRI imaging in women with known breast carcinoma. *Radiology*. 2013;266:743–51.
- Dupont WD, Page DL. Risk factors for breast cancer risk associated with proliferative breast disease and atypical hyperplasia. *Cancer*. 1993;71:1258–65.
- Orr B, Kelley JL III. Benign breast diseases: evaluation and management. *Clinical Obstet Gynecol*. 2016;59(4):710–26.
- Goel NB, Knight TE, et al. Fibrous lesions of the breast: imaging-pathologic correlation. *Radiographics*. 2005;25:1547–59.
- Dupont WD, Di P, et al. Long term risk of breast cancer in women with fibroadenoma. *N Engl J Med*. 1994;331:10–5.
- Houssami N, Irwig L, Ung O. Review of complex breast cysts: implications for cancer detection and clinical practice. *ANZ J Surg*. 2005;75:1080–5.
- Venta LA, Kim JP, Pelloski CE, et al. Management of complex breast cysts. *AJR Am J Roentgenol*. 1999;173:1331–6.
- Jensen RA, Page DL, Dupont WD, et al. Invasive breast cancer risk in women with sclerosing adenosis. *Cancer*. 1989;64:1977–83.
- London SJ, Connolly JL, Schnitt SJ, et al. A prospective study of benign breast disease and the risk of breast cancer. *JAMA*. 1992;267:941–4.
- Hines N, Slanetz PJ, et al. Cystic masses of the breast. *AJR*. 2010;194:W122–33.
- Chen J, Nalcioğlu O, et al. Fibrocystic change of the breast presenting as a focal lesion mimicking breast cancer in MR imaging. *J Magn Reson Imaging*. 2008;28(6):1499–505.
- Chen J, Liu H, et al. MR imaging features of fibrocystic change of the breast. *Magn Reson Imaging*. 2008;26(9):1207–14.
- Tse GM, Law BK, et al. Hamartoma of the breast: a clinical pathological review. *J Clin Pathol*. 2002;55:951–4.
- Linda A, Zuiani C, et al. The wide spectrum of hyperechoic lesions of the breast. *Clin Radiol*. 2011;66:559–65.
- Linda A, Zuiani C, Lorenzon M, et al. Hyperechoic lesions of the breast: not always benign. *AJR Am J Roentgenol*. 2011;196:1219–24.
- Adrada B, Wu Y, Yang W. Hyperechoic lesions of the breast: radiologic-histopathologic correlation. *AJR Am J Roentgenol*. 2013;200:W518–30.
- Presazzi A, Di Giulio G, et al. Breast hamartoma: ultrasound, elastosonographic, and mammographic features. Mini pictorial essay. *J Ultrasound*. 2015;18:373–7.



32. Knogler T, Homolka P, et al. Application of BI-RADS descriptors in contrast enhanced dual-energy mammography: comparison with MRI. *Breast Care*. 2017;12:212–6.
33. Tuffarelli M, Pellegrini A, et al. Positive predictive value of breast lesions of uncertain malignant potential (B3): Can we identify high risk patients? The value of a multidisciplinary team and implications in the surgical treatment. *Surg Oncol*. 2016;25:119–22.
34. Rakha EA, Ho BC, et al. Outcome of breast lesions diagnosed as lesion of uncertain malignant potential (B3) or suspicious of malignancy (B4) on needle core biopsy, including detailed review of epithelial atypia. *Histopathology*. 2011;56:626–32.
35. Rageth CJ, O'Flynn EAM, et al. First International Consensus Conference on lesions of uncertain malignant potential in the breast (B3 lesions). *Breast Cancer Res Treat*. 2016;159:203–203.
36. Eidi R, Chong J, et al. Papillary lesions of the breast: MRI, ultrasound, and mammographic appearances. *AJR Am J Roentgenol*. 2012;198:264–71.
37. Tan PH, Lai LM, et al. Fat necrosis of the breast: a review. *Breast*. 2006;15:313–8.
38. Taboada J, Stephens T, et al. The many faces of fat necrosis in the breast. *AJR Am J Roentgenol*. 2009;192:815–25.
39. Dromain C, Thibault F, Diekmann F, et al. Dual energy contrast-enhanced digital mammography: initial clinical result of a multireader, multicase study. *Breast cancer Res*. 2012;14:R94.
40. Luczynka E, Heinze-Paluchowska S, et al. Contrast enhanced spectral mammography: comparison with conventional mammography and histopathology in 152 women. *Korean J Radiol*. 2014;15:689–96.
41. Luczynka E, Niemiec J, et al. Degree of enhancement on contrast enhanced spectral mammography (CESM) and lesion type on mammography (MG): comparison based on histological results. *Med Sci Monit*. 2016;22:3886–93.
42. Covington MF, Pizzitola VJ, et al. The future of contrast enhanced mammography. *AJR Am J Roentgenol*. 2018;210:1–9.



## High-Risk (B3) Lesions

# 12

Giulia Bicchierai, Jacopo Nori,  
and Francesco Amato

### 12.1 Introduction

Breast lesions classified as lesions of uncertain malignant potential (B3) represent a wide range of non-malignant breast pathologies with a borderline histological spectrum and a variable risk of associated malignancy, which may predispose a patient to an increased risk of developing breast cancer in the future. The lesions in this B3 group include atypical ductal hyperplasia (ADH), flat epithelial atypia (FEA), classical lobular neoplasia (LN), papillary lesions (PL), benign phyllodes tumours (PT), radial scars (RS) and other uncommon abnormalities such as mucocele-like lesions. These lesions are diagnosed in 4–9% of all core needle biopsies (CNB), with increasing rates as breast imaging techniques and interventional tools such as vacuum-assisted biopsy (VAB) advance. The post-biopsy management of these lesions has changed in recent years from the previously recommended surgical excision of all lesions to a more conservative approach involving VAB and imaging follow-up [1]. Therefore, it is very important to find imaging modalities that identify B3 lesions associated with malignancy to distinguish patients who need surgery from those for whom imaging follow-up is sufficient.

---

G. Bicchierai (✉) · J. Nori · F. Amato  
Diagnostic Senology Unit, Department of Radiology,  
Azienda Ospedaliero Universitaria Careggi,  
Florence, Italy

Breast magnetic resonance imaging (MRI) has been evaluated in some studies for this purpose, but no specific imaging features that predict the upgrade of high-risk lesions have been definitively identified [2]. Contrast-enhanced digital mammography (CEDM) is a new breast imaging modality in which endovenous administration of iodinate contrast medium is used with digital mammography to depict lesion vascularity, similar to MRI. CEDM has been demonstrated to have a sensitivity similar to MRI for the detection of breast cancer, with increased specificity in addition to lower costs and greater availability. Therefore, it is an emerging technology that may help in predicting the malignant potential of breast lesions classified as B3 with CNB and VAB [3].

All B3 lesions, excepted for PL, are characterized by poor neoangiogenesis. As in MRI, CEDM identifies benign or malignant lesions based on the release of contrast medium from the vessels and its diffusion into the interstitium. Therefore, it is not surprising that B3 lesions often show minimal enhancement patterns. With this rationale, CEDM is able to identify associated occult malignant lesions.

In this chapter, we will review each category of B3 lesions and describe their appearance by CEDM based on our own experience and the limited data available in the literature. We will conclude this chapter by describing our evaluation of the diagnostic performance of CEDM in predicting the malignant potential of B3 lesions.

## 12.2 Atypical Ductal Hyperplasia

The histopathology features of ADH are essentially the same as those of low-grade ductal carcinoma in situ (DCIS). If less than 2 mm, the lesion is classified as ADH, and if greater than 2 mm, it is classified as low-grade DCIS [4, 5]. This comprises the fundamental problem underlying ADH diagnosis by cutaneous needle biopsy (CNB) which often only excises parts of the lesion. Hence, techniques such as vacuum-assisted biopsy (VAB) or surgical excisions are more accurate and may result in a more accurate upgrade of the diagnosis from a B3 to a B5 malignant lesion [6–9]. Furthermore, many believe that ADH is a direct precursor of low-grade ductal breast cancer (BC) because molecular studies have discovered shared molecular characteristics between atypical proliferative lesions such as ADH and low-grade DCIS [10, 11].

For this reason, most guidelines recommend surgical excision following a CNB diagnosis of ADH. Surveillance is only considered if a unifocal ADH lesion has been completely removed by VAB [1].

The appearance of ADH with CEDM is variable, ranging from non-enhancing lesions to areas of inhomogeneous or clumped non-mass enhancement, with a focal or ductal distribution, reflecting the similarity of the intraductal growth patterns of these lesions to DCIS. It is not uncommon that ADH lesions appear as masses with irregular margins. The kinetics of ADH enhancement patterns is often progressive, and the appearance of these lesions may be affected by the consequences of VAB biopsy (haematomas), which create an area of false-positive rim enhancement, frequently with the post-biopsy clip inside. However, we can easily differentiate this lesion

from a post-biopsy haematoma based on the patient's history and by performing a second-look ultrasound (Figs. 12.1, 12.2 and 12.3).

---

## 12.3 Papillary Lesion

Papillary lesions represent up to 5% of all biopsied breast lesions. PLs are intraductal solid formations consisting of a fibrous vascular axis covered with epithelium, which may be the site of atypia. Indeed, the term PL comprises a heterogeneous group of epithelial lesions such as intraductal papilloma, intraductal papilloma with ADH, intraductal papilloma with DCIS, papillary DCIS, encapsulated papillary carcinoma, solid papillary carcinoma and invasive papillary carcinoma. PLs demonstrate intralésional heterogeneity and are associated with small foci of ADH or DCIS within the PL or in the adjacent tissue, which may be missed by limited sampling with CNB [12–15]. When describing PL, only PL without atypia should be considered because lesions with atypia should be categorized among the higher-grade lesions (ADH) and are usually offered therapeutic surgical excision.

Upgrade rates after the surgical excision of benign papillomata diagnosed following CNB or VAB vary from 0 to 28% with atypical cells and from 0 to 20% for invasive cancer. Generally, understaging of invasive malignancy is reduced if multiple biopsy cores are taken or if larger biopsy needles are employed, such as those used in VAB. According to the recommendations of the recent First International Consensus Conference on B3 breast lesions [1], a PL lesion that is visible by imaging should undergo therapeutic excision with VAB, after which surveillance is justified [16–19].

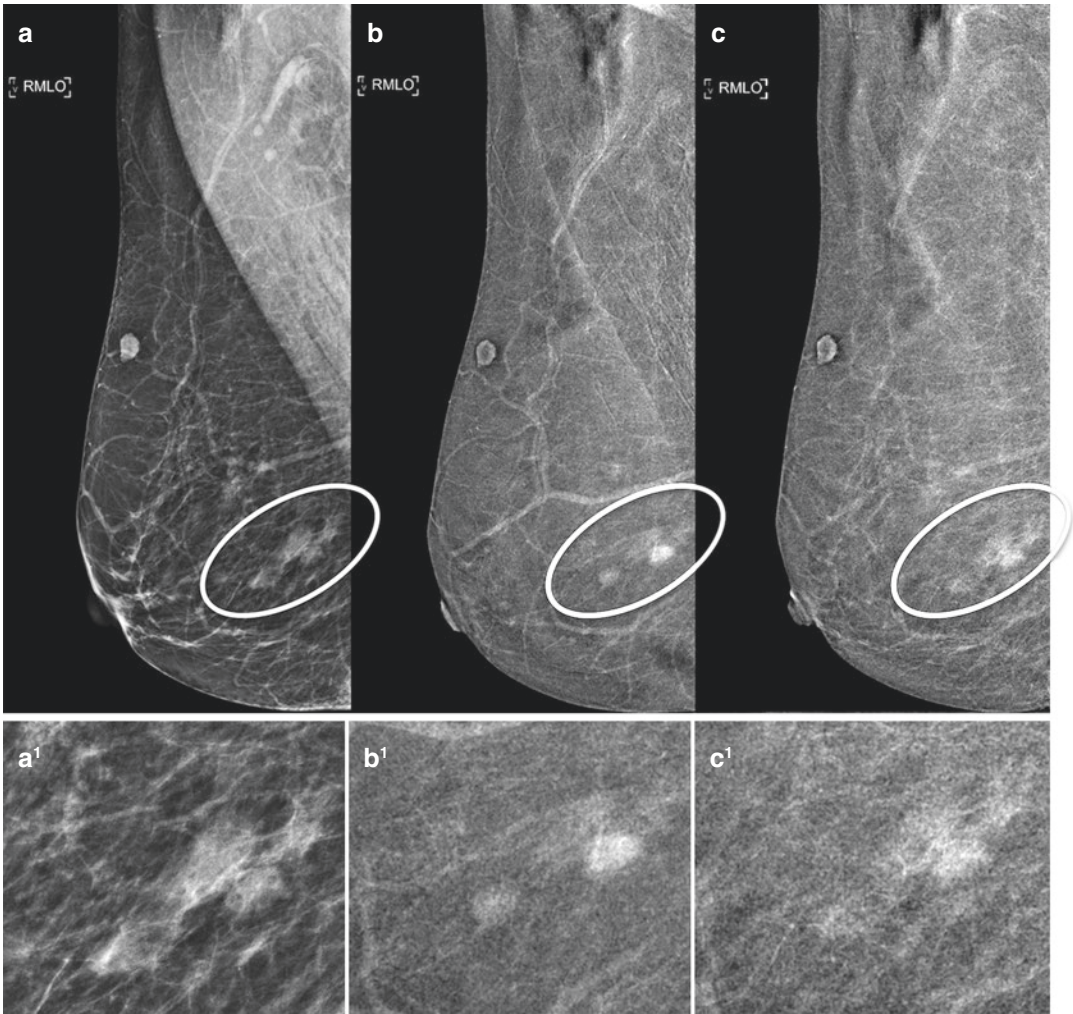


**Fig. 12.1** CEDM study in a 63-year-old woman with atypical ductal hyperplasia (ADH). (**a, a<sup>1</sup>**) Mediolateral oblique low-energy view, with magnification. (**b, b<sup>1</sup>**) Mediolateral oblique recombined images, with magnification, showing an 8.0 mm mass with heterogeneous enhancement, oval shape and ill-defined margins, in the

right lower outer breast (ADH). Behind this is an 8.5 mm mass with heterogeneous enhancement, oval shape and ill-defined margins, not previously known. (**c, c<sup>1</sup>**) Mediolateral oblique late recombined images, with magnification, showing a slightly progressive enhancement of the two masses

These lesions are generally pedunculated formations that can completely fill the duct from which they originate or the cystic cavity in which they grow.

The morphological and dynamic aspect of these lesions by CEDM depends on the size of the vascular component in the stromal axis. With CEDM, PL usually appears as oval-



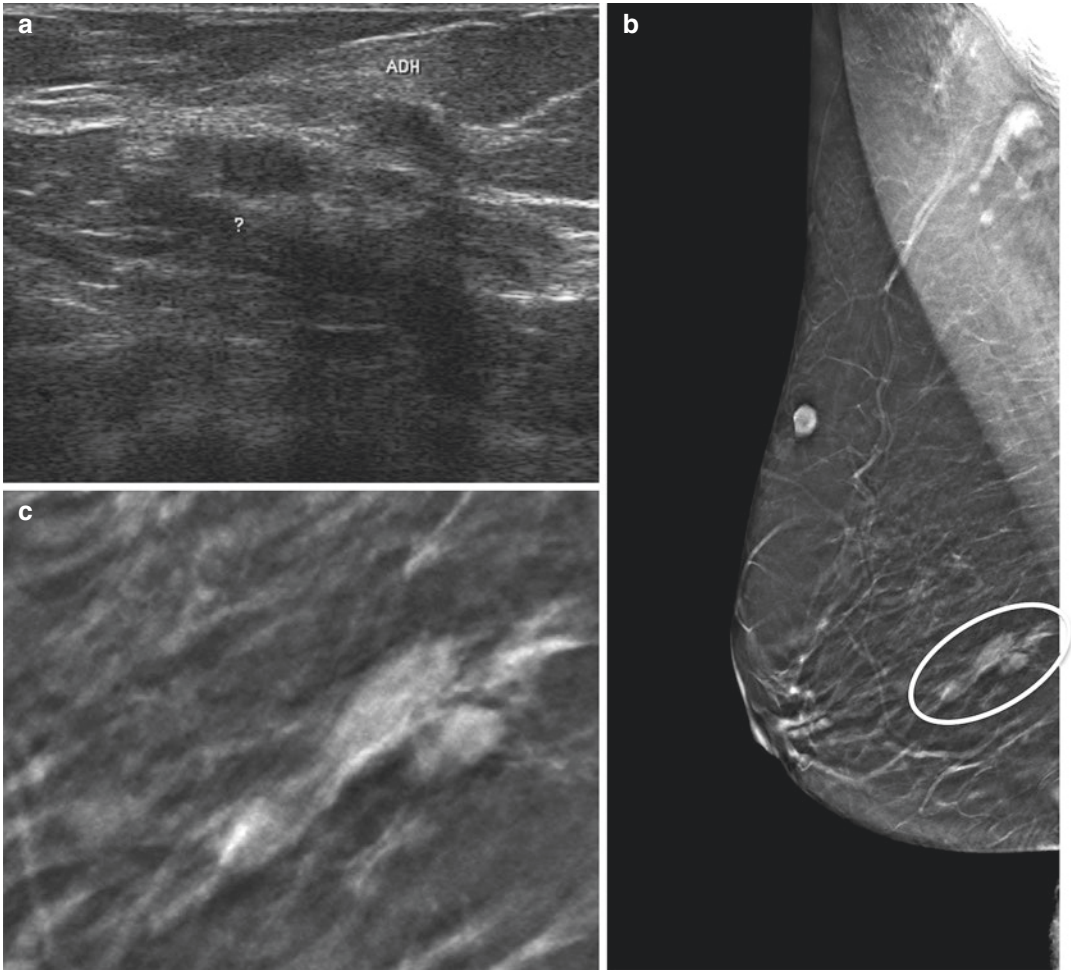


**Fig. 12.2** (a) Second-look ultrasonography after CEDM of the previous patient with ADH shows two hypoechoic lesions from refer to the two lesions showed by CEDM; (b, c) mediolateral oblique tomosynthesis slice

view, with magnification. The second lesion identified by CEDM resulted after ultrasound-guided core needle biopsy another ADH lesion

shaped masses with relatively well-circumscribed margins, which demonstrate intense or moderate enhancement and rapid washout (Figs. 12.4 and 12.5).

## 12.4 Classical Lobular Neoplasia

Classical LN encompasses a spectrum of atypical epithelial proliferations in the terminal ductal-lobular unit (TDLU) of the breast mainly consisting of proliferating of epithelial cells that fill and

extend the acinus. The histology consists of non-cohesive proliferating epithelial cells with or without pagetoid involvement of the terminal ducts. These proliferations consist of small, round, uniform cells that do not overlap, appear more dyshesive and have an increased nuclear to cytoplasmic ratio. Nuclear atypia should be minimal. Loss of E-cadherin staining is characteristic of LN and is also seen in advanced lesions such as invasive lobular carcinoma. An important distinction between LN and lobular carcinoma in situ is that there must be less than 50% involve-

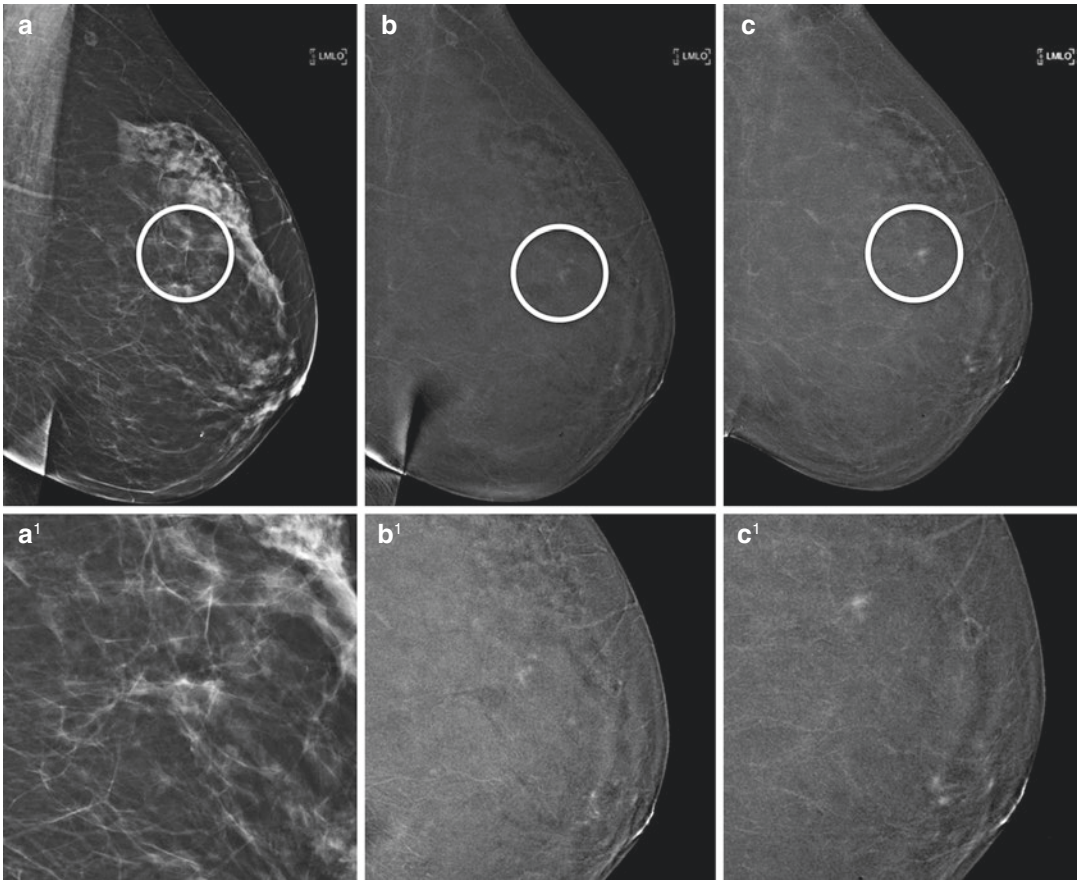


**Fig. 12.3** CEDM study in a 59-year-old woman with atypical ductal hyperplasia (ADH). (**a**, **a**<sup>1</sup>) Mediolateral oblique low-energy view, with magnification. (**b**, **b**<sup>1</sup>) Mediolateral oblique recombined images, with magnification, showing a 6.0 mm mass with a mild and heteroge-

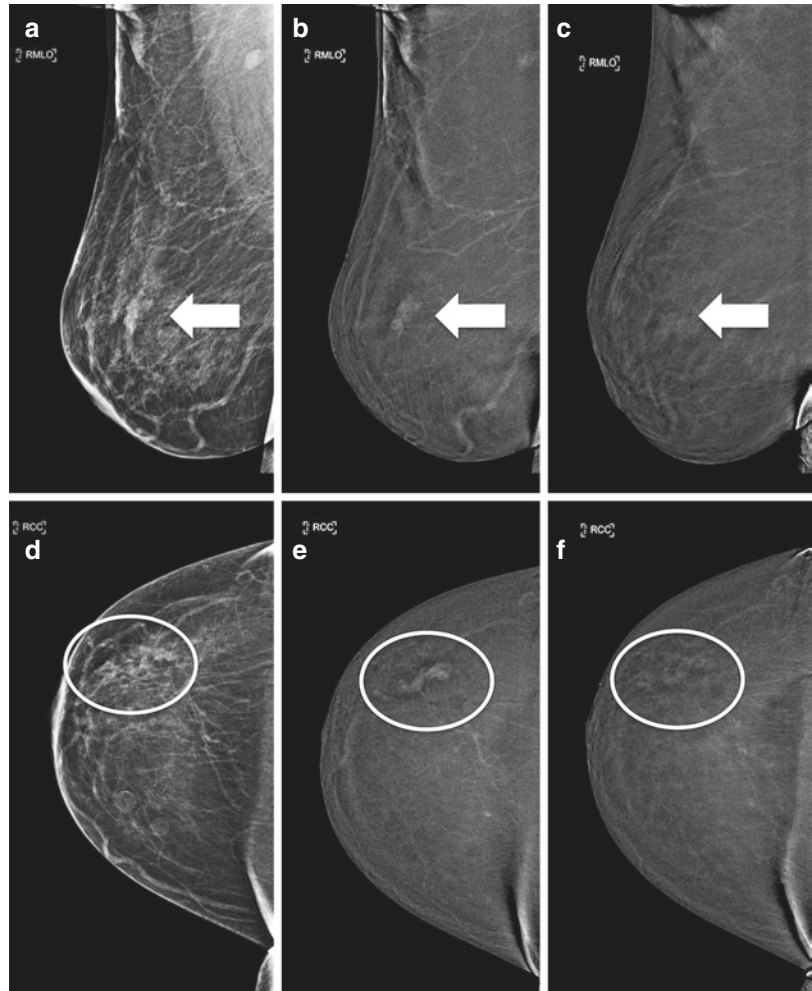
neous enhancement, oval shape and ill-defined margins, in the left upper outer breast. (**c**, **c**<sup>1</sup>) Mediolateral oblique recombined images, with magnification, showing progressive enhancement of the mass

ment of the acini in the TDLU to make the diagnosis of ALH [10, 20].

There are several nomenclatures used for LN. The classical type of LN covers all lobular lesions that develop in the TDLU, with the exception of those with pleomorphic or extensive variants. The older nomenclature of atypical lobular hyperplasia (ALH) and lobular carcinoma in situ (LCIS) refers to the same lesion but to a different extent; it is defined as ALH if less than 50% of the given TDLU is involved and LCIS if more than 50% is involved. The World Health Organization (WHO) also applies the term lobular intraepithelial lesion (LIN), which

is classified as LIN1, LIN2 and LIN3. LIN1 is formally equivalent to ALH, LIN2 to LCIS and LIN3 to the pleomorphic or extensive LN variants with or without necrosis [21]. The Swiss Minimally Invasive Breast Biopsies Working Group (MIBB), a subgroup of the Swiss Society of Senology classification of lobular neoplasia, categorizes all lesions (classical LN, ALH, LCIS, LIN1 and LIN2) as B3; however, LIN3 or pleomorphic LN or lesions with extensive necrosis are classified as B5a [22]. The MIBB classification and WHO recommend the use of histological terms: classical LN as B3 and pleomorphic LN as B5a [21, 22]. Some studies have

**Fig. 12.4** CEDM study in a 51-year-old woman with papillary lesion. (a, d) Mediolateral oblique and craniocaudal low-energy views. (b, e) Mediolateral oblique and craniocaudal recombined image showing a 2.0 cm oval mass with circumscribed margins and intense enhancement in the right central outer breast. (c, f) Mediolateral oblique and craniocaudal late recombined image showing the rapid “washout” of the papillary lesion



suggested that LN is predominantly a condition found in premenopausal women. Most lesions present incidentally without any palpable mass, and the predominant radiological features of LN are punctate microcalcifications or stromal deformity [23, 24].

LN is considered a non-obligate precursor of malignancy and a risk indicator. This interpretation is based on the fact that the presence of LIN is associated with an increased risk of bilateral malignancy that may include DCIS, invasive ductal carcinoma or invasive lobular

carcinoma. However, invasive malignancy is three times more frequent in the involved breast, and ILC is more frequent than IDC. The reported upgrade rates after LN is diagnosed at CNB or VAB vary between 0 and 58%, and upgrades are more frequent with LIN3 and pleomorphic LIN than with classical LIN grades 1 and 2 [4, 25–28].

According to the recent First International Consensus Conference on lesions of uncertain malignant potential [1], a classical LN lesion that is visible by imaging should undergo



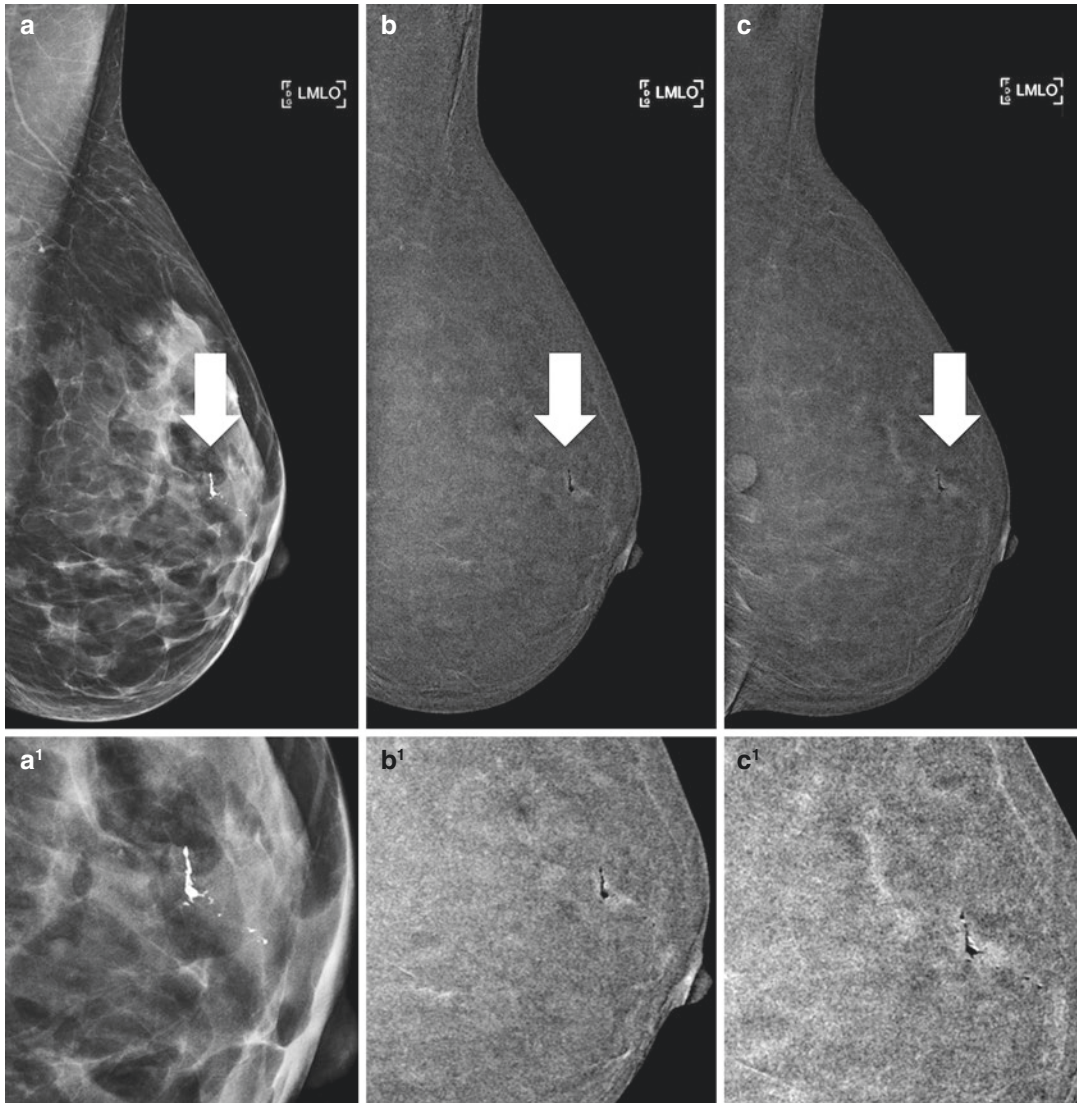


**Fig. 12.5** CEDM study in a 49-year-old woman with papillary lesion. (a, a<sup>1</sup>) Mediolateral oblique low-energy view with magnification. (b, b<sup>1</sup>) Mediolateral oblique early recombined image shows a 13 mm mass

with heterogeneous enhancement, oval shape and ill-defined margins with intense enhancement, in the left upper outer breast. (c, c<sup>1</sup>) Mediolateral oblique late recombined image shows a persistence of enhancement

therapeutic excision with VAB, and thereafter surveillance is justified. Due to the poor angiogenesis associated with these lesions, they often do not show enhancement with CEDM. However, when enhancement is present, more often the internal enhancement pat-

terns are non-mass-like, asymmetrical clumped or heterogeneous with a linear, focal or regional distribution. In some cases, the appearance may indicate a mass-like lesion with round or irregular shape and a heterogeneous enhancement pattern (Figs. 12.6 and 12.7).



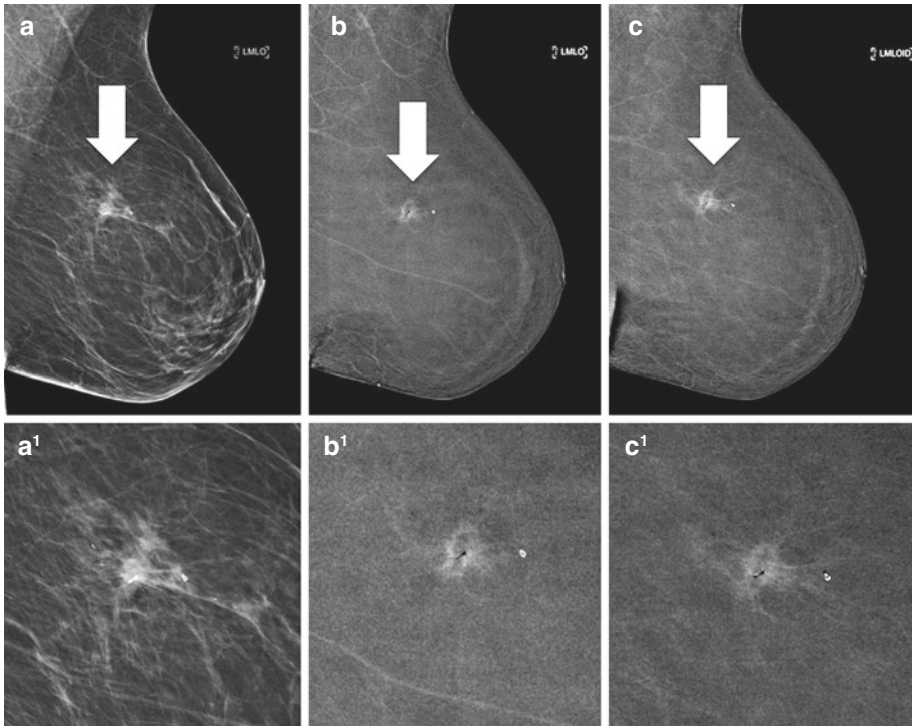


**Fig. 12.6** CEDM study in a 62-year-old woman with lobular neoplasia (LN). **(a, a<sup>1</sup>)** Mediolateral oblique low-energy view, with magnification. **(b, b<sup>1</sup>)** Mediolateral oblique early recombined image, with magnification, shows a 1.2 cm mass with heterogeneous enhancement,

oval shape and ill-defined margins, in the left upper outer breast. **(c, c<sup>1</sup>)** Mediolateral oblique late recombined image, with magnification, shows a progressive enhancement of the mass

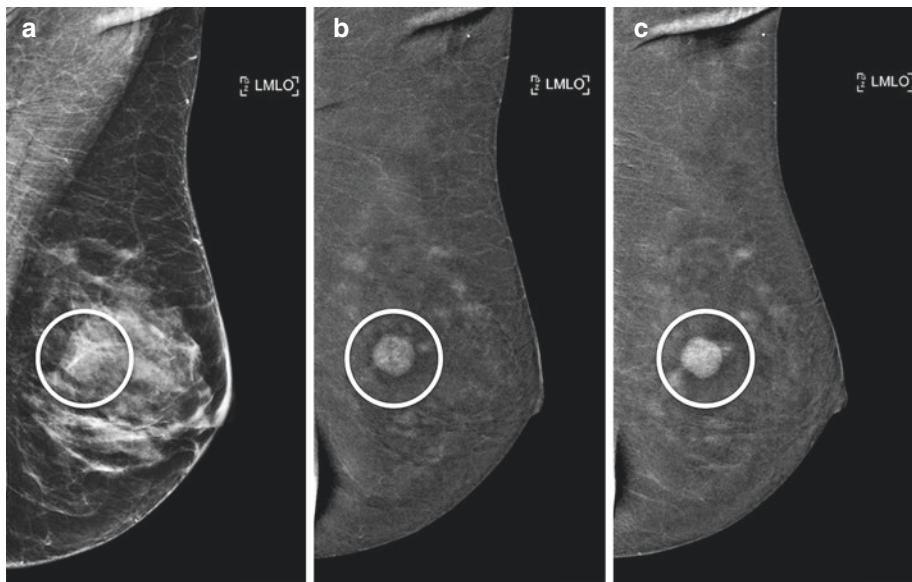


**Fig. 12.7** CEDM study in a 55-year-old woman with lobular neoplasia (LN). **(a)** Mediolateral oblique low-energy view. **(b)** Mediolateral oblique early recombined image shows a 1.5 cm mass with heterogeneous enhance-

ment, round shape and ill-defined margins, in the left slightly upper outer breast. **(c)** Mediolateral oblique late recombined image shows a slightly progressive enhancement of the mass

## 12.5 Radial Scars

RS or complex sclerosing lesions (CSL) of the breast are characterized by a stellate-like distortion.

Radial scar lesions are small (<10 mm), non-palpable and stellate or spiculated lesions usually detected by mammography. Complex sclerosing lesions are larger (>10 mm) and may be palpable, but both lesions are regarded as part of a continuum.

Histologically, these lesions are characterized by a central fibroelastotic core with entrapped ducts and surrounding radiating ducts and lobules with or without the presence of associated lobulocentric cysts, usual ductal hyperplasia, adenosis and microcalcifications. The adenosis may evolve the elastic fibres resulting in entrapped glands, which may mimic a highly differentiated neoplastic glandular proliferation. Post-mortem studies indicate that these lesions are commonly present in the population, especially in association with benign breast disease [29, 30].

On mammography, radial scars cannot be reliably differentiated from invasive malignancies; in particular, invasive lobular carcinoma and calcifications are also a common feature associated with RS. Therefore, based on the existing literature, any spiculated masses without a known cause (e.g. previous surgery) would require biopsy for definitive diagnosis [31].

The prognosis of RS/CSL depends on the presence of associated atypia. Based on the correlation between imaging and pathology, RS/CSL without atypia following CNB or VAB are unlikely to be malignant lesions in the surgical excision specimen. The relative risk of developing breast cancer given the presence of RS/CSL without atypia varies between 1.1 and 3.0%. Conversely, RS/CSL showing cytological or histological atypia have a relatively higher risk of malignant potential ranging from 2.8 to 6.7%, particularly in patients over 50 years of age. Upgrade rates vary from 0 to 43%, with significantly lower upgrade rates shown in studies using larger-gauge vacuum-assisted sampling devices [30, 32–37].

The recommendation for RS/CSL lesion in the recent First International Consensus Conference

on lesions of uncertain malignant potential in the breast [1] indicates that if the RS/CSL lesion is visible by imaging, it should undergo therapeutic excision with VAB, after which surveillance is justified.

The typical mode of presentation of RS in mammography is an architectural distortion with a hypodense centre, also known as a “black star”. Rarely, it presents as a spiculated opacity or microcalcifications.

On CEDM, radial scars often appear as masses with irregular or oval shape and heterogeneous or rim enhancement. Rarely, these radial scars may be seen as an asymmetric non-mass enhancement with a variable intensity of enhancement.

The degree of enhancement is often progressive or steady (Figs. 12.8 and 12.9).

---

## 12.6 Flat Epithelial Atypia

FEA is defined as a neoplastic proliferation of the terminal ductal-lobular units (TDLU) by a few layers of cells with low-grade (monomorphic) atypia. The histopathology of FEA lesions encompasses the proliferation of round and uniform cells (defined as low-grade atypia) exhibiting inconspicuous nuclei, often associated with calcifications. A FEA lesion lacks secondary architecture such as roman bridges or cellular tufts and exhibits a characteristic immunophenotype of negative low molecular weight cytokeratins and high regulation of oestrogen receptors.

With mammography, it typically presents as grouped amorphous calcifications, and with sonography, it is seen as an irregular hypoechoic or complex mass [38, 39].

Other lesions that are often associated with FEA, both by imaging and histopathology, encompass classical LN, other benign columnar cell lesions and low-grade intraductal proliferations such as ADH/DCIS or tubular carcinoma. Multiple studies have demonstrated a wide variability in FEA upgrade rates, leading to uncertainty about its clinical significance and management. The risk of malignancy associated with FEA has been estimated to be between 0 and

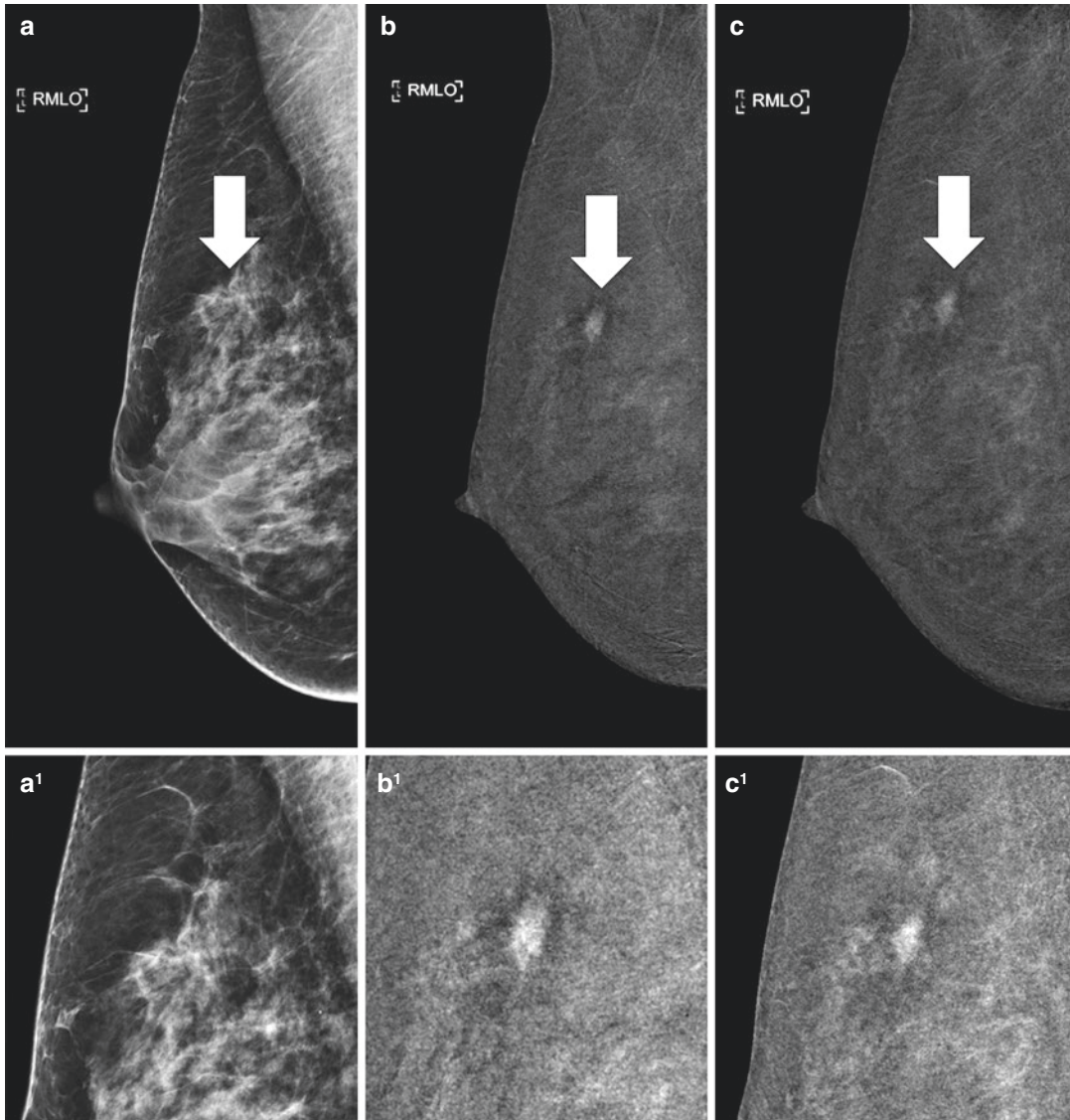
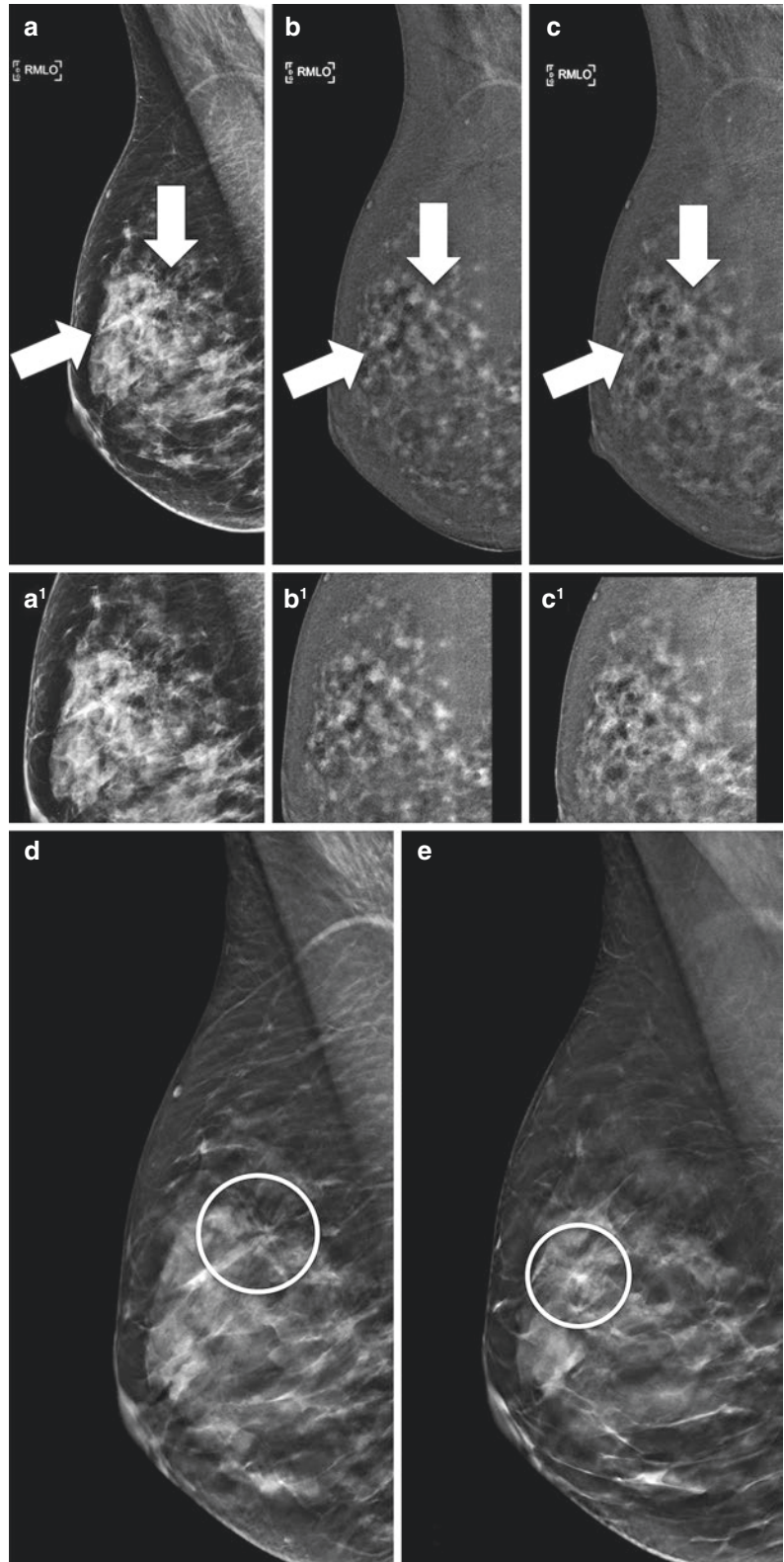


**Fig. 12.8** CEDM study in a 53-year-old woman with a radial scar. **(a, a<sup>1</sup>)** Mediolateral oblique low-energy view, with magnification. **(b, b<sup>1</sup>)** Mediolateral oblique early recombined image, with magnification, shows a 1.0 cm mass with

heterogeneous enhancement, oval shape and ill-defined margins, in the right upper outer breast. **(c, c<sup>1</sup>)** Mediolateral oblique late recombined image, with magnification, shows a slightly progressive enhancement of the mass



**Fig. 12.9** CEDM study in a 51-year-old woman with two radial scars. **(a, a<sup>1</sup>)** Mediolateral oblique low-energy view, with magnification. **(b, b<sup>1</sup>)** Mediolateral oblique early recombined image, with magnification, shows a 10 mm mass with heterogeneous enhancement, irregular shape and ill-defined margins, in the right upper outer breast, and another 7.0 mm mass with heterogeneous enhancement, irregular shape and ill-defined margins, in the right upper central breast. **(c, c<sup>1</sup>)** Mediolateral oblique late recombined image, with magnification, shows a slightly progressive enhancement of the masses. **(d–e)** Tomosynthesis slices images





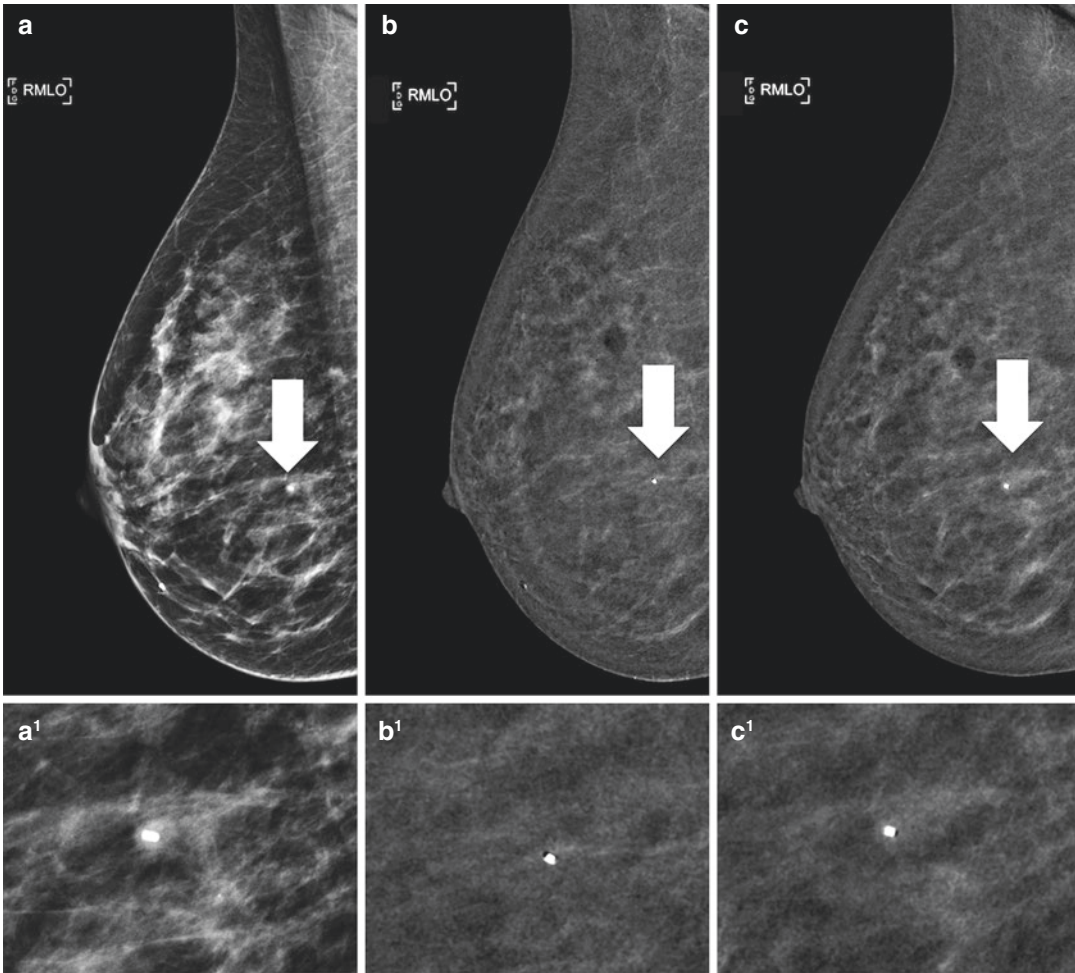


**Fig. 12.10** CEDM study in a 48-year-old woman with columnar cell hyperplasia. (**a**, **a**<sup>1</sup>) Mediolateral oblique low-energy view, with magnification, shows a clip in the site of the previous biopsy. (**b**, **b**<sup>1</sup>) Mediolateral oblique early recombined image shows a mild focal non-mass

enhancement in correspondence with the clip. (**c**, **c**<sup>1</sup>) Mediolateral oblique late recombined image shows a slightly progressive enhancement in correspondence with the clip

40% [40–44]. ADH and DCIS are the most frequent pathologies found following surgical excision.

Current recommendations of the First International Consensus Conference on lesions of uncertain malignant potential in the breast [1] do not suggest therapeutic open surgical excision of FEA diagnosed by CNB or VAB if the lesion is small (maximum two TDLU) and if the imaging abnormality was completely removed by VAB. Surgical excision is only recommended if there is radiopathological discrepancy, i.e. if the

lesion is visible with imaging and the imaging classification is BIRADS 4. However, for BIRADS 3 lesions that have been completely removed by VAB, open surgery is not considered necessary [1].

In CEDM, FEA lesions may be non-enhancing; however, if enhancement is present, most often it is a non-mass-like enhancement pattern with a focal or regional distribution, or there may be a rim enhancement secondary to post-biopsy complications. If enhancement is seen, it is usually weak or mild and progressive (Figs. 12.10 and 12.11).

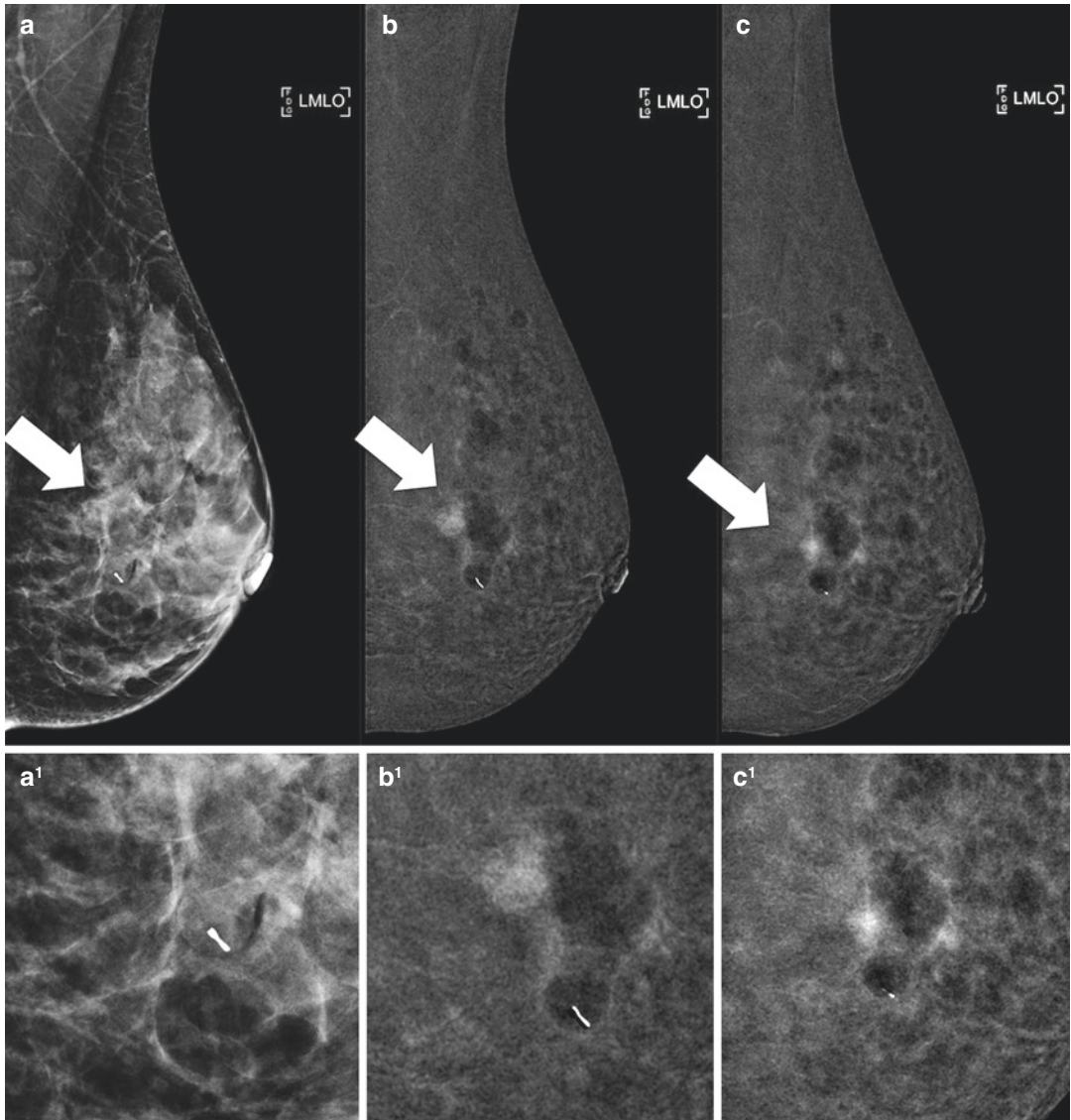


**Fig. 12.11** CEDM study in a 52-year-old woman with columnar cell hyperplasia. (a, a<sup>1</sup>) Mediolateral oblique low-energy view, with magnification, shows a clip in the site of the previous biopsy and a post-biopsy haematoma. (b, b<sup>1</sup>) Mediolateral oblique early recombined image

shows a mild focal non-mass enhancement in behind the clip, where there can see a rim enhancement in the site of post-biopsy haematoma. (c, c<sup>1</sup>) Mediolateral oblique late recombined image shows a progressive enhancement of the focal NME behind the clip

### 12.7 Potential Role of CEDM for Predicting Malignancy of B3 Lesions

We have described how the post-biopsy management of B3 lesions has changed in recent years, from the previously recommendation of

surgical excision for all lesions to a more conservative approach with VAB and imaging follow-up. Therefore, it is very important to find imaging modalities that identify B3 lesions associated with malignancy to distinguish patients who need surgery from those in whom imaging follow-up is sufficient. Based on our

experience, CEDM may play an important role in this setting.

Breast magnetic resonance imaging (MRI) has been evaluated in some studies for this purpose, but no specific imaging features that predict the upgrade of high-risk lesions have been definitively identified [45–52]. Worldwide, CEDM is a rapidly evolving technology that may be an alternative to MRI for the same clinical indications. CEDM has been demonstrated to have sensitivity comparable to that of MRI for the detection of breast cancer and also has increased specificity, in addition to lower costs and greater availability.

Based on our experience, CEDM has shown excellent results in the pre-surgical assessment of B3 lesions. We observed that B3 lesions that were upgraded to malignancy after surgical excision frequently demonstrated enhanced mass lesions with an oval or irregular shape and heterogeneous internal enhancement by CEDM. These morphological descriptors, analysed in Chapter 9 of this book, allow us to correctly classify B3 lesions as suspicious, especially if a mass shows a marked enhancement. We also observed that all upgraded lesions demonstrate a moderate or marked enhancement and it is the intensity of enhancement of the B3 lesions that best correlates with malignancy. Therefore, if you find a B3 lesion appearing as a mass with marked enhancement by CEDM, malignancy should be suspected, and you must consider surgical biopsy rather than follow-up.

However, post-biopsy haematoma, which usually appears as a mass with rim enhancement (as shown in Chapter 9), may mask a possible enhancement. To avoid the presence of a haematoma, we usually perform the CEDM examination when the haematoma (monitored with ultrasound) has resolved, which is at least 2–3 weeks post-biopsy.

We also observed that if minimal or no enhancement is seen at the site of a B3 lesion, there is a high likelihood that no invasive cancer is present. To date, the only false-negative lesions we have observed in our experience (i.e. a lesion with absent or minimal enhancement at CEDM that was found to be malignant at histological post-surgical analysis) were ductal carcinomas in situ. In our opinion, the lack of diagnosis of low-grade DCIS we encountered

may be tolerated in light of a close follow-up or by considering the recommended therapeutic excision of B3 lesions with VAB. In our false-negative lesions, the lack of detectable enhancement may have been the result of a small tumour size or weak angiogenesis. However, another factor that may hinder the interpretation of CEDM images is a moderate or marked background parenchymal enhancement (BPE) level, which we encountered in our study of false-negative lesions and found, may have been a masking element [53–56].

Therefore, the routine use of CEDM in the diagnostic-therapeutic path for B3 breast lesions allows better patient management. We also observed that approximately 87% of surgical excisions can be spared if all patients with negative CEDM examination results are hypothetically referred for follow-up, missing only low-grade DCIS. This, combined with the high negative predictive value for the detection of malignant lesions by CEDM, confirms the marked potential of this new diagnostic technique to exclude malignancy in a large proportion of B3 cases, potentially sparing the patient unnecessary surgical intervention.

CEDM is also useful in the follow-up of B3 lesions, combining the advantages of contrast medium with those of conventional mammography imaging, with total costs approximately six times lower than MRI [57].

---

## References

1. Rageth CJ, O'Flynn EA, Comstock C, et al. First International Consensus Conference on lesions of uncertain malignant potential in the breast (B3 lesions). *Breast Cancer Res Treat.* 2016;159(2):203–13.
2. Pediconi F, Padula S, Dominelli V, et al. Role of breast MR imaging for predicting malignancy of histologically borderline lesions diagnosed at core needle biopsy: prospective evaluation. *Radiology.* 2010;257(3):653–61.
3. Fallenberg EM, Schmitzberger FF, Amer H, et al. Contrast-enhanced spectral mammography vs. mammography and MRI – clinical performance in a multi-reader evaluation. *Eur Radiol.* 2017;27(7):2752–64.
4. Page DL, Dupont WD, Rogers LW, Rados MS. Atypical hyperplastic lesions of the female breast. A long-term follow-up study. *Cancer.* 1985;55(11):2698–708.

5. Tavassoli FA, Norris HJ. A comparison of the results of long-term follow-up for atypical intraductal hyperplasia and intraductal hyperplasia of the breast. *Cancer*. 1990;65:518–29.
6. AGO. Guidelines of the AGO Breast committee: lesions of uncertain malignant potential (B3) (ADH, LIN, FEA, Papilloma, Radial Scar).
7. Brem RF, Behrndt VS, Sanow L, Gatewood OM. Atypical ductal hyperplasia: histologic underestimation of carcinoma in tissue harvested from impalpable breast lesions using 11-gauge stereotactically guided directional vacuum-assisted biopsy. *AJR Am J Roentgenol*. 1999;172:1405–7.
8. Bedei L, Falcini F, Sanna PA, Casadei Giunchi D, Innocenti MP, Vignutelli P, et al. Atypical ductal hyperplasia of the breast: the controversial management of a borderline lesion: experience of 47 cases diagnosed at vacuum-assisted biopsy. *Breast*. 2006;15:196–202.
9. Gumus H, Mills P, Gumus M, Fish D, Jones S, Jones P, et al. Factors that impact the upgrading of atypical ductal hyperplasia 2013. *Diagn Interv Radiol*. 2013;19:91–6.
10. Hartmann LC, Radisky DC, Frost MH, Santen RJ, Vierkant RA, et al. Understanding the premalignant potential of atypical hyperplasia through its natural history: a longitudinal cohort study. *Cancer Prev Res (Phila)*. 2014;7(2):211–7.
11. Myers DJ, Bhimji SS. *Breast, atypical hyperplasia*. StatPearls. Treasure Island: StatPearls Publishing; 2017. p. 8.
12. Bianchi S, Bendinelli B, Saladino V, Vezzosi V, Brancato B, Nori J, et al. Non-malignant breast papillary lesions - b3 diagnosed on ultrasound-guided 14-gauge needle core biopsy: analysis of 114 cases from a single institution and review of the literature. *Pathol Oncol Res*. 2015;21:535–46.
13. Liberman L, Bracero N, Vuolo MA, Dershaw DD, Morris EA, Abramson AF, et al. Percutaneous large-core biopsy of papillary breast lesions. *AJR Am J Roentgenol*. 1999;172:331–7.
14. Mercado CL, Hamele-Bena D, Singer C, Koenigsberg T, Pile-Spellman E, Higgins H, et al. Papillary lesions of the breast: evaluation with stereotactic directional vacuum-assisted biopsy. *Radiology*. 2001;221:650–5.
15. Reynolds HE. Core needle biopsy of challenging benign breast conditions: a comprehensive literature review. *AJR Am J Roentgenol*. 2000;174:1245–50.
16. Yamaguchi R, Tanaka M, Tse GM, Yamaguchi M, Terasaki H, Hirai Y, et al. Management of breast papillary lesions diagnosed in ultrasound-guided vacuum-assisted and core needle biopsies. *Histopathology*. 2015;66:565–76.
17. Chang JM, Moon WK, Cho N, Han W, Noh DY, Park IA, et al. Management of ultrasonographically detected benign papillomas of the breast at core needle biopsy. *AJR Am J Roentgenol*. 2011;196:723–9.
18. Youk JH, Kim MJ, Son EJ, Kwak JY, Kim EK. US-guided vacuum-assisted percutaneous excision for management of benign papilloma without atypia diagnosed at US-guided 14-gauge core needle biopsy. *Ann Surg Oncol*. 2012;19:922–8.
19. Chang JM, Han W, Moon WK, Cho N, Noh DY, Park IA, et al. Papillary lesions initially diagnosed at ultrasound-guided vacuum-assisted breast biopsy: rate of malignancy based on subsequent surgical excision. *Ann Surg Oncol*. 2011;18:2506–14.
20. Danforth DN. Molecular profile of atypical hyperplasia of the breast. *Breast Cancer Res Treat*. 2018;167(1):9–29.
21. Tavassoli FA, Millis RR, Boecker W, Lakhani SR. Lobular neoplasia. In: Lakhani SR, Ellis IO, Tan PH, Van de Vijver MJ, editors. *WHO classification of tumours of the breast*. 4th ed. Lyon: IARC; 2012. p. 60–2.
22. Saladin C, Haueisen H, Kampmann G, Oehlschlegel C, Seifert B, et al. Lesions with unclear malignant potential (B3) after minimally invasive breast biopsy: evaluation of vacuum biopsies performed in Switzerland and recommended further management. *Acta Radiol*. 2016;57(7):815–21.
23. Portschy PR, Marmor S, Nzara R, Virnig BA, Tuttle TM. Trends in incidence and management of lobular carcinoma in situ: a population-based analysis. *Ann Surg Oncol*. 2013;20:3240–6.
24. Maxwell AJ, Clements K, Dodwell DJ, Evans AJ, Francis A, et al. The radiological features, diagnosis and management of screen-detected lobular neoplasia of the breast: findings from the Sloane Project. *Breast*. 2016;27:109–15.
25. Heywang-Köbrunner SH, Nährig J, Hacker A, Sedlacek S, Höfler H. B3 lesions: radiological assessment and multi-disciplinary aspects. *Breast Care (Basel)*. 2010;5(4):209–17.
26. Bodian CA, Perzin KH, Lattes R. Lobular neoplasia. long term risk of breast cancer and relation to other factors. *Cancer*. 1996;78:1024–34.
27. D'Alfonso TM, Wang K, Chiu YL, Shin SJ. Pathologic upgrade rates on subsequent excision when lobular carcinoma in situ is the primary diagnosis in the needle core biopsy with special attention to the radiographic target. *Arch Pathol Lab Med*. 2013;137:927–35.
28. Elsheikh TM, Silverman JF. Follow-up surgical excision is indicated when breast core needle biopsies show atypical lobular hyperplasia or lobular carcinoma in situ: a correlative study of 33 patients with review of the literature. *Am J Surg Pathol*. 2005;29:534–43.
29. Kennedy M, Masterson AV, Kerin M, Flanagan F. Pathology and clinical relevance of radial scars: a review. *J Clin Pathol*. 2003;56(10):721–4.
30. Douglas-Jones AG, Denson JL, Cox AC, Harries IB, Stevens G. Radial scar lesions of the breast diagnosed by needle core biopsy: analysis of cases containing occult malignancy. *J Clin Pathol*. 2007;60(3):295–8.
31. Cohen MA, Newell MS. Radial scars of the breast encountered at core biopsy: review of histologic, imaging, and management considerations. *AJR Am J Roentgenol*. 2017;209(5):1168–77.



32. Kalife ET, Lourenco AP, Baird GL, Wang Y. Clinical and radiologic follow-up study for biopsy diagnosis of radial scar/radial sclerosing lesion without other atypia. *Breast J*. 2016;22:637–44.
33. Hou Y, Hooda S, Li Z. Surgical excision outcome after radial scar without atypical proliferative lesion on breast core needle biopsy: a single institutional analysis. *Ann Diagn Pathol*. 2016;21:35–8.
34. Linda A, Zuiani C, Furlan A, Londero V, Girometti R, Machin P, et al. Radial scars without atypia diagnosed at imaging-guided needle biopsy: how often is associated malignancy found at subsequent surgical excision, and do mammography and sonography predict which lesions are malignant? *Am J Roentgenol*. 2010;194:1146–51.
35. Sloane JP, Mayers MM. Carcinoma and atypical hyperplasia in radial scars and complex sclerosing lesions: importance of lesion size and patient age. *Histopathology*. 1993;23:225–31.
36. Jacobs TW, Byrne C, Colditz G, Connolly JL, Schnitt SJ. Radial scars in benign breast-biopsy specimens and the risk of breast cancer. *N Engl J Med*. 1999;340:430–6.
37. Miller CL, West JA, Bettini AC, et al. Surgical excision of radial scars diagnosed by core biopsy may help predict future risk of breast cancer. *Breast Cancer Res Treat*. 2014;145:331–8.
38. Solorzano S, Mesurole B, Omeroglu A, et al. Flat epithelial atypia of the breast: pathological-radiological correlation. *AJR Am J Roentgenol*. 2011;197:740–6.
39. Senetta R, Campanino PP, Mariscotti G, Garberoglio S, Daniele L, Pennecci F, et al. Columnar cell lesions associated with breast calcifications on vacuum-assisted core biopsies: clinical, radiographic, and histological correlations. *Mod Pathol*. 2009;22:762–9.
40. Lamb LR, Bahl M, Gadd MA, Lehman CD. Flat epithelial atypia: upgrade rates and risk-stratification approach to support informed decision making. *J Am Coll Surg*. 2017;225(6):696–701.
41. Piubello Q, Parisi A, Eccher A, Barbazeni G, Franchini Z, Iannucci A. Flat epithelial atypia on core needle biopsy: which is the right management? *Am J Surg Pathol*. 2009;33:1078–1084.
42. Chivukula M, Bhargava R, Tseng G, Dabbs DJ. Clinicopathologic implications of “flat epithelial atypia” in core needle biopsy specimens of the breast. *Am J Clin Pathol*. 2009;131:802–808.
43. Acott AA, Mancino AT. Flat epithelial atypia on core needle biopsy, must we surgically excise? *Am J Surg*. 2016;212:1211–3.
44. Dialani V, Venkataraman S, Frieling G, et al. Does isolated flat epithelial atypia on vacuum-assisted breast core biopsy require surgical excision? *Breast J*. 2014;20:606–14.
45. Linda A, Zuiani C, Bazzocchi M, Furlan A, Londero V. Borderline breast lesions diagnosed at core needle biopsy: can magnetic resonance mammography rule out associated malignancy? Preliminary results based on 79 surgically excised lesions. *Breast*. 2008;17(2):125–31.
46. Sardanelli F, Houssami N. Evaluation of lesions of uncertain malignant potential (B3) at core needle biopsy using magnetic resonance imaging: a new approach warrants prospective studies. *Breast*. 2008;17(2):117–9.
47. Cheeney S, Rahbar H, Dontchos BN, Javid SH, Rendi MH, Partridge SC. Apparent diffusion coefficient values may help predict which MRI-detected high-risk breast lesions will upgrade at surgical excision. *J Magn Reson Imaging*. 2017;46(4):1028–36.
48. Heller SL, Moy L. Imaging features and management of high-risk lesions on contrast-enhanced dynamic breast MRI. *AJR Am J Roentgenol*. 2012;198(2):249–55.
49. Londero V, Zuiani C, Linda A, Girometti R, Bazzocchi M, Sardanelli F. High-risk breast lesions at imaging-guided needle biopsy: usefulness of MRI for treatment decision. *AJR Am J Roentgenol*. 2012;199(2):W240–50.
50. Linda A, Zuiani C, Furlan A, Lorenzon M, Londero V, Girometti R, Bazzocchi M. Nonsurgical management of high-risk lesions diagnosed at core needle biopsy: can malignancy be ruled out safely with breast MRI? *AJR Am J Roentgenol*. 2012;198(2):272–80.
51. Crystal P, Sadaf A, Bukhanov K, McCready D, O'Malley F, Helbich TH. High-risk lesions diagnosed at MRI-guided vacuum-assisted breast biopsy: can underestimation be predicted? *Eur Radiol*. 2011;21(3):582–9.
52. Strigel RM, Eby PR, Demartini WB, Gutierrez RL, Allison KH, Peacock S, Lehman CD. Frequency, upgrade rates, and characteristics of high-risk lesions initially identified with breast MRI. *AJR Am J Roentgenol*. 2010;195(3):792–8.
53. Kuhl CK, Schrading S, Bieling HB, et al. MRI for diagnosis of pure ductal carcinoma in situ: a prospective observational study. *Lancet*. 2007;370(9586):485–92.
54. Sardanelli F, Bacigalupo L, Carbonaro L. What is the sensitivity of mammography and dynamic MR imaging for DCIS if the whole-breast histopathology is used as a reference standard? *Radiol Med*. 2008;113(3):439–51.
55. Sogani J, Morris EA, Kaplan JB, D'Alessio D, Goldman D, Moskowitz CS, Jochelson MS. Comparison of background parenchymal enhancement at contrast-enhanced spectral mammography and breast MR imaging. *Radiology*. 2017;282(1):63–73.
56. Savaridas SL, Taylor DB, Gunawardana D, Phillips M. Could parenchymal enhancement on contrast-enhanced spectral mammography (CESM) represent a new breast cancer risk factor? Correlation with known radiology risk factors. *Clin Radiol*. 2017. pii: S0009-9260(17)30403-8.
57. Patel BK, Gray RJ, Pockaj BA. Potential cost savings of contrast-enhanced digital mammography. *AJR Am J Roentgenol*. 2017;208(6):W231–7.



## 13.1 Introduction

Breast cancer is the most common cancer in women, with over 230,000 new cases diagnosed in the United States and 1.5 million new cases of invasive carcinoma diagnosed worldwide each year. For women, there is an approximately 12.4% (1 in 8) individual lifetime chance of developing invasive breast cancer. Breast cancer death rates declined 39% from 1989 to 2015 among women, and this progress was attributed to improvements in early detection [1]. Therefore, the ultimate goal for any breast imaging modality is to decrease the mortality from breast cancer by improving detection at its early stage and diagnosis.

Angiogenesis is the process by which new blood vessels are formed and has been recognized as a key element in the pathophysiology of tumour growth and metastases [2]. Tumours can only grow up to a diameter of 1–2 mm, beyond which neovascularization becomes a necessity, as passive diffusion is no longer sufficient to support the viability of malignant cells [3, 4].

Oncologic research has focused on the development of antiangiogenic and antivascular agents, bringing with it a demand for an accurate means of diagnosing tumour angiogenesis and monitoring treatment responses [5].

At present, magnetic resonance imaging (MRI) is regarded as the gold standard modality to provide functional information on neovascularity as a tumour-specific feature, improving the detection and characterization of breast cancers. MRI demonstrates relatively good spatial resolution and specificity, without ionizing radiation, and has limited side effects [6]. However, despite this increased ability for cancer detection, MRI is limited by its high cost, long acquisition times and low availability.

Contrast-enhanced digital mammography (CEDM) is an emerging breast imaging modality in which contrast enhancement is used with digital mammography to depict tumour neovascularity in a fashion similar to MRI [7–11].

Based on previous literature, CEDM has been demonstrated to be more sensitive than mammography for the detection of breast cancer. It has also shown to have sensitivity comparable to that of MRI at 96–100% for breast cancer detection, with fewer false positive findings in the pre-operative setting [12–14]. CEDM is becoming a promising addition to current breast imaging techniques due to its low cost, increasing availability and its ability to be used in women who are contraindicated for MRI [15].

J. Nori (✉) · C. Bellini  
Diagnostic Senology Unit, Department of Radiology,  
Azienda Ospedaliero Universitaria Careggi,  
Florence, Italy  
e-mail: [jakopo@tin.it](mailto:jakopo@tin.it)

C. Piccolo  
Department of Medicine and Health Science,  
University of Molise, Campobasso, Italy

In this chapter, we aim to review the imaging features of the malignant breast lesions frequently observed during our daily diagnostic work-up and to describe their morphologic and kinetic patterns, with particular mention of CEDM manifestations in our single-institution experience.

---

## 13.2 CEDM Malignant Findings

CEDM is an imaging modality which combines digital mammography with intravenous injection of iodinated contrast media to detect hypervascularized lesions. The rationale behind this modality lies in the digital subtraction between two images: one image containing information about breast vascularization and the second about its morphology. Based on the interaction between X-rays and iodine, it is possible to distinguish vascular structures, saturated by contrast agent, by a “high-energy” image (above the k-edge of iodine of 33 keV) and the morphological information by a “low-energy” image (below the 33 keV energy). The subtraction of the two images reveals the “hypervascularized” regions of the mammary gland [16].

CEDM is typically performed as a second-level technique for patients with suspicious focal lesions, when conventional mammography and additional ultrasound (US) examinations fail to make a definitive diagnosis. It is particularly useful in dense breasts or heterogeneously dense breasts (BI-RADS grades C and D), where cancer detection is lowered due to reduced mammographic sensitivity [17].

The hypervascularized appearance of malignant tumours has been emphasized since the first work on contrast-enhanced mammography. Breast cancers are usually characterized by an intense enhancement with spiculated contours in contrast-enhanced digital mammography, as opposed to the rest of the mammary gland, which is little or not at all enhanced. When breast cancer is clinically or radiologically suspected, CEDM may be performed to detect additional

homo- or contralateral lesions, enhancing those localizations not spontaneously visible by standard mammograms.

CEDM has been shown to have an excellent correlation with MRI for evaluating the disease extent, although current study results are still based on limited sample sizes [18, 19].

CEDM is also useful in the setting of a second-look examination by ultrasound, helping to identify additional lesions and to more easily decide on those that require a biopsy.

---

## 13.3 Malignant Breast Neoplasms

### 13.3.1 Ductal Carcinoma In Situ (DCIS)

DCIS is a non-invasive malignancy and a non-obligate precursor to invasive cancer. It is characterized by proliferation of malignant ductal epithelial cells lining the terminal ductal-lobular unit, without invasion through the basement membrane, leading to a dilatation of the duct itself [20].

The incidence of DCIS has risen dramatically since the use of screening mammography has strongly increased. According to the literature, multicentricity is observed in 8–33% of cases. In a case series by Lagios et al. [21], they reported that the likelihood of multicentricity increased with tumour size and DCIS lesions measuring over 2.5 cm in diameter were multicentric 47% of the time. Similar results were obtained by Dershaw et al. [22], who observed that all cases of DCIS measuring over 2.5 cm were characterized by multicentric disease and were associated with an increased risk of microinvasive components.

According to these data, it is easy to understand why a correct pre-operative assessment of the disease is mandatory, since it has been demonstrated that patients with positive margins after surgery, as well as patients with residual synchronous foci of DCIS, have increased risk for relapse. The frequency of local recurrence differs

according to the nuclear grade of the lesion, the presence and extent of necrosis or both [23, 24].

The traditional pathologic classification of DCIS is based on the architectural pattern, including cribriform, micropapillary, solid and comedo subtypes. However, this architectural subtype is not prognostic and is independent of the presence of necrosis and the histologic grade. Other classification systems for DCIS have tried to be more reproducible with a significant prognostic impact; among these, the simplest and fittest is the Van Nuys prognostic index system, which divides DCIS into three groups, based on the size, nuclear grade and presence or absence of comedo necrosis. Later, recommendations from the committee of the Consensus Conference on the Classification of DCIS identified three nuclear grades: low, high and intermediate [25, 26].

This digression is essential to better understand the kinetic behaviour of DCIS in CEDM examinations, as explained thereafter.

### 13.3.1.1 DCIS Findings

- *On mammography*, approximately 80% of DCIS lesions appear as a cluster of calcifications, which may be amorphous, coarse, heterogeneous or fine pleomorphic with a clustered, linear or segmental distribution [27]. The relationship between the histologic grade of DCIS and mammographic calcifications has been a subject of several studies, although only a few have shown a significant correlation; owing to the considerable overlap between the mammographic appearances of the different histologic subtypes, the pathologic grading cannot be determined prospectively with any accuracy on the basis of imaging findings [27]. Fine linear and fine linear branching calcifications seen in a grouped or segmental distribution are usually associated with higher-grade DCIS, whereas amorphous calcifications have been associated with low-grade DCIS. A significant association was found between fine pleomorphic or fine linear branching calcifications and necrosis; furthermore, a significant correlation was

encountered between round calcifications and low-grade DCIS.

In 10% of cases, DCIS can also appear as a mass at mammography, possibly related to two different conditions: the opacity could be a direct manifestation of an existing soft-tissue mass or may be a result of periductal fibrosis or elastosis producing an irregular or spiculated margin around a non-mass lesion. Low-grade DCIS appears as masses or asymmetries at imaging, differently from high-grade lesions, which usually manifest as calcified abnormalities. In 7–13% of cases, DCIS may manifest as an architectural distortion [28].

- *On US*, DCIS is infrequently seen, appearing as an intraductal, iso to hypoechoic, microlobulated soft tissue nodule with normal acoustic transmission. Sometimes, suspicious calcifications can be seen, and in those cases, a biopsy could also be performed based on US findings.
- *On MRI*, The sensitivity of MRI for the detection of DCIS has been shown to be higher for high-grade and intermediate-grade DCIS compared with low-grade DCIS (98%, 91% and 80%, respectively) [29, 30]. This observation was also demonstrated by Kuhl et al. [31], where they studied 89 cases of high-grade DCIS, of which 43 (48%) were missed by mammography but diagnosed by MRI alone. In contrast, MRI detected 87 (98%) of these lesions; the two cases missed by MRI were detected by mammography. They concluded that MRI could help improve the ability to diagnose DCIS, especially those with high nuclear grade type. Therefore, MRI is by far more sensitive than mammography in the detection of all grades of DCIS.

DCIS most commonly appears as an area of non-mass enhancement (NME) (60–81%) and less frequently as a mass (14–41%) or as a focus (1–12%) [29, 30].



DCIS may not be visible or hypointense on pre-contrast T1-weighted images and on non-fat-saturated or fat-saturated T2-weighted images because it could be masked by the normal breast parenchyma. DCIS may sometimes appear bright on T2-weighted images because of ductal secretions or necrosis.

In the MRI BIRADS lexicon, NME is defined as an area of enhancement distinct from the surrounding parenchyma, larger than a mass but without space-occupying effect features. The NME area shows stippled or patchy normal glandular tissue or fat within its borders. It is often not detected on pre-contrast images even when correlated with post-contrast images, and follows the distribution of glandular tissue. This imaging entity was unique to MRI until the appearance of CEDM and is usually not detected on mammography and US. The features of NME have been described extensively in Chapter 9 of this book.

Briefly, NME distribution descriptors include symmetric or asymmetric enhancement of the breast tissue. The BIRADS lexicon describes NME distribution as focal, linear, linear branching, segmental, regional, multiple regions and diffuse. NME internal enhancement descriptors are homogeneous, heterogeneous, stippled, clumped or clustered ring enhancement (a recently introduced internal enhancement descriptor).

Stippled enhancement refers to multiple, often innumerable punctuate foci and is usually typical of benign background parenchymal enhancement or fibrocystic changes. Clumped enhancement refers to cobblestone or beaded enhancement, with occasional confluent areas, often suggesting a DCIS in 60–80% of cases [32]. The term “clustered ring enhancement” is a new internal enhancement descriptor, describing “minute ring enhancements”, mostly associated with ductal carcinoma in situ and invasive cancers associated with ductal carcinoma in situ. Tozaki and colleagues [33] described this pattern in 63% of malignant lesions, compared with only 4% of benign lesions; a wash-out kinetic pattern was seen in 55% of malignant lesions with clustered

ring enhancement. Segmental distribution is the most common pattern of contrast distribution in DCIS (14–77% of cases) [34].

DCIS may appear as an enhancing mass in 14–34% of cases; focal enhancement, the least common finding, is seen in 1–12% of cases. On the other hand, the mixed forms of invasive and DCIS lesions appear as an enhancing mass in 76% of cases [35].

High-grade DCIS more frequently manifests as an enhancing mass than intermediate or low-grade DCIS does. According to Heywang-Köbrunner [36], there is significant variability in DCIS enhancement kinetics, with some lesions showing delayed enhancement. Furthermore, several studies have demonstrated that the qualitative enhancement patterns differ significantly according to lesion type. Mass lesions more often exhibit rapid uptake of contrast medium in the initial phase and rapid wash-out compared with non-mass lesions.

- *On CEDM*, detecting and staging DCIS is still under debate: similar to MRI, CEDM is capable of detecting non-calcified DCIS, providing a better tumour size assessment, in comparison with full-field digital mammography (FFDM). Unlike MRI, CEDM can also spot calcifications, which are seen as “negative contrast enhancement” artefacts, thus improving the diagnostic performance.

A recent study by Cheung et al. [37] focused on screening patients referred for CEDM to evaluate the presence of enhancement of areas of suspicious calcifications. They found that enhancement of areas with calcifications on CEDM significantly improved the cancer prediction rate, with a PPV of 46.15% for amorphous and 90% for pleomorphic calcifications and that all these types of findings were characterized by a high NPV of approximately 95%. The authors concluded that the enhancement detected in CEDM could be considered an adjuvant tool for assessing the study of calcifications. Another study by Luczynska et al. [38],

which compared the degree of enhancement on CEDM with mammographic findings and histopathological results, reported that 87.5% of DCIS lesions (presenting as calcifications or a mass with associated calcifications on FFDM) showed weak enhancement, with no false-negative cases.

- In our preliminary experience with 157 malignant lesions detected on CEDM, DCIS accounted for 13%, and DCIS associated with invasive elements accounted for 6%; there was no dominant pattern of presentation observed, with mass, NME and ring enhancement all manifesting with the same frequency for pure DCIS, while the pattern associated with invasive ductal carcinoma (IDC) presented itself in 42% of cases as a mass, in 42% of cases as NME and in 16% of cases as ring enhancement.

The kinetics of enhancement was characterized by a delayed enhancement in the majority of cases. A possible explanation for this finding may rely on the relative lack of blood supply and the diffusibility of contrast media to the ducts. As addressed by Fallenberg et al. [39], the possible explanation for this would be that the amount of contrast reaching the tissue by diffusion is time dependent. Therefore, longer time delays between contrast injection and CEDM exposure can result in stronger enhancement and better visibility of DCIS (Figs. 13.1 and 13.2).

For DCIS associated with IDC, 58% of lesions showed a progressive enhancement, and 42% exhibited a prompt wash-out.

### 13.3.2 Invasive Ductal Carcinoma, Not Otherwise Specified (IDC NOS)

Invasive ductal carcinoma accounts for 65–80% of breast cancers [40–42].

IDC is the most common invasive malignant breast tumour. At gross analysis, it appears as a

solid mass, with various degrees of necrosis and haemorrhage.

The morphologic patterns can have a wide variation, depending on its clinical and biological features.

#### 13.3.2.1 IDC Findings

- *On mammography*, IDC usually appears as a scirrhous, radiodense and irregular mass, often associated with a stromal desmoplastic reaction, responsible for spiculated margins; when calcifications manifest, they generally suggest an associated intraductal component. Less frequently, invasive ductal carcinomas are well defined, with a lobulated shape and circumscribed margins.
- *On US*, the typical finding is an inhomogeneous and hypoechoic lesion with irregular margins surrounded by a hyperechoic rim with posterior shadowing and increased vascularity on colour Doppler analysis.
- *On MRI*, owing to its high cellularity, IDC appears as a hypointense lesion on T2-weighted images. However, some of them may manifest as a high signal intensity on T2-weighted images because of the presence of necrosis, a finding suggesting a poorly differentiated high-grade carcinoma; extensive necrosis within an invasive breast carcinoma may be indicative of a rapid growth rate and an unfavourable prognosis [36, 41].

The majority of IDCs follow the “90/90 rule”: they enhance by 90% within the first 90 seconds after contrast medium injection.

The kinetics of IDC is typical of a malignant lesion, characterized by early enhancement with rapid uptake of contrast medium followed by wash-out (type III) in half of the cases and by a plateau in 40% of cases (type II). Just a few (5%) manifest a type I curve with a mild and progressive enhancement, a pattern reflecting a low-density lesion with abundant fibrosis, as occurs in the scirrhous type [36].

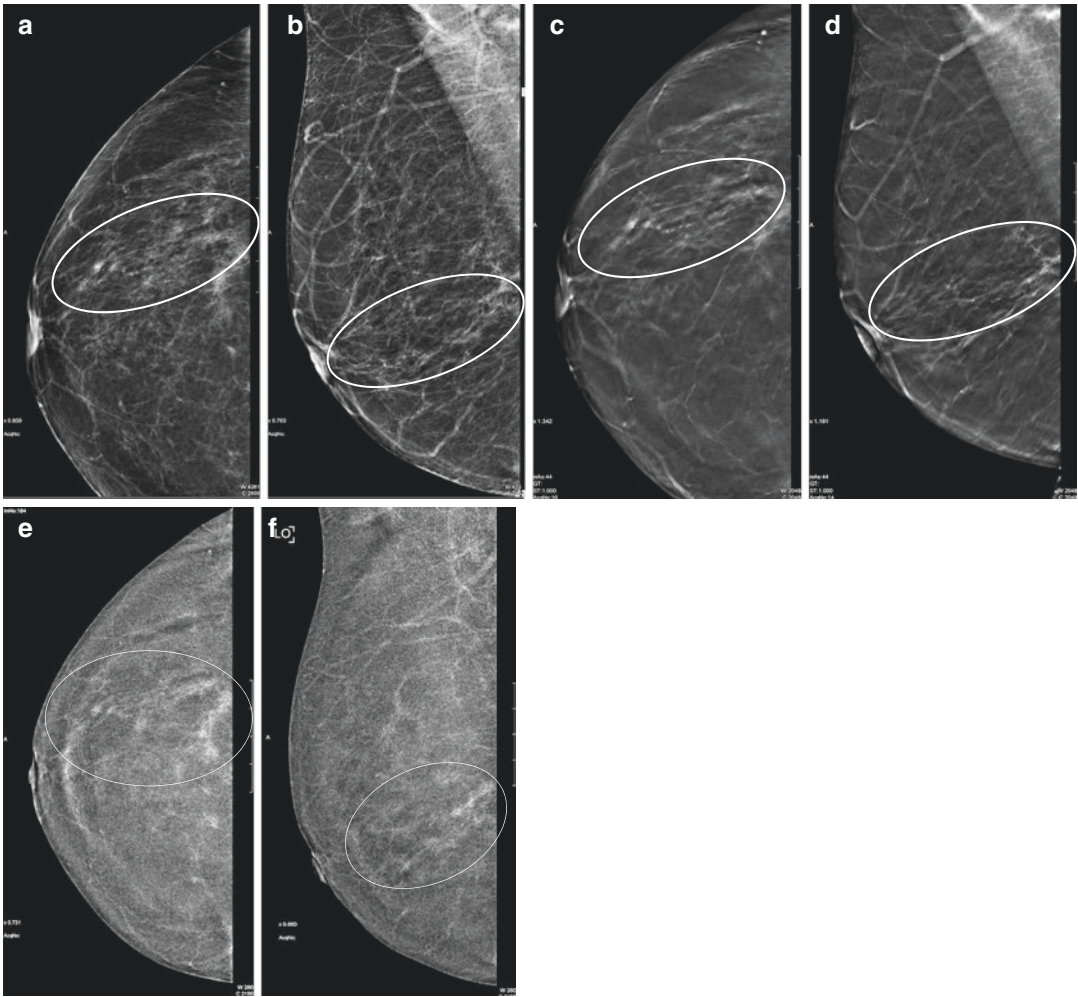


**Fig. 13.1** Pre-surgical staging in a patient with a BI-RADS 5 lesion in the mid-outer quadrant of the right breast, already biopsied. **(a, b)** Low energy 2D images in CC and MLO projections show a cluster of fine pleomorphic calcifications in a linear pattern of distribution (*circles*). **(c, d)** 3D in CC and MLO projection demonstrates a linear pattern of architectural distortion along the

segmental distribution of the calcifications (*circles*). **(e, f)** CEDM recombined image in CC and MLO projection. The examination demonstrates a faint non-mass enhancement in the lower-outer quadrant of the right breast, tracking along the distribution of the calcifications. *Diagnosis: The pathology was a ductal carcinoma in situ (DCIS)*

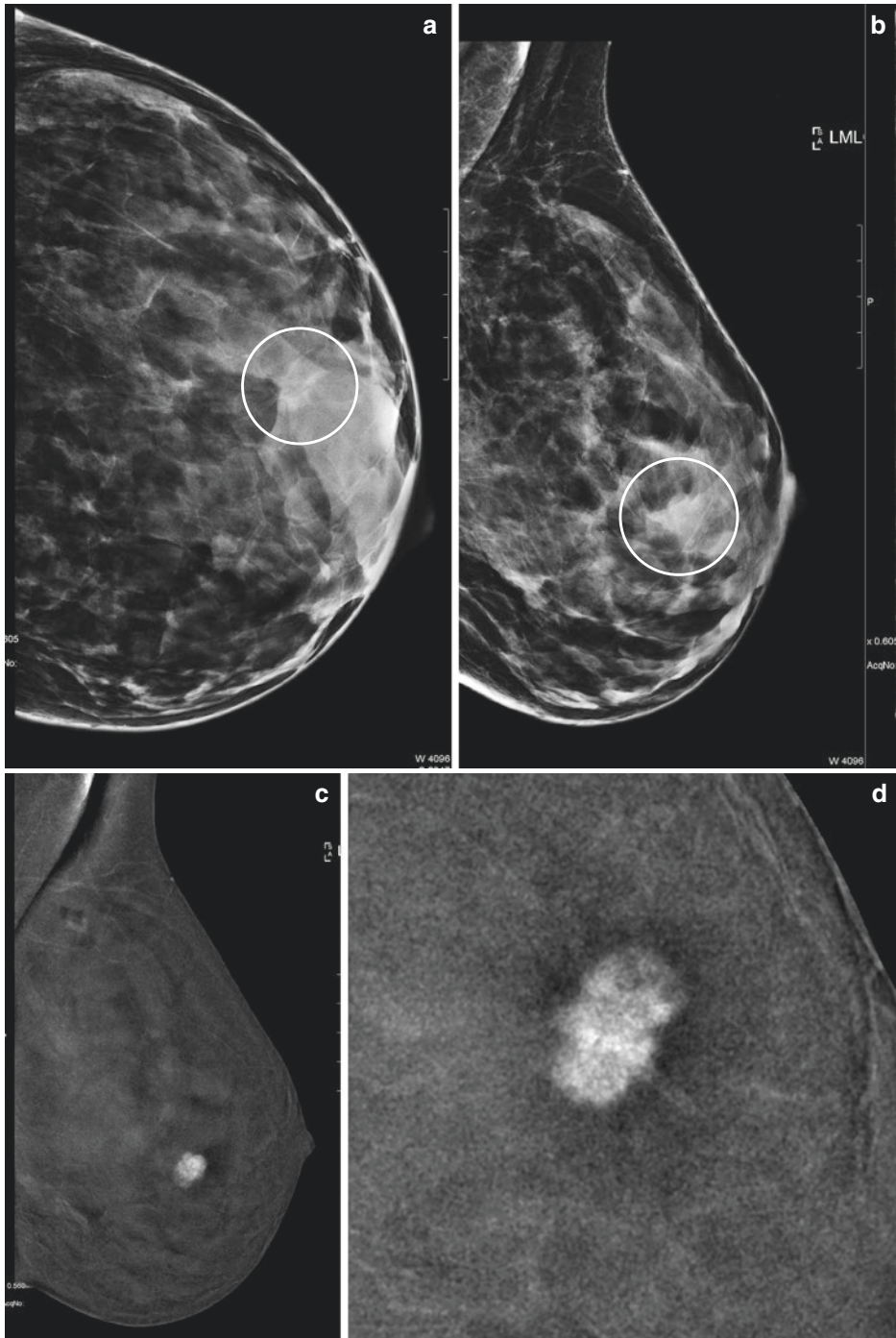


**Fig. 13.2** Pre-surgical staging in a patient with a BI-RADS 5 lesion in the central-outer quadrant of the left breast. (a, b) Low energy 2D images in CC and MLO projections demonstrate a dense breast with reduced diagnostic capability. However, there appears to be a lobulated mass with spiculated margins and associated architectural

distortion (*circles*) at the lower outer quadrant. (c, d) CEDM recombined image in CC projection and magnification view of the lesion. The examination shows an intensely enhancing malignant lesion with irregular borders, better depicted on the magnified view. *Diagnosis: The pathology was an invasive ductal carcinoma*



- *On CEDM*, invasive ductal carcinoma may present as a mass characterized by a prompt intense enhancement with irregular and/or spiculated margins [26]. Less frequently, IDC can present as a round, regular mass or as a NME. It often shows an early wash-out and thus is less enhanced in the delayed images. Small foci of enhancement, near the index lesion, should be considered suspicious for satellite lesions in the differential diagnosis of multicentric/multifocal disease. If there are any new enhancing lesions identified, we usually perform a second-look US and also a second-look review of the tomosynthesis images. This will be followed by either an US or tomosynthesis guided biopsy if they are visible. In addition, the association with a NME or a linear enhancement (“comet tail sign”) may be suggestive of an associated in situ component. Comparison with the contralateral breast helps to differentiate between a new lesion and normal bilateral parenchymal background enhancement (BPE), especially in cases with a severe BPE.
- In our experience, ductal invasive carcinoma accounted for 50% of invasive carcinomas. CEDM detected 71 tumours out of 74, with a specificity of 96% and three false negative results, due to severe background parenchymal enhancement. IDC appeared as a mass with spiculated and irregular margins in 96% of cases and as NME in 4% of cases and displayed no ring enhancement. The IDC kinetics reflects that of a highly vascularized lesion with anarchic vessels, showing prompt wash-out in 69% of cases, progressive enhancement in 27% of cases and the absence of enhancement in the remaining 4% of cases (Figs. 13.3, 13.4, 13.5, 13.6, 13.7, 13.8, 13.9, and 13.10).

### 13.3.3 Subtypes of Invasive Ductal Carcinoma

#### 13.3.3.1 Mucinous Carcinoma

Mucinous carcinomas, known also as colloid carcinomas, account for 1–7% of all breast cancers

and have a better 5- to 10-year survival than the usual infiltrating duct carcinoma. Histologically, mucinous carcinoma is characterized by “large amounts of extracellular epithelial mucus, sufficient to be visible grossly, and recognizable microscopically surrounding and within tumour cells” [42].

Two subtypes of mucinous carcinoma may be differentiated histologically: pure and mixed. Of these two subtypes, pure mucinous carcinoma is characterized by less aggressive growth and less frequently metastasizes to axillary lymph nodes [42].

#### Mucinous Carcinoma Findings

- *On mammography*, mucinous carcinoma usually appears as a round and well-defined mass with regular borders without calcifications.
- *On US*, mucinous carcinoma often displays mixed echogenicity with solid and cystic components. Posterior acoustic enhancement is common. At times the lesion can be isoechoic to breast tissue on ultrasound which can make diagnosis difficult. Due to its high intraleisional mucinous component, it may not demonstrate increased vascularity on colour Doppler analysis. All these findings may make it difficult to differentiate mucinous carcinoma from inflamed cysts or benign lesions.
- *On MRI*, mucinous carcinoma appears as a homogeneous and lobular mass. They are one of the few cancers that are markedly hyperintense on T2-weighted images, which relates to the water component in mucin, and they demonstrate a persistent enhancement pattern on dynamic MRI images (including a rim-like peripheral or heterogeneous internal enhancement). Thus, mucinous carcinoma has MRI features of both benignity and malignancy (i.e. rim-like or heterogeneous enhancement). The combination of these MRI findings is useful for accurate diagnosis of the tumour [43, 44].
- *On CEDM*, in our personal series, mucinous tumours, which accounted for 4% of all cancers at our centre, manifested as a mass in all the cases. The kinetics was typical for a malig-

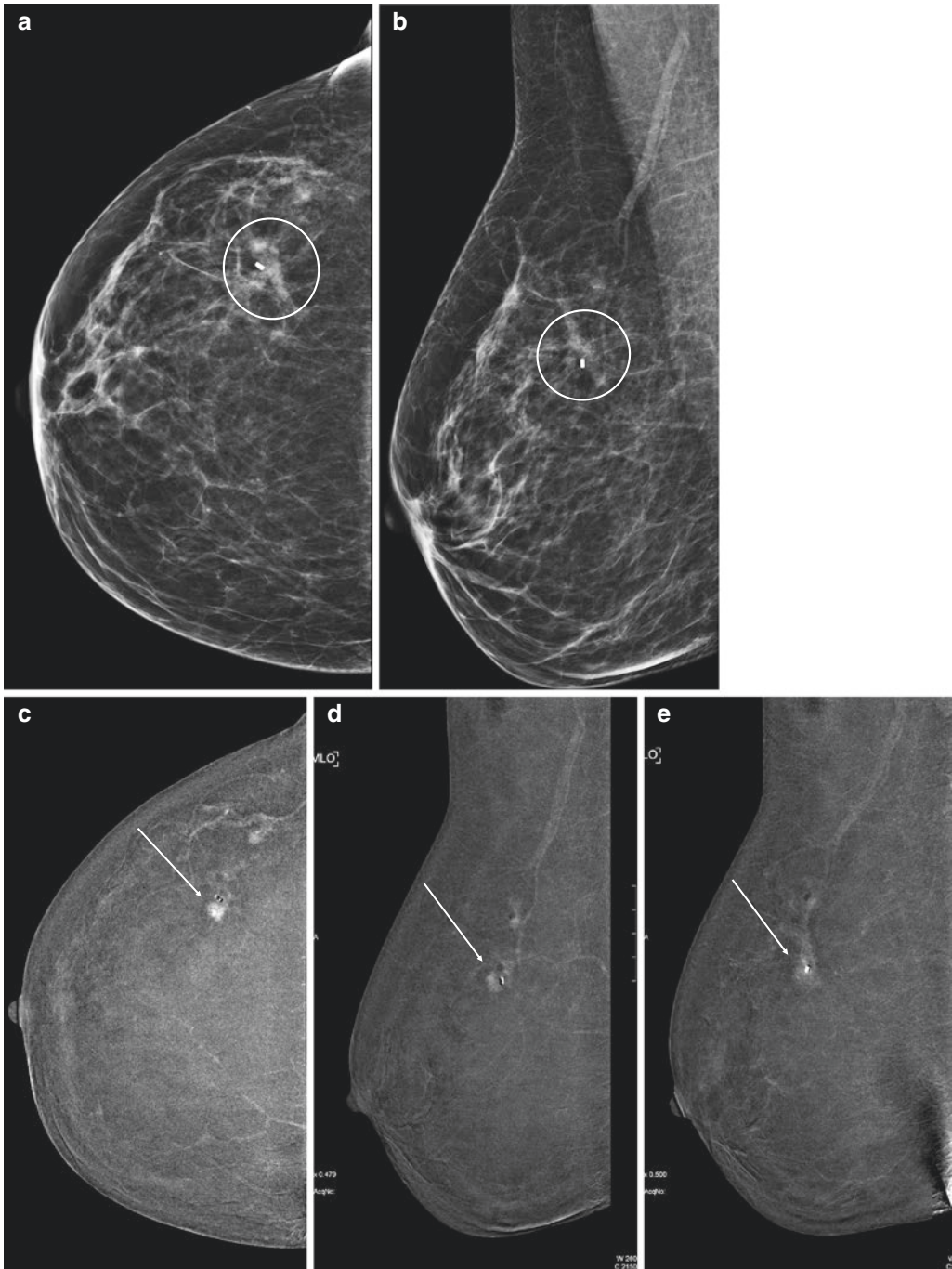


**Fig. 13.3** Pre-surgical staging in a patient with a BI-RADS 6 lesion in the upper-outer quadrant of the right breast. (a, b) Low energy 2D images in CC and MLO projections show a subcentimeter opacity with spiculated margins in the right upper-outer quadrant associated with a small cluster of calcifications and a post vacuum assisted biopsy (VAB) marker in situ (circle). (c) CEDM recombined image in CC projection. (d, e) CEDM recombined

image in the early and late phase in MLO projection. The examination demonstrates an intensely enhancing mass together with a non-mass linear enhancement, tracking along the distribution of the calcifications. The lesion is better delineated in the delayed MLO phase. *Diagnosis: The pathology was an invasive ductal carcinoma associated with a ductal carcinoma in situ component*

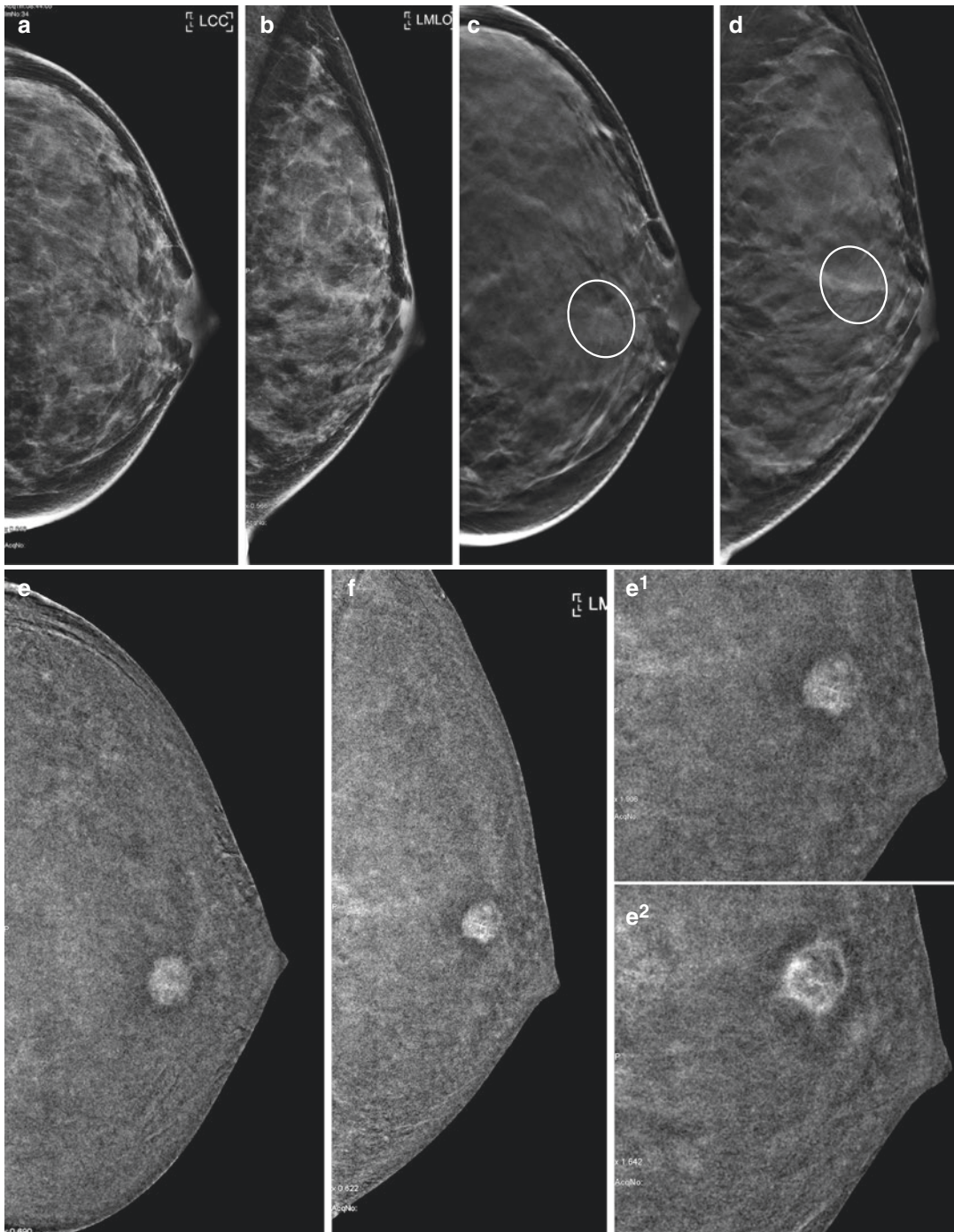


**Fig. 13.4** Pre-surgical staging in a patient with a BI-RADS 6 lesion in the upper-outer quadrant of the left breast. (a, b) Low energy 2D images in CC and MLO projections demonstrated dense breast parenchyma with no significant abnormality. (c, d) 3D in CC and MLO projection demonstrates a suspicious opacity and architectural distortion in the retro-areolar region (circle). (e, f) CEDM

recombined image in CC and MLO projection. (e<sup>1</sup>, e<sup>2</sup>) Magnification views of the lesion in early and late phases. The examination shows a suspicious intensely enhancing mass with no significant wash-out seen in delayed images (magnification views). *Diagnosis: The pathology was an invasive ductal carcinoma*



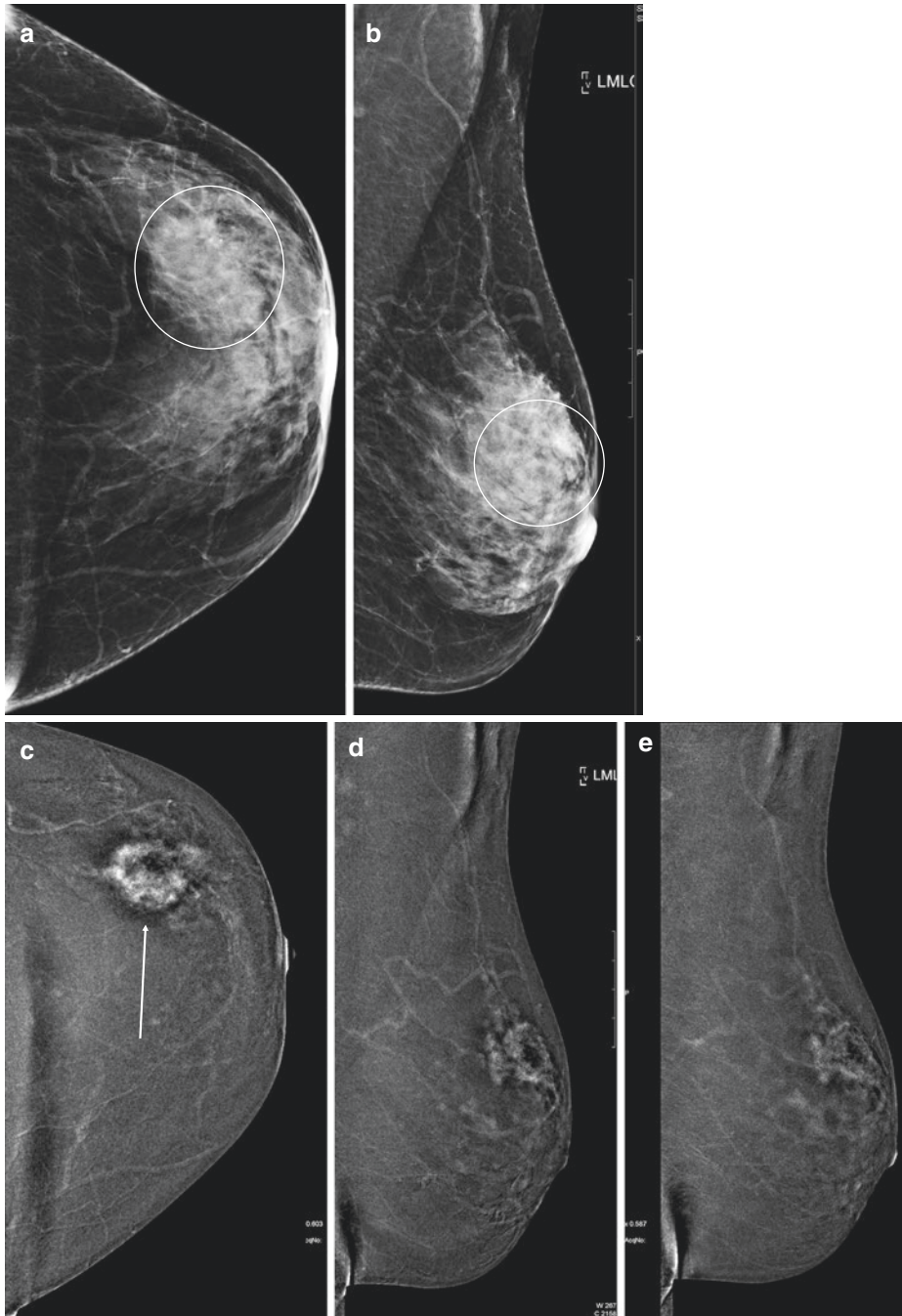


**Fig. 13.5** Pre-surgical staging in a patient with a palpable mass in the upper-outer quadrant of the left breast. (a, b) Low energy 2D images in CC and MLO projections show a dense breast, with an asymmetrical area of increased density (with respect to the other side, not shown) particularly in the left upper-outer quadrant. (c)

CEDM recombined image in CC projection. (d, e) CEDM recombined image in the early and late phase in MLO projection. The examination reveals an enhancing mass with irregular borders and a non-enhancing necrotic core (arrow) with wash-out in the delayed phase. *Diagnosis: The pathology was an invasive ductal carcinoma*



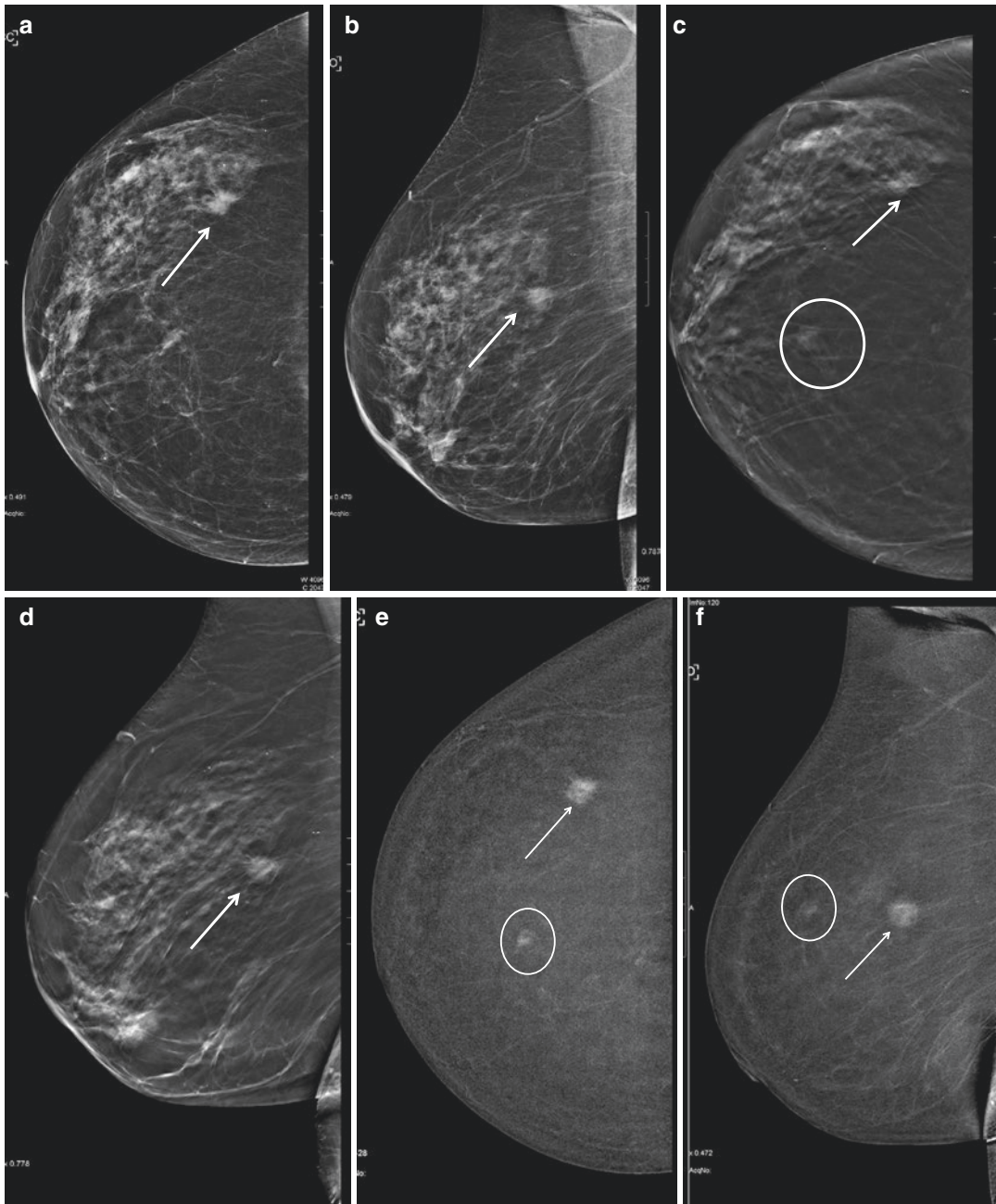


**Fig. 13.6** Pre-surgical staging in a patient with a BI-RADS 6 lesion in the central-outer quadrant of the right breast. (a, b) Low energy 2D images in CC and MLO projections show a highly suspicious mass with irregular borders in the central-outer quadrant (arrows). (c, d) 3D in CC and MLO projections better depicts the features of the suspected mass, and it also demonstrates another new smaller lesion anterior to it (circle). (e, f)

CEDM recombined image in CC and MLO projection. The examination shows an intensely enhancing malignant lesion (arrow) with irregular borders in the upper outer quadrant, and the other smaller lesion (circle) seen on 3D also demonstrated a similar enhancement pattern. *Diagnosis: The pathology of both lesions was invasive ductal carcinoma*

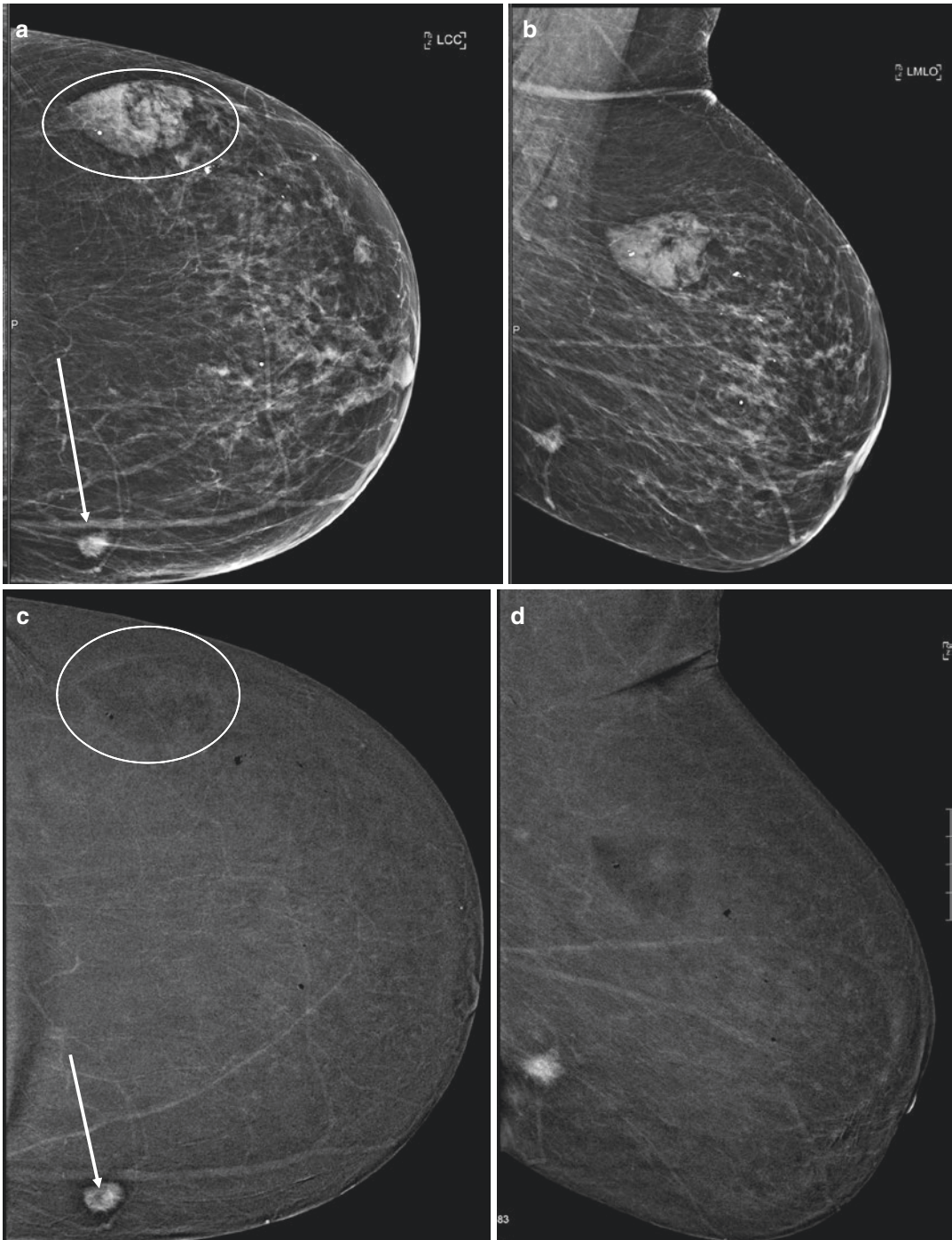


**Fig. 13.7** Pre-surgical staging in a patient with a BI-RADS 6 lesion in the lower-inner quadrant of the left breast (*arrow*). (**a, b**) Low energy 2D images in CC and MLO projections show a deep-seated suspicious opacity in the lower inner quadrant. There is also a large opacity with lobulated borders seen in the upper outer quadrant

(*circle*). (**c, d**) CEDM recombined images in CC and MLO projection. The examination shows an intensely enhancing malignant lesion, with irregular borders (*arrow*). The lesion in the upper-outer quadrant showed no enhancement. *Diagnosis: The pathology was an invasive ductal carcinoma (arrow) and a fat lobule (circle)*

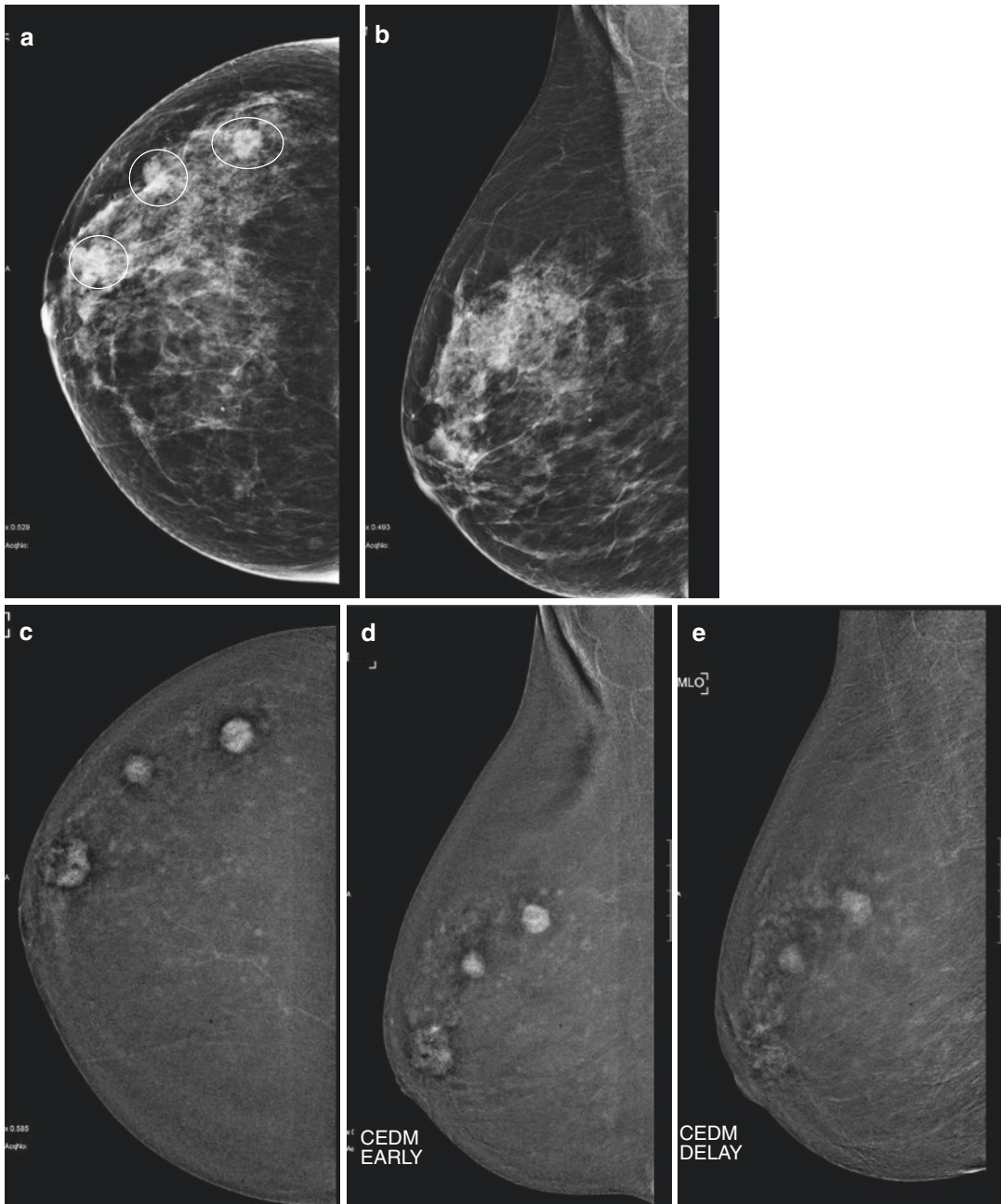


**Fig. 13.8** Further evaluation of a patient with a palpable mass in the retro-areolar area of the right breast. (a, b) Low energy 2D images in CC and MLO projections show an area of increased density in the retro-areolar region, with at least two other masses further away in the outer quadrant. (c) CEDM recombined image in CC projection. (d, e) CEDM recombined image in the early and late

phase in MLO projection. The examination shows the known lesion in the retroareolar region that demonstrates enhancement in the early phase with wash-out in the late phase; it also depicts two other lesions with the similar kinetics of enhancement, indicating multifocality. *Diagnosis: The pathology was colloid tumour*



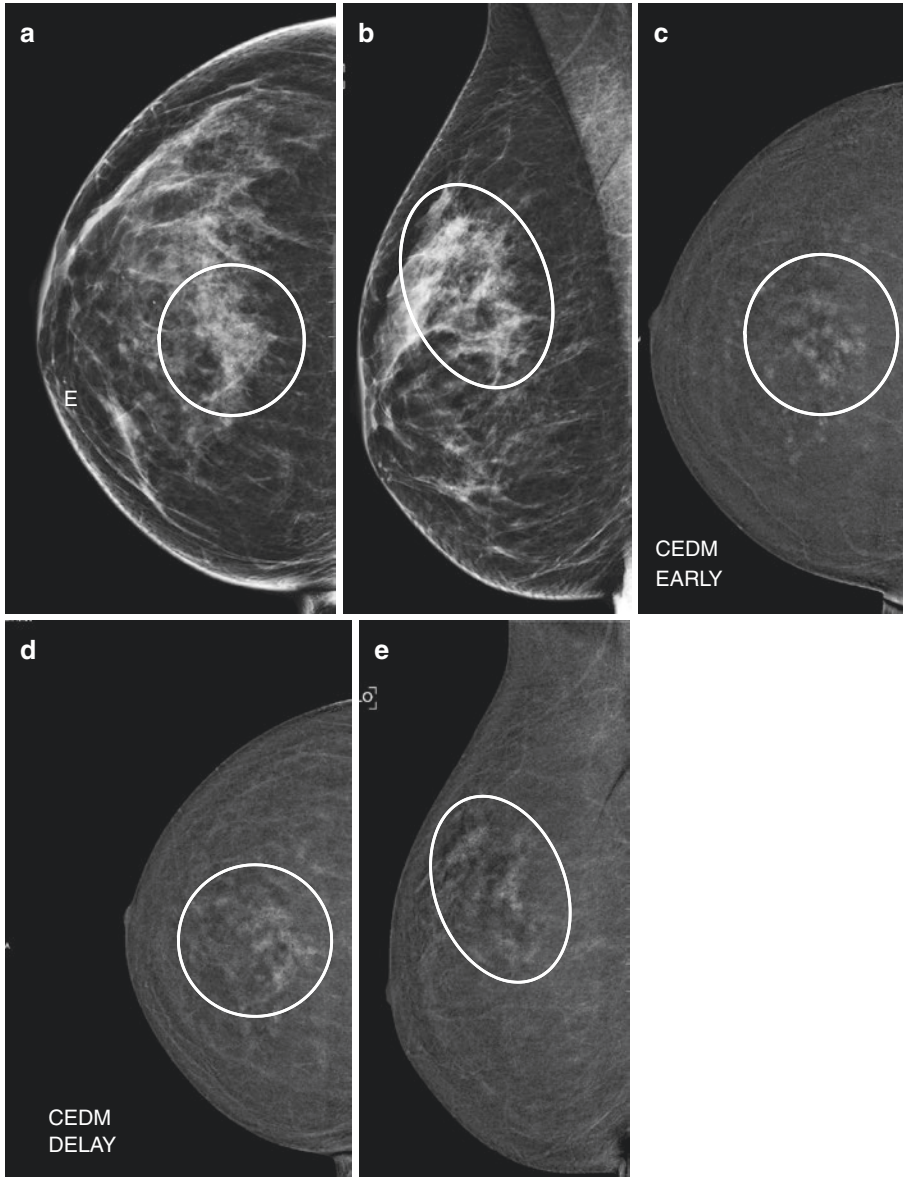


**Fig. 13.9** Pre-surgical staging in a patient with a BI-RADS 6 lesion in the central-upper quadrant of the right breast. (a, b) Low energy 2D images in CC and MLO projections show an asymmetrical area of increased density (*with respect to the other side, not shown*) in the central upper quadrant. (c, d) CEDM recombined image in the early and late phase in CC projection. (e) CEDM recombined image in MLO projection. The examination shows the known lesion presenting as a non-mass enhancement with a clustered distribution demonstrating progressive enhancement on the recombined CC views (*circles*). Owing to the discordance between the mammogram, US (*not shown*), and CEDM findings, the patient

underwent a MR examination. (a'–e') Subtracted images of the dynamic T1-weighted sequence on axial plane. MR also demonstrated progressive enhancement kinetics, as observed on CEDM examination. In the upper-central quadrant of the right breast one can observe the lesions (*circles*) associated with a clustered non-mass enhancement also extending to the upper-inner quadrant. (e') STIR T2-weighted image on axial plane depicts an asymmetric glandular distortion, with respect to the other side (*not shown*). (f') MIP reconstruction demonstrates the angiogenic vessels (*arrows*) associated with the index lesion. *Diagnosis: The pathology was a colloid tumour*



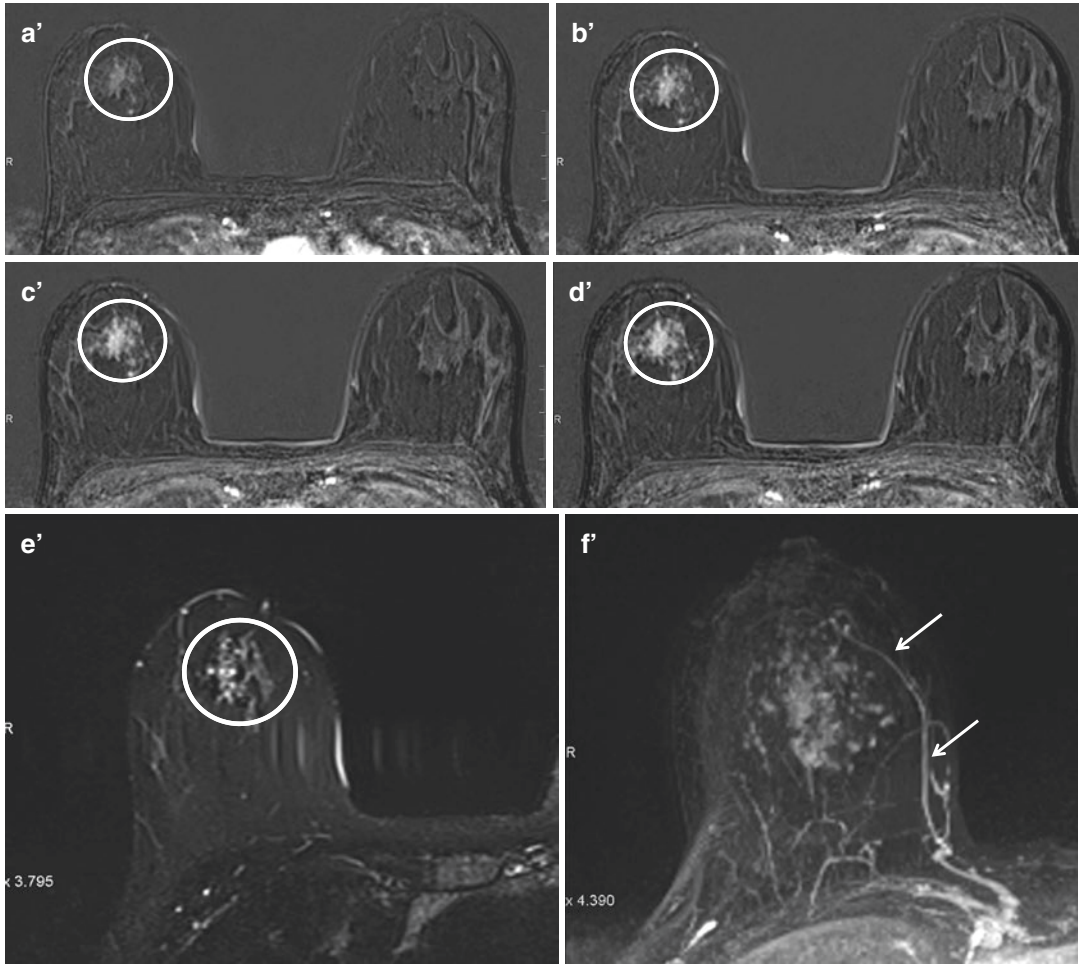


**Fig. 13.9** (continued)

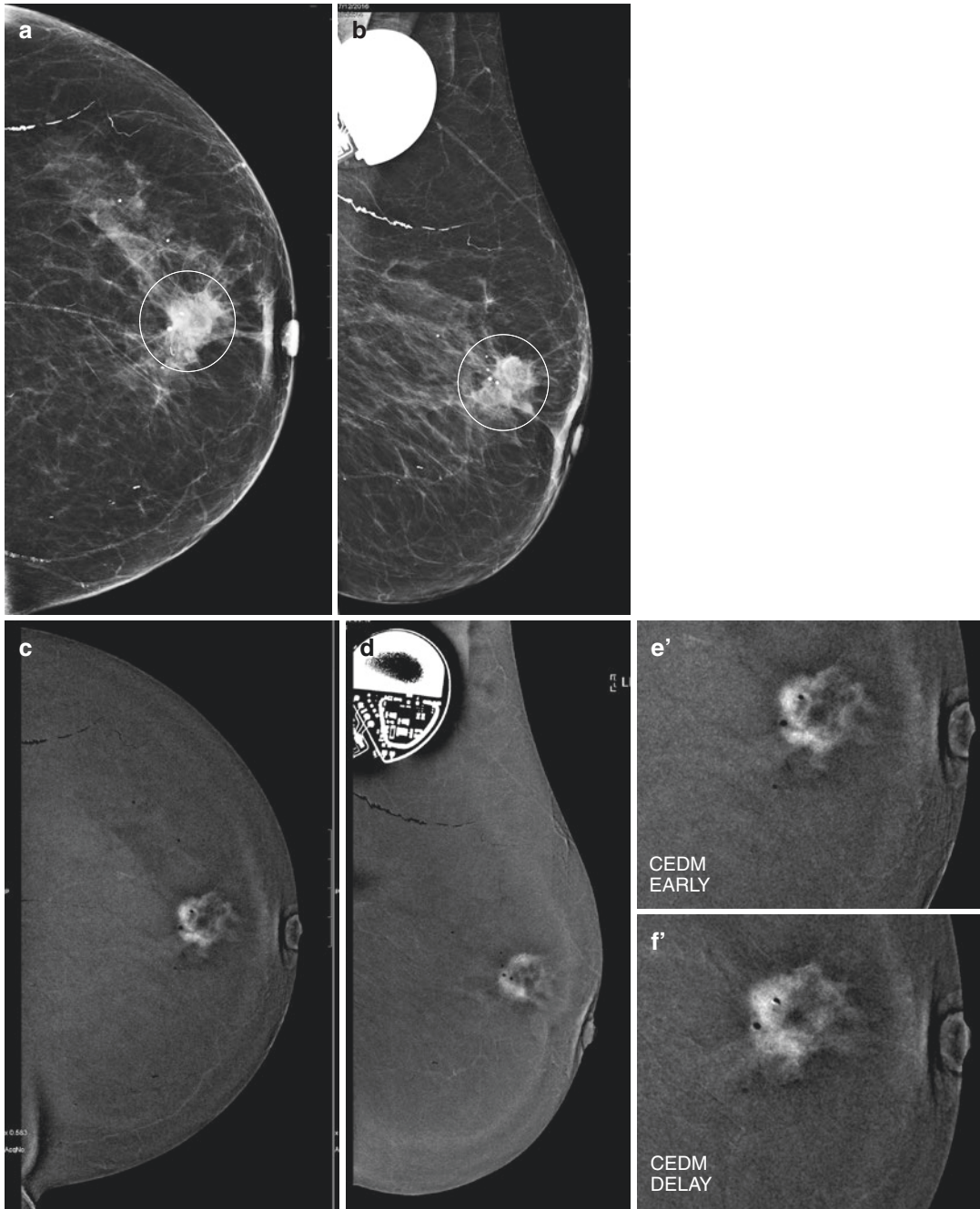


**Fig. 13.10** Pre-surgical staging in a patient with a BI-RADS 6 non-palpable lesion in the central-outer quadrant of the left breast. (a, b) Low energy 2D images in CC and MLO projections show a highly suspicious mass with irregular borders in the central-outer quadrant. (c, d) CEDM recombined image in CC and MLO projections. (e, f) Magnification views of the lesion in the early and

late phase. The examination shows an intensely enhancing mass demonstrating an early enhancement with no wash-out, as demonstrated by the comparison between the two phases, in the magnification views. The presence of a cardiac pacemaker device was a contraindication for the patient to undergo a MR examination. *Diagnosis: The pathology was a colloid infiltrative carcinoma*

nant lesion, with wash-out in 72% of cases; in 14% of cases, we observed an early and rapid uptake of contrast medium with a subsequent plateau phase, and in the remaining 14% of cases, we observed a gradual and steady persistent enhancement (Figs. 13.11, 13.12, and 13.13).

### 13.3.3.2 Papillary Carcinoma

Papillary carcinoma is a rare tumour, accounting for 1–2% of breast cancers [45]. The histologic hallmark of all papillary tumours, whether benign or malignant, is arborization of the fibrovascular stroma supporting the epithelial component. The cytomorphology is distinctive, with the presence of single papillae and papillary clusters. An absent myoepithelial layer distinguishes papillary carcinomas from benign papillary lesions.

The tumour is described as an intracystic papillary carcinoma in the presence of a cystic component.

#### Papillary Carcinoma Findings

- *On mammography*, the features of papillary carcinoma resemble those of medullary carcinoma, with more peripherally located calcifications and a higher density.
- *On US*, papillary carcinoma usually appears as a hypoechoic and solid mass, often with posterior acoustic enhancement; alternatively, they may present as complex cyst with solid components within.
- *On MRI*, the characteristics have been described as an intensely enhancing mass with irregular or rounded borders and non-enhancing internal septae. It is typically heterogeneous, with multiple nodular masses of intermediate signal intensity pro-

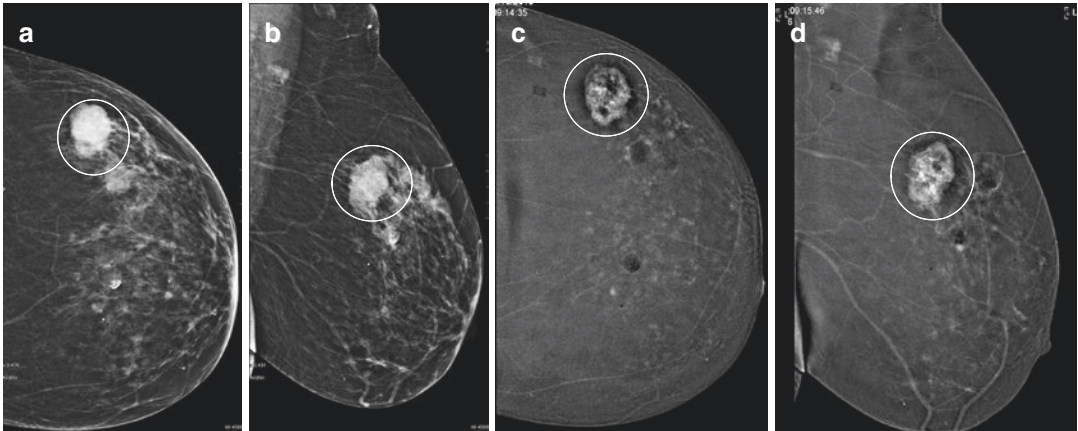


**Fig. 13.11** Pre-surgical staging in a patient with a BI-RADS 6 palpable lesion in the upper-outer quadrant of the left breast. (a, b) Low energy 2D images in CC and MLO projections show a suspicious mass with spiculated borders in the upper-outer quadrant. (c, d) CEDM recom-

bined image in CC and MLO projection demonstrates an intensely enhancing mass with irregular borders, associated with non-enhancing necrotic areas within it. *Diagnosis: The pathology was a papillary carcinoma*

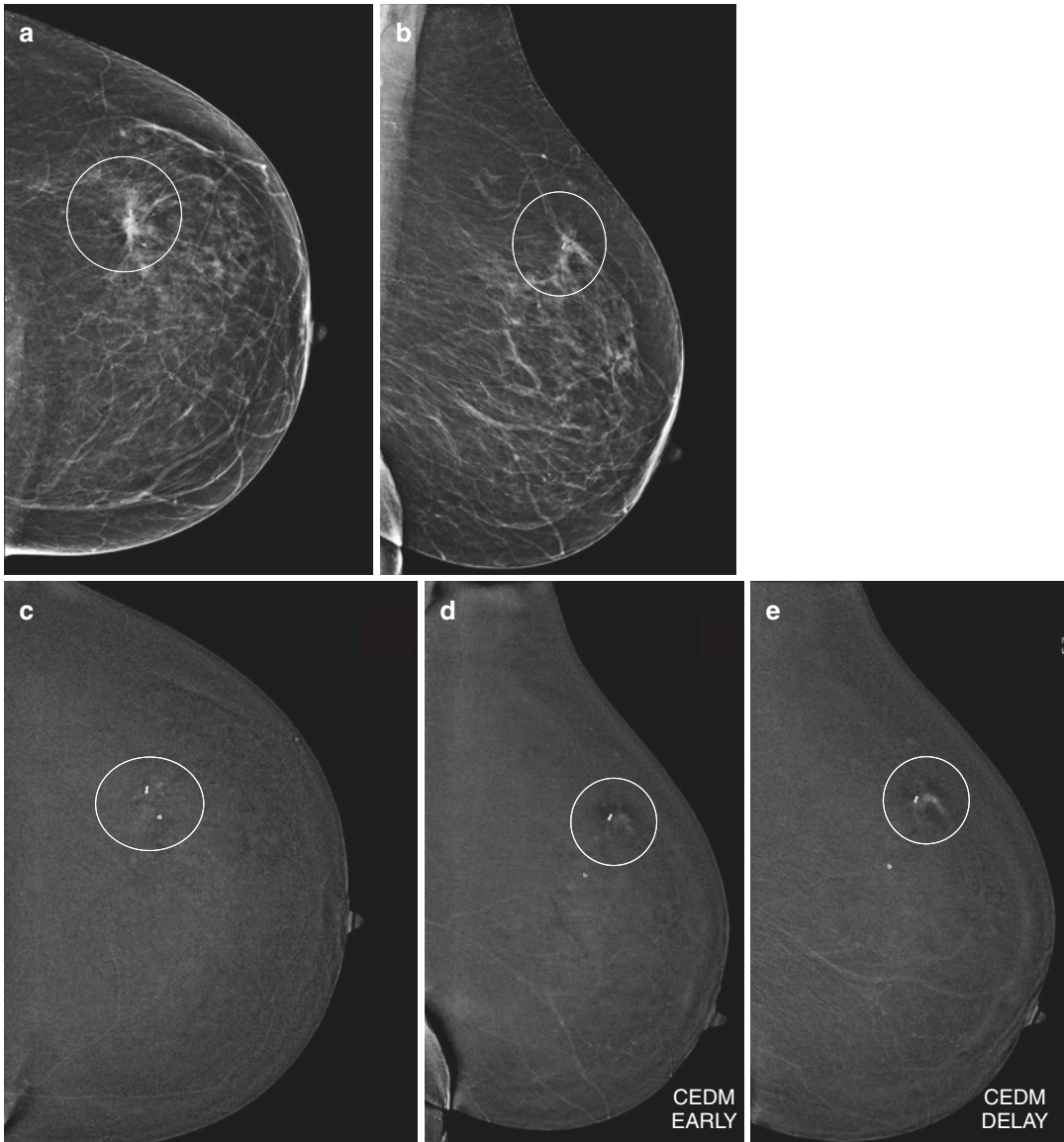


**Fig. 13.12** Pre-surgical staging in a patient with a BI-RADS 6 lesion in the upper-outer quadrant of the left breast. (a, b) Low energy 2D images in CC and MLO projections show an area of architectural distortion in the upper-outer quadrant with post biopsy markers in situ.

(c, d) CEDM recombined image examination in CC and MLO projections demonstrates a small area of non-mass enhancement with persistent to progressive enhancement kinetics as seen on the MLO early and delayed phase. *Diagnosis: The pathology was a tubular carcinoma*



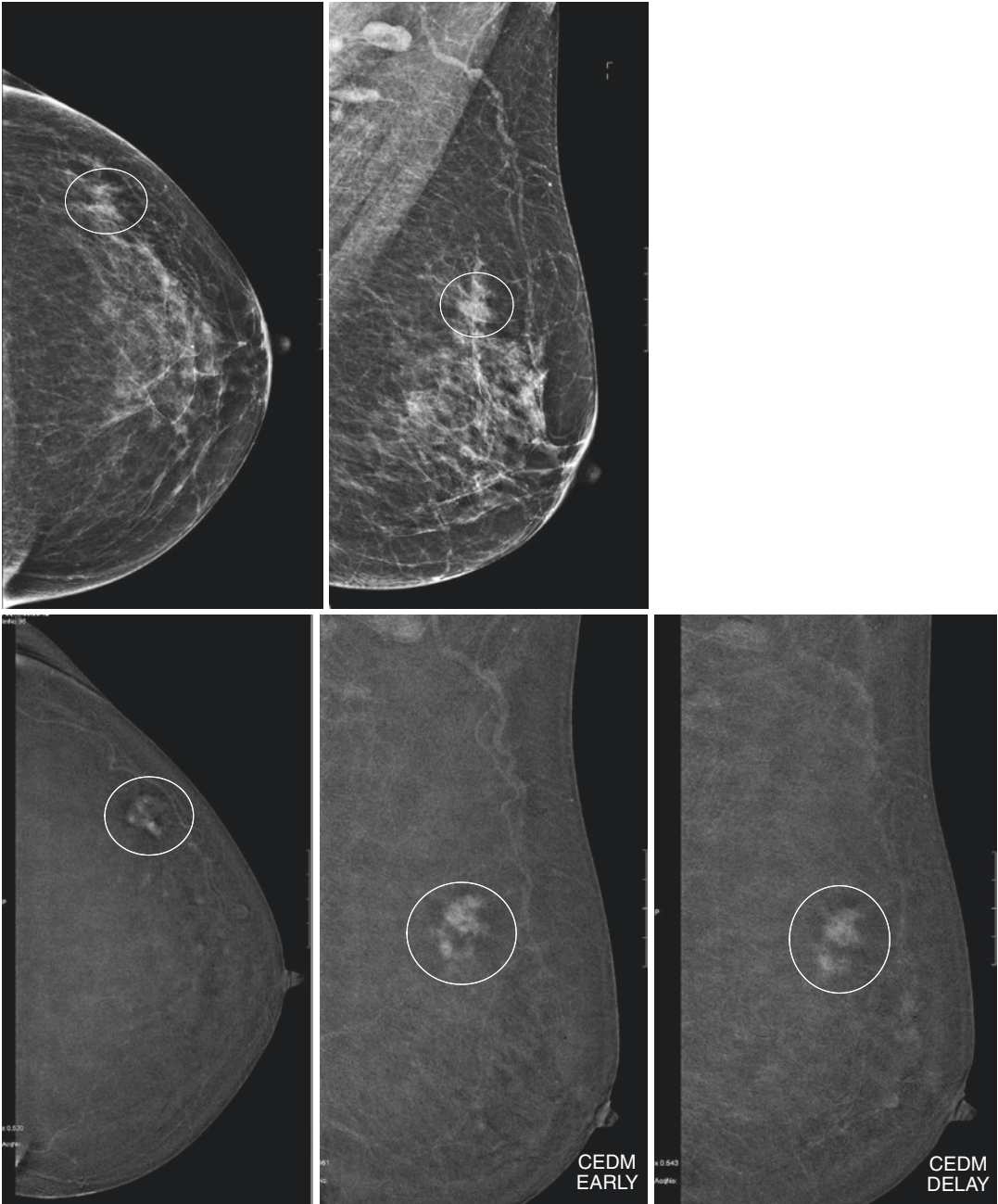


**Fig. 13.13** Pre-surgical staging in a patient with a BI-RADS 6 non-palpable lesion in the upper-outer quadrant of the left breast. (a, b) Low energy 2D images in CC and MLO projections show a suspicious mass with spiculated borders in the upper-outer quadrant. (c) CEDM recombinant image in CC projection. (d, e) CEDM recom-

bined image in the early and late phase in MLO projection. The examination shows an intensely enhancing mass with spiculated borders, which is seen to demonstrate a subtle wash-out in the late phase. *Diagnosis: The pathology was a tubular carcinoma*

jecting from the periphery into the lumen [46, 47].

The signal intensity is also dependent on the intracystic fluid composition:

- If serous, it will be hypointense on T1-weighted images and hyperintense on T2-weighted images.
- If there are haemorrhagic contents, it will be hyperintense on both T1- and T2-weighted images, and fluid-fluid levels may be seen on T2-weighted images.
  - On *CEDM*, papillary cancer accounted for 4% of all malignant lesions in our personal series. The morphologic pattern of presentation was a mass in 63% of cases, NME in 25% of cases and rim enhancement in the remaining 12% of cases. The kinetics pattern was characterized by a progressive enhancement in 62% of cases and as an early wash-out in 38% of cases (Fig. 13.14).

### 13.3.3.3 Tubular Carcinoma

Tubular carcinoma accounts for less than 2% of all breast cancers and for approximately 20% of cancers detected by mammography. It usually affects women in their mid-to-late 40s, slightly younger than for breast cancer in general. At gross examination, tubular carcinoma appears as a small, solid nodule with spiculated borders.

#### Tubular Carcinoma Findings

- On *mammography*, tubular carcinoma often presents as a small spiculated mass, associated with suspicious calcifications in half of cases. Frequently, it manifests as a small architectural distortion, increasing the diagnostic challenge with sclerosing adenosis and radial scar.
- On *US*, tubular carcinoma typically mimics IDC NOS (not otherwise specified), manifesting

as a hypoechoic solid mass with ill-defined margins and posterior acoustic shadowing.

- On *MRI*, it presents as a mass with the typical kinetics of a malignant lesion.
- On *CEDM*, in our series, tubular carcinomas accounted for 6% of breast cancers; the kinetics pattern was characterized by a progressive enhancement in 69% of cases and by wash-out in 31% of cases. The morphology of enhancement presented as a mass in 92% of cases and as NME in 8% of cases (Figs. 13.15 and 13.16).

### 13.3.4 Invasive Lobular Carcinoma

Invasive lobular carcinoma (ILC) is the second most common histologic type of breast cancer, accounting for 10–15% of all invasive breast neoplasms [48]. Although ILC is associated with a higher rate of multiplicity and bilaterality (approximately 30%) than invasive ductal cancers at diagnosis, the overall survival rate for patients with ILC is slightly higher than that for patients with the usual types of invasive ductal carcinomas.

Mammographically, ILC is very difficult to diagnose because of its high rate of false negative results (up to 19%), with a sensitivity ranging from 57 to 81%; a possible explanation for this behaviour can be found in its histological features: in fact, tumour cells have the tendency to infiltrate the stroma in a single-file arrangement without formation of a mass or development of associated fibrosis [49, 50]. Malignant cells may surround acini or ducts, creating a characteristic “bull’s-eye” pattern. The diffuse spread of neoplastic cells in ILC is also reflected by its unusual metastatic pattern: ILC is far more likely to metastasize to the peritoneum-retroperitoneum, gastrointestinal tract, urogenital tract, leptomeninges and myocardium with respect to IDC. Histological variants of ILC include signet ring, alveolar, solid and pleomorphic types.

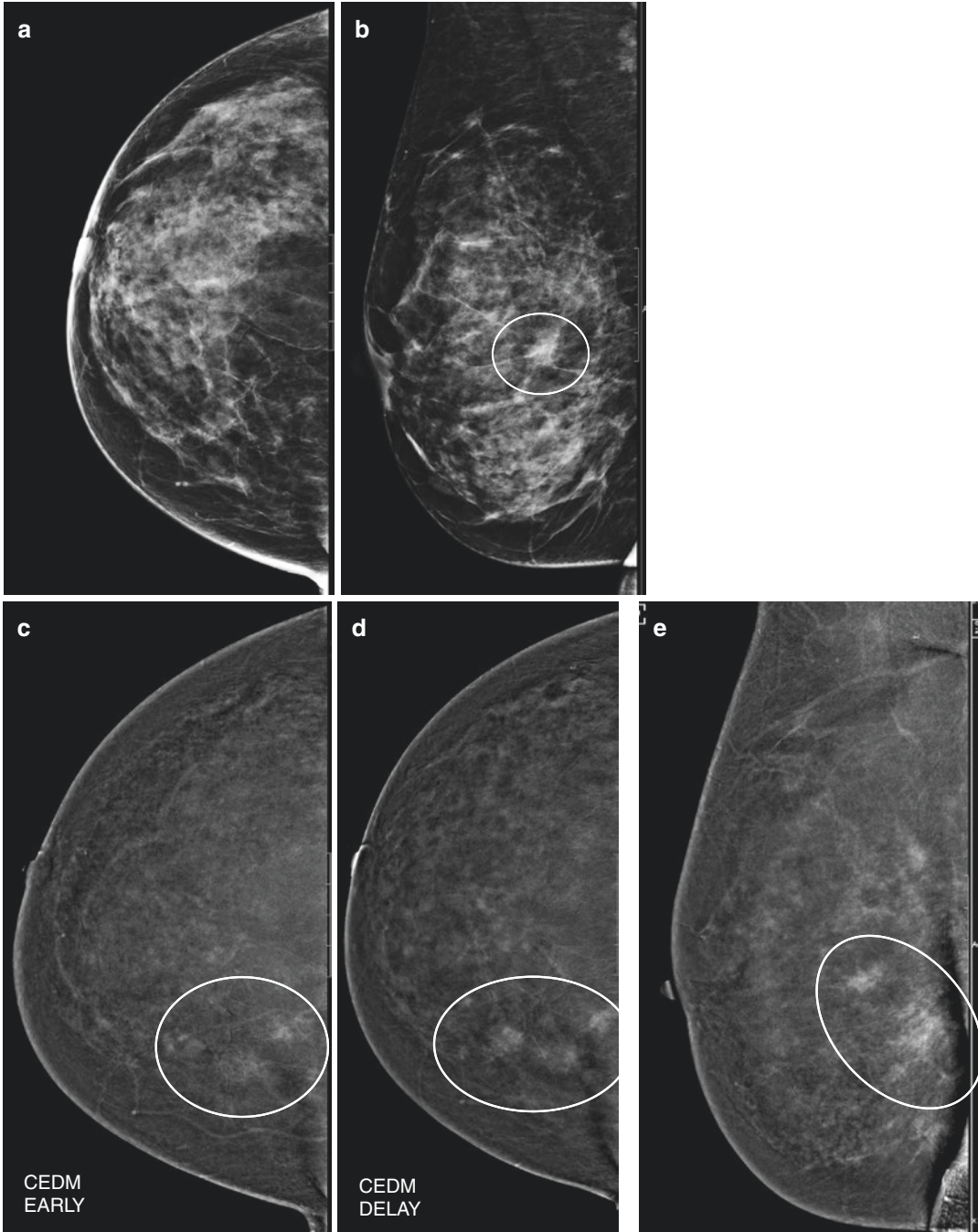


**Fig. 13.14** Pre-surgical staging in a patient with a palpable BI-RADS 6 lesion in the central quadrants of the right breast. (a, b) Low energy 2D images in CC and MLO projections show a deep-seated suspicious mass with spiculated borders in the central-outer quadrant (circle). (c, d) CEDM recombined image in the early and

late phase in CC projection. (e) CEDM recombined image in MLO projection. The examination shows the known lesion as an area of non-mass enhancement in the lower-inner quadrant (circle), demonstrating progressive enhancement kinetics. *Diagnosis: The pathology was an infiltrative lobular carcinoma*

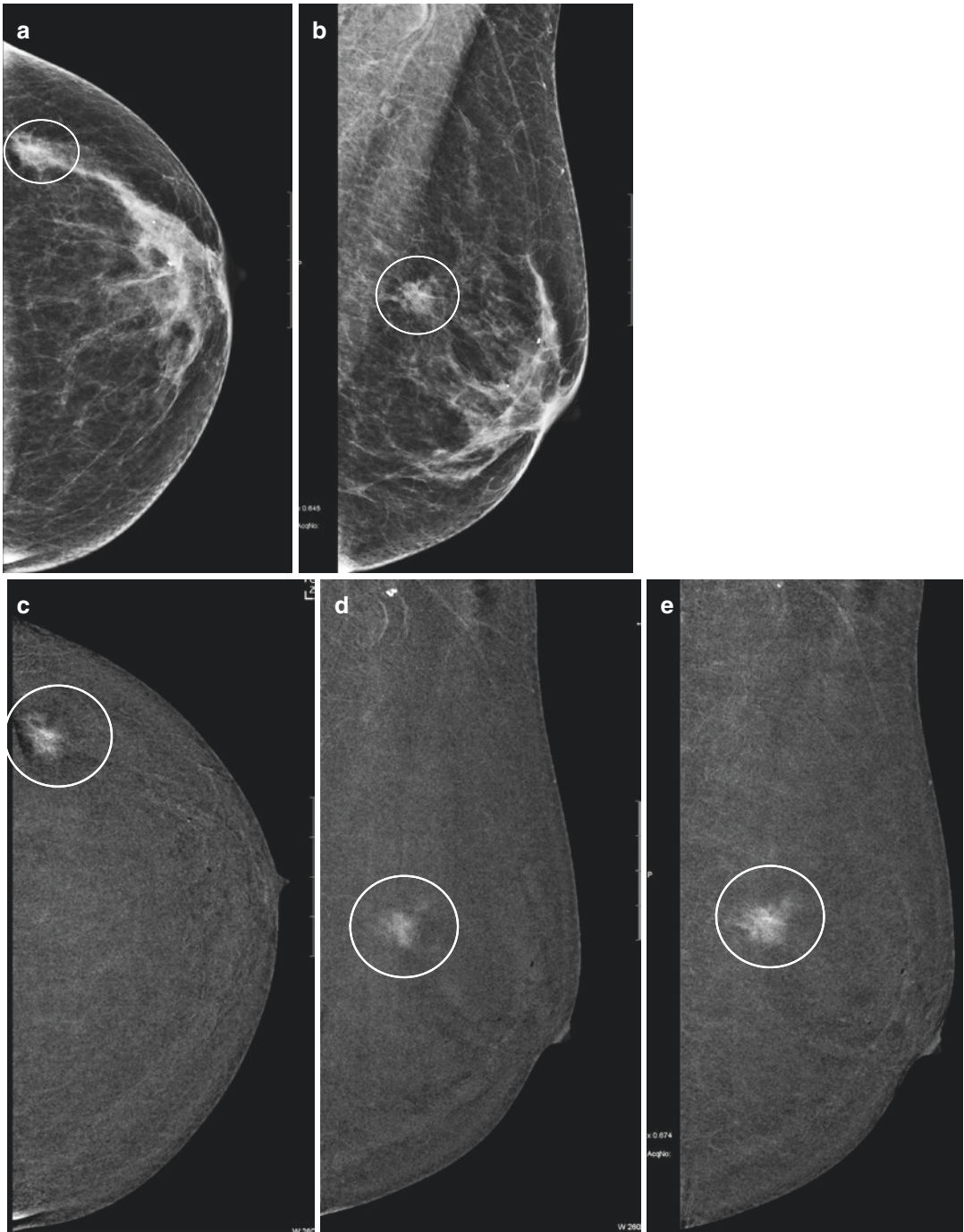


**Fig. 13.15** Pre-surgical staging in a patient with a palpable BI-RADS 6 lesion in the central-outer quadrant of the left breast. (a, b) Low energy 2D images in CC and MLO projections show a deep-seated suspicious mass with spiculated borders in the central-outer quadrant (circle). (c) CEDM recombined image in CC projection.

(d, e) CEDM recombined image in the early and late phase in MLO projection. The examination demonstrates the known mass as an intensely enhancing lesion with spiculated borders, showing progressive enhancement kinetics. *Diagnosis: The pathology was an infiltrative lobular carcinoma*



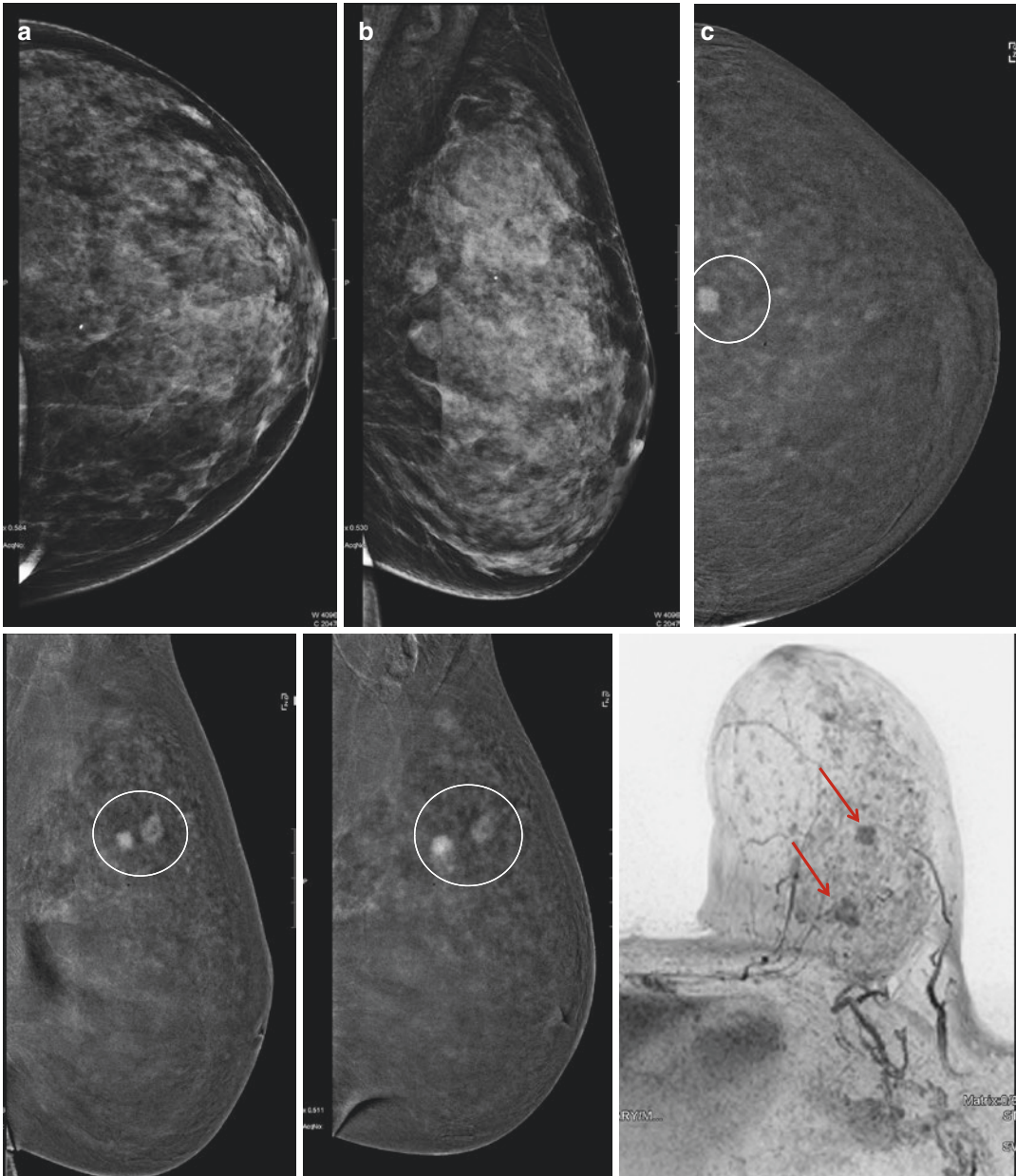


**Fig. 13.16** Pre-surgical staging in a patient with a BI-RADS 6 lesion in the upper-outer quadrant of the left breast. (a, b) Low energy 2D images in CC and MLO projections show a relatively dense breast parenchyma. (c) CEDM recombined image in CC projection. (d, e) CEDM recombined image in the early and late phase in MLO projection. The examination demonstrates two intensely enhancing masses in the upper outer quadrant. However,

the second lesion is not visualised on the CC view in view of the deep-seated location, which is among the limitations of CEDM. These lesions are seen to demonstrate a progressive enhancement. (f) MIP reconstruction on axial plane depicts both the lesions (red arrows) well, including the posteriorly located lesion, which was not seen on the CC view of the recombined images. *Diagnosis: The pathology was an infiltrative lobular carcinoma*

### 13.3.4.1 Invasive Lobular Carcinoma Findings

- *On mammography*, ILC commonly manifests as an opacity (44–65% of cases), usually with spiculated or ill-defined margins. Round masses account for only 1–3% of cases. Architectural distortion and subtly increased asymmetric density are the other forms of appearance, with a reported incidence of 10–34% and 1–14%, respectively [50]. For its peculiar presentation, ILC's diagnosis may be very difficult, presenting often completely negative mammography.
  - *On US*, the detection rate of ILC rises dramatically, ranging from 68 to 98% [51]; in fact, it has been proven that US is superior to mammography for identifying multicentricity and multifocality and more accurately reflects the size of a mass than does mammography or clinical examination. US may show a mass with hypoechoic and heterogeneous internal echoes, and posterior acoustic shadowing in an area of clinically palpable mass or mammographic asymmetric density or abnormality. More specifically, classic ILC tends to manifest as focal shadowing without a significant mass, whereas the pleomorphic type typically manifests as a shadowing mass. Signet ring, alveolar and solid subtypes are more likely to manifest as a lobulated, well-circumscribed mass [51–53].
  - *On MRI*, the morphologic and kinetic appearance of ILC is variable, reflecting its histological features. To date, MRI has been shown to be superior to mammography and US in detecting multifocality and multicentricity and is the most reliable technique in estimating tumour size [54]. The most common manifestation of ILC on MRI is a focal enhancing mass with spiculated or ill-defined margins (31–43% of cases). Additional manifestations include a dominant lesion surrounded by multiple small enhancing foci, multiple small enhancing foci with interconnecting enhancing strands, architectural distortions, diffuse enhancement patterns resembling normal glandular patterns and normal findings [54, 55]. A typical dynamic feature of ILC is the tendency to demonstrate a delayed progressive enhancement, with wash-out exhibited by only a minority of lesions.
  - *On CEDM*, the MRI kinetics are similar to those observed in CEDM, in our experience; ILC, which accounted for 12% of all tumours, presented a delayed enhancement in 72% of cases, whereas only 28% of ILCs showed wash-out. An irregular mass was observed in 83% of cases and NME in 17% of cases. A possible explanation of this behaviour may rely on the histologic tendency of ILC to spread diffusely through the breast stroma in a lipid-filled pattern without exhibiting a nodular mass; thus, the enhancing portion may correspond to the normal parenchyma, which manifests as progressive enhancement.
- Nevertheless, these data need further confirmation. In 28% of cases, CEDM detected an unsuspected cancer in the contralateral breast, proving the importance of functional imaging in staging multicentric/multifocal tumour: of these five new lesions, four were ILCs, and one was a lobular intraepithelial neoplasia (LIN1) (Figs. 13.17, 13.18, and 13.19).

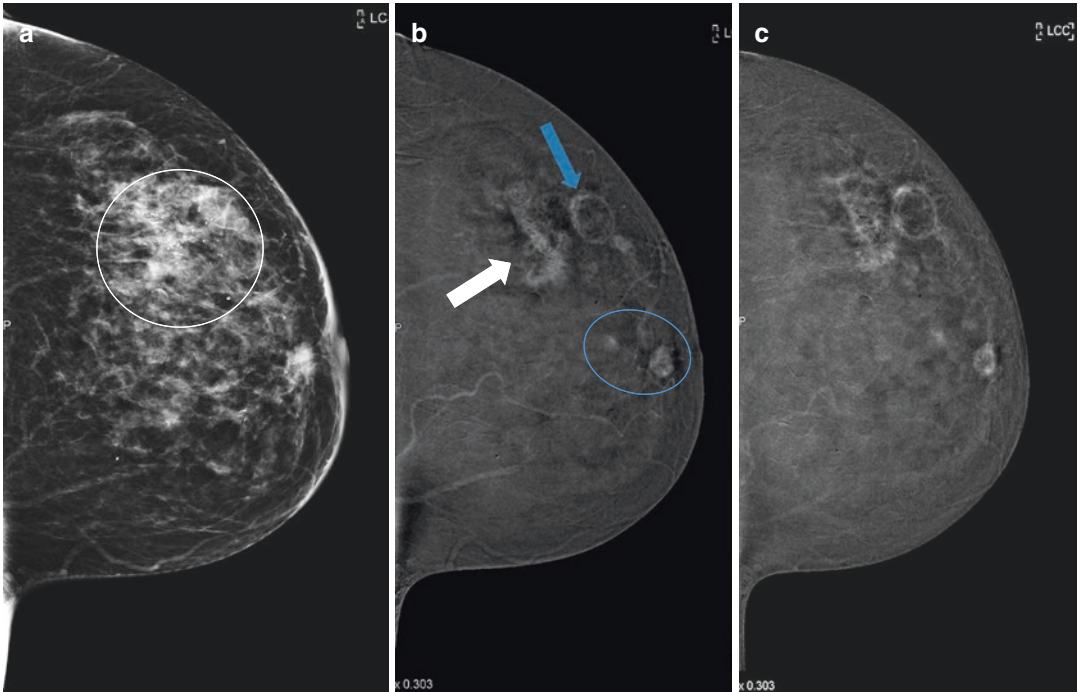


**Fig. 13.17** Pre-surgical staging in a patient with a BI-RADS 6 lesion in the upper-outer quadrant of the left breast. **(a)** Low-energy 2D images in the CC projection show a cluster of heterogeneous calcifications with a regional distribution (*white circle*). **(b, c)** CEDM recombined image in the early and late phase in the CC projection. The examination shows a rim-enhancing lesion at the

site of previous biopsy (*blue arrow*) in keeping with a post-biopsy haematoma. There is an associated area of non-mass enhancement seen posterior to it (*white arrow*), and there are two retroareolar masses which demonstrate wash-out in late images (*blue circle*). *Diagnosis: The pathology was ductal carcinoma in situ*

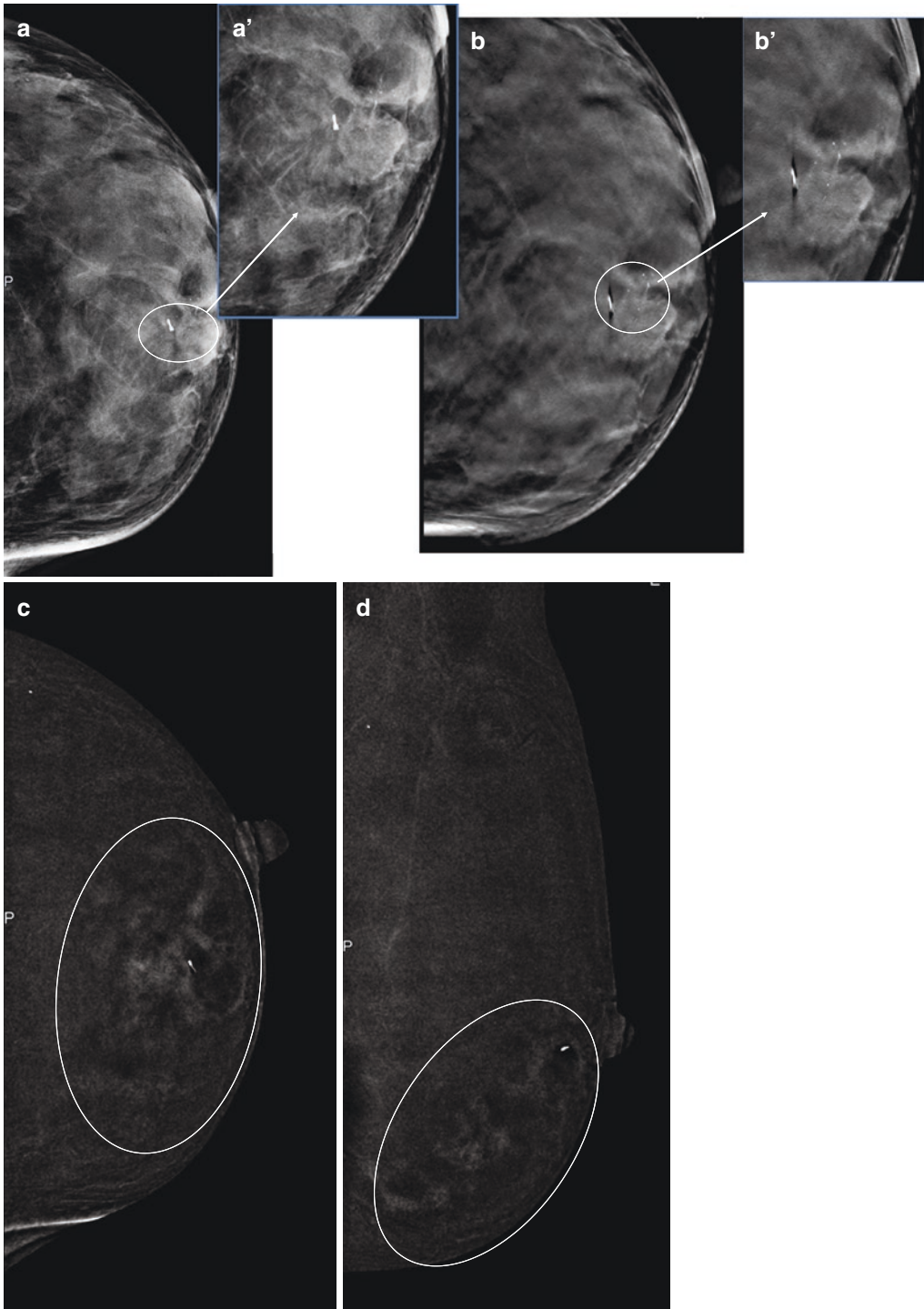


**Fig. 13.18** Pre-surgical staging in a patient with a BI-RADS 6 lesion in the lower-inner quadrant of the left breast, already biopsied. **(a, a')** Low-energy 2D images in the CC projection demonstrating a very dense breast with a suspicious cluster of fine pleomorphic cluster of calcifications (*circle*). **(b, b')** 3D in CC projection depicts the calcifications and its distribution better (*circle*). **(c, d)**

CEDM recombined image in the CC and MLO projections demonstrates an area of non-mass enhancement with regional distribution in the lower-inner and central-inner quadrants. The area of enhancement was much larger than the focal distribution of calcifications seen on the non-contrasted images. *Diagnosis: The pathology was a multicentric invasive ductal carcinoma*



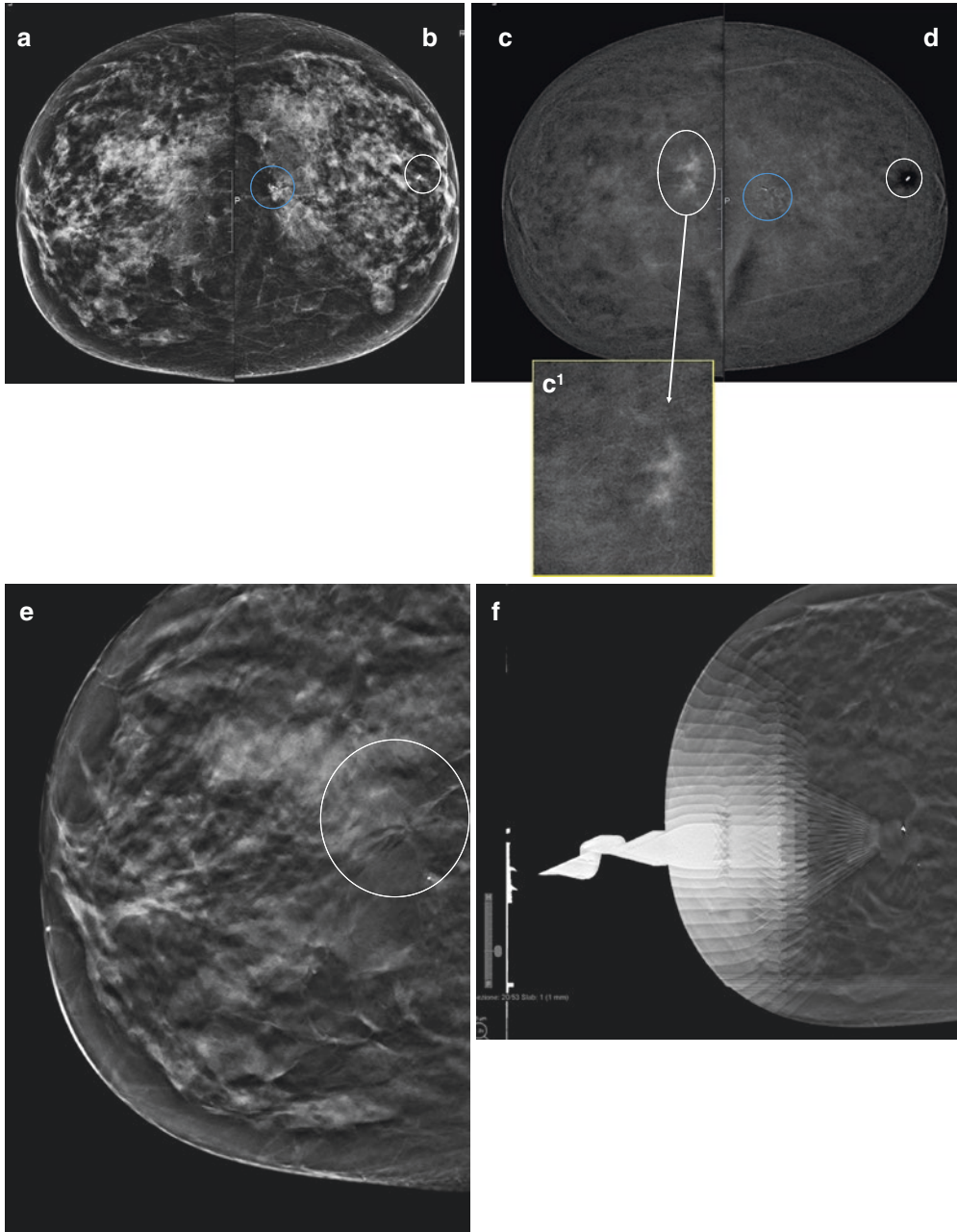


**Fig. 13.19** A problem-solving case in a woman with dense breast and discordances between mammogram findings and histology results. (a, b) 2D FFDM low-energy 2D images in the CC projection show the two post-biopsy clips (*circles*), one at the lower-central quadrant and one at the superior-central quadrant both of the left breast. No obvious abnormalities are evident in the right breast. The histologic result of the two biopsy sites was B2, benign lesions, but the radiologic appearances of the architectural distortion were highly suggestive for malignancy. (c, d) CEDM recombined image in the early phase in CC projection shows a mild enhancement of the lesion

in the posteriorly biopsied site (*blue circle*) of the left breast. (c, c') However, there was an intense non-mass enhancement seen in the right breast in the central quadrant, which is better depicted in the magnified image. (e, f) 3D images were retrospectively reviewed after the CEDM exam, which showed an area of distortion corresponding to the enhancing site on recombined images. We later performed a tomosynthesis-guided stereotactic biopsy on the right breast. *Diagnosis: The pathology of the right lesion was a 10 mm multifocal ductal carcinoma in situ (DCIS), while the left breast lesion (blue circle) was a 4.5 mm infiltrating carcinoma*

## References

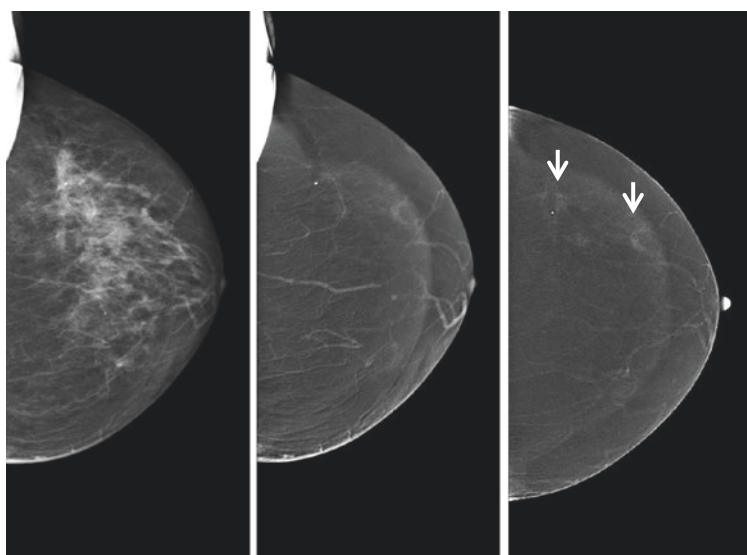
1. Siegel RL, Miller KD, Jemal A. Cancer statistics, 2017. *CA Cancer J Clin*. 2017;65:5–29.
2. Folkman J. Role of angiogenesis in tumor growth and metastasis. *Semin Oncol*. 2002;29(6 Suppl 16):15–8.
3. Folkman J. New perspectives in clinical oncology from angiogenesis research. *Eur J Cancer*. 1996;32A:2534–9.
4. Gasparini C, Harris A. Clinical importance of the determination of tumor angiogenesis in breast carcinoma: much more than a new prognostic tool: review. *J Clin Oncol*. 1995;13:765–82.
5. Chu JS, Lee WJ, Chang TC, Chang KJ, Hsu HC. Correlation between tumor angiogenesis and metastasis in breast cancer. *J Formos Med Assoc*. 1995;94:373–8.
6. Barrett T, Brechbiel M, Bernardo M, Choyke PL. MRI of tumor angiogenesis. *J Magn Reson Imaging*. 2007;26:235–49.
7. Jong RA, Yaffe MJ, Skarpathiotakis M, et al. Contrast-enhanced digital mammography: initial clinical experience. *Radiology*. 2003;228(3):842–50.
8. Lewin JM, Isaacs PK, Vance V, Larke FJ. Dual-energy contrast-enhanced digital subtraction mammography: feasibility. *Radiology*. 2003;229(1):261–8.
9. Dromain C, Balleyguier C, Adler G, Garbay JR, Delaloge S. Contrast-enhanced digital mammography. *Eur J Radiol*. 2009;69(1):34–42.
10. Diekmann F, Freyer M, Diekmann S, et al. Evaluation of contrast-enhanced digital mammography. *Eur J Radiol*. 2011;78(1):112–21.
11. Jochelson M. Contrast-enhanced digital mammography. *Radiol Clin North Am*. 2014;52(3):609–16.
12. Diekmann F, Marx C, Jong R, Dromain C, Toledano AY, Bick U. Diagnostic accuracy of contrast enhanced digital mammography as an adjunct to mammography. *Eur Radiol*. 2007;17(12):3086–92.
13. Dromain C, Thibault F, Muller S, et al. Dual-energy contrast-enhanced digital mammography: initial clinical results. *Eur J Radiol*. 2011;21:565–74.
14. Jochelson MS, Dershaw DD, Sung JS, et al. Bilateral contrast-enhanced dual-energy digital mammography: feasibility and comparison with conventional digital mammography and MR imaging in women with known breast carcinoma. *Radiology*. 2013;266:743–51.
15. Sogani J, Morris EA, Kaplan JB, et al. Comparison of background parenchymal enhancement at contrast-enhanced spectral mammography and breast MR imaging. *Radiology*. 2017;282(1):63–73. <https://doi.org/10.1148/radiol.2016160284>.
16. Bhimani C, Matta D, G Roth R, et al. Contrast enhanced spectral mammography: techniques, indications and clinical applications. *Acad Radiol*. 2017;24:84–8.
17. Lalji U, Lobbes M. Contrast-enhanced dual-energy mammography: a promising new imaging tool in breast cancer detection. *Womens Health*. 2014;10(3):289–98.
18. Lobbes MB, Smidt ML, Houwers J, et al. Contrast-enhanced mammography: techniques, current results, and potential indications. *Clin Radiol*. 2013;68:935–44.
19. Hobbs MM, Taylor DB, Buzynski S, Peake RE. Contrast-enhanced spectral mammography (CESM) and contrast enhanced MRI (CEMRI): patient preferences and tolerance. *J Med Imaging Radiat Oncol*. 2015;59(3):300–5.
20. Silverstein MJ, Poller DN, Waisman JR, et al. Prognostic classification of breast ductal carcinoma-in-situ. *Lancet*. 1995;345(8958):1154–7.
21. Lagios MD. Heterogeneity of duct carcinoma in situ (DCIS): relationship of grade and subtype analysis to local recurrence and risk of invasive transformation. *Cancer Lett*. 1995;90(1):97–102.
22. Dershaw DD, Abramson A, Kinne DW. Ductal carcinoma in situ: mammographic findings and clinical implications. *Radiology*. 1989;170(2):411–5.
23. Holland R, Hendriks JH, Vebeek AL, Mravunac M, Schuurmans Stekhoven JH. Extent, distribution, and mammographic/histological correlations of breast ductal carcinoma in situ. *Lancet*. 1990;335(8688):519–22.
24. Yang WT, Tse GMK. Sonographic, mammographic, and histopathologic correlation of symptomatic ductal carcinoma in situ. *AJR Am J Roentgenol*. 2004;182(1):101–10.
25. Douglas-Jones AG, Morgan JM, Appleton MA, et al. Consistency in the observation of features used to classify duct carcinoma in situ (DCIS) of the breast. *J Clin Pathol*. 2000;53(8):596–602.
26. Consensus Conference Committee. Consensus conference on the classification of ductal carcinoma in situ. *Cancer*. 1997;80(9):1798–802.
27. Lee KS, Han BH, Chun YK, Kim HS, Kim EE. Correlation between mammographic manifestations and averaged histopathologic nuclear grade using prognosis-predict scoring system for the prognosis of ductal carcinoma in situ. *Clin Imaging*. 1999;23(6):339–46.
28. Berg WA, Gutierrez L, NessAiver MS, et al. Diagnostic accuracy of mammography, clinical examination, US, and MR imaging in preoperative assessment of breast cancer. *Radiology*. 2004;233(3):830–49.
29. Orel SG, Mendonca MH, Reynolds C, Schnell MD, Solin LJ, Sullivan DC. MR imaging of ductal carcinoma in situ. *Radiology*. 1997;202(2):413–20.
30. Mokbel K. Current management of ductal carcinoma in situ of the breast. *Int J Clin Oncol*. 2003;8(1):18–22.
31. Kuhl CK, Schrading S, Bieling B, et al. MRI for diagnosis of pure ductal carcinoma in situ: a prospective observational study. *Lancet*. 2007;370:485–92.
32. Yamada T, Mori N, Watanabe M, et al. Radiologic-pathologic correlation of ductal carcinoma in situ. *Radiographics*. 2010;30(5):1183–98.

33. Tozaki M, Igarashi T, Fukuda K. Breast MRI using the VIBE sequence: clustered ring enhancement in the differential diagnosis of lesions showing non-mass like enhancement. *AJR Am J Roentgenol.* 2006;187(2):313–21.
34. Morakkabati-Spitz N, Leutner C, Schild H, Traeber F, Kuhl C. Diagnostic usefulness of segmental and linear enhancement in dynamic breast MRI. *Eur Radiol.* 2005;15(9):2010–7.
35. Mossa-Basha M, Fundaro GM, Shah BA, Ali S, Pantelic MV. Ductal carcinoma in situ of the breast: MR imaging findings with histopathologic correlation. *Radiographics.* 2010;30(6):1673–87.
36. Heywang-Köbrunner SH. Contrast-enhanced magnetic resonance imaging of the breast. *Invest Radiol.* 1994;29(1):94–104.
37. Cheung YC, Juan YH, Lin YC, et al. Dual-Energy Contrast enhanced spectral mammography: enhancement analysis on BI-RADS 4 non mass microcalcifications in screened women. *PLoSOne.* 2016;11(9):e0162740. <https://doi.org/10.1371/journal.pone.0162740>.
38. Luczynska E, Niemiec J, Hendrick E, et al. Degree of enhancement on contrast enhanced spectral mammography (CESM) and lesion type on mammography (MG): comparison based on histological results. *Med Sci Monit.* 2016 Oct 21;22:3886–93.
39. Fallenberg E, Dromain C, Diekmann F, et al. Contrast-enhanced spectral mammography versus MRI: initial results in the detection of breast cancer and assessment of tumour size. *Eur J Radiol.* 2014;24:256–64.
40. Carriero A, Ambrossini R, Mattei PA, et al. Magnetic resonance of the breast: correlation between enhancement patterns and microvessel density in malignant tumors. *J Exp Clin Cancer Res.* 2002;21(Suppl 3):83–7.
41. Yamaguchi R, Furusawa H, Nakahara H, et al. Clinicopathological study of invasive ductal carcinoma with large central acellular zone: special reference to magnetic resonance imaging findings. *Pathol Int.* 2008;58(1):26–30.
42. World Health Organization. Histological typing of breast tumors. *Tumori.* 1982;68:181–98.
43. Okafuji T, Yabuuchi H, Sakai S, et al. MR imaging features of pure mucinous carcinoma of the breast. *Eur J Radiol.* 2006;60(3):405–13.
44. Kawashima M, Tamaki Y, Nonaka T, et al. MR imaging of mucinous carcinoma of the breast. *AJR Am J Roentgenol.* 2002;179(1):179–83.
45. Soo MS, Williford ME, Walsh R, Bentley RC, Kornguth PJ. Papillary carcinoma of the breast: imaging findings. *AJR Am J Roentgenol.* 1995;164(2):321–6.
46. Lam WW, Tang AP, Tse G, Chu WC. Radiology-pathology conference: papillary carcinoma of the breast. *Clin Imaging.* 2005;29(6):396–400.
47. Kuhl CK, Klaschik S, Mielcarek P, Gieseke J, Wardelmann E, Schild HH. Do T2-weighted pulse sequences help with the differential diagnosis of enhancing lesions in dynamic breast MRI? *J Magn Reson Imaging.* 1999;9(2):187–96.
48. Arpino G, Bardou VJ, Clark GM, Elledge RM. Infiltrating lobular carcinoma of the breast: tumor characteristics and clinical outcome. *Breast Cancer Res.* 2004;6(3):R149–56.
49. Dixon JM, Anderson TJ, Page DL, Lee D, Duffy SW, Stewart HJ. Infiltrating lobular carcinoma of the breast: an evaluation of the incidence and consequence of bilateral disease. *Br J Surg.* 1983;70(9):513–6.
50. Lopez JK, Bassett LW. Invasive lobular carcinoma of the breast: spectrum of mamographic, US, and MR imaging findings. *Radiographics.* 2009;29:165–76.
51. Paramagul CP, Helvie MA, Adler DD. Invasive lobular carcinoma: sonographic appearance and role of sonography in improving diagnostic sensitivity. *Radiology.* 1995;195(1):231–4.
52. Butler RS, Venta LA, Wiley EL, Ellis RL, Dempsey PJ, Rubin E. Sonographic evaluation of infiltrating lobular carcinoma. *AJR Am J Roentgenol.* 1999;172(2):325–30.
53. Selinko VL, Middleton LP, Dempsey PJ. Role of sonography in diagnosing and staging invasive lobular carcinoma. *J Clin Ultrasound.* 2004;32(7):323–32.
54. Mann RM, Hoogveen YL, Blickman JG, Boetes C. MRI compared to conventional diagnostic work-up in the detection and evaluation of invasive lobular carcinoma of the breast: a review of existing literature. *Breast Cancer Res Treat.* 2008;107(1):1–14.
55. Weinstein SP, Orel SG, Heller R, et al. MR imaging of the breast in patients with invasive lobular carcinoma. *AJR Am J Roentgenol.* 2001;176(2):399–406.

Jacopo Nori, Maninderpal Kaur, Marc B. I. Lobbes,  
Felix Diekmann, Giulia Bicchierai,  
and Diego de Benedetto

### 14.1 Contrast Media in CEDM

#### Case 1



Tumour is hardly visible on the initial craniocaudal CEDM image, while multiple arteries are filled with contrast. A delayed image shows tumour areas with better enhancement (*arrows*). If too many arteries are seen in the first image, one should consider repeating the image 1 minute later to make sure it wasn't too early for visualization of contrast enhancement (*Image courtesy of Felix Diekmann, St. Joseph-Stift Bremen, Germany*)

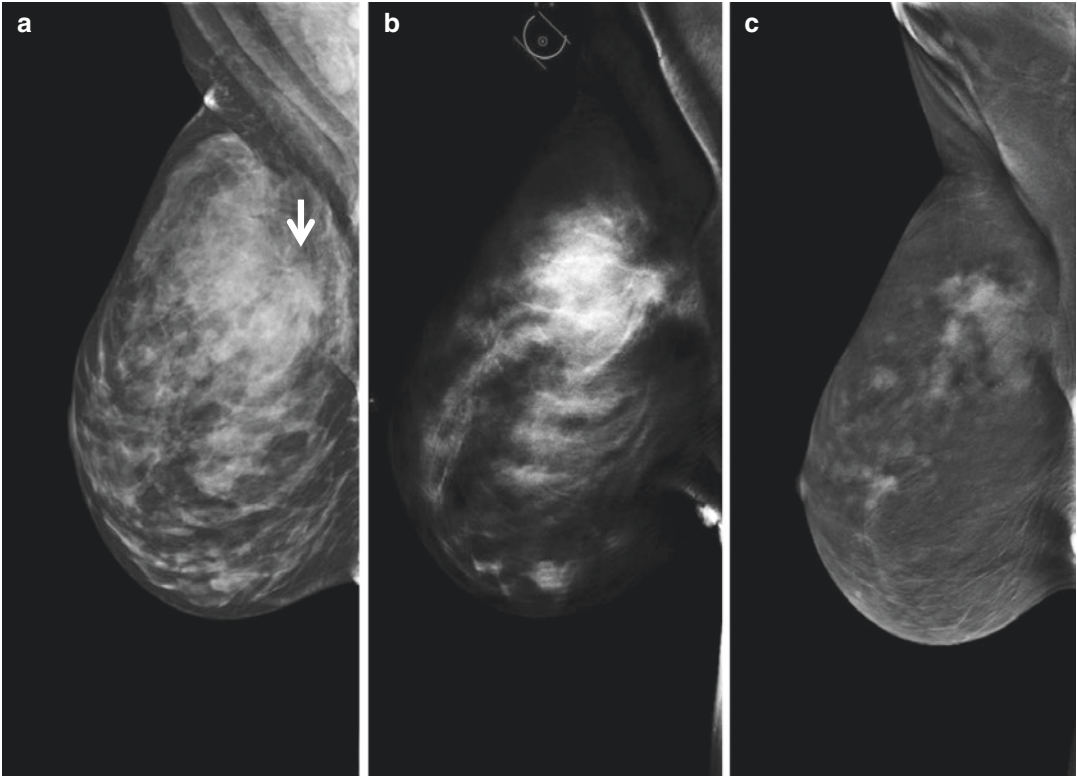
J. Nori (✉) · G. Bicchierai · D. de Benedetto  
Diagnostic Senology Unit, Department of Radiology,  
Azienda Ospedaliero Universitaria Careggi,  
Florence, Italy

Maninderpal Kaur  
Department of Radiology, Kuala Lumpur Hospital,  
Kuala Lumpur, Malaysia

M. B. I. Lobbes  
Department of Radiology and Nuclear Medicine,  
Maastricht University Medical Center,  
Maastricht, The Netherlands  
e-mail: [marc.lobbes@mumc.nl](mailto:marc.lobbes@mumc.nl)

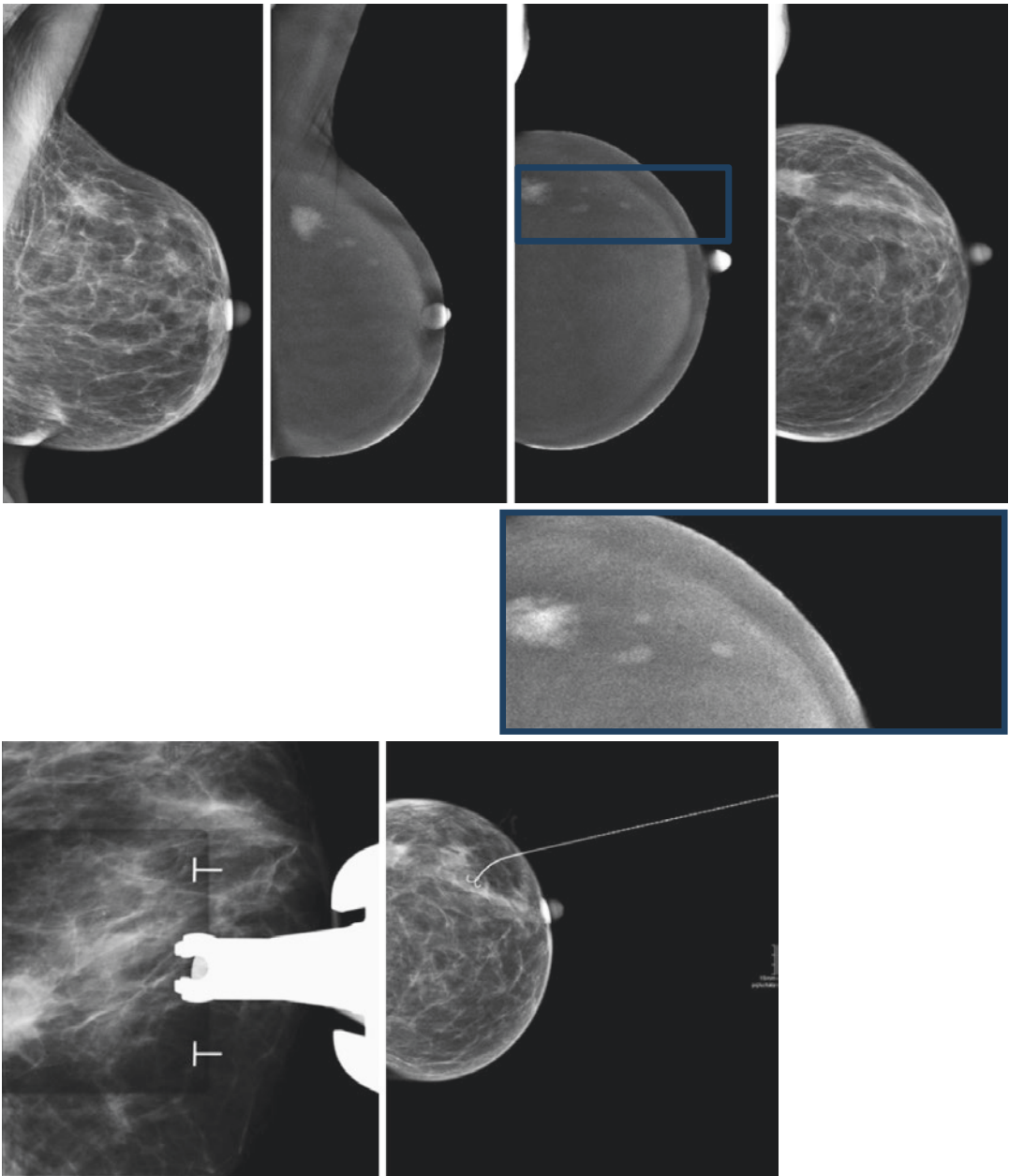
F. Diekmann  
Department of Radiology, St. Joseph-Stift Bremen,  
Bremen, Germany  
e-mail: [FDiekmann@sjs-bremen.de](mailto:FDiekmann@sjs-bremen.de)



**Case 2**

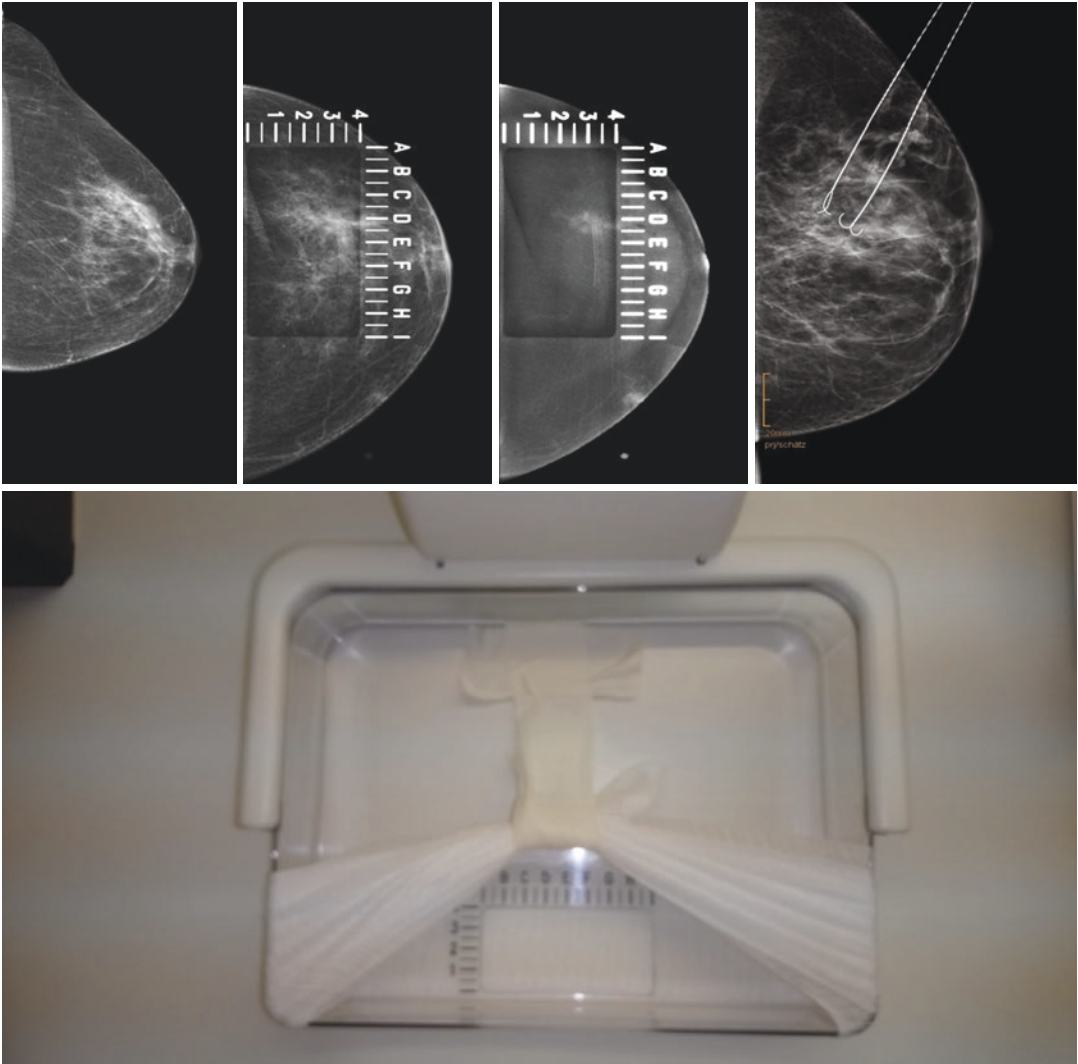
(a) 2D mammography shows an architectural distortion (*arrow*). (b) Distortion is better visualized in tomosynthesis. (c) The large extension of the tumour with various satellite lesions, which is seen only in the recombined CEDM image (*Image courtesy of Felix Diekmann, St. Joseph-Stift Bremen, Germany*)

Case 3



Correlation of a left upper outer quadrant lesion seen on 2D mammography and CEDM. The tumour is visible without contrast, but additional satellite lesions that were not visualized on 2D are clearly demonstrated on the CEDM images. When the radiologist is aware of the entire area of involvement, based on the CEDM findings, it is possible to perform a hook wire localization in the area, even without contrast enhancement (*Image courtesy of Felix Diekmann, St. Joseph-Stift Bremen, Germany*)

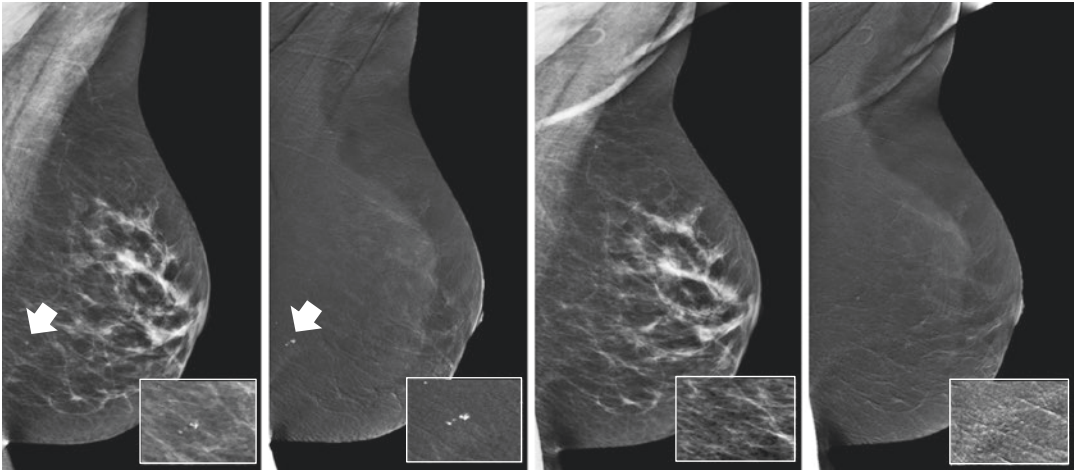
Case 4



This image shows an example of a possible method of intervention in CEDM with a picture of the compression paddle, which has been prepared prior to biopsy. Preparation of the compression paddle with a sterile gauze bandage is necessary to make sure that the breast thickness is not influenced by the compression paddle. On 2D mammography, the tumour is hardly visible. However, on the CEDM low-energy and recombined images with the compression paddle in the middle, the tumour is well visualised. Wire localization was done under CEDM-guidance (as seen in the final image on the right) (Image courtesy of Felix Diekmann, St. Joseph-Stift Bremen, Germany)

## 14.2 Artefacts and Limitations

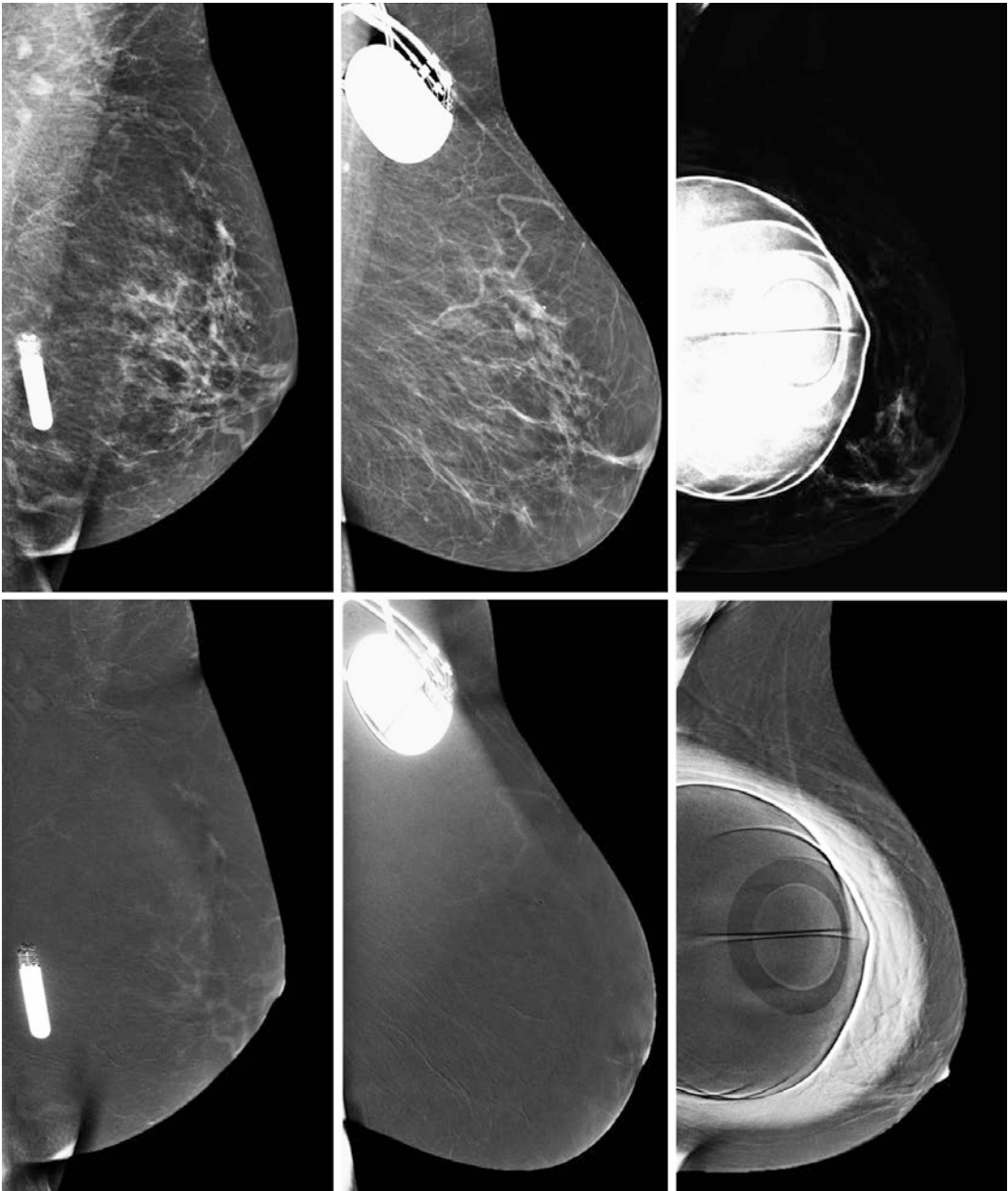
### Case 1



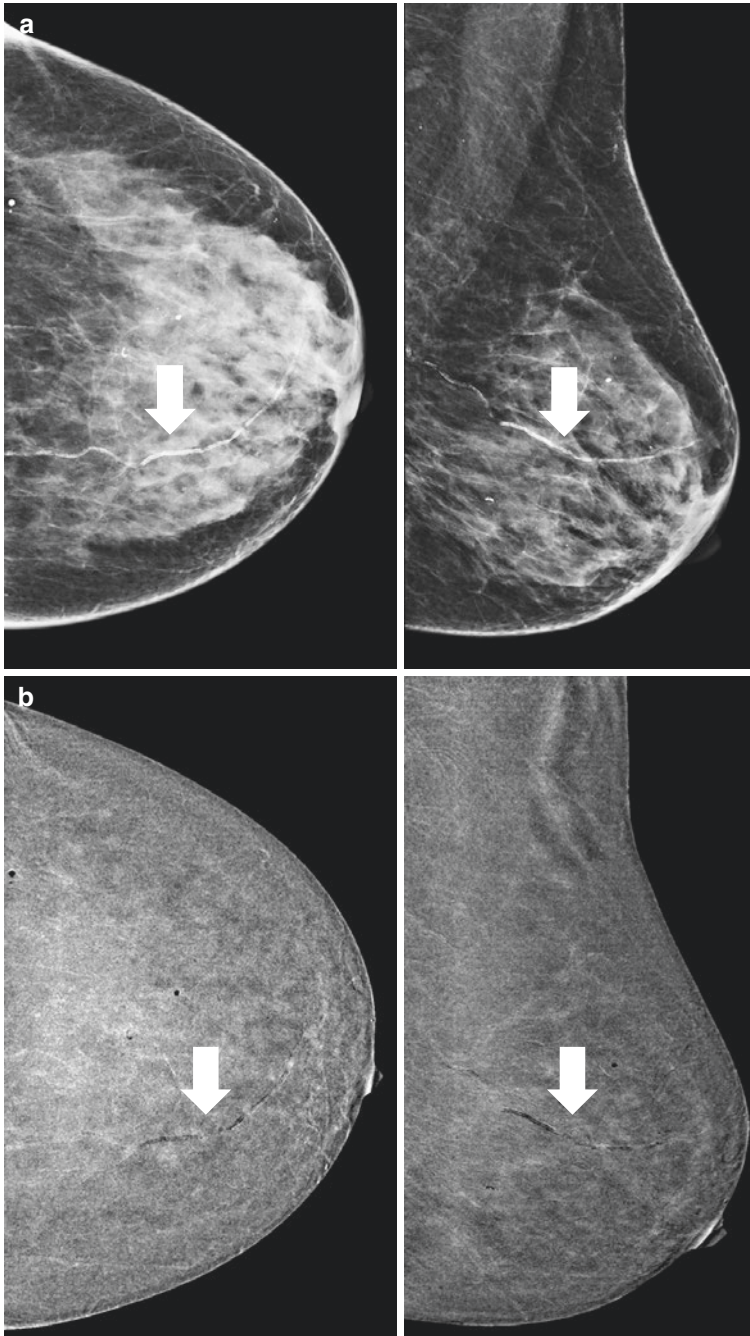
A 49-year-old female undergoing CEDM as an alternative of breast MRI for high-risk screening. On the initial images (*left side*), grouped calcifications were suggested on the low-energy images, which showed a very high opacity on the recombined images. True calcifications are extremely dark on the recombined images. Therefore, contrast splatter on the detector was suspected. After this first image, the detector was cleaned and the exam repeated immediately, which showed that the findings had disappeared (*right images*) (*Image courtesy of Marc B.I. Lobbes, Maastricht University Medical Center*)



Case 2



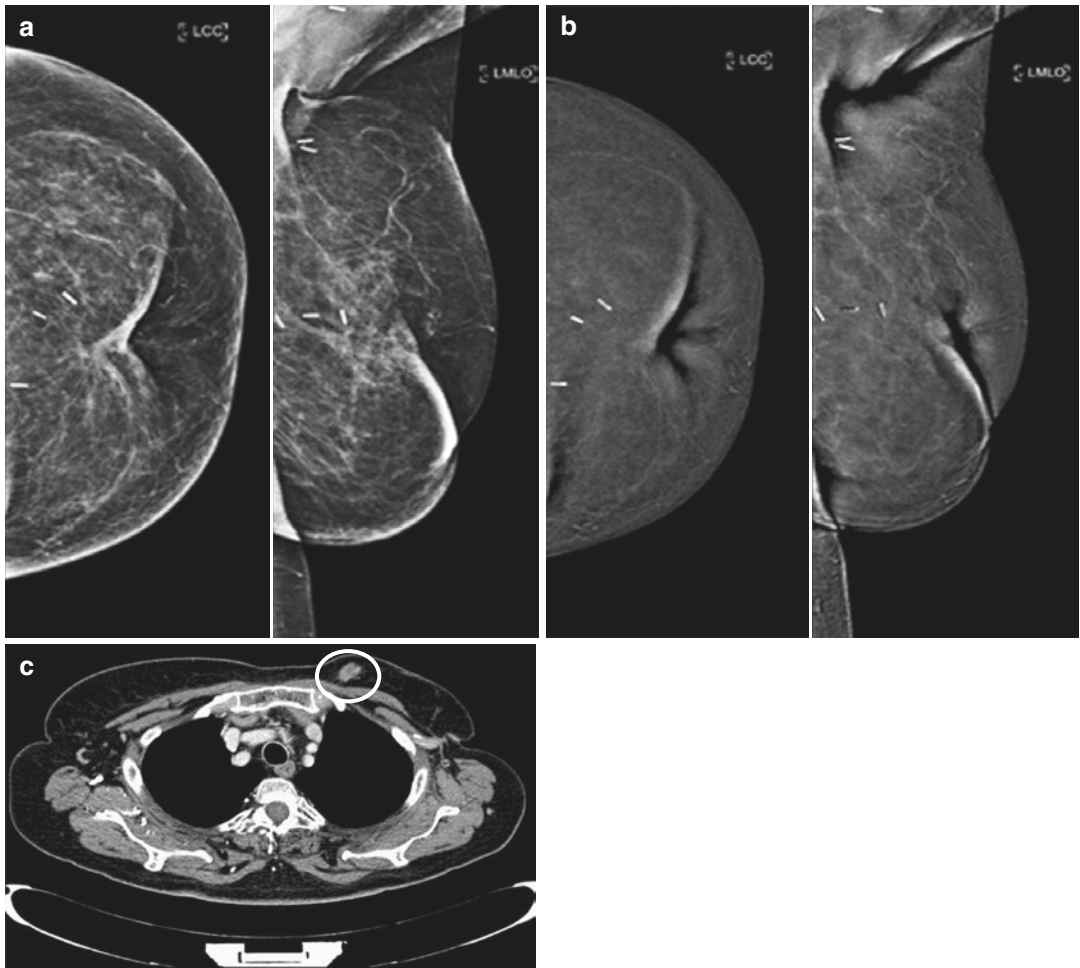
Implantable cardiac devices do not seem to hamper the image quality of CEDM exams, as demonstrated by these exams of an implantable cardiac monitoring device (*left column*) or a cardiac defibrillator (*middle column*). However, breast implants are a contraindication for performing CEDM, as they reduced imaging quality significantly, especially the recombined images (*right column*) (*Image courtesy of Marc B.I. Lobbes, Maastricht University Medical Center*)

**Case 3**

An 80-year-old woman with diffuse calcifications in the left breast, post-lumpectomy in the contralateral breast. **(a)** Craniocaudal and mediolateral oblique low-energy views show a dense breast and a calcific vessel in the upper inner quadrant. **(b)** Craniocaudal and mediolateral oblique recombined images show the “negative contrast enhancement” due to the calcific vessel, which appears darker with respect to the background

*Diagnosis: Negative contrast enhancement of vascular calcification (Image courtesy of Jacopo Nori, Careggi University Hospital, Florence, Italy)*

Case 4

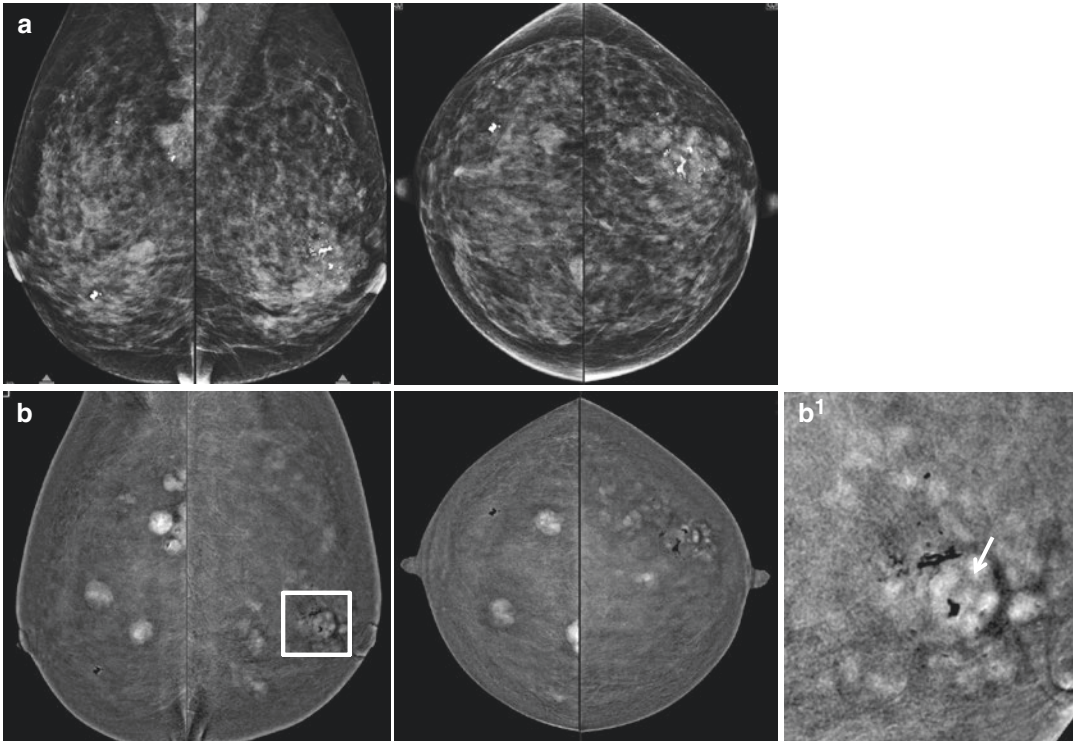


Pre-surgical staging in a 77-year-old patient, with a palpable mass at the left breast (chest wall). An ultrasound-guided biopsy confirmed a malignant lesion. (a, b) The mass is deep-seated; neither the low-energy image nor CEDM could detect the lesion. (c) Patient underwent a staging CT examination; it confirmed the presence of a deep-seated mass at the left upper inner quadrant. This is a limitation of CEDM, which is non-visualisation of deep-seated masses and inability to assess the extent of posteriorly located masses

Diagnosis: Invasive carcinoma (Image courtesy of Jacopo Nori, Careggi University Hospital, Florence, Italy)

### 14.3 Benign Lesions

#### Case 1

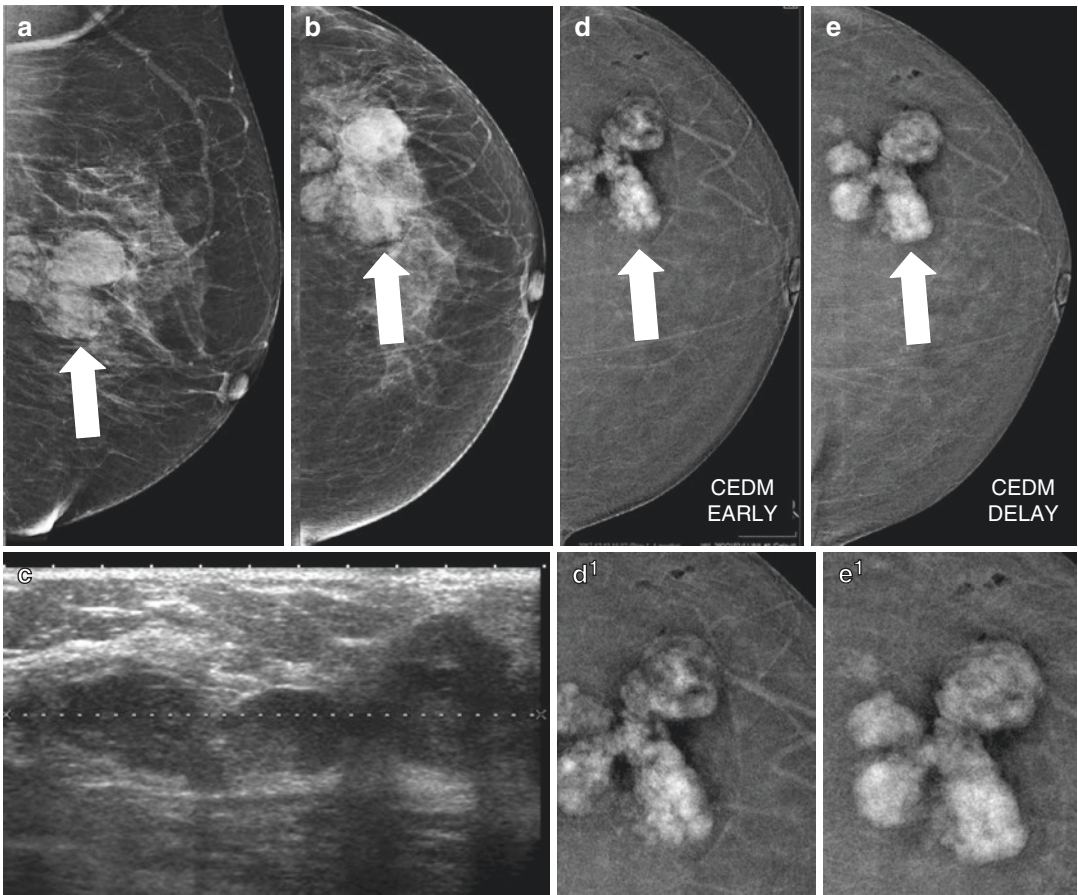


A young 38-year-old female referred from a primary healthcare centre for an irregular deep-seated mass in the right breast. **(a)** Low-energy images in CC and MLO view showed a lobulated deep-seated opacity in the right upper outer quadrant and multiple bilateral relatively well-defined opacities with associated coarse calcifications. **(b)** CEDM recombinant images in CC and MLO view show intense enhancement in all the lesions. Negative contrast enhancement artefacts are seen at the regions of coarse calcifications. **(b<sup>1</sup>)** note the non-enhancing internal septations (*white arrow*) within the left enhancing lesion (*box*), which is a typical feature of fibroadenoma. The largest lesions in both breasts were biopsied under ultrasound guidance

*Diagnosis: Benign lesions favouring bilateral fibroadenomas (Image courtesy of Maninderpal Kaur, Kuala Lumpur Hospital, Malaysia)*

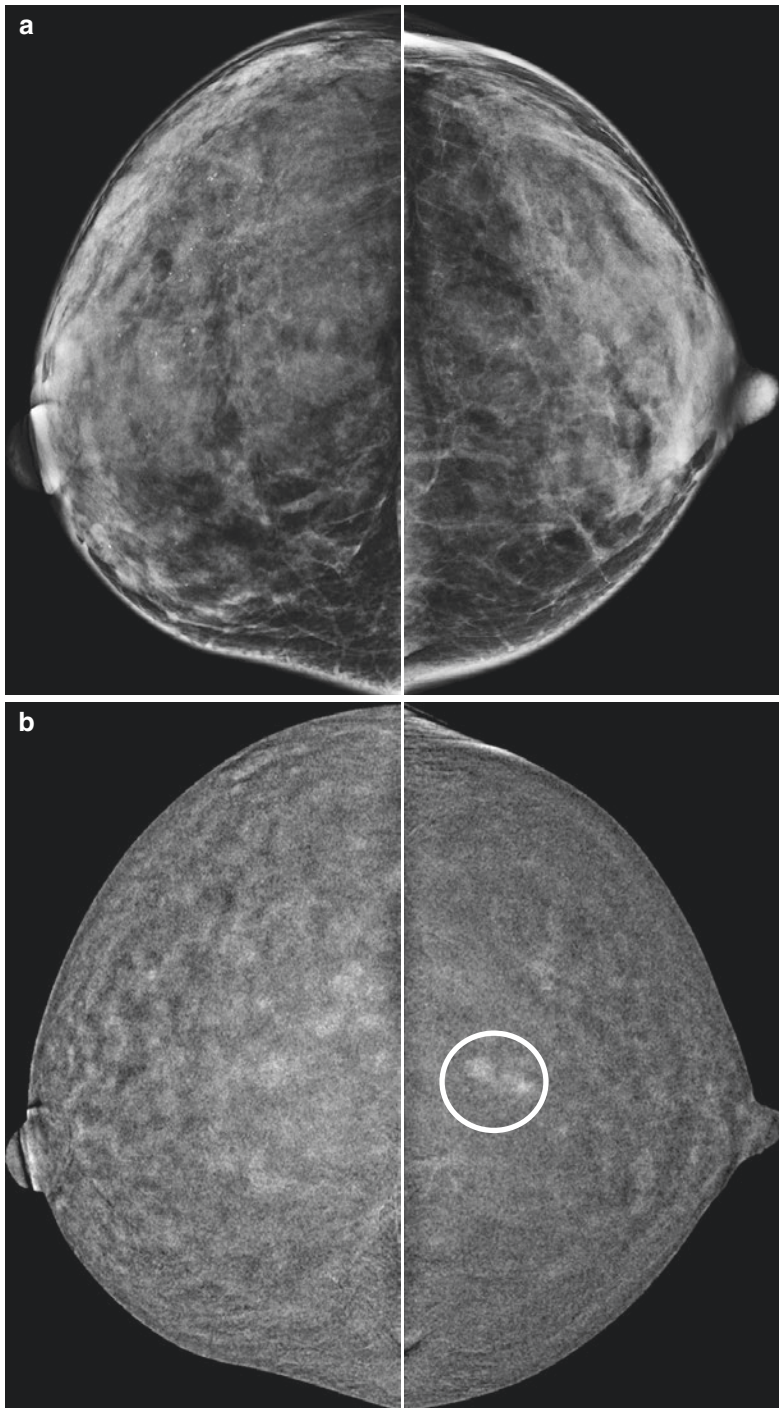


## Case 2



A 59-year-old female presented to the surgical clinic with an ill-defined irregular mass in the left breast. CEDM was performed as first-line imaging. (a–b) Low-energy images in CC and MLO view showed a lobulated opacity (*block arrows*) in the left upper outer quadrant. (c) It was identified as a suspicious ill-defined heterogeneously hypoechoic lesion on ultrasound which was biopsied. CEDM recombined images in (d) early and (e) delayed phase showed heterogeneous enhancement of the lobulated mass in the left upper outer quadrant. (d<sup>1</sup>–e<sup>1</sup>) However, there was progressive enhancement of the lesion seen in the delayed CEDM recombined image

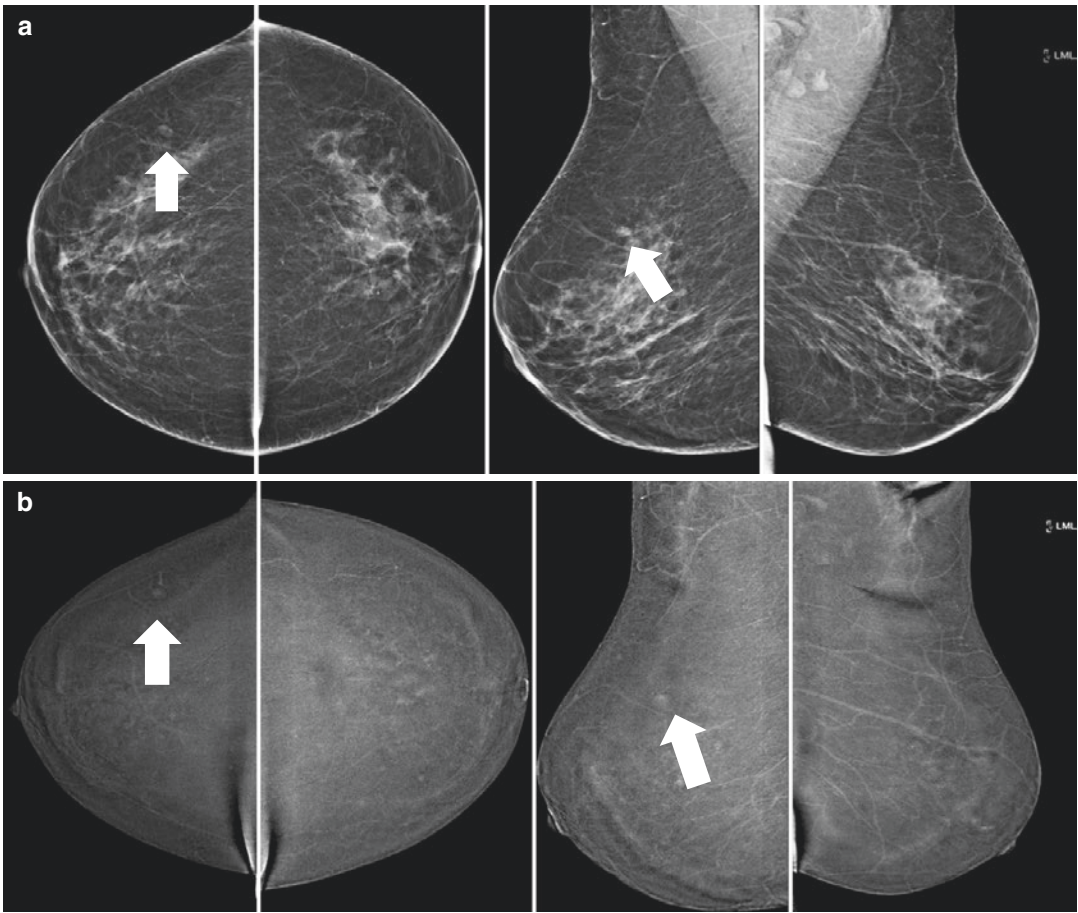
*Diagnosis: Final pathology showed fibroadenomatoid hyperplasia of the breast (FAHB), which is a rare benign breast lesion, and its clinical features are similar to fibroadenoma and fibrocystic changes. Hence the benign enhancement kinetics was seen on CEDM (Image courtesy of Maninderpal Kaur, Kuala Lumpur Hospital, Malaysia)*

**Case 3**

Screening mammogram in a 43-year-old woman with extremely dense parenchyma with a known benign lesion in the left breast. **(a)** Craniocaudal low-energy views. **(b)** Craniocaudal recombined images show a round mass with circumscribed margins and mild enhancement

*Diagnosis: Fibroadenoma (Image courtesy of Jacopo Nori, Careggi University Hospital, Florence, Italy)*

Case 4

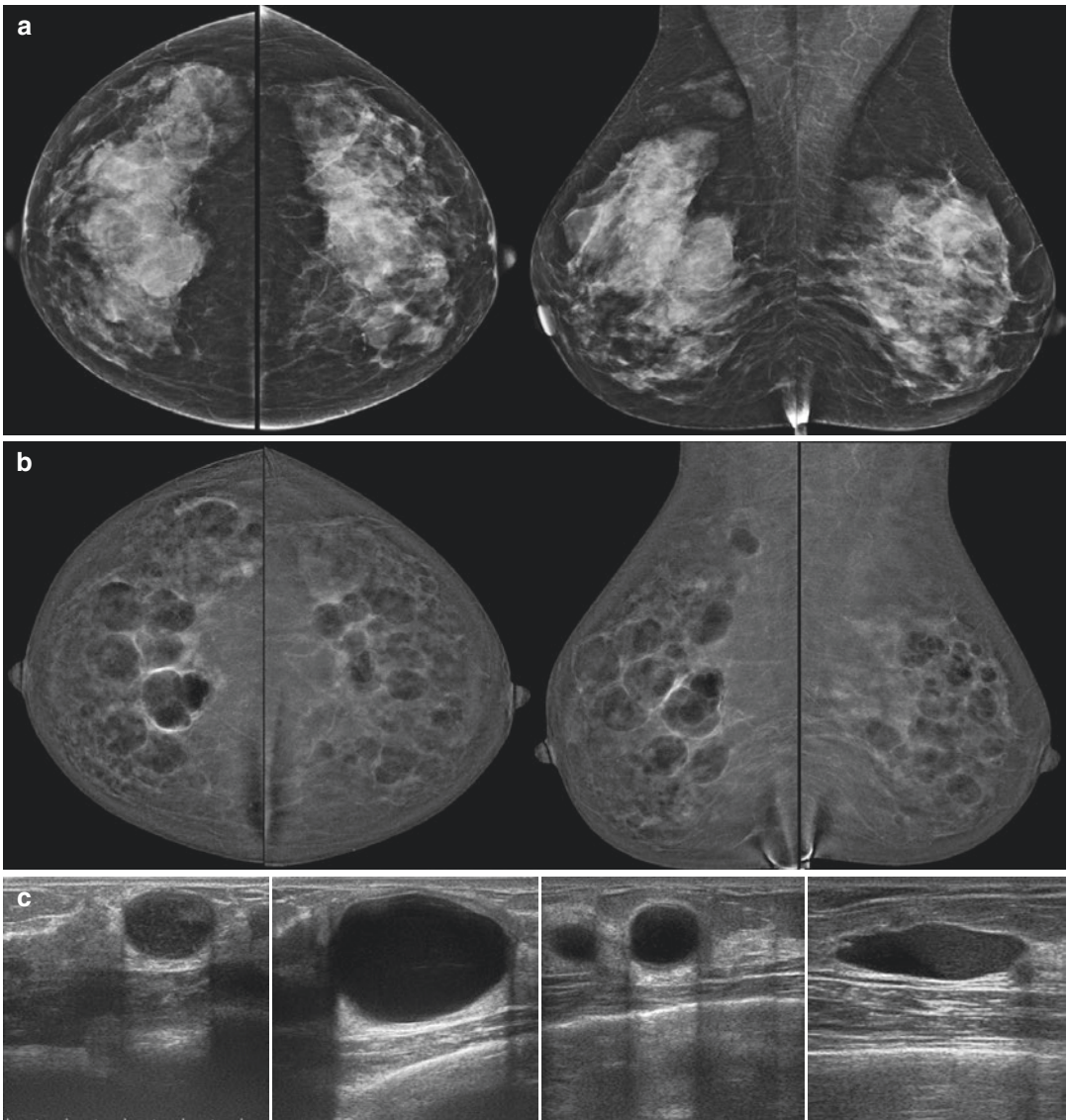


Screening mammogram in a 54-year-old woman with trabecular thickening in the right breast. (a) Craniocaudal and mediolateral oblique low-energy view shows an oval mass in the upper outer quadrant of the right breast. (b) Craniocaudal and mediolateral oblique recombined images show an oval mass with circumscribed margins and moderate enhancement

*Diagnosis: Intramammary lymph node (Image courtesy of Jacopo Nori, Careggi University Hospital, Florence, Italy)*



## Case 5

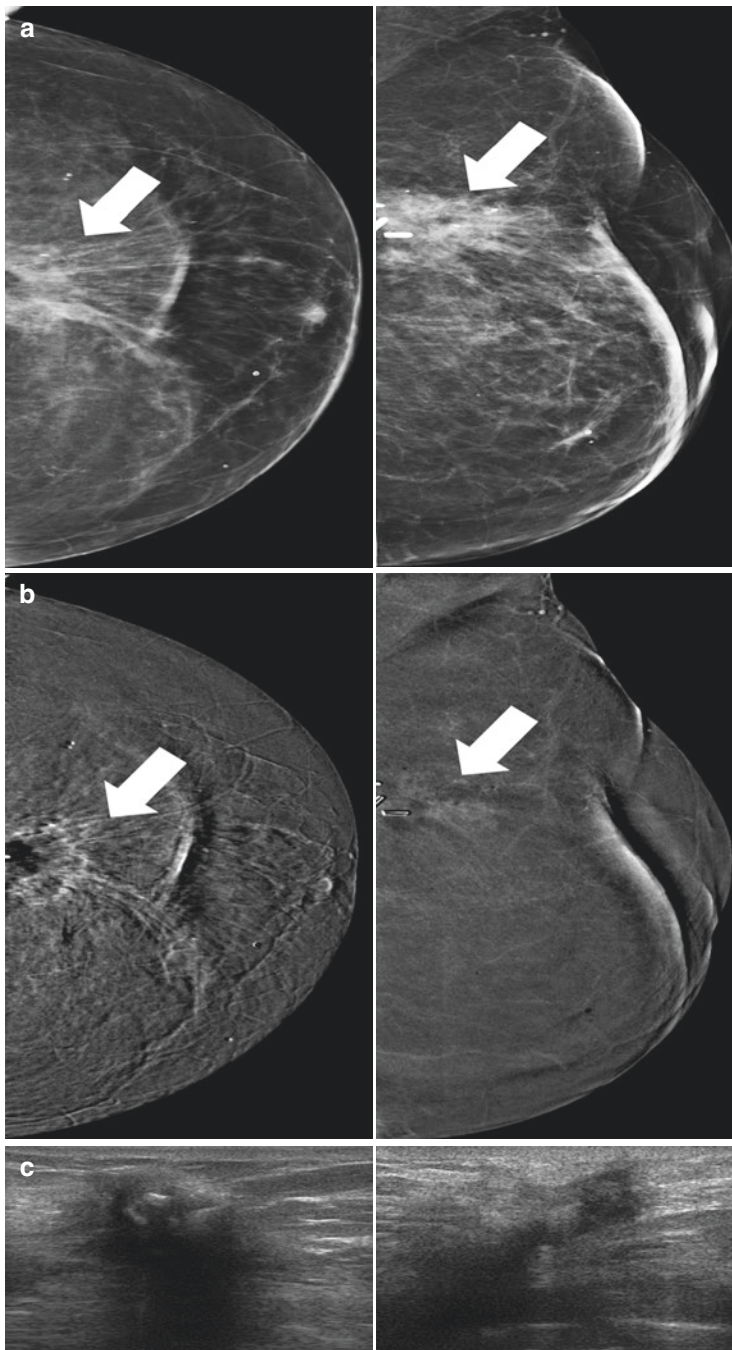


A 44-year-old woman with extremely dense parenchyma and multiple opacities seen on screening mammogram. (a) Craniocaudal and mediolateral oblique low-energy views show multiple scattered round opacities, with well-circumscribed margins. (b) Craniocaudal and mediolateral oblique recombined images show multiple radiolucent areas, surrounded by thin uniform mural enhancement and peripheral thin rim enhancement. (c) Ultrasound (US) images show many simple cysts that are well circumscribed, anechoic and with a thin echogenic capsule

*Diagnosis: Diffuse bilateral breast cysts (Image courtesy of Jacopo Nori, Careggi University Hospital, Florence, Italy)*

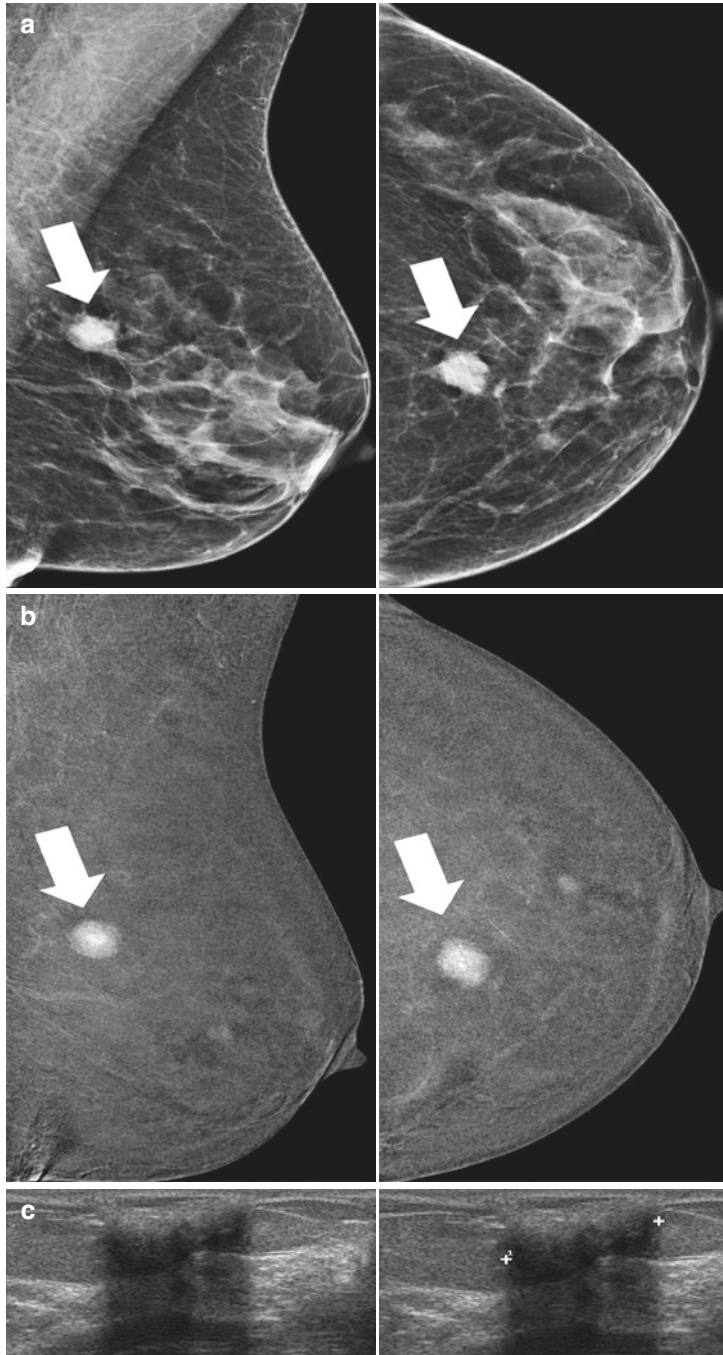


## Case 6



A 70-year-old woman with a history of left quadrantectomy for breast cancer. (a) Low-energy CEDM image in cranio-caudal view of the left breast shows a hypertrophic surgical scar of previous quadrantectomy. (b) Mediolateral CEDM recombined images show a slight enhancement of the scar. (c) It is seen as an inhomogeneous hypoechoic area on US. US-guided biopsy of the lesion was performed

*Diagnosis: Fat necrosis with inflammatory changes (Image courtesy of Jacopo Nori, Careggi University Hospital, Florence, Italy)*

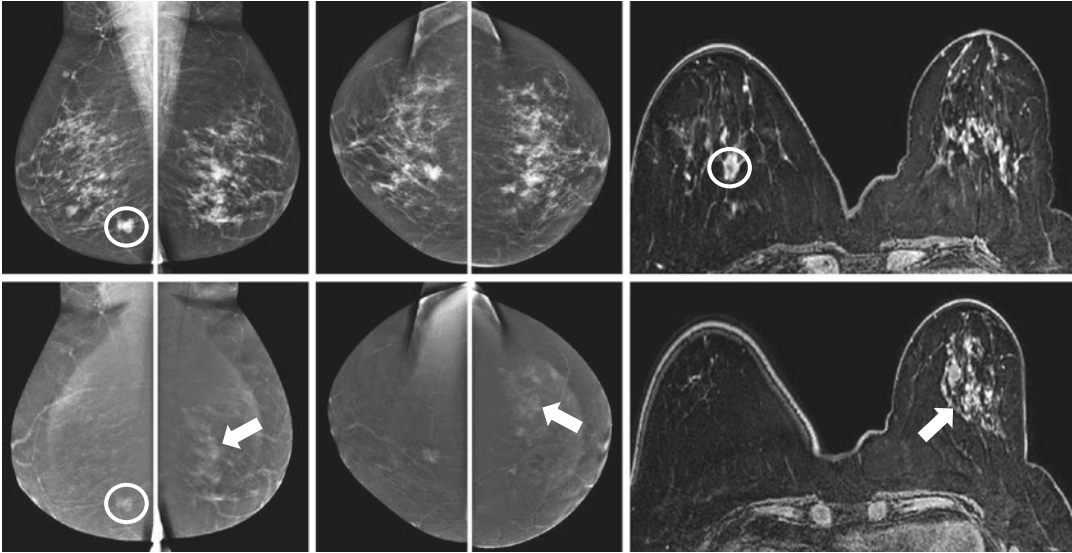
**Case 7**

A 70-year-old woman with previous core biopsy on a suspicious left breast nodule and marking with liquid coal solution. **(a)** Low-energy CEDM image in mediolateral oblique and craniocaudal low-energy views showing a relatively well-defined opacity in the left upper inner quadrant. **(b)** Mediolateral oblique and craniocaudal recombined images demonstrate a solitary mass with intense homogenous enhancement. **(c)** The lesion corresponds to an inhomogeneous hypoechoic area with strong posterior acoustic shadowing on ultrasound. An ultrasound-guided core biopsy was performed

*Diagnosis: An inflamed granuloma due to marking with liquid coal solution was revealed (Image courtesy of Jacopo Nori, Careggi University Hospital, Florence, Italy)*

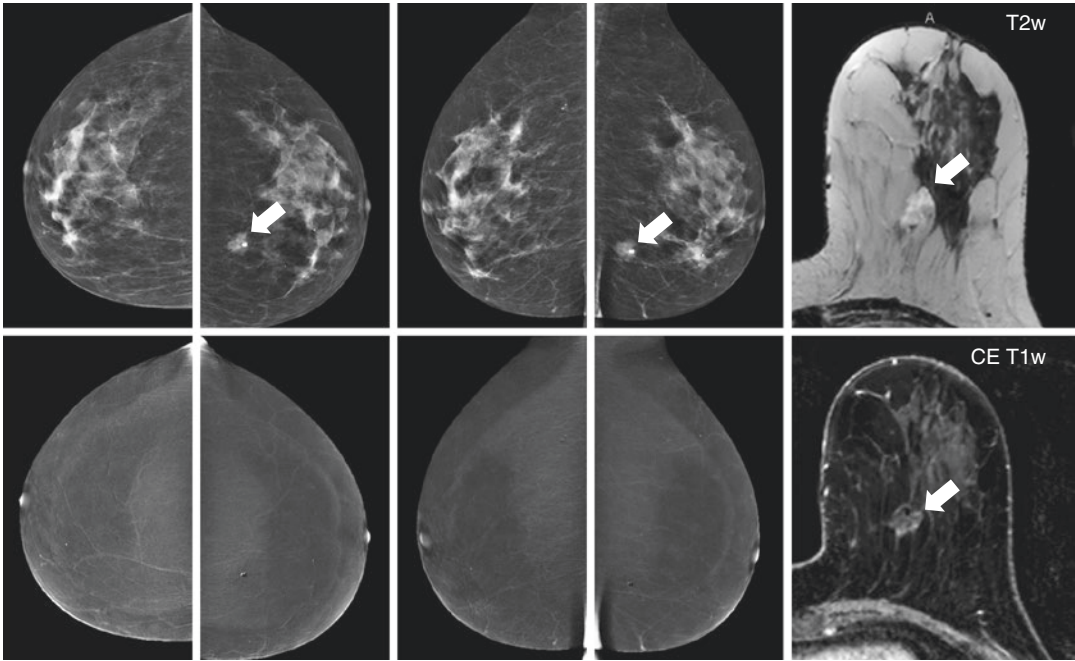
## 14.4 Malignant Lesions

### Case 1



A 57-year-old female referred from a private practice for an ill-defined irregular mass in the right breast, enhancing on both CEDM and MRI (*circles*). However, CEDM also showed diffuse enhancement throughout the left breast, for which random biopsies were taken, showing lobular carcinoma in situ (LCIS). Because of its extent, a MR-guided biopsy was recommended, again showing LCIS. Based on these findings and patient's preference, a bilateral mastectomy with reconstruction was performed. Final pathology showed invasive carcinoma of no special type (NST) in the right breast, but ten (!) invasive lobular cancer foci varying from 3 to 10 mm in the left breast surrounded by LCIS (*Image courtesy of Marc B.I. Lobbes, Maastricht University Medical Center*)

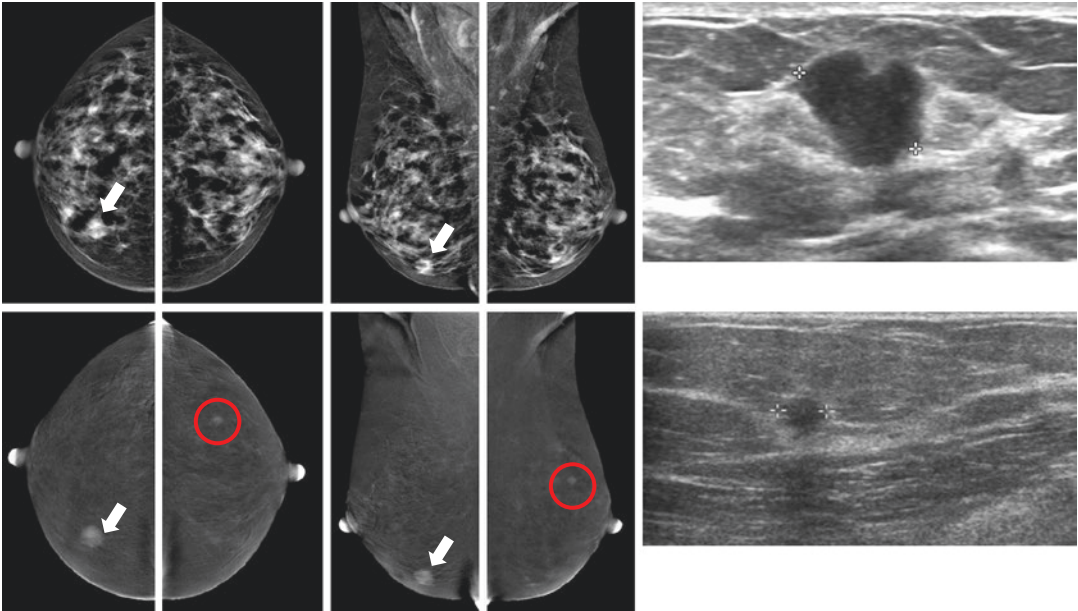
## Case 2



A 50-year-old female recalled from a first-round breast cancer screening. There is an ill-defined mass in the lower inner quadrant of the left breast (*arrows*). On the recombined images, no enhancement whatsoever is observed in the mass. A similar phenomenon was observed on the dynamic, contrast-enhanced T1W sequence of a subsequent breast MRI. On the T2W images, the mass showed increased signal intensity, suggesting a cystic content. Final histopathology showed a mucinous carcinoma. Due to their high water content relative to the small number of tumour cells, mucinous carcinomas might show no or only subtle enhancement on either CEDM or breast MRI. Therefore, they should be considered as a potential pitfall in CEDM (*Image courtesy of Marc B.I. Lobbes, Maastricht University Medical Center*)

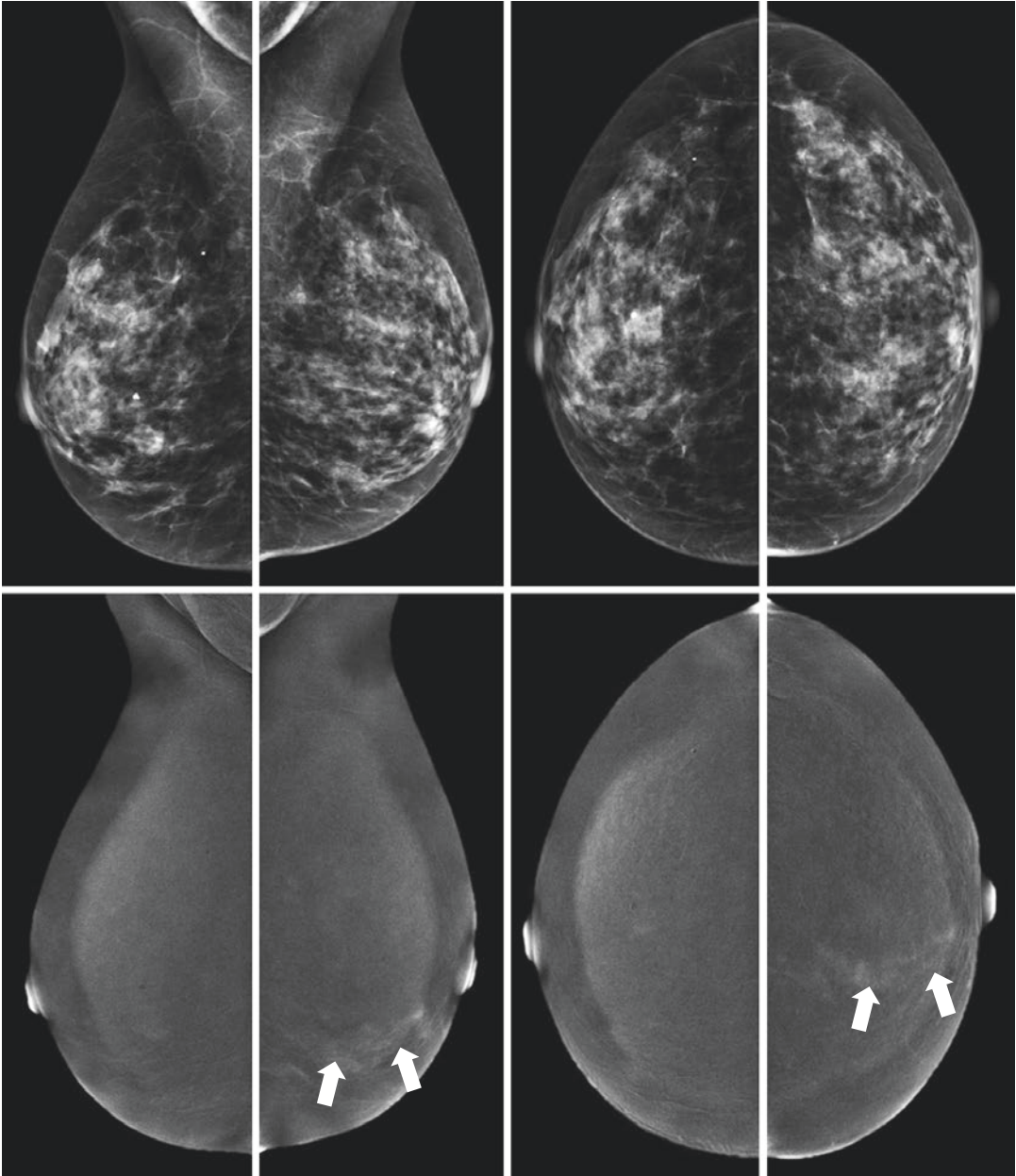


Case 3



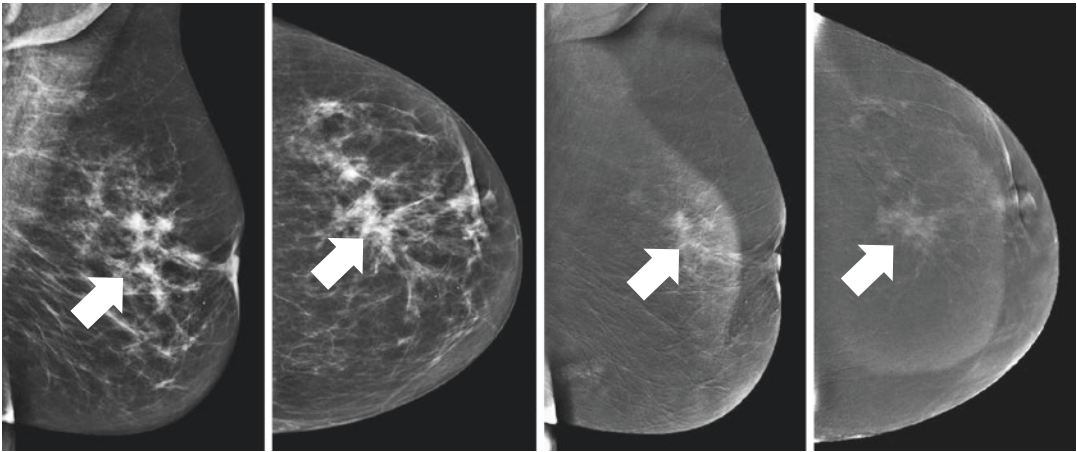
A 68-year-old female recalled from breast cancer screening for an ill-defined mass in the lower inner quadrant of the right breast (*white arrows*). However, on the recombined images of the left breast, an enhancing mass was observed without any correlation on the low-energy images. Both masses were found with targeted ultrasound (*images on the right*) and biopsied. In both breasts an invasive carcinoma was diagnosed (*Image courtesy of Marc B.I. Lobbes, Maastricht University Medical Center*)

## Case 4



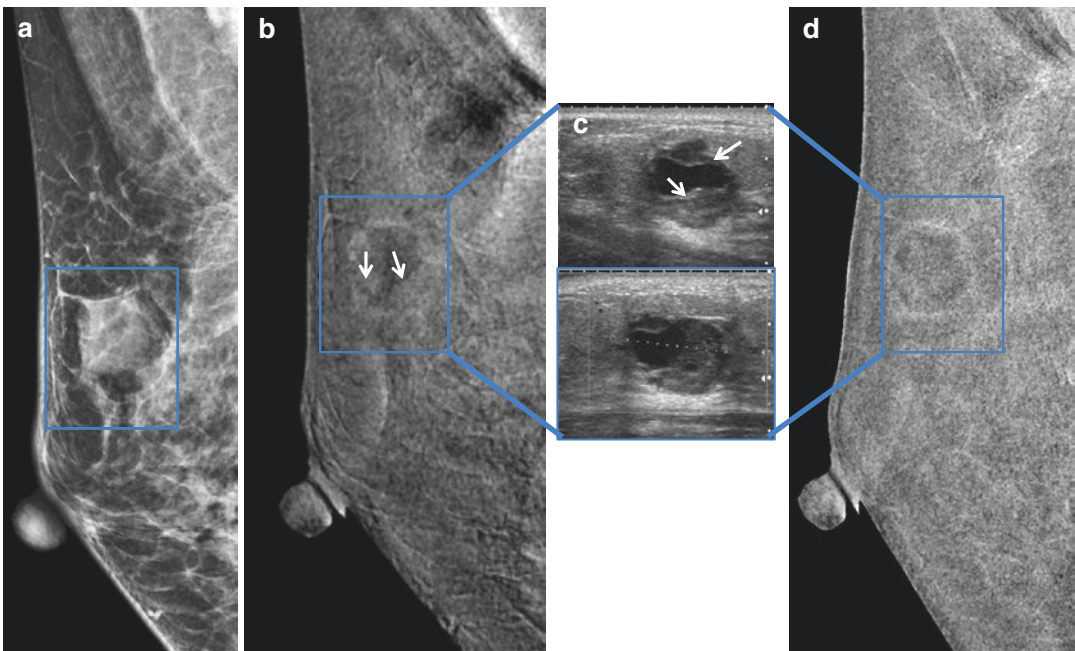
A 55-year-old female presented with a subtle swelling and tenderness in the lower inner quadrant of the left breast, without any abnormal findings on prior mammography and ultrasound. CEDM was performed for inconclusive findings and showed a segmental non-mass enhancement in the lower inner quadrant. Biopsies were randomly performed in this area using ultrasound. Final pathology showed extensive high-grade ductal carcinoma in situ (DCIS). Although some symmetric background parenchyma can also be observed in CEDM (like in breast MRI), the asymmetry of this enhancement should cause suspicion and warrant further action (i.e. minimum BI-RADS 4 classification) (Image courtesy of Marc B.I. Lobbes, Maastricht University Medical Center)

### Case 5



A 72-year-old female recalled for an evolving architectural distortion in the central part of the left breast (*arrows*). This distortion showed (*heterogeneous*) enhancement and was found by targeted ultrasound and biopsied, revealing an invasive lobular carcinoma (*Image courtesy of Marc B.I. Lobbes, Maastricht University Medical Center*)

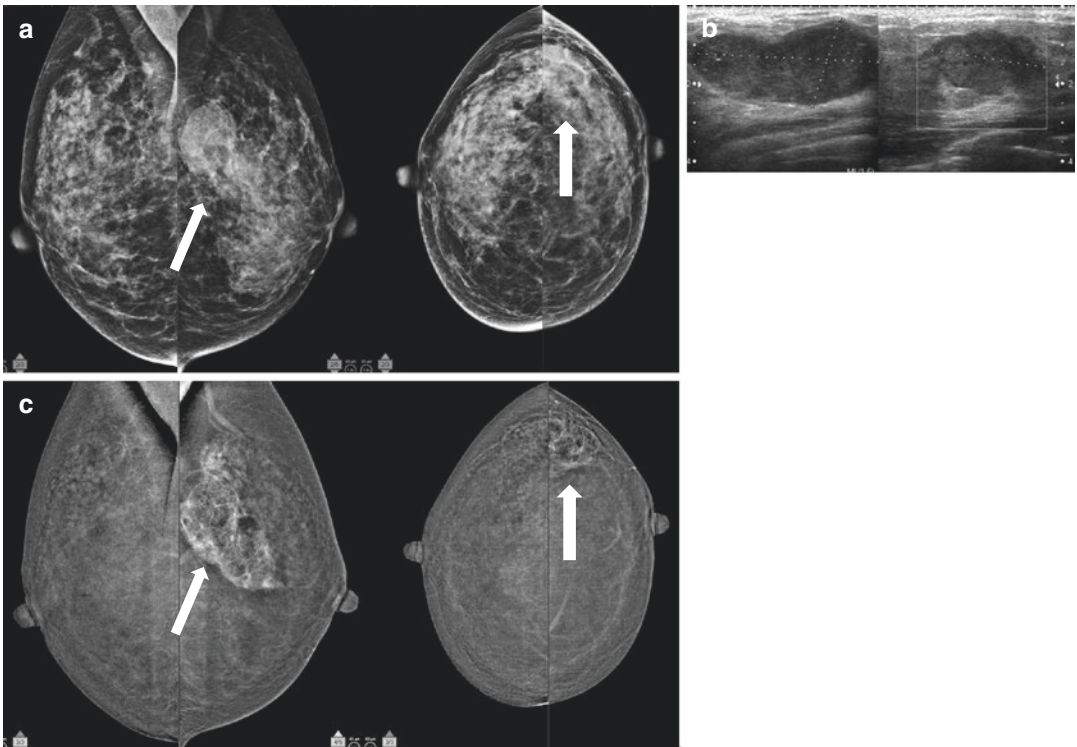
### Case 6



A 40-year-old female referred for a palpable right upper outer quadrant mass. (a) Low-energy image in MLO view shows an opacity in the right upper quadrant. (b) Early CEDM recombined image demonstrates a subtle thick rim-enhancing lesion suggestive of a cystic lesion with intracystic enhancement (*arrows*). Note the motion artefacts in this image. (c) On ultrasound, the lesion was seen as a lobulated complicated cyst with solid and cystic components within and posterior acoustic enhancement. It was subsequently biopsied. (d) Delayed CEDM recombined image nicely demonstrates wash-out of the intracystic solid components

*Diagnosis: The pathology was an invasive carcinoma, Grade 2 (Image courtesy of Maninderpal Kaur, Kuala Lumpur Hospital, Malaysia)*

## Case 7

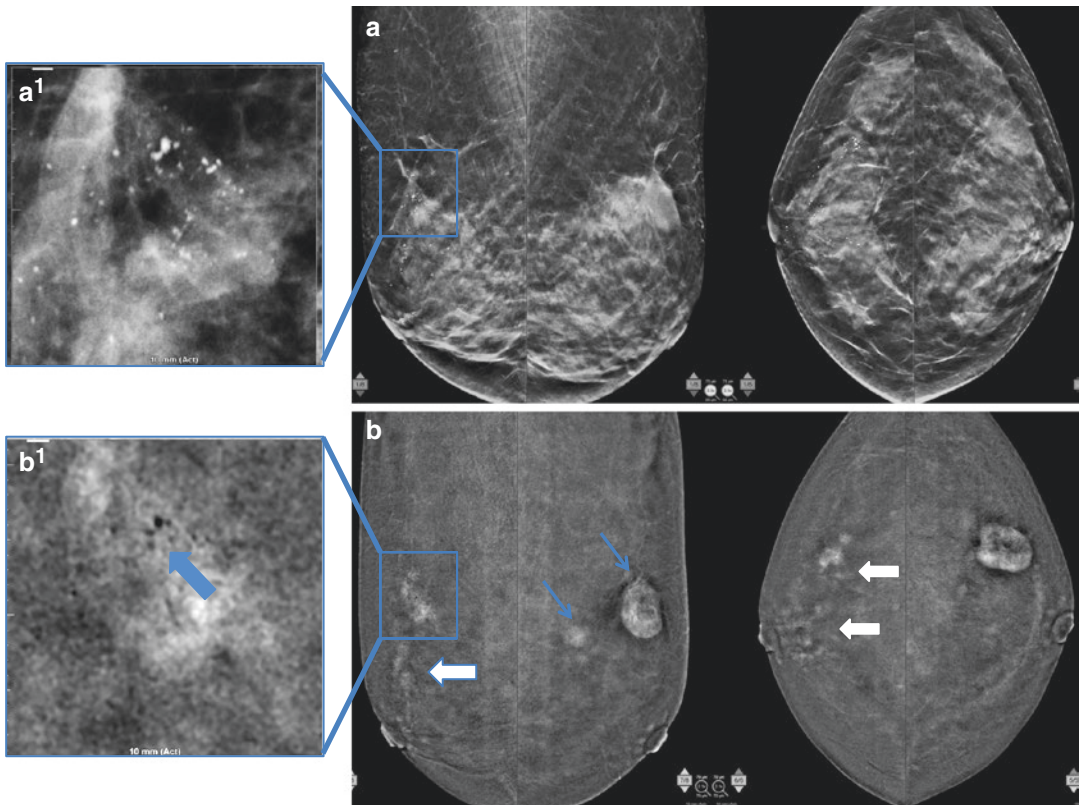


A young 30-year-old female referred from a primary healthcare centre for a large irregular mass in the left breast. **(a)** Low-energy images in CC and MLO view showed a large deep-seated opacity in the left upper outer quadrant (*arrows*). **(b)** The lesion was seen as a 5.1 cm hypoechoic, oval-lobulated mass with posterior acoustic enhancement on ultrasound. It was subsequently biopsied. **(c)** CEDM recombined images demonstrating a large heterogeneously enhancing lesion seen in the left upper outer quadrant, the posterior extent of which is not clearly demarcated in the CC view (*arrows*)

*Diagnosis: The pathology was invasive carcinoma of no special type with ductal carcinoma in situ (Image courtesy of Maninderpal Kaur; Kuala Lumpur Hospital, Malaysia)*



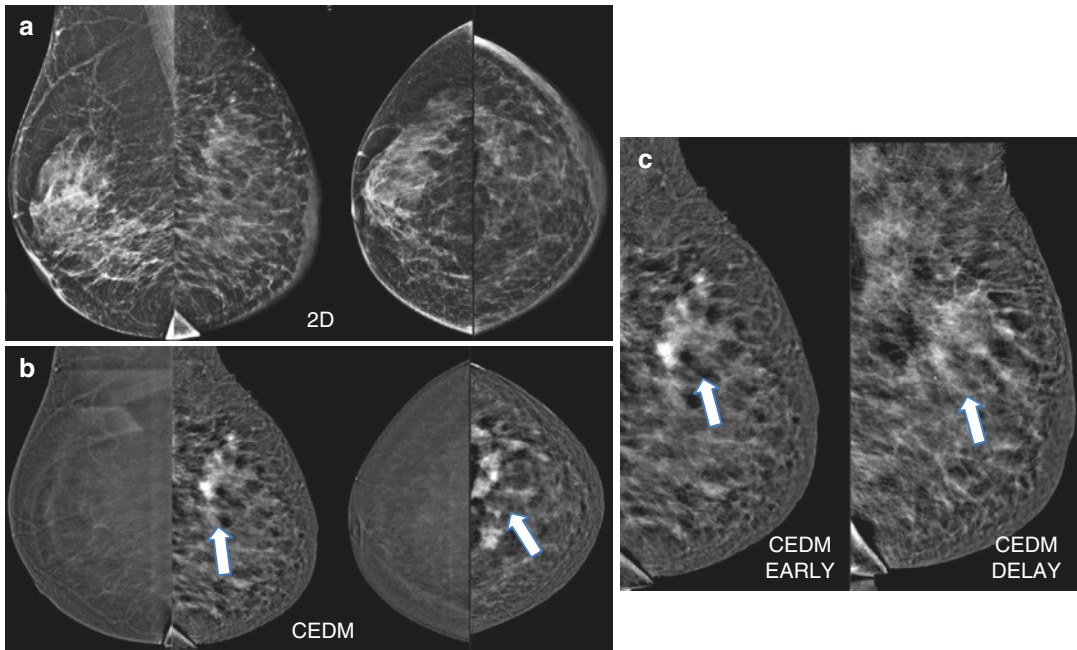
## Case 8



A 45-year-old female presented with a palpable mass in the left breast. **(a)** Low-energy images in CC and MLO view showed an asymmetric opacity in the left upper outer quadrant which were identified as two suspicious solid lesions on ultrasound and biopsied. **(a<sup>1</sup>)** The mammogram also demonstrated a segmental cluster of pleomorphic calcifications in the right upper outer quadrant. Stereotactic biopsy of these calcifications was performed. **(b)** CEDM performed as pre-operative staging showed intense enhancement of the two masses in the left upper outer quadrant (*blue arrows*). There was also an area of non-mass enhancement (*white block arrows*) seen in the distribution of right calcifications, **(b<sup>1</sup>)** the calcifications are seen as dark foci (*blue block arrow*) over the enhancing areas

*Diagnosis: Right calcifications were invasive carcinoma of no special type with ductal carcinoma in situ, while the left breast mass was invasive carcinoma of non-specific type (Image courtesy of Maninderpal Kaur, Kuala Lumpur Hospital, Malaysia)*

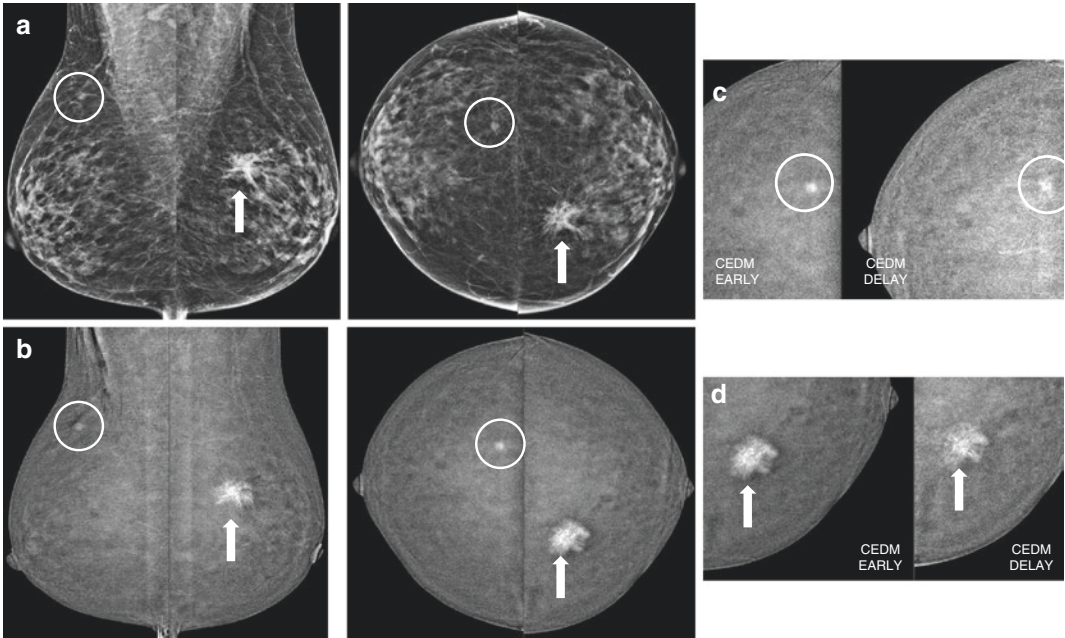
## Case 9



A 62-year-old female presented with a large tender left breast swelling involving the entire breast. CEDM was performed as first-line imaging. (a) Low-energy images in CC and MLO view shows diffuse architectural distortion, skin thickening and nipple retraction in the left breast. (b) CEDM recombined images demonstrating a diffuse patchy non-mass enhancement throughout the left breast with focal areas of intense enhancement demonstrated at the upper mid-quadrant. (c) Mediolateral oblique recombined images in early and delayed phase demonstrating wash-out of the intensely enhancing lesions on the delayed images

*Diagnosis: Final pathology showed a multifocal invasive carcinoma of non-specific type (Image courtesy of Maninderpal Kaur, Kuala Lumpur Hospital, Malaysia)*

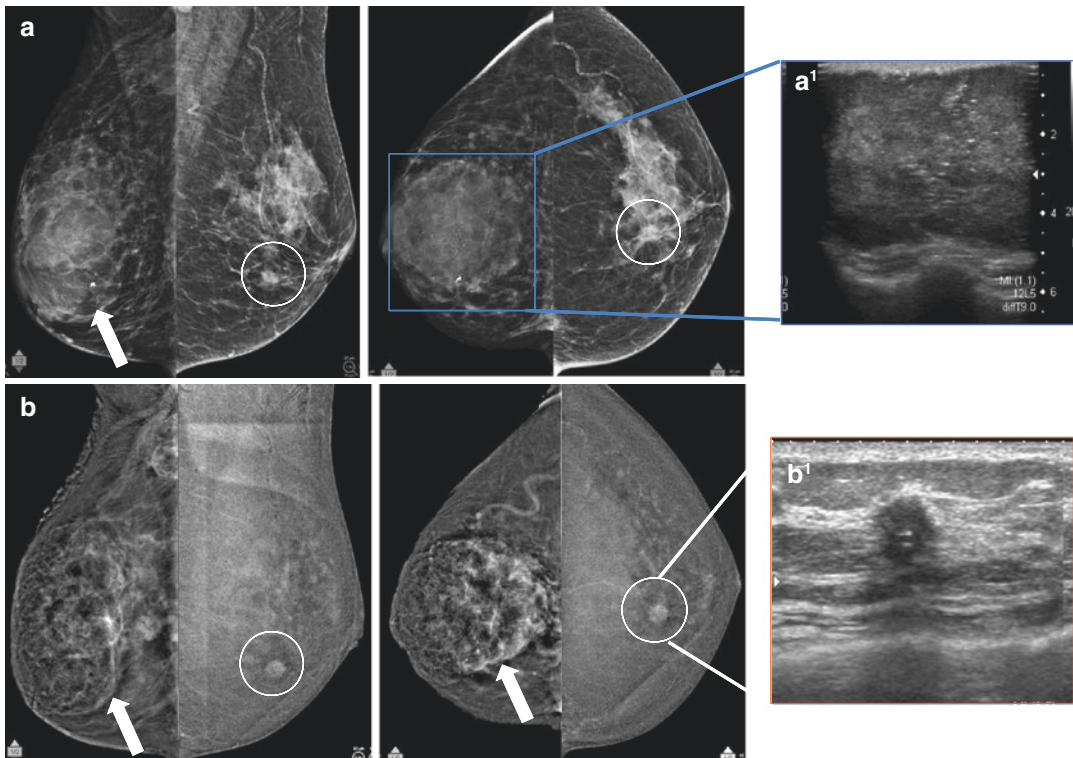
## Case 10



A 62-year-old female presented with a palpable left breast mass. (a) Low-energy image in CC and MLO view showed a spiculated opacity in the left upper inner quadrant (*arrow*) with a small opacity seen in the right upper outer quadrant (*circle*). (b) CEDM recombined images demonstrate an intense enhancement of the left spiculated mass (*arrow*), and there is also a small focus of enhancement seen in the right upper outer quadrant (*circle*). (c) Right CC recombined images in early and delayed phase demonstrating contrast wash-out of the right focus of enhancement. (d) Left CC recombined images in early and delayed phase demonstrating contrast wash-out of the left spiculated mass

*Diagnosis: Left breast invasive carcinoma and the focus in the right breast was also an invasive carcinoma (Image courtesy of Maninderpal Kaur, Kuala Lumpur Hospital, Malaysia)*

## Case 11

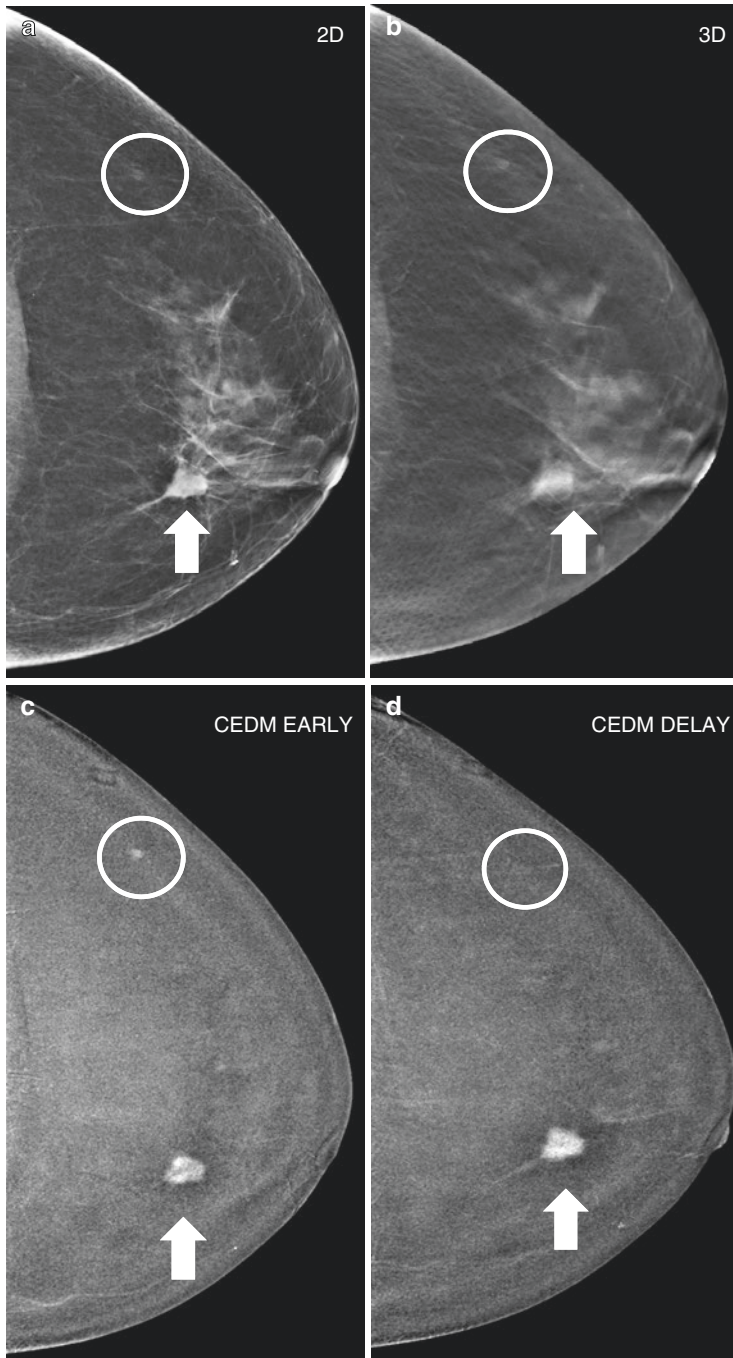


A 63-year-old female presented with a large tender right breast swelling. (a) Low-energy images in CC and MLO view shows a large right breast mass (arrow) with pleomorphic calcifications within, diffuse architectural distortion, skin thickening and nipple retraction in the right breast. There is also a spiculated lesion seen in the left lower inner-quadrant (circle). (b) CEDM recombined images demonstrated a large 9.0 cm heterogeneously enhancing right breast mass with evidence of angiogenic vessels adjacent to it. There was also moderate enhancement of the left spiculated lesion seen. (a<sup>1</sup>–b<sup>2</sup>) The ultrasound of the highly suspicious right breast lesion and the lesion in the left breast (circle) was also identified as a hypoechoic lesion with ill-defined margins and posterior acoustic shadowing. Bilateral breast lesions were immediately subjected to biopsy

*Diagnosis: Final pathology of both lesions showed a multifocal invasive carcinoma on the right and left invasive carcinoma indicating bilateral disease (Image courtesy of Maninderpal Kaur, Kuala Lumpur Hospital, Malaysia)*



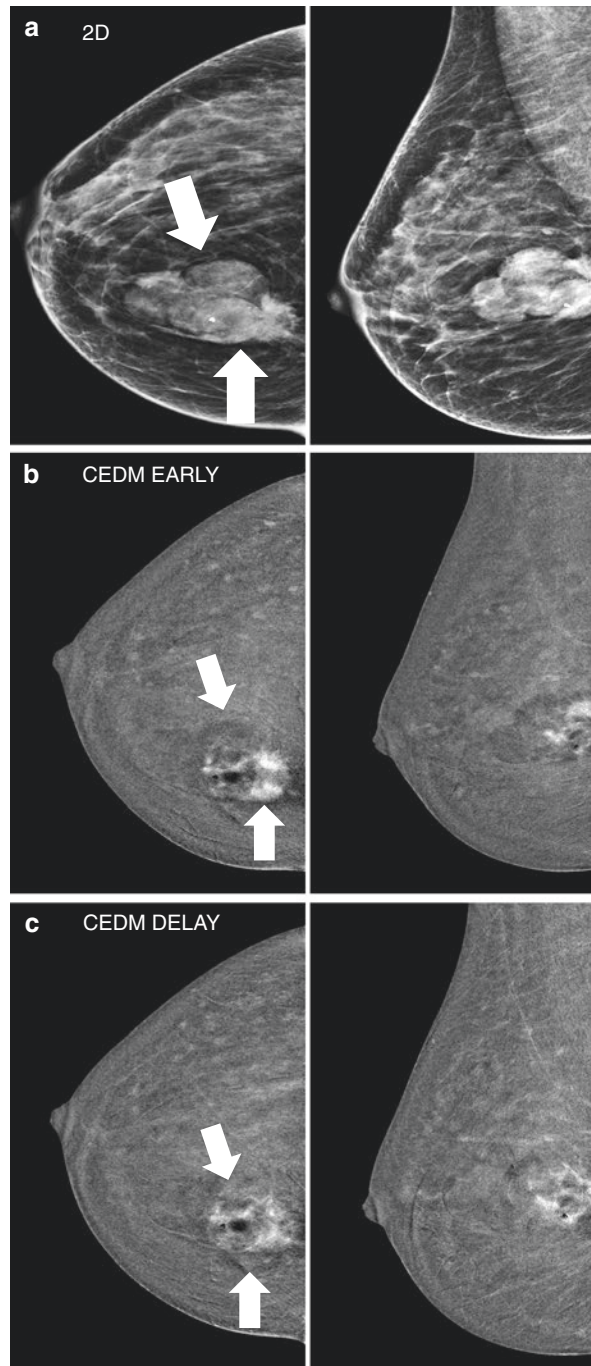
## Case 12



A 73-year-old woman with two opacities in the left breast seen on screening mammogram. (a) Craniocaudal low-energy (2D) and (b) tomosynthesis (3D) views show a spiculated mass in the inner quadrant and a small focus in the outer. (c) Craniocaudal recombined early and (d) craniocaudal recombined late views show a rapid wash-out of the enhancing focus in the outer quadrant and intense progressive enhancement of the inner quadrant mass

*Diagnosis: Outer quadrant enhancing focus with rapid wash-out was a cutaneous angioma (white circle), while the inner quadrant mass with intense progressive enhancement is an invasive carcinoma (white arrow) (Image courtesy of Jacopo Nori, Careggi University Hospital, Florence, Italy)*

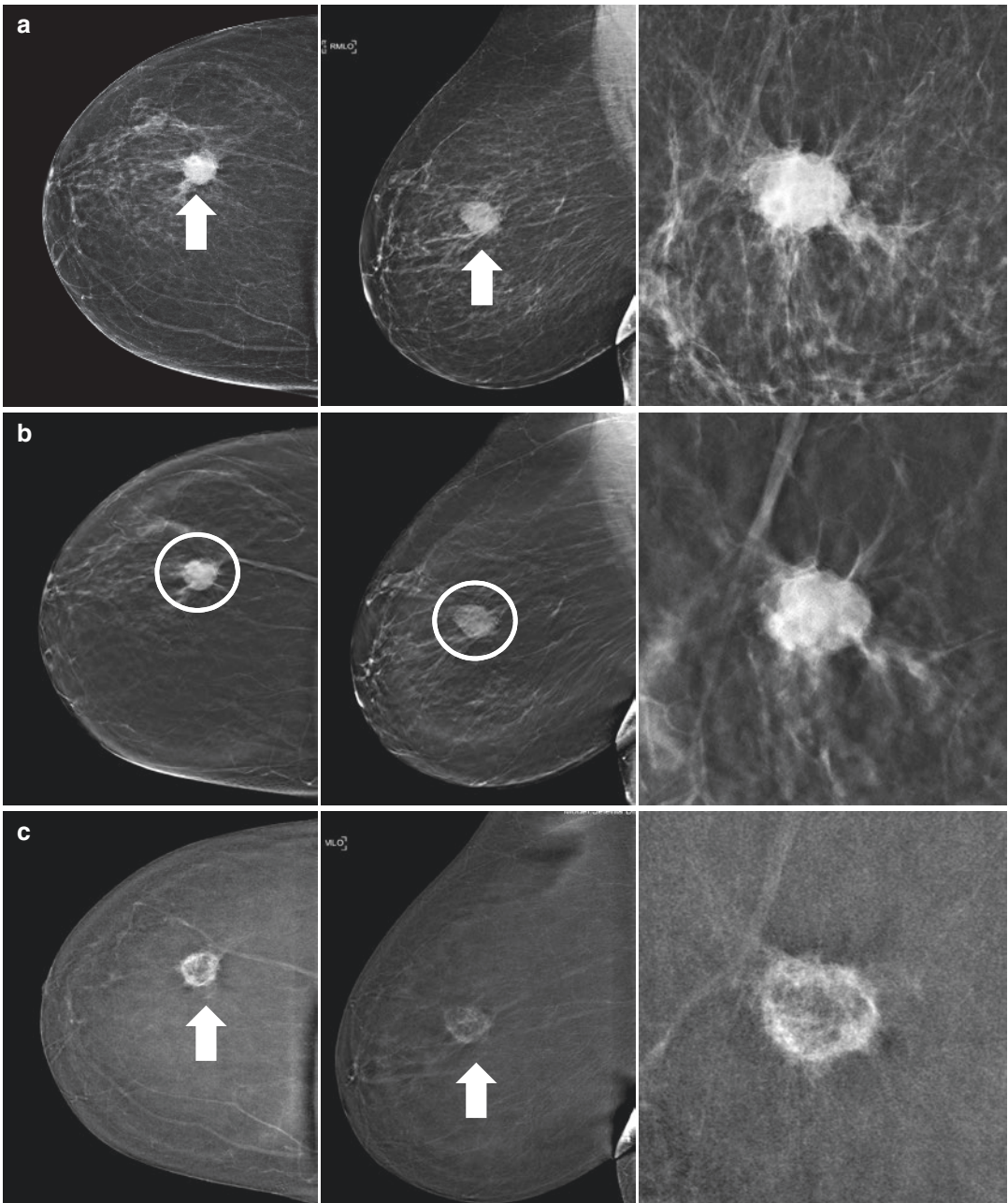
## Case 13



A 49-year-old woman with an invasive ductal carcinoma in the right breast obscured by a known fibroadenoma. CEDM examination demonstrated a unifocal mass corresponding to the carcinoma behind the fibroadenoma. (a) Craniocaudal and mediolateral oblique low-energy (2D) views. (b) Craniocaudal and mediolateral oblique and early recombined images show intense enhancement of the carcinoma. (c) Delay recombined images show a rapid wash-out of the carcinoma and the faint progressive enhancement of the fibroadenoma

*Diagnosis: Invasive carcinoma obscured by a fibroadenoma (Image courtesy of Jacopo Nori, Careggi University Hospital, Florence, Italy)*

## Case 14

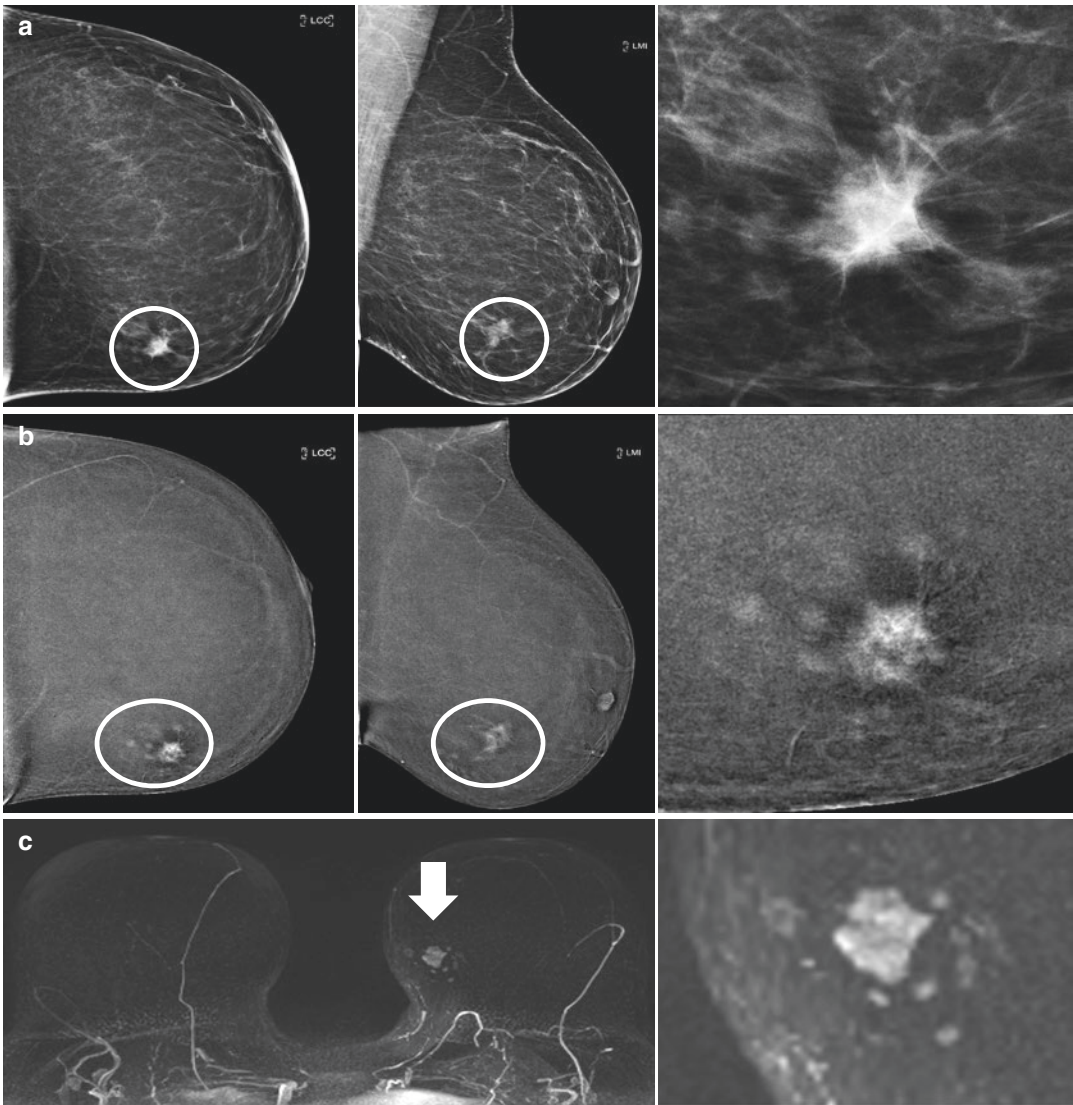


A 43-year-old woman with a fine-needle aspiration on a nodule in the right breast performed in private centre yielded malignant cells. CEDM was performed as pre-surgical staging. (a) Craniocaudal and mediolateral oblique low-energy views with magnification showing a spiculated mass at the right upper outer quadrant. (b) Craniocaudal and mediolateral oblique tomosynthesis with magnification. (c) Craniocaudal and mediolateral oblique recombined images with magnification showing an enhancing lesion with central necrosis. Note the thick irregular rim enhancement

*Diagnosis: Invasive ductal carcinoma, poorly differentiated with focal lobular growth pattern (Image courtesy of Jacopo Nori, Careggi University Hospital, Florence, Italy)*



## Case 15

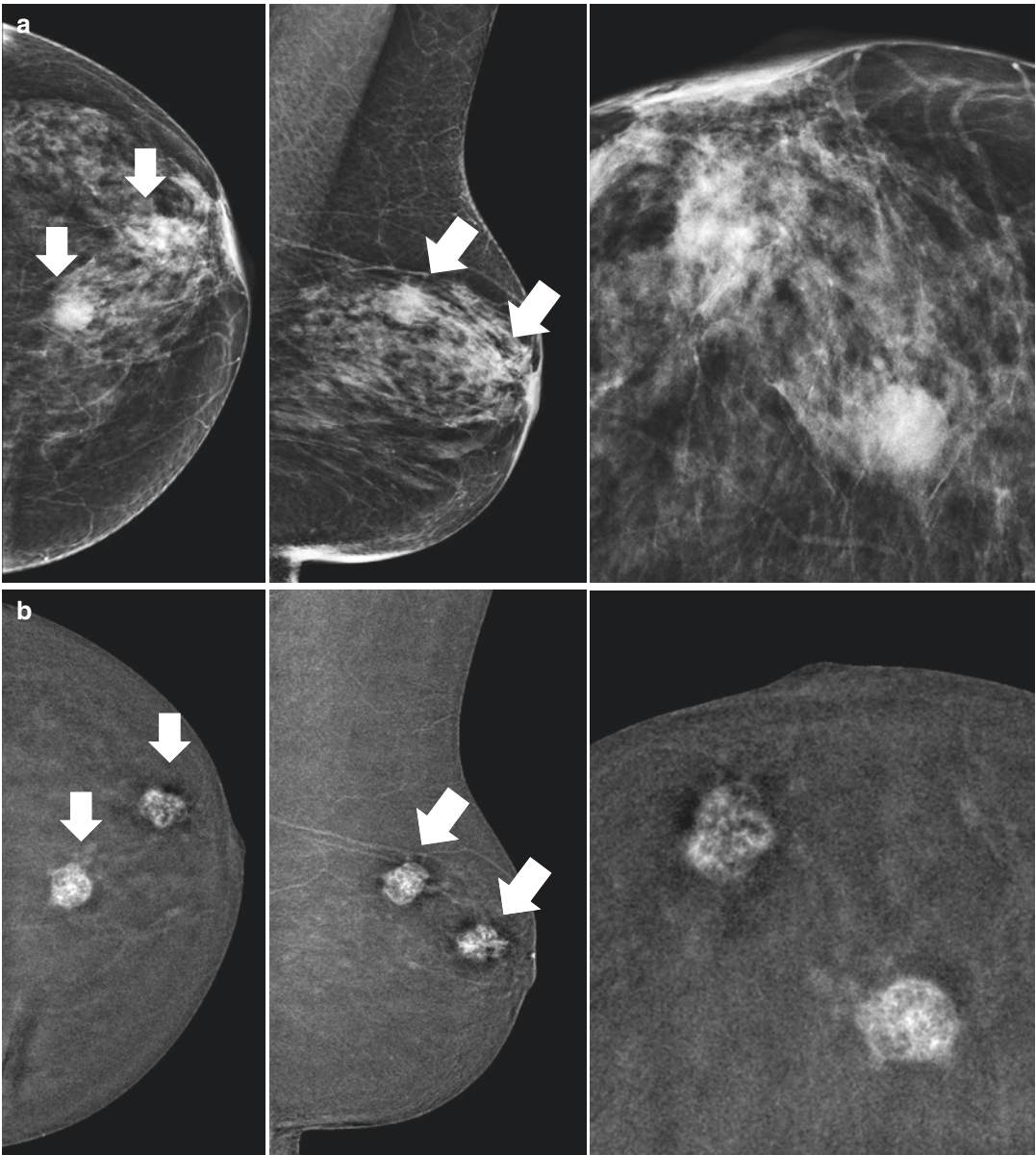


A 41-year-old woman presented with a palpable left breast mass. **(a)** Craniocaudal and mediolateral oblique low-energy views with magnification. **(b)** Craniocaudal and mediolateral oblique recombined images with magnification show the intense enhancement of the dominant mass and some satellite nodules in a framework that is perfectly comparable to that of MRI. **(c)** MRI MIP (maximum intensity projection) with magnification

*Diagnosis: Invasive ductal carcinoma, not otherwise specified (Image courtesy of Jacopo Nori, Careggi University Hospital, Florence, Italy)*

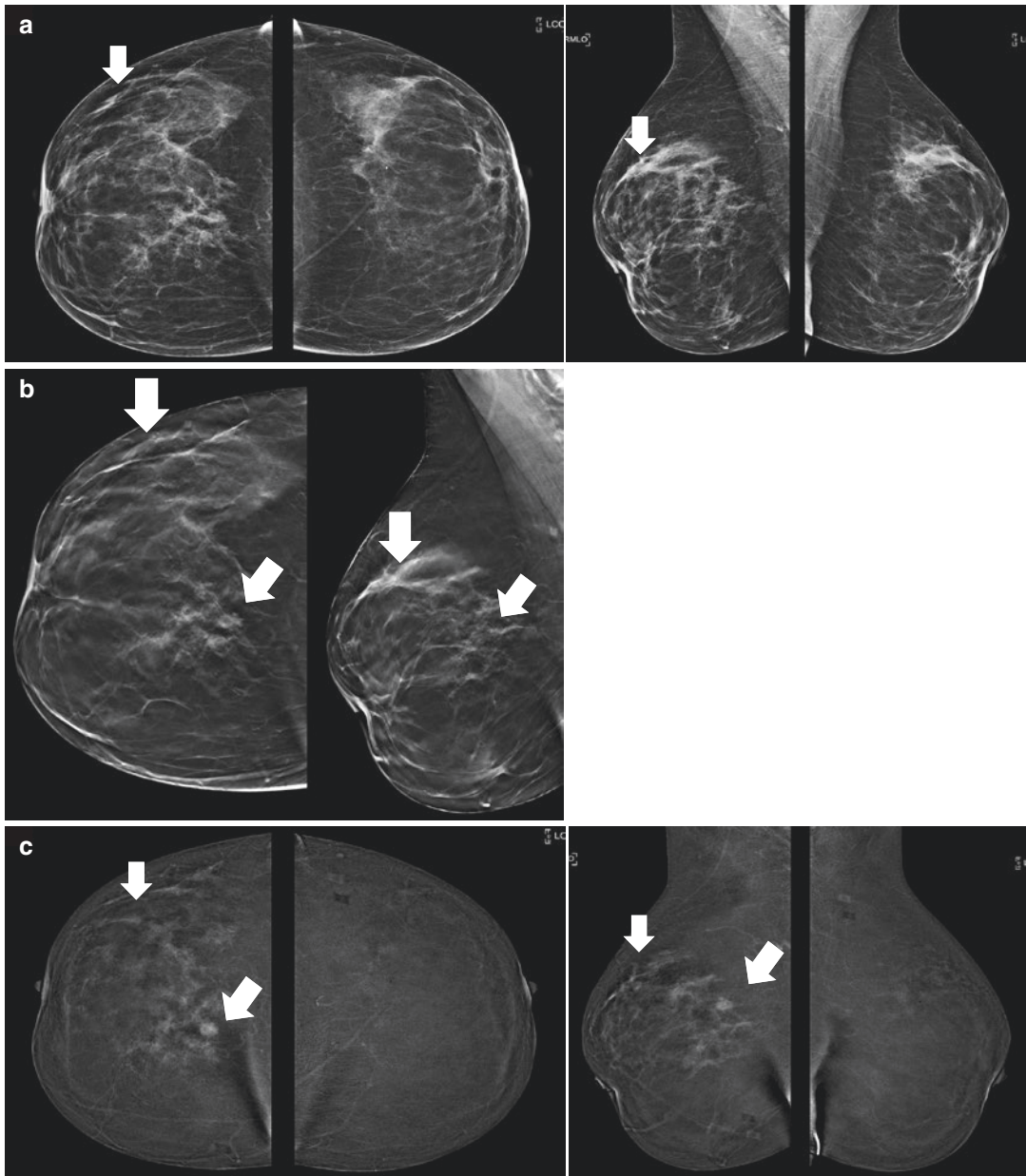


Case 16



A 41-year-old woman with palpable masses in the left breast. (a) Craniocaudal and mediolateral oblique low-energy views with magnification. (b) Craniocaudal and mediolateral oblique recombined images with magnification shows the intense enhancement of the two masses and the angiogenic vessels are also seen on the MLO view  
*Diagnosis: Invasive ductal carcinoma, not otherwise specified (Image courtesy of Jacopo Nori, Careggi University Hospital, Florence, Italy)*

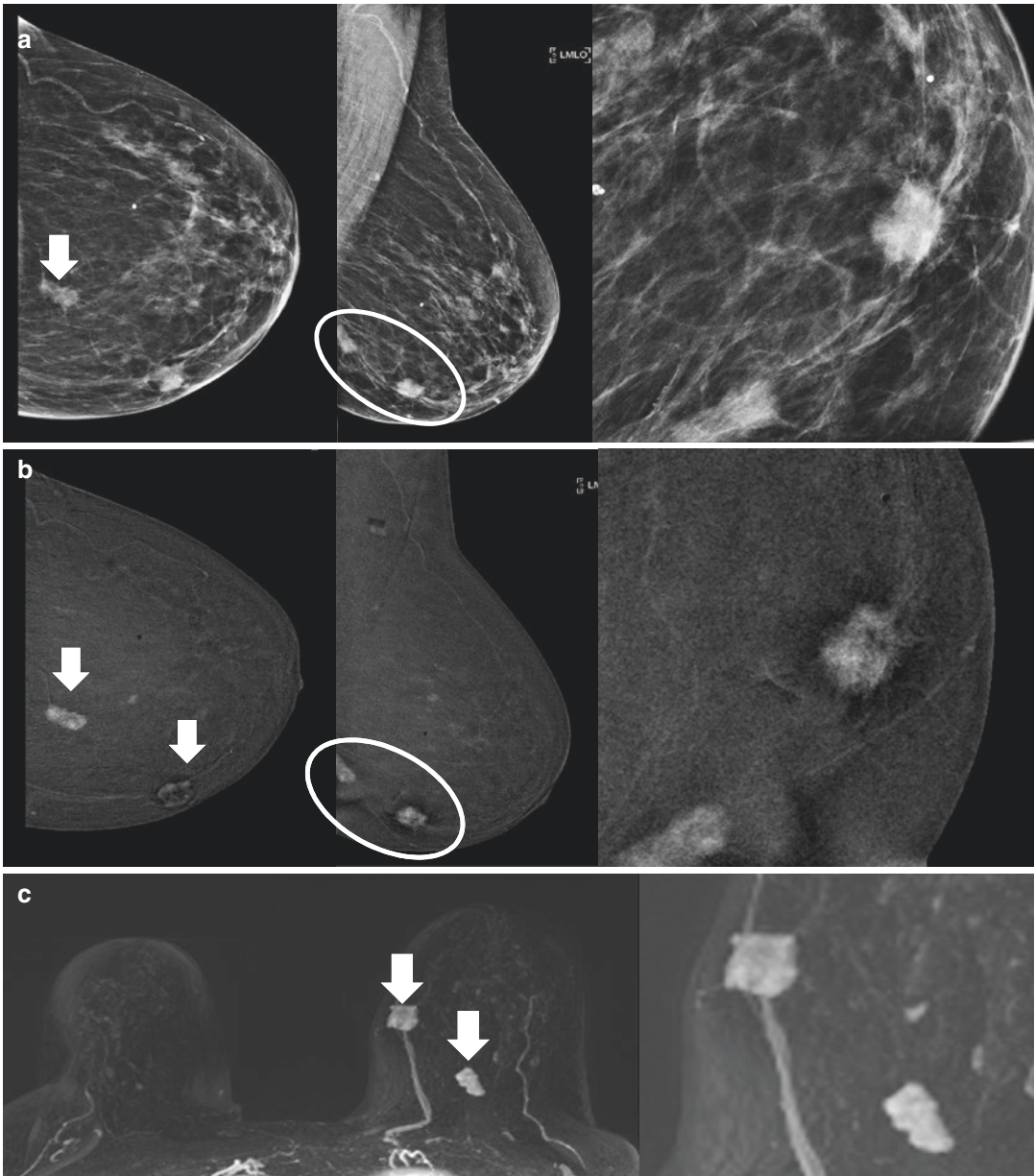
## Case 17



In a 47-year-old woman, the mammogram and tomosynthesis demonstrated areas of architectural distortion involving the upper outer quadrant of the right breast. An ultrasound-guided core biopsy revealed invasive ductal carcinoma. CEDM examination demonstrated an asymmetrical multiregional non-mass enhancement in the upper outer and central quadrant and a mass in the upper central quadrant. (a) Bilateral craniocaudal and mediolateral oblique low-energy views demonstrating a distortion in the upper outer quadrant of the right breast. (b) Right craniocaudal and mediolateral oblique tomosynthesis with more areas of distortion seen involving the upper outer quadrant. (c) Craniocaudal and mediolateral oblique recombined images demonstrating a large area of markedly asymmetric non-mass enhancement involving the entire mid- to upper outer quadrant of the right breast

*Diagnosis: Mastectomy was performed and confirmed an invasive ductal carcinoma not otherwise specified, G3 multicentric (Image courtesy of Jacopo Nori, Careggi University Hospital, Florence, Italy)*

Case 18

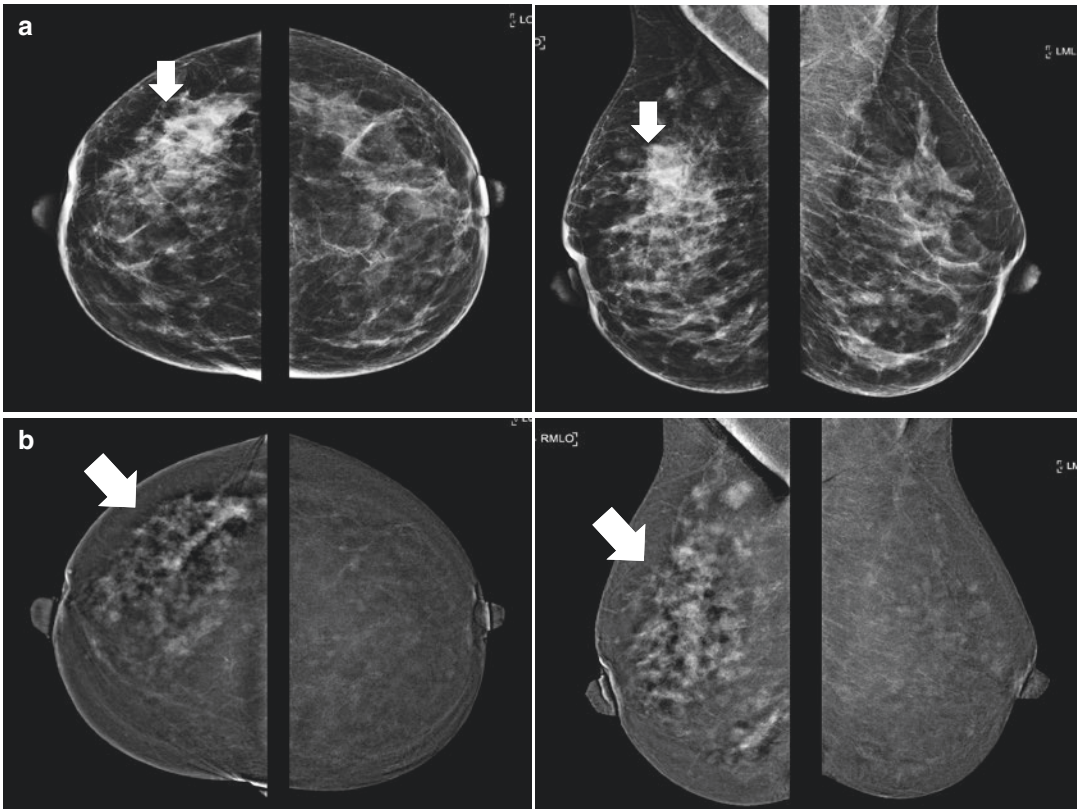


A 46-year-old woman presented with two palpable masses in the left breast. (a) Craniocaudal and mediolateral oblique low-energy views with magnification show two ill-defined opacities in the left lower inner quadrant. (b) Craniocaudal and mediolateral oblique recombined images with magnification show the two masses with intense enhancement exactly corresponding to findings on the MRI maximum intensity projection (MIP) images. (c) MRI MIP with magnification

*Diagnosis: Poorly differentiated invasive ductal carcinoma (Image courtesy of Jacopo Nori, Careggi University Hospital, Florence, Italy)*



## Case 19

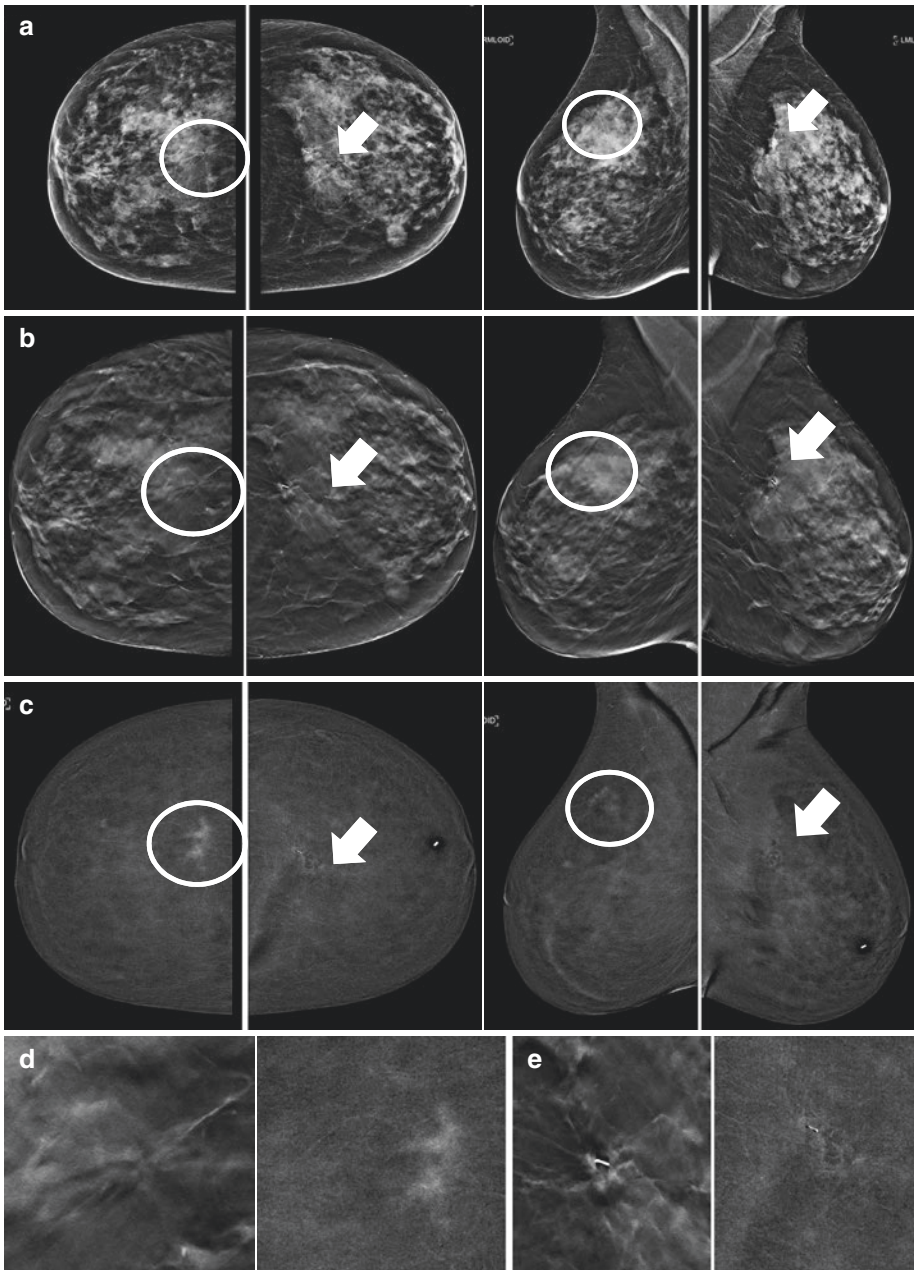


A 51-year-old woman with palpable mass in the upper outer quadrant of the right breast. **(a)** Craniocaudal and mediolateral oblique low-energy views showing an area of asymmetric increased density in the right upper outer quadrant. **(b)** Craniocaudal and mediolateral oblique recombined images demonstrating a markedly asymmetric multiregional non-mass enhancement

*Diagnosis: Pathology post-right mastectomy was a multicentric invasive ductal carcinoma with metastatic lymph nodes (Image courtesy of Jacopo Nori, Careggi University Hospital, Florence, Italy)*



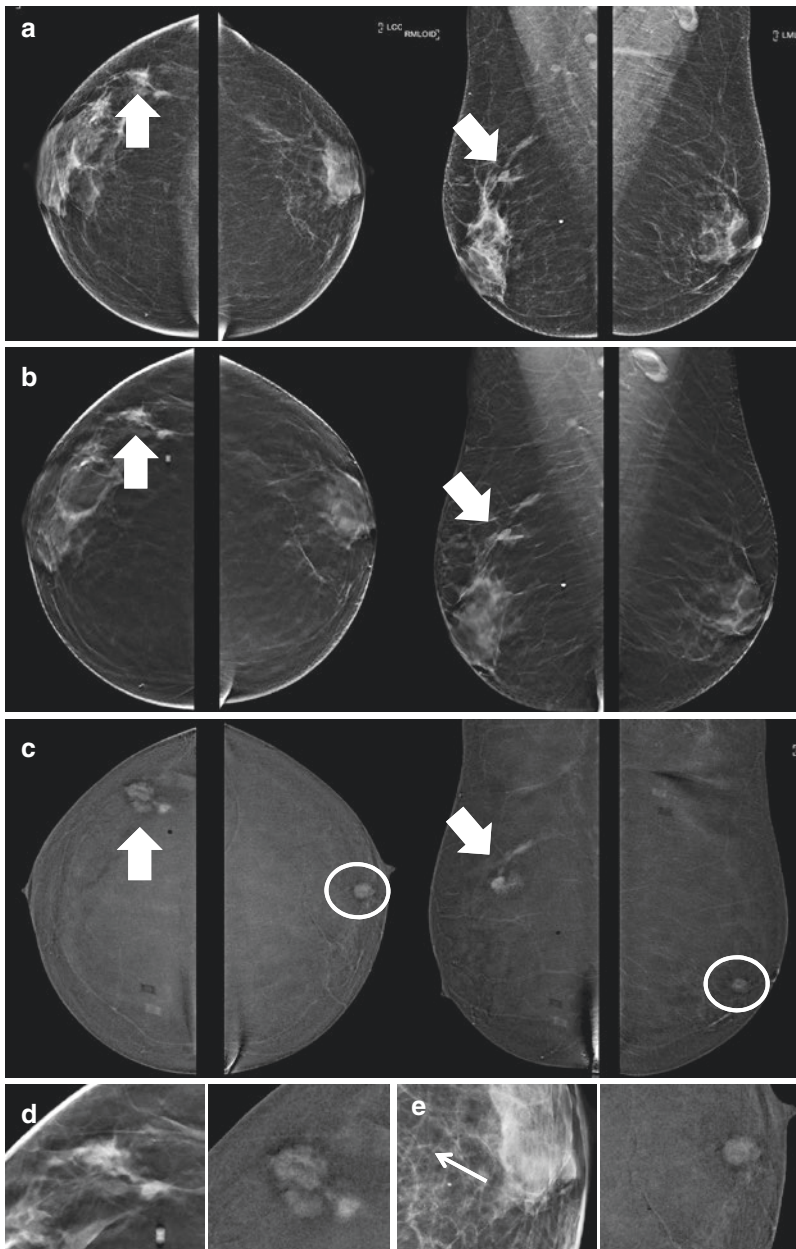
## Case 20



Screening mammogram on a 70-year-old woman who was being worked up for a distortion in the left breast. CEDM demonstrated a non-mass enhancement in the contralateral breast, which was retrospectively seen to be corresponding to a distortion in tomosynthesis views. **(a)** Craniocaudal and mediolateral oblique low-energy views showing bilateral upper mid-quadrant distortions (*white circle and white arrow*). **(b)** Craniocaudal and mediolateral oblique tomosynthesis slice where the distortions are more prominent. **(c)** Craniocaudal and mediolateral oblique recombined images demonstrating non-mass enhancement corresponding to the bilateral areas of distortions. **(d)** 3D and recombined magnified image of the right breast distortion and enhancement. **(e)** 3D and recombined magnified image of the left breast distortion and cystic non-mass enhancement with post-biopsy marker in place

*Diagnosis: Right breast was a 10 mm ductal carcinoma in situ, and the left breast lesion was a 4.5 mm infiltrating carcinoma (Image courtesy of Jacopo Nori, Careggi University Hospital, Florence, Italy)*

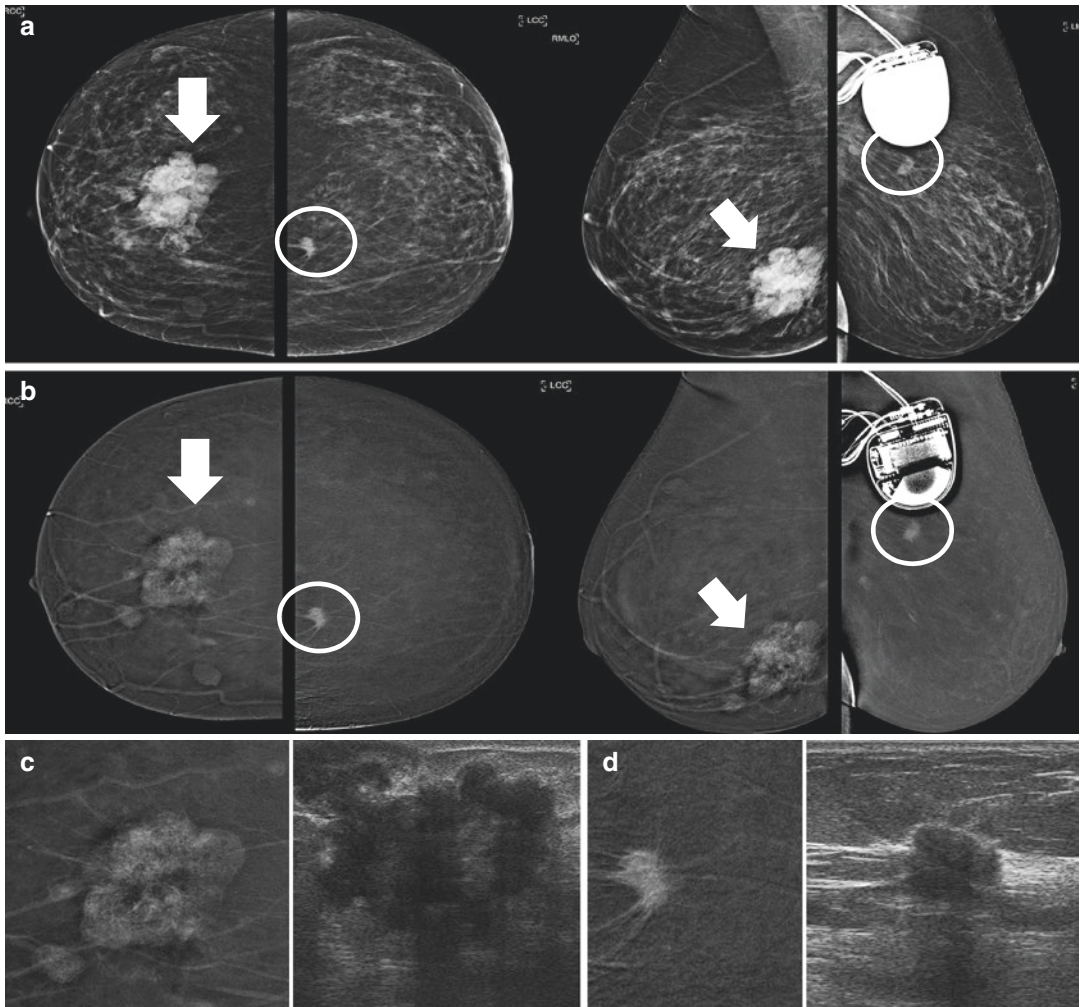
## Case 21



A 55-year-old woman presented with a palpable right breast mass. (a) Craniocaudal and mediolateral oblique low-energy views with an increased asymmetric density with no obvious mass seen in the left breast. (b) Craniocaudal and mediolateral oblique tomosynthesis showing evidence of architectural distortion associated with the right asymmetric density with still no obvious lesion seen in the left breast. (c) Craniocaudal and mediolateral oblique recombined images demonstrating an enhancing round retroareolar mass (*white circle*) in the contralateral breast and an ill-defined enhancing mass with satellite nodules (*block arrow*) in the upper outer quadrant of the right breast, corresponding to the asymmetric density in the low-energy views. (d) Low-energy and recombined magnification views of the right breast lesion. (e) Low-energy and recombined magnification views of the left breast lesion and a cluster of calcifications (*arrow*) are also visualised in this magnified view

*Diagnosis: The right breast mass was an invasive ductal carcinoma, and the left breast mass was an invasive ductal carcinoma and the calcifications were DCIS after core needle biopsy and stereotactic biopsy, respectively (Image courtesy of Jacopo Nori, Careggi University Hospital, Florence, Italy)*

Case 22

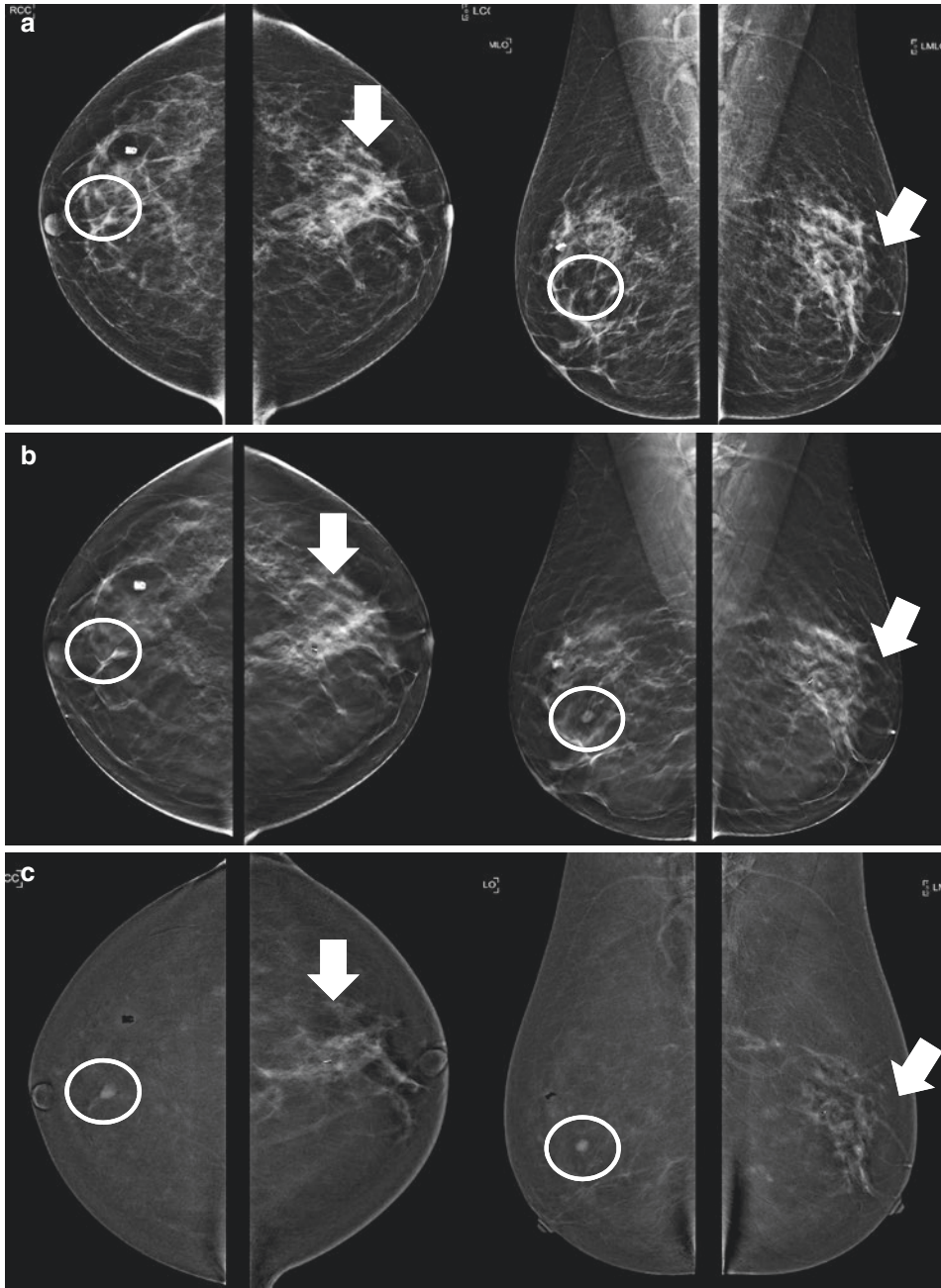


A 61-year-old woman with a cardiac pacemaker presented with a palpable mass in the right breast. CEDM demonstrated multiple masses in the right breast and another mass in the contralateral breast. (a) Craniocaudal and mediolateral oblique low-energy views demonstrating a large lobulated right lower mid-quadrant mass (black arrow) and another small spiculated opacity in the left upper inner quadrant (white circle). (b) Craniocaudal and mediolateral oblique recombined images show multifocal enhancement in the right breast (black arrow), and the left breast nodule (white circle) is also seen to enhance. (c) Recombined image magnification and ultrasound of the right breast masses. (d) Recombined images magnification and ultrasound of the left breast mass

*Diagnosis: The right breast mass was an invasive ductal carcinoma, and the left breast mass was also invasive ductal carcinoma after core needle biopsy. The patient underwent mastectomy on the right that confirmed the multicentric pathology and a lumpectomy on the left (Image courtesy of Jacopo Nori, Careggi University Hospital, Florence, Italy)*



## Case 23

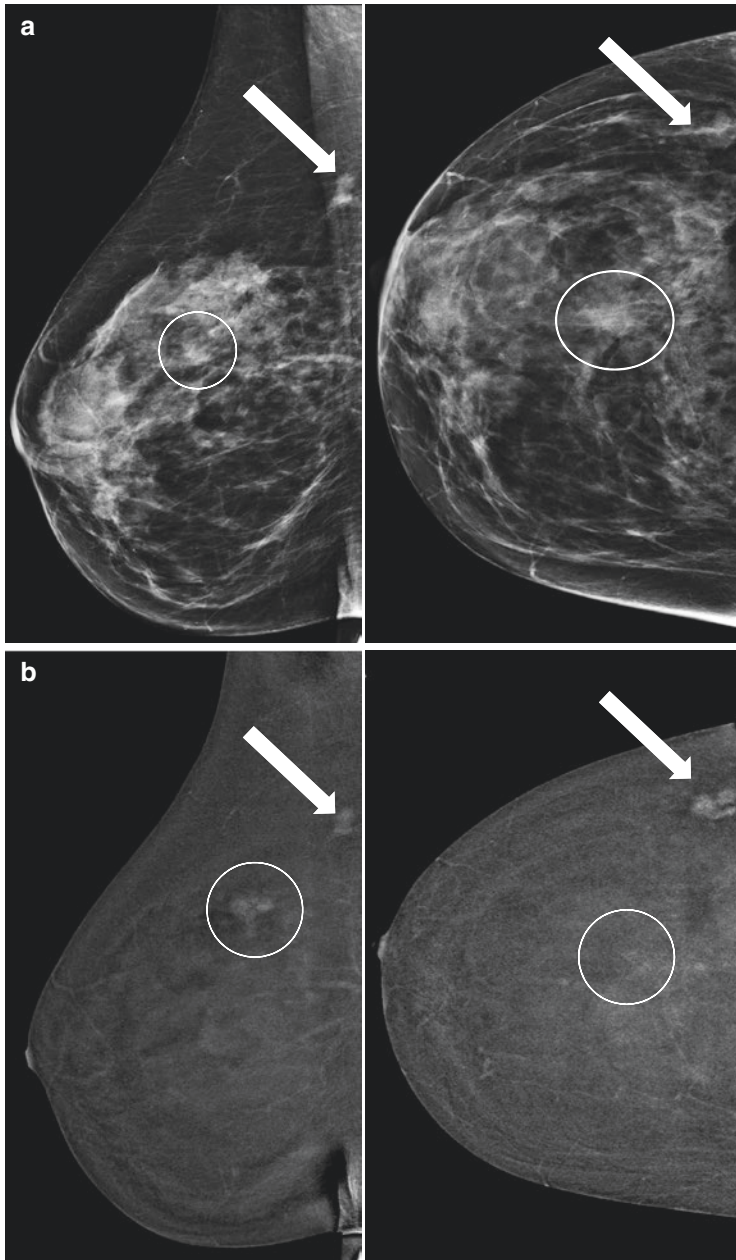


A 58-year-old woman with biopsy-proven ductal carcinoma in situ of the left breast undergoes CEDM to assess disease extent. (a) Craniocaudal and mediolateral oblique low-energy views show an area of increased asymmetric density and architectural distortions in the left breast (*block arrow*). There is also a well-defined nodule (*white circle*) seen in the right retroareolar region. (b) Craniocaudal and mediolateral oblique tomosynthesis slice demonstrates similar findings. (c) Craniocaudal and mediolateral oblique recombined images demonstrate a large segmental heterogeneous non-mass enhancement (*block arrow*) in the left breast, and in the right breast, there was a well-defined oval mass (*white circle*)

*Diagnosis: The left breast mass was a multifocal ductal carcinoma, not otherwise specified, microinvasive, and the right breast mass was a fibroadenoma (Image courtesy of Jacopo Nori, Careggi University Hospital, Florence, Italy)*



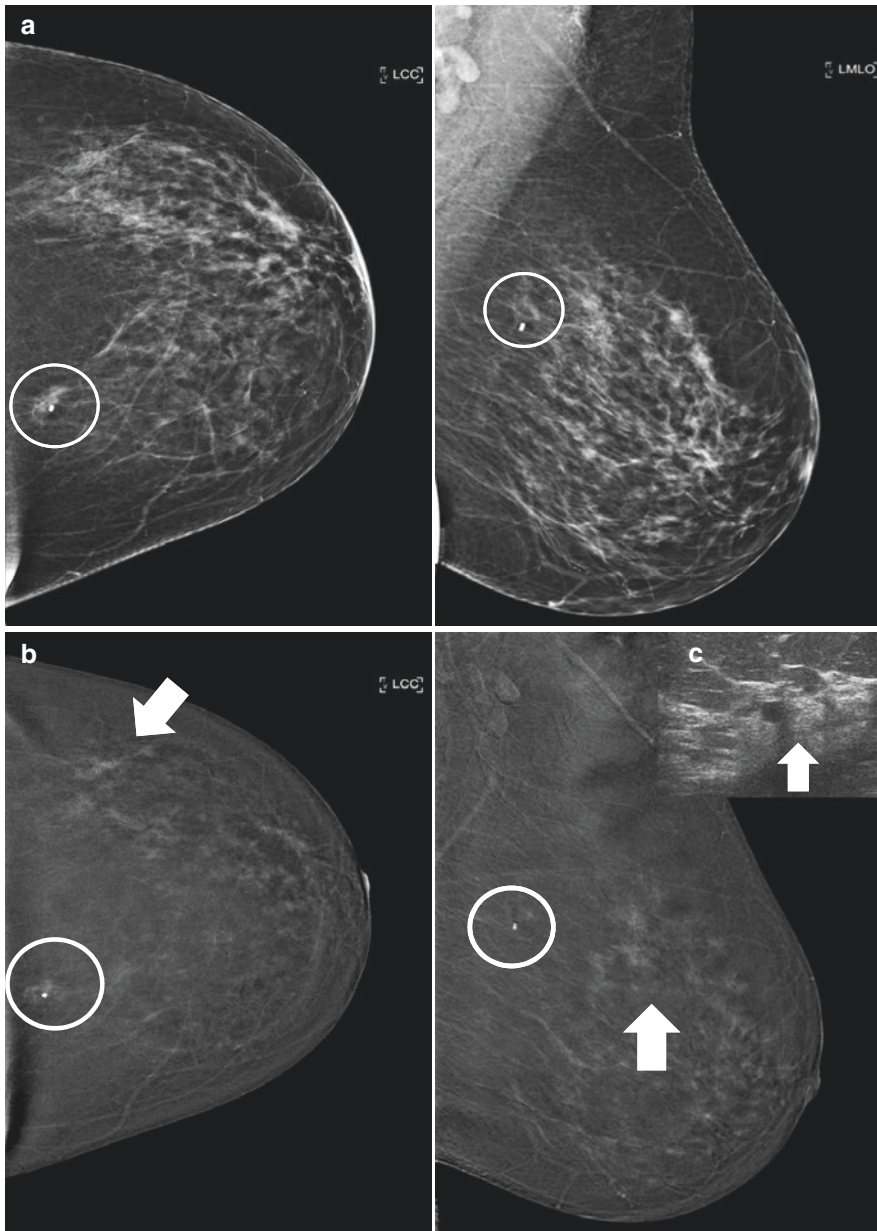
## Case 24



A 64-year-old woman with a biopsy-proven invasive mucinous carcinoma in the upper outer quadrant of the right breast had a CEDM examination to assess for disease extent. **(a)** Mediolateral oblique and craniocaudal low-energy view which shows an ill-defined opacity (*white circle*) in the right upper outer quadrant corresponding to the previously biopsied lesion. There was another smaller ill-defined opacity seen at the right axillary tail region (*black arrow*). **(b)** Mediolateral oblique recombined images demonstrated an intensely enhancing 13 mm mass with irregular margins in the upper outer quadrant of the right breast (*white circle*) which is seen to wash out in the subsequent craniocaudal view. There is another intensely enhancing mass seen in the axillary tail region (*black arrow*)

*Diagnosis: Pathology post-surgery confirmed a multifocal invasive mucinous carcinoma (Image courtesy of Jacopo Nori, Careggi University Hospital, Florence, Italy)*

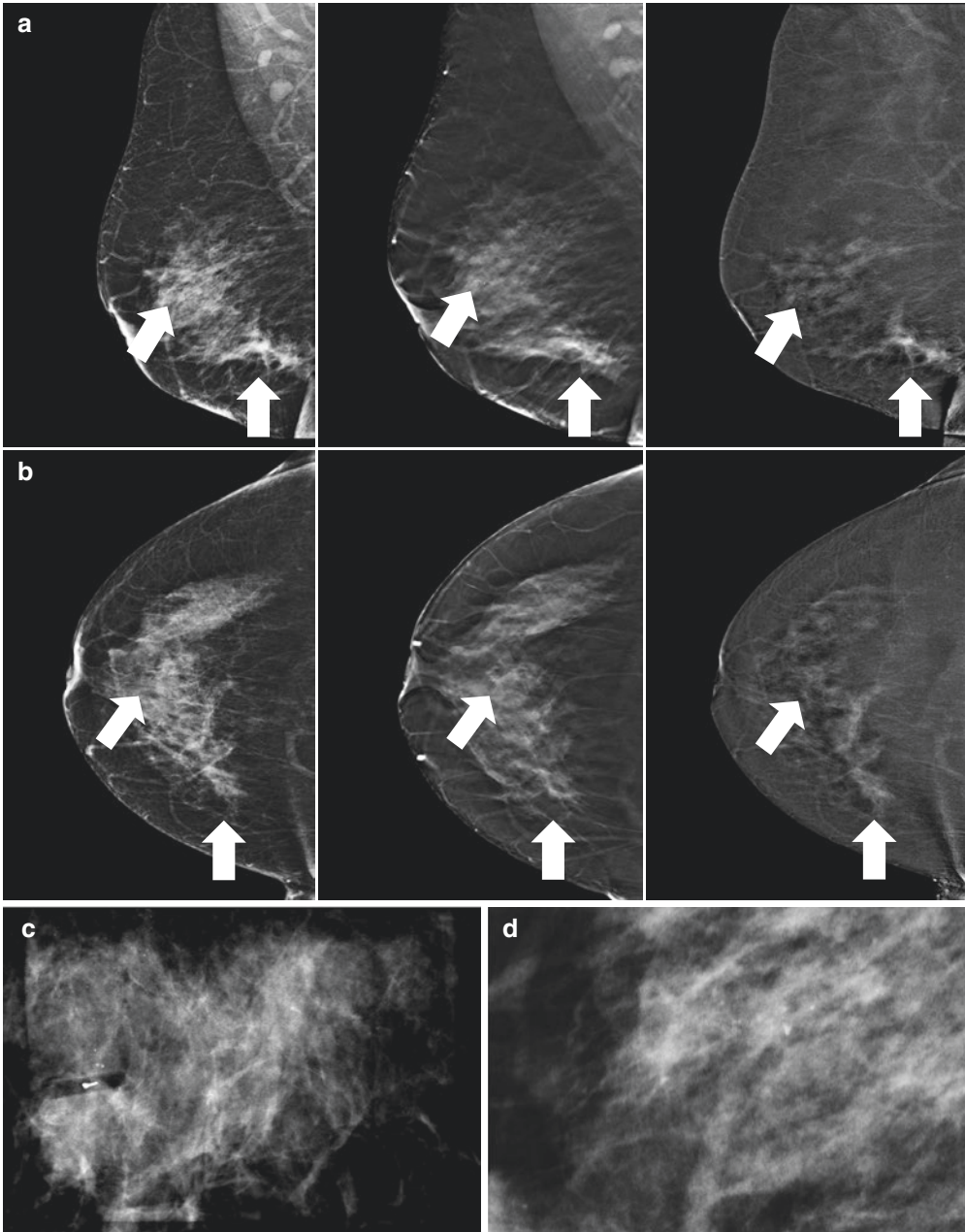
## Case 25



A 56-year-old woman with a proven invasive tubular carcinoma in the upper-inner quadrant of the left breast after a tomosynthesis-guided vacuum-assisted breast biopsy (VABB) with post-biopsy marker placement. (a) Mediolateral oblique and craniocaudal low-energy views showing an increased opacity post-biopsy marker at the biopsy site (*white circle*). (b) Mediolateral oblique and craniocaudal recombined images of CEDM examination demonstrate a post-biopsy marker with adjacent regional non-mass enhancement in the upper inner quadrant of the breast (*white circle*). However, there was also an 8 mm area of faint non-mass enhancement seen in the upper outer quadrant of the left breast (*white arrow*). (c) A second-look ultrasound (US) showed a 9 mm hypoechoic pseudonodular area in the upper outer quadrant

*Diagnosis: Known case of an invasive tubular carcinoma at the left upper inner quadrant. The pathology of the lesion in the upper outer quadrant was also an invasive tubular carcinoma after core needle biopsy (Image courtesy of Jacopo Nori, Careggi University Hospital, Florence, Italy)*

## Case 26



A 67-year-old woman who had an ultrasound-guided biopsy done at another centre, which yielded a lobular invasive carcinoma in the lower inner quadrant of the right breast, was referred to us for a pre-surgical staging CEDM. **(a)** Mediolateral oblique low-energy, tomosynthesis and CEDM recombined images. **(b)** Craniocaudal low-energy, tomosynthesis and CEDM recombined images. **(c)** Post-VABB mammographic detail with a clip released at the biopsy site. **(d)** Magnification view of the calcifications. The CEDM study shows a 27 mm regional non-mass enhancement (NME) in the lower inner quadrant of the right breast, in keeping with the previously biopsied lobular carcinoma. In the retroareolar area, there is another 15 mm non-mass enhancement corresponding to a focal cluster of polymorphic calcifications that was diagnosed as a ductal carcinoma in situ (DCIS) post-stereotactic biopsy  
*Diagnosis: Lobular invasive carcinoma in the lower inner quadrant of the right breast with a DCIS in the retroareolar region (Image courtesy of Jacopo Nori, Careggi University Hospital, Florence, Italy)*

# Index

## A

- Adenosis, 140, 150, 151, 177
- Allergic reaction, 123
- Antiperspirant artefacts, 77–78
- Architectural distortions (AD), 39, 40, 52, 66, 151, 209, 251
- Aromatase inhibitors (AI), 12
- Artefacts
  - abnormal timing of contrast bolus, 80–81
  - contrast retention in veins, 81
  - contrast splatter, 79–80
  - full-field digital mammogram (FFDM)
    - air gap and high-attenuation artefacts, 78–80
    - antiperspirant artefacts, 77–78
    - hair artefacts, 76–77
    - hardware-related factors, 75
    - patient motion, 76
    - patient-related factors, 75
    - software-related factors, 76
  - ghosting artefact, 89–90
  - halo artefact, 82–83
  - high-risk screening, 219
  - implantable cardiac monitoring device, 220
  - invasive carcinoma, 222
  - misregistration artefacts, 87–88
  - negative contrast enhancement, 82, 84, 85, 221
  - QC processes, 88–89
  - ripple artefacts, 84–86
  - skin-line enhancement artefact and enhancing skin lesions, 85–87
- Atypical ductal hyperplasia (ADH), 108, 148, 169–171, 173
  - appearance of, 170
  - histopathology features, 170
  - hypoechoic lesions, 172
  - mediolateral oblique late recombined images, 171
  - mediolateral oblique low-energy view, 171, 173
  - mediolateral oblique recombined images, 173
  - mediolateral oblique tomosynthesis slice view, 172
  - vacuum-assisted biopsy, 170
- Average glandular dose (AGD), 38, 41, 42, 62, 119

## B

- Background parenchymal enhancement (BPE), 93, 94
  - bilateral symmetric NME, 114

- CEDM pitfalls and limitations, 128, 134, 137
  - stippled enhancement, 188

## Benign lesions

- bilateral fibroadenomas, 223
- breast cysts, 141
- complex cyst findings, 147, 148, 150
- complicated cyst findings, 146, 147, 149
- diffuse bilateral breast cysts, 226
- false-positive finding, 140
- fat necrosis
  - conservative management, 158
  - examination and imaging, 158
  - mammography, 158
  - MRI, 158
  - negative contrast enhancement, 158, 165
  - post quadrantectomy surgical scar, 158, 165
  - slow progressive enhancement, 158, 164
  - surgical scar and area of radiotransparency, 158, 162–164
  - US, 158
- fat necrosis with inflammatory changes, 227
- fibroadenoma, 224
  - biopsy-proven fibroadenoma, 140
  - CEDM early phase and delayed phase, 141–143
  - complex fibroadenoma, 140
  - enhancing patterns, 145
  - incidence, 140
  - mammography, 140
  - multiple fibroadenoma, 144–145
  - and papilloma, 143
  - US, 142
- fibroadenomatoid hyperplasia of the breast (FAHB), 224
- fibrocystic changes
  - enhancement patterns, 152–154
  - histologic classification system, 151
  - hormonal imbalance, 150
  - mammography, 151
  - microcystic and macrocystic formation, 150
  - segmental distribution, 155–156
  - ultrasound, 151
- hamartoma
  - glandular tissue and lipomatous elements, 151
  - high risk B3 lesion, 156–157
  - mammography, 151–152



- Benign lesions (*cont.*)
  - MRI, 152–153
  - slow heterogeneous initial enhancement pattern, 153
  - US, 152
- inflamed granuloma, 228
- intraductal papilloma
  - mammography, 156
  - MRI, 156, 158
  - oval opacity, 158, 160
  - retroareolar irregular opacity, 158, 159
  - US, 156
- intramammary lymph node, 225
- simple cyst findings, 141, 146–148
- ultrasound examination, 139–140
- Benign phyllodes tumours, 169
- Bland-Altman plots, 50
- Breast cancer
  - antiangiogenic and antivascular agents, 185
  - breast implant evaluation, 54
  - CEDM, 185
  - death rates, 185
  - imaging-guided breast biopsy procedures, 54–55
  - metastases, diagnosis, 50–51
  - MRI, 185
  - neoadjuvant chemotherapy, 51
  - neovascularization, 185
  - preoperative staging
    - Bland-Altman plots, 50
    - conventional imaging methods, 48
    - imaging modalities, 50
    - invasive lobular cancers, 50
    - Pearson's correlation coefficient (PCC), 49
    - tumour size measurements, 49
  - screening of, 53–54
- Breast conservative therapy (BCT), 52–53
  
- C**
- Claustrophobia, 58
- Clinical implementation, 37
- Complementary test, 61
- Contrast-enhanced digital mammography (CEDM)
  - acquisition costs, 58
  - anatomic and functional information, 57
  - artefacts (*see* Artefacts)
  - BI-RADS lexicon and classification system, 6
  - breast tomosynthesis, 3
  - clinical applications
    - high-risk patients, screening of, 68, 70–72
    - inconclusive findings in conventional imaging, 64–67
    - neoadjuvant chemotherapy (NAC), 68, 70
    - preoperative staging, 68, 69
    - unknown primary cancer, 71
  - clinical indications, 6, 44–45
  - compression paddle
    - preparation of, 37
    - for wire localization, 30–31
  - contrast reactions, 63
  - copper filter installation, 26, 28
  - cost-effectiveness and space allocation, 4
  - dense breast imaging, 20
  - diagnostic accuracy, 36, 37
  - examination interpretation and results
    - communication, 62
  - exposure techniques and radiation dose, 19
  - and full-field digital mammography
    - architectural distortions (AD), 39, 40
    - diagnostic accuracy, 38
    - limitations and pitfalls, 38
    - meta-analysis, 37
    - microcalcifications, 38–39
    - PRISM, 37
    - ROC analysis, 38
    - tumour size estimation, 38
  - functional assessment and lesion localization, 3
  - future aspects of, 71
  - gadolinium-contrast breast MRI indication, 23
  - image acquisition, 63–64
  - imaging procedure workflow, 21–22
  - implementation, 4
  - inconclusive findings, 48
  - in dense breasts
    - clinical assessment, 41
    - clinical performance, 41
    - conventional imaging, 41
    - glandular dose, 42
    - imaging modalities, 40
    - Mammography Quality Standards Act (MSQA), 42
    - sensitivity and specificity values, 41
  - indications, 5
  - interventions in, 30
  - invasive carcinoma, 4, 5
  - iodine-containing contrast agents, 29, 32
  - iodine images, 19, 20
  - lesion vascularity, 4
  - lexicon and interpretation criteria
    - background parenchymal enhancement (BPE), 93, 94
    - focus enhancement, 95–97
    - kinetic enhancement pattern, 94
    - mass enhancement, 97–107
    - non-mass enhancement, 107–118
    - pathology-proven ductal invasive carcinoma, 95
  - low-and high-energy images, 26
  - low energy CEDM, 142, 143, 146–150, 152–156, 159, 160, 162, 164
  - with MRI
    - diagnostic performance, 43
    - lesion size measurements, 43
    - sensitivity and specificity values, 42
  - neovascularity, 3
  - patient handling, 62–63
  - patient issues, for examination
    - claustrophobia, 58
    - complementary test, 61
    - MRI examination, 58

patient anxiety, 58  
 patient compliance and tolerance, 58  
 patient fact card, 59–60  
 patient screening, 58  
 pharmacokinetic simulation, 29  
 physics theory  
   adipose and fibroglandular tissue, 17  
   background subtraction, 17  
   dual-energy subtraction, 17–18  
   practical commercial system, 18  
   X-ray spectra, 19  
   X-ray tubes and X-ray filters, 18  
 pitfalls and limitations  
   abnormal areas of enhancement, 125  
   accurate screening and selection strategies,  
     123–124  
   allergic reaction, 123  
   background parenchymal enhancement, 128, 134,  
     137  
   benign lesion enhancement, 128, 130, 131  
   false-negative lesions, 125–128  
   radiation exposure, 119–123  
 radiation dose considerations, 61–62  
 radiologist and technologist considerations, 61  
 sampling design, 35  
 satellite nodule involvement, 36  
 in symptomatic patients, 7  
 temporal contrast-enhanced mammography  
   dual-energy technique, 35, 36  
   low-energy images, 35  
   pre-contrast image, 35  
   recombined image, 35  
 temporal subtraction, 26–28  
 theoretical considerations, 30  
 3D iodine imaging procedure, 22–23  
 tissue-specific constants, 30  
 tumour extension, 35  
   2D iodine imaging procedure, 17, 22–23  
   2D mammography finding, 36  
   visualization of contrast enhancement, 34  
 Contrast-enhanced spectral mammography (CESM), 57  
 Contrast media  
   architectural distortion, 216  
   compression paddle preparation, 218  
   dynamics, 32–33  
   initial craniocaudal CEDM image, 215  
   satellite nodules/additional areas of involvement, 217  
   2D mammography finding and enhancing lesion, 217  
   X-ray absorption of iodine, 33  
 Contrast splatter, 79–80

**D**

Dense breasts  
   clinical assessment, 41  
   clinical performance, 41  
   conventional imaging, 41  
   cranio-caudal low-energy views, 94  
   glandular dose, 42

  imaging modalities, 40  
   Mammography Quality Standards Act (MSQA), 42  
   sensitivity and specificity values, 41  
 Dual energy subtraction, 17, 18, 35  
 Ductal carcinoma in situ (DCIS)  
   architectural distortion, 190  
   faint non-mass enhancement, 190  
   high-grade DCIS, 188  
   incidence of, 186  
   mammography, 187  
   MRI, 187  
   MRI BIRADS lexicon, 188  
   pathologic classification, 187  
   pathology of, 190  
   pleomorphic calcifications, 190  
   stippled enhancement, 188  
   T1-weighted images, 188  
   T2-weighted images, 188  
   US, 187  
   Van Nuys prognostic index system, 187

**E**

European Reference Organisation for Quality Assured  
   Breast Screening and Diagnostic Services  
   (EUREF) criteria, 123  
 Europe is the guideline of the European Society of  
   Uroradiology (ESUR), 32

**F**

Fibroadenomatoid hyperplasia of the breast (FAHB), 224  
 Fibrocystic changes  
   enhancement patterns, 152–154  
   histologic classification system, 151  
   hormonal imbalance, 150  
   mammography, 151  
   microcystic and macrocystic formation, 150  
   segmental distribution, 155–156  
   ultrasound, 151  
 Flat epithelial atypia, 177, 180–181  
 Full-field digital mammogram (FFDM)  
   air gap and high-attenuation artefacts, 78–80  
   antiperspirant artefacts, 77–78  
   hair artefacts, 76–77  
   hardware-related factors, 75  
   patient motion, 76  
   patient-related factors, 75  
   software-related factors, 76

**G**

Ghosting artefact, 89–90  
 Glomerular filtration rate (eGFR), 124

**H**

Hair artefacts, 76–77  
 Halo artefact, 82–83

- Hamartoma  
 glandular tissue and lipomatous elements, 151  
 high risk B3 lesion, 156–157  
 mammography, 151–152  
 MRI, 152–153  
 slow heterogeneous initial enhancement pattern, 153  
 US, 152
- High-risk (B3) lesions  
 atypical ductal hyperplasia (ADH)  
 appearance of, 170  
 histopathology features, 170  
 hypoechogenic lesions, 172  
 mediolateral oblique late recombined images, 171  
 mediolateral oblique low-energy view, 171, 173  
 mediolateral oblique recombined images, 173  
 mediolateral oblique tomosynthesis slice view, 172  
 vacuum-assisted biopsy, 170
- breast magnetic resonance imaging (MRI), 169  
 CEDM role of, 181–182  
 classical lobular neoplasia (LN)  
 bilateral malignancy, 174  
 histology, 172  
 internal enhancement patterns, 175  
 invasive malignancy, 174  
 loss of E-cadherin staining, 172  
 mass-like lesions, 175  
 mediolateral oblique early recombined image, 175, 176  
 mediolateral oblique low-energy view, 175, 176  
 MIBB classification and WHO, 173  
 nomenclatures, 173  
 nuclear atypia, 172  
 premenopausal women, 174
- flat epithelial atypia, 177, 180–181  
 hamartoma, 156–157  
 imaging follow-up, 169  
 minimal enhancement patterns, 169  
 papillary lesion  
 internal enhancement patterns, 175  
 intra-lesional heterogeneity, 170  
 mediolateral oblique early recombined image, 175, 179  
 mediolateral oblique low-energy view, 175, 176  
 morphological and dynamic aspects, 171  
 papillary DCIS, 170  
 therapeutic excision, 170  
 upgrade rates, 170
- radial scars  
 adenosis, 177  
 asymmetric non-mass enhancement, 177  
 central fibroelastotic core, 177  
 mammography, 177  
 mediolateral oblique early recombined image, 178  
 mediolateral oblique late recombined image, 178  
 mediolateral oblique low-energy view, 178  
 recommendation for, 177  
 therapeutic excision, 177
- risk factor, 169  
 vacuum-assisted biopsy (VAB), 169
- I**
- Image acquisition, 63–64  
 Intraductal papilloma  
 mammography, 156  
 MRI, 156, 158  
 oval opacity, 158, 160  
 retroareolar irregular opacity, 158, 159  
 US, 156
- Intramammary lymph node, 225  
 Invasive carcinoma, 234  
 Invasive ductal carcinoma, 241, 242, 245  
 CEDM, 192  
 colloid tumour, 198–200  
 fat lobule, 201  
 and fat lobule, 197, 201  
 kinetics of, 189  
 mammography, 189  
 morphologic patterns, 189  
 MRI, 189  
 mucinous carcinoma, 192, 202–204  
 multicentric invasive ductal carcinoma, 194  
 papillary carcinoma, 202, 205, 206  
 pathology, 191, 195, 196  
 in situ component, 193  
 tubular carcinoma, 205, 207, 208  
 US, 189
- Invasive lobular carcinoma, 205, 209–212  
 Iodine contrast, 21, 22
- K**
- Kinetic enhancement, 94, 102, 109, 140, 150, 188, 199, 203, 207, 210, 224
- L**
- Lifetime attributable risk (LAR), 122  
 Lobular neoplasia (LN)  
 bilateral malignancy, 174  
 histology, 172  
 internal enhancement patterns, 175  
 invasive malignancy, 174  
 loss of E-cadherin staining, 172  
 mass-like lesions, 175  
 mediolateral oblique early recombined image, 175, 176  
 mediolateral oblique low-energy view, 175, 176  
 MIBB classification and WHO, 173  
 nomenclatures, 173  
 nuclear atypia, 172  
 premenopausal women, 174
- M**
- Magnetic resonance imaging (MRI)  
 contrast-enhanced breast MRI, 47

- diagnostic performance, 43
  - hamartoma, 152–153
  - high-risk (B3) lesions, 169
  - intraductal papilloma, 156, 158
  - invasive ductal carcinoma, 189
  - lesion size measurements, 43
  - malignant lesions
    - ductal carcinoma in situ (DCIS), 187
    - MRI BIRADS lexicon, 188
  - MRI BI-RADS lexicon, 98
  - patient issues, for examination, 58
  - sensitivity and specificity values, 42
  - Malignant lesions
    - architectural distortion, 234
    - breast swelling, 238, 239
    - CEDM finding, 186
    - distortion, 248
    - ductal carcinoma in situ (DCIS)
      - architectural distortion, 190
      - faint non-mass enhancement, 190
      - high-grade DCIS, 188
      - incidence of, 186
      - mammography, 187
      - MRI, 187
      - MRI BIRADS lexicon, 188
      - pathologic classification, 187
      - pathology of, 190
      - pleomorphic calcifications, 190
      - stippled enhancement, 188
      - T1-weighted images, 188
      - T2-weighted images, 188
      - US, 187
      - Van Nuys prognostic index system, 187
    - first-round breast cancer screening, 231
    - ill-defined irregular mass, 230, 232, 235
    - inner quadrant mass, 240
    - invasive ductal carcinoma, 241, 242, 245
      - CEDM, 192
      - colloid tumour, 198–200
      - and fat lobule, 197, 201
      - kinetics of, 189
      - mammography, 189
      - morphologic patterns, 189
      - MRI, 189
      - mucinous carcinoma, 192, 202–204
      - multicentric invasive ductal carcinoma, 194
      - papillary carcinoma, 202, 205, 206
      - pathology, 191, 195, 196
      - in situ component, 193
      - tubular carcinoma, 205, 207, 208
      - US, 189
    - invasive lobular carcinoma, 205, 209–212
    - invasive tubular carcinoma, 253
    - lobular invasive carcinoma, 254
    - multifocal ductal carcinoma, 251, 252
    - non-mass enhancement, 236
    - palpable masses, 243, 244, 246, 247, 249, 250
    - palpable right upper outer quadrant mass, 234
    - segmental cluster of pleomorphic calcifications, 236
    - segmental non-mass enhancement, 233
    - subtle swelling and tenderness, 233
  - Mammographic breast density (MBD)
    - computer-assisted methods, 11
    - definition, 9
    - diagnostic tools, 13–14
    - glandular tissue and stromal tissue, 9
    - independent risk factors, 12–13
    - masking effect, 12
    - visual methods
      - ACR classification criteria, 10
      - BI-RADS categories, 10
      - parenchymal patterns, 9
      - quantitative method, 9
  - Mammography Quality Standards Act (MSQA), 42, 119
  - Mass enhancement
    - fibroadenoma, 106
    - heterogeneous enhancement, 104
    - homogeneous enhancement, 98, 101–103
    - intensity of enhancement, 104
    - invasive ductal carcinoma, 105
    - irregular margins, 98, 99
    - lobular carcinoma, 107
    - margin analysis, 97
    - morphology descriptors of, 97, 98
    - MRI BI-RADS lexicon, 98
    - papillary lesion, 105–106
    - regular margins, 98
    - rim enhancement, 100, 101
    - spiculated margins, 98
  - Metastases, diagnosis of, 50–51
  - Microcalcifications, 38–39
- N**
- Neoadjuvant chemotherapy (NAC), 51, 68, 70
  - Non-mass enhancement (NME)
    - asymmetric enhancement, 114
    - background parenchymal enhancement (BPE), 107
    - bilateral symmetric NME, 114
    - causes, 107
    - clumped enhancement, 108
    - clumped non-mass enhancement, 113–114
    - clustered ring enhancement pattern, 109
    - diffuse NME, 108
    - distribution descriptor, 113
    - heterogeneous enhancement, 108
    - internal enhancement patterns, 108
    - invasive (IDC) and in situ (DCIS) ductal carcinoma, 110
    - LE and eventual enhancement pattern, 116–117
    - linear NME, 108
    - microcalcifications, 115
    - multiregional NME, 108, 112
    - regional NME, 108, 111
    - segmental NME, 108
    - symmetric enhancement, 114
  - Nuclear atypia, 172



**P**

- Papillary lesion (PL)
  - internal enhancement patterns, 175
  - intra-lesional heterogeneity, 170
  - mediolateral oblique early recombined image, 175, 179
  - mediolateral oblique low-energy view, 175, 176
  - morphological and dynamic aspects, 171
  - papillary DCIS, 170
  - therapeutic excision, 170
  - upgrade rates, 170
- Patient anxiety, 58
- Patient fact card, 59–60
- Pearson's correlation coefficient (PCC), 49
- Problem-solving, 36, 41, 48, 64, 66, 67

**Q**

- Qualitative assessment, 9, 11
- Quantitative assessment, 9, 11
- Quality control processes, 88–89

**R**

- Radial scars
  - adenosis, 177
  - asymmetric non-mass enhancement, 177
  - central fibroelastotic core, 177
  - mammography, 177
  - mediolateral oblique early recombined image, 178
  - mediolateral oblique late recombined image, 178
  - mediolateral oblique low-energy view, 178
  - recommendation for, 177
  - therapeutic excision, 177
- Radiation exposure
  - automatic exposure control (AEC), 122
  - dosage of, 122
  - dose optimization, 122
  - dose reduction, 122–123
  - dual acquisition, 122
  - factors for CEDM, 119, 120

- high-energy exposure, 119, 122
- intravenous iodinated contrast, 123
- lifetime attributable risk (LAR), 122
- low-energy exposure, 119, 122

**Radiology, 62**

Ripple artefacts, 84–86

**S**

- Satellite nodule involvement, 36
- Skin-line enhancement artefact, 85–87
- Supplemental screening, 13, 14, 45

**T**

- Tamoxifen (TAM), 12
- Temporal subtraction, 26–28
- Tomosynthesis, 3

**U**

- Ultrasound
  - benign mass, 142
  - complex cysts, 141
  - ductal carcinoma in situ (DCIS), 187
  - fat necrosis, 158
  - fibroadenoma, 141
  - hamartoma, 152
  - hypoechoic ill-defined lesions, 13
  - intraductal papilloma, 156
  - invasive ductal carcinoma, 189
  - multiple fibroadenomas, 144

**V**

- Vacuum-assisted biopsy (VAB), 169

**W**

- Wolfe's qualitative method, 10